



C Cranfield UNIVERSITY

C Cranfield HEALTH

EngD THESIS

Academic Years 2003-2007

William St John Roberts

SCANNING ELECTROCHEMICAL MICROSCOPY FOR THE
INTERROGATION OF BIOLOGICALLY MODIFIED SURFACES

Supervisor: Professor Séamus P. J. Higson
Industrial Supervisors: Dr. G. Johnson, Dr. D. Lonsdale, Dr. J. Griffiths
Management Supervisor: Dr. P. Smart

Presented January 2007

This thesis is submitted in partial fulfilment of the requirements for the
degree of
Doctor of Engineering (EngD)

©Cranfield University 2007. All rights reserved. No part of this publication
may be reproduced without written permission of the copyright owner.

For my family and friends

Acknowledgements

Over the course of this research programme, I have been fortunate enough to meet and work with many very talented individuals, to whom I am most indebted. First and foremost I am enormously grateful to my supervisor, Professor Seamus Higson for all his support over the past few years – not only for his academic input, but also for his unerring enthusiasm and energy for what he does. Thanks also go to other senior members of the group – Dr. Frank Davis for his technical input and Dr. Stuart Collyer for his technical, moral and comedic support. My thanks also go to more recent additions to the group – Duncan, Stuart, Tim, Phil and Sarah – all of whom have been a great source of support and all of whom I wish the very best in their research over the coming years. Thanks are also due to Dr. Lee Larcombe for his technical insights into my project (and of course, introducing me to the daily Dilbert cartoon strip) and Dr. Sarah Morgan for her advice and guidance. Additionally, I would like to thank my management supervisor, Dr. Palie Smart for her time in both her supervision and advice.

This project could not have been possible without the financial support of the EPSRC and the support of my industrial sponsors, Uniscan Instruments Ltd. The technical support I received from Dr. Daniel Lonsdale was invaluable and I cannot thank him enough for his help and encouragement over the course of this project. Additionally I am truly thankful to Dr. Graham Johnson for his significant support and valuable insights into the commercial aspects of this work.

During my time at Cranfield, I have met some inspirational individuals who continue to entertain, support and truly mystify me – Swifty, Damo, Wakster, Dan, Kathryn and Helen – cheers guys. Outside Cranfield - to all my friends who have been patiently waiting for me to finally finish - thanks for always being there or thereabouts when I needed you.

Finally, to my Mum, Dad and sister Alice, for a lifetime of support and encouragement, Pappa, for your inspirational pep talks (the 4F's) and of course Gran, who is a true inspiration to us all.

Declaration

This is a declaration to certify that no portion of the work referred to in this thesis has been submitted in support of an application for another degree or qualification of this or any other university, or institute of learning.

William St John Roberts

January 2007

Abstract

This thesis describes two novel applications of scanning electrochemical microscopy (SECM) to biological systems.

The first involves the characterisation of a novel, impedance based genomic DNA biosensor - previously developed within the group. SECM in feedback mode was used to interrogate a DNA-polyelectrolyte film to determine whether the changes observed by impedance were detectable by SECM. Using the SECM micropositioning device to pattern a carbon ink substrate, a dotted array of polyethylenimine (PEI) and single stranded DNA (ssDNA) was fabricated. Using hexamine ruthenium chloride as the redox couple, the array was then interrogated by a SECM area scan before and following exposure to complementary and non-complementary DNA. Upon the exposure of the DNA/PEI array to complementary DNA, the feedback current over the functionalised region was observed to increase, whereas on exposure of the array to non-complementary DNA, an increase in feedback current was also observed - but to a lesser degree.

The second SECM application described involves the use of SECM to detect protein expression in cells. Using an established immunochemical protocol, the transmembrane protein, CD44, expressed by cultured RT112 cells was labelled via a primary/secondary antibody complex to horseradish peroxidase. Using hydrogen peroxide and hydroquinone, the activity of the HRP label was subsequently detected by SECM in feedback mode. The microelectrode tip was biased at a potential of -0.4V , a potential sufficient for the reduction of benzoquinone - the redox active product of the HRP catalysed reaction. The work presented represents the first application of SECM to detecting protein expression in cells and effectively demonstrates the promise this technique holds for immunochemical applications.

An analysis of Uniscan's innovation network is also presented, which provides a valuable insight into the management of such resources and how they may be orchestrated to extract maximal innovative value for all parties involved in a collaborative relationship.

Table of Contents

List of figures and tables	i
Nomenclature	viii
1. Research rationale	1
2. Introduction and literature review	5
2.1 Electrochemistry	6
2.1.1 Electron transfer and energy levels	7
2.1.2 Non-faradaic processes and the nature of the double layer	12
2.1.3 The electrode/solution interface	13
2.1.4 The Electrical Double Layer	15
2.1.5 Voltammetry	18
2.1.6 The electrochemical cell and electrodes	18
2.1.7 Working electrodes (WE)	21
2.1.8 Reference electrodes (RE)	21
2.1.9 Counter electrodes (CE)	21
2.2 Processes affecting the electrode reaction rate and current	22
2.3 Mass Transport	23
2.3.1 Diffusion	24
2.3.2 Convection	28
2.3.3 Migration	29
2.4 Microelectrodes	30
2.4.1 Definition	30
2.4.3 Advantages of microelectrodes	39
2.5 A review of existing microelectrode fabrication methodologies	41
2.5.1 Glass-encapsulated microelectrodes	41
2.5.2 Pulled Pt Wires/Pipette puller	41
2.5.3 Gold microbead electrodes	41
2.5.4 Microelectrode fabrication by Chemical Vapor Deposition	42
2.5.5 Spherical microelectrodes	42
2.5.6 Ring-disk microelectrodes	43
2.5.7 Finite conical microelectrodes	43
2.5.8 Microelectrodes by microfabrication	44
2.5.9 Feedback independent electrodes	44
2.6 Scanning electrochemical microscopy	46
2.6.1 Feedback mode	48
2.6.2 Substrate generation / tip collection mode	49
2.6.3 Tip generation / substrate collection mode	49
2.6.4 Penetration mode	51
2.7 Application of SECM to biological systems	53
2.7.1 Living cells	54
2.7.2 Mammalian cells	62
2.7.3 Monitoring cellular status and drug viability testing	65

2.7.4	Multicellular organisms and their interrogation by SECM	67
2.7.5	Single celled organisms, microbial chips and bioassays	68
2.7.6	Cellular models	70
2.7.7	Enzymes	71
2.7.8	DNA imaging by SECM	80
2.7.9	Conclusions and future outlook	84
3.	Materials and methods	87
3.1	Introduction	88
3.1.1	Reagents	88
3.1.2	Materials	88
3.1.3	Equipment	89
3.1.4	Solution preparation	90
3.2	DNA sensor characterisation methodology	91
3.2.1	Additional reagents	91
3.2.2	Substrate	91
3.2.3	Polyelectrolyte film deposition	91
3.2.4	ssDNA/polyelectrolyte film formation	91
3.2.5	SECM interrogation and hybridisation detection	92
3.3.	Horseradish peroxidase patterning and imaging	93
3.3.1	Additional reagents	93
3.3.2	Silanised glass formation	93
3.3.3	Enzyme deposition	93
3.3.4	SECM interrogation	93
3.4	Imaging of cell membrane protein expression	95
3.4.1	Additional reagents and equipment	95
3.4.2	Solutions used	95
3.4.3	Cell lines	95
3.4.4	Recovery from cryogenesis	96
3.4.5	Passage	96
3.4.6	Cell growth for SECM experimentation	96
3.4.7	Preparation of slides for immunocytochemistry	97
3.4.8	Poly-L-Lysine coated slides	97
3.4.9	Patterning cells by cyto-spinning	98
3.4.10	Immunocytochemistry	99
3.4.11	SECM experiments	100
4.	An overview of the Uniscan SECM270	101
4.1	Uniscan SECM270	103
4.1.1	Dimensions	104
4.1.2	XYZ stage	104
4.1.3	Probe clamp	105
4.1.4	Potentiostats	106
4.1.5	Software	106
4.1.6	Tip positioning and microscope	107
4.2	Experiment capabilities	109

4.2.1 Approach curve macro	109
4.2.2 Area scan	109
4.2.3 Sloping scan macro	111
4.2.4 Repetitive scans	114
4.3 Constant distance imaging	114
4.4 Conclusions	117
5. The development of a microelectrode fabrication protocol	118
5.1 Introduction	119
5.2 A review of commercially available electrodes	120
5.2.1 Rg Ratio	120
5.2.2 Electrode robustness	121
5.2.3 Build quality and encapsulation	122
5.3 Performance comparison	123
5.4 Fabrication of microelectrode probes for SECM	124
5.4.1 Equipment	124
5.4.2 Method	125
5.5 Microelectrode characterisation	131
5.5.1 Optical Microscopy	131
5.5.2 Cyclic voltammtery	133
5.5.3 Simulating current/distance curves and subsequent estimation for fabricated microelectrodes	136
5.5.4 Polishing	138
5.5.5 Review of microelectrodes	140
5.6 Conclusions	141
6. Characterisation of DNA biosensor and detection of changes in DNA/polyelectrolyte film charge transfer properties by SECM	143
6.1 Introduction	144
6.2 Results and discussion	148
6.2.1 Carbon electrode substrate	148
6.2.2 Characterisation of carbon inks by SECM	149
6.2.3 Polyelectrolyte films	153
6.3 Mediator selection	157
6.3.1 Cyclic voltammetry	157
6.4 Scan height	159
6.4.1 Effect of mediator charge on feedback response	161
6.4.2 Interrogation of film integrity by SECM	165
6.5 Statistical analysis of array data by region of interest analysis tool	168
6.6 Control experiments	171
6.7 Hybridisation detection by SECM	174
6.8 Conclusions	189
7. Imaging horseradish peroxidase activity by SECM	191
7.1 Introduction	192
7.1.1 Horseradish peroxidase	192

7.1.2 HRP enzymatic mechanism	194
7.1.3 Hydroquinone / Benzoquinone redox couple	196
7.1.4 Immobilisation of horseradish peroxidase on glass and SECM detection method	197
7.2 Results and discussion	199
7.2.1 SECM approach curves	199
7.2.2 Approach curve control experiments	201
7.2.3 Experimental approach curves	202
7.2.4 Effect of enzyme concentration in loading solution on tip current	204
7.2.5 Effect of reaction time on product concentration	206
7.2.6 Calculation of benzoquinone concentration gradients	209
7.2.7 Imaging horseradish peroxidase activity	213
7.2.8 Area scans	214
7.2.9 Effect of substrate concentration on area scan resolution	214
7.3 Conclusions	226
8. The development of a novel approach to imaging the expression of the transmembrane protein CD44 in RT112 cells by SECM	229
8.1 Introduction	230
8.1.1 Immunochemistry	230
8.1.2 Enzymatic/chromogenic detection	231
8.1.3 Fluorescent labelling	231
8.1.4 A brief introduction to cell adhesion molecules and CD44	233
8.2 Visualising protein expression – the existing HRP/DAB staining method and the proposed detection method involving SECM	235
8.3 Results and discussion	240
8.3.1 Control experiments	240
8.3.2 Approach curves over HRP labelled RT112 cells	242
8.3.3 Change in approach curve response over time	243
8.3.4 Area scans	246
8.3.5 Effect of cell confluence/density on SECM response	255
8.3.6 Intracellular redox activity	257
8.3.7 Area scans	260
8.3.8 Effect of scan height on image resolution	264
8.4 Conclusions	270
9. Exploitation of innovation networks as a resource to create and maintain competitive advantage	271
9.1 Introduction	272
9.2 Models of strategic management	273
9.3 Innovation networks	283
9.3.1 Innovation networks – a definition	283
9.4 Relationship strength	287
9.5 Network configuration	291
9.6 Centrality	291

9.7 Network diversity	293
9.8 Communication environment	295
9.9 Geographical clustering in innovation networks and embeddedness	295
9.10 Strategic relationship management	297
9.11 Network orchestration	298
9.11.1 Knowledge mobility (KM)	298
9.11.2 Appropriability	299
9.11.3 Network stability	299
9.12 Uniscan Instruments Ltd	301
9.12.1 Introduction	301
9.12.2 Company profile	301
9.12.3 Skills and core competencies	302
9.12.4 Strategic direction	304
9.13 The Uniscan Network	306
9.13.1 Universities and research institutes	307
9.13.2 Sponsored projects	307
9.13.3 Start-ups and spin-outs	308
9.13.4 Distributors and agents	309
9.13.5 Joint research initiatives	309
9.13.6 Sub-contractors	309
9.13.7 Suppliers	310
9.13.8 Network infrastructure	311
9.13.9 Relationship ties	314
9.13.10 Network management	315
9.13.11 The academic/commercial boundary	317
9.13.12 Enhancing learning across the commercial/academic boundary and the development of best practice	318
9.14 Conclusions	320
10. General conclusions	322
11. Suggestions for further work	327
12. References	329
Appendix	350

List of figures and tables

Figure No.	Legend	Page
2.1	Free energy profile for a single electron reduction of species O(aq)	9
2.2	Schematic diagram illustrating the principle of oxidation and reduction of redox active species	11
2.3	The electrode-solution interface has been shown to behave like a capacitor; this is illustrated schematically here for an electrode with an excess (A) and deficiency (B) of charge at its surface. Alternatively, with a negative (a) and a positive (b) charge	14
2.4	Schematic diagram of the electrical double layer	17
2.5	Schematic detailing a two electrode cell and three electrode cell with a counter electrode	19
2.6	A schematic illustrating the potential drop between working and auxiliary electrodes in solution and iR_u measured at the reference electrode	20
2.7	Schematic diagram depicting the processes which may affect the rate of the reaction at the electrode surface	23
2.8	Schematic diagram illustrating diffusion from left to right and the concentration gradient from right to left	24
2.9	Schematic detailing the growth of the diffusion layer into bulk solution with time	26
2.10	A schematic diagram detailing the nomenclature used when describing microelectrodes	31
2.11	Schematic illustrating planar diffusion at a macroelectrode and hemispherical diffusion at a micro electrode.	34
2.12	Schematic diagram illustrating the flattening of a hemispherical microelectrode to a disc conformation	35
2.13	Schematic detailing the growth of the diffusion layer into bulk solution with time from a microelectrode	37
2.14	Schematic diagrams illustrating the difference in the faradaic current response to variation in applied potential for a macroelectrode and a microelectrode	38
2.15	Schematic diagram depicting the instrumentation necessary in SECM	47
2.16	Schematic illustrating the principles of positive and negative feedback and of SECM in substrate generation, tip collection mode	50
2.17	Schematic diagram illustrating the combination of feedback mode with substrate generation/collection mode in enzyme imaging	52
2.18	Schematic diagram detailing imaging of cells by detection of reduction in oxygen concentration in the vicinity of the immobilised cell	56
2.19	Imaging surface topography and stomatal activity by SECM	57

2.20	SECM image of <i>Brassica Juncea</i>	58
2.21	Linescans over wood surface achieved simultaneously by using SECM in GC mode with shear force feedback	59
2.22	Schematic detailing use of mediators to probe intracellular redox activity	61
2.23	Optical Micrographs and the corresponding SECM images of the cell bodies and axons of NGF-differentiated PC12 neuronal cells	63
2.24	Topographical and electrochemical images of live PC12 neuronal cells	64
2.25	Schematic diagram detailing the principle of enzyme mediated positive feedback over a GDH-functionalised surface	73
3.1	Slide flask from nunc™	97
3.2	Photographs of the cell patterning assembly and the Boeco C-28 centrifuge	98
4.1	Photographs of the Uniscan SECM270	103
4.2	Exploded schematic of the microelectrode probe clamping mechanism	105
4.3	Possible alternative video microscope camera configurations	108
4.4	Schematic diagrams depicting the movement of the microelectrode probe during an area scan	110
4.5	Series of approach curves detailing how substrate slope may be calculated	112
4.6	Area scan over sloped glass substrate using the area scan macro and the sloping scan macro	113
5.1	Optical micrograph of a 25µm microelectrode Ultramicroelectrodes Inc.	120
5.2	Optical micrograph of commercially available electrode from Thomas Recording GmbH	121
5.3	Optical Micrograph of 30µm probe fabricated by Sycopel International	122
5.4	Value gap analysis for commercially available electrodes and in-house electrodes	123
5.5	Optical Micrograph of a pulled capillary	125
5.6	Platinum quartz fibre with 5micron diameter platinum core	127
5.7	Optical micrograph of pulled capillary with Pt-quartz fibre	128
5.8	Platinum-quartz fibre-mercury junction in lumen of capillary	129
5.9	Schematic diagram illustrating the use of silver conductive paint to enhance contact between Pt quartz fibre and electrical lead	130
5.10	Optical micrograph of a 10 µm Pt microdisk electrode	131
5.11	Optical micrograph of 5µm probe tip	132
5.12	Series of cyclic voltammograms in mediators of differing concentrations and with electrodes of differing effective diameters	135

5.13	Approach curve obtained using electrode fabricated in-house plotted against simulated approach curves	137
5.14	Approach curves for four 25 μ m tips before and after polishing illustrating the importance of a consistent polishing protocol	139
6.1	Schematic illustrating principle of DNA biosensor	145
6.2	An image of the carbon paste electrode used in the study. The working electrode was patterned with the polyethylenimine array	148
6.3	A) Area scan over border between carbon (green/yellow region) substrate and millinex printing substrate (dark blue region) ; (B) Linescan across border at a tip position of 800microns	150
6.4	A) 3D representation of the data obtained from area scan images of a carbon ink electrode	151
6.5	Schematic detailing construction of a A) general multilayer polyelectrolyte film B) DNA/polyethylenimine film	153
6.6	Schematic illustration of patterned polyelectrolyte film which allows the monitoring of the change in background current over an unmodified surface against the change in feedback response over PEI/DNA modified carbon	154
6.7	Photograph of polyethylenimine deposition on carbon electrode by pulled microcapillary using the XYZ micro-positioning stage of the SECM270	155
6.8	Optical Micrographs of polyethylenimine dots on carbon paste electrode using capillaries of differing internal diameters; 100micron (A) 30micron (B)	156
6.9	Cyclic voltammograms for A) hexamine ruthenium (III) chloride and ferrocenecarboxylic acid and potassium ferricyanide (III) and B) potassium ferricyanide only (5mM in pH 7.1 buffer)	158
6.10	Consecutive linescans over carbon ink border. Scans were carried out at the height at which the tip current was equal to 80%, 70%, 60% and 50% of the tip current observed in bulk	159
6.11	Area scan profile over polyethylenimine array patterned on a carbon ink electrode using 5mM potassium ferricyanide mediator	161
6.12	Area scan over polyethylenimine array using 5mM ferrocenecarboxylic acid. Please note that the Z axis is opposite to that in Figure 6.11 . Also, note the colour bar: Red to blue on the colour bar indicates a direction of low to high current	163
6.13	Schematic diagram illustrating the electrostatic forces of attraction and repulsion between the mediators A) ferricyanide and B) ferrocenecarboxylic acid with the positively charged polyethylenimine film and the negatively charged carbon substrate respectively	164
6.14	Consecutive area scans over PEI array on carbon at T=0min, T=100min, T=200min, T=300min using 5mM ferrocenecarboxylic acid	166

6.15	Consecutive scans over a PEI array on carbon at T=0min, T=100min, T=200min, T=300min using 5mM hexamine ruthenium chloride mediator	167
6.16	Screen captures of the GUI developed to allow extraction of data from area scan data	169
6.17	Screen capture of ROI output in excel, detailing extraction of data from an area scan array	170
6.18	Area scan arrays before (A) and after (B) rinsing and 3hrs exposure to control solution (0.015mM phosphate buffer solution)	172
6.19	A) Array obtained from the subtraction of 'before' array from 'after' array; B) Representative linescans from before and after rinsing and exposure	173
6.20	Linescan across array obtained by the subtraction of array 'before' and 'after' exposure to 'control' hybridisation solution	174
6.21	Area scans over PEI/ssDNA array before and after exposure to complementary ssDNA solution (0.2mg/ml)	176
6.22	Absolute change in tip current after exposure to complimentary single stranded DNA	177
6.23	Linescans showing change in feedback current following exposure to complementary DNA	178
6.24	Area scans over ssDNA/PEI spotted array before and after exposure to non-complementary DNA	180
6.25	Absolute change in tip current after exposure to non-complementary DNA	181
6.26	A) Series of linescans extracted from arrays represented in Figure 6.24 – the current profile across a spotted array before and after exposure to non-complementary DNA B) linescan extracted from Figure 6.25 depicting change in tip current after exposure to non-complementary DNA	182
6.27	Linescans illustrating difference in feedback response after exposure to single stranded complementary and non-complementary DNA	183
7.1	Three dimensional representation of X-ray crystal structure of HRP isozyme C	193
7.2	Simplified schematic of HRP enzymatic reaction	194
7.3	Catalysis of hydrogen peroxide by HRP, forming Complex I and its return to its native state via complex II	195
7.4	Proposed mechanism for the catalysis of hydrogen peroxide to water by HRP using hydroquinone as the oxidising substrate	196
7.5	Reaction mechanism of HRP immobilisation	197
7.6	Schematic diagram of proposed detection mechanism of horseradish peroxidase using the hydroquinone / benzoquinone redox couple and the SECM in GC mode	198
7.7	Approach curve over HRP functionalised glass in 2mM hydroquinone in pH 7.1 buffered solution	200
7.8	Normalised approach curve [i (tip) / i (bulk)] used to position tip	200

	over HRP-modified surface	
7.9	Control approach curves over a non-functionalised glass substrate and a heat treated, HRP functionalised substrate	202
7.10	Normalised approach curves over a control substrate and a normal, HRP functionalised glass substrate	203
7.11	Variation in peak tip current with enzyme concentration in loading solution. Error bars are 95% confidence intervals for calculated means	204
7.12	Variation in peak tip current with enzyme concentration in loading solution. Error bars are 95% confidence intervals for calculated means	205
7.13	A series of approach curves obtained at various time intervals after the introduction of hydrogen peroxide to the system	207
7.14	Graph illustrating change in peak tip current over time obtained by approach curve over HRP-functionalised glass	208
7.15	Linegraphs illustrating changing benzoquinone concentration from bulk solution towards the enzyme functionalised surface	210
7.16	Average concentration gradient of benzoquinone plotted as a function of time, calculated using data from approach curves	212
7.17	Schematic diagram illustrating the importance of distance in fabricating an array and avoiding merging of diffusion layers	213
7.18	Area scans over HRP arrays. Using 1mM and 0.6mM H ₂ O ₂ respectively	215
7.19	Area scans over HRP modified array using 0.6mM and 0.4mM H ₂ O ₂	216
7.20	Linescan extracted from area scan data to allow construction of background current array	217
7.21	Background current array for subtraction from experimental array	218
7.22	Background subtracted area scan over HRP modified array using 1mM H ₂ O ₂ and 0.6mM H ₂ O ₂	220
7.23	Background subtracted area scan over HRP modified array using 0.4mM H ₂ O ₂ and 0.2mM H ₂ O ₂	221
7.24	Schematic illustrating the effect of topography on interrogating diffusion layers of differing depths as a result of substrate concentration	222
7.25	Cross section extracted from the area scan array and resulting line scan plot	223
7.26	Linescans over HRP array	224
8.1	Schematic detailing the immunochemistry of the DAB staining methodology	236
8.2	Eppendorf containing DAB after addition of 1µl hydrogen peroxide	237
8.3	Schematic detailing the mechanism by which SECM may be used in the detection of membrane protein expression (not to scale)	238
8.4	An example optical micrograph of highly confluent RT112 cells used in control experiments; cells are stained with the nuclear counterstain hematoxylin	240

8.5	Approach curves over glass ('glass'), un-labelled cells ('un-treated cells') and cells exposed to blocking and secondary antibodies only ('negative control')	241
8.6	Approach curve over HRP labelled RT112 cells	243
8.7	Normalised approach curves over glass, untreated RT112 cells, RT112 cells with no primary antibody binding and RT112 cells which have undergone complete labelling procedure ('HRP-treated cells')	244
8.8	Consecutive approach curves over HRP-labelled CD44 expressing RT112 cells	245
8.9	Optical micrograph of highly confluent RT112 cells stained with hematoxylin	246
8.10	Area scan over highly confluent cells using 1% secondary antibody dilution	248
8.11	Cross section of Figure 8.10 taken at Y=200 μ m	248
8.12	Approach curve over low current area in area scan from Figure 8.10	249
8.13	Approach curve over area over which a comparatively higher tip current was obtained in the area scan	250
8.14	Area scan over highly confluent cells with HRP labelled CD-44. Labelling undertaken using a 0.5% solution of secondary antibody	252
8.15	Cross section of Figure 8.14 at X =200 μ m	252
8.16	Area scan over RT112 cells expressing CD44 which has been labelled with horseradish peroxidase. Substrate prepared using secondary antibody dilution of 0.1%	253
8.17	Cross section of Figure 8.16 at Y = 1000	253
8.18	Comparison of linescans over fields of RT112 cells treated with secondary antibodies of differing dilutions (1%, 0.5%, 0.01%)	254
8.19	Poly-L-lysine coated slide patterned with RT112 cells stained with hematoxylin	255
8.20	Optical micrograph of the border of the cells immobilised to the poly-L-lysine functionalised slide using the cyclospin technique	256
8.21	Linescan across border between glass / cell functionalised region	258
8.22	Normalised linescans across glass/cell border (at approximately 500 μ m). Scans were normalised to the tip current measured over non-functionalised glass	259
8.23	Optical micrograph of substrate prepared using cell suspension of 19×10^6 cells ml ⁻¹ . Cells have undergone treatment with DAB	261
8.24	Area scan across glass / cell border. Scan was conducted in pH 7.1 buffered solution containing 1mM hydroquinone and 1mM hydrogen peroxide; 19.5×10^6 cells ml ⁻¹	262
8.25	Cross sectional linescan across glass / cell functionalised region. (From Y = 20 μ m in Figure 8.24.	262
8.26	Area scan across glass / cell border. Conducted in pH 7.1 buffered solution of 1mM hydroquinone / 1mM hydrogen peroxide. Pattern fabricated using cell suspension of 10×10^6 cells ml ⁻¹ growth media	264
8.27	Cross section of area scan in Figure 8.26 where Y = 280 μ m	264

8.28	Border of cell functionalised surface prepared using cell suspension of 5×10^6 cells ml^{-1} . After treatment with both DAB and hematoxylin	265
8.29	Area scan across glass / cell border. Conducted in pH 7.1 buffered solution of 1mM hydroquinone / 1mM hydrogen peroxide. Pattern fabricated using cell suspension of 5×10^6 cells ml^{-1} growth media	266
8.30	Cross section of area scan in Figure 8.29 where $Y = 20\mu\text{m}$	266
8.31	Area scan over cell-functionalised glass prepared using a cell suspension of 10×10^6 cells ml^{-1} growth media; scan conducted at it $= 0.5i_{\text{bulk}}$	268
9.1	Schematic diagram illustrating Porters Five Forces Model	274
9.2	Schematic diagram illustrating the re-organisation and re-bundling of internal resources to meet new competitive environments	278
9.3	Schematic diagram illustrating the three kinds of dynamic capabilities	279
9.4	Schematic illustration of the concept of innovation networks and the movement of the locus of innovation outside the boundary of the firm	282
9.5	A schematic illustrating the potential loss of flexibility a firm may experience as a result of collaboration and single loop learning	286
9.6	Schematic diagram illustrating the transition from weak informal tie to strong tie	288
9.7	Schematic representation of role of weak and strong ties in the innovation pipeline	290
9.8	Schematic illustration of innovation associated advantages of upstream interaction with suppliers	294
9.9	Schematic diagram illustrating the factors involved in the orchestration of an innovation network by a firm	300
9.10	Schematic illustration of the innovation trajectories of the SVET, SECM, SKP and LEIS before and after the M370	304
9.11	Schematic illustration of Uniscan's innovation network	306
9.12	Schematic depicting Uniscan's network infrastructure - the mechanism by which alliances may be initiated and maintained	311
9.13	Illustration of what the Uniscan Innovation Net may look like	313

Table No.		Page No.
2.1	The diffusion limited plateau current for each of the predominant microelectrode tip geometries	33
2.2	Proteins interrogated by SECM in feedback mode	74
2.3	Proteins interrogated by SECM in generation/collection mode	75
4.1	Weight and dimensions of the SECM270	104
6.1	Resolution as a function of scan height – calculated over the 400-440 μ m range of line scans	160
8.1	Summary of the advantages and disadvantages associated with using enzymatic and fluorescent labels in immunochemistry	232

Nomenclature

Term	Description
a	tip radius in SECM (μm)
A	geometric electrode area (cm^2)
Ab	antibody
ABC	avidin-biotin complex
AC	alternating current (V)
AFM	Atomic Force Microscopy
Ag	antigen
BQ	benoquinone
C	capacitance (Farads, F)
$C_0(x=0)$	concentration of species O at a distance $x = 0$ from the electrode
$C_{0\infty}$	concentration of species O in bulk solution
CVD	chemical vapour deposition
CT	charge transfer
d	tip to substrate distance
D	diffusion coefficient (cm^2/s)
DAB	diaminobenzidine
DNA	deoxyribonucleic acid
Dp	diaphorase
E	potential of an electrode versus a reference
E^0	standard potential
EBL	electron beam lithography
ET	electron transfer
f	F/RT
F	Faraday's constant ($9.6 \times 10^4 \text{ Cmol}^{-1}$)
FB	feed back mode
FIB	focussed ion beam
FMA	Ferrocene methanol
G^Φ	Gibbs Free energy of transition state
ΔG_{red}^Φ	Gibbs Free energy change in reduction reaction
ΔG_{ox}^Φ	Gibbs Free energy change in oxidation reaction
GC	generation collection mode
GDH	glucose dehydrogenase
GFP	green fluorescent protein
GOx	glucose oxidase
HQ	hydroquinone
HUVEC	human umbilical vein epithelial cells
HRP	horseradish peroxidase
i_c	oxidative current (A)
i_l	limiting current
i_r	reductive current (A)
i_s	substrate current (A)

i_T	tip current (A)
$i_{T\infty}$	tip current in bulk solution
IHP	inner helmholtz plane
IPE	ideal polarised electrode
ITIES	interface between two immiscible fluids
J	diffusional flux ($\text{molcm}^{-2}\text{s}^{-1}$)
K_{ox}	first order heterogenous rate constant for the reductive ET reaction
K_{red}	first order heterogenous rate constant for the oxidative ET reaction
L	normalised tip to substrate distance
m_O	mass transfer coefficient
n	number of electrons involved in electrode reaction
NADPH	nicotinamide adenine dinucleotide phosphate oxidase
NGF	neuronal growth factor
NHE	normal hydrogen electrode
O	oxidised form of a redox couple ($O \rightarrow R + ne^-$)
OHP	outer Helmholtz plane
PAP	p-aminophenol
PAP-G	p-aminophenyl- β -D-galactopyranoside
PBS	phosphate buffer solution
PQI	p-Quinone Imine
POD	peroxidase
PDMS	poly(dimethoxysilane)
PQQ-GDH	pyrroloquinoline quinone-dependent glucose dehydrogenase
q	charge stored on a capacitor
qe	charge on an electrode (C)
qs	charge in solution (C)
rg	ratio of radius of insulating sheath to radius of electroactive area
r_{disk}	radius of a microdisk electrode
$r_{\text{hemisphere}}$	radius of a hemispherical electrode
R	a) Reduced form of a redox couple ($O \rightarrow R + ne^-$) b) Resistance
R_u	uncompensated resistance
R	gas constant ($\text{Jmol}^{-1}\text{K}^{-1}$)
RE	reference electrode
ROS	reactive oxygen species
SCE	saturated calomel electrode
SCFM	scanning confocal microscope
SCID	severe combined immunodeficiency
SCLM	scanning chemi-luminescence microscope ()
SECM	Scanning Electrochemical Microscopy
SG/TC	substrate generation/tip collection mode
SHE	standard hydrogen electrode
ssDNA	single stranded DNA
t	time (s)
T	absolute temperature ($^{\circ}\text{K}$)
TBS	trizma base solution

UME	ultramicroelectrode
WE	working electrode
x	distance from electrode (cm)
X	X axis on SECM stage
Y	Y axis on SECM stage
Z	Z axis on SECM stage

Symbol

α	transfer coefficient
δ_j	diffusion layer thickness for species j
η	overpotential (E-E _{eq})
σ_d	charge density of diffuse layer
σ_i	charge density arising from IHP
σ_s	charge density on solution side of double layer
Φ_e	electrostatic potential of electrode
Φ_s	electrostatic potential of solution
Φ_{REF}	electrostatic potential of reference electrode
$\Delta\Phi$	electrostatic potential drop

Chapter 1

Research rationale

1. Research Rationale

Scanning electrochemical microscopy (SECM) is a novel, scanning probe technique which allows for the collection of high resolution electrochemical data at a range of surfaces. The primary aim of this research programme was to develop SECM and explore its applicability to interrogating biologically modified surfaces.

SECM offers significant advantages over other microscopic techniques. It does not require the biological sample to undergo complex pre-treatment; it does not suffer from artefacts such as background fluorescence since the technique is not optically based and the system under interrogation may be numerically modelled, allowing the subsequent capture of information relating to the kinetics of the reaction under observation. Additionally, samples may be interrogated repeatedly due to the non-destructive nature of the imaging process.

The technique has been applied to a wide selection of bioanalytical problems (Roberts *et al*, 2007; Gyurcsanyi *et al*, 2004; Edwards *et al*, 2006; Wittstock *et al*, 2001; 2007; Amemiya *et al*, 2006; Sun *et al*, 2007). To name but a few examples, SECM has been used successfully in the investigation of diffusion through biological membranes, the respiratory and intracellular redox activity of cancerous cells, the topography of neurons and in the quality control of biosensing devices (Yasukawa *et al*, 1998; Liu *et al*, 2001; Takii *et al*, 2003; Uitto and White, 2003).

Within the work described in this thesis, two different avenues of SECM application were explored. The first involved the characterisation of a DNA biosensor previously developed within the group (Davis *et al*, 2005) which revealed the possibility for the development of SECM as an approach to detecting DNA hybridisation in polyelectrolyte films.

Electrochemical approaches to the detection of DNA hybridisation promise to offer significant advantages over the established optical detection methods based on the use of fluorescent labels – potentially offering high sensitivity, cost effectiveness and synergy with microfabrication technologies. Whilst the electrochemical labelling approach offers much in the development of rapid sensing technologies, there is much scope for the direct, label-less detection of DNA hybridisation by electrochemical methods. By removing the necessity for

labelling, sensors offer the promise of faster responses while requiring fewer reagents so making them an extremely attractive route for investigation.

The second route of investigation was the development of SECM as a novel approach to detecting cell membrane protein expression. The predominant immunochemical staining techniques currently employed in the visualisation of protein expression in cytological and histological samples involve either fluorescent labels or enzymatic labels combined with chromogenic substrates. Each of these techniques comes with their own relevant advantages and disadvantages – and so the development of an alternative approach to imaging protein expression would be of significant value to the cell biologist. By developing SECM as an approach to detecting protein expression, not only is there the opportunity to visualise protein expression with considerable sensitivity - there is also the possibility for numerically modelling the system and making quantitative estimations of the levels of protein expression. To explore the potential of SECM to serve as a new immunochemical technique, the expression of the transmembrane protein CD44 in RT112 cells was investigated.

The quality of the images obtained by SECM is highly dependent on the quality of the microelectrode probes used. The development of an appropriate methodology by which robust microelectrodes with small critical dimensions may be fabricated hence represented an additional aim in this research programme.

This research programme was sponsored by Uniscan Instruments Ltd, the designer and manufacturer of the SECM 270 workstation used in this research programme. A key aspect of their strategy is the production of high quality instrumentation which fulfils and if possible, exceeds the requirements and expectations of customers looking to purchase electrochemical instrumentation. By their involvement in this project, valuable feedback would be provided regarding the usability of the SECM270, how it may be improved and possible future design considerations. The use of the SECM in this programme also represented a means by which new product developments may be tested and evaluated.

Cranfield Health at Cranfield University is just one of Uniscan's strategic alliances. In today's competitive environment, such alliances are becoming increasingly prevalent. By forming relationships outside the boundary of the company, the skills and competencies

needed to generate innovative products, processes or services may be accessed, with the effect of increased competitive advantage over other industry incumbents. An additional focus of this research was hence to explore the theoretical aspects of innovation networks in a comprehensive literature review and to see whether any of these aspects or principles emerges from the way in which Uniscan manages its relationship ties.

In summary, the aims of the research programme were as follows:

1. To develop and explore new, novel SECM applications
 - i. To characterise a DNA biosensor previously developed within the group (Davis *et al*, 2005) and in doing so, investigate the potential of SECM to detect DNA hybridisation in polyelectrolyte films.
 - ii. To investigate the application of SECM to detecting protein expression by hybridisation with existing immunochemical techniques.
2. To develop a methodology by which robust microelectrodes of small critical dimensions may be fabricated.
3. To provide Uniscan Instruments Ltd with valuable feedback regarding the usability of the SECM270 and possible improvements which could be incorporated into its product development programme.
4. To investigate the leverage of competitive advantage from Uniscan Instruments Ltd's innovation network.

Chapter 2

Introduction and literature review

2. Introduction

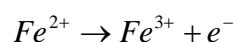
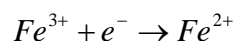
The aim of this chapter is to provide a background and an insight into the principles behind the experimental work reported in this thesis. First, an introduction to electrochemistry is given, followed by an overview of scanning electrochemical microscopy as an analytical technique. The chapter concludes by discussing the advantages SECM offers to studying biological systems.

2.1 Electrochemistry

In electrochemical systems, interest lies with the parameters and processes that affect charge transfer across the boundaries between chemical phases; such as, for example, an electrode and an ionic conductor immersed within an electrolyte. In the solid phase, i.e. the electrode, charge is passed by the flow of electrons (or 'holes') through the material, whereas in the electrolyte phase, charge is carried by the movement of ions. Within electrochemical cells, the difference between the potential at each electrode may be measured using a high impedance voltmeter. This cell potential is measured in volts (V) where $1\text{V} = 1\text{JC}^{-1}$. The magnitude of the potential difference at the interface of an electrode affects the relative energies of the carriers in the two phases and in doing so, the potential difference controls the rate and direction of the charge transfer process.

The overall reaction taking place in an electrochemical cell is composed of two independent half cell reactions which describe the chemical changes occurring at each of the electrodes, where each half cell responds to the interfacial potential difference at the corresponding electrode. The electrode at which the reaction of interest occurs is called the working electrode (WE). A standard, reference electrode, with a known and constant composition is often included. As a result of this constant composition, the potential of the standard, reference electrode remains fixed, allowing any variation in the potential difference to be attributable to changes at the working electrode; the potential of the WE is hence said to be controlled or observed with respect to the reference electrode. Commonly employed reference electrodes include saturated calomel electrodes (SCE), standard hydrogen electrodes (SHE) and the normal hydrogen electrode (NHE).

The transfer of electrons between the electrode and a molecule (in this example, $Fe^{2+/3+}$) may occur in either direction - using the example below, a molecule in solution may either accept an electron from the electrode, in which case it is said to be reduced, or it may donate an electron to the electrode and become oxidised.

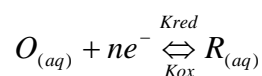


Equation 2.1

For the reduction of Fe^{3+} at the electrode/solution interface, the passage of current through the cell converts Fe^{3+} to Fe^{2+} , resulting in an increase in the concentration of Fe^{2+} at the electrode; this is because the rate of reduction is greater than the rate at which the reactant may be replenished by diffusion from the bulk solution to the interfacial region. It hence follows that the faradaic current arising from the oxidation or reduction of molecules in solution is dependent on two core factors – the transport of reactants to, and products from, the electrode surface (rate determining mass transport) or the rate of heterogeneous electron transfer (rate-determining electrode kinetics). Whilst Bard and Faulkner (2001) give a significant account of the latter, the salient points are given below.

2.1.1 Electron transfer and energy levels

Consider the following equation depicting the transfer of electrons to O forming R, where both species are soluble and in solution.



Equation 2.2

The electrons in the electrode have a maximum energy distributed proximal to the Fermi level (the energy of the highest occupied atomic orbital), where electrons may only be supplied or received at energy levels around this level. On the application of an external potential however, the Fermi level may be altered to either supply electrons to, or remove electrons from the electrode. For the reduction of a molecule in solution, electrons in the

electrode must have a minimum amount of energy in order to be transferred from the electrode to the receptor molecule, O; whilst on the other hand, for oxidation to take place, the electrons in the donor orbital of R must be equal to or higher than the Fermi level of the electrodes. In order to study the relationship between a species' energy levels and their propensity to donate or receive electrons, it is necessary to quantify the potential dependence of the heterogenous rate constant for the electron transfer reaction. In Equation 2.2, it is assumed that there are arbitrary quantities of O and R present in the solution and that K_{red} and K_{ox} describe the first order heterogenous rate constants for the reductive and oxidative ET reactions.

$$i_a = -FAk_{red}[O]_O$$

Equation 2.3

$$i_c = FAk_{ox}[R]_O$$

Equation 2.4

Equation 2.3 and Equation 2.4 represent the reductive and oxidative components of Equation 2.1, where $k_{red}[O]_O$ and $k_{ox}[R]_O$ represent the respective fluxes of the electroactive species to the electrode, where F = Faraday's constant ($9.6 \times 10^4 \text{ Cmol}^{-1}$), A is the electrode area (cm^2) and i_a and i_c are the oxidative and reductive currents (A) respectively.

From this, it may be stated that the total current flowing is equal to:

$$i = i_a + i_c$$

Equation 2.5

It follows that by the substitution of Equation 2.3 and Equation 2.4 into Equation 2.5, we derive:

$$i = FA(k_{ox}[R]_O - k_{red}[O]_O)$$

Equation 2.6

It can be seen from this equation that when the fluxes of the reductive and oxidative elements are equal as Equation 2.2 is in equilibrium, current flow will be zero.

$$k_{ox} [R]_o = k_{red} [O]_o$$

$$i = FA(0) = 0$$

Equation 2.7

The process of electron transfer (ET) may be described by the transition state model, the theory of which is described comprehensively by Cox (1994). The model envisages the ET reaction as one that occurs via a path involving two reactants ($O_{(aq)} + e^-$) and one product ($R_{(aq)}$). For the reaction to occur however, the reactants must overcome an energy barrier, the height of which is given by G^Φ , the transition state. Transition state theory predicts that the rate of the reduction reaction, k_{red} will be given by:

$$k_{red} = Af \exp\left(\frac{-\Delta G_{red}^\Phi}{RT}\right)$$

Equation 2.8

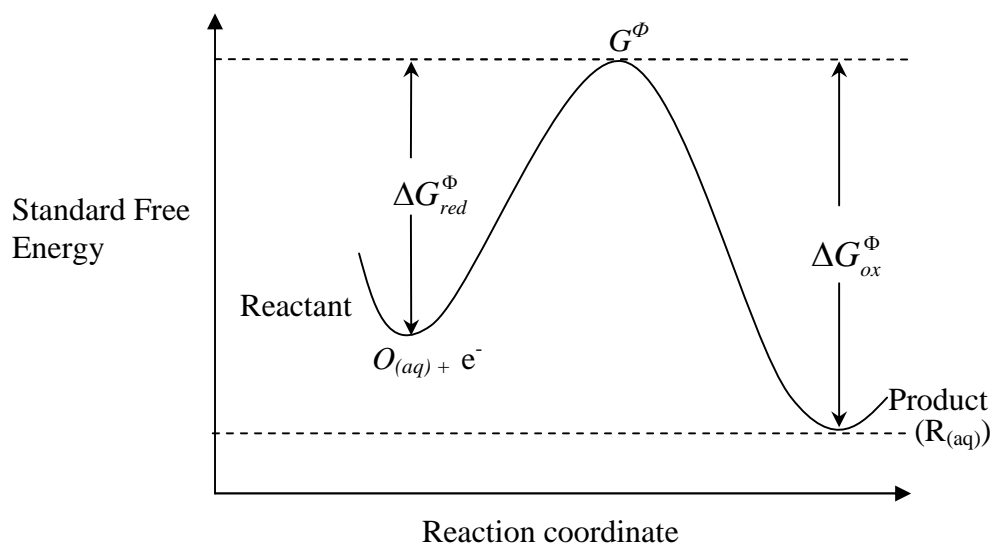


Figure 2.1: Free energy profile for a single electron reduction of species $O_{(aq)}$

At a fixed pressure and temperature, the activation free energies for the reduction and oxidation reactions may be derived, where G_{ox} and G_{red} represent the free energy changes of the reactant and product respectively.

$$\Delta G_{red}^{\Phi} = G^{\Phi} - G_{ox}$$

Equation 2.9

$$\Delta G_{ox}^{\Phi} = G^{\Phi} - G_{red}$$

Equation 2.10

Unlike homogenous chemistry, which has an analogous kinetic model, electrochemical reactions can be influenced by altering the energy levels of the electrode – i.e. changing the interfacial potential. When the applied potential is equal to the equilibrium potential / open circuit potential, no current flows through the system. On biasing the electrode to a more negative potential, the energy of the electrons within the electrode phase is raised, which, depending on the energy state of the species in the electrolyte phase, may result in the transfer of the electrons from the electrode and into vacant electronic states on species in the electrolyte (Figure 2.2). The current that results from this flow of electrons from the electrode to the solution is termed a reduction current. Similarly, an oxidation current is said to flow when electrons in solution move to a more favourable energy level on the electrode, as a result of driving the potential of the electrode towards a more positive value. The critical potentials at which these processes occur are related to the standard potentials, E^0 for the specific chemical substances in the system.

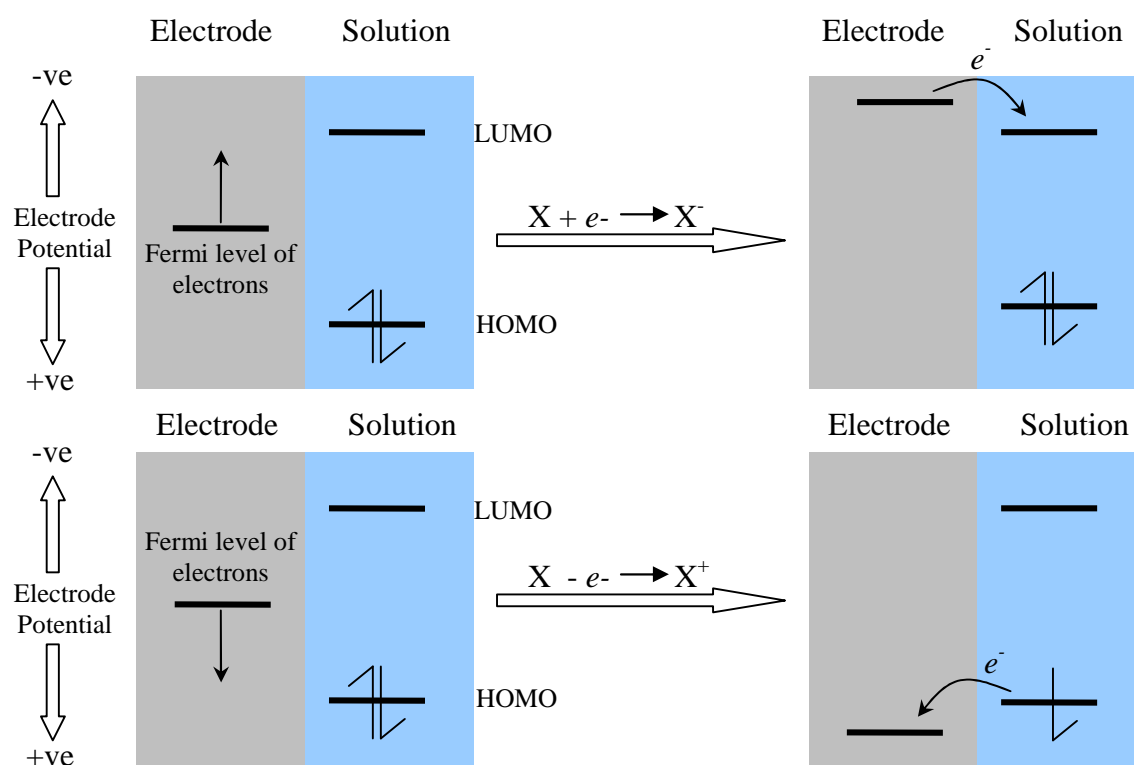


Figure 2.2: Schematic diagram illustrating the principle of oxidation and reduction of species X. HOMO is the highest occupied molecular orbital and LUMO is the lowest unoccupied molecular orbital.

When the potential of the electrode is raised or decreased to a level E to drive the electrode reaction, the amount by which it differs from the equilibrium potential is termed the ‘overpotential (η)’:

$$\eta = E - E_{eq}$$

Equation 2.11

In most experimental systems however, the interest lies with how the Faradaic current varies with the over-potential applied to an electrochemical system (a ‘cell’) comprising two or three electrodes. The inter-relationship between over-potential and the current observed in the electrochemical cell is described by the Butler-Volmer equation (Butler, 1924; Volmer, 1930). The equation predicts how the observed current, i , varies as a function of η and the transfer coefficient, α . Assuming the electrolyte solution is well stirred, the concentrations of the electroactive species at the electrode surface will be equal to their concentrations in bulk.

$$i = i_o \left(\exp \left\{ \frac{(1-\alpha)F\eta}{RT} \right\} - \exp \left\{ \frac{-\alpha F\eta}{RT} \right\} \right)$$

Equation 2.12

In irreversible systems, the standard exchange current (i_o) is small, whereas in reversible systems it is large. It should be noted that the terms ‘Large’ and ‘Small’ used here are relative terms, and signify the time scale of the electrode kinetics relative to the transport of material in and out of the electrode/solution interface. For irreversible processes, Tafel analysis may be used to determine the transfer coefficient and the exchange current (Tafel, 1905).

2.1.2 Non-faradaic processes and the nature of the double layer

The processes that occur at electrodes may be divided into two types. The first comprises reactions in which charge, in the form of electrons, is transferred across the electrode-solution interface causing oxidation or reduction to occur, whereby the amount of chemical

reaction caused by the flow of current is in proportional to the charge passed. These processes are termed faradaic processes and they are governed by Faraday's Law.

An electrode-solution interface may however, over a range of potentials, exhibit no charge transfer (CT) reactions as the reactions are thermodynamically or kinetically unfavourable. Adsorption and desorption may occur at the electrode surface however, as may the structure of the electrode-solution interface with potential or solution composition. Termed non-faradaic processes, these contribute to the flow of an external current when the potential, electrode area or solution composition is varied, even though charge does cross the electrode solution interface.

Whilst the faradaic charge transfer processes are usually those of primary interest, both non faradaic and faradaic processes occur when electrode reactions take place and for a complete interpretation of electrochemical data regarding the charge transfer processes of a specific system, the role of non faradaic processes in the system must be taken into account.

2.1.3 The electrode/solution interface

The electrode/solution interface is the region in the electrochemical system where CT reactions occur and where the most significant differences in potential across the electrical circuit appear; the structure of the region is of great interest because it may control the rate at which CT reactions occur.

Consider an ideal polarised electrode, an electrode at which no charge transfer can occur across the metal-solution interface, irrespective of the potential applied by an outside source of voltage. As charge cannot cross the IPE interface when the potential across it is changed, the electrode-solution interface behaves similarly to a capacitor, a circuitry element composed of two metal sheets separated by a dielectric whereby its behaviour is described by the following equation (Equation 2.13):

$$\frac{q}{E} = C$$

Equation 2.13

where q = charge stored on capacitor (coulombs, C)

E = potential across capacitor (volts, V)

C = Capacitance (Farads, F)

On the application of a potential across a capacitor, charge accumulates until q satisfies the equation above. During this accumulation of charge, a charging current flows. In a similar manner to a capacitor, the electrode-solution interface has been shown to exhibit capacitative properties.

Consider an electrode simply as a source of electrons: depending on the applied potential, there may be a surplus or deficiency of electrons at the electrode surface. As a result, a net charge will manifest itself at the surface, which will attract charged species in solution, which may be electrolyte ions or the re-orientation of dipoles in solvent molecules, as depicted in Figure 2.3.

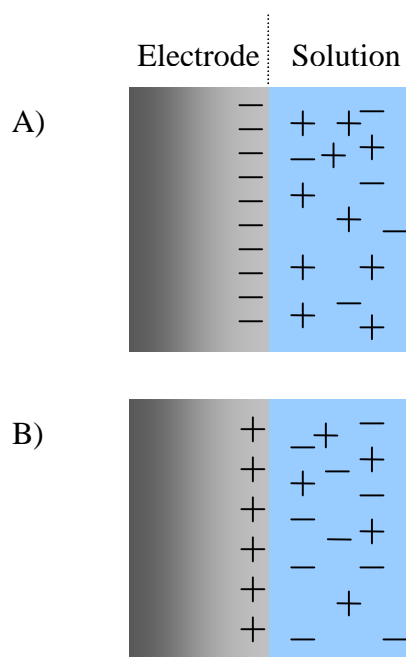


Figure 2.3: The electrode-solution interface has been shown to behave like a capacitor; this is illustrated schematically here for an electrode with an excess (A) and deficiency (B) of charge at its surface. Alternatively, with a negative (a) and a positive (b) charge

At a specific potential, a charge exists on the electrode, q^e and in the solution, q^s . Depending on the nature of the potential applied to the electrode, the charge may be negative or positive relative to the solution, however in all cases, the magnitude of each is identical:

$$q^e = -q^s$$

Equation 2.14

The charge on the electrode, which may represent an excess or deficiency of electrons, exists on the electrode surface in a layer less than 0.1 Å thick, whereas the charge in solution is composed of either an excess of cations or anions in the vicinity of the electrode surface. The charges q^e and q^s are often expressed with reference to the area of the electrode in the form of charge density, calculated by the division of the charge by the area of the electrode surface.

$$\sigma^e = \frac{q^e}{A}$$

Equation 2.15

$$\text{Units} = \mu\text{C}/\text{cm}^2$$

As a result of this redistribution of charged species, a potential difference therefore exists across the electrode/solution interface.

2.1.4 The Electrical Double Layer

The electrical double layer is the array of charged species and oriented dipoles at the electrode-solution interface, thought to be made up of several layers (see Figure 2.4). The inner layer, also known as the ‘compact’, ‘Helmholtz’ or ‘Stern’ layer, which is located closest to the electrode, contains solvent molecules that are specifically adsorbed on the electrode surface. With reference to the Figure 2.4, the locus of the electrical centres of these adsorbed ions is called the inner Helmholtz plane (IHP), located a distance x_l from the electrode surface. It should be noted however, that although the IHP may be dominated by solvent molecules, it may be possible for some ionic or even uncharged species from

the electrolyte solution to penetrate this region as a result of the loss of the solvation shell and become ‘specifically adsorbed’ to the electrode surface (the term ‘specific’ is used here to account for the fact that the interaction occurs only for certain ions or molecules and is usually unrelated to the charge on the ion) (Grahame, 1947). The total charge density arising from this layer of specifically adsorbed ions is defined as σ^i . Solvated ions, non-specifically adsorbed to the electrode surface by long range electrostatic forces of attraction, can approach the electrode to a distance of x_2 only, making the locus of these centres the outer Helmholtz plane (OHP). As these forces are relatively weak, thermal agitation and subsequent Brownian motion causes this layer to be diffusely distributed, where the OHP extends into the bulk of the solution. The charge density of this diffuse layer, given by σ^d , contributes to the total charge density on the solution side of the double layer, σ^S so that (Guoy, 1910; Chapman, 1913):

$$\sigma^S = \sigma^i + \sigma^d = -\sigma^e$$

Equation 2.16

As highlighted by Stern (1924), electrode processes may be significantly affected by the structure of the double layer; a non-specifically adsorbed electroactive species can approach the electrode only to the OHP, resulting in the potential it experiences being less than that between the electrode and the solution (potential drop). Whilst sometimes one can neglect the double layer effects in considering electrode reaction kinetics, one cannot usually neglect the existence of a charging current in electrochemical experiments; to the contrary, during electrode reactions using very low concentrations of electroactive species, the charging current can be much larger than the faradaic current corresponding to the oxidation or reduction of the redox system under interrogation.

Much of the modern models of the electrical double layer are based on statistical mechanics which are not within the boundaries of this thesis.

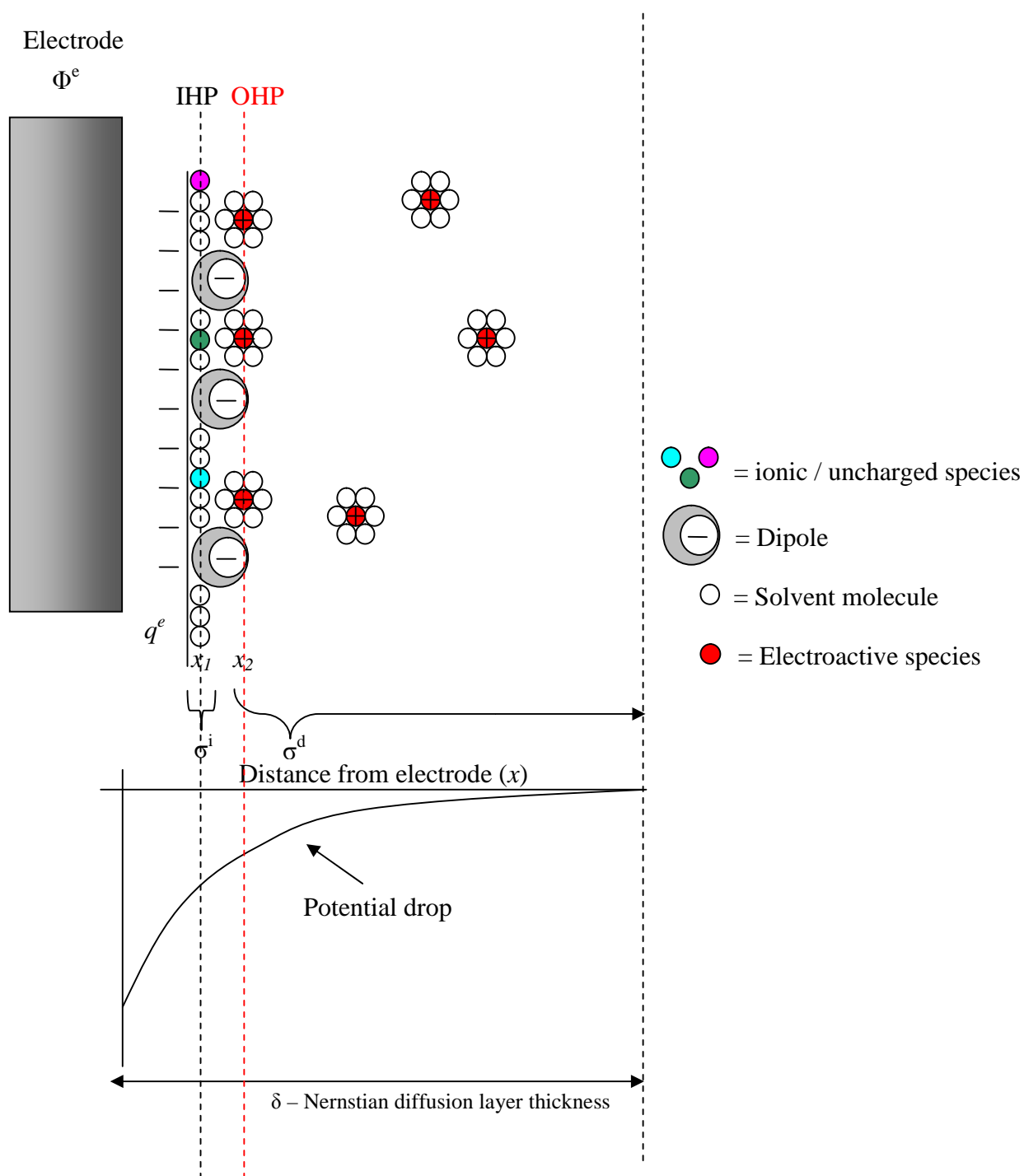


Figure 2.4: Schematic diagram of the electrical double layer

2.1.5 Voltammetry

The analysis of the effect of cell potential on charge transfer reactions within an electrochemical cell can provide a plethora of information about the reaction of interest. Voltametric techniques are based on the observation of a current in response to a constant or changing applied potential. Within this section, a brief overview is given of the instrumentation and experimental approach required for such analyses.

2.1.6 The electrochemical cell and electrodes

A typical apparatus assembly necessary for an electrochemical experiment consists of a container vessel in which at least two independent electrodes are immersed in a solution containing the electroactive species of interest - and in most cases, an electrolyte. These are linked through solution and through external connectors to form an electrical circuit (Figure 2.5). The working electrode (WE) is the electrode at which the reaction of interest occurs; the reference electrode (RE) provides a stable and fixed potential so that when a potential (E) is applied between the two electrodes, the potential drop between the WE and the solution is defined according to Equation 2.17.

$$\text{Potential Drop } (\Delta\Phi) = \Phi_e - \Phi_s$$

Equation 2.17

In this two electrode arrangement, complementary oxidation and reduction reactions occur at each electrode. In systems where a tiny current is passed, a two electrode arrangement will often suffice. However, in the case of larger electrodes, problems frequently arise with potential drop.

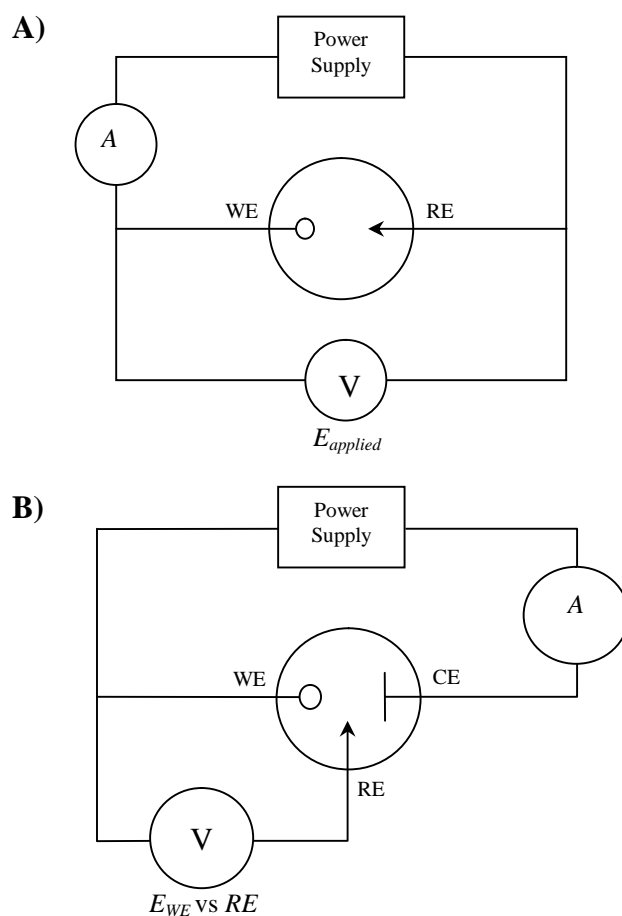


Figure 2.5: A) Two electrode cell B) Three electrode cell with a counter electrode

When a potential (E) is applied to a two electrode system, a finite current flows between the RE and WE, where E may be split into three components:

$$E = (\Phi_e - \Phi_s) + iR_s + (\Phi_s - \Phi_{REF})$$

Equation 2.18

Where Φ_e , Φ_s , and Φ_{REF} represent the electrostatic potential of the electrode, solution and reference electrode respectively. The first term refers to the over-potential required to drive the redox reaction at the WE/solution interface, the second term refers to the potential drop due to the passage of current through solution (where i = current flowing, R_s = solution

resistance) and the final term refers to the potential drop at the RE/solution interface which is fixed via the chemical composition of the chosen reference solution.

In the case of a small electrode, the current flowing is small, so the second term is almost negligible and as such, may be ignored. This, combined with the fact that the potential drop at the RE is constant, results in changes in E being reflected directly in the driving force applied to the WE. In the case of larger electrodes however, solution resistance becomes a significant element as changes in E do not solely control the potential at the working electrode. Problems associated with this phenomenon may be overcome by the use of a third electrode, a 'counter' or 'auxiliary' electrode (CE). In this arrangement, the current is passed between the WE and the CE and the potential of the working is monitored with respect to the reference electrode. The potential applied to the WE is controlled via a potentiostat which maintains the potential across the electrodes irrespective of the current measured. This instrument ensures that the only current which flows is between the WE and CE. It should be noted however, that not all of the iR_S term is removed from the reading made by the potentiostat – if this reference electrode is anywhere but exactly at the working electrode surface, some fraction of iR_S will be included in the measured potential; this is defined as iR_u where R_u is defined as the uncompensated resistance. This concept is illustrated schematically in Figure 2.6 .

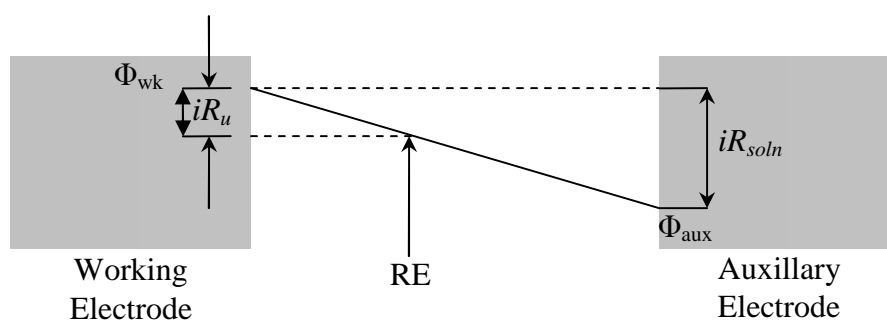


Figure 2.6: A schematic illustrating the potential drop between working and auxiliary electrodes in solution and iR_u measured at the reference electrode

2.1.7 Working electrodes (WE)

If the WE is to be used under non-equilibrium conditions, the WE should be a good electron conductor. As a consequence, WEs are often precious inert metals such as platinum (Pt) or gold (Au), although recently in the drive to produce inexpensive electrode systems, carbon in its various forms is being increasingly used. It is also essential that the electrode remains inert through the potential range over which the electrochemical experiment is to be conducted. Within the realms of SECM, the resolution of the information that may be obtained about the electrochemistry of a surface is very much determined by the physicochemical properties of the microelectrode probe. The different materials and methodologies employed in their fabrication are detailed in section 2.5.

2.1.8 Reference Electrodes (RE)

The standard hydrogen electrode (SHE) is the RE used for the calculation of the standard electrode potentials. Due to its cumbersome nature however, it is impractical to use it on a routine basis. As a result, a number of other electrodes have been developed which are much more suited to electrochemical analysis in smaller volumes. These include the saturated calomel electrode (SCE) and the silver/silver chloride (Ag/AgCl) electrode. Ideally, on the application of a potential to the WE, no current should cross the RE/solution interface and they should be able to exhibit a stable potential difference that can be referred to.

2.1.9 Counter electrodes (CE)

As the role of the CE is to provide a sink/supply of electrons and minimise potential drop, the CE should be a magnitude larger than the WE. In cases where the products of the reaction occurring at the CE should not be allowed to reach the WE, the CE should be placed sufficiently far away from the WE so as to prevent the diffusion of unwanted reaction products from the CE to the WE.

2.2 Processes affecting the electrode reaction rate and current

The reaction rate observed at an electrode is governed by the rates of a variety of processes including:

1. Mass transport
2. Electron transfer at the electrode surface
3. Chemical reactions preceding or following the electron transfer reaction
4. Surface reactions such as adsorption, desorption or crystallisation/electrodeposition.

Considering the redox reaction $O + ne \leftrightarrow R$, whereby O is reduced to R at the electrode surface, the role of these various factors in determining the rate of electron transfer at the electrode surface is depicted in Figure 2.7, where each of these factors in turn are dependent on the potential.

On obtaining a steady state current, the magnitude of the current is limited by the rate determining step. The effects of mass transport processes in limiting the charge transfer reaction at the electrode will now be discussed in more detail.

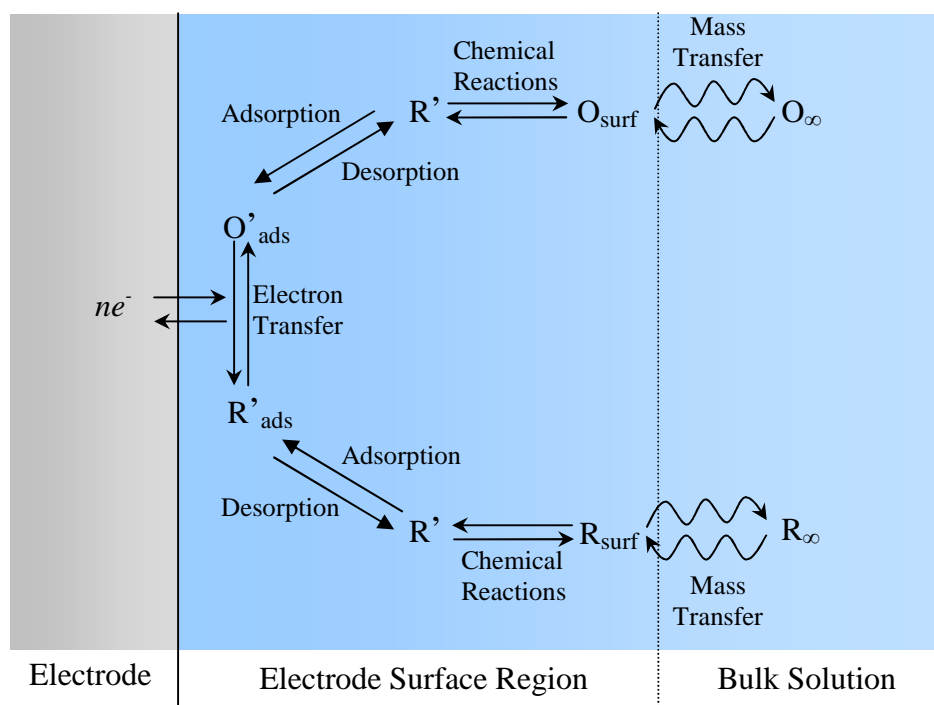


Figure 2.7: Schematic diagram depicting the processes which may affect the rate of the reaction at the electrode surface

2.3 Mass Transport

When electrochemical reactions are induced rapidly by the application of a potential to an electrode surface, the flux of reactants and products to and from the electrode surface may have a significant effect on the resultant faradaic current; this is especially so when the reactions occur rapidly and the rate at which the electroactive species arrives at the electrode surface is not fast enough to deliver at the surface a sufficient quantity of reactant for the ET reaction to occur.

Mass transport is the term used to describe the movement of a reactant to and from the electrode surface. In order for a reaction to occur, the reactant molecule must move from the bulk solution and towards the electrode surface and after the reaction has occurred, the products must themselves diffuse away from the electrode/solution interface. Three modes of mass transport are said to occur – namely diffusion, convection and migration, each of which will now be discussed.

2.3.1 Diffusion

Diffusion may be described as the natural movement of species down a concentration gradient – from a region of high concentration to a region of low concentration. The driving forces behind diffusion phenomenon are entropy based which work to equalise these differences in reactant concentration. Schematically depicted below (Figure 2.8), diffusion is the flux of J (the number of moles of material diffusing through a unit area per second) into and out of an area with boundaries ' x ' and ' $x + dx$ ' which are separated by distance dx .

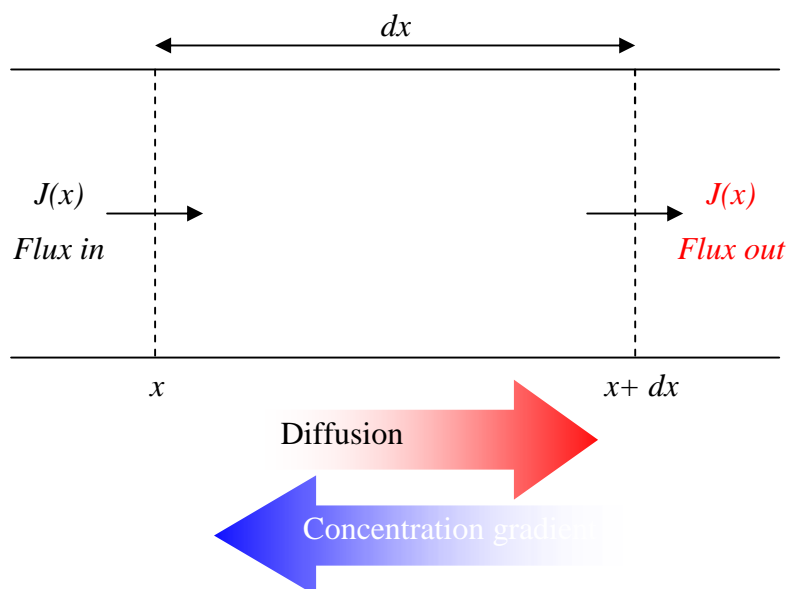


Figure 2.8: Schematic diagram illustrating diffusion from left to right and the concentration gradient from right to left

Fick's first law of diffusion describes diffusion phenomena mathematically (Equation 2.19). Fick (1855) showed experimentally that the diffusional flux, J is equal to the negative of the product of the concentration gradient ($\partial [C] / \partial x$) and the diffusion coefficient (D), the latter of which is a unique characteristic of the diffusing molecule in that particular solvent. Values of D in aqueous solution are generally found to be between 1×10^{-5} and $1 \times 10^{-6} \text{cm}^2 \text{s}^{-1}$.

$$J = \frac{-D\partial[C]}{\partial x}$$

Equation 2.19

Ficks first law of diffusion is then extended in Ficks second law of diffusion to yield information about the variation in concentration at a specific point in space and time – where $\partial[C]/\partial t$ represents the concentration of the species of interest with respect to space and time and $\partial^2[C]/\partial x^2$ is the concentration gradient.

$$\frac{\partial[C]}{\partial t} = D\left(\frac{\partial^2[C]}{\partial x^2}\right)$$

Equation 2.20

This equation may then be used to derive the Cottrell equation which gives the variation in Faradaic current as a function of time where n is the number of electrons transferred in the oxidation or reduction of the species per mol, F = Faraday's Constant, A = Electrode area (cm^2) and $[C]_\infty$ is the concentration of the electroactive species of interest in bulk solution.

$$i = nFAJ = \frac{nFAD^{1/2}[C]_\infty}{(\pi t)^{1/2}}$$

Equation 2.21

Now consider the following redox couple:



When the electrolysis of O begins, its concentration at the electrode surface ($C_{O(x=0)}$) falls to a value less than that in bulk, i.e. ($C_{O(x=0)} < C_{O\infty}$). As the concentration gradient grows perpendicularly to the electrode, it acts to force a flux of unreacted O from the bulk solution and towards the electrode surface. As the electrolytic process proceeds, consuming more and more O, the diffusion layer grows as depicted in Figure 2.9.

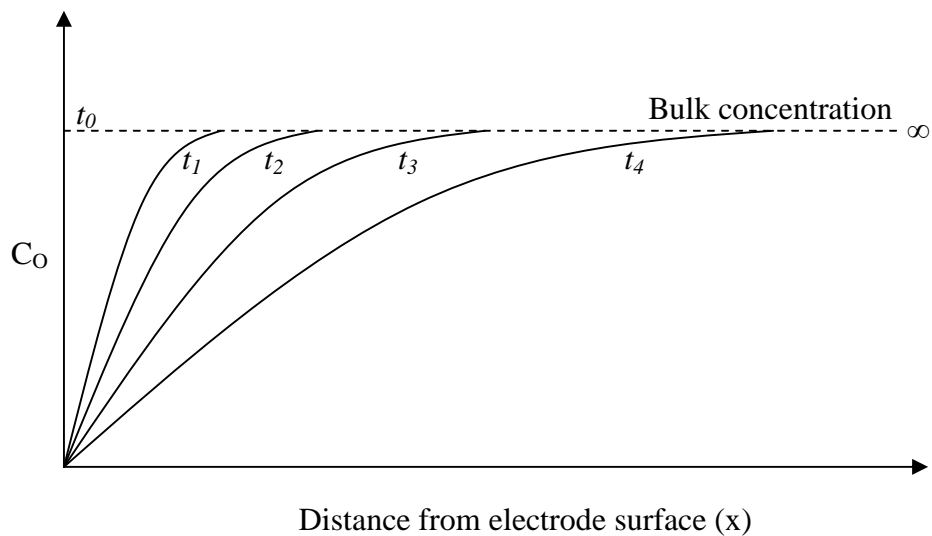


Figure 2.9: Schematic detailing the growth of the diffusion layer into bulk solution with time

At time t , if the reaction is Nernstian, the following will be true:

$$\frac{i}{nFA} = D \left(\frac{\partial[C]}{\partial x} \right)_0 = \frac{D_o [C_{o\infty} - C_o(x=0)]}{\delta_o(t)}$$

Equation 2.22

Now consider when $[C]_0 = 0$:

$$\frac{i}{nFA} = D \left(\frac{\partial[C]}{\partial x} \right)_0 = \frac{D_o [C_{o\infty}]}{\delta_o(t)} = m_o [C]_{\infty}$$

Equation 2.23

where m_o is the mass transfer coefficient ($m_o = D_o/\delta_o$). On combining this finding with the Cottrell equation, the diffusion layer thickness and the mass transfer coefficient may be given by:

$$\delta = (\pi Dt)^{1/2}$$

Equation 2.24

$$k_d = (D / \pi t)^{1/2}$$

Equation 2.25

At points where $x > \delta_0$, $C_O = C_{O\infty}$. Combining δ_0 and the diffusion coefficient as a single constant, m_O , the following relationship is obtained for C_O (Equation 2.26) and C_R (Equation 2.27) considering that in a net cathodic reaction, where C_R is produced at the electrode so that $C_R(x=0) > C_{R\infty}$.

$$\frac{i}{nFA} = m_O [C_{O\infty} - C_O(x=0)]$$

Equation 2.26

$$\frac{i}{nFA} = m_O [C_R(x=0) - C_{R\infty}]$$

Equation 2.27

From these equations, it may be seen that when $C_O \ll C_{O\infty}$ (Equation 2.26), the largest rate of mass transfer and therefore, the largest current under these conditions is achieved. When this occurs, the current value is termed the limiting current (i_l) and is given by:

$$i_l = nFAm_O C_{O\infty}$$

Equation 2.28

when this limiting current flows, the electrode process is occurring at the maximum rate under the given conditions as O reduced immediately on arrival at the electrode surface and the resultant current is dependent on how quickly it can diffuse to the electrode. Rearranging Equation 2.26 and Equation 2.27, the concentration of O at the surface of the electrode may be given by Equation 2.29, which shows that C_O is linearly related to i and varies from $C_{O\infty}$ to a value approaching zero when the current approaches the limiting value, i_l .

$$\frac{C_o(x=0)}{C_{o\infty}} = 1 - \frac{i}{i_l}$$

Equation 2.29

As the diffusion layer is typically less than a few hundred micrometers, the direct observation of concentration profiles within this layer demand an analytical approach with high spatial resolution. One of the first procedures developed in this context was that of McCreery and co-workers; here, a beam of light is made to travel parallel to the electrode surface, which permits the collection of spatially resolved data in a plane perpendicular to the surface of the electrode (Pruiksma *et al*, 1979, Pruiksma *et al*, 1981). The initial approach employed involved the use of a small, movable slit positioned at the edge of the electrode through which a laser was passed. Absorption measurements were then made within a 25µm window to allow a concentration profile to be constructed. The group then went on to monitor the diffusional properties of species down to 5µm from the electrode surface by the use of diffractive spectroelectrochemistry (Rossi *et al*, 1981, Rossi *et al*, 1983). A resolution of 1.2µm was later achieved by the magnification and subsequent detection of a light beam onto a diode array detector (Jan *et al* 1985). Iontophoresis was also used (Engstrom *et al* 1984). In a later publication by Engstrom *et al* (1986), a microelectrode probe with an active area diameter of 10µm was used to interrogate the diffusion layer of an electrode with conventional (i.e. macro) dimensions. By translating the probe through the diffusion layer using a three-dimensional translational stage, concentration profiles within the diffusion layer were obtained as close as 5µm to the macroelectrode surface with 2µm resolution – this was to represent a key step in the development of the Scanning Electrochemical Microscope.

2.3.2 Convection

Convection may be defined as the movement of species within a solution due to the application of a mechanical force or energy to the system. There are generally two forms of convection – natural convection and forced convection. Natural convection arises as a result of thermal gradients or differential densities within solution, whereas forced convection is a result of the application of kinetic energy into the system by, for example, stirring or pumping.

In electrochemical systems incorporating large electrodes, natural convection may limit the distance that the diffusion layer may extend into the bulk solution. As a result of this, the larger the convective forces, the smaller the diffusion layer. When convection forces are large, the faradaic current may be enhanced two fold: by the physical movement of species from bulk towards the electrode and by the enhancement of the rate of diffusion by increasing the concentration gradient through the narrowing of the diffusion layer.

In large electrodes, natural convection may become a significant problem. As the phenomenon is not controlled by the experimenter and is essentially random, the process may add a significant error component to an experiment. As this is highly undesirable, experiments may be conducted under forced convection conditions with the aim of swamping contributions from natural convection and enabling reproducible experiments involving measurements past the 10-20 second boundary.

2.3.3 Migration

Migration is the third mass transport mechanism encountered within electrochemistry and may be defined as the movement of charged species through a medium under the influence of an applied potential gradient. The mechanism is the route by which charge flows between two electrodes immersed in an electrolyte, with the effect of maintaining the charge balance between electrodes. Whilst the mechanism may be considered essential for this, it does not significantly affect the mass transport of redox active species since in most cases, an inert supporting electrolyte is present which enables the passage of charge and negates (or at least mitigates) any potential gradients that may arise in the electrochemical cell.

On the addition of electrolytic ions to the electrochemical cell, there is a redistribution of the anions and cations of which the supporting electrolyte is comprised and this has the effect of maintaining near electrical neutrality in the entire interfacial region. By adding surplus electrolyte to an electrochemical system, the risk of electrical fields building up in solution around the cell's electrodes is minimised.

When all three processes are taking place in a system however, it is difficult to determine the contribution of each process to the observed faradaic current. To counter this, electrochemical experiments are designed so there is one principle mass transfer component in action. For example, convection and migration effects may be avoided by, respectively, the prevention of stirring and the use of an excess of inert electrolyte in the mediator solution.

2.4 Microelectrodes

2.4.1 Definition

Few advances in the world of electrochemistry have changed electrochemical science to a greater degree than the advent of microelectrodes, which occurred principally through the independent work of Wightman, Fleischmann and co-workers circa 1970 -1990 (Ponchon *et al* 1979; Fleischmann *et al* 1987). A microelectrode *may* be defined as an electrode that has a characteristic surface dimension smaller than the thickness of the diffusion layer on the timescale of the electrochemical experiment (Dayton *et al* 1980). Such a definition does not, however, take into account any kinetic parameters of the electroanalytical technique employed and under certain experimental conditions relatively large electrodes may respond like microelectrodes (Stulik *et al* 2000). A definition specifying solely a geometric dimension is therefore inappropriate. It follows that a microelectrode may be defined as:

“...any electrode whose characteristic dimension is, under the given experimental conditions, comparable to or smaller than the diffusion layer thickness, δ . Under these conditions, a steady state or pseudo steady state (cylindrical electrodes) is attained.”

In more quantitative terms, a UME may be defined as an electrode with a critical dimension of $<25\mu\text{m}$ (Wang, 2000), but no less than 10nm - when the electrodes critical dimensions becomes less than this lower limit, the experimental behaviour of the electrode appears to deviate from theoretical expectations based on larger electrodes (Zoski, 2000,

2002). As a consequence of their smaller size, microelectrodes possess some significantly different properties to their larger counterparts. It is these properties that are discussed next, along with their subsequent advantages over macroelectrodes that makes them exploitable in SECM. A schematic diagram detailing the nomenclature used when describing microelectrodes is given in Figure 2.10.

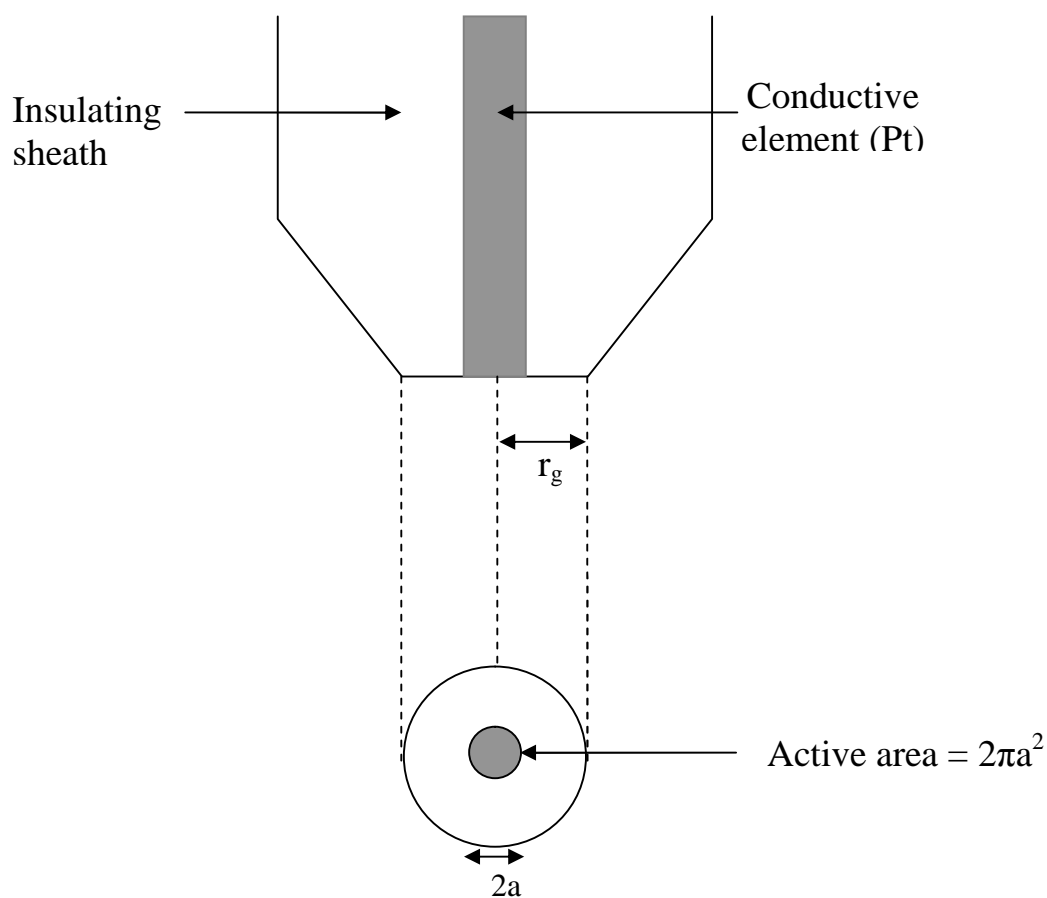


Figure 2.10: A schematic diagram detailing the nomenclature used when describing microelectrodes the r_g ratio is the ratio of the radius of the electroactive area to that of the insulating sheath.





2.4.2 An introduction to microelectrode behaviour

Despite being present in the world of electrochemistry for over 25 years, only recently has the true potential of electrodes with small dimensions been realised. It is only now that the scientific community has really gained an understanding of what microelectrodes have to offer analytical science – i.e. the ability to glean a vast amount of information about a myriad of living, chemical and physiochemical systems.

Diffusion to and from a macro-electrode surface can pose significant problems as diffusion occurs at a much slower rate than convection. As a result, if convective forces are not eliminated from a system, current fluctuations will occur that cannot be attributed to any known experimental variable and so a significant error component may be introduced to the data. This problem may be overcome if the convection force is either eliminated or the rate of diffusion is enhanced to a level significantly larger than that of convection. This can be achieved using microelectrodes.

As the current measured at an electrode is a function of its area, the current measured at a microelectrode is significantly lower than that at a conventional macroelectrode (often nano-amps or below). By virtue of passing minute currents, micro electrodes induce only a tiny amount of electrolysis in solution. It hence follows that the diffusion layer of microelectrodes is very thin (in the order of micrometers) meaning that the concentration gradient induced across them is correspondingly very high. Consequently, the rate of mass transport, namely diffusion, to the microelectrode is much greater than that for macroelectrodes. The current measured is also highly dependent on the geometry of the microelectrode (Table 2.1).

Table 2.1: The diffusion limited plateau current for each of the predominant UME tip geometries, where: n = no. of electrons, F = Faraday constant, D = Diffusion coefficient, c^b = bulk concentration of electroactive species, r_0 = radius of hemisphere, a = radius of base of cone or radius of disk, c = outer ring radius, H = finite cone height (See Zoski, 1990; Zoski, 2002)

Electrode Geometry		Plateau Current
Hemisphere		$2\pi nFDc^b r_0$
Disk		$4nFDc^b a$
Ring		$nFDc^b l_0$
Finite cone		$4nFDc^b a(1+qH^p)$

The variation of current at a hemispherical electrode (Figure 2.11) with time, derived from the Cottrell equation, is as follows:

$$i = nFAD[C]_{\infty} \left[\frac{1}{(\pi Dt)^{1/2}} + \frac{1}{r} \right]$$

Equation 2.30

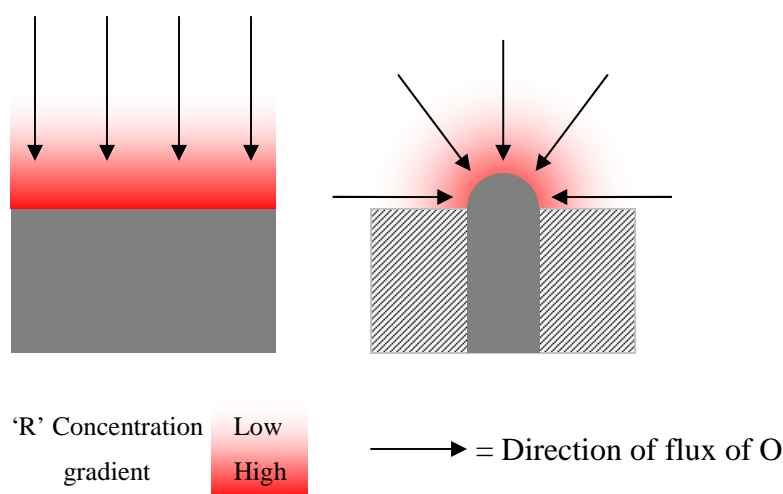


Figure 2.11: Schematic illustrating planar diffusion at a macroelectrode and hemispherical diffusion at a micro electrode.

Where r is the radius of the sphere and A is given by $4\pi r^2$ and $2\pi r^2$ for a sphere and a hemisphere respectively. In microelectrodes, the limiting current is achieved in a fraction of the time required for the limiting current to be reached in a planar microelectrode. As a result of this, the term t is suppressed, yielding the following equation which describes the current at a hemispherical microelectrode:

$$i = \frac{nFAD[C]_{\infty}}{r_{\text{hemisphere}}} = 2\pi nr_{\text{hemisphere}} FD[C]_{\infty}$$

Equation 2.31

In SECM and many other electrochemical experimental arrangements however, one of the main geometries employed is that of the embedded disk electrode. Now, if the hemispherical dimension is close to the diffusion layer thickness (approx. $10\mu\text{m}$), the current will be the same if the hemisphere were to be flattened into a disc shape (Oldham and Zoski, 1988) in which microdisc and microhemisphere electrodes of equal superficial dimensions are found to give identical steady-state voltammograms.

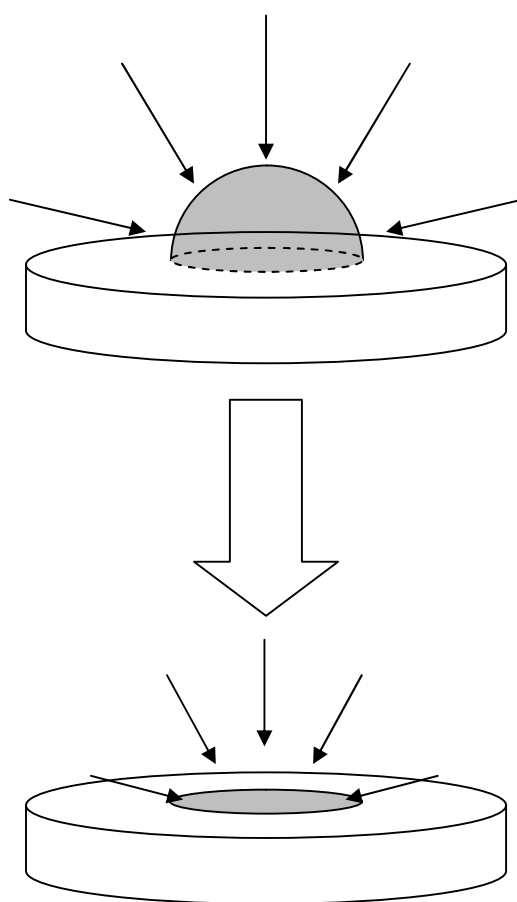


Figure 2.12: Schematic diagram illustrating the flattening of a hemispherical microelectrode to a disc conformation

In this flattening, the disc radius becomes a quarter of the perimeter of the sphere ($2\pi r$):

$$r_{disc} = \frac{2\pi r_{hemisphere}}{4}$$

Equation 2.32

$$r_{hemisphere} = \frac{2r_{disc}}{\pi}$$

Equation 2.33

It follows that by substituting Equation 2.33 into Equation 2.31, the steady state current measured a few seconds after applying a potential step to a disc microelectrode may be given by Equation 2.34. A body of further research also exists on the effect of other electrode geometries, the steady-state equations of which are given in Table 2.1 (Zoski, 1990).

$$i = 4nFr_{disc}D[C]_{\infty}$$

Equation 2.34

The Cottrell equation which describes the planar diffusion of electroactive species towards an electrode predicts that on the application of sufficient electrical potential to an electrode, products of the redox reaction will form a diffusion gradient which extends from the surface of the electrode out into solution to a point where $C_0 \rightarrow C_{0\infty}$. In the case of a microelectrode however, the concentration profile is quite different (Figure 2.13).

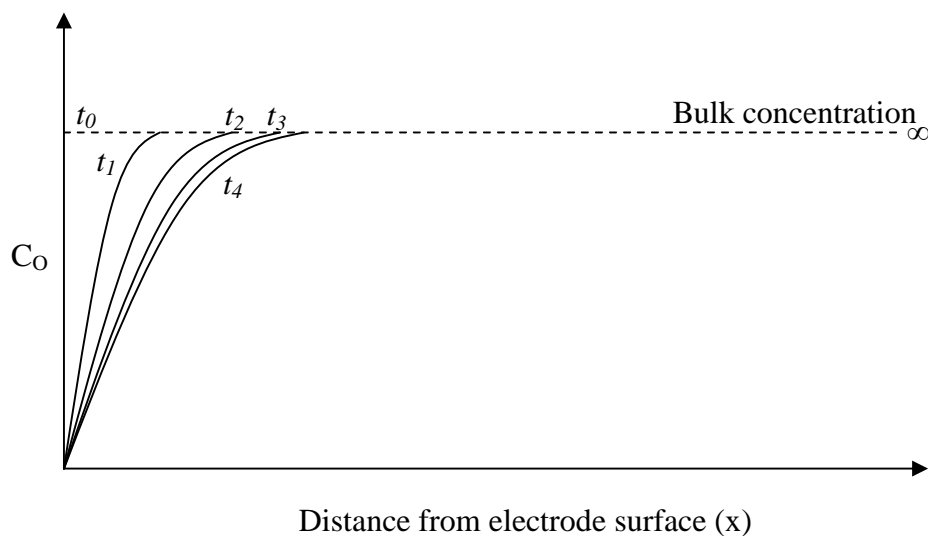


Figure 2.13: Schematic detailing the growth of the diffusion layer into bulk solution with time from a microelectrode

At the immediate onset of electrolysis, the diffusion layer may be said to be similar to that observed at a planar microelectrode – the diffusion layer extends out into the solution adopting an expanding hemispherical conformation – i.e. the diffusion occurs both in the planar direction and radially (Figure 2.13). As a consequence of this bi-lateral diffusion, the flux of electroactive species to the electrode surface is substantially greater than is observed at a typical macro-electrode.

As a consequence of this enhanced rate of mass transport, when the electrode is scanned from a potential which causes no electrolysis of the electroactive species towards a potential that does, the faradaic current that results from the oxidation or reduction of the species exhibits a sigmoidally shaped response (Figure 2.14).

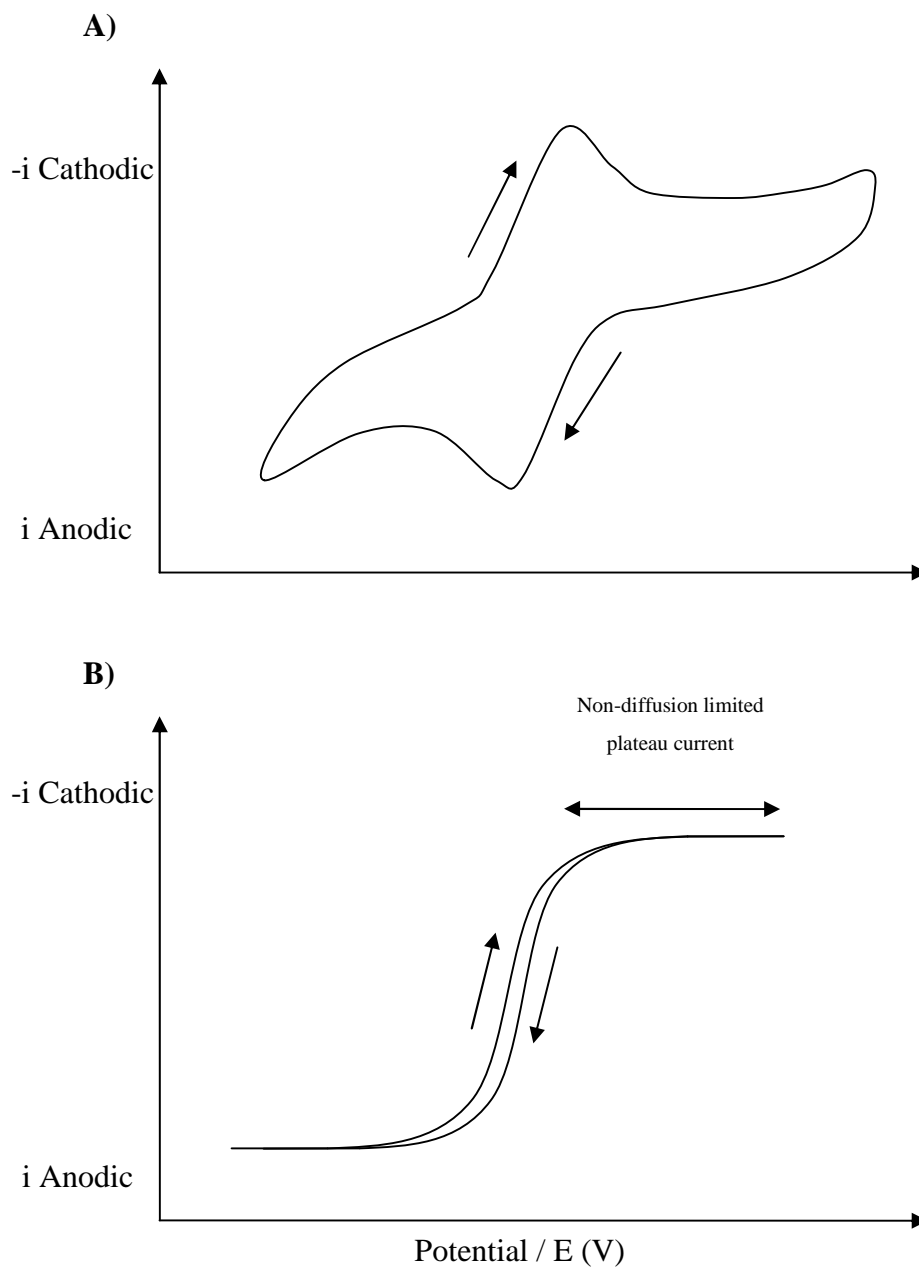


Figure 2.14: Schematic diagrams illustrating the difference in the faradaic current response to variation in applied potential for a macroelectrode (A) and a microelectrode (B)

2.4.3 Advantages of microelectrodes

The relatively small, thin diffusion layer (δ) at a microelectrode means that when the electrode is brought into close proximity to the substrate of interest for scanning, the 'sensing' is performed within the diffusion layer, which induces a very low dependence on hydrodynamic conditions (i.e. stir independence). Hence, when the microelectrode is translated through the mediator solution across the substrate, the current observed may be attributed to the properties of the substrate, mediator and tip - and not the movement of the tip through solution. If the process under investigation is fast in comparison to the rate of mass transport, then electrochemical experiments simply reflect the rate of the slowest step in the process and provide information on the rate of diffusion in solution only. With microelectrodes, the substantially increased rate of mass transport means that this limitation is less likely to arise and much faster chemical steps are available for study by electrochemical methods.

The second advantage to using microelectrodes is the reduced iR or 'ohmic drop' effect. 'Ohmic drop' represents a considerable distortion factor in the derivation of data in electrochemical experiments. Ohmic drops occur as the current that flows through solution generates a potential that opposes the applied potential. The true potential (E) of the working electrode can only be determined by subtracting the product of current (i) and resistance (R) from the applied potential (E_{app}) (Equation 2.35).

$$E = E_{app} - iR$$

Equation 2.35

In highly resistive solutions such as organic solvents or aqueous systems with no added electrolyte, there are fairly severe iR distortions at conventional electrodes because the current is relatively large (due to the large surface area). Microelectrodes however, avoid these problems, making experiments in such environments possible. They do this in two ways. First, microelectrodes performing at or near steady state show minimal iR problems compared with electrodes operating under planar diffusion – it has actually been shown that the iR drop is insignificant and independent of size and geometry of the electrode with

conditions under which true steady-state currents are observed (Bruckenstein, 1987). Secondly, the distribution of current through the solution in the vicinity of the electrode surface is different at microelectrodes, resulting in enhanced electrochemical behaviour.

Much information about electrode processes can be found by sweeping the electrode potential whilst monitoring the current. This effect of changing potential, in addition to electrolysis, also changes the ionic distribution of the electrolyte (background or otherwise) near the electrode surface, causing a charging current to flow which can mask the phenomena under study. As the faradaic-to-charging current ratio, i_F/i_c increases with the reciprocal of the characteristic dimension, microelectrodes have much smaller electrode areas which give rise to significantly smaller transient currents. It hence follows that microelectrode systems suffer less distortion from so-called ‘capacitive charging’. This in practice means that the rate at which the potential is swept can be made much greater in microelectrode systems (Munteanu, 2002).

In summary, as a consequence of their properties discussed above, microelectrodes show the following capabilities:

- Can rapidly attain a steady state for a faradaic process
- Improved I_c/I_F reduces risk of masking the phenomena under study and allows rapid scan rates
- Minimised ohmic drop minimises risk of signal distortion
- Improved signal to noise ratio as a result of minimal charging current
- The smaller size of microelectrodes permits measurements in very small solution volumes
-

2.5 A review of existing microelectrode fabrication methodologies

2.5.1 Glass-encapsulated microelectrodes

Much literature exists on the encapsulation of fine metal (Au, Pt) or Carbon in glass in the fabrication of microelectrodes. A description of this fabrication technique is given in chapter 4, where the technique is employed to fabricate electrodes in-house.

2.5.2 Pulled Pt Wires/Pipette puller

To fabricate microelectrodes of smaller dimensions, one may employ a pipette puller, which involves inserting the metal wire into the open glass capillary and then simultaneously pulling the two together, which leads to a drastic decrease in the diameter of the UME (Pendley, 1990; Katemann, 2001). As one is able to program the pipette puller with the required temperature and rate of pulling of the capillary; the technique allows for the repeatable fabrication of small microelectrodes with a very uniform shape (Zoski, 2002). With the introduction of laser pipette pullers, electrodes with dimensions down to 10nm have been reported using quartz capillaries and 25 μ m hard Pt wire (Katemann, 2001).

2.5.3 Gold Microbead Microelectrodes

Miles et al (1997), reported using gold microbeads of diameters down to 1.5 μ m in the construction of microelectrodes of dimensions $\leq 5\mu$ m. First, gold beads in solution were injected into the lumen of a pyrex capillary (with an internal glass filament). This was then heated to enable the evaporation of the water from the capillary (at 120°C) before heating further at 580°C so as to sinter the gold microbeads to form a solid mass. Epoxy was then used to provide a leak proof seal for the gold beads in glass. An advantage of this microbead approach is that microelectrodes are less expensive to manufacture and available in smaller dimensions than their respective wires. Using these micro-beads in suspension also circumvents the problems associated with working with fragile microwires.

Additionally, Demaille et al (1997) constructed spherical gold microelectrodes with diameters of 1-30 μm by self assembly of Au nanoparticles and 1,9-nonanedithiol molecules at the tip end of glass micropipettes. This technique led to perfectly spherical electrodes in the size range of 1-30 μm and was described as being perfectly controlled and reproducible.

2.5.4 Microelectrode fabrication by Chemical Vapour Deposition (CVD)

In CVD, an insulating film is deposited on a carbon fibre or metal wire from a gas phase precursor. The film is formed by the deposition of silica from a SiCl_4 , H_2 and O_2 gas phase onto a resistively heated carbon fibre or metal wire (Zhao 1995). Due to the existence of a temperature gradient at the extremes of the wire or fibre, deposition rates are variable, which has the effect of generating an insulating covering of a uniform and concentric film that tapers down to the bare fibre/metal tip. Films of thicknesses varying between 1 and 600 μm have been deposited using this technique to generate microelectrodes of a diameter of 5-10 μm (Zhao, 1994).

In comparison to other tip fabrication methodologies, CVD offers many advantages. Because of the nature of deposition, the need for sealants as used in glass encapsulation is alleviated; the concentric deposition of the film according to the temperature gradient means that the resultant geometry is highly predictable and so conforms to theoretical predictions; finally, by altering the precursor formulae, one is able to cover an array of electrode materials of differing physiochemical properties with films of different thicknesses and properties.

2.5.5 Spherical microelectrodes

As mentioned previously, by the self-assembly of gold nano-particles and 1,9-nonanedithiol cross linking molecules at the tip of a capillary pulled by a laser micropipette puller, spherical microelectrodes have been fabricated with diameters of 1-30 μm (Demaille, 1997). The spherical geometry of these fabricated tips were perfectly

controlled and reproducible, and their electrochemical properties the same as for solid metallic Au, showing ideal micro-electrode behaviour.

2.5.6 Ring-disk microelectrodes

Au/Pt ring disk

Glass encapsulated Pt disk microelectrodes may be fabricated and sharpened to the required Rg ratio (see Fig. 2.10, page 31). A thin Au film may be sputtered onto the continuously rotated tip producing a thin Au film of a thickness of about 500nm. This outer ring can then be insulated by the application of a layer of varnish. Ring-disks of this type can then be exposed by polishing with aluminium oxide grinding paper (Liljheroth, 2002).

Carbon disk microelectrodes

Zhao et al (1995), reported a 10 μ m diameter carbon fibre insulated with an Si film by CVD. A layer of pyrolytic carbon was then deposited from acetone. The silica coating process was then repeated to insulate the newly deposited Carbon ring layer. The ring disk was then prepared by cutting the end of the coated fibre at a position that produces the desired outside diameter for the analytical tip and polished. Tip diameters down to 25-30 μ m have been fabricated.

2.5.7 Finite Conical (Etched) microelectrodes

A substantial quantity of literature exists on the fabrication of electrodes down to diameters of 10nm using electrochemical etching, which involves the anodic dissolution of a metal as a result of the application of an AC voltage (Lee, 1991). The alternating voltage is applied between the microwire and a Pt coil in which the microwire is centrally located to try and ensure symmetrical etching. The sharpness of the tip is a product of the etching current and the length of time etching is allowed to proceed. After etching, the wire is then coated with an insulating material to create a microelectrode with a very small area. Coating techniques employed include dipping the wire into a varnish, translating the tip through a bead of molten glass, or the deposition of electrophoretic paints. Even though

electrodes of nanometre dimensions may be produced in this way, it has, however, been shown that one-step insulation processes often result in recessed electrodes, the apparent electrochemical size of which is solely related to the dimension of the 'hole' left in the coating film at the extremity of the electrode.

Although the etching process allows the fabrication of very small tips, it is very difficult to perform reproducibly - and uncertainty often remains as to the exact shape of the resultant electrode (Thiebaud *et al*, 2000).

2.5.8 Microelectrodes by microfabrication

As the field of SECM is focussing on exploring smaller and smaller dimensions of space, so must microelectrode fabrication techniques focus on generating smaller probes with reproducible, exact geometries. A technique such as this is that employed by Thiebaud *et al* (2000), which involved the use of Si anisotropic etching and thin-film Pt deposition techniques to fabricate well controlled Pt-tip microelectrodes. Used primarily for extracellular monitoring of brain slices *in vitro*, the technique may be one day applied to fabricating tips for SECM applications. If this is to ever happen however, a systematic investigation into the diffusional characteristics of these tips is needed.

Microfabrication techniques are again illustrated in Kranz *et al's* work (2001) in which they present a novel approach to developing and processing a microelectrode integrated in an AFM tip. Here, an AFM tip was sputter coated with Au, then insulated with silicon nitride and then milled using an FIB (focussed ion beam). The batch-microfabrication of SECM-AFM probes was recently reported by Dobson *et al* who used direct write electron beam lithography (EBL) to produce sharp AFM tips with a triangular-shaped electrode at the apex with a base width of 1 μ m and a height of just 0.65 μ m (Dobson, *et al* 2005). The technique was particularly successful with over 80% of probes exhibiting reproducible physicochemical behaviour.

2.5.9 Feedback independent electrodes

A significant problem in classical SECM experiments is that the observed map of surface electrochemical activity may be attributed to variations in topography and electrochemical

activity unless the user has complementary information about either variable. Whilst one approach has been to develop methods such as shear force feedback to modulate the tip to substrate distance, a recent approach described by Etienne *et al* (2006) reports the fabrication of feedback independent nanoelectrodes. By positioning the electroactive area of the electrode off-centre in the insulating sheath, the tip does not exhibit SECM feedback while approaching the sample surfaces even to distances within a few hundred nanometres. It is important to note however, that when microelectrode sizes of less than 10nm are fabricated, the experimental behaviour of the electrode may deviate from theoretical expectations based on larger electrodes, meaning developments in fabrication techniques producing increasingly smaller microelectrodes should be accompanied by concomitant developments in the associated theory.

The use of tip current feedback information for positioning and imaging is only possible for well characterised systems however, and is not suitable for the interrogation of topographically complex surfaces or those which exhibit variable conductive properties.

The size of the UME is a critical factor in SECM – for feedback to be observed, the tip must be positioned within one radius of the effective electrode from the substrate for feedback to be sufficiently large to allow feedback to be observed. This problem is obviously negated by the use of larger electrodes, but is exacerbated by the implementation of smaller electrodes – for feedback to be measured using these, the tip must be positioned even closer, thereby increasing the risk of tip crash. With tip crash prevention in mind, several approaches have been developed to maintain a constant tip to substrate distance over substrates with heterogeneous topographies, namely shear force feedback and the hyphenation of the technique with AFM.

2.6 Scanning electrochemical microscopy

Scanning electrochemical microscopy (SECM) is a surface scanning probe technique that allows for the collection of high resolution electrochemical data at a variety of surfaces. SECM exploits several of the unique electrochemical properties of microelectrodes described above, including the hemispherical diffusion profile of solutes towards a microelectrode and the stir independence of microelectrode responses. SECM builds on a body of work conducted by Engstrom *et al* and Liu *et al* in the late 1980's in which the possibility of using microelectrodes to probe diffusion layers and study conductor and semi-conductor surfaces was first demonstrated (Engstrom *et al* 1986; Liu *et al* 1986). During these early years much of the theory underpinning SECM was developed and expanded by Bard and co-workers allowing a theoretical description of (i) how the faradaic current measured at the tip may be described as a function of substrate charge transfer properties (ii) the relationship between the faradaic current detected at the tip and the tip to substrate distance, and (iii), the relationship between mass transport and homogenous reaction kinetics in the inter tip-substrate gap (Liu *et al* 1986, Kwak 1989; Kwak 1989b; Bard *et al* 1989; Bard *et al* 1990, Bard *et al* 1991; Unwin, *et al* 1991; Bard *et al* 1992).

The SECM instrument is composed of (1) an electrochemical cell, (2) a translational stage capable of high resolution movement in the X,Y and Z planes (sub-micron), (3) a bipotentiostat for the accurate control of the potential applied at the tip and/or the substrate, (4) a hardware interface enabling the control of (1) and (2), and (5) a PC which ideally provides an easy to use interface with the hardware and allows the experimenter to control the parameters of the SECM experiment (Figure 2.15).

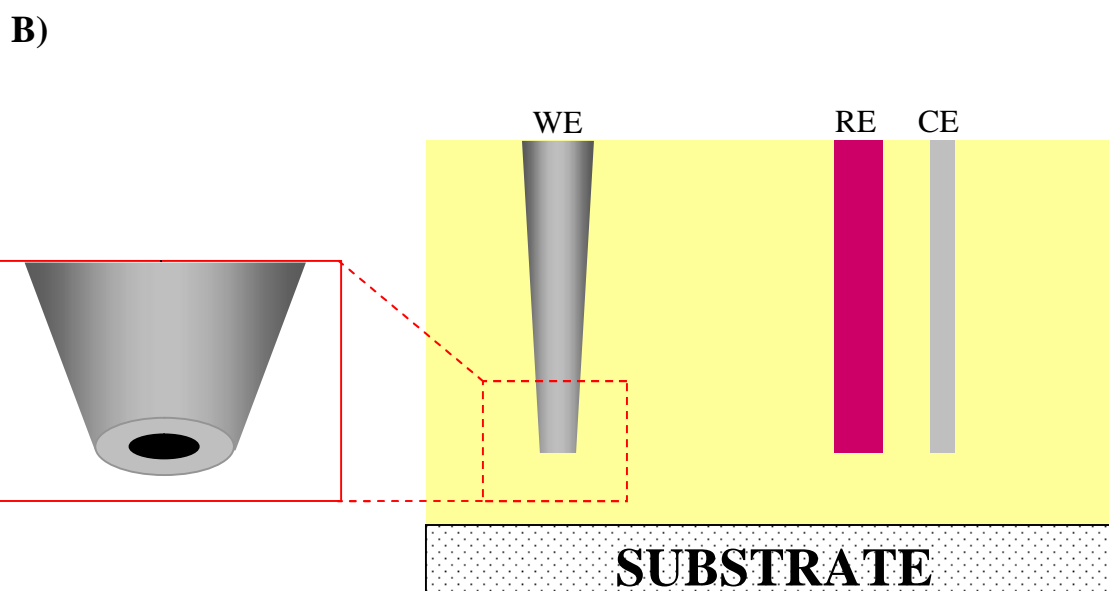
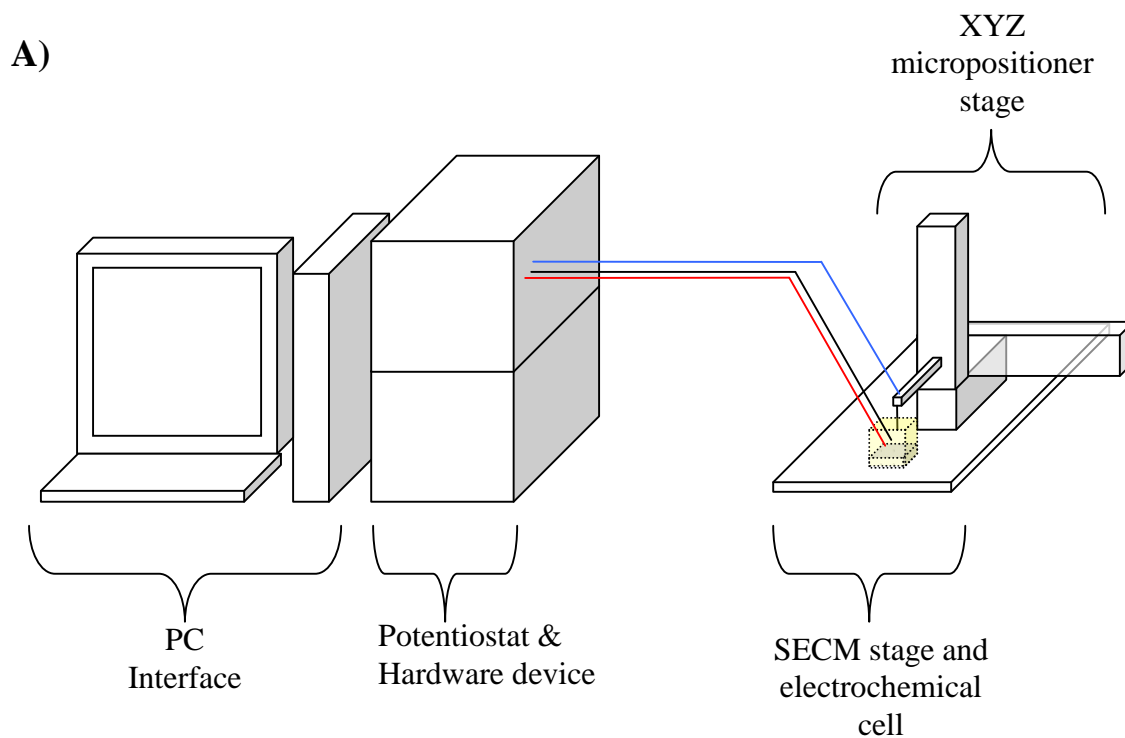


Figure 2.15: Schematic diagram depicting the instrumentation necessary in SECM (A) and the arrangement of electrodes in the electrochemical cell – i.e. WE, RE and the CE (bottom)

In a general SECM experiment, the microelectrode probe, most usually in the form of a disc conformation embedded in an insulating substrate, is immersed in a mediator solution with a reference and counter electrode. The three main SECM principles that may then be employed to collect data about the electrochemical properties of the substrate are: feedback mode (FB), generation collection mode (GC) (Figure 2.16), or, the generally less used, penetration mode.

2.6.1 Feedback mode

When a microelectrode is biased at a potential sufficient to drive an electron transfer reaction at the tip, a small faradaic current is generated - the magnitude of which is dependent on the radius of the active area and is termed ' i_T ' (Equation 2.34). The current observed at this position, a relatively infinite distance away from the substrate – i.e. in bulk solution, is termed $i_{T\infty}$. Now, as the tip is moved towards the substrate, through the mediator solution, the faradaic current may be observed to change. If the substrate is conductive, or, more accurately, has a high rate of heterogeneous electron transfer, the electroactive species reduced or oxidised at the microelectrode tip diffuses to the substrate and is recycled as it donates electrons to or receives electrons from the conductive substrate. As a consequence of this mediator recycling, the rate at which fresh mediator molecules arrive at the microelectrode is enhanced to a rate greater than that due to diffusional processes only, as is observed in bulk, resulting in an increase in tip current ($i_T > i_{T\infty}$). This enhancement of tip current is termed 'positive feedback'. The equation for the tip current as a function of the normalised tip to substrate distance, L is as follows (where $L = d/a$) (Kwak and Bard, 1989).

$$(i_T / i_{T\infty}) = 0.68 + 0.7838/L + 0.3315 \exp(-1.0672/L)$$

Equation 2.36

Conversely, if the substrate is insulating, as the tip approaches the substrate surface, the diffusion of the mediator to the tip of the microelectrode is hindered, resulting in the rate of diffusion becoming a limiting factor. As a consequence of this, as the microelectrode

approaches distances increasingly less than the depth of the diffusion layer, the tip current is observed to drop exponentially. This reduction in tip current in response to approaching the substrate is termed negative feedback ($i_T < i_{T\infty}$), where the normalised current is given by (Kwak and Bard, 1989).

$$(i_T / i_{T\infty}) = \frac{1}{0.292 + 1.515/L + 0.655 \exp(-2.4035/L)}$$

Equation 2.37

Apart from the ‘feedback modes’ described above, the other main type of data collection by SECM is via generation collection mode (GC).

2.6.2 Substrate generation / tip collection mode

This is the more frequently employed of the collection-generation modes and involves the tip probing reactions taking place on the substrate under investigation. For example, a scan in the z direction can produce the concentration profile, whilst a scan over the surface can identify hot spots, where reactions are seen to be occurring at a higher rate. This approach has been used significantly in the study of enzymatic reactions and the diffusion of electroactive species through, for example, membrane pores and biological materials.

2.6.3 Tip generation / substrate collection Mode

The TG/SC mode is somewhat similar to the feedback mode of the SECM (Fernandez et al 2003). Here, the microelectrode tip is held at a potential where an electrode reaction occurs and the substrate is held at a different potential where the product of the tip reaction will react and thus be collected. In the majority of cases the substrate is infinitely larger than the tip, yielding a collection efficiency, given by i_s/i_t , of 1 (100%) for a stable tip-generated species, R. If R reacts, i_s/i_t becomes smaller and its change with separation, d , allows the determination of the rate constant of the homogenous reaction (Bard, 2001).

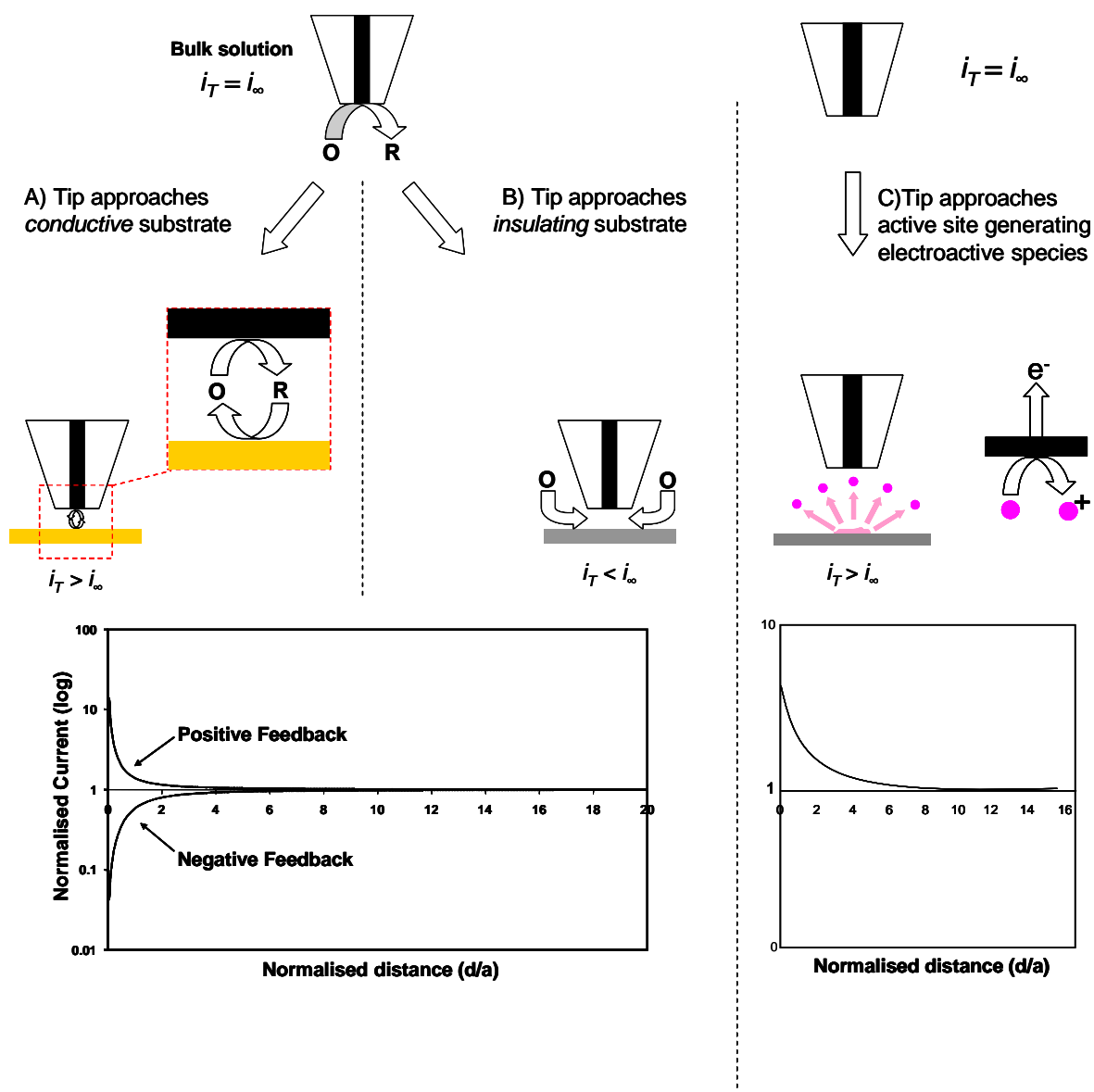


Figure 2.16: Schematic illustrating the principles of positive and negative feedback (A and B respectively) and of SECM in substrate generation, tip collection mode (C). A) Mediator recycling at the boundary interface results in enhanced mass transport and increase in faradaic current. B) Hindered diffusion of mediator to active electrode results in decrease in faradaic current. C) SECM may be used to detect electroactive species generated at an active site (SG/TC mode)

2.6.4 Penetration mode

In penetration mode, the SECM UME tip is translated through the substrate of interest to obtain spatially resolved electrochemical information. An example of such an experiment may be seen in an early investigation by Csoka et al (2003a) who used SECM in the penetration mode to investigate concentration profiles of oxygen and hydrogen peroxide in a biosensor devised for the detection of sucrose in glucose containing samples by Scheller *et al* (1983). The multilayer electrode comprised a glucose-eliminating outer layer of glucose oxidase and catalase together with a sucrose detecting inner layer of invertase, mutarotase and glucose oxidase. The analytical signal of interest was the current obtained from the oxidation of the hydrogen peroxide generated by the enzymatic reaction. Using the SECM technique, they were able to measure enzymatic activity, activity ratios and reaction layer thickness, as well as sucrose and glucose concentrations.

The different approaches to SECM imaging both have their associated advantages. In feedback mode, the reaction at the surface, be it the simple recycling of the mediator species or the involvement of the redox species in an enzymatic reaction, only occurs if the tip is in close proximity to the reaction site generating the necessary reactants. On the other hand, in SG/TC mode, the reaction under observation occurs at the electrode surface regardless of the presence of the microelectrode tip. As a consequence of this, the microelectrode, when scanned across a surface is imaging the diffusion layer, i.e. the products of the reaction at the substrate. As a result of the accumulation of these products, the microelectrode shows high sensitivity but lower resolution than SECM in the feedback mode.

The two imaging techniques do not have to remain distinct techniques though and it is possible to combine the sensitivity of SG/TC together with the high resolution of the feedback mode, although the applications to which this may be applied are somewhat limited. In an example such as this, Zhao et al (2004) used the FB-SG/TC mode to image the activity of the enzyme glucose dehydrogenase (GDH). With reference to Figure 2.17, PQI - a cofactor to GDH, diffuses to the substrate and is converted to p-aminophenol (PAP) by GDH in the presence of D-Glucose. PAP then diffuses back to the microelectrode, closing the feedback loop. The microelectrode tip current may in this way

be attributed to the oxidation of PAP from galactosidase activity (GC mode) and from PQI at the GDH modified surface (FB mode); GC mode provides the sensitivity and FB allows signal amplification over GDH regions only, so enhancing resolution (Zhao, C. and Wittstock, G., 2004a; Zhao, C. and Wittstock, G., 2004b).

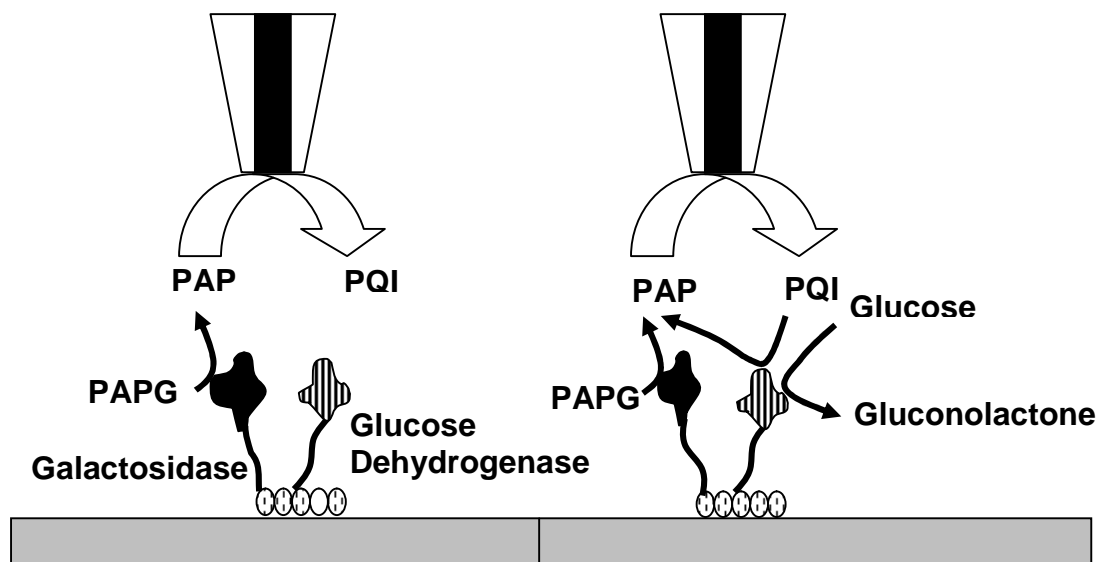


Figure 2.17: Schematic diagram illustrating the combination of FB mode with SG/SC to combine the sensitivity of the SG/TC mode with the high resolution of the FB mode (Zhao, C. and Wittstock, G., 2004). Figure depicts an immobilised Gal-GDH multi-enzyme system. A) Conventional GC mode for Galactosidase in the absence of glucose; B) Signal amplification in the presence of glucose

2.7 Application of Scanning Electrochemical Microscopy to Biological systems

Since its inception, scanning electrochemical microscopy has been applied to a diverse array of bio-analytical problems and represents a tool that is capable of bringing together a number of previously dissociated analytical techniques. SECM is capable of providing quantitative information about the topography and electrochemical properties of a surface.

In contrast to other microscopic techniques such as fluorescence or scanning electron microscopy, SECM does not require the biological sample to undergo complex pre-treatment, with a sample only having to be submerged in a mediator solution or thin film. SECM moreover does not suffer from artefacts such as background fluorescence since the technique is not optically based. A further advantage of SECM over alternative imaging technologies, is that the system under interrogation may be numerically modelled, allowing the subsequent capture of information relating to the kinetics of the reaction under observation. This makes SECM uniquely suitable for the study of biological specimens, since they may be studied under simulated conditions close to those experienced *in-vivo* and may be interrogated repeatedly due to the non-destructive nature of the imaging process. SECM has allowed numerous, distinctly different bioanalytical problems to be tackled, and these have included; determining the electroosmotic flow of ions through mouse and human skin (Bath *et al*, 2000; Uitto and White, 2003), the imaging of methyl viologen permeability in bovine cartilage (Gonsalves *et al*, 2000), bone reabsorption by osteoclasts (Berger *et al*, 2001), convective flow rates through dentine (Macpherson and Unwin, 2005), the interrogation of redox activities of cancer cells - and as a quality control tool for biosensor fabrication.

Other techniques, however, have undergone rigorous development and have established, well characterised protocols. Further, as a consequence of this and their greater commercial availability, they are more widely used in academic and other research laboratories. A significant caveat to SECM imaging however, (which is one experienced by most scanning probe techniques), is the slow scanning speed and hence, low sample throughput. The use of a probe as opposed to a lens is also a significant issue – for positive feedback to occur, the tip must be positioned within one critical dimension of the working electrode from the surface under interrogation. This in itself gives rise to the problem of tip

crash and the potential damage of the tip and substrate, which can lead to wasted time and effort. A key point to remember, however, is that one should not be tempted to directly compare SECM directly against other imaging technologies. SECM is a technique which does not directly image these biological entities, but the processes in which they are involved. When SECM is used to image an enzyme immobilised on a surface for example, it is the enzyme mechanism and the behaviour of products, co-factors or substrates that it is imaging not the enzyme itself. The technique gives complementary information that can allow an improved understanding of the images obtained by other techniques such as fluorescence.

In this section, recent advances in the application of SECM to biological systems are reported. For additional reviews on SECM and biological systems, the reader is also directed to Gyurcsanyi *et al* (2004), Edwards *et al* (2006), Wittstock *et al* (2001; 2007), Amemiya *et al* (2006) and Sun *et al* (2007).

2.7.1 Living Cells

Unlike many other microscopic techniques, SECM may be used to image living specimens under *in-vivo* conditions, so negating the need for complex preparation techniques that can give rise to artefacts. Combined with its ability to interrogate substrates non-invasively, SECM offers a unique approach to the study of intracellular processes with high spatial resolution (Yotter and Wilson, 2004). Using SECM, Lee *et al* (1990) studied the photosynthetic activity of a variety of plant leaf structures by monitoring the concentration profiles of oxygen evolved during photosynthesis and their topography via negative feedback imaging using potassium ferricyanide (Lee *et al* 1990). Since this first application of SECM to a biological substrate, the technique has since been considerably refined and subsequently applied to a variety of biological systems. Here we discuss how SECM techniques have been applied to derive information on living cells and the processes that occur within them.

The first approach to monitoring cellular activity by SECM is based upon monitoring the depletion of molecular oxygen in the immediate environment of cells as they respire (Yasukawa *et al*, 1998). In bulk solution, oxygen is present at higher concentrations than in

the immediate vicinity to a respiring cell as oxygen moves down a concentration gradient and is consumed by the cell. If an electrode is placed in close vicinity to a respiring cell, the faradaic current arising from the reduction of oxygen near the specimen will be less than that recorded by the electrode in bulk solution, Figure 2.18. Conversely, if a cell is producing oxygen, as in the case of a photosynthetic cell, oxygen concentration around the cell increases. This approach may be used in the study of plant physiology (Tsionsky, 1997); SECM's ability to obtain high resolution electrochemical maps of a surface has enabled the activity of single stomata to be monitored and has allowed an investigation into the effects of cadmium induced stress on the plant *Brassica Juncea* (Zhu, 2005) (Figure 2.19 and Figure 2.20). It was also used in the retrospective chemical analysis of tree rings by modifying the amino groups on the wood surface with glucose oxidase; using a shear force feedback approach, it was possible to obtain both topographical and chemical composition information about the sample wood surface obtained from the spruce, *Picea abies* (Garay *et al* 2004) (Figure 2.21). The 2%-4% difference observed between early and late wood regions was attributed to a greater deposition of nitrogen during high growth phases (during early wood growth in spring and summer). The results were in strong agreement with other, more classical analyses of the wood, illustrating SECM's applicability to a wide variety of bioanalytical problems. It is perhaps surprising that to date SECM has not been employed more widely in the study of plant physiology.

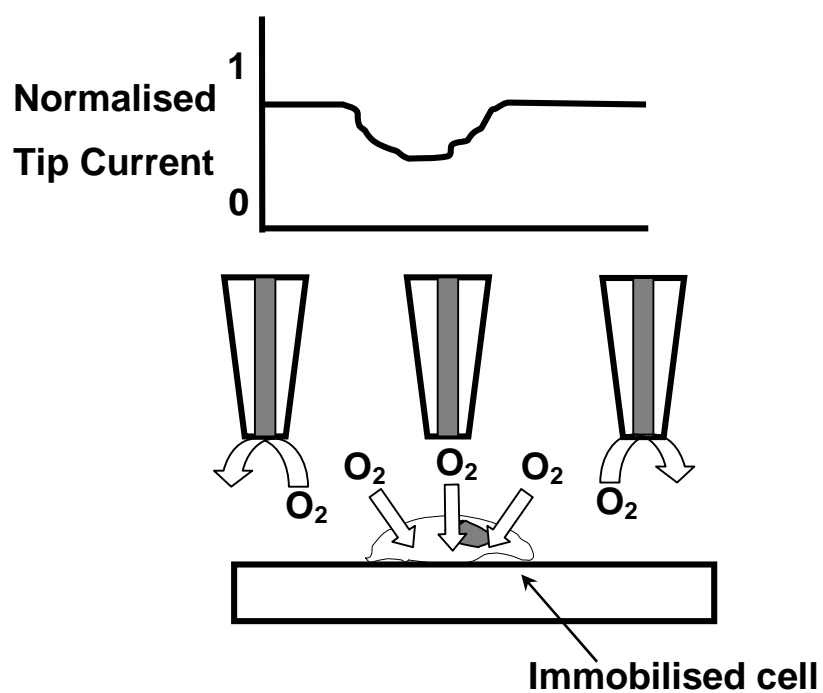


Figure 2.18: Schematic diagram detailing imaging of cells by detection of reduction in oxygen concentration in the vicinity of the immobilised cell

Oxygen was used further by SECM in a study of the differentiation process of human monocytic cell lines. Leukocytes, which play a central role in the immune system, produce reactive oxygen species (ROS), ($O_2^{\bullet-}$, H_2O_2 and OH^{\bullet}) during “respiratory burst” which involves the conversion of molecular oxygen to $O_2^{\bullet-}$ by NADPH oxidase in human monocytic leukaemia cells. Using SECM, the rate of ROS production was found to be reflective of the cellular differentiation process and when combined with chemiluminescence methodologies, could represent an easy approach to monitoring the differentiation process in real time (Kasai *et al* 2005).

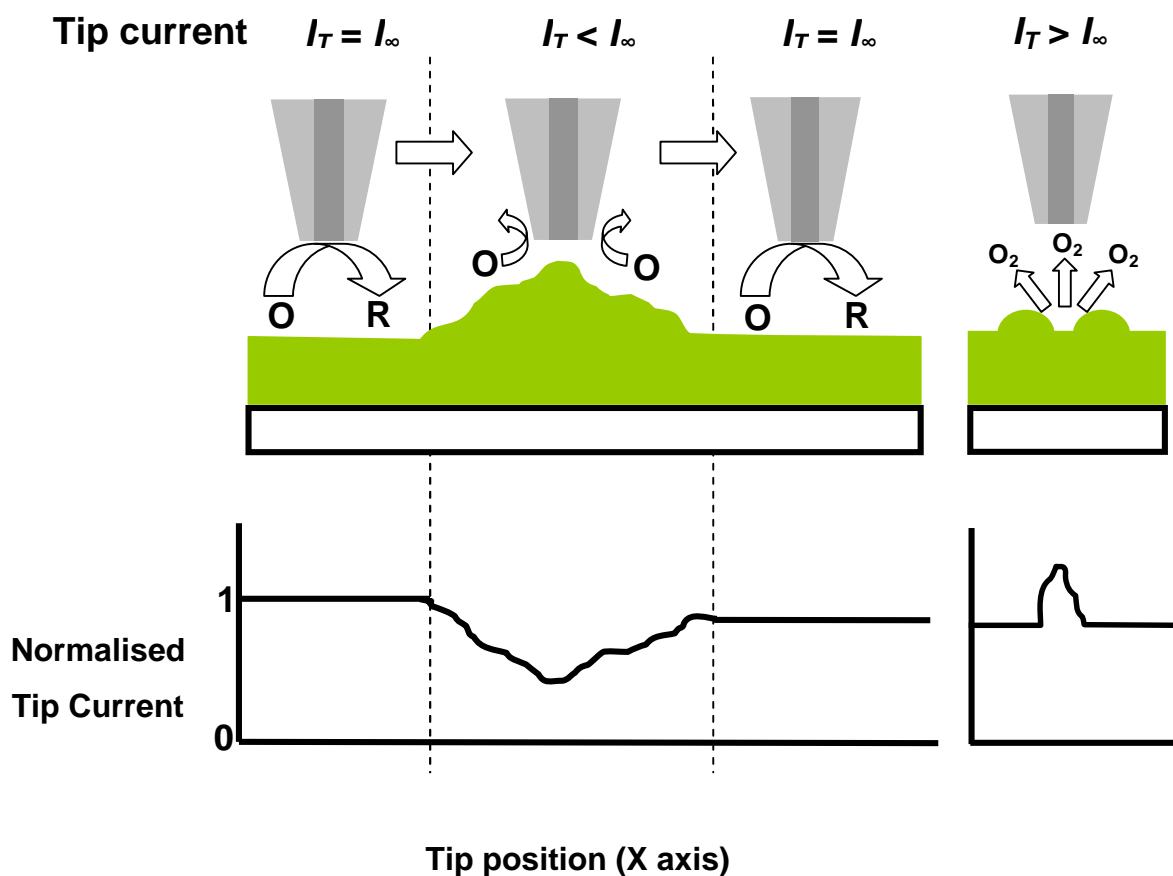


Figure 2.19: A) ‘O’ represents the mediator in its oxidised form and ‘R’ in its reduced form. In bulk solution, faradaic current is maximal at the applied potential and diffusion controlled; however, when brought into close proximity to a cell or a raised region of the specimen surface the diffusion of the mediator to the UME is hindered and negative feedback is observed. B) When interrogating stomatal behaviour, an increase in tip current is observed over oxygen-generating regions of the specimen surface – i.e. over stomata

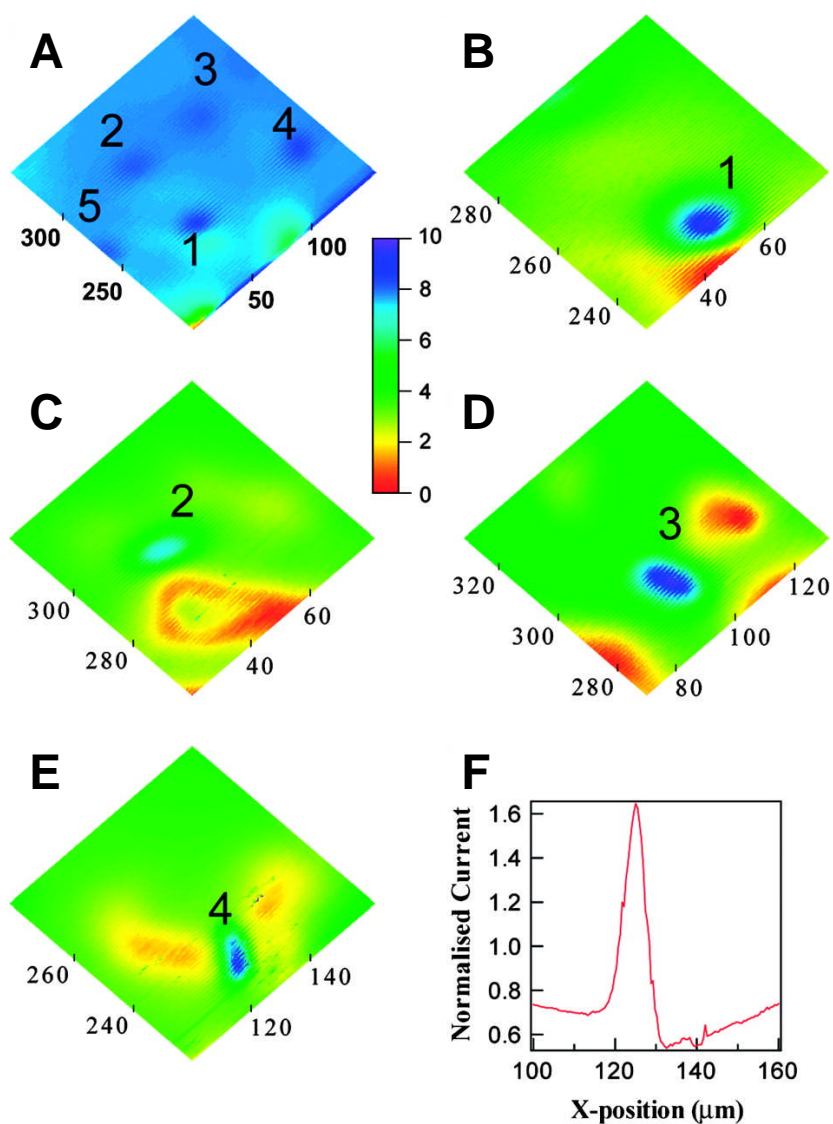


Figure 2.20: A) SECM image of a 150x150 μm area of *Brassica Juncea* (tip current, i_T was normalised by: i_T / i_{∞} where $i_{\infty} = 0.77 \text{ nA}$) B-E) Zoomed in image of areas 1-4 in A. F) Cross-sectional linescan over stomata with high peripheral oxygen concentration. (Zhu, R., Macfie, S.M. and Ding, Z. (2005) Cadmium-induced plant stress investigated by scanning electrochemical microscopy. (Journal of Experimental Botany 56, 2831-2838 by permission of Oxford University Press)

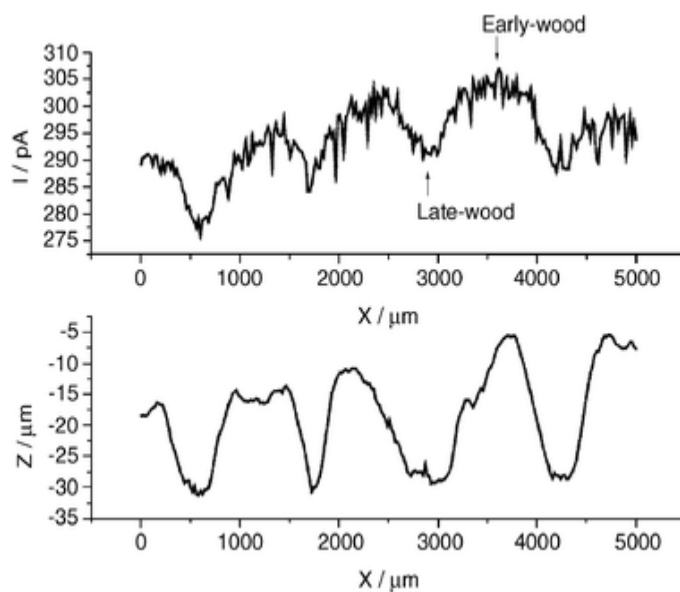


Figure 2.21: Linescans over wood surface achieved simultaneously by using SECM in GC mode with shear force feedback. Glucose oxidase was immobilised on nitrogenous compounds on the wood surface and imaged under a 0.1M phosphate buffer + 50mM glucose solution (Garay, M.F., Ufheil, J., Borgwarth, K., Heinze, J., (2004) Retrospective chemical analysis of tree rings by means of the scanning electrochemical microscopy with shear force feedback *Physical Chemistry Chemical Physics*, 6, 4028-4033 - Reproduced by permission of the PCCP Owner Societies)

An alternative method to the imaging of cells using oxygen is described by Liu et al (2001). The approach involves the depletion of oxygen in the vicinity of the cell and monitoring the resultant increase in tip current as oxygen diffuses from the cell into its immediate surroundings. Whilst this is not necessarily a direct measurement of respiratory activity, it was only used here as a means of locating cells in the absence of a potentially harmful mediator. The tip current near the cell surface is enhanced as a result of the diffusion of oxygen trapped within the cell membrane to the tip down a concentration gradient, so increasing the effective mass transport rate.

Cellular activity may also be followed by approaches including the monitoring of the efflux of acid species from cells, since this is often an indicator used to monitor metabolic rate (McConnell *et al* 1992). Using antimony electrodes to monitor the efflux of acid from immobilised cells, pH measurements were possible which allowed pH profiles to be composed and inferences about cellular activity to be made (Liu *et al*, 2001). Given

advances in the detection of pH changes at the molecular level, it is possible that more spatially resolved data may be able to be obtained to allow more detailed inferences to be drawn about the role of pH in cellular and metabolic regulation (Boldt *et al* 2004).

All of the approaches discussed so far do not include the use of electroactive mediators, i.e. redox active species that act as intermediaries between the ultramicroelectrode probe and the substrate under interrogation. The advantage of this approach is that the use of potentially harmful reagents can be avoided, maintaining conditions as close as possible to those experienced *in-vivo*. Whilst this type of experiment is useful for studying cellular respiration and has been used extensively in SECM experiments, their usefulness in probing cellular biology and physiology is somewhat limited. There is hence much scope for the development of alternative techniques, such as the use of electroactive mediators. By introducing a mediator to the system it is possible to interrogate the topography of cells, changes in morphology and changes in intracellular processes - as well as the mixed intracellular potentials, concentration and location of redox centres (Liu, 2001).

Of the vast array of tightly regulated cellular metabolic pathways, many function by the involvement of specific redox couples such as NAD^+/NADH , cysteine/cystine and the oxidised and reduced forms of glutathione and metalloenzymes (Rabinowitz, 1998). It follows that as extracellular conditions vary and these pathways are regulated to allow the cell to tolerate these changes, the intracellular concentrations of these couples also change. SECM techniques were first applied to investigating transmembrane charge transfer in a study into the different redox activities of nonmetastatic and metastatic human breast cells; this followed work in which intracellular redox activity was probed by detecting ferri/ferrocyanide regeneration by menadione/menadiol redox membrane permeable mediators at a gold electrode (Rabinowitz, 1998; Liu, 2000; Mirkin, *et al* 2002).

A schematic detailing some of the ways in which mediators of differing hydrophobicities may be utilised to interrogate living cells are shown in Figure 2.22.

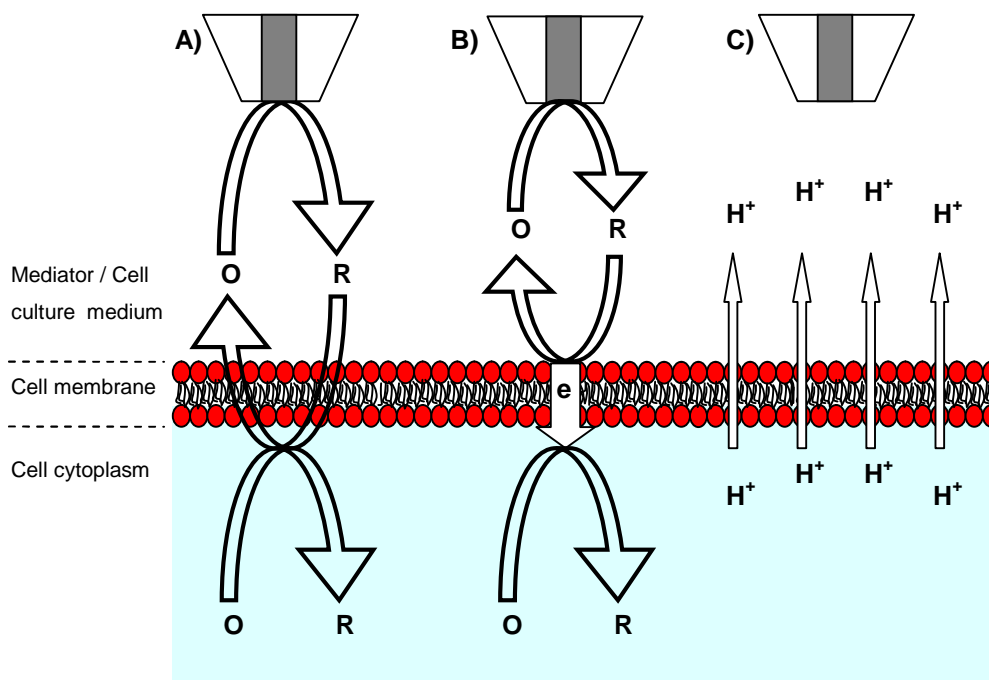


Figure 2.22: A) Positive feedback is observed as the hydrophobic reduced species generated at the tip diffuses through the cell membrane and is re-oxidised by a different intracellular redox centre confined within the boundaries of the cell. B) Positive feedback is observed as a result of a self-exchange electron transfer reaction. Hydrophobic mediator diffuses to the cell membrane where it is re-oxidised by ET occurring across the cell membrane C) Schematic diagram illustrating the potentiometric measurement of the pH profile around a single cell

2.7.2 Mammalian cells

It has become possible to conduct studies exploring the intracellular redox potential of cells and the redox reactions that take place within them through the use of mediators with differential hydrophobicities - and hence abilities to permeate through cellular membranes.

Using a range of hydrophilic mediators, namely $\text{Ru}(\text{NH}_3)_6^{3/2+}$, $\text{Fe}(\text{CN})_6^{3/4-}$ and $\text{Ru}(\text{CN})_6^{3/4-}$ the topography and intracellular redox behaviour of metastatic and non-metastatic breast cell lines has been investigated (Liu *et al* 2001). Metastatic and non-metastatic cell lines were observed to exhibit significantly different intracellular redox behaviour; normal, healthy MCF-10A cells regenerated naphthoquinone at a substantially greater rate than the metastatic MDA-MB-231 cells, a pattern which was observed with each of the other mediators used. Using SECM in combination with single cell chronocoulometry, it was established that the difference in the redox activity between non-transformed breast cells and metastatic breast cells arose from different concentrations of redox-active moieties in the cells and that the same intracellular moieties participate in the oxidation of all three quinols used as mediators. The occurrence of 'hotspots' of mediator regeneration within the cell also raised the question of whether specific redox events are confined to specific spatial localities in the cell (Liu *et al* 2001). The capability of SECM to detect hotspots of activity is highlighted further by Takii *et al* (2003) who employed SECM techniques to characterise the spatial distribution of respiratory activity in PC12 neuronal cells (Figure 2.23). Using the oxygen reduction current as an indicator of respiratory intensity, areas in which negative feedback was obtained were correlated to areas of high respiratory activity as the cell consumes oxygen from its immediate environment. Using this technique, the location of mitochondria in the axon could be identified together with the role of neuronal growth factor (NGF) in mitochondrion distribution and excitation (Takii *et al* 2003) (Figure 2.23).

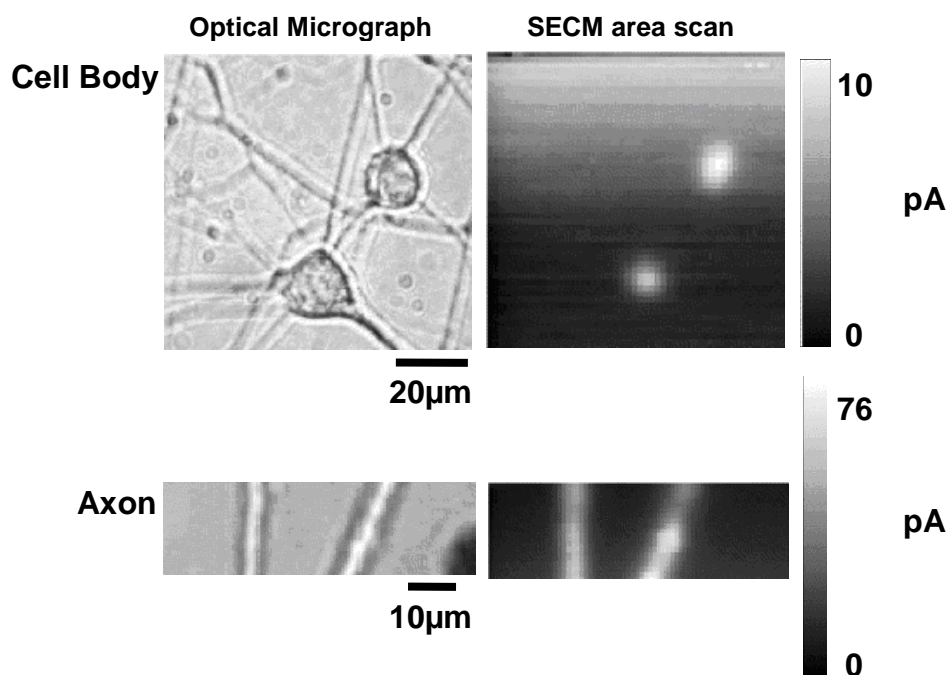


Figure 2.23: Optical Micrographs and the corresponding SECM images of the cell bodies and axons of NGF-differentiated PC12 neuronal cells. SECM images were recorded with a Pt microelectrode scanned at $9.8\mu\text{ms}^{-1}$ in a HEPES based saline solution. This figure was published in *Electrochimica acta*, 48, Takii, Y., Takoh, K., Nishizawa, M. and Matsue, T.; 3381-3385 Copyright Elsevier (2003)

A significant limitation on this study however, was that it was not possible to simultaneously image the axon and cell body due to the height differential between the two cell structures. This problem was later overcome by the use of a ‘standing approach mode’, a feedback mechanism which allowed the simultaneous imaging of PC12 cell topography and respiratory activity for the first time (Takahashi *et al* 2006) (Figure 2.24). SECM has also been used in the development of a sensor for the neurotransmitter acetylcholine (Lin, 2004).

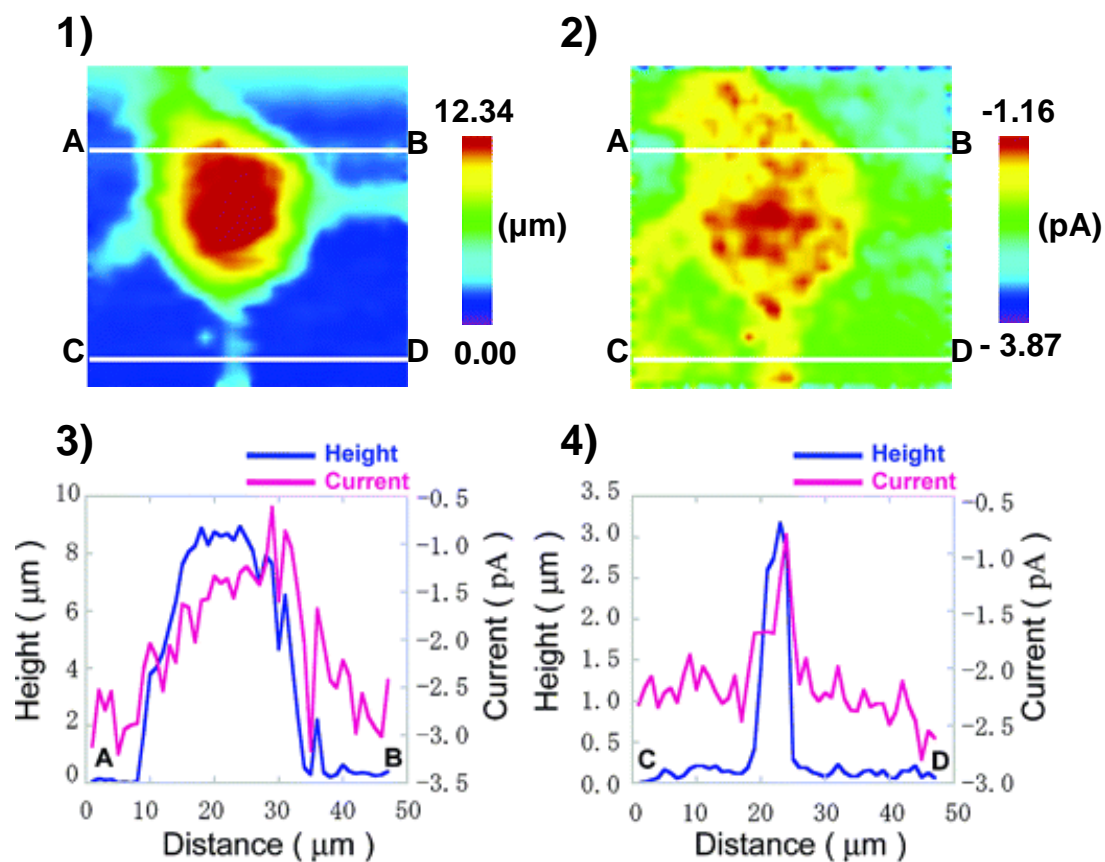


Figure 2.24: Topographical (1) and electrochemical (2) images of live PC12 neuronal cells in PBS solution. Cross sections (white lines on images, A-B, C-D) across these images yield profiles (3&4) across the cell body and axon respectively. Images were recorded by SECM in STA (standing approach mode) using a capillary electrode probe, which allowed constant distance imaging. Scan range: $47\mu\text{m} \times 47\mu\text{m}$; step size: $1.0\mu\text{m}$. Reprinted with permission from Langmuir (2006), 22(25) 10299-10306. Copyright (2006) American Chemical Society

SECM provides information at the single cell level that may be very difficult to obtain by observing the average response from fields of cells - as well as allowing measurements on a much smaller time scale. However, SECM may be applied to larger fields of cells with good effect. By measuring the redox activity of a heterogeneous field of cells, it is possible to identify cancerous cells and so identify malignant cells in human tissues. Metastatic breast cells were loaded with fluorescent nanospheres and placed in a densely packed monolayer with unlabelled normal breast cells. Fluorescent images and SECM profiles were then superimposed on one another to show that SECM was capable of differentiating between the two closely packed cell lines (Feng, *et al* 2003).

It is possible via the use of hydrophobic mediators, to obtain quantitative information relating to the morphology of living cells by observing changes in the tip current arising from variations in topography. Using SECM, cell structure-function relationships may be investigated. With a specific interest in the differentiation of PC12 cells into a neuron phenotype on exposure to nerve growth factor, Liebetrau *et al* (2003) found that the images produced by the occurrence of negative feedback gave valuable insights into cell topography that could not be attained via light microscopy. SECM successfully recorded real-time morphological changes ($\pm < 1\mu\text{m}$) induced by modulating the ionic strength of the surrounding medium. However, using the constant height approach to image the cells, it was not possible to image a complete neuron with the cell body and associated neurites due to the height difference between the two types of structure, much like the aforementioned study of Takii *et al* (2003). To image samples with such a height differential, the SECM must be used in the constant distance mode and was later adopted to study undifferentiated and differentiated PC12 neurons. Here the tip to substrate distance was maintained by monitoring the impedance of the solution between the tip and substrate and then moving the tip in the Z plane accordingly (Kurulugama, 2005).

2.7.3 Monitoring cellular status and drug viability testing

There are various approaches available for monitoring the physiology of cultured cells, including following pH changes through to impedance measurement and extracellular potential recording. The principal technique for measuring drug efficacy is however via

fluorescence imaging. Stains such as GFP, Calcein-AM and propidium iodide interact with intracellular components to emit fluorescence which may subsequently be measured by a fluorometer. A drop in fluorescence may be attributed either to a decrease in cellular status or the photo-degradation of the fluorescing species, which means that care must be taken since the data can be ambiguous. This creates a perfect niche for the use of SECM since the approach does not depend on such chrono-dependent reactions – but rather measures respiratory activity directly through the uptake of oxygen. A further advantage of using this non-invasive approach over these other approaches, is that continuous monitoring of the dose effect is possible - and so there is no need for loading the system with cytotoxic fluorescent dyes.

In a study by Kaya *et al* (2003c), SECM was used to study the impact of KCN, ethyl alcohol and Antimycin A on HeLa cells (see also Nishiwaza *et al* 2002). Measuring cellular activity by observing the oxygen reduction current, SECM successfully monitored cellular activity and the effects of cellular inhibitors. In a similar manner, Torisawa *et al* (2003) used the SECM imaging system to investigate the differential anticancer drug sensitivity of the human erythroleukemia (K562) cell line and its adriamycin-resistant subline (K562/ADM). On comparing the results obtained to the succinic dehydrogenase inhibition (SDI) assay, it was found that they were highly correlated, despite the underlying principles of the tests being fundamentally different. The same SECM assay was later applied to cancer cells isolated from xenografts implanted into severe combined immunodeficiency (SCID) mice as a model of a human tumor (Torisawa, Y-S. *et al* 2004). By using SECM, the substrate and the sensing equipment are separated, so removing the necessity to incubate the cell with the chip, which in turn allows results to be attained in 4 days as opposed to 9 using the CD-DST assay.

SECM has been used in the development of a multi-channel 3-D cell culture device for use in an anticancer drug sensitivity test. The device, which consisted of 4 x 5 panels of pyramidal activities micromachined on a silicon wafer, when combined with SECM allowed for the continuous quantification of the oxygen consumption rate by the immobilised cells (Torisawa *et al* 2005). Using this 3-D culture system combined with

SECM, the simultaneous detection of the effects of multiple chemical stimuli on the cells arrayed in the chip was possible (Torisawa *et al* 2005b).

2.7.4 Multicellular organisms and their interrogation by SECM

SECM has been used to study several different multi-cellular systems in a similar manner to the approach used for individual cells. For example, SECM has been used to quantify the embryogenesis, oxygen consumption and quality of individual bovine embryos and the respiratory, photosynthetic and peroxidase (POD) activities of *Bryopsis plumosa*, an algal protoplast, breast cancer spheroids and bovine embryos (Shiku *et al* 2001; Shiku *et al* 2004; Shiku *et al*, 2005; Aoyagi, 2006; Agung *et al*, 2005; Abe and Hoshi, 2003; Hoshi, 2003). With reference to the work on bovine embryos, this is of particular interest since it involved the entrapment of the embryos within a cone-shaped microwell to amplify the oxygen concentration changes due to respiration, giving considerable support for the use of this substrate in constructing multi-sample arrays. SECM has also been used to quantify the local permeability of the nuclear envelope of *Xenopus Oocyte* nuclei (Guo, 2005). Using approach curve and chronoamperometric experiments, findings supported existing conclusions that most nuclear pore complexes spanning the nuclear envelope are open. An advantage of using SECM over alternative methods used to study membrane transport such as patch-clamping, is that SECM is non-destructive and this allows the same nucleus or membrane to be used for several different experiments.

An alternative approach for monitoring the activity of specific electrochemically active species is by chemically modifying the tip of the bare microelectrode. Tip modifications such as these were undertaken by Pailleret *et al* (2003) to target nitric oxide, a key intracellular messenger, which is generated by adherently grown human umbilical vein endothelial cells (HUVEC) upon stimulation with bradykinin. Using SECM approach curves it was possible to position the tip accurately and non-destructively near the cell population and allow the detection of spontaneous NO release by the HUVEC population on stimulation by bradykinin. In a later study, a 50µm diameter platinum disk probe was modified by the electrodeposition of Ni^{II} tetrakis (p-nitrophenylporphyrin) and combined

in a double-barrel electrode arrangement to study the signal transduction pathway of NO release from transformed HUVEC cells (Borgmann, *et al*, 2006).

Whilst SECM is capable of imaging fields of cells, problems arise in comparing cells with differing treatments. A technique has been developed that allows for a local dose to be administered to part of the cell culture, allowing the simultaneous comparison of cellular status of neighbouring cells undergoing different treatments. By juxtaposing a microporous alumina membrane with a poly-(dimethoxysilane) (PDMS) mask, ethanol was administered to a well defined area of a HeLa cell culture which was subsequently imaged by SECM via the measurement of the oxygen reduction current (Takoh *et al* 2004). SECM has also been used quite extensively in patterning cells on substrates, examples of which involved switching the cytophobic behaviour of albumin-coated substrates to cell adhesive by exposure to HBrO, an oxidising agent, generated at an ultramicroelectrode held in close proximity to the surface (Kaji *et al*, 2003).

2.7.5 Single Celled Organisms, Microbial Chips and Bioassays

SECM has been used extensively in the characterisation of microbial behaviour, largely due to its ability to facilitate non-invasive studies. As a consequence, SECM offers many advantages for both studying and incorporation into microbial bio-sensing systems. SECM has been used to interrogate the impact of the antibiotics ampicillin and streptomycin on the electron transport chain and membrane synthesis of *Escherichia Coli* (Kaya 2001), the effect of high osmotic stress on bacterium *E. Coli* and *Staphylococcus aureus* (Nagamine *et al*, 2004; Nagamine *et al* 2005) and the respiratory activity of immobilised *E.Coli* in response to exposure and subsequent uptake of Ag^+ , which is known to be an antibacterial agent (Holt *et al*, 2005). In the latter study, the well characterised ferricyanide mediator was used to monitor cellular status as bacteria are known to reduce ferricyanide to ferrocyanide during respiration; it was found that Ag^+ affected cellular viability by inhibiting electron transfer. The possibility of using *E.Coli* microbial chips as sensors for glucose was explored using SECM (Kaya *et al* 2003b). On scanning a microelectrode across the collagen microstructure in which the *E. coli* cells were immobilised, a significant increase in the oxidation current was observed on the addition of D-(+)-glucose. This increase in oxidation current indicates the localised increase in the concentration of

ferrocyanide released from the embedded *E. Coli* cells. In the same study, the possibility to use SECM to detect changes in microbial population size, and hence, growth rates, was investigated and a detection limit of just 100 cells was achieved in a later study (Kaya *et al* 2003b), revealing the sensitivity of the technique and the promise it holds for application to interrogating microbial arrays (Kaya, *et al*, 2004).

Whilst the evolution of DNA microarray technologies has allowed the survey of intracellular gene networks and pathways by the comparison of transcriptional profiles in response to environmental stimuli, the data it provides is discontinuous and as such, it is not suitable for the investigation of temporal changes in cellular behaviour. Taking this into account, it would be of great benefit if we could probe genetic changes that eventually manifest themselves at the cellular level. SECM, by its non-invasive nature and wide applicability offers a novel way to probe microbial behaviour on array chips, (Nagamine *et al*, 2005; Nagamine *et al* 2005b). Using a microfluidic device, *E. Coli* cells were transformed with various plasmid DNAs and the resulting change in phenotype monitored by a variety of techniques, including SECM. By monitoring β -Galactosidase activity induced by the insertion of different plasmid DNAs, SECM successfully allowed differentiation between transformed and normal *E. Coli* cells (Nagamine *et al*, 2005). The approach was later applied to screening for mutagens in a whole cell sensor containing *Salmonella Typhumurium*. Using P-aminophenyl- β -D-galactopyranoside (PAPG) as the enzymatic substrate, in comparison to the conventional assay, the SECM measurements were taken in a much smaller volume, were less time consuming and offered a lower detection limit for the mutagens used (Matsui, *et al* 2006). SECM was also used to investigate the production of ferrocyanide by *Paracoccus Denitrificans* in response to a changing carbon source.

The technique also been used in the study of menadione uptake in the yeast *Saccharomyces Cerevisa*. As menadione is toxic to yeast, the cell employs a defence system, based on Glutathione, a non-protein sulfhydryl compound that conjugates with menadione to form a complex (thiodone) which is then exported from the intracellular space by a specific membrane pump. As thiodone is detectable by electrochemical means, it was possible to determine its rate of efflux from the cell and from that, to calculate the

rate of uptake of menadione by the yeast cells, which, it was found, was the rate determining process (Mauzeroll, 2004). The technique was similarly used to detect the efflux of the same compound from hepatocytes (Mauzeroll, 2004b). These studies highlight the unique potential for the use of SECM techniques in studying cellular behaviour and response to environmental stress.

By investigating the difference in the charge transfer mechanism between mammalian cells and bacteria, SECM has been used to probe the redox behaviour of *Rhodobacter sphaeroides*, a purple bacteria that contains a number of bound redox co-factors and a membrane bound reaction centre protein (Cai *et al*, 2002). By using a variety of hydrophobic and hydrophilic mediators it was possible to both interrogate different compartments of the cell due to their differential permeabilities and secondly to establish the effective concentration of intracellular redox centres. SECM revealed that the irradiation of the bacteria with visible light affects their redox response and that rate constants for the regeneration of mediators were being significantly lowered by illuminating the cells. The same membrane bound reaction centre was interrogated further but in chromatophores and liposomes (Longobardi, 2006).

2.7.6 Cellular models

Cells interrogated by SECM described so far, have primarily consisted of the positioning of an ultramicroelectrode in close proximity to a cell and the measurement of the resultant current due to changes in topography, the emission of cellular products - or the recycling of a redox mediator. However, whilst this provides a great deal of information regarding the redox state of the cell, it would be hugely beneficial to monitor redox processes occurring within the cell directly. This would allow the more precise determination of the location of redox activities and their subsequent characterisation - and may even allow for the development of techniques that would enable the study of the redox behaviour of intracellular compartments. With the long term aim of one day carrying out such an intracellular investigation, a simpler analogous system was interrogated to determine the viability of monitoring the intracellular redox conditions by SECM (Zhan *et al*, 2006). Giant liposomes of diameters 30-50 μm were constructed by the double-emulsion method and filled with $\text{Ru}(\text{bpy})_3^{2+}$; their redox properties were then probed by a flame-etched

carbon fibre SECM ultramicroelectrode tip. Over the course of the experiments, the tip current was monitored as the tip was firstly lowered into close proximity and then through the lipid membrane. The results illustrate SECM's suitability in studying membrane transport and its promise as an alternative technique to those based on fluorescence and radioactivity. The application of this technique to studying membrane transport also represents a departure from the existing paradigm of membrane transport investigations via the use of bi-layer lipid membranes and allows measurements to be conducted over a longer period of time (Zhan *et al* 2006). One of the first SECM studies involving the penetration of a cell with an electrode was reported by Fasching *et al* (2006). Tips of a radius < 50nm were fabricated using focus ion beam technology and inserted into an 8 micron diameter rat fibroblast cell (Fasching *et al*, 2005; Fasching *et al*, 2006). Using the ultra small tip, it was possible to penetrate the cell membrane and so to measure the potential of the cytosolic cell environment. A key area for consideration for future 'overlap' with single cell analysis by SECM is that of ITIES (interface between two immiscible fluids) and the study of membrane transfer, a key process in cellular processes. Lee *et al* for example describe the stochastic electrophoretic capture of individual nanometer-scale particles at a pore in a synthetic membrane (Lee *et al* 2004).

2.7.7 Enzymes

With a strong trend towards the development of miniaturised analytical devices, there is much scope for the use of SECM in the fabrication (with regards to substrate patterning), characterisation and optimisation of enzyme based sensing systems. Through the determination of enzymatic activity, SECM may be used to characterise a variety of different sensors with various applications, from those that use enzymes as a label for a binding event through to sensors in which the enzyme forms the primary recognition element (Turcu *et al* 2005; Zhang *et al* 2006). By obtaining spatially resolved data relating to the distribution of electrochemical activity on the sensor substrate, the effectiveness of the patterning technique may be established and problems associated with cross talk between different sensing regions may be detected (Strike, D.J., 1999). For example, SECM was recently used to validate an ink-jet microdispensing technique for the production of a sensor with differently composed sensing regions (Turcu *et al*, 2005). A

brief overview of imaging enzyme activity the highlights of recent advances in the field since the publication of the comprehensive review of enzymatic imaging by Wittstock (2001) is given in the following section. The different enzymes previously interrogated by SECM are given in Table 2.2 and Table 2.3.

An immobilised enzyme may be imaged by SECM in either feedback or SG/TC mode of operation, with the usual trade-off between resolution and sensitivity. Enzyme mediated feedback imaging, or ‘enzyme-mediated positive feedback’ involves the replacement of the enzymes co-factor, or ‘electron acceptor’ by a mediator. To illustrate this principle of feedback imaging through mediator regeneration, one may use the catalysis of glucose to gluconolactone by glucose dehydrogenase (GDH) using the redox active mediator ferrocenemethanol as a cofactor (Zhao *et al*, 2005). Biotinylated GDH was immobilised on streptavidin coated paramagnetic microbeads at a surface concentration of 2.8×10^6 molecules/ $4\pi r_{\text{bead}}^2$ (1.8×10^{-11} molcm⁻²) and deposited in a well defined, mound-shaped 100µm diameter microspot (Figure 2.25).

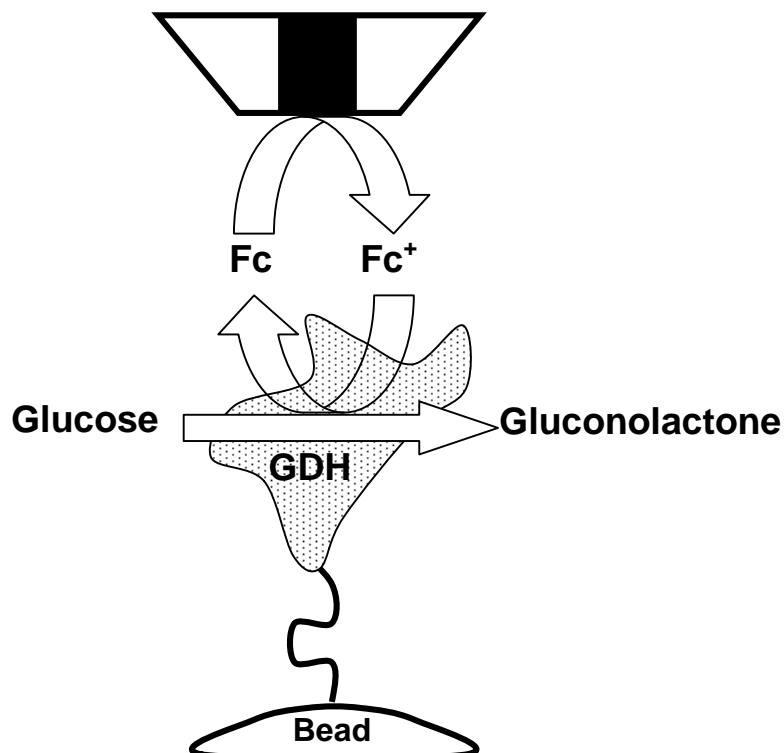


Figure 2.25: Schematic diagram detailing the principle of enzyme mediated positive feedback. The mediator replaces oxygen as the electron acceptor, resulting in mediator recycling over a GDH-functionalised surface and hence, positive feedback. In this system, the reaction only occurs if the tip is present, which has the effect of increasing the resolution of the system

Polarised at a potential of +400mV at a scan height of 30 μ m above the surface, the scan was conducted in a buffered solution of Ca²⁺, D-glucose and FcCH₂OH. Positive feedback was obtained as a result of the reduction of the ferroceniummethanol (Fc) complex that occurs with the oxidation of glucose and its subsequent diffusion to the tip (Figure 2.25).

On the removal of the D-glucose from the system, the feedback signal was halted. The detailed catalytic mechanism of GDH has not yet been fully defined due to the limited structural information available, however, a simplified over-arching mechanism has been proposed as (Zhao *et al* 2004):



Table 2.2: Proteins interrogated by SECM in feedback mode

Protein	Substrate	Mediator	Reaction at UME	Ref
Cytochrome c NADH- Cytochrome reductase	NADH	$\text{Fe}(\text{CN})_6^{4-}$	Oxidation	Holt, K., 2006
		TMPD ⁺	Oxidation	Pierce, D.T., 1993;
Glucose Oxidase	β -D Glucose	FcCOOH	Oxidation	Pierce, D.T., 1992;
Glucose Dehydrogenase	Glucose	FcCH ₂ OH	Oxidation	Zhao, C., 2005; Zhao, C., 2004; Zhao, C., 2004;
		FcCOOH	Oxidation	Zhao, C., 2004;
		p-Aminophenol	Oxidation	Zhao, C., 2004;
Glucose Oxidase	Glucose	Dimethylaminome thyl ferrocene	Oxidation	Wittstock, G., 2001;
		Hydroquinone (HQ)		Pierce, D.T., 1993;
PQQ-dependant Glucose Dehydrogenase (GDH)	Glucose	$\text{Fe}(\text{CN})_6^{3-/4-}$ (with Os-redox relay)	Oxidation	Niculescu, M., 2004
		PAPG/PAP	Oxidation	Zhao, C., 2004.
Quinohemoprotein Alcohol Dehydrogenase	Ethanol	$\text{Fe}(\text{CN})_6^{3-/4-}$ (with Os-redox relay)	Oxidation	Niculescu, M., 2004
Diaphorase (Dp)	NADH	FMA ⁺	Oxidation	Shiku, H., 1995; Suzuki, M., 2004; Oyamatsu, D., 2003a, 2003b, 2003c;
Nitrate Reductase	NO_3^-	Methyl Viologen	Reduction	Zaumseil, J., 2000; Wittstock, G., 2001;
Lactate Oxidase	L-Lactate	Hydroxymethylfe rocene	Oxidation	Parra, A. <i>et al</i> 2006.

Table 2.3: Proteins characterised by SECM in generation collection mode

Protein	Substrate	Signal Product	Reaction at UME	Ref
Horse Radish Peroxidase (HRP)	Hydrogen Peroxide	Hydroxyl Methyl Ferrocene	Oxidation	Kranz, C., 2004; Wilhelm and Wittstock, 2002; Glidle, A., 2003) Oyamatsu, D., 2003c;
HRP	Hydroquinone (H ₂ Q)	Benzoquinone (BQ)	Reduction	Zhang, 2006; Zhou, J., 2002.
Glucose Oxidase	D-glucose	Hydrogen Peroxide (H ₂ O ₂)	Oxidation	Turcu, F., 2005; Kueng, A., 2003; Wilhelm and Wittstock, 1999, 2002; Evans, S.A.G., 2005; Turyan, I., 2000; Strike, D.J., 1999; Hirata, Y., 2004; Kasai, S., 2002; Csoka, B., 2003.
	D-Glucose (<i>p</i> -benzoquinone as Co-substrate)	Hydroquinone		Fuyun, Ge., 2001
GOx in Multienzyme step (mutuarose + Glucosidase)	D-Glucose	Hydrogen Peroxide	Oxidation	Gaspar, S., 2001
Diaphorase	NADH	FMA	Reduction	Yamada, H., 2005;
Bilirubin Oxidase	Oxygen	Hydrogen Peroxide	Oxidation	Mano, N., 2003;
Glucose Dehydrogenase	Glucose	Fe(CN) ⁴⁻	Oxidation	Zhao, C., 2004. Zhao, C., 2004.
Galactosidase (in multienzyme system with GOx)	PAPG	<i>p</i> -aminophenol	Oxidation	Zhao, C., 2004
Uricase	Uric Aid	Hydrogen Peroxide	Oxidation	Kasai, S., 2002;

For feedback imaging to be possible none of the mediator solution components should undergo oxidation or reduction at the working electrode or be capable of interfering with enzyme activity in any way (Wittstock, 2001). Taking into account the observation that SECM in feedback mode is somewhat less sensitive than SG/TC mode, the detection limit of the technique in feedback mode was determined. Horseradish peroxidase (HRP) was immobilised both within a hydrogel in a polycarbonate filter membrane and by biotin-avidin chemistry to a glass slide; both were subsequently imaged using the benzoquinone/hydroquinone redox couple. The work demonstrated a detection limit of less than 7×10^5 HRP molecules within a $\sim 7 \mu\text{m}$ diameter area (Zhou, 2002).

Until recently, a significant limitation to the use of oxidases as a recognition element in biosensors has been their dependence on the oxygen concentration in the surrounding media. However, significant improvements have been achieved by the replacement of the oxidase with a quinoprotein – one example being the pyrroloquinoline quinone-dependent glucose dehydrogenase (PQQ-GDH). The promise of this enzyme to replace its oxygen dependent predecessor, glucose oxidase, is illustrated in a study by Zhao and Wittstock (2004), who undertook a qualitative and quantitative study into the activity of this immobilised enzyme by SECM. Using four different mediators, of which *p*-aminophenol was found to be the most sensitive, they found that despite a degree of deactivation (during the biotinylation and immobilisation steps), PQQ-GDH had a turnover rate significantly larger than immobilised glucose oxidase. It was hence concluded that the high activity of PQQ-GDH and its independence of oxygen make this enzyme a very promising substitute for glucose oxidase as the recognition element in glucose sensors and as the labelling enzyme in chip-based bioassays.

The second mode of imaging enzymatic activity, substrate generation / tip collection (SG/TC) mode, is different to the feedback mode in that it does not involve the use of a mediator but rather the direct reduction or oxidation of the enzymatic product. Here, the microelectrode tip is rastered across the specimen surface to produce a map of the local concentration of a molecule generated or consumed by the enzyme. In contrast to the feedback mode, the biochemical process in this mode is independent of the presence of the tip. A distinct advantage of GC over the feedback mode is that the background current

detected at the tip is negligible, increasing the signal to noise ratio by allowing any change in the faradaic current to be attributed to enzymatic activity. Additionally, many immobilisation techniques involve the immobilisation of the enzyme on gold substrates, meaning that if the feedback approach was to be adopted, the contribution of mediator regeneration by the electrochemical reaction at the gold surface under the enzyme layer would have to be de-coupled from the faradaic current arising from the oxidation or reduction of electroactive species generated by the immobilised enzyme (Kranz *et al*, 1997; Oyamatsu *et al*, 2003).

Despite its high sensitivity however, in contrast to the FB mode, this technique does suffer from a lack of spatial resolution; this comes as a result of the diffuse distribution of the biocatalytic products which diffuse away from the substrate down a concentration gradient into the surrounding medium preventing the accurate determination of the location of the enzyme. This may further be distorted by the movement of the electrode through the surrounding medium and the disturbance of the diffusion shell around the enzyme functionalised region. A further disadvantage of this technique arises when the process at the tip is reversible which means that there may be a feedback component to the current. This problem may be overcome by increasing the tip to substrate distance or by using a potentiometric tip which does not perturb the local concentration of the reactant. The sensitivity of the GC mode may be enhanced by increasing the concentration of the generated product, which may be achieved by minimising the volume of solution between the tip and the substrate. A problem with this however, is that the diffusion of the substrate or cofactor from bulk to the enzyme may be physically hindered by the tip, resulting in a lowering of the tip current akin to that observed when approaching an insulating substrate (Zhao *et al*, 2004). Further, unless the SECM system is equipped with a constant distance mechanism, by positioning the tip closer to the substrate, the user increases the risk of tip crash and hence damaging the microelectrode probe and substrate.

The interrogation of horseradish peroxidase by SECM in GC mode is illustrated by Zhang *et al* (2006) who used the technique in the development of an immunoassay. This immunoassay was designed to detect the circulating CA15-3 antigen, a specific marker used by clinicians to identify and diagnose breast cancer patients, and was constructed

with the aim of simplifying the conventional, time consuming, costly and complex assays currently being adopted. The assay involves the sandwiching of the antigen between an antibody immobilised on a streptavidin coated plate and an antibody labelled with horseradish peroxidase. On exposure of the complete system (Ab-Ag-Ab*HRP) to H_2O_2 and hydroquinone, HRP catalyses the reduction of hydrogen peroxide to water via the oxidation of hydroquinone to benzoquinone which then diffuses to the microelectrode and is reduced, thus generating a faradaic current. The immunoassay was sensitive to 2.5U/ml, which makes the approach suitable for detecting CA15-3 antigens. Similarly, SECM has been used in a number of other immunoassays and immunosensors involving the use of a variety of other enzyme linked systems including alkaline phosphatase (Wittstock *et al* 1995; Wijayawardhana *et al*, 2000a), horseradish peroxidase (Shiku *et al* 1996; Shiku *et al* 1997; Kasai *et al* 2000) and biotinylated glucose oxidase (Wijayawardhana *et al* 2000b). Building on the advantageous analytical properties that the SECM provides the immunoassay analyst, a self contained microelectrochemical enzyme-linked immunosorbant assay device was developed – the integration of all electrodes in the microwell in very close proximity to the modified surface allowed reproducible low detection limits of 9pg/mL of mouse IgG in a 1 μ L drop (Aguilar *et al* 2001).

SECM imaging is unique in the information it can provide and serves as an excellent complimentary technique, allowing an opportunity for hybridisation with other imaging techniques. By hybridisation it may also be possible to address the recurrent problem of differentiating the variation in current due to surface reactivity from that due to surface topography. For example, SECM was combined with a scanning chemi-luminescence microscope (SCLM) to generate electrochemical/chemiluminescence maps of HRP activity; the SCLM images generated are based on the detection of localised chemiluminescence and show the activity and distribution of the immobilised enzyme, whereas the SECM image based on the reduction current of oxygen gives information on the topography of the area of enzyme immobilisation (Zhou *et al*, 2001). In a further example, Oyamatsu *et al* (2003b) utilised a novel hybrid SECM/Scanning Confocal microscope (SCFM) system to image diaphorase (Dp) patterns generated by spotting, laser induced patterning and patterning through the electrogeneration of HOBr in order to deactivate the immobilised enzyme. Unlike the SECM which only generates an image when NADH is introduced to

the system, SCFM is capable of imaging D_p alone, which makes these ideal complimentary techniques since one can image the localised enzyme and the *activity* of the enzyme only. Together however, these techniques could be used to good effect in the patterning and imaging of enzymes in the fabrication and characterisation of bio-devices.

In order to describe the function of different enzyme based biosensors, or to design optimal, efficient devices, it is necessary to determine the distribution of the different electroactive species inside the differently made, sized and formed reaction layers during their operation. Using SECM it is possible to make these determinations, in order to allow for the optimisation of the biosensor. Such is the effectiveness and usefulness of the technique, this area of research is one of the most frequent situations where SECM is used as a quality control technique.

In this context, in a series of papers by Csoka *et al*, SECM has been used to quantify the effectiveness of an interference-eliminating layer and to determine the reaction layer thickness to give an optimum enzyme response (100 μ m) and to calculate the distribution of enzyme products within a less complex glucose oxidase biosensor in order to determine the optimum polymer:enzyme ratio in a wired enzyme electrode (Csoka *et al*, 2003; Csoka *et al*, 2003b). The research demonstrated the capability of SECM in determining the distribution of different species within the reaction layer of biosensors which may allow their optimisation by the alteration of the structure of the sensor. Interference elimination was also the focus for Maciejewska *et al* who used SECM to visualise the spatial variability of GOx/resydrol dots; using selected data collected from SECM area scans, Principle Component Analysis (PCA) and trained Neural Networks were used to successfully quantify the concentration of glucose, 2-deoxy-D(+)-glucose and ascorbic acid in a solution (Maciejewska *et al* 2006; Maciejewska *et al* 2006b). SECM was used further in the visualisation of redox hydrogel-based micropatterned complex biosensor architectures; using SECM in feedback mode, the biochemical activity of immobilised enzyme microstructures were determined with high spatial resolution through the use of $K_4[Fe(CN)_6]$ as the electroactive mediator (Niculescu *et al* 2004).

Extensive work has also been conducted on evaluating the efficiency of different linkage chemistries and methods for the immobilisation of enzymes on a variety of substrates. In a comprehensive review by Wittstock (2001), a variety of techniques available for the immobilisation of enzymes are described, including enzyme-modified patterned monolayers, polymer and metal microstructures. SECM studies published after this review which detail new immobilisation combinations include: GOx immobilisation on biotinylated polypyrrole films deposited by SECM in direct mode (Evans *et al.*, 2005; see also Kranz *et al.* 1997); biotinylated β -Galactosidase on streptavidin coated paramagnetic beads (Zhao *et al.* 2004); ‘wired’ spots of bilirubin oxidase (laccase) in a redox hydrogel (Fernandez, *et al.* 2004); horseradish peroxidase in β -Cyclodextrin (Wang, X.L., 2004 Chemistry Letters); horseradish peroxidase and glucose oxidase immobilisation on amino-thiol- and disulphide- functionalised gold patterned by a variety of soft lithographic techniques (Wilhelm and Wittstock, 2002; Wilhelm and Wittstock, 2003; Oyamatsu *et al.* 2003c; see also Gaspar, 2002). Also, recently, Lactate Oxidase, LOx absorbed directly on glassy carbon and highly ordered pyrolytic graphite was detected by SECM and AFM, giving scope for the development of these materials as platforms for a biosensor for lactate, an important analyte in food and clinical science (Parra, 2006).

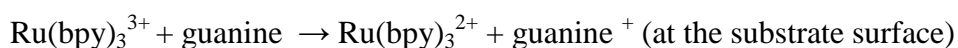
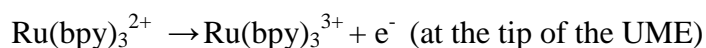
On reviewing the extensive literature concerning the application of SECM to the interrogation of immobilised enzymes, it is clear that only a limited number of enzymes have been characterised to date. There is clearly a vast array of proteins that remain uncharacterised by SECM.

2.7.8 DNA Imaging by SECM

As discussed by Fan (2001), the first SECM images of DNA were reported by Guckerberger *et al.* in 1994. Since these images were first produced, much progress has been made and effort devoted to, the development of the fabrication techniques of DNA microarrays and their associated high-throughput DNA microarray chip detectors. The reliable detection of mismatched base pairs is critical for the study, diagnosis and treatment of genetic disease, as well as the identification of SNPs (single nucleotide polymorphisms). Of the assays proposed for large scale mutational analysis those employing “DNA chips” are by far the most widely investigated. Existing techniques often

rely on the detection of a label tagged on to the target sequence on the formation of a duplex between the probe sequence (on the chip) and targets in the sample analyte (which may have a fluorophore or a chemiluminescent label). However, the size, complexity and capital-intensive nature of these techniques represent major drawbacks, meaning there is plenty of scope for the development of alternative methods of detecting hybridisation events (Turcu, 2004). As a consequence of this, numerous electrochemical biosensors and assays have been successfully developed which represent realistic alternatives to identifying sequence specific DNA in addition to the mass-sensitive devices and optical biosensors dominating this biomedical niche today.

The employment of SECM techniques in studying hybridisation events is extremely appealing for a number of reasons – the detection level is potentially sufficiently low for most applications involving gene expression and SECM detection is relatively inexpensive and substrate general. With regards to its suitability in comparison to other modes of scanning probe microscopy, it represents the most viable approach because of the congruency of the spatial resolution of SECM tips with dimensions of microarray wells or spots. Micro arrays printed by ink jet technology, for example, produce droplets ~67 μm in diameter, which is well within the resolution capabilities of an SECM and does not require the possibly costly fabrication of sub-micrometer UME tips. The simplest form of nucleic acid detection has been described by Wang *et al* who exploit the intrinsic electrochemical properties of the guanine residue in the DNA duplex (Wang *et al*, 2002). Surface-confined DNA molecules were detected through the guanine oxidation induced by the tip-generated $\text{Ru}(\text{bpy})_3^{3+}$:



Equation 2.38

On the application of a sufficient potential at the tip (+1.1V), $\text{Ru}(\text{bpy})_3^{3+}$ is generated which then diffuses to the substrate and irreversibly oxidises the guanine residues on the immobilised substrate, generating $\text{Ru}(\text{bpy})_3^{2+}$ for re-oxidation at the tip. In this way

positive feedback is observed over the surface confined DNA molecules. In the same study, the applicability of SECM to the detection of DNA hybridisation was also illustrated also by exposing a Poly[G] target to an immobilised Poly[C] probe sequence. A distinct disadvantage of this approach is that due to the irreversible oxidation of the guanine residue, the same surface cannot be repeatedly scanned. In addition to this, the success of the technique is wholly dependent on the DNA sequence containing a significant amount of guanine residues in order to produce a sufficiently large oxidation current, which somewhat limits its applicability (Wang *et al*, 2002).

The second approach to imaging DNA and the hybridisation event is to use electrochemically active labels. Yamashita *et al* (2001) were one of the first teams to investigate the SECMs applicability to visualising DNA microarrays. Using an amino based ligand to immobilise DNA duplexes on glass in a mediator solution of ferrocenyl naphthalene, the microarray was imaged. This ligand was concentrated on the double stranded DNA region of the DNA array only, meaning that because of the ligand's electrochemistry, it can interact with the scanning tip to generate a signal (The reader is also referred to Komatsu, 2006). The DNA hybridisation detection levels of this system however, were significantly less than those reported for alternative, existing techniques. In a later study by Wang *et al* (2002b), these weaknesses of Yamashita *et al* were highlighted. They subsequently reported using the silver staining approach in combination with SECM to image a DNA microarray. Here, silver nanoparticles were deposited at sites where hybridisation had occurred as they conjugate onto the biotin/streptavidin-colloidal gold conjugate that has been sequentially constructed at the site of hybridisation. The result was an area over which positive feedback could occur as a consequence of mediator recycling at the site of silver deposition. Hence, the SECM can be used to detect hybridisation events. In addition to these findings, it was also revealed that by altering the hybridisation temperature, highly sequence-specific DNA analysis was possible down to the level of a single base-pair mismatch.

A significant caveat of current approaches to imaging DNA microarrays is the use of numerous reagents – a costly and time consuming factor. The development of reagentless means by which DNA hybridisation could be detected would clearly be highly beneficial.

Exploiting the highly negatively charged properties of the sugar phosphate back bone of DNA, Turcu *et al* (2004) developed an electrostatic approach to visualising the status of surface bound DNA probes (Turcu *et al* (2004); Turcu *et al* (2004b)). Hybridisation detection was achieved through coulomb interactions between the negatively charged sugar phosphate back bone of the immobilised oligonucleotide and the free diffusing redox mediator. Using $[\text{Fe}(\text{CN})_6]^{3-}$ as a mediator, it was found that when the tip was scanned across a gold electrode functionalised with DNA, the tip current dropped as a result of the repulsive forces preventing the diffusion of the mediator to the gold electrode beneath for recycling. Additional differences were found between the repulsive forces of ssDNA dots and dsDNA, indicating that the increase in repellent charges due to duplex formation is sufficient for detection by their repellent mode of SECM operation. In a further study by Liu and Bard *et al*, the role of mediator charge in investigating DNA films was highlighted further (Liu and Bard *et al* 2005). Using the anionic mediators $\text{Fe}(\text{CN})_6^{-3/4}$ and $\text{Fe}(\text{III})\text{EDTA}^-$, they interrogated ds-DNA and M-DNA immobilised on thiolated gold (M-DNA is dsDNA in which a divalent metal cation is inserted in place of one of the protons at the interface between two of the nitrogenous bases at the centre of the duplex – which has been shown by electrochemical methods to enhance the ET properties of the DNA strand). Whilst initial results from approach curves suggested that M-DNA showed enhanced ET transfer properties, it was later revealed that this observation may be due to changes in the electrostatic repulsion forces between the mediator and the polyanionic sugar-phosphate backbone of the DNA; on adding the metal cations they may have been attracted to the phosphate groups, resulting in charge compensation, diminishing the overall negative charge on the immobilised DNA and allowing anionic mediators to diffuse through the film to the gold substrate, resulting in the surface exhibiting positive feedback when interrogated by SECM approach curves.

Preliminary experiments were conducted in order to evaluate the feasibility of SECM for detecting hybridisation events via the use of enzyme labelling (Gyurcsanyi, R.E. *et al* 2004). Complementary probe sequences were first dropped onto a microarray slide and allowed to hybridise. A 2.5% glutaraldehyde solution was then applied to the surface for the subsequent covalent crosslinking and attachment of GOx via the amino group on the

complementary nucleotide. By monitoring the activity of the enzyme labels, it was possible to follow the hybridisation event.

As our knowledge of the human genome expands, there is an accompanying drive to develop increasingly specific DNA-targeting drugs, possibly acting on specific genes, effectively switching them on or off by preventing their transcription. With this comes the need to develop techniques that allow the characterisation of their behaviour to answer questions regarding the nature of the drug and characteristics of the binding site. Using electrochemical methods, including SECM approach curves, the electrochemical behaviour of minor-groove binding electroactive, antitubercular compound Hoechst 33258 was characterised (Wang, S., 2002; also see Soderlind, *et al* 1999). Using these techniques they successfully developed a relationship for examining the interaction of irreversible redox active compounds intercalated with DNA.

2.7.9 Conclusions and future outlook

Since the first description of SECM in the late 1980's, SECM has become a key tool in the interrogation of a variety of biological systems. Since samples require little or no pre-treatment, the technique permits high resolution imaging of electrochemical processes under in-situ conditions, making this technique an invaluable tool for studying living cells. Using mediators with different hydrophobicities, a number of studies have been conducted into the redox behaviour of cells. Additionally, SECM has been used extensively to study transmembrane processes and the role of trans-membrane pumps. The further interrogation of intracellular domains is a significant possibility with the fabrication of increasingly small electrodes – Takahashi *et al* for example have just recently reported the successful imaging of biological samples using an electrode with an effective radius of just 35nm (Takahashi *et al* 2006) – it has already been demonstrated that it may be sensitive enough to determine the locus of enhanced mitochondrial activity within a cell; with developments in SECM probes capable of insertion into the intracellular domain, more accurate determination of the locus of redox activity may be attained. However, with the fabrication of these electrodes must come the development of the accompanying theory,

since electrodes with progressively smaller critical dimensions may exhibit electrochemical behaviour that departs from existing models.

The major group of organisms not yet interrogated by SECM are the fungi – major, extra-cellular producers of enzymes which play a central role in the major nutrient cycles. Given SECM's ability to detect enzymatic activity in both generation collection- and feedback- mode, it is believed that the technique is ideally suited to mapping the extracellular production of enzymes by fungi. By doing so, the technique may give a useful insight into the metabolism of fungi, with specific relevance to selecting the appropriate organisms with the optimal suitability to industrial processes. Many fungal enzymes are capable of performing chemically difficult reactions under harsh conditions and have been harnessed in a variety of industrial processes, including pulp and paper processing, bioremediation and biocatalysis in the production of fine chemicals.

Since SECM has been successfully used in monitoring cellular respiration by measuring the oxygen oxidation current in the vicinity of a living cell, it is apparent SECM has significant promise as a research tool for use within drug discovery. Since the technique may be used to non-invasively monitor cellular status, it is believed that it will be increasingly adopted in this field.

There is a strong trend towards the exploitation of developments in manufacturing techniques to allow the miniaturisation of biological devices such as biosensors, micro-fluidic devices and “lab-on-a-chip” sensing technologies. Whilst the fabrication techniques are available, it is important that for these systems there is a technique sufficiently flexible to characterise the resulting product appropriately, with particular reference to imaging immobilised enzymes by SECM. Using this technique it is possible to locate immobilised entities, determine their spatial distribution and to interrogate the movement of substrates and products in and around the functionalised surface. The SECM is hence a hugely versatile system for application to sensor development, not only in their characterisation and quality control of sensing systems, but also in their fabrication via the controlled direct deposition of polymers and other biosensor scaffolds. The SECM's capability to pattern substrates, either by selective desorption of self assembled

monolayers or by the localised deposition of polymers, has significant implications for the construction of multi-enzyme arrays.

A significant amount of effort is continuing to be focussed towards the development of electrochemical methods by which to detect DNA hybridisation. The reasons are several; the technique potentially offers great sensitivity, the sensors themselves exploit micro-fabrication techniques and they are also highly cost effective. With the current drive to develop electrochemical approaches for monitoring DNA, it is possible that the spatial resolution attainable using SECM offers great potential for the development of DNA microarray sensing systems to rival the benchmark fluorescent approach currently used.

As a stand-alone technique, SECM is a powerful tool for particular applications, but beyond this, when combined with other imaging tools such as atomic force and confocal microscopy, the power and resolution of the technique, in terms of information provided, is very much enhanced. By this 'hyphenation' or 'hybridisation' with other techniques, the shortcomings of the technique in tackling bioanalytical problems are partly addressed.

Chapter 3

Materials and Methods

3. Materials and methods

3.1 Introduction

This chapter provides details of the materials and methods employed in the preparation of mediator solutions and the fabrication of substrates for interrogation by SECM. The protocol for each kind of SECM experiment is also described.

3.1.1 Reagents

Potassium ferricyanide, hexamine ruthenium chloride, ruthenium bi-pyridine, hydroquinone, benzoquinone, hydrogen peroxide, nitric acid (70%), sulphuric acid (95-98%), 3-(aminopropyl) triethoxysilane (98%), poly(sodium 4-styrenesulfonate) 30wt% in water and poly-L-lysine were all purchased from Sigma Aldrich.

Sodium hypochlorite solution was obtained from Fluka.

Aniline hydrochloride, disodium hydrogen orthophosphate 12-hydrate, sodium chloride, diaminobenzene dihydrochloride and polyvinyl alcohol (all 'AnalR' grade) were purchased from BDH (Poole, Dorset, UK). Polyethylenimine (50% solution) was obtained from Sigma Aldrich.

3.1.2 Materials

Menzel® 'Superfrost' microscope slides were purchased from Fisher Scientific (Loughborough, Leics), Superfrost® microscope slides were obtained from Menzel-Glaser GmbH & Co, Germany.

A cold mounting Serifix kit was used for the preparation of inlaid disk substrates and was purchased from Struers, Solihull, Midlands.

Epoxy resin (Araldite®) and Acheson Electrodag conductive silver paint were purchased from AGAR Scientific Limited.

Platinum wires were obtained from Goodfellow Cambridge Limited, Huntingdon, Cambridgeshire and Platinum-Quartz fibres were obtained from Thomas Recording GmbH, Germany.

All wires, crocodile clips and other consumer electronics were purchased from Maplin Electronics (Luton, Bedfordshire, UK).

Conductive inks (carbon type 422SS and Ag/AgCl type 6088SS) were obtained from Acheson Industries Europe and printed onto Melinex plastic sheets.

Standard Calomel Electrode was purchased from ABB Limited, Gloucs.

3.1.3 Equipment

Scanning Electrochemical Microscope (SECM)

A Uniscan Instruments Ltd SECM270 was used for all SECM experiments. Further details about this instrument are given in chapter 4.

Gold Sputter Coater

An Agar B7341 auto sputter coater (Agar Scientific Ltd, Essex) was used in conjunction with a Pfeiffer rotary vacuum pump (Pfeiffer Vacuum Ltd, Newport Pagnell, UK) for the production of gold counter electrodes.

Potentiostats

A Sycopel analytical electrochemical workstation model AEW2-10 potentiostat (Sycopel Scientific Ltd, Tyne and Weir, UK) was used in conjunction with an ECProg3 (version 3.6) user interface in the interrogation of macroelectrodes.

Microscopy

An Olympus SZX12 bifocal microscope (max 90X magnification), a Schott KL 1500 LCD light source and a KPM1E/K CCD camera with Leutron Vision software package were used for some image captures. An Axiovision microscope and Axiovision CCD digital camera were used to image the cells in chapter 8.

Pipette Puller

A Narashige PP-830 pipette puller was used in the fabrication of microelectrodes.

Electrode polishing

Electrode surfaces were polished using a combination of the Struers-DP10 grinder and the Narashige EG-400 microgrinder. Silicon carbide grinding discs, lapping paper and alumina powder were obtained from Buehler (Windsor, Berks).

3.1.4 Solution preparation

Unless stated otherwise, all solutions were prepared using water from the Elga Purelab UHQ-II water system (Vivendi Water Systems, High Wycombe, Buckinghamshire, UK).

3.2 DNA sensor characterisation methodology

3.2.1 Additional reagents

Herring and Salmon DNA were obtained from Sigma chemical company (Poole, Dorset, UK).

3.2.2 Substrate

A screen printed electrode was used as the substrate in this series of experiments (obtained from Microarray Ltd). Conductive inks (carbon type 422SS and Ag/AgCl type 6088SS) were obtained from Acheson Industries Europe and printed onto melinex plastic sheets.

3.2.3 Polyelectrolyte film deposition

A borosilicate glass capillary was drawn to an internal diameter between 20-100 μ m using the Narashige PP-830 pipette puller. This capillary was then filled with a 1% solution of polyethylenimine solution and fixed into the clamp of the XYZ stage on the SECM270. The substrate for functionalisation (the screen printed electrode) was fixed onto the platform and levelled before positioning under the polymer-filled microcapillary. The microcapillaries were lowered at a rate of 5 μ m per step to lightly touch the carbon substrate via the use of a combination of eye and microscope viewing. At this point a small droplet of the polyethylenimine solution was transferred from the capillary to the carbon surface. Following deposition, the microcapillary was then retracted and translated away to a fixed distance in the X or Y axis for the deposition of another polyethylenimine dot. Using this technique, a polyelectrolyte array was fabricated. After patterning, excess polyethylenimine was rinsed from the surface with an excess of RO (reverse osmosis) H₂O and allowed to air dry.

3.2.4 ssDNA/Polyelectrolyte film formation

A solution of Herring or Salmon DNA (0.2mg/ml in H₂O) was boiled for 5 minutes to denature the DNA into its constituent single stranded counterparts; this solution was then flash cooled in ice. The resulting ssDNA solution was applied to the patterned region of the

carbon electrode for ten minutes to allow the adsorption of the negatively charged DNA onto the positively charged polyethylenimine-functionalised regions. The substrate was then rinsed with an excess of UHQ H₂O.

3.2.5 SECM interrogation and hybridisation detection

The patterned PEI/ssDNA substrate above was first fixed to the SECM stage and the substrate levelled. The microelectrode probe, reference electrode and counter electrode was then positioned above the area of interest. 1ml of the 5mM solution of the respective mediator was then introduced to the system, which was large enough to cover the functionalised area and deep enough to immerse the working, reference and counter electrodes. The microelectrode probe was then moved to an inert (Melinex) region of the substrate and an approach curve conducted so as to allow the positioning of the probe relative to the substrate. The approach curve was stopped at $i_T = 0.5 i_\infty$ and a linescan conducted to locate the carbon substrate – indicated by a large increase in the faradaic current observed at the tip as a result of positive feedback. The area scan was then conducted at $i_T = 0.5 i_\infty$. After tip positioning, the tip was then set to the relevant potential and scanned across the substrate at a step rate of 5-20 μ m per step.

After the first area scan was conducted, the microelectrode tip was retracted from the mediator solution and the mediator solution removed from the substrate, taking care not to touch the substrate. The substrate was then rinsed five times with 1ml of UHQ before 1ml of the hybridisation solution was applied to the substrate (0.2mg/ml ssDNA herring/salmon). The system was then left for three hours to allow hybridisation to occur. After three hours, the solution was removed and the system rinsed as discussed previously. 1ml of the mediator solution was then introduced to the substrate and the tip repositioned before conducting the area scan once more.

3.3 Horseradish peroxidase patterning and imaging

3.3.1 Additional reagents

3-aminopropyltriethoxysilane (APTES) and horseradish peroxidase were obtained from Sigma Aldrich. Hydroquinone was obtained from Sigma Aldrich and buffers used were as discussed previously.

3.3.2 Silanised glass slide preparation

Glass slides were cleaned by immersion in a 1:1 solution of 95% H₂SO₄ and 70% HNO₃ for ten minutes. These were then removed from the acid, washed, rinsed with sterile UHQ water and dried. Following drying, slides were immersed in acetone and dried before immersion in a 1% v/v aqueous solution of APTES in UHQ for 2 minutes - after which they were allowed to dry.

3.3.3 Enzyme deposition

5mg of horseradish peroxidase was dissolved in 1ml of 1% glutaraldehyde and consecutive dilutions prepared down to 0.0625mgml⁻¹. Using a pulled microcapillary, this enzyme/glutaraldehyde solution was then deposited onto the silanised glass slides by micromanipulation of the tip position using the SECM270 XYZ stage. After patterning, the substrate was rinsed with UHQ water and stored in pH 7 phosphate buffer until required.

For experiments involving approach curves only, a small volume (50µl) was deposited onto the surface and the excess rinsed off after 10 minutes. In all cases, the location of the deposited enzyme was marked by the use of a glass-cutter pen on the underside of the glass slide.

3.3.4 SECM interrogation

The patterned substrate was positioned on the SECM stage and the entire assembly levelled. 1ml of 2mM hydroquinone in pH 7 buffer was then introduced to the substrate and the three electrodes positioned within the droplet. The microelectrode tip was then set at +0.8V which

was sufficient for the oxidation of hydroquinone to benzoquinone – and an approach curve was conducted over the functionalised region. When the tip current was observed to begin to fall, the approach curve was halted and the tip retracted 1000 μm . The tip was stopped at this stage so as to prevent tip crash and any damage to the immobilised enzyme layer. 1ml of 2mM H_2O_2 was then injected into the system, resulting in a mediator solution composed of 1mM hydroquinone and 1mM H_2O_2 . After a specific period (0, 2, 4, 6, 8 or 10min), the tip was biased at -0.4V to detect the benzoquinone produced by the immobilised enzyme and an approach curve was conducted over the enzyme modified region at a rate of 10 μm per step; the tip was stopped when the approach curve profile began to fall off – i.e. when negative feedback was observed. For patterned substrates, area scans were conducted over the region of interest at a rate of 20 μm per step over areas up to 1500 μm^2 .

3.4 Imaging of cell membrane protein expression

3.4.1 Additional reagents and equipment

Cell culture media and various additives were supplied by Gibco (Invitrogen, Paisley, UK); all cell culture plastics were manufactured by Nalge Nunc (Fisher Scientific, Leicestershire, UK). All cell culture work was performed in a class II laminar flow hood (HeraSafe, Heraeus, Germany). Trizma base and sodium chloride were obtained from Sigma Aldrich.

3.4.2 Solutions used

Phosphate Buffered Saline (PBS)

PBS was made using tablets purchased from Gibco dissolved in 500ml of UHQ H₂O. PBS for cell culture was sterilised by autoclaving.

Tris buffered saline (TBS)

A 20X stock solution of TBS was prepared and diluted down for use as and when required (20 x TBS = 121.1g Trizma base, 175.3g NaCl in 1 litre H₂O).

Cell growth media

Cells were grown in McCoy media which was composed of DMEM or RPMI media (Gibco), 50mls foetal calf serum, 1ml glutamine and 200µl penicillin/streptomycin antibiotic mix.

3.4.3 Cell lines

The cells used were human RT112/84 cells (ECACC number 85061106). This cell line is a bladder line derived from a transitional cell carcinoma (TCC) of the bladder with epithelial morphology.

3.4.4 Recovery from cryogenesis

Frozen cells stored in vials in liquid nitrogen were carefully thawed by immersion in a 37°C water bath. 10ml of growth media was then slowly added drop-wise to the thawed cells over the course of five minutes. The suspension was then centrifuged (for 5min at 4000rpm) before resuspension in growth media and then transferred to culture flasks.

3.4.5 Passage (re-seeding new flasks etc)

As RT122 cells are adherent, passage required the use of Trypsin to detach the cells from the surface of the culture flasks. First, existing (used) media was removed from the cell flask and the flask rinsed with sterile PBS. 5ml of 1 x Trypsin solution was then added to each flask and incubated at 37°C for between 2-4 min or until a sufficient proportion of the cells has become detached. The trypsin/cell suspension was removed from the cell flask and placed into a 15 ml microfuge tube with 5 ml of the growth media required to deactivate the trypsin. This cell suspension was then centrifuged at 4000rpm for 5 min in a constant temperature 4°C room. The supernatant was subsequently discarded and the cells resuspended in the required volume of media and subcultured into fresh sterile culture flasks.

3.4.6 Cell growth for SECM experimentation

Cells required for interrogation by SECM were either grown in cell culture flasks, on slide flasks or on glass slides in sterile petri dishes. Slide flasks are small culture flasks with a detachable polystyrene slide as their base (Figure 3.1). Cells were introduced into these flasks and grown for one or two days until the cells were at the required level of confluence.

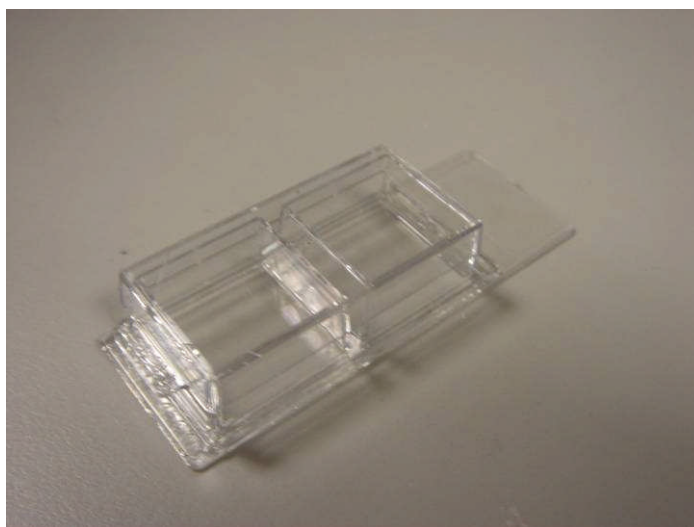


Figure 3.1: Slide flask from nunc™

3.4.7 Preparation of slides for immunocytochemistry

When cells had reached the required level of confluence, the media was removed and the slides and the flask rinsed three times with cold (4°C) PBS before detaching the slides. These slides were then placed in cold methanol for 10 min and allowed to dry, with the effect of fixing the cells to the slide surface. The slides were then either used immediately or wrapped carefully in foil and stored at -20°C until required.

3.4.8 Poly-L-Lysine coated slides

For some experiments involving the patterning of cells, poly-L-lysine was used to coat microscope slides. The polycationic nature of this polymer allows interaction with anionic sites of tissue sections, resulting in strong adhesive properties. Poly-L-lysine solution (0.1% w/v) obtained from Sigma Aldrich was diluted 1:10 with deionised water. At room temperature, clean slides were submerged into diluted poly-L-lysine for five minutes and removed. They were then either placed in an oven at 60°C for 1 hour - or allowed to dry at room temperature overnight depending on time limitations.

3.4.9 Patterning cells by cytospinning

For some experiments it was necessary to form well defined patterns of cells. This was achieved by the use of a Boeco C-28 centrifuge (Figure 3.2).

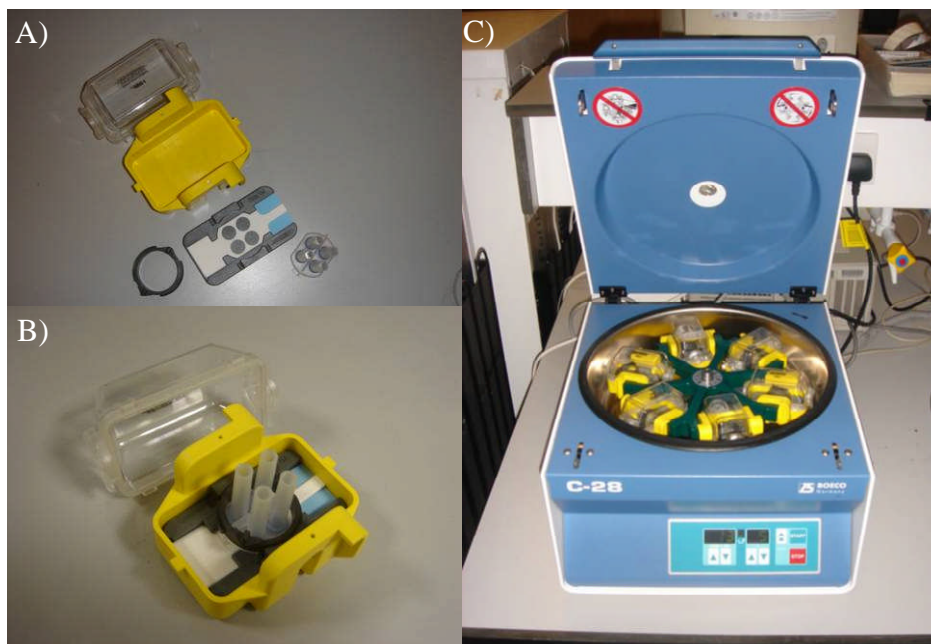


Figure 3.2: Photographs of the cell patterning assembly (A + B) and the Boeco C-28 centrifuge (C).

The parts in A) of Figure 3.2 were assembled into the arrangement in B) of Figure 3.2 and solutions containing different concentrations of cells were placed into each vertical channel. A lid was then locked onto each unit which was then placed into the centrifuge. The units, which contained a poly-L-lysine coated slide, were then centrifuged for 10 minutes at 3000rpm. Over the course of this period of time, cells in the solution would be forced down onto the poly-L-lysine slide, in a spatially defined pattern.

3.4.10 Immunocytochemistry

CD44-HRP labelling

Prepared slides were removed from -20°C storage and allowed to thaw for 10 minutes before removing the foil. When required, an ImmEdge pen (Vector Laboratories, Peterborough, UK) was then used to divide the slide into a grid conformation allowing the differential treatment of areas of the same slide.

After thawing, in order to block non-specific antibody reaction, neat goat serum (Gibco/Invitrogen, Paisley, UK) was applied to the slides which were then incubated in a humid environment for one hour.

The blocking serum was removed and dilutions (1/100,1/200,1/400) of the anti-CD44 (mouse anti-human) primary antibody in neat goat serum were applied to the cell grids. Slides were then placed in a humid atmosphere at 4°C to incubate overnight.

Slides were removed from the 4°C atmosphere and allowed to return to room temperature over 30 minutes before they were rinsed via three five minute washes. Where required, they were incubated for 10 min in a 3% solution of hydrogen peroxide (to exhaust endogenous peroxidases) followed by a further three washes in 1X TBS. Biotinylated rabbit-anti-mouse secondary anti-body was applied at a dilution (1/100) and slides were incubated at 37°C for 30 min.

Excess antibody/TBS solution was removed and the slides washed 3 times in 1X TBS before the addition of 100µl of ABC (avidin-biotin conjugate) (Dako Ltd, Cambridgeshire, UK) which was prepared in the dark 30 minutes before - as per the kit instructions. Slides were then left for 30 minutes in the dark at 37°C. The slides were then washed as before (3x5 min in 1X TBS). These were then ready for interrogation by SECM.

3.4.11 SECM Experiments

Slides were fixed onto the imaging stage and the microelectrode probe, reference and working electrodes placed above the region of interest. Depending on the area under interrogation, a sufficient volume of 2mM Hydroquinone in pH 7.1 phosphate buffer was used to submerge the cells and contain all three electrodes.

For the placement of the electrode at the correct tip to substrate distance, an approach curve was then conducted with the tip biased at 0.8V and the tip positioned where the tip current was equal to half that observed in bulk solution. When the tip had been positioned at the correct height, the same volume of 2mM hydrogen peroxide was then added to the system (making a final solution of 1mM hydroquinone and 1mM hydrogen peroxide).

After the introduction of the hydrogen peroxide, a linescan across the surface was conducted to find an area of interest. An area scan was then carried out at a specified scan rate (1,10 or 20 μ m per step) over a specified area of the substrate (e.g. 500x500 μ m).

Chapter 4

An overview of the Uniscan SECM270

4. Introduction

In all SECM experiments reported in this thesis, the scanning electrochemical microscope used was the SECM270, designed and manufactured by Uniscan Instruments Ltd. Within this short chapter, a brief overview of the SECM system is given, together with a section detailing some of the possible recommendations that may be incorporated into forthcoming instrument improvements.

User input is an essential facet of Uniscan's product development strategy. Customers and users represent an invaluable source of constructive criticism which allows for the development of products which are well aligned to the needs of the customer. By using this information, ideas for incremental and even, perhaps, disruptive innovations may be internalised for incorporation into future product developments.

4.1 Uniscan SECM270

The Uniscan SECM270 is a versatile, scanning electrochemical microscope that may be used in the modification, characterisation and interrogation of a variety of substrates on a sub-micrometer scale. The system is composed of a bi-potentiostat (two PG580R potentiostats), a precision xyz micro-positioning stage and the SECM270 control unit for motion control (Figure 4.1). Via the user interface on a connected PC, the user is able to control all experimental variables detailing the movement of the tip and the potential applied to the system.

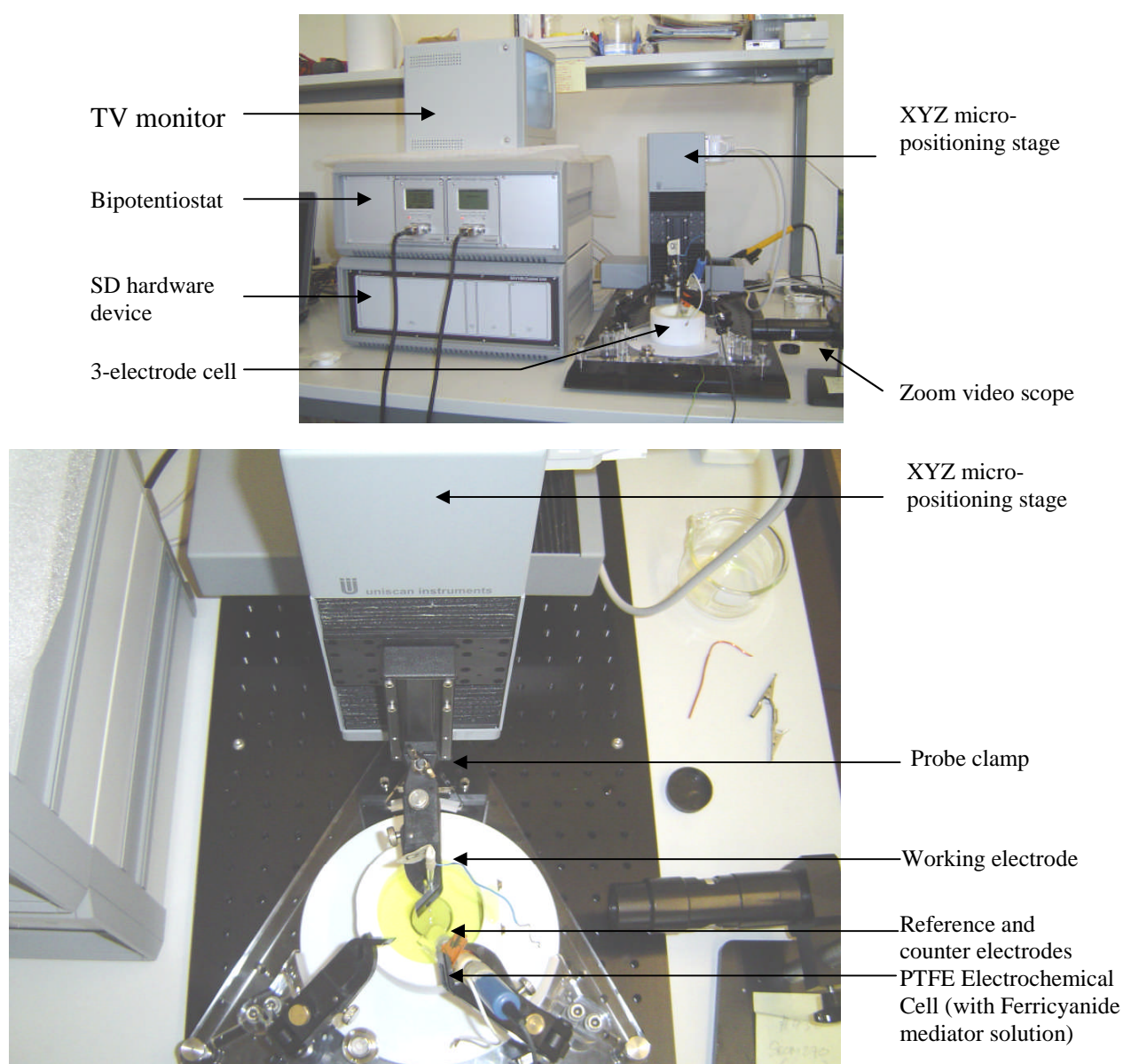


Figure 4.1: Photographs of the Uniscan SECM270 and electrochemical cell

4.1.1 Dimensions

Space is very much a premium in today's laboratory. The continual miniaturisation of the system is hence of paramount importance.

Table 4.1: Weight and dimensions of the SECM270

SECM270 Part	Weight	Dimensions
XYZ Scanning System:	17kg	350mm x 650mm x 400mm
SCV100 Hardware Device (motion control)	3kg	450mm x 320mm x 185mm
Bi-Potentiostat:	3kg	450mm x 320mm x 185mm

4.1.2 XYZ stage

The precision micropositioner in the SECM270 is composed of precision motors on fine pitch lead screws allowing a combination of speed, accuracy and excellent reproducibility (i.e. zero hysteresis). The reproducibility of a scan is an essential criterion in time-dependent work – when a scan is conducted, the user must be confident that after the required time period, the scan will be conducted over exactly the same region as the first experiment (so the experimenter may observe changes in the behaviour of the substrate over time). Each motor on each axis has a resolution of 100nm and is capable of scanning at a rate of 2mm per second. One of the most attractive aspects of the SECM technique and indeed, the Uniscan SECM270 in particular, is that images or scans may be acquired over relatively large distances; the maximum scan range of this instrument is 70mm in all X, Y and Z dimensions. By the use of linear encoders, the user is fully aware of the position of the probe at all times via a readout of the sensor position given in the toolbar of the user interface.

4.1.3 Probe clamp

The probe clamp is the point of contact between the XYZ stage and the microelectrode probe; as such, it must provide a firm point of contact without risking damaging the probe while providing a reproducible positioning mechanism. In SECM experiments, the tip is translated in all X, Y and Z axes. During this movement, it is essential that there is no movement of the tip due to creep or slippage at the fixing point in the clamp. An exploded schematic of the clamp used in this study is given below (Figure 4.2). The number of connection points and rotational joints in this assembly means that there is quite a lot of movement when inserting the probe and movement in this region during scanning may introduce the risk of variation in tip current not attributable to variations in substrate activity or topography. It is hence suggested that this clamping mechanism be replaced by a single, one piece unit.

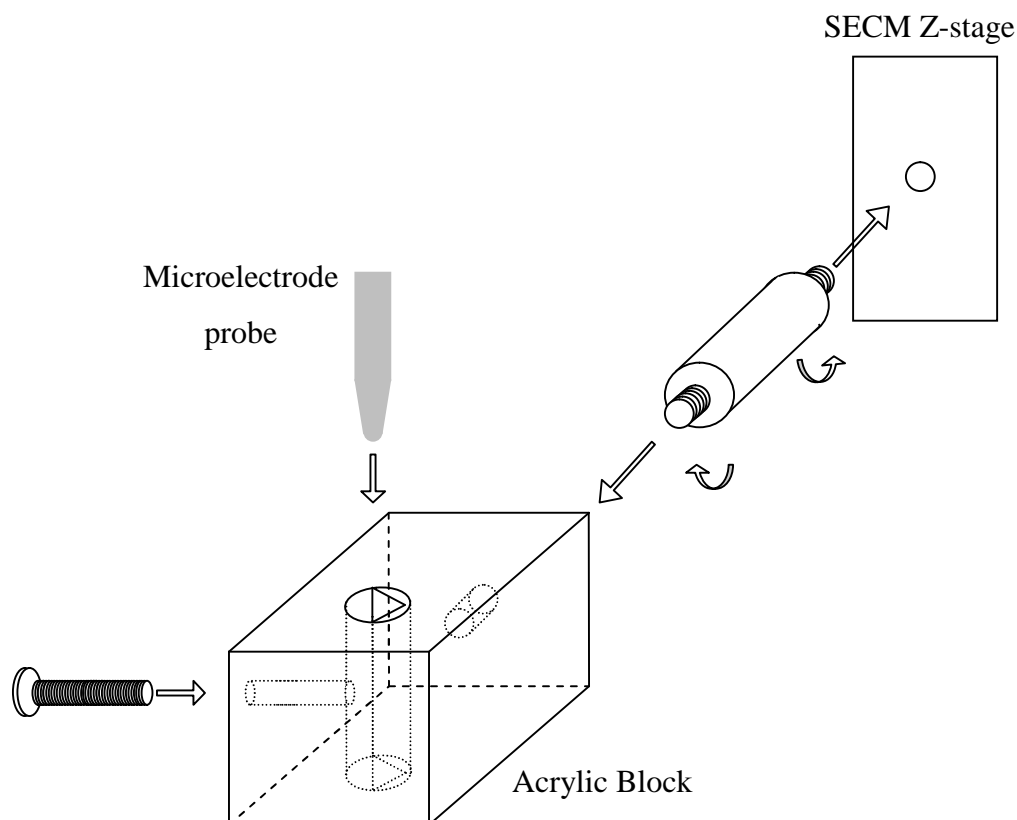


Figure 4.2: Exploded schematic of the microelectrode probe clamping mechanism

4.1.4 Potentiostats

Two Uniscan PG580R potentiostats are incorporated into the Uniscan SECM270. This allows the experimenter flexibility in their experimental design and allows scope for the use of the instrument for interrogating biased substrates. Via the PC interface and by direct, manual control, the user may specify the electrochemical parameters of the experiment. As currents measured at microelectrodes are very small in comparison to those measured at larger, planar electrodes used in more general electrochemical experiments, the PG580s have been designed with relatively low limits, with a maximum current of just $\pm 10\text{mA}$ and a potential range of $\pm 2\text{V}$ for both potentiostats (i.e. substrate and probe potentiostats). Whilst this may allow the measurement of small currents with relatively high resolution, it does limit the flexibility of the system. For instance, if the user wished to modify a planar electrode or set it at a particularly high potential for subsequent interrogation by the SECM, they may be limited in what they can do by the potential and current range of the system.

Prior to running an experiment, the user may set the experimental parameters and adjust potentiostat settings. With respect to the latter, this concerns setting the default, initial potential and the current range – the range across which the system will record the current passing at the working electrode, which may be between 1nA and 10mA . If the experiment is conducted and the current arising at the tip exceeds the specified current range however, the system does not readjust and will not record any data past the upper and lower limits of the range. It is hence suggested that an additional functionality be added that allows the step-wise change of the current range in accordance to the current measured at the electrode as the experiment progresses.

4.1.5 Software

The user interface software is Uniscans Windows based control and analysis software. The interface is highly intuitive and the user can be conducting experiments almost immediately. Whilst the interface is perfectly effective for specifying experiment type, experimental parameters, potentiostat settings and probe position, the utility the software offers the user in terms of post-data acquisition analysis is very limited. Whilst the user is provided with IsoPlot software which allows them to produce aesthetically pleasing images with shading

and colour manipulation tools, it provides little value in terms of allowing the user to leverage any additional information from the data – i.e. there are no statistical analysis tools. Ideally the user would have the option to directly extract statistical information from the experimental data, possibly with smoothing and background subtraction functions. Additionally, the option to conduct experimental simulations would be useful – for example, to estimate Rg ratios and active electrode areas (see chapter 5).

4.1.6 Tip Positioning and microscope

The SECM270 is supplied with a video microscope and TV which aids the user in tip positioning prior to conducting an SECM experiment. A problem with this approach is that not only is valuable space taken up by this additional equipment, but also the user has to monitor two different screens. It is hence suggested that there is some integration between the SECM user interface and the video capture software which allows simultaneous monitoring of both tip current and the physical positioning of the probe.

A further possibility is the addition of an inverted microscope to the system. Placed underneath the stage, the microscope would relay an image which would give direct information as to the positioning of the tip with respect to the X and Y axes (Figure 4.3). This would be particularly useful in the study of cells and other functionalised transparent substrates.

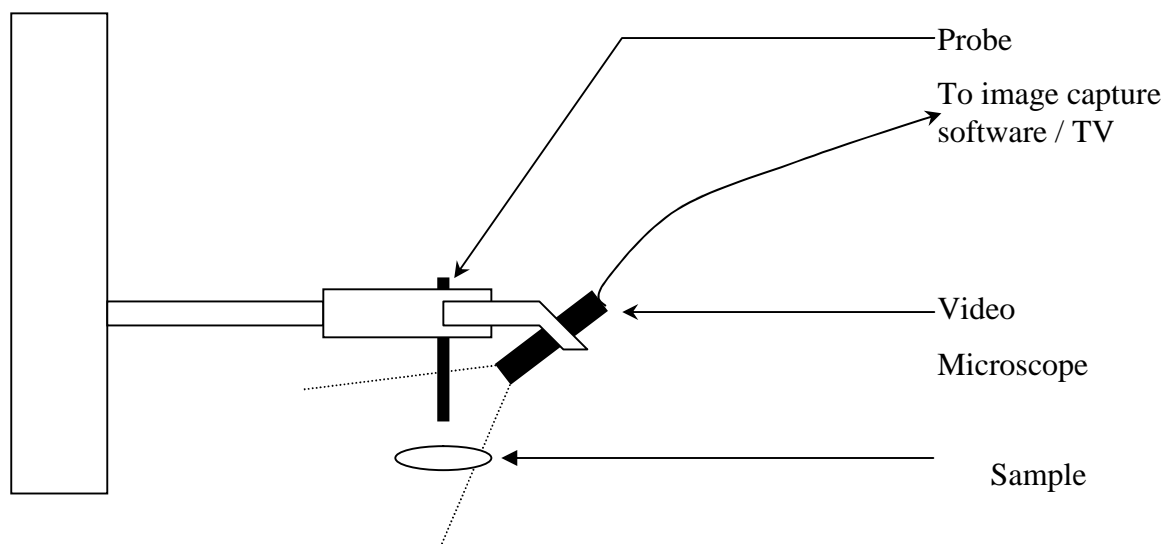
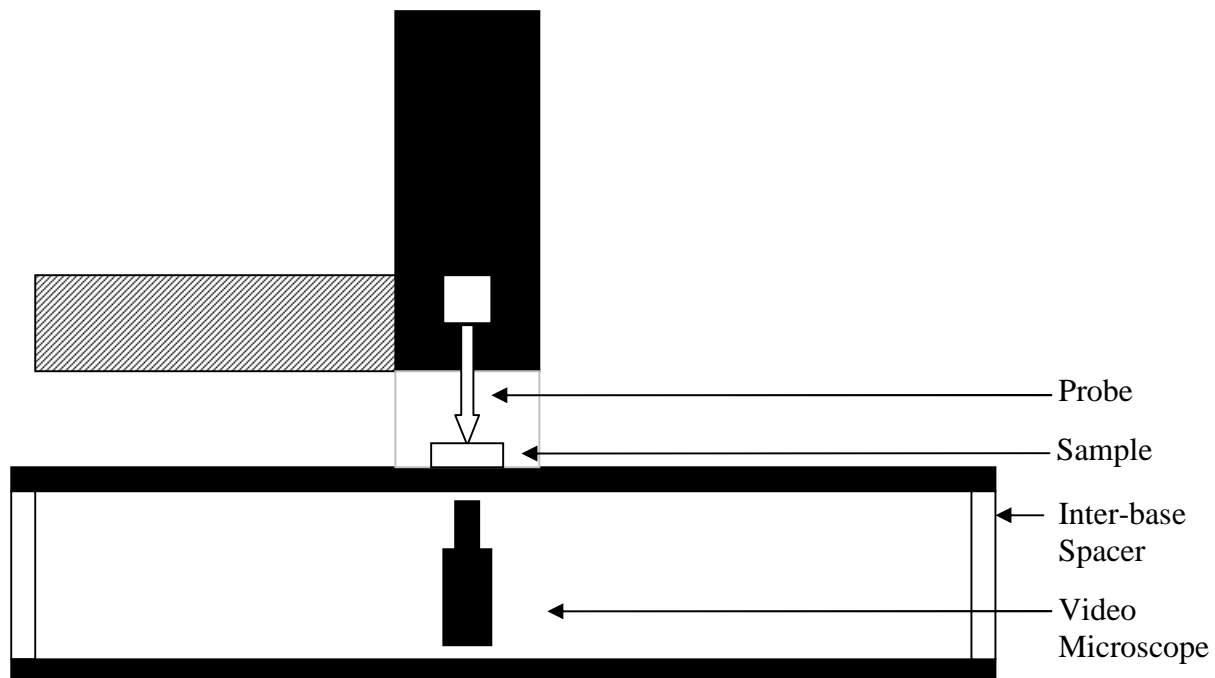


Figure 4.3: Possible alternative video microscope camera configurations

4.2 Experiment capabilities

The SECM is capable of a wide variety of electrochemical experiments. Relating to SECM specifically, the user may conduct line scans, approach curves and area scans. Recent additions also include a sloping scan macro. Outside SECM applications, the user may conduct a number of other, general electrochemical experiments including cyclic voltammetry, chronoamperometry, chronopotentiometry, square-wave voltammetry, normal pulse voltammetry and differential pulse voltammetry.

4.2.1 Approach curve macro

To conduct an approach curve, the user stipulates the distance of the scan, tip potential and the step size required. However, in order to avoid tip crash, it is necessary for the user to continually monitor the tip current and to halt the experiment manually. A recommendation is hence to develop a functionality which allows the user to stipulate a particular current value or at a specific i_{∞} / i_T value at which the approach curve should be halted.

Following on from this, it is suggested that the area scan macro should be developed to incorporate an approach curve function. In this proposed function, prior to each area scan experiment, an approach curve is automatically conducted which allows the tip to be positioned at the required tip to substrate distance, so minimising set-up time.

4.2.2 Area scan

In an SECM area scan, the microelectrode tip is translated across a substrate of interest to generate a map of the electrochemical activity or topography of a specified area of that substrate. In the SECM270, the tip is moved repeatedly from left to right in the X axis and moved incrementally in the Y axis after each sweep (Figure 4.4(A +B)). After each linescan, the potential applied to the tip is switched off, the tip repositioned on the left hand side of the scan area (recovery sweep) and the potential re-applied for another scan. This can have the effect of creating a high current area on the left hand side of the area scan due to the brief occurrence of a charging current. It is hence suggested that as opposed to having this

‘recovery sweep’ where the probe is switched off, the potential of the probe is maintained and the scan is conducted as depicted in Figure 4.4(C).

This new scanning path would not only reduce the time required to conduct a scan, but it would also minimise the disturbance to any diffusion fields emanating from the surface. Additionally, it may extend the lifetime of the micropositioning device by minimising the distance travelled in each experiment.

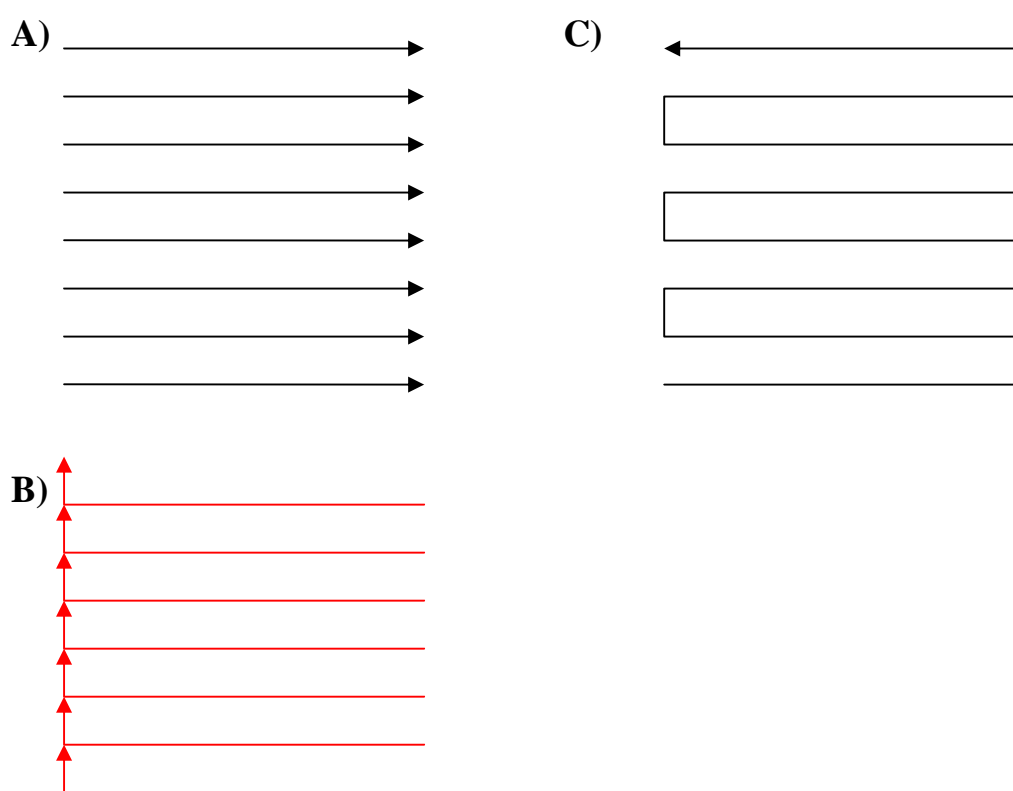


Figure 4.4: Schematic diagrams depicting the movement of the microelectrode probe during an area scan. A) and B) are the scanning and tip recovery paths respectively and C) is the new, proposed scanning path which has no recovery phase

4.2.3 Sloping Scan macro

A recurring problem with the SECM approach is the difficulty in differentiating variation in tip current due to variations in topography and those due to variation in the electrochemical properties of the surface. Different options that may be considered to address this are discussed later, but a partial solution is presented in the sloping scan macro. This macro allows the user to conduct an area scan over a sloped but topographically flat substrate; in doing so, any variation in current due to the slope of the substrate is accounted for, preventing such variation from masking the signal current. First, the slope of the substrate in the X and Y axes is calculated by conducting approach curves 1000 μm from the origin in both the X and Y dimensions as in Figure 4.5.

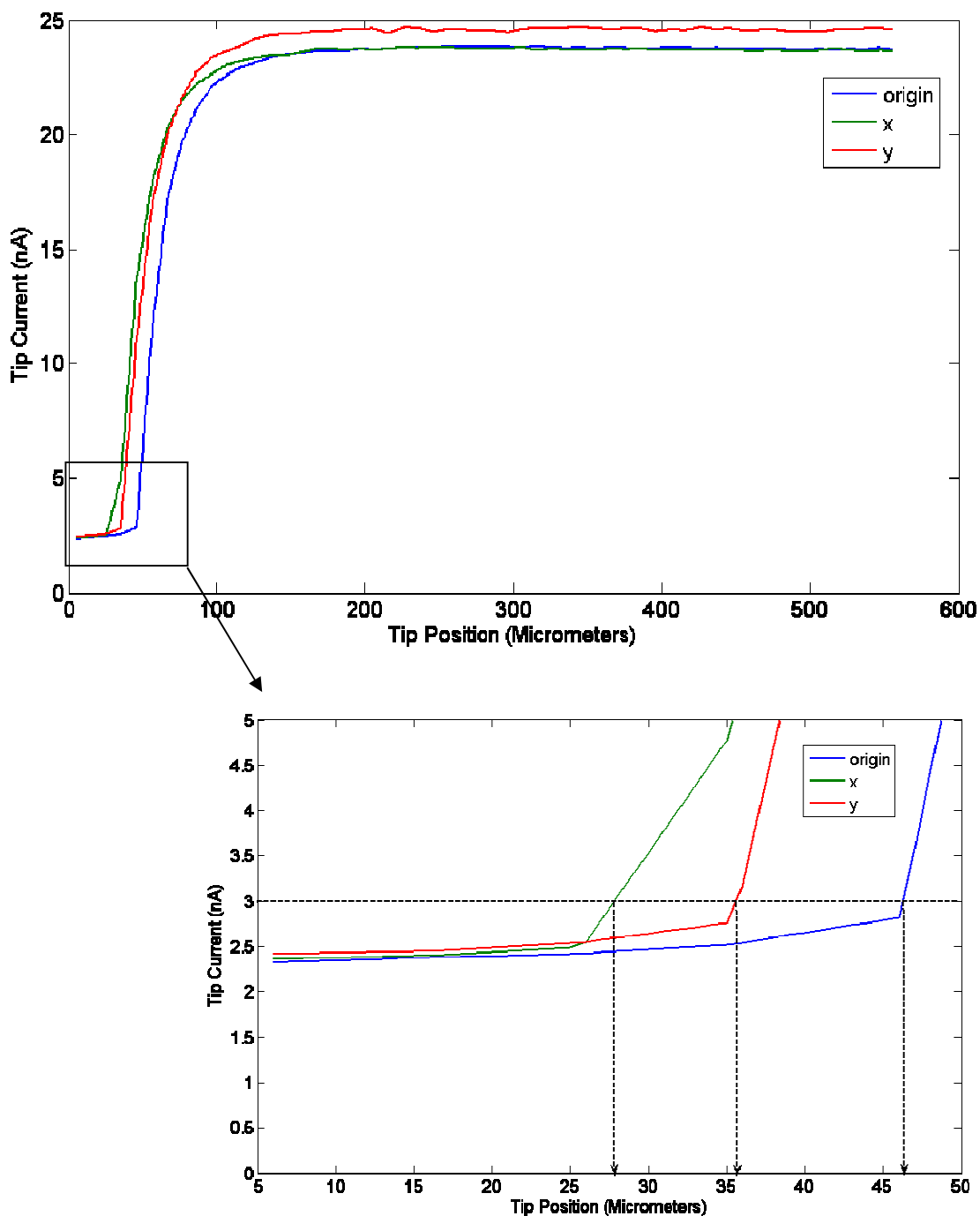


Figure 4.5: Series of approach curves detailing how substrate slope may be calculated

By calculating the point at which a specific current value is reached, the tip to substrate distance may be estimated; from this, the slope in X and Y may then be calculated by trigonometric methods. These values were then input into the macro and the scan conducted, whereby the microelectrode probe was moved in the respective direction in the Z plane with movement along the X or Y axis. The effectiveness of this technique in eliminating substrate slope is demonstrated below (Figure 4.6).

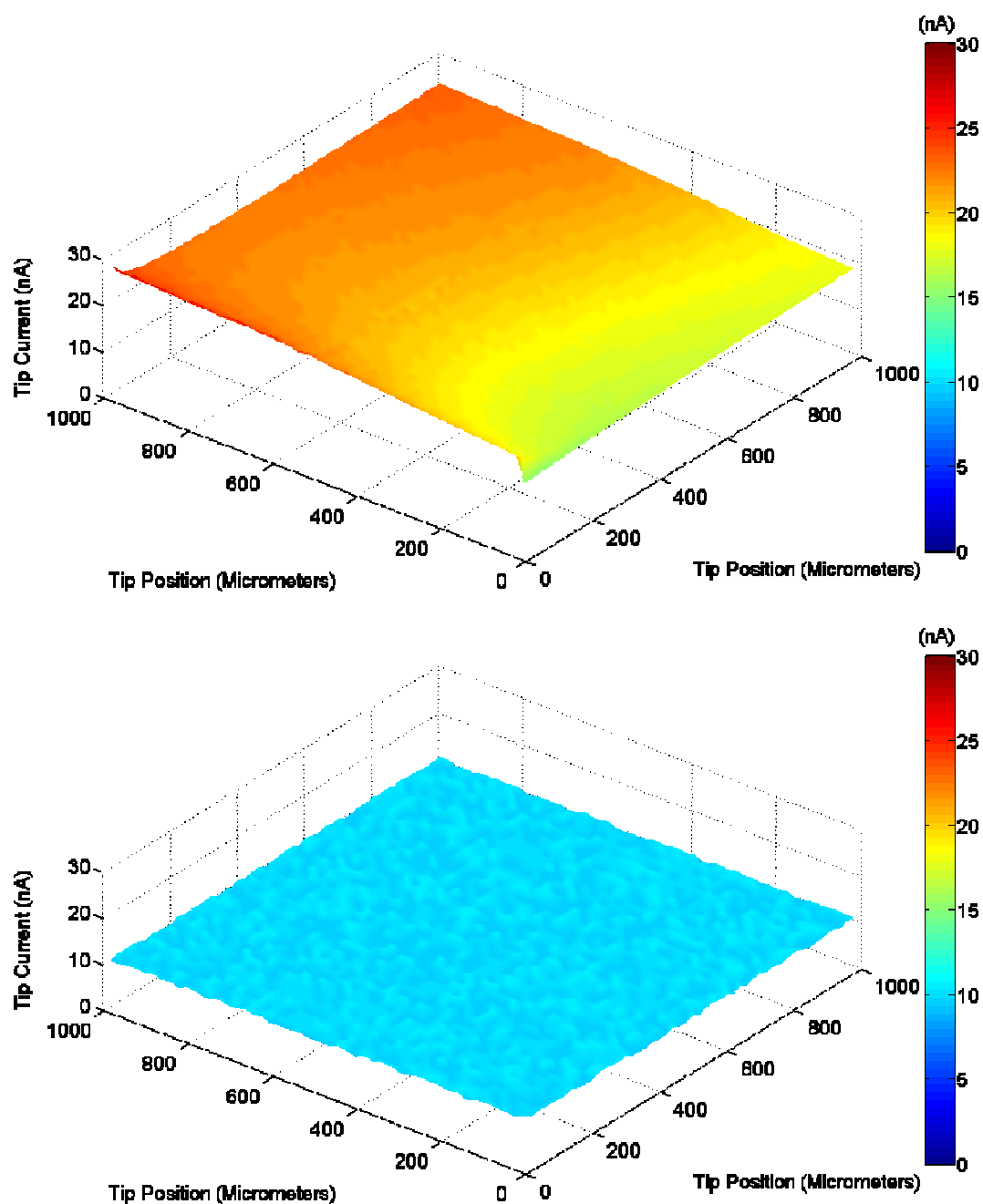


Figure 4.6: Area scan over sloped glass substrate using the area scan macro (A) and the sloping scan macro (B)

4.2.4 Repetitive Scans

A key advantage of SECM is that it may be used to investigate changes in living systems. It follows that the system may be used to monitor temporal changes in biological systems. For example, in experiments monitoring the oxygen consumption (respiration rate) of living cells with exposure to an environmental stimulant, the user may want area scans to be conducted at specific time intervals, or to be repeated several times so they may compare changes at the substrate level over a period of time. It is hence suggested that the SECM270 incorporates a temporal function which allows the user to conduct experiments at specific time intervals over a specified period.

4.3 Constant distance imaging

A recurring problem in SECM imaging is that changes observed in tip current may be attributable to one of two factors – changes in the topography of the surface, which causes negative or positive feedback, or changes in the nature or properties of the surface. Such devices have been constructed, but have been done so by individuals in university and laboratory environments – no system with such capabilities is currently in the commercial domain. Delivering a constant distance SECM to market would be a significant strategic step for Uniscan.

In order for one to make accurate inferences with regards to the physiochemical properties of a surface, one must know the tip-substrate distance to allow the differentiation of current due to changes in topography from changes in the local electrochemical reactivity - i.e. a constant distance mode needs to be in place. In such a mode, the tip is moved in the Z-plane as it is translated across the surface in the X and Y direction, maintaining a constant distance from the area of the substrate under interrogation. Several such constant distance modes have been developed.

One system is based on a feedback mechanism which relies on the detection of shear forces occurring between a vibrating UME and the sample surface. Here, the specially designed UME is vibrated at a resonant frequency using a piezo electric tube for agitation ('tuning fork feedback'). A laser focussed on the tip then generates a fresnel diffraction pattern which is

projected onto split photodiodes. The closer the UME is to the surface, the greater the vibrations are dampened by the increasing shear forces. It has been shown that such feedback allows distance regulation of the order of 10nm. By attaining such small sample to probe separation distances, higher resolution images were made possible (Buchler, et al 2000).

The problem with such an optical approach is that the operator is confined to special electrochemical chambers and transparent solutions. In heed of this, a non-optical shear-force based detection scheme was developed where the detection of the shear force is accomplished by mechanically attaching a set of two piezo electric plates to the scanning probe – one vibrates the SECM tip, causing it to resonate, whilst the other detects the amplitude of tip oscillation (Katemann, 2003). Increasing shear forces in close proximity to the sample surface lead to a damping of the vibration amplitude and a phase shift, effects that are registered by connecting the second plate to a dual-phase analogue lock-in amplifier. The shear force and hence distance-dependent signal of the lock-in amplifier is used to establish an efficient, computer-controlled closed feedback loop enabling SECM imaging in a constant-distance mode of operation. An additional technique is that of Lee et al, who integrated scanning optical microscopy and SECM whilst using both tip current and shear force to maintain a constant tip to substrate distance (Lee et al 2002).

A more advanced system, described by Kranz et al (2001 and 2004) involves the integration of a microelectrode into a standard AFM tip, allowing the electroactive area to be scanned at an exactly defined tip to substrate distance. This allows the complete separation of topographical and electrochemical information. The problem with this approach however, is the generation of frictional forces at the sample surface. These were overcome however by an elegant system developed by Kueng et al (2003) which uses SECM-AFM cantilevers oscillated at their resonance frequency. However, whilst the combination of AFM and SECM affords the generation of higher resolution images, the system is unable to scan the large areas that the SECM device is capable of, which may be of the order of several mm².

A further alternative involves the use of impedimetric techniques (Alpuche-Aviles *et al* 2001). The approach is based on the principle that the impedance between the SECM tip and auxiliary electrode varies as a function of the distance between the scanning probe and the

sample, much like current varies when conducting approach curves over insulating or conducting surfaces with a DC current. The central idea is as follows: the UME is biased at a high frequency potential which causes a small ac current to flow through the solution between the tip and substrate and the amount of current depends on the impedance of the solution in the gap, providing information about the tip to substrate distance which is then translated to a feedback controller which modulates the tip-substrate distance. The tip impedance is monitored by the application of a high frequency ac voltage bias between the tip and auxiliary electrode and is separated from the DC-level faradaic current electrochemistry by the use of an RC filter which allows impedance measurements during feedback or generation/collection mode. Alpuche-Aviles *et al* (2001) demonstrate that it is possible to simultaneously measure impedance and the faradaic current so as to allow the collection of orthogonal topographic and electrochemical properties of the surface by multiplexing the two components and then separating them later.

4.4 Conclusions

A major objective of this research project was to give feedback to Uniscan Instruments Ltd on their SECM system, the SECM270. By combining insights obtained by the use of the SECM270 over the course of this project and through the analysis of the capabilities of a competing SECM system, a number of suggestions were made as to how Uniscan may focus product development.

In summary, these are as follows:

1. Work towards the miniaturisation of the scanning head and table.
2. Develop an approach curve function to incorporate current / ratio searching function.
3. Develop an accurate levelling mechanism, ensuring no creep or non-powered movement of axes.
4. Eliminate 'recovery sweep' and alter scanning path.
5. Incorporate an inverted microscope to aid tip positioning.
6. Incorporate smoothing and simulation functions and data visualisation tools into user interface.
7. Develop a constant distance imaging mechanism.

Chapter 5

The development of a microelectrode fabrication protocol

5. The development of a microelectrode fabrication protocol

5.1 Introduction

The quality of the microelectrode used is a key parameter in any SECM study. A poorly constructed probe will impact on the spatial resolution of an area scan, the signal to noise ratio and may have implications for the reproducibility of the experiment. The development of a robust methodology for the fabrication of high quality probes which exhibit reproducible electrochemical behaviours is therefore of paramount importance. The subsequent characterisation of microelectrodes following fabrication is hence an essential step and by conducting a variety of electrochemical approaches it is possible to determine whether an individual electrode exhibits good microelectrode behaviour (i.e. as close as possible to 'ideal' with respect to behaviour as predicted by microelectrode theory). Approaches such as these also allow the quantification of the area of the active electrode and the thickness of the insulating sheath in which it is embedded.

The development of a robust, reproducible methodology for the fabrication of high quality microelectrodes with well characterised dimensions was also of significant importance to Uniscan Instruments Limited. The electrodes available from commercial suppliers were found to be of variable quality as well as being expensive. Uniscan wished to supply in-house microelectrodes to customers purchasing the SECM270 and by supplying high quality electrodes with reproducible electrochemical behaviour, the performance of the instrument could be demonstrated.

Within this chapter, a brief critique of current electrode suppliers' electrodes is given, followed by several different methods developed for the fabrication of the microdisk electrodes employed in this work. The techniques employed in the characterisation of these electrodes will then be presented.

5.2 A review of commercially available electrodes

Some of the problems experienced with commercially available electrodes are briefly explained below and these include poor construction, large Rg ratios and fragility.

5.2.1 Rg Ratio

The Rg ratio may be defined as the ratio between the radius of the active electrode area and the radius of the insulating sheath surround and is an essential consideration in microelectrode fabrication. High Rg ratios were a recurring problem we encountered. For negative or positive feedback to be observed on approaching a surface, the microelectrode tip must be positioned within one radius of the effective electrode from the substrate. If the Rg ratio is too large, the likelihood of tip crash is increased. It is hence of paramount importance that the electrode produced has as small an Rg ratio as possible.

As can be seen from the optical micrographs of a 25 μ m electrode below, in some cases the Rg value was in excess of 20 (Figure 5.1).

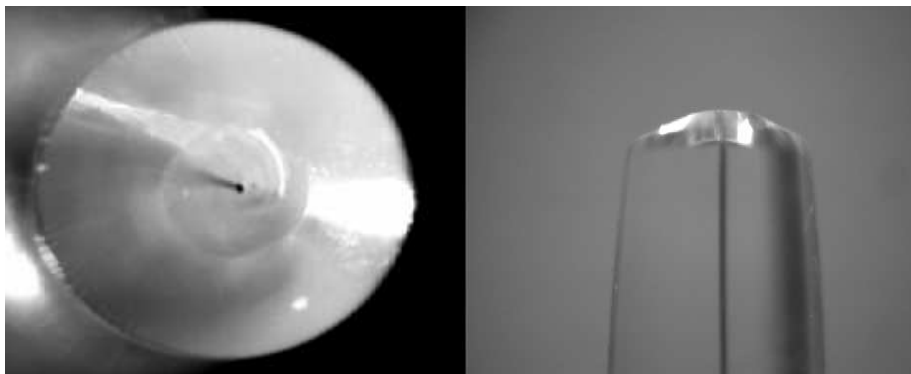


Figure 5.1: Optical micrograph of a 25 μ m microelectrode. Rg ratio >20. (Microelectrode is sample from Ultramicroelectrodes Inc.)

5.2.2 Electrode robustness

Following consultation with Uniscan Instruments, it was revealed that a key user requirement was that the electrode should be highly robust. When customers were learning the SECM technique and conducting their first SECM experiments, many did not feel confident using small, fragile probes and needed a more robust solution.

Many current product offerings, whilst offering the small electrode areas and the small Rg ratio, were often very fragile. The example given below is an example of a 5 μ m microelectrode with an Rg ratio of 10 (Figure 5.2). Whilst this electrode offered the small Rg ratio required, its overall construction was not particularly robust and a small misjudgement during an area scan or approach curve often resulted in a broken probe. During testing, these probes also suffered badly from poor electrical connection – on testing, just one of the three probes tested gave any response. Their fragility also raised questions about the ease with which they could be polished and their day to day usability. The lack of suitability of this probe for SECM applications was perhaps a consequence of the manufacturers focus on the application of electrodes to neurophysiology and their failure to take into account key criteria required by SECM users.



Figure 5.2: Optical micrograph of commercially available electrode from Thomas Recording GmbH

5.2.3 Build quality and encapsulation

In the majority of cases, the electroactive area of the microelectrode was embedded in an insulating sheath of borosilicate glass. However, one manufacturer produced electrodes using epoxy as the insulating material (Sycopel Ltd) (Figure 5.3). The resulting product was poorly constructed, with a poorly defined active area. The disk was not well embedded in the substrate, resulting in a non-disk conformation and an indeterminable surface area. None of the probes supplied exhibited microelectrode behaviour and were hence of no use to SECM applications.



Figure 5.3: Optical Micrograph of 30 μ m probe fabricated by Sycopel International

5.3 Performance Comparison

In order to effectively compare these electrodes and identify the areas for development, each of the commercially available electrodes were subsequently scored from 0-10 on seven criteria – rg ratio, microelectrode behaviour, robustness, build quality, suitability to the clamping mechanism on the SECM, electrode geometry and cost (Figure 5.4).

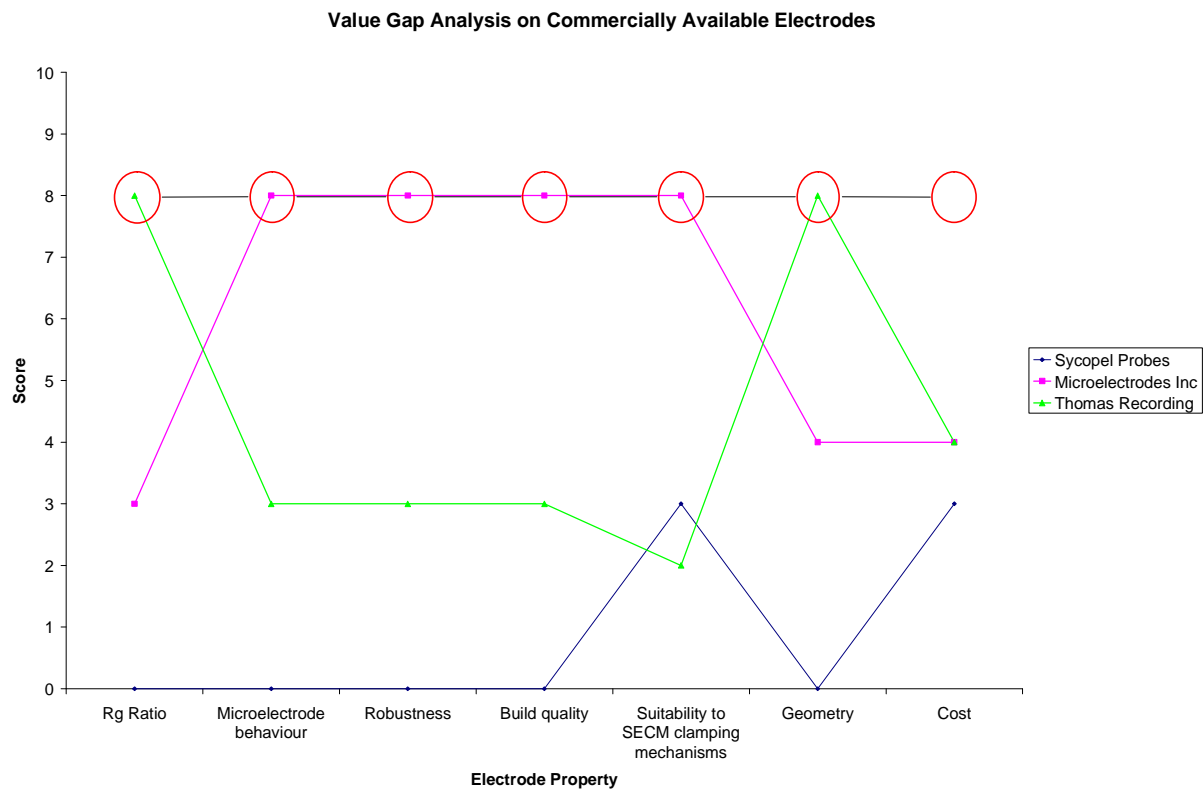


Figure 5.4: Value gap analysis for commercially available electrodes and in-house electrodes

Observing the results of this simple analysis it is observed that electrodes do score well, but in different categories; it hence follows that an electrode needs to be developed that scores highly for all criteria, taking aspects of each design and incorporating it into a single model - the value path of which is illustrated on the graph above (red circles).

5.4 Fabrication of microelectrode probes for SECM

In this section, methods are described for the fabrication of embedded disk microelectrodes suitable for use with the Uniscan SECM 270. The aim of this area of work was to develop a standard, well characterised method for the construction of robust electrodes with a small Rg ratio and excellent geometry which reproducibly exhibit microelectrode behaviour in accordance with microelectrode theory. The fabrication of electrodes using platinum wire and platinum quartz fibres will be described followed by a description methods employed in their characterisation.

5.4.1 Equipment

Pipette pulling and microelectrode polishing described below were achieved by the use of a Narashige pipette puller and a Narashige microgrinder.

5.4.2 Method

A glass capillary (2.0mm O.D x 1.16mm I.D) was pulled with ~250g weight whilst being heated at 99.8°C at its midsection using the pipette puller. On reaching the point at which the capillary is plastic and may be pulled, the descending weight is allowed to pull the capillary to the end of its axis of travel. The weight is lowered and not allowed to fall. The resulting (upper half) capillary section appears as in Figure 5.5.

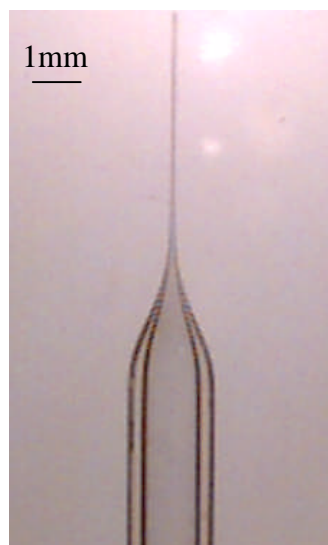


Figure 5.5: Optical Micrograph of a pulled capillary

Platinum wire inlaid disk

Fine platinum wires of the desired thickness (10-100 μ m) were placed in to the lumen of the pulled capillary which was then re-inserted into the nichrome wire coil. On heating, a vacuum was applied to the open end of the capillary to draw the heated glass around the platinum wire, encapsulating the platinum in the insulating glass sheath. The electrode was then inspected to ensure the wire was completely sealed.

Following sealing, the microelectrode was polished using silicon paper of a progressively finer grade to reveal the conductive surface. To ensure a square finish, and where required, to fabricate a bevelled tip and lower the Rg ratio, the Narashige microgrinder was used. This allowed a controlled polishing of the microelectrode tip whilst under close observation. Depending on the size of the electrode, lapping paper may have been used to complete the polishing process.

Electrical connection was made using iridium (heated until molten using a heat gun) or silver conductive paint to connect the Pt wire to a Cu multi-core wire. Using quick setting epoxy resin, the open end of the capillary was subsequently sealed.

Platinum-quartz fibre electrodes

Platinum quartz fibres were obtained from Thomas Recording GmbH. The Platinum core is accurately centred in the quartz fibre, offering excellent geometry and reducing the necessity for bevelling and polishing to produce an electrode with the required positioning (Figure 5.6).

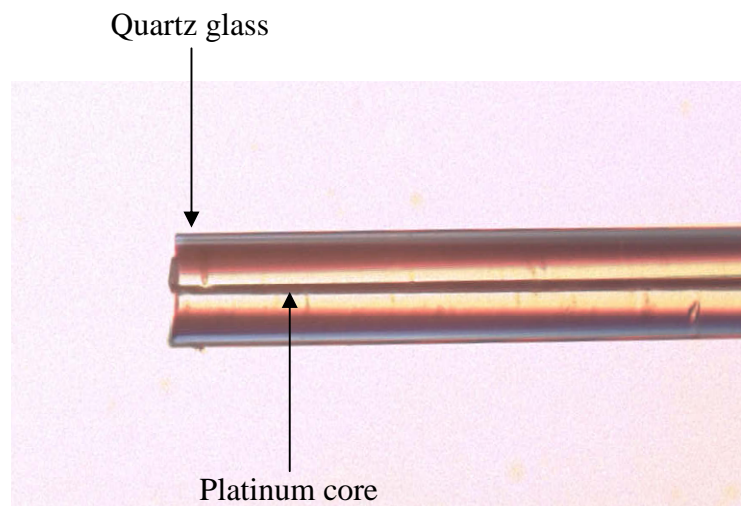


Figure 5.6: Platinum quartz fibre with 5micron diameter platinum core

The platinum fibre is cut to a length of approximately 5-10mm and placed into a pulled capillary. The capillary is then gently tapped to allow the fibre to move down to the tip and into the finely drawn out section of the capillary. The capillary should be pulled so that the thickness of the capillary is minimal (so as not to increase the Rg ratio) with the pulled region of the probe being as short as possible – i.e. the probe is robust. This point actually represents a significant compromise - between Rg ratio and robustness.

A mark is then made at the furthest point along the tip where the fibre reaches (Figure 5.7). The fibre is then removed so as to allow the tip to be cut to length and polished as far as possible before sealing and polishing the tip. This is to minimise the risk of damaging the fibre at this early stage of fabrication.

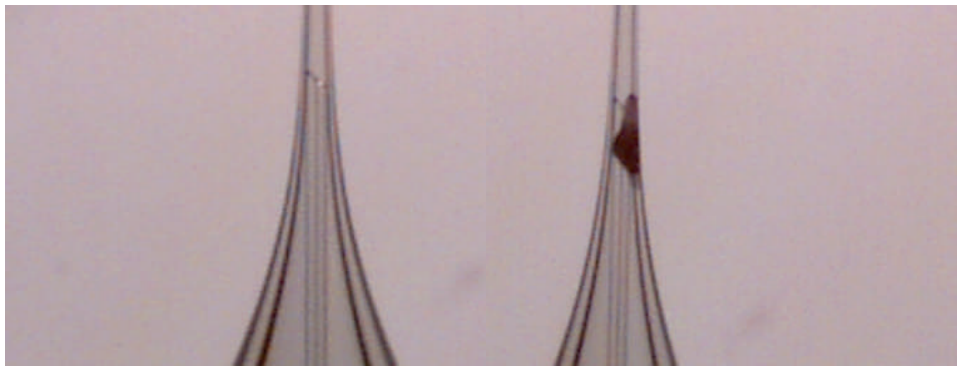


Figure 5.7: Optical micrograph of pulled capillary with Pt-quartz fibre

Additionally, by reducing the length of the ‘excess’ section of the capillary before heating and the application of a vacuum, the geometry of the electrode after sealing is improved. This also prevents the formation of a ‘teardrop’ tip. Once this is achieved, the tip is then taken and the fibre sealed in the borosilicate glass by the application of a vacuum to the inside of the capillary during heating.

The next step involves making an electrical connection between the embedded Pt fibre and the electrical lead. This represented a significant problem as it was found to be exceptionally difficult to achieve a successful electric connection with the Pt quartz fibre due to the very small conductive area at the end of the fibre. The first approach, which involved syringing mercury into the lumen of the capillary, achieved this, but the weight and corrosive nature of the mercury often damaged the fibre, resulting in unreliable and often poor electrical connections Figure 5.8.



Figure 5.8: Platinum-quartz fibre-mercury junction in lumen of capillary

The second approach, which achieved some success, involved coating the internal walls of the capillary and the Pt-quartz fibre with silver by the Tollens reaction. Ammoniacal silver nitrate ($[\text{Ag}(\text{NH}_3)_2]^+$) was mixed with a small quantity of glucose solution and the resultant solution injected into the lumen of the capillary and gently heated with a heat gun. After approximately five minutes the lumen of the entire assembly was coated with silver as a consequence of the reduction of the ammoniacal silver nitrate by the glucose. Subsequent electrical connection was normally successful, but the quality of the connection quickly deteriorated – as a consequence of the various chemically and electrochemically active species present in the lumen of the capillary.

An alternative approach was subsequently developed which involved the use of silver conductive paint. First, the Pt quartz fibre was fixed to a multicore wire with epoxy, taking care to keep the conductive end revealed. Then, the entire assembly was covered with conductive silver paint. This fibre-wire assembly was then placed into the lumen of the capillary, heat sealed and the entire assembly fixed with epoxy (Figure 5.9).

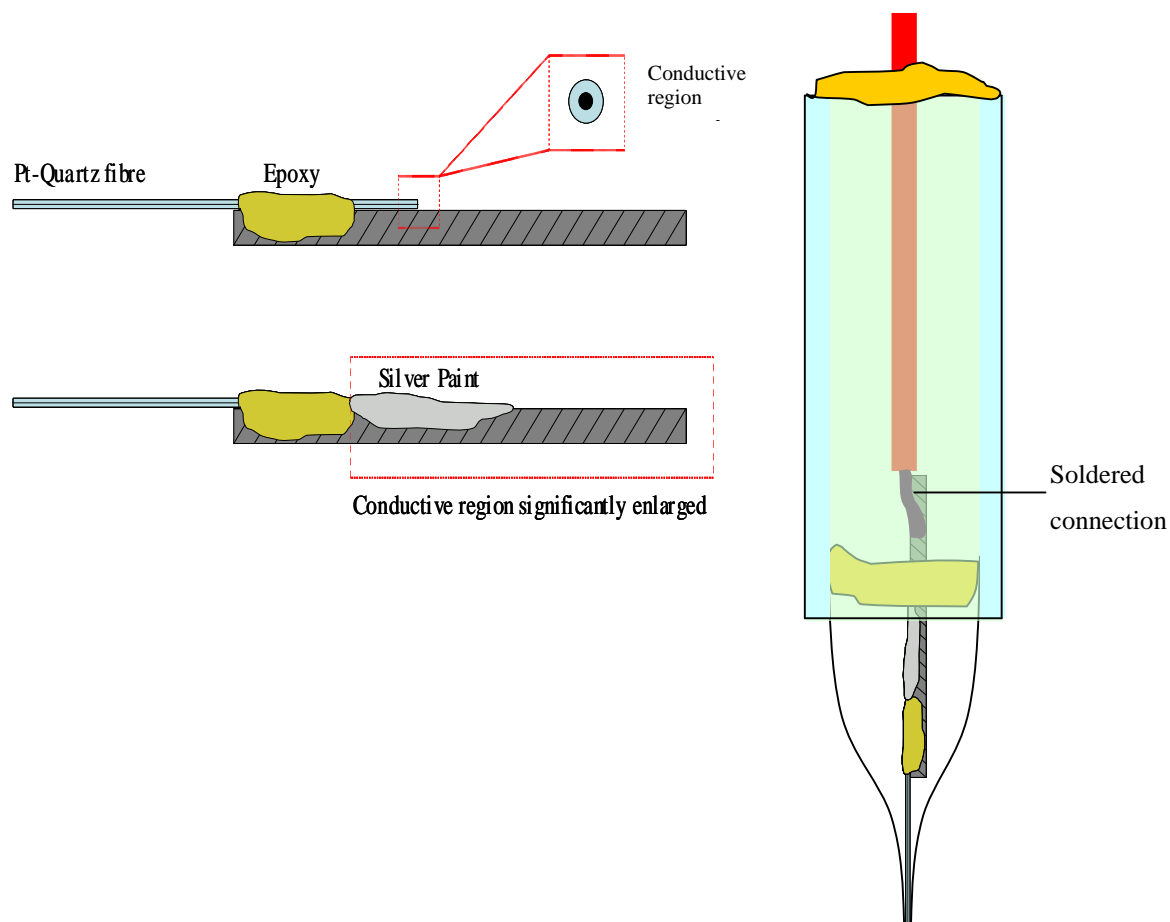


Figure 5.9: Schematic diagram illustrating the use of silver conductive paint to enhance contact between Pt quartz fibre and electrical lead

An electrical connection was then made by soldering the section to a multicore wire and the completed article was placed within a larger-bored capillary. This has the effect of increasing the robustness of the electrode and reducing risk of damage during clamping in the SECM stage or transit.

5.5 Microelectrode characterisation

Following fabrication, microelectrodes were characterised by cyclic voltammetry and their Rg ratios calculated by both measurement and comparison with simulated negative feedback approach curves.

5.5.1 Optical Microscopy

To ensure the microelectrodes produced had the desired geometries (i.e. active embedded disk centrally located in insulating glass sheath), optical micrographs were taken using Video Capture software (as in Figure 5.10 and 5.11). If the disk was found to be non-centrally positioned, it was polished further to obtain the required geometry. If the microelectrode is not directly in the centre of the insulating substrate in which it is embedded, the resulting mass flow of the mediator solution in a horizontal direction *may* contribute to an additional current component.

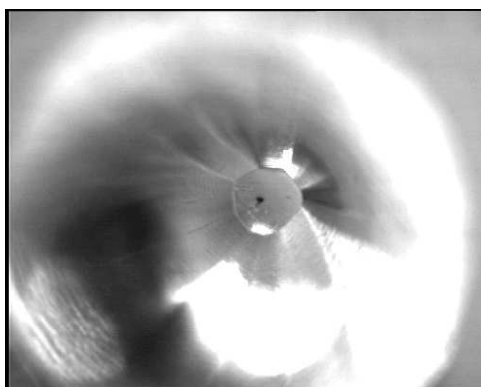


Figure 5.10: Optical micrograph of a 10 µm Pt microdisk electrode

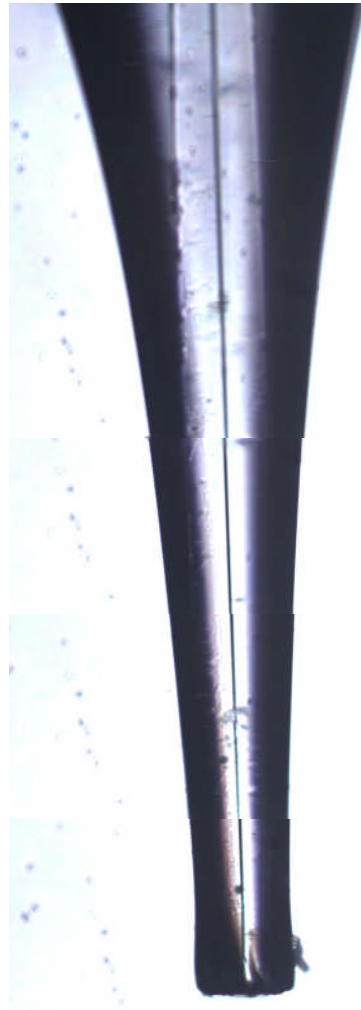


Figure 5.11: Optical micrograph of 5µm probe tip. Image demonstrates highly central position of platinum core in pulled capillary

5.5.2 Cyclic Voltammetry

Cyclic voltammograms represent one of the simplest electrochemical techniques that can be employed for the characterisation of electrochemical processes (Bollo, 2003; Cannes, 2003).

Cyclic voltammograms were conducted at a series of scan rates using a variety of different mediators at different concentrations with the aim of comparing the microelectrodes' behaviour with that theoretically expected. Mediators used include ferricyanide, hexamine ruthenium chloride and ferrocenecarboxylic acid. Representative cyclic voltammograms are given in Figure 5.12.

As the current measured at an electrode is a function of its area, the current measured at a microelectrode is significantly lower than that at a conventional macroelectrode (often nanoamps or below). By virtue of passing minute currents, microelectrodes induce very little electrolysis in solution. As a result, the diffusion layer associated with microelectrodes is very thin, (in the order of micrometers) meaning that the concentration gradient induced across them is correspondingly very high. Consequently, the rate of mass transport, namely diffusion, to the microelectrode is much greater than for macroelectrodes, leading to an absence of the 'diffusion limited' peak in the oxidation phase of the cyclic voltammogram for the microelectrode. It is this difference that allows one to make inferences concerning the quality of a microelectrode and ensure that on using it in an SECM system.

A series of cyclic voltammograms for ferrocenecarboxylic acid at four different concentrations (5mM, 2.5mM, 1.25mM and 0.625mM) is shown below for a microelectrode fabricated by the method described in section 5.4.

Initially the electrode is polarised at a potential that is insufficient to initiate the oxidation reaction, but on sweeping the potential to 0.55V at a sweep rate of 50mVs^{-1} , the tip current is observed to increase to a plateau current of approximately -12nA when the applied potential is approximately 350mV. This current arises as the reduced form of the redox couple is oxidised to form the oxidised ferricenium species. The sigmoidal plateau current with no diffusion limited peak is a clear indication of microelectrode behaviour.

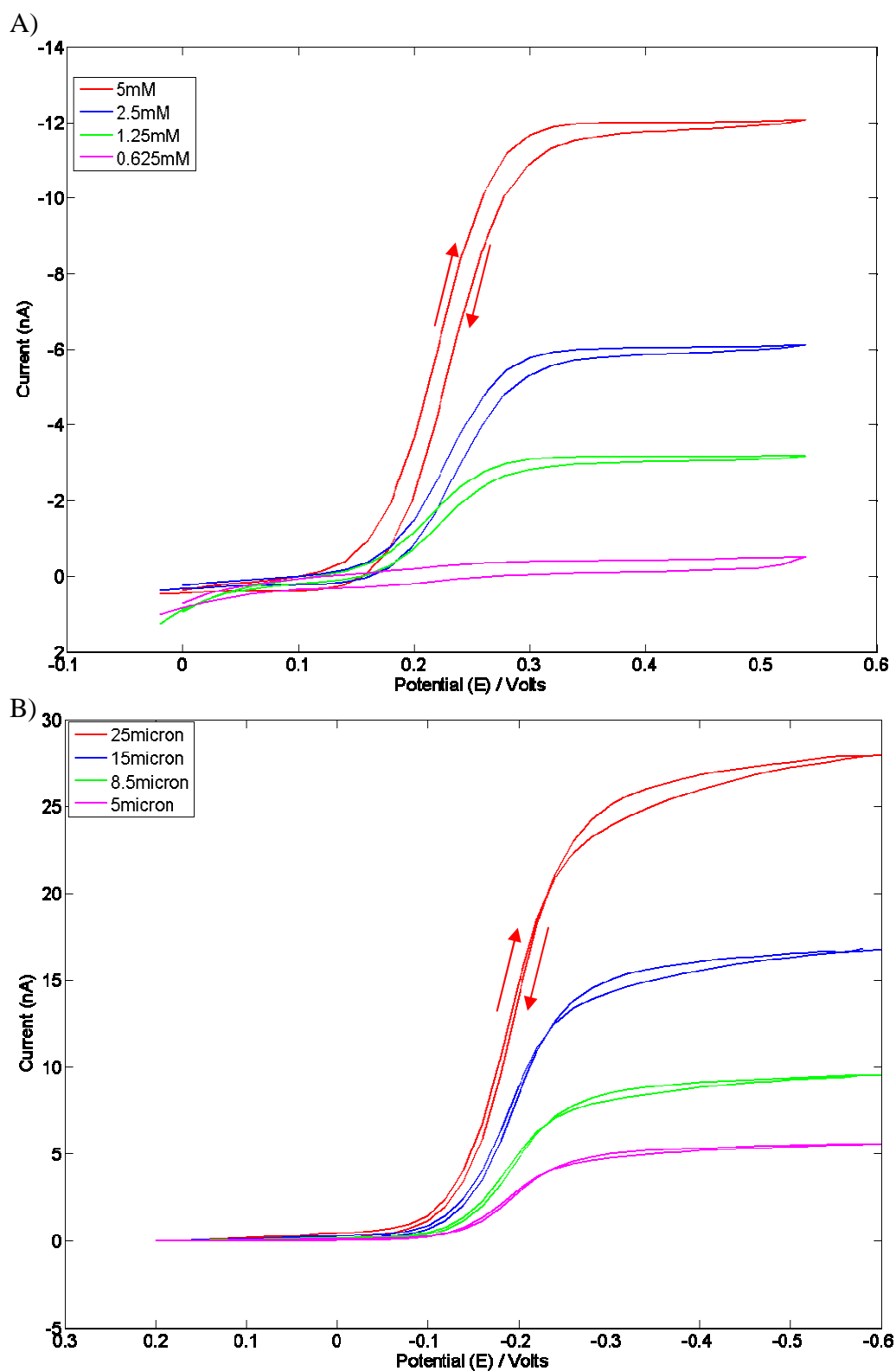


Figure 5.12: Series of cyclic voltammograms in mediators of differing concentrations and with electrodes of differing effective diameters. A) CVs conducted in 5mM ferrocenecarboxylic acid B) CVs conducted in 5mM hexamine ruthenium chloride using electrodes of progressively smaller diameters

5.5.3 Simulating current/distance curves and subsequent estimation of R_g value for fabricated UMEs

Kwak and Bard (1989) have reported the effect of tip geometry on amperometric tip responses. It was shown that the ratio of the insulating glass sheath radius had a strong influence on the faradaic tip current when the tip was moving in the vicinity of an inert substrate, an effect explained in terms of the hindered diffusion of a redox mediator from the bulk solution to the tip. In an article expanding on this work, Amphlett and Denault (1998) developed a simulation using an alternating direction implicit algorithm implementing expanding space and time grids to account for the diffusion of the redox species around the corner of the insulating sheath, something not accounted for in previous simulations. The equations for each of these simulations is given below for negative and positive feedback scenarios:

$$\text{Negative feedback: } i_{tip} / i_{tip,\infty} = 1 / \left[k_1 + \left(\frac{k_2}{L} \right) + k_3 \exp\left(\frac{k_4}{L} \right) \right]$$

$$\text{Positive Feedback: } i_{tip} / i_{tip,\infty} = k_1 + \left(\frac{k_2}{L} \right) + k_3 \exp\left(\frac{k_4}{L} \right)$$

Where d = tip-substrate distance

a = disk radius

$L = d/a$, the dimensionless tip-substrate distance

k_1, k_2, k_3, k_4 = constants dependent on R_g and L values

Using these equations, simulated negative approach curves were generated for microelectrodes of varying R_g ratios.

On obtaining the approach curve experimentally, the data was subsequently plotted against that data generated by the above simulation (Figure 5.1). On comparing the data, quantitative support for an estimation of the R_g value may be obtained. It should be noted that only negative feedback curves were used to estimate the R_g value. This is because it has been shown that insulator thickness has been shown to affect SECM approach curves over insulating substrates more than for conductive substrates (Lee, 2001; Mirkin, 1992). The R_g ratio of the fabricated probe was subsequently estimated according to the curve's fit to the simulated curves. From reference to the curves below, the fabricated electrode appears to have an R_g ratio of approximately 10; this is in contrast to the approximate R_g ratio of 12 calculated by optical microscopy.

Normalised approach curves obtained by simulation and by experimentation are given below. Curves obtained experimentally were conducted at a scan rate of $1\mu\text{m}$ per step.

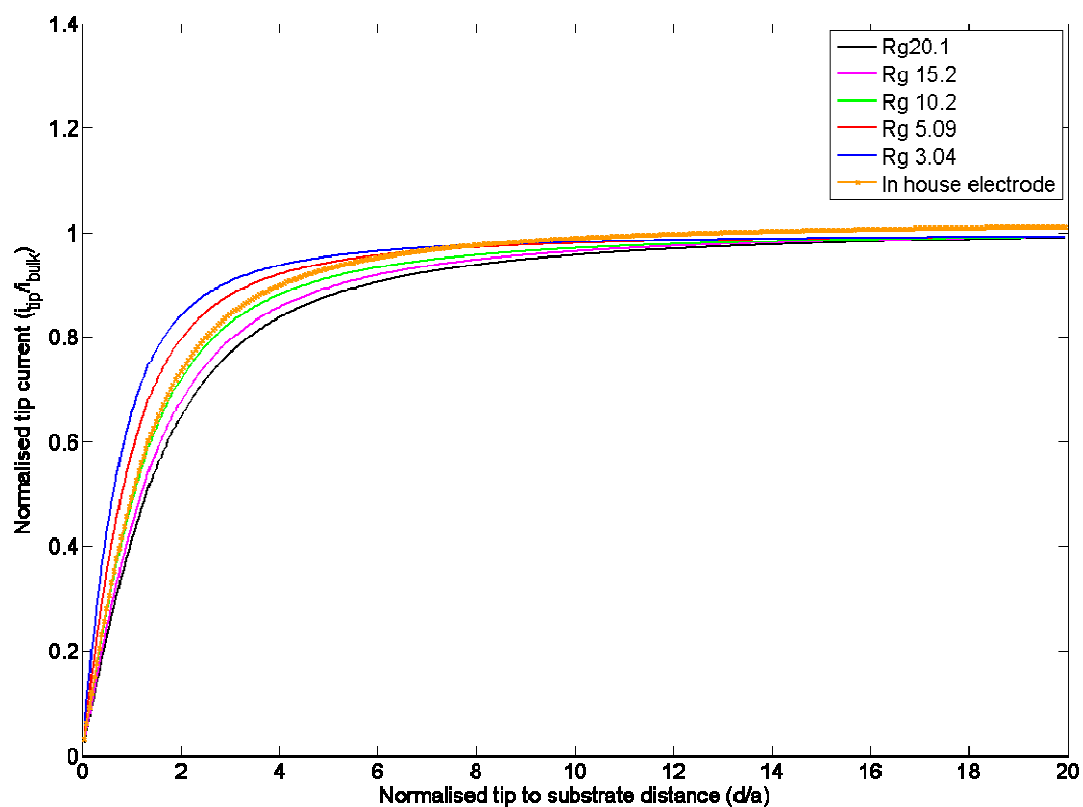


Figure 5.13: Approach curve obtained using electrode fabricated in-house plotted against simulated approach curves

The deviation often observed between the measured R_g value and that expected by theory may be attributed to the tips slight deviation from either exact 'concentric' geometry, or perhaps an uneven substrate. However, as a diagnostic tool and an approximator of R_g values, this method does hold some value. It also gives a target for the fabrication of high quality microelectrodes with repeatable geometries.

Another observation can be made from the production of such approach curves; the topographical sensitivity of the microelectrode (i.e. how sensitive the electrode is to small changes in the tip-substrate distance) can be perceived by considering the derivative of the curve. A high rate of change of the tip current with respect to tip-substrate distance means that the microelectrode will be able to detect small topographical features on the substrate – a considerable advantage if the microelectrode is being used for topographical imaging. However, topographical imaging is very much a shared art, as it is accomplished by other scanning probe techniques. The advantage of the SECM is that it is able to differentiate between areas of the substrate that have differing levels of surface reactivity. It hence follows that there is a great drive to increase the resolution of the SECM system, where 'resolution' may be defined as the ability of the microelectrode to resolve two closely positioned areas of differing levels of reactivity.

5.5.4 Polishing

The importance of a reproducible, effective approach to polishing microelectrodes is illustrated. Immediately after electrode construction but before polishing, a batch of 25 μ m electrodes were characterised by approach curves. From Figure 5.14, it is evident that each of these probes exhibited a distinctly different tip current when in bulk solution. However, on polishing all probes using the same protocol, their behaviour became more homogenous and the inter-batch variation was significantly lowered.

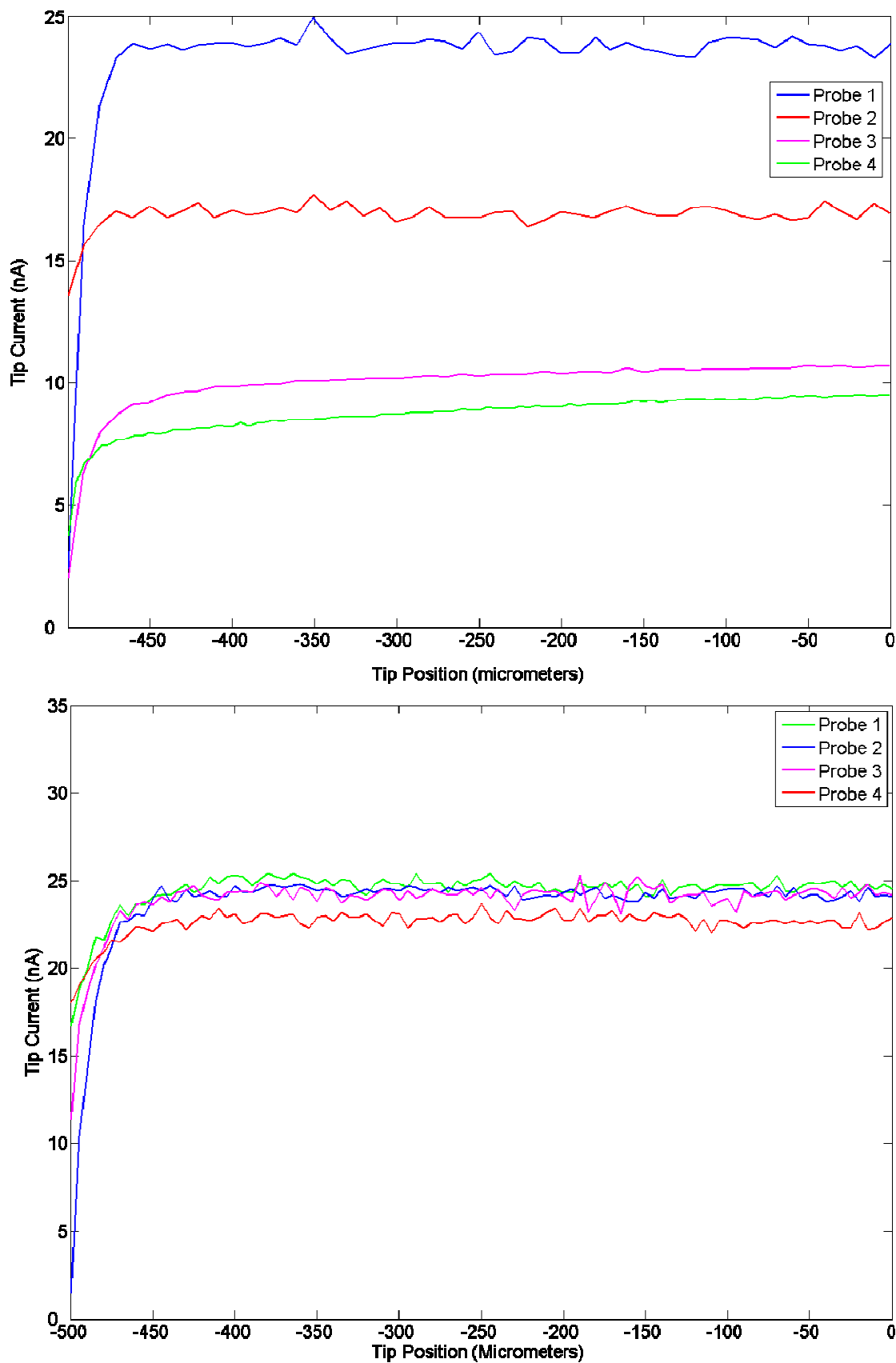


Figure 5.14: Approach curves for four 25 μ m tips before (top) and after (bottom) polishing illustrating the importance of a consistent polishing protocol

5.5.5 Review of microelectrodes

The production of robust, well characterised electrodes with a variety of different active area dimensions represented a key step in this thesis as the quality of data obtained is very much dependent on the quality of the electrode used. The development of a reproducible methodology for the fabrication of electrodes with an active surface diameter down to 5 μm is reported here. The fragile nature of the fibres used, make polishing exceptionally difficult and problems were frequently encountered with getting an electrical connection between the platinum quartz fibre and the wire which was to be connected to the potentiostat cabling. As a result of using the platinum quartz fibre as opposed to the platinum wire, the geometry of the tips is much improved since there was little deviation in the fibres position relative to the insulating glass surround during sealing. Beveling the tip to produce a microelectrode with a smaller Rg ratio was found to be exceptionally difficult as the risk of damaging the tip was exceptionally high. Those electrodes that were constructed successfully however, exhibited excellent electrochemical behaviour.

In comparison to electrodes currently available, the electrodes developed here represent a significant alternative offering, taking aspects from each commercial design and applying them in one model. The electrodes are robust, exhibit excellent electrochemical behaviour, and the construction methodology means a highly concentric geometry. Additionally, the robust construction makes it highly suited to the clamping mechanism on the SECM270. By taking aspects of existing electrode designs and incorporating them into a single model, an electrode with a unique combination of desirable qualities can be produced.

5.6 Conclusions

A reproducible methodology for the production of microelectrodes down to an active area diameter of 5 μ m has been described. The electrodes produced are well suited to the SECM technique as they are robust, exhibit concentric geometry and reproducible electrochemical behaviour. Whilst they are not as small as the electrodes produced by other methods such as those employing micro-fabrication techniques (see microelectrode section of introductory chapter), their dimensions are well within those required for most applications.

The quality of the electrodes produced by this methodology is highly dependent on the skill of the individual involved in the fabrication process. There is hence considerable scope for minimising the human element in the process. One suggestion for future consideration is the purchase and use of a laser pipette puller. This instrument, an example of which is given below, allows for the simultaneous pulling of platinum in glass, to allow the controlled manufacture of platinum disk electrodes with diameters down to the nanometer range. By the appropriate programming of the system, electrodes may be made to a much higher level of reproducibility and errors associated with the polishing and electrical connection steps may be partially removed.

The provision of high quality microelectrodes is a key issue for Uniscan Instruments Ltd. Whilst this has been partially achieved by the development of the fabrication process above, ensuring electrodes are supplied to the customer in good working order is difficult and movement in transit has been known to damage the electrode's response, even if, superficially, the electrode looks unharmed. One option for consideration perhaps is the supply not of working electrodes to the customer, but the fabricating equipment. By provision of the fabricating equipment, the customer is no longer dependent on Uniscan for microelectrodes and becomes self-sufficient. Such a move would reduce the time Uniscan spend managing the fabrication of microelectrodes and their quality control. This approach would also reduce the risk of any kind of damage to the electrodes that may occur during transit. The proposition is hence that Uniscan Instruments develop a range of accessories for the fabrication of microelectrodes and incorporate it with the current SECM270 product offering. A strategic alliance with manufacturers of such equipment may not only provide an additional income stream, free up human resources from the management of their supply but

also give scope for further collaborative agreements with the various alliance ties. A suitable collaborating company may be one which provided a laser pipette puller, optical microscopes and the raw materials required for their fabrication. Uniscan customers, on purchasing the SECM270 then not only receive a high quality piece of equipment, but also the equipment necessary for them to be self sufficient and access to the knowledge and expertise of a company with the specialised knowledge and skills required for microelectrode fabrication.

Chapter 6

**Characterisation of DNA biosensor and
detection of changes in
DNA/polyelectrolyte film charge transfer
properties by SECM**

6. Characterisation of DNA biosensor and detection of changes in DNA/polyelectrolyte film charge transfer properties by SECM

6.1 Introduction

This chapter describes the use of scanning electrochemical microscopy for the characterisation of a DNA biosensor previously developed within the group (Davis *et al*, 2005). The work successfully demonstrates the usefulness of the technique in biosensor development, whilst also highlighting the possibility of using SECM for the label-less detection of DNA hybridisation.

The development of technologies capable of detecting specific DNA sequences in real time has significant implications for studies and diagnostic tests associated with clinical applications, environmental regulation, food science, agriculture and forensics (MacPherson *et al*, 1993; Wang, 1997; Lucarelli *et al*, 2002; Babkina, 2004).

The concept of the DNA biosensor was first introduced by Millan and Mikkelsen in 1993. The DNA biosensor is an analytical device which allows the recognition of a DNA hybridisation event and its conversion into a detectable signal (see Figure 6.1). Generally speaking, the system is composed of a detection component in which a single stranded DNA sequence is immobilised onto a surface which is then exposed to a hybridisation solution containing the target sequences. If the solution contains a sequence complementary to the immobilised probe DNA, complementary binding may occur. Complementary binding may then be detected by the transducer - which may be based on optical, gravimetric or electrochemical approaches (Okumura, 2005).

Electrochemical techniques for the detection of DNA hybridisation events have received a considerable amount of attention over recent years – partially as a result of the success of the blood-glucose sensing technologies - but also because of the numerous advantages they offer over alternative approaches to DNA assaying. Such techniques potentially offer high sensitivity and are compatible with modern microfabrication technologies.

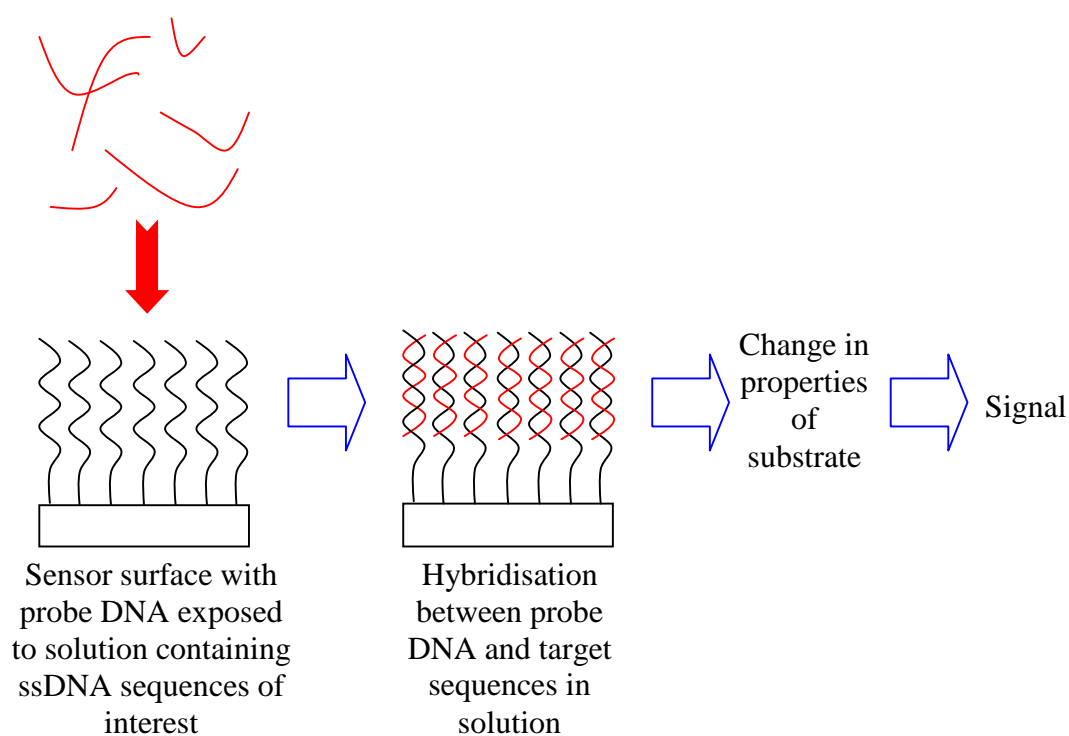


Figure 6.1: Schematic illustrating principle of DNA biosensor

The most frequently employed electrochemical strategies for detecting the hybridisation event rely on redox-active hybridisation indicators which have a greater affinity for double stranded rather than single stranded DNA (e.g. Hashimoto, 1994). In these systems, electrodes are functionalised with single stranded oligonucleotides with which target sequences bind to form a duplex. On the formation of a duplex, the indicator (which may be a cationic metal complex, a groove binder or intercalator) binds preferentially to the double stranded region, resulting in an increase in the local concentration of the indicator at the surface of the electrode. This may be detected by electrochemical approaches such as cyclic or chronoamperometric voltammetry (Hashimoto *et al*, 1994; Millan and Mikkelsen, 1993; Kelley *et al*, 1997). Zhou *et al* for example recently reported danthron (1,8-dihydroxy-anthraquinone) as having the ability to intercalate with DNA; due to its planar structure, it was found that Danthron slots between adjacent base pairs and in doing so, discriminates between DNA in its single and double stranded forms (Zhou *et al*, 2005). Daunomycin, a more well characterised intercalator, is known to bind to the guanine residue within the DNA duplex - Cheng *et al* recently reported a detection limit of 2.3 x

10^{-14} mol/L of target oligonucleotide using daunomycin and mercaptoacetic acid coated magnetite nanoparticles (Cheng, 2005;). Navarro *et al* directly labelled the probe DNA with ferrocene phosphoramidites (Navarro *et al*, 2004).

Whilst the electrochemical labelling approach has much potential in the development of a rapid sensing technology, there is much scope for the direct, label-less detection of DNA hybridisation by electrochemical methods. By removing the necessity for labelling, sensors are capable of offering faster responses and require fewer reagents, making them an extremely attractive route of investigation. A label-less detection mechanism such as this involves monitoring the changes in the physicochemical properties of the film by electrochemical methods. An example of a label-less system such as this was developed by Wang *et al*, who reported the label-free detection of DNA hybridisation by doping electropolymerised conducting polypyrrole films and monitoring the current-time profiles on the addition of complementary DNA sequences to the system (Wang *et al* 1999; see also Hui, 2005). In a similar system, detection limits of 1.6fmol of complementary oligonucleotide target in 0.1ml was reported by Komarova *et al* (2005). For a comprehensive review of electrochemical DNA biosensors, the reader is referred to Wang *et al* (1997), Thorp (1998), Pividori *et al* (2000), Gooding (2002) and Kerman *et al* (2004).

Within this chapter, a DNA biosensor previously developed within the group is interrogated by scanning electrochemical microscopy (Davis *et al* 2005). The biosensor is based on the modification of a carbon electrode with a genomic DNA/polyelectrolyte film which is then exposed to a solution containing either non-complementary or complementary single stranded genomic DNA. In this work, changes in the charge transfer properties of the film were monitored by impedimetric approaches. It was found that on exposing a carbon electrode modified with a polyethylenimine (PEI)/ssDNA film to a solution containing complementary ssDNA, the impedance of the system dropped approximately 10% over the course of three hours, after which time the impedance was observed to plateau. In contrast, on exposing the ssDNA/PEI film to non-complementary DNA, the impedance of the system increased slightly.

By interrogating the same system using SECM, valuable insights may be obtained regarding the fabrication of this biosensor and the applicability of SECM to detecting DNA hybridisation. SECM offers a route for non-contact electrochemical interrogation, negating the need for hard-wired electrodes; this in turn offers the potential for developing an array based approach which may be interrogated via a scanning probe tip.

In brief, the aim of the work presented in this chapter is two-fold:

1. To investigate the different components of the DNA biosensor developed by Davis *et al* by SECM, which will provide a useful insight into the methodologies employed in its fabrication.
2. To conduct a preliminary investigation into whether SECM may be used to differentiate between non-complementary and complementary DNA hybridisation.

6.2 Results and Discussion

6.2.1 Carbon electrode substrate

As described earlier, the substrate used in this series of experiments was the same as that used in the original study by Davis *et al.* An image of the sensor used is given below (Figure 6.2).

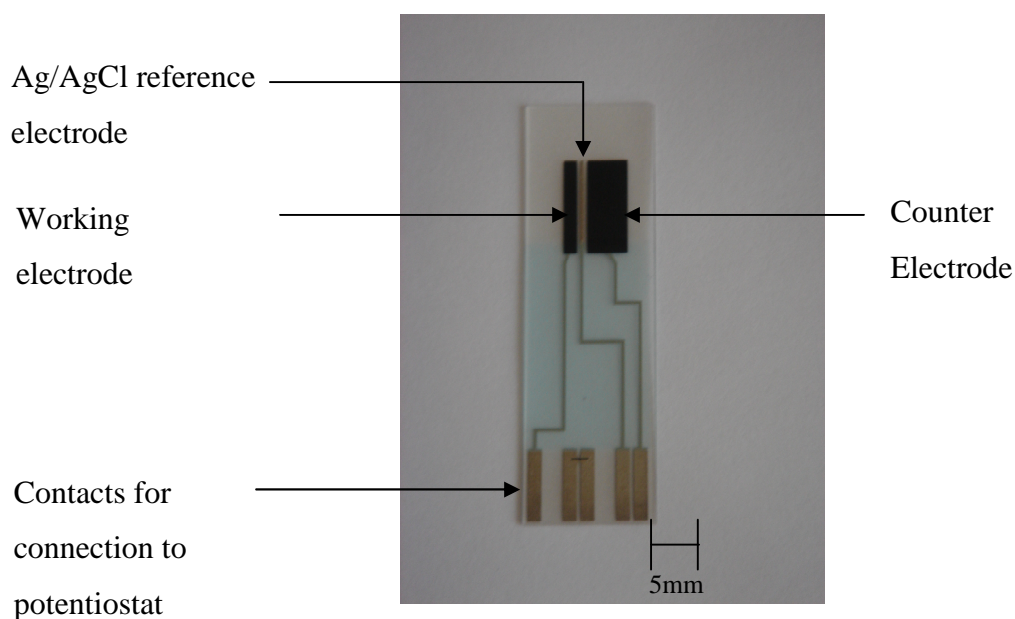


Figure 6.2: An image of the carbon paste electrode used in the study. The working electrode was patterned with the polyethylenimine array

The application of thick film, screen printing techniques to the fabrication of electrodes represents the most promising route towards the mass production of inexpensive yet highly reproducible biosensing devices (Alvarez-Icaza *et al.*, 1993).

As a result of the ease with which screen printed electrodes may now be fabricated and their application to blood glucose sensing, screen printing technologies have undergone intense development (Hart and Wring, 1997; Albareda-Silvert *et al.* 2000). Screen printed electrodes are now the substrate of choice for a wide range of sensing applications.

The screen printing of the functional sensing electrode has two main stages: the first is the deposition of the conductive film, which is achieved by forcing a conductive ink through a patterned screen. The second is the curing phase, achieved by either heating or photocuring; during this step, the solvent within the ink evaporates. This process is then repeated depending on how complex the pattern is. Insulating dielectric films may also be used to define electrode areas.

Silver based inks are generally used for reference electrodes, whilst carbon or metallic inks (e.g. Pt, Au, Ag) are used for the working and counter electrodes of the sensor.

There are various advantages associated with the use of carbon inks; they exhibit lower background currents over a wider potential window than metal electrodes which improves the signal/noise ratio and lowers the detection limits of the system under investigation (Niwa *et al*, 1994; Gilmartin *et al*, 1995). The graphite based carbon electrodes are also extremely robust and this allows them to be used in turbulent conditions (Wring *et al*, 1990). Moreover, they are extremely cost effective, making them ideal for single use applications. Screen printed electrodes additionally offer a clean electrode substrate electrode for each analyte and negate the need for electrode cleaning between analytical determinations.

6.2.2 Characterisation of carbon inks by SECM

Generally, carbon inks are composed of graphite particles bound by a polymer and a selection of additives which allow the dispersion, printing and adhesion of the ink to the base substrate (Adams, 1958; Svancara *et al*, 1996a, 1996b; Grennan *et al*, 2001). As a result of this heterogeneous composition, there is a great deal of topographical variation in the conductivity of the electrodes produced. These heterogeneities were investigated by SECM.

Prior to each area scan, the microelectrode tip was positioned at a height where the tip current was equal to half of that obtained in bulk solution. The area scan shown in Figure 6.3 was conducted using the hexamine ruthenium chloride redox couple (5mM). On scanning across the carbon/millinex border, a 30% increase in the tip current is observed as

a consequence of positive feedback due to the recycling of the hexamine ruthenium redox couple at the conductive substrate. On further interrogation of the carbon substrate at a decreased tip to substrate distance, (see Figure 6.4) it is evident that there is a considerable amount of variation in the feedback response.

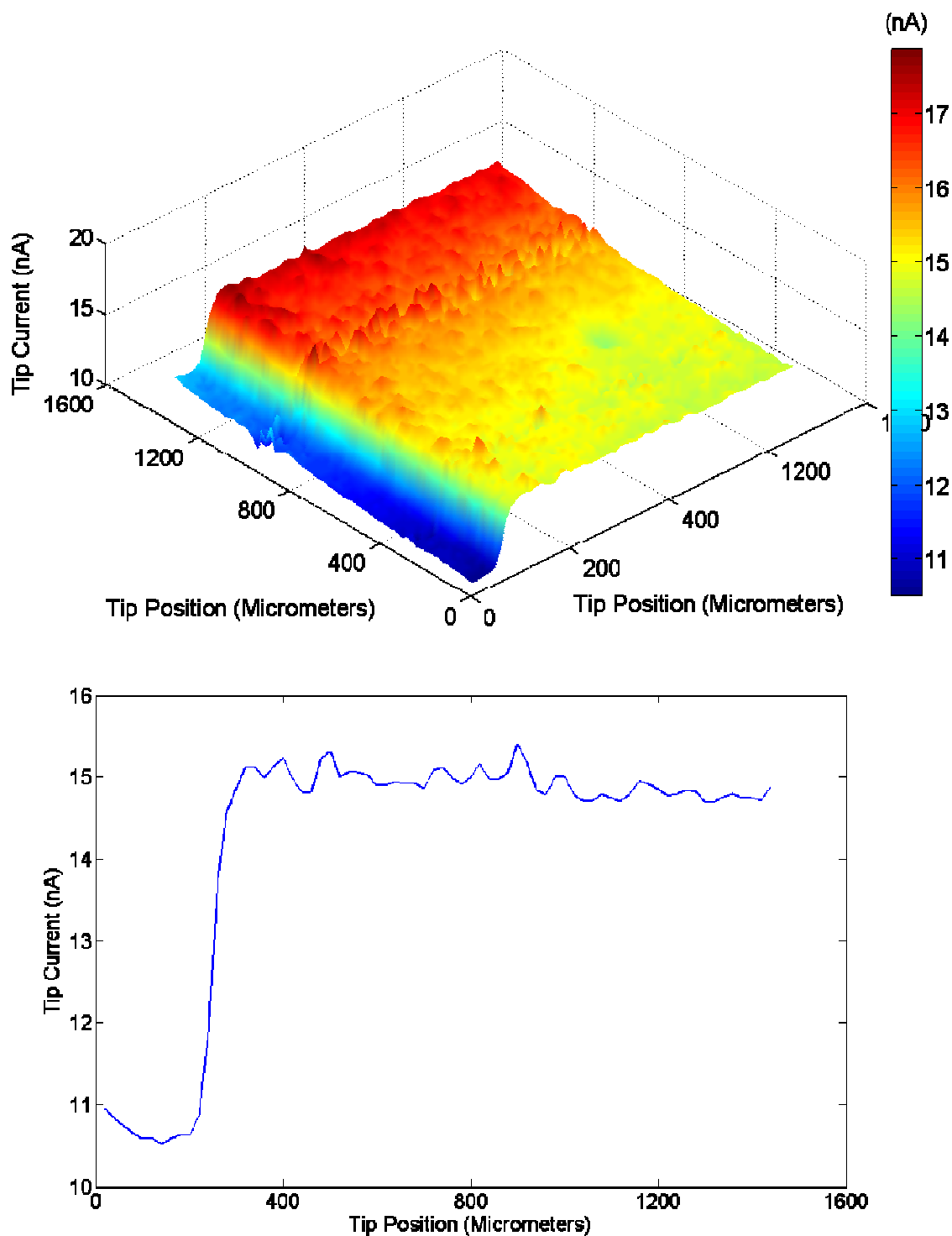


Figure 6.3: (A) Area scan over border between carbon (green/yellow region) substrate and millinex printing substrate (dark blue region) ; (B) Linescan across border at a tip position of 800microns

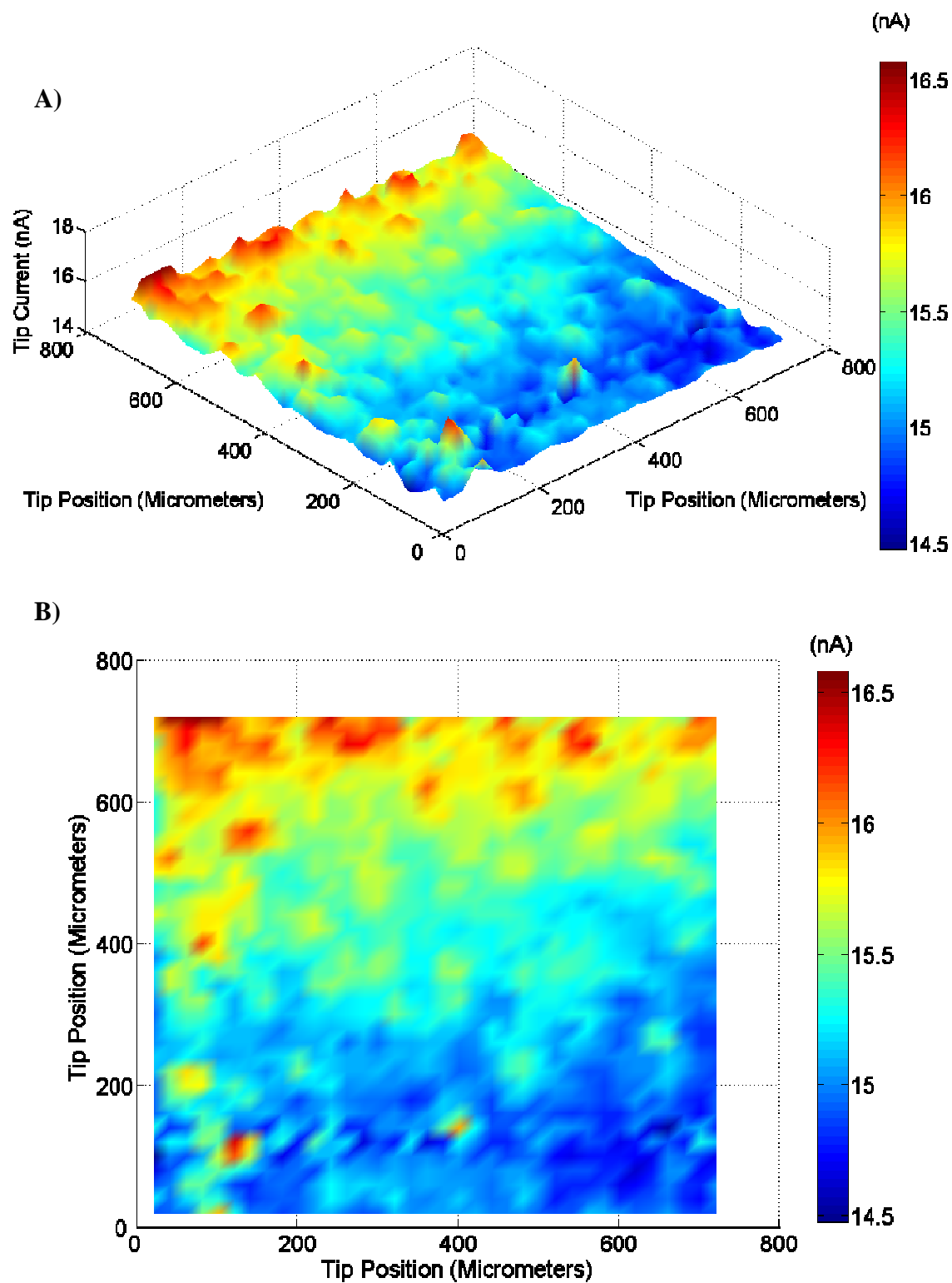


Figure 6.4: A) 3D representation of the data obtained from area scan images of a carbon ink electrode. Current hotspots show areas of raised topography and/or increased conductivity arising from the heterogeneous nature of the carbon ink used. B) A 'birds eye view' of 'A'

The observed heterogeneity may be due to variation in the conductivity of the substrate, arising as a result of the composition of the carbon ink. Electrical conductivity within the bulk system occurs by physical contact between graphite particles, providing a conductive route through the polymeric medium (Svancara *et al*, 2000), although an alternative mechanism involving indirect electron tunnelling between proximal particles has been suggested (Svancara *et al*, 2000). However, although the addition of conductive particles such as carbon black are added to the ink to enhance conductivity, regions of higher conductivities and hence, higher rates of heterogeneous charge transfer may still exist as a result of the physical properties of graphite. Graphite, an allotrope of carbon, consists of carbon atoms arranged in a hexagonal sheet, with each atom covalently bound to three other surrounding atoms; the remaining fourth electron is donated to a delocalised system of electrons between sheets. As a result of this delocalised system, there is high electron mobility parallel to the plane of the sheets, yielding excellent conductivity – of the order of $\sim 0.1 \Omega\text{cm}$ (McCreery, 1991). This is in contrast to the conductivity of graphite across the sheets – of the order of $\sim 1 \times 10^{-4} \Omega\text{cm}$. As a result of this differential conductivity, the edge plane of graphite exhibits excellent conductivity, whilst the basal plane is highly insulating. Considering that there is no mechanism by which to orientate the graphite particles in the carbon ink, the result of this differential conductivity is a surface with highly heterogeneous charge transfer, with some areas exhibiting higher rates of heterogeneous rates of charge transfer than others.

A further possible reason for the observed heterogeneity in feedback response is the variation in the topography of the substrate. When the tip is translated across the substrate, raised regions are closer to the tip, resulting in an enhanced positive feedback effect as the distance across which the recycled mediator has to travel is less than for areas that are topographically further away from the tip. This may either be as a result of the topography of the underlying millinex substrate, variation caused by the screen printing process, or be due to variations in the size of particles incorporated into the ink.

These two hypotheses for the observed variation in tip current highlight one of the central problems in interpreting SECM data. Without the aid of a constant distance approach, it is not possible to differentiate current variation due to differences in the electrochemical properties of the surface from those variations due to topographical variations.

6.2.3 Polyelectrolyte films

Polyelectrolyte films have been used extensively in the preparation of biosensing elements. Films such as these may be assembled by taking advantage of the strong forces of attraction between oppositely charged polyelectrolytes, a technique first reported by Decher *et al* (1992). The procedure is very simple and is demonstrated schematically in Figure 6.5. First, a charged solid substrate (in this case a negatively charged carbon ink electrode) is submerged in a dilute solution of an oppositely charged polymer (polyethylenimine) where strong multiple charge interactions result in the formation of a thin film of the polyelectrolyte across the substrate surface. After rinsing, the film coated sample is exposed to an alternately charged polymer (DNA) which has the effect of reversing (or perhaps only neutralising) the charge of the substrate by the adsorption of the polymer onto the substrate surface. If this process is repeated, a polyelectrolyte multilayer may be constructed.

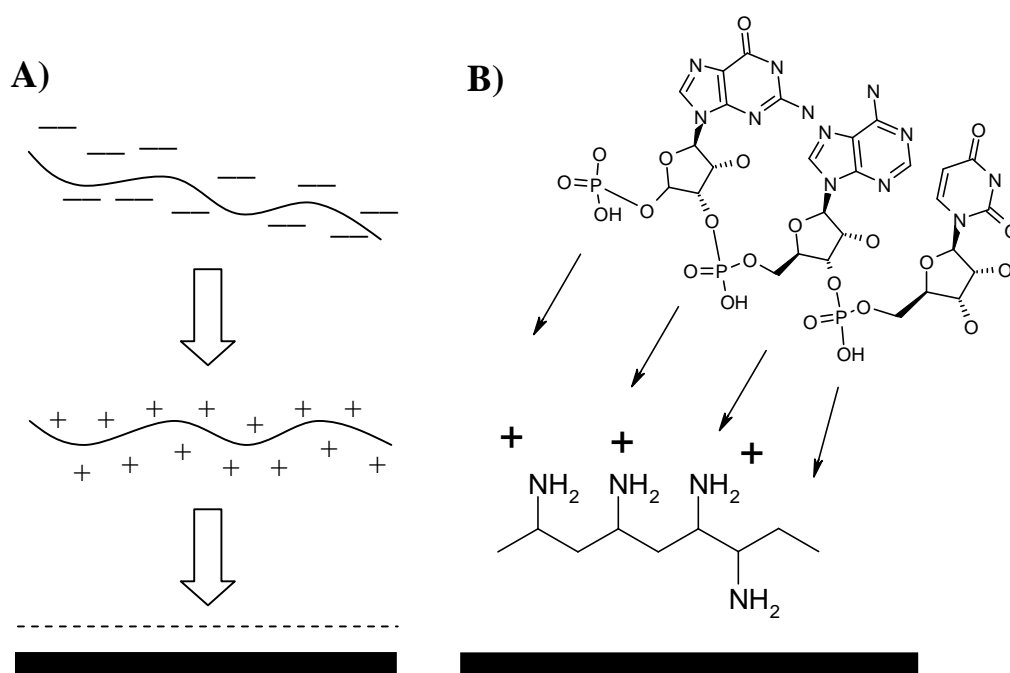


Figure 6.5: Schematic detailing construction of a A) general multilayer polyelectrolyte film B) DNA/polyethylenimine film

The use of polyelectrolyte films in the immobilisation of DNA was first reported in the early 1990s (Lvov *et al* 1993; Sukhorukov *et al* 1996). Since then, the technique has become widely employed in the development of DNA immobilisation and biosensing technologies, in which both oligonucleotides and complete DNA molecules have been used (Xi, *et al* 2000; Travas-Sejdic *et al* 2006). The technique has also been used to immobilise single stranded probe DNA on support structures, allowing hybridisation to complementary sequences in solution (Nicollini *et al*, 1997; Davis *et al* 2005).

In the biosensor developed within the group, a carbon ink electrode was dip coated with the polycationic polyethylenimine (Davis *et al* 2005). Whilst this was a suitable approach for sensor preparation for impedimetric analysis, it was not appropriate for the preparation of electrodes to be interrogated by SECM. The reason for this was that by imaging a homogeneously treated surface, it is not possible to compare a modified region with an unmodified region. Any changes in the tip current may be due to changes in the background current and not due to changes in the charge transfer properties of the modified substrate. It was therefore decided that for SECM interrogation, the polyelectrolyte film should be patterned in an array format. By producing this pattern, background changes in the feedback current could be determined by comparing the feedback signals over unmodified carbon (Figure 6.6).

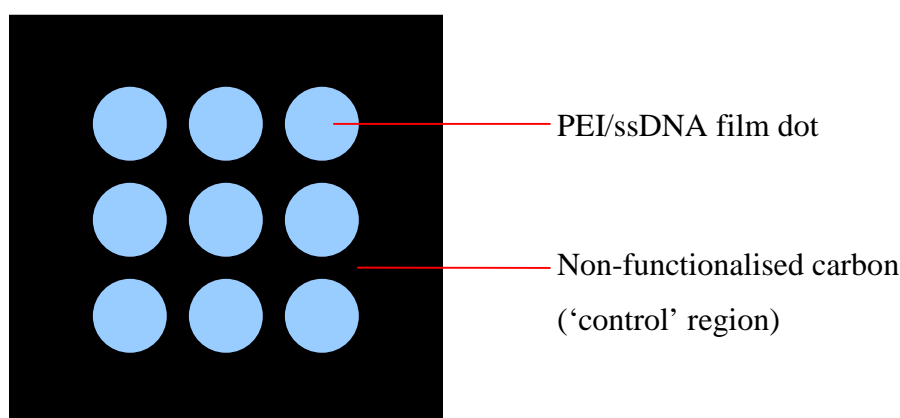


Figure 6.6: Schematic illustration of patterned polyelectrolyte film which allows the monitoring of the change in background current over an unmodified surface against the change in feedback response over PEI/DNA modified carbon

As described in the methods section (Chapter 3) the patterned array was achieved by using the SECM micro-positioning XYZ stage. A capillary was filled with the polyelectrolyte (polyethylenimine – PEI) and lowered towards the carbon substrate (Figure 6.7). The deposition process was accomplished by monitoring the tip to substrate distance by video microscope and by eye. By observing the small meniscus at the tip of the pulled capillary it was possible to determine the point at which contact was made and when the deposition of the PEI droplet was achieved. After deposition, the tip was retracted and moved in the X or Y direction respectively and the process repeated. Arrays with a variety of spot sizes and densities were possible (Figure 6.8). After deposition, arrays were rinsed. Problems arose with using larger dots however, as the surplus polymer attached to the non-functionalised regions during rinsing, resulting in poorly defined arrays.

As mentioned previously, this aspect of the work effectively illustrates the promise of the system to be used in micropatterning solution arrays and represents a significant route for investigation by Uniscan Instruments Ltd.

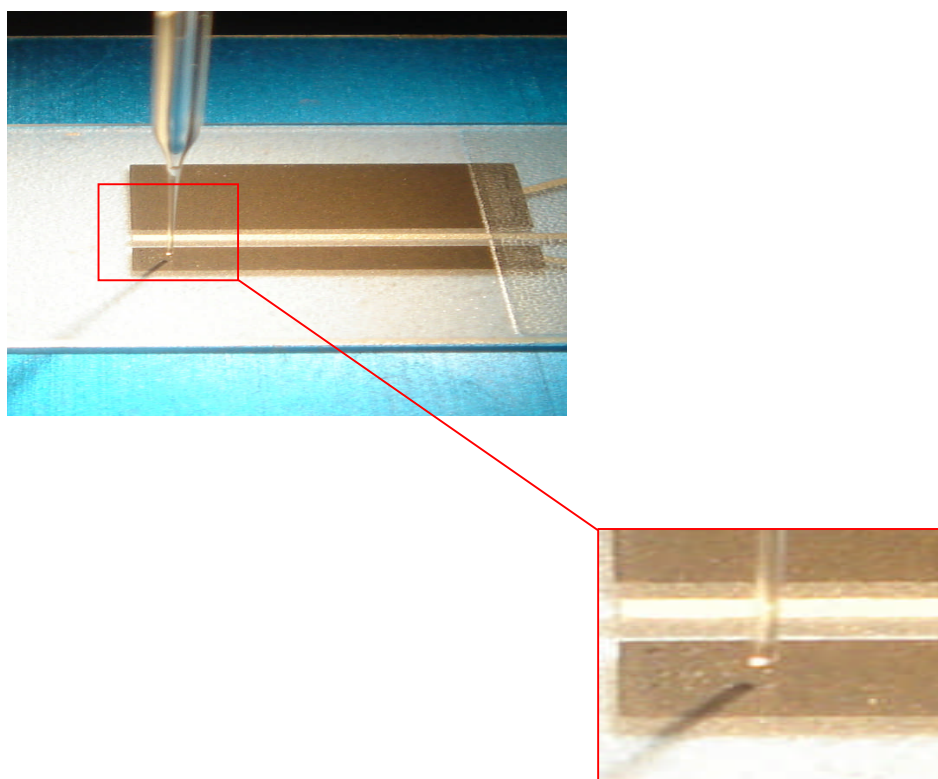


Figure 6.7: Photograph of polyethylenimine deposition on carbon electrode by pulled microcapillary using the XYZ micro-positioning stage of the SECM270

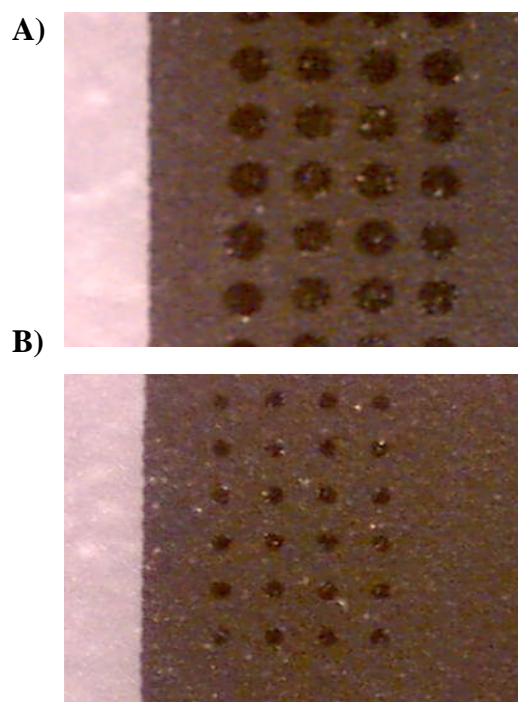


Figure 6.8: Optical Micrographs of polyethylenimine dots on carbon paste electrode using capillaries of differing internal diameters; 100micron (A) 30micron (B)

6.3 Mediator selection

A selection of mediators was considered for use in the interrogation of the DNA/PEI polyelectrolyte array, including ferrocenecarboxylic acid, ferricyanide and hexamine ruthenium chloride. Ruthenium bi-pyridine was not considered as it is known to irreversibly oxidise the guanine residue in DNA – and this could have implications for later use in the interrogation of DNA functionalised polyelectrolyte films.

6.3.1 Cyclic Voltammetry

To determine the suitability of each mediator to the study of a modified carbon electrode, the behaviour of each was characterised by cyclic voltammetry and then compared. Cyclic voltammetry was conducted using 5mM of the respective mediator dissolved in pH 7.1 phosphate buffer at a scan rate of 50mVs^{-1} . The cyclic voltammograms for these are shown in Figure 6.9.

The carbon ink was seen to exhibit quasi-reversible electron-transfer properties for both ferrocenecarboxylic acid and hexamine ruthenium (III) chloride. In contrast, the peak current for the potassium ferro/ferricyanide redox couple was significantly smaller than that obtained for the other two redox couples. This non-reversible electrochemical behaviour was exhibited in previous work involving the characterisation of inks. Erlenkotter *et al* (2000) for example reported peak separations of over 300mV, well beyond the 59mV expected for a Nernstian, diffusion controlled single electron transfer reaction.

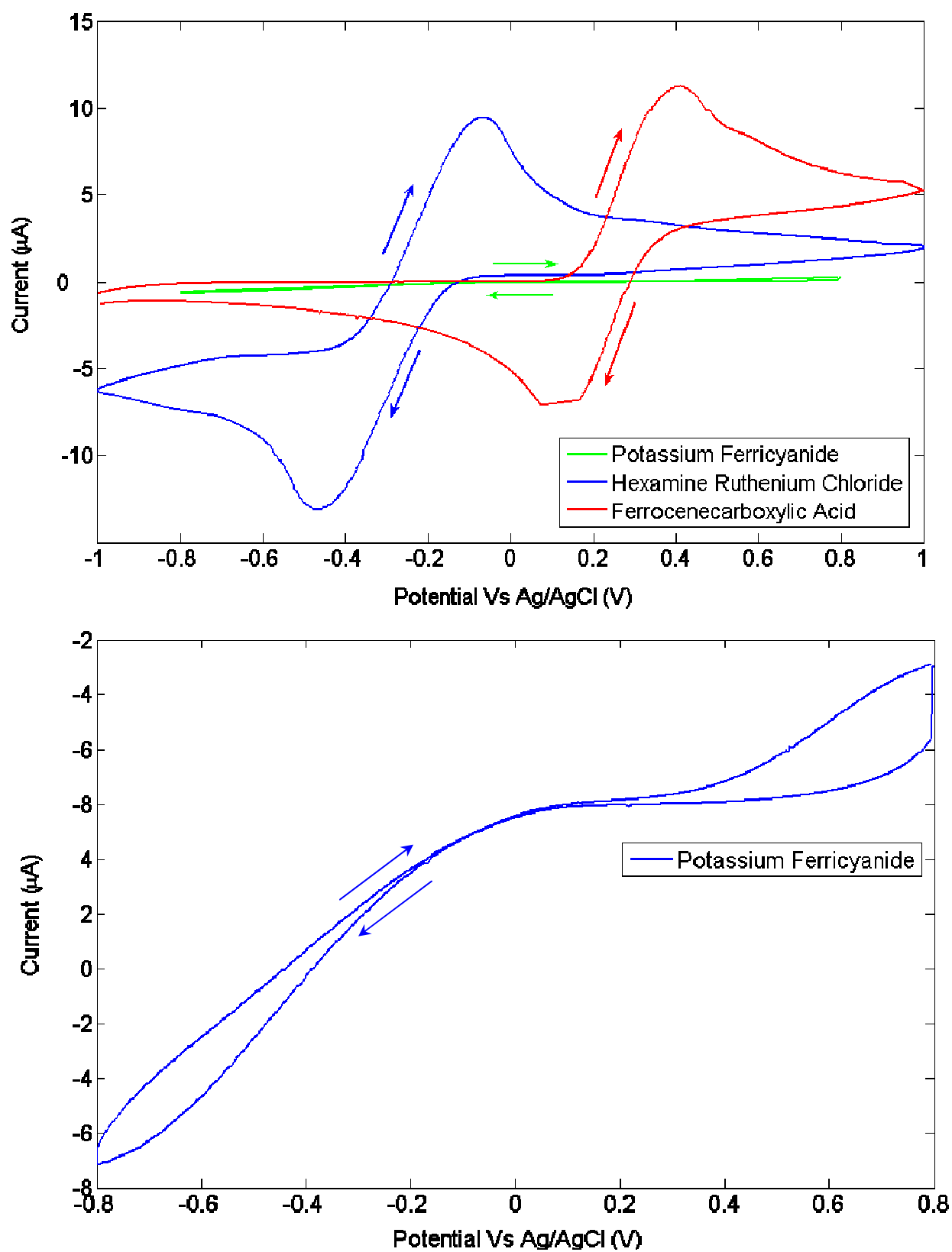


Figure 6.9: Cyclic voltammograms for A) hexamine ruthenium (III) chloride and ferrocenecarboxylic acid and potassium ferricyanide (III) and B) potassium ferricyanide only (5mM in pH 7.1 buffer)

The stark contrast between the cyclic voltammograms obtained for hexamine ruthenium chloride and ferrocencarboxylic acid and those obtained for potassium ferricyanide offers further support for the hypothesis that the carbon substrate has a slightly negative charge (Deakin *et al.*, 1985; Cui *et al.*, 2001). This negative charge hinders the diffusion of the negatively charged mediator species to the carbon substrate by electrostatic repulsion; as a consequence of this, charge transfer kinetics are slowed, resulting in the departure of the system from ideal behaviour. These results also exhibit the suitability of the carbon as a base substrate for the construction of a polyelectrolyte film due to its negative charge.

6.4 Scan height

A series of linescans were conducted across the border of the carbon ink substrate to determine the optimum height at which area scans could be conducted. Using 5mM hexamine ruthenium chloride, approach curves were conducted and line scans across the carbon border were performed where the tip current was equal to 80, 70, 60 and 50% of the current measured in bulk (Figure 6.10).

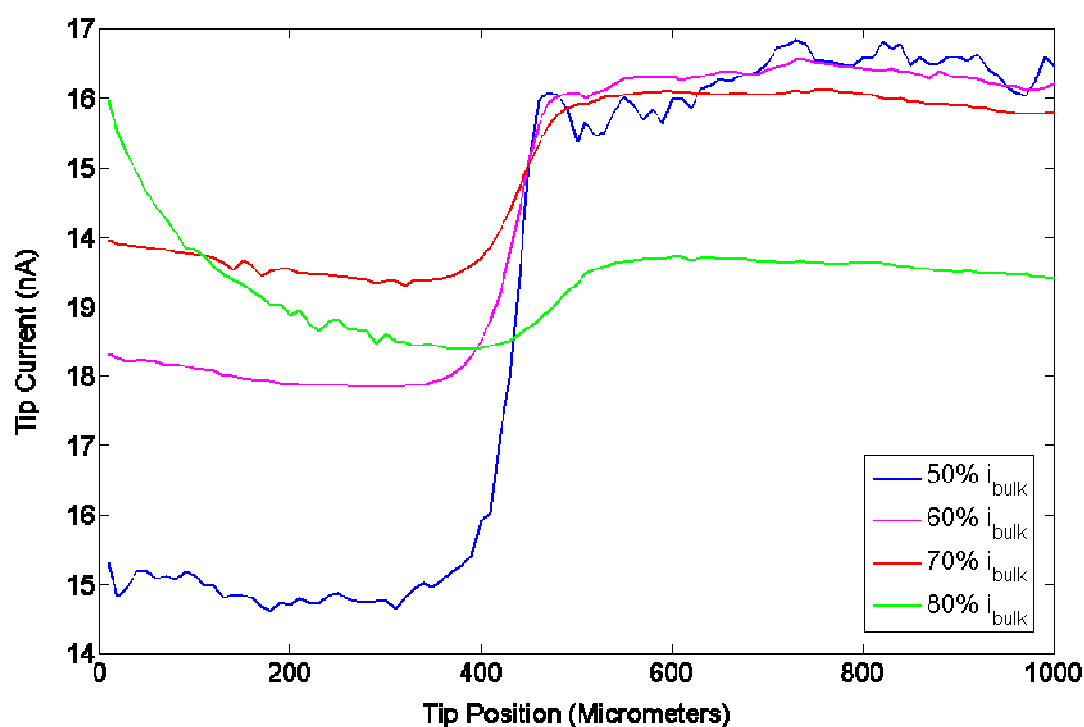


Figure 6.10: Consecutive linescans over carbon ink border. Scans were carried out at the height at which the tip current was equal to 80%, 70%, 60% and 50% of the tip current observed in bulk

The resolution of each linescan is observed to increase with a reduction in the tip to substrate distance (Figure 6.10). On comparing the gradient of the line over the region of inflexion, which represents the movement of the tip across the insulator/carbon border, it is evident that the scan which produces the greatest rate of change is the scan conducted at the height at which the tip current is equal to 50% of that obtained in bulk solution (see Table 6.1

This improved resolution is also apparent on observing the variation in tip current over the portion of the linescan conducted over the carbon surface. Because conducting linescans at lower scan heights increases the likelihood of tip crash, it was deemed prudent to conduct area scans within this work with the tip positioned where $i_{\text{tip}} = 0.5 \times i_{\text{bulk}}$.

Table 6.1: Resolution as a function of scan height – calculated over the 400-440 μm range of line scans

Scan height as a % of bulk current	Resolution ($\Delta I/\text{distance}$)(nA/ μm)
80	3.32×10^{-03}
70	1.48×10^{-03}
60	2.87×10^{-03}
50	6.29×10^{-03}

6.4.1 Effect of mediator charge on feedback response

The feedback response when interrogating polyelectrolyte films is strongly influenced by the charge of the mediator used. In the images below, ferricyanide and ferrocenecarboxylic acid were both used as the mediator to interrogate a polyethylenimine array patterned on a carbon ink electrode. The results also give greater insights into the observations made in section 6.3.1 where potassium ferricyanide was observed to exhibit poor electrochemical behaviour at the surface of the carbon electrode.

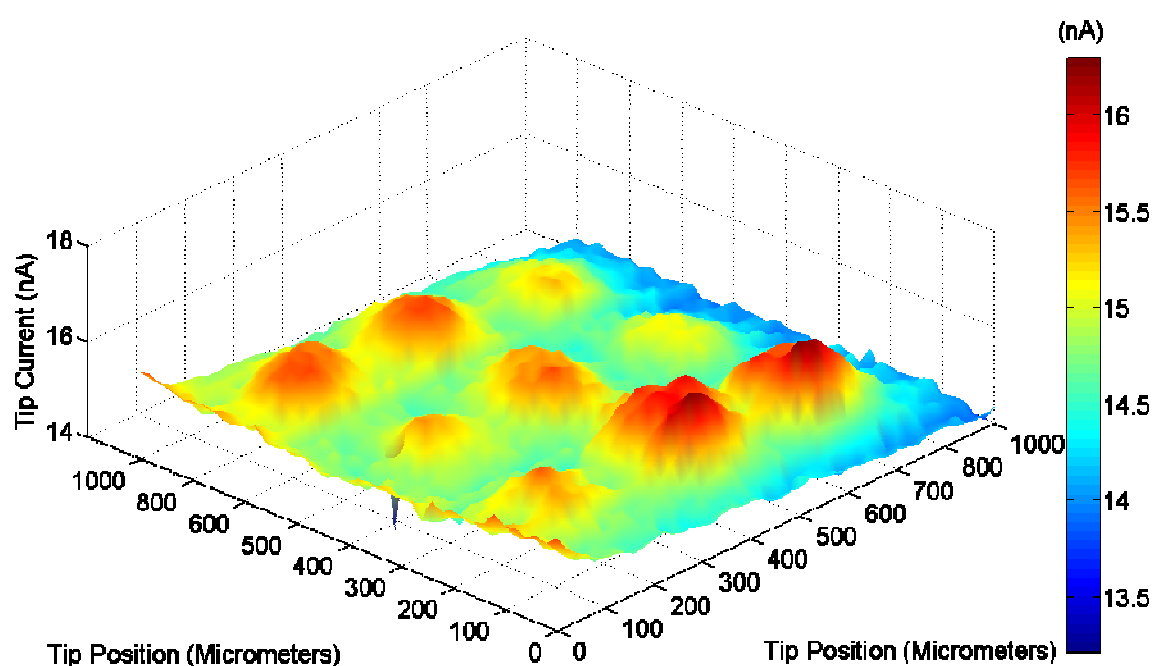


Figure 6.11: Area scan profile over polyethylenimine array patterned on a carbon ink electrode using 5mM potassium ferricyanide mediator

With reference to Figure 6.11, it is evident that the functionalisation of the carbon ink with the polyelectrolyte film had the effect of enhancing the rate of charge transfer between the carbon electrode and the ferricyanide mediator solution. In the case of unmodified carbon, following reduction at the tip of the microelectrode, the ferrocyanide mediator diffuses to the carbon surface, where it is recycled (oxidised) to ferricyanide and is made available for re-reduction. In the case of polyethylenimine functionalised carbon, however, the rate at which the ferrocyanide is oxidised to ferricyanide is enhanced. For an enhancement of current to be observed, there must be some mechanism by which the transfer of charge

from the carbon to the mediator is being facilitated. As polyethylenimine has no delocalised electron systems, the transfer of charge from the carbon substrate to the mediator is unlikely to occur by the passage of electrons through the polymer film. It is therefore thought that charge transfer occurs as a result of the diffusion of the mediator through the polymer, promoted by the electrostatic forces of attraction between the polymer and negatively charged mediator species. Polyelectrolyte films such as those used here are not highly ordered films with a crystalline structure – like Langmuir Blodgett films for example. Rather, they tend to be more amorphous in nature, with layers interpenetrating one another (Decher, 1997; Decher *et al.*, 1998). As a consequence of this, gaps in the film allow the diffusion of the mediator towards the electrode substrate, resulting in an enhancement in the faradaic current measured at the tip.

This enhancement of charge transfer properties is in contrast with the diminution in charge transfer properties observed when using the positively charged mediator, ferrocenecarboxylic acid. On modifying the carbon ink with the polyethylenimine array, the functionalised region is observed to behave similarly to an insulating substrate when interrogated by SECM (Figure 6.12). This is thought to be a result of the electrostatic forces of repulsion between the positively charged mediator and the positively charged polyethylenimine film. As a result of these repulsive forces, the mediator is inhibited from approaching the conductive carbon substrate, resulting in the diminution of positive feedback. The result is a lowering in the feedback current when compared to the feedback response over blank, unmodified carbon. This argument is illustrated schematically in Figure 6.13.

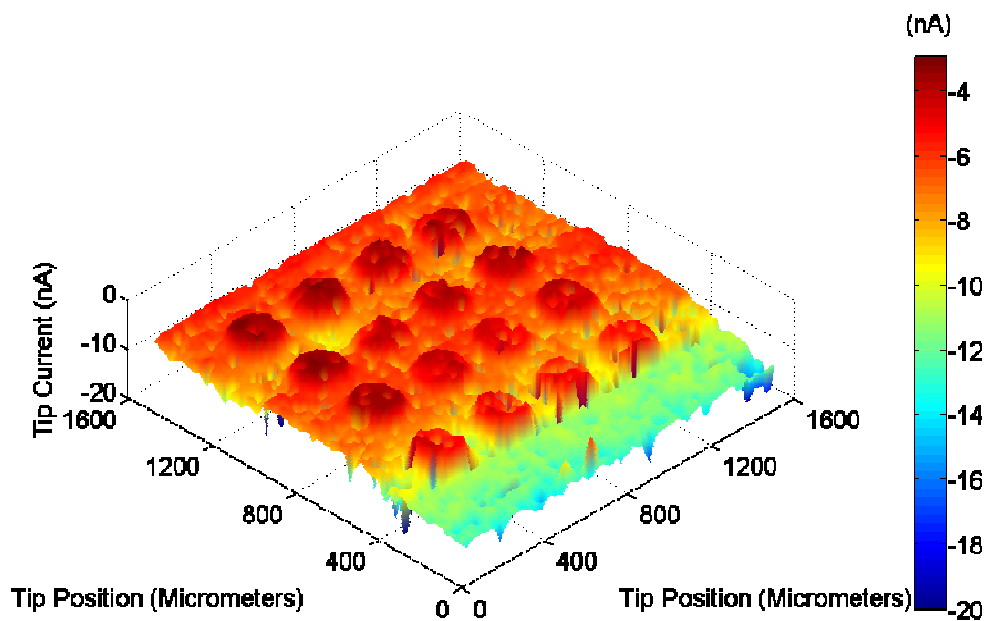


Figure 6.12: Area scan over polyethylenimine array using 5mM ferrocenecarboxylic acid. Please note that the Z axis is opposite to that in Figure 6.11. Also, note the colour bar: Red to blue on the colour bar indicates a direction of low to high current

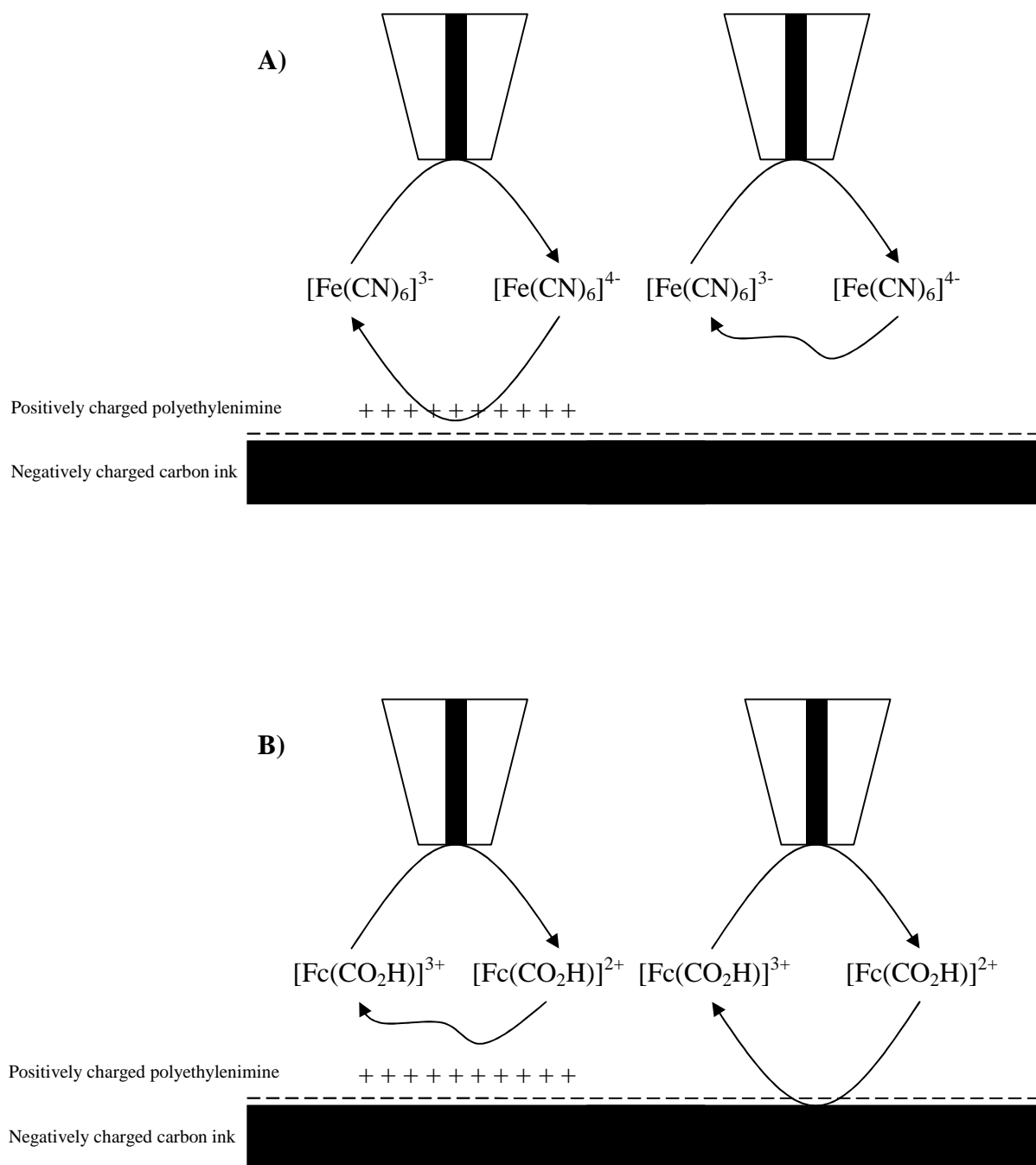


Figure 6.13: Schematic diagram illustrating the electrostatic forces of attraction and repulsion between the mediators A) ferricyanide and B) ferrocenecarboxylic acid with the positively charged polyethylenimine film and the negatively charged carbon substrate respectively

6.4.2 Interrogation of film integrity by SECM

To determine the stability of the polyethylenimine film during multiple scans, to the scanning process, the polyethylenimine film was scanned repeatedly over a period of time. If the integrity of the film was put at risk by the scanning process, it would not be possible to determine whether any changes occurring in the film were due to DNA hybridisation or not in future experiments. With reference to Figure 6.14, it is apparent that over the course of four area scans in which the polyethylenimine film was submerged in ferrocenecarboxylic acid mediator, the image became significantly distorted. Initially it was thought that this noise may have been a result of the degradation of the film, but because the distortion is seen to occur across the entire region, it is felt that this may be due to either the fouling of the electrode or the degradation of the substrate as a whole – perhaps as a consequence of precipitation of the ferrocenecarboxylic acid out of solution.

On performing the same experiment using hexamine ruthenium chloride however, there was no such distortion. Whilst a small increase in noise is apparent on comparing visually, there is little apparent change in the area scan data as a whole (Figure 6.15). A paired t-test was carried out on both datasets to determine whether there was any statistically significant difference between the change in feedback response using the mediators ferrocenecarboxylic acid and hexamine ruthenium chloride. It was found that there was no statistically significant difference between arrays at $T = 0\text{min}$ and $T = 300\text{min}$ using the hexamine ruthenium chloride mediator ($p \gg 0.05$), but there was a statistically significant difference between those scans obtained using ferrocenecarboxylic acid (the null hypothesis of no difference was rejected for 29 of the 76 columns of the array of data obtained by the use of ferrocenecarboxylic acid (p-value range 0 to 0.7746)).

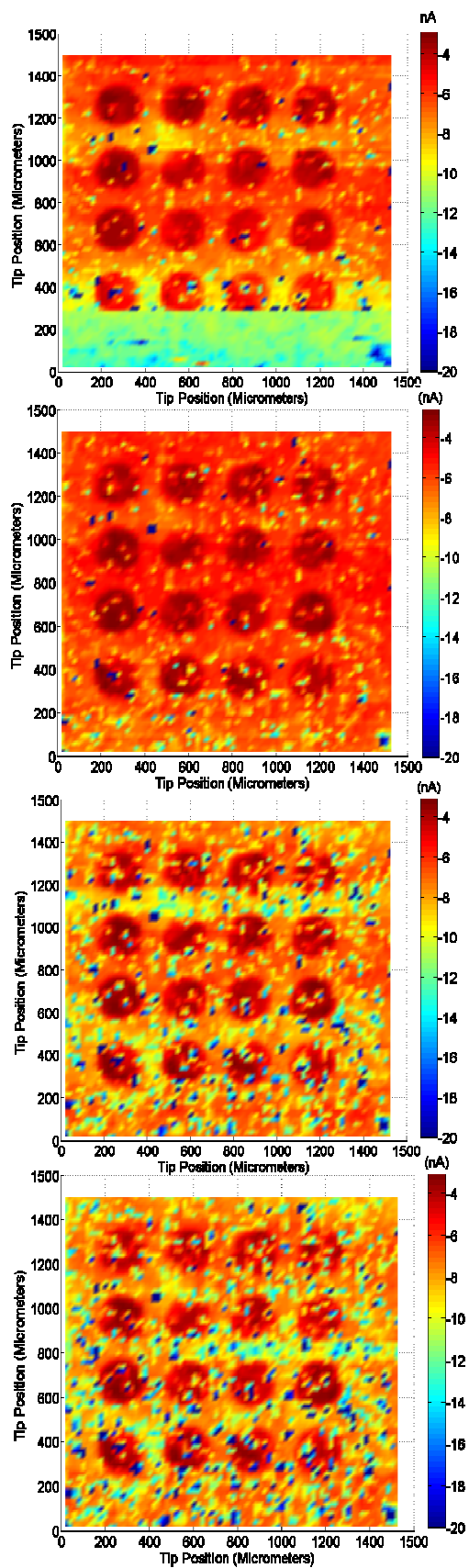


Figure 6.14: Consecutive area scans over PEI array on carbon at T=0min, T=100min, T=200min, T=300min using 5mM ferrocenecarboxylic acid

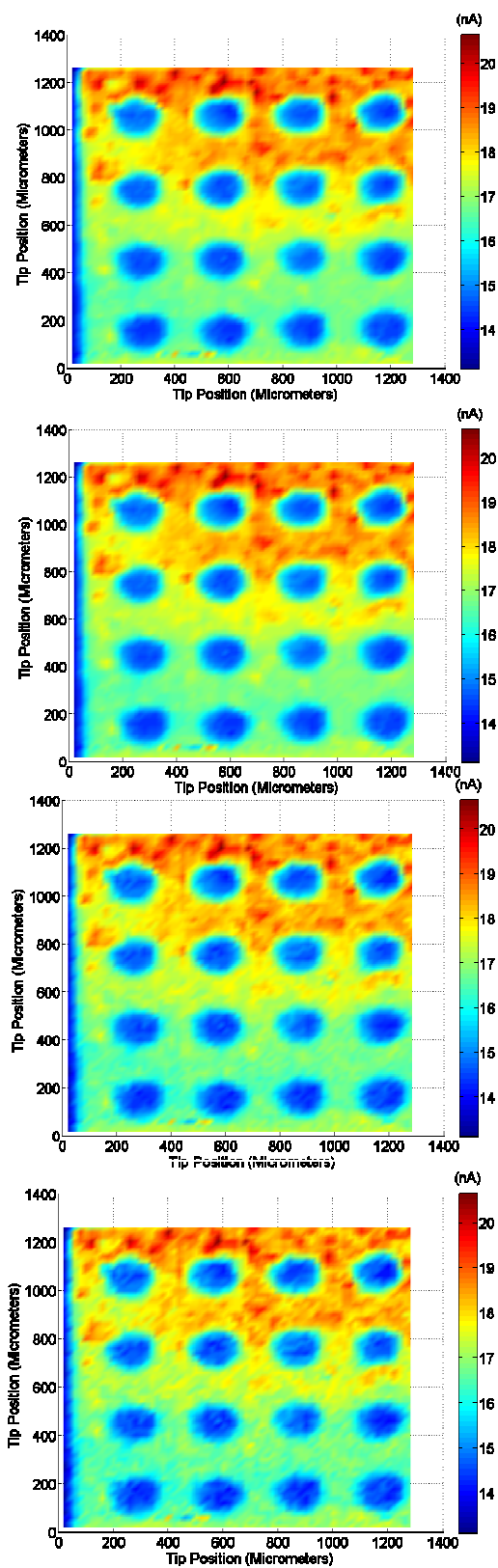


Figure 6.15: Consecutive scans over a PEI array on carbon at T=0min, T=100min, T=200min, T=300min using 5mM hexamine ruthenium chloride mediator

Building on this analysis, it was decided that hexamine ruthenium chloride would be used as the mediator in the interrogation of the DNA/polyethylenimine array as it has been shown that the films show good stability when immersed in the hexamine ruthenium chloride mediator.

6.5 Statistical interrogation of array data by region of interest (ROI) analysis tool

In the previous section, a simple statistical analysis was undertaken to determine whether the changes observed in the charge transfer properties of the surfaces before and after the exposure of the ssDNA/PEI film to complementary and non-complementary genomic DNA were statistically significant. The way in which this was initially achieved was by a simple paired t-test, in which each column of data was paired with its respective column in the second array. A significant problem with this is that by doing so, data points not exposed to the experimental treatment become part of the population dataset, which may affect the test statistic obtained. Whilst the test statistics obtained support the observations – i.e. the apparent enhancement in charge transfer properties over ssDNA/PEI regions, it was decided that an alternative approach to analysing these arrays should be developed. In conjunction with a bioinformatician within our department, a simple graphical user interface (GUI) tool was developed to allow the calculation of descriptive statistics about a specific region of the area scan (Clarke, 2007).

The ROI GUI was developed to allow the extraction of information about regions of interest (ROI) in an array of data obtained by the use of the area scan macro in the SECM270 software. Data is extracted from the SECM user interface and saved as an excel file which is then imported into the Matlab GUI. The user is then able to highlight a region of the area scan with a polygon. Information regarding the number of data points, the average current value and relevant statistics are then saved to a chosen excel file for further interpretation and analysis. The GUI, screen captures of which are shown in Figure 6.16, provided an ideal platform for the analysis of the PEI/DNA arrays fabricated in this study. Such a tool, which allows the interrogation of area scan data, would be an excellent addition to the SECM270 as it would significantly curtail the time spent by the user in post-scan analysis.

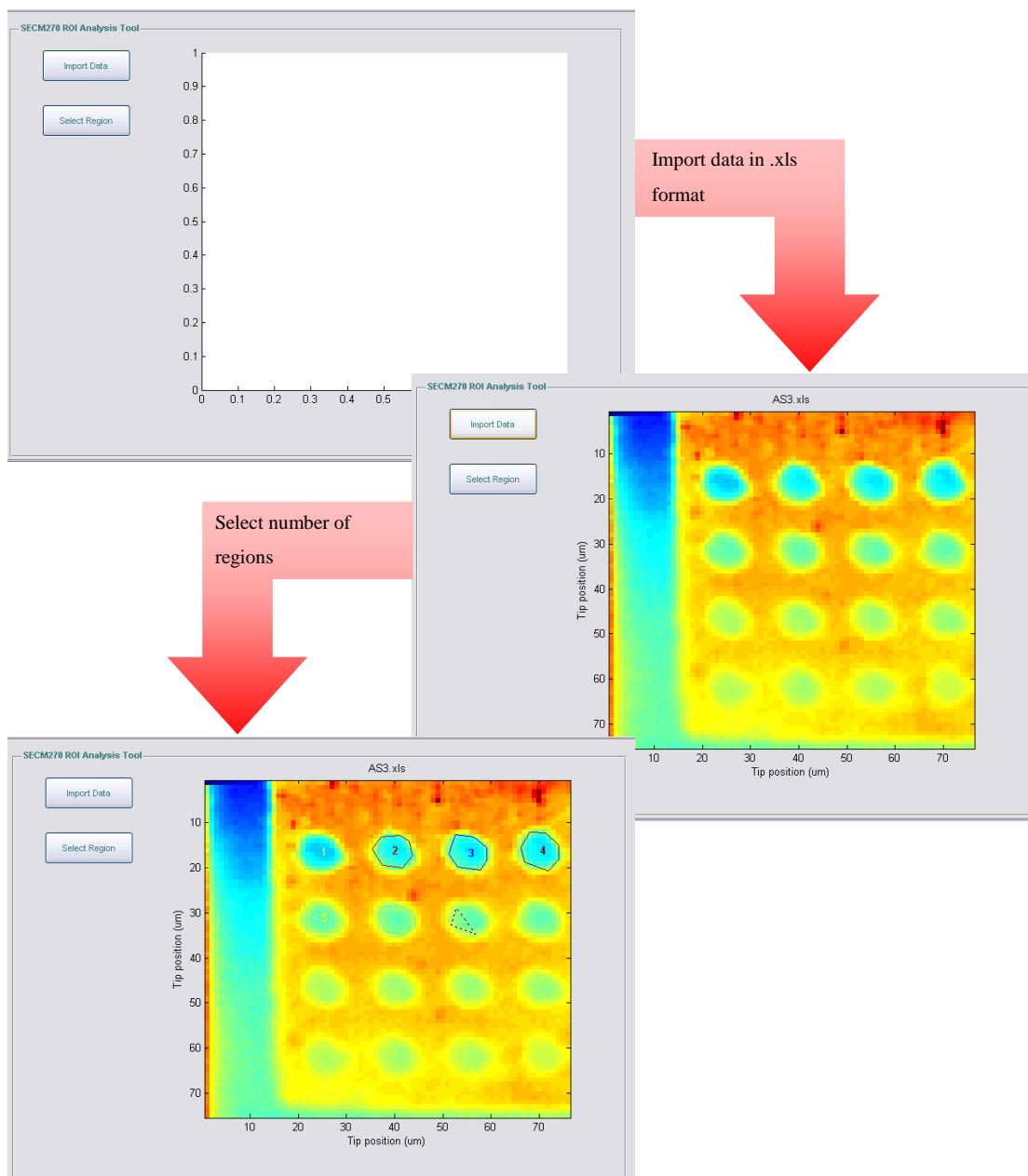


Figure 6.16: Screen captures of the GUI developed to allow extraction of data from area scan data

As the user highlights regions of the array, descriptive statistics are calculated for the highlighted regions encapsulated by the polygon, including the mean, minimum, maximum, range, standard deviation and ROI centre (coordinate). By the selection of the functionalised regions, discrete data points are obtained which may then undergo statistical analysis. A screen capture of the ROI GUI output in excel is given in Figure 6.17.

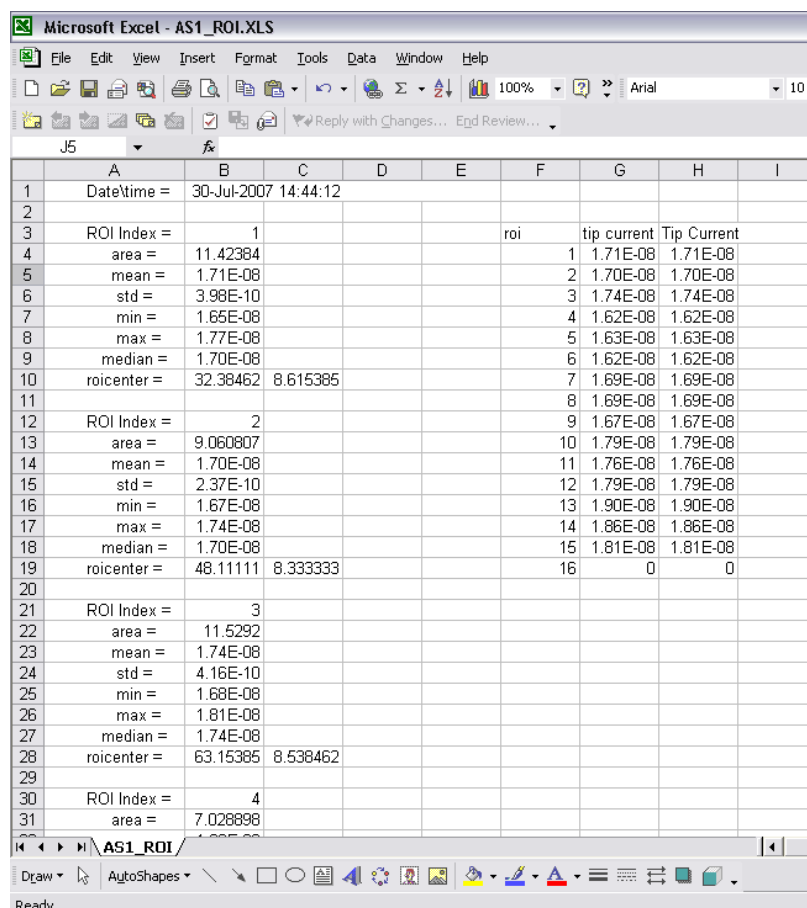


Figure 6.17: Screen capture of ROI output in excel, detailing extraction of data from an area scan array

6.6 Control experiments

In the hybridisation experiment, different solutions are introduced and removed from the polyelectrolyte substrate. To ensure that the introduction and removal of these solutions did not affect the integrity of the film or have an impact on its charge transfer properties, a control experiment was conducted. In this experiment, all steps of the hybridisation studies were replicated but with the omission of the single stranded DNA from the hybridisation solution. All other aspects of the investigation, from imaging to rinsing protocols were identical to those of the hybridisation studies. In Figure 6.18, the two area scans, before and after the 3hr exposure to the hybridisation solution, are presented. On subtracting the 'post-exposure' scan from the 'pre-exposure' scan, the resulting 'difference' array is relatively homogenous with an approximate range of 0 to 0.08nA Figure 6.19(A). If there was some change in the charge transfer properties of the film, then one would see larger changes over those regions functionalised with the ssDNA / polyethylenimine film. On conducting a paired t-test on the average current over each dot measured before and after exposure to the buffered control hybridisation solution, it was revealed that whilst there was a statistically significant difference between the average current value, it was very small ($t = 8.1$; $df = 15$; $p = 7.1 \times 10^{-7}$; $CI = 0.04 \times 10^{-9}$ to 0.07×10^{-9}). Representative linescans are also presented (Figure 6.19 (B)), which depict graphically the very small change in the feedback current after exposure to the buffered hybridisation solution (Figure 6.20). It may be concluded that the PEI/ssDNA film does not appear to undergo any changes on exposure to the hybridisation solution that would produce a significant change in the charge transfer properties of the film observable by SECM.

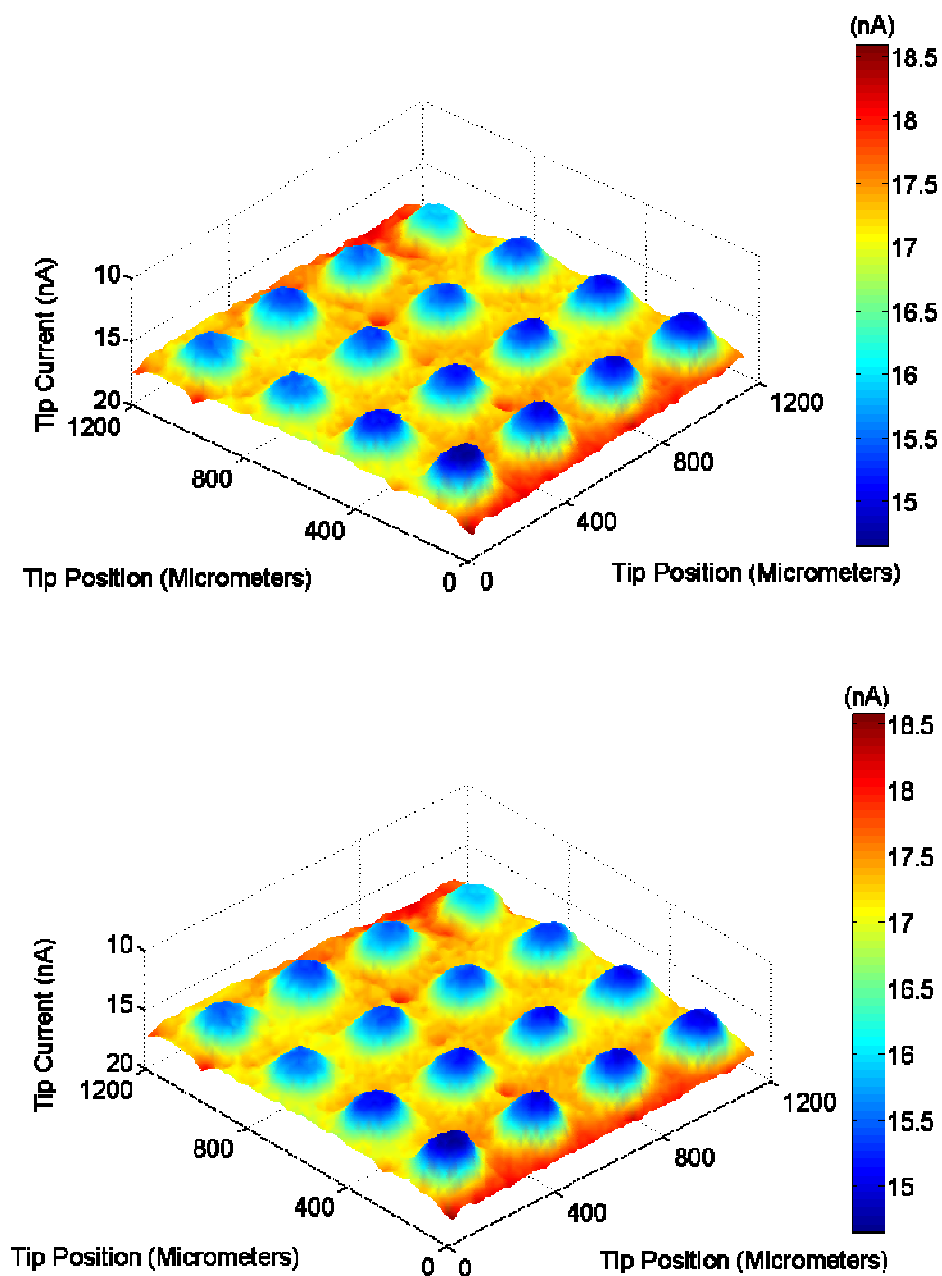
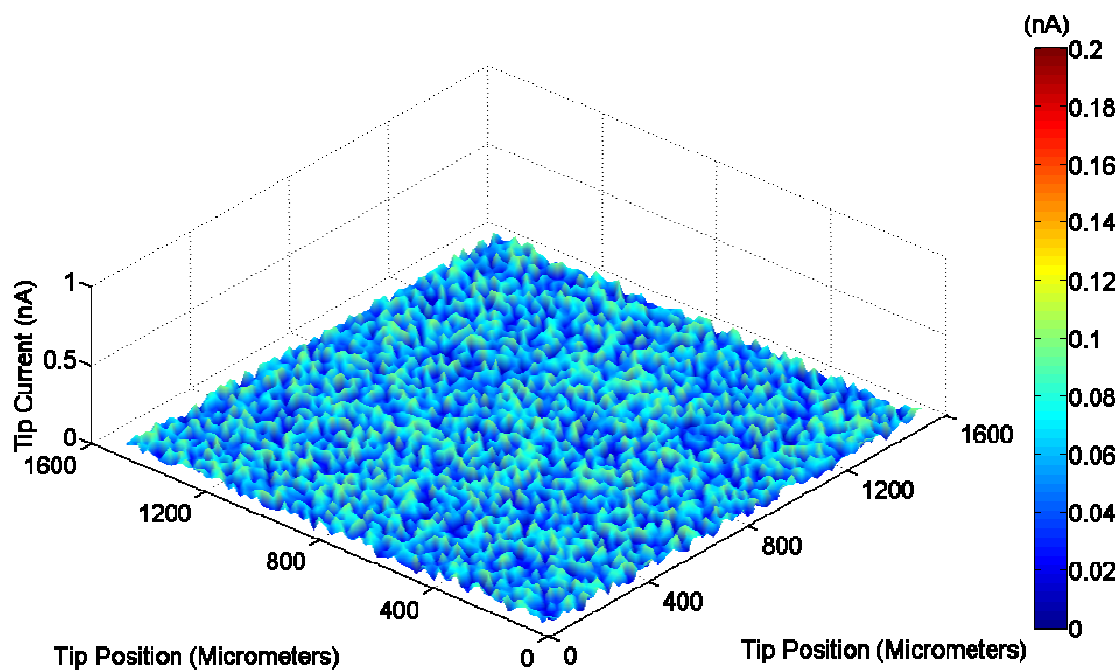


Figure 6.18: Area scan arrays before (A) and after (B) rinsing and 3hrs exposure to control solution (0.015mM phosphate buffer solution)



B)

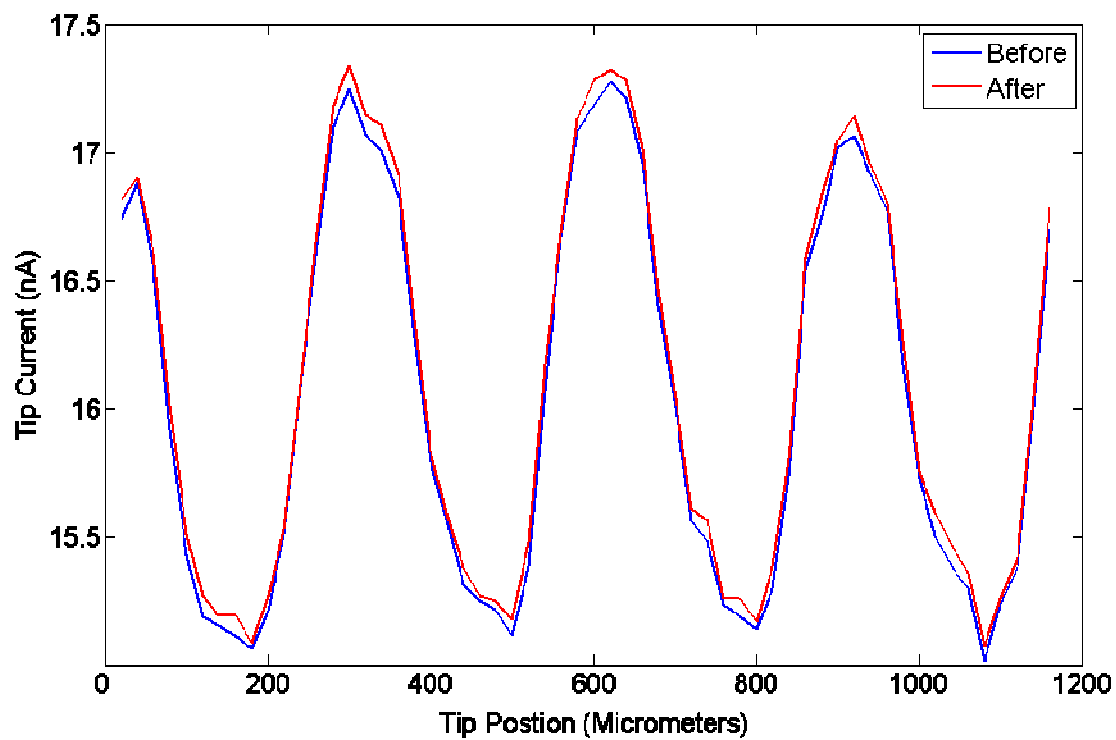


Figure 6.19: A) Array obtained from the subtraction of 'before' array from 'after' array; B) Representative linescans from before and after rinsing and exposure

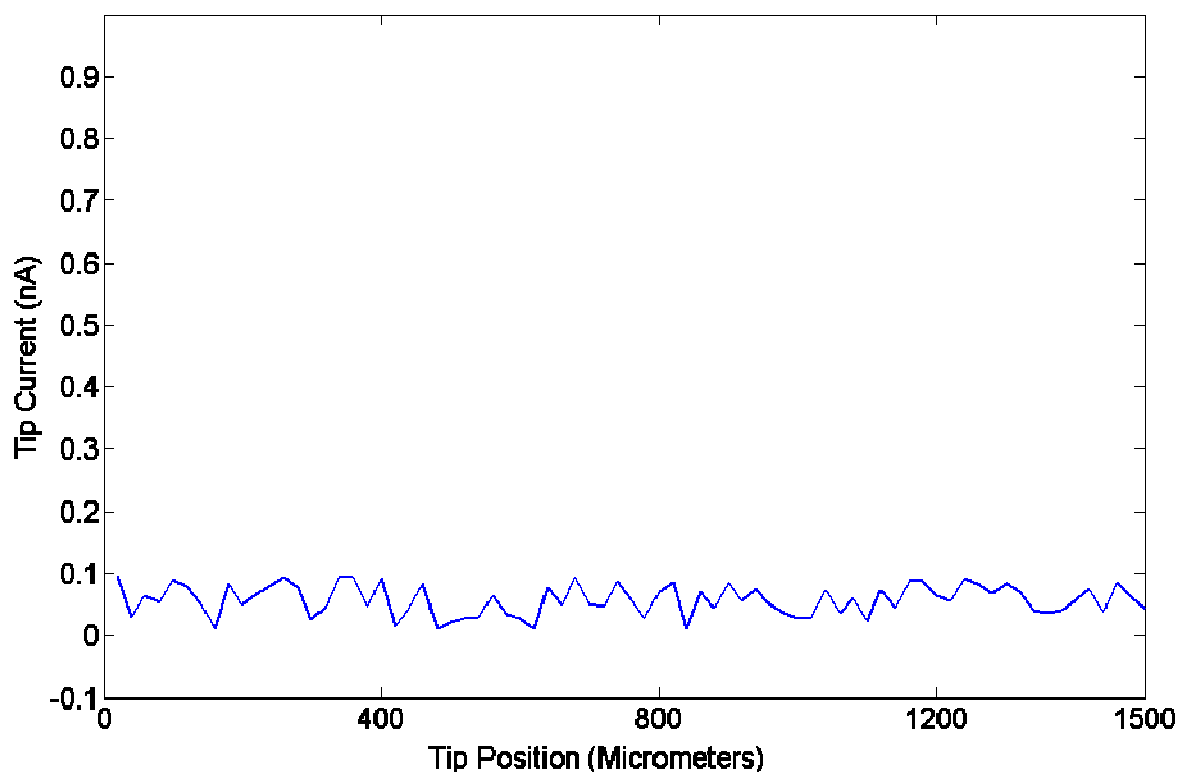


Figure 6.20: Linescan across array obtained by the subtraction of array 'before' and 'after' exposure to 'control' hybridisation solution

6.7 Hybridisation detection by SECM

After the preparation of the ssDNA/PEI arrays on the carbon electrode, the substrate was interrogated by SECM area scan. Following the successful completion of the scan, the mediator solution was removed and the substrate was rinsed with 5ml UHQ H₂O which was then also removed. 1ml of the hybridisation solution containing 0.015mM phosphate buffer and 0.2mg/ml of either complementary or non-complementary DNA in its single stranded form was then applied to the substrate and left at room temperature for 3hrs (ssDNA, formed by boiling dsDNA was also an approach used by Ding *et al* (2005)). After this time, according to Davis *et al*, changes in the impedimetric response are observed to plateau. Following the 3hr exposure period, the hybridisation solution was removed and the substrate rinsed once more with 5ml UHQ H₂O before the introduction of the electroactive mediator to the system – 5mM hexamine ruthenium chloride. Any possible

dilution effects were minimised by the removal and re-introduction of the mediator solution three times. Every precaution was taken in all cases to prevent moving the substrate and the tip. After the re-introduction of the mediator solution, the tip was re-positioned and the scan conducted once more using exactly the same parameters as the previous scan. Representative images of the data obtained by this technique are given in sections Figure 6.21.

Whilst the data used in the analysis of the arrays before and after exposure to complementary and non-complementary DNA were well resolved replicates, a number of problems arose relating to scanning height, substrate crash, tip fouling, and substrate slope. Much time was spent trouble-shooting these issues and making slight modifications to the experimental setup which would allow the collection of data of sufficient resolution and reproducibility for analysis. The dependence of the tip current on the tip to substrate distance was also a key consideration and care had to be taken to minimise any movement of the system.

On the initial comparison of the 'before' and 'after' scans (Figure 6.21), the exposure of the system to the complementary DNA solution appears to have had no effect on the charge transfer properties of the ssDNA/PEI film. However, on the subtraction of the 'before' scan from the 'after' scan, it becomes evident that there has indeed been a change (Figure 6.22).

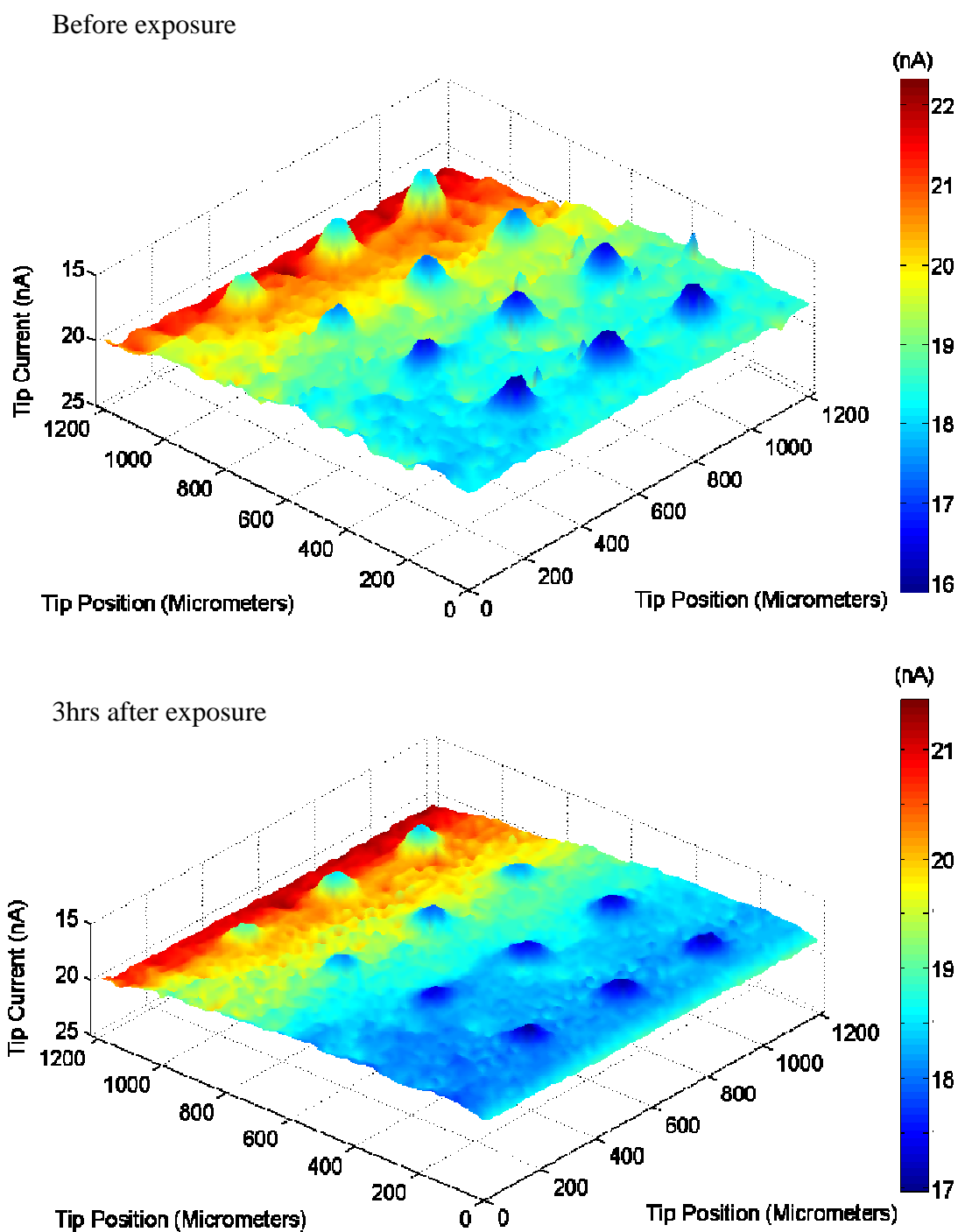


Figure 6.21: Area scans over PEI/ssDNA array before and after exposure to complementary ssDNA solution (0.2mg/ml)

Referring to Figure 6.22, the feedback current over the PEI/ssDNA array has increased – more specifically, the insulating effect of the PEI/ssDNA on the carbon electrode has fallen by 1.2nA, which represents an increase in the feedback current of approximately 7.5% in this representative example. In contrast, the feedback current over the non-functionalised carbon is unaffected.

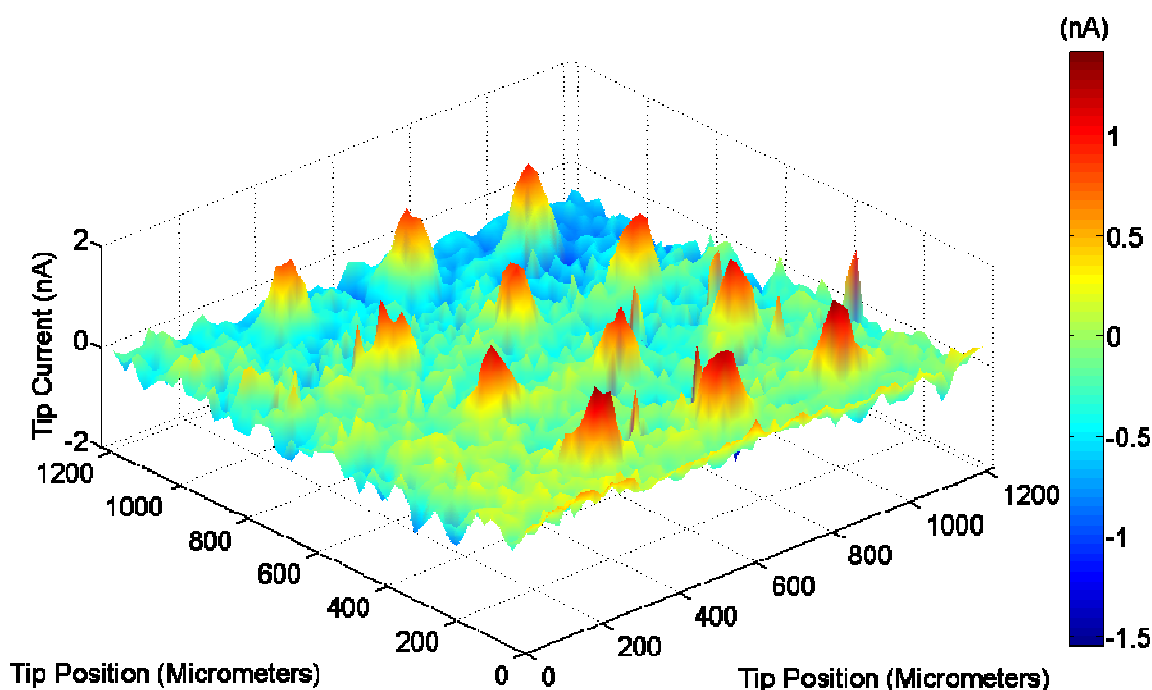


Figure 6.22: Absolute change in tip current after exposure to complimentary single stranded DNA

To aid the comparison of the two scans and the change in current between them, a cross section of each scan was plotted on the same axis (Figure 6.23 (A)). It can be seen from these linescans that there is a significant enhancement in the feedback current obtained following exposure of the system to the complementary DNA, which is in contrast to the observation that the non-functionalised regions do not given rise to such a change. The absolute change in the feedback current measured in each of these scans is given in (Figure 6.23 (B)).

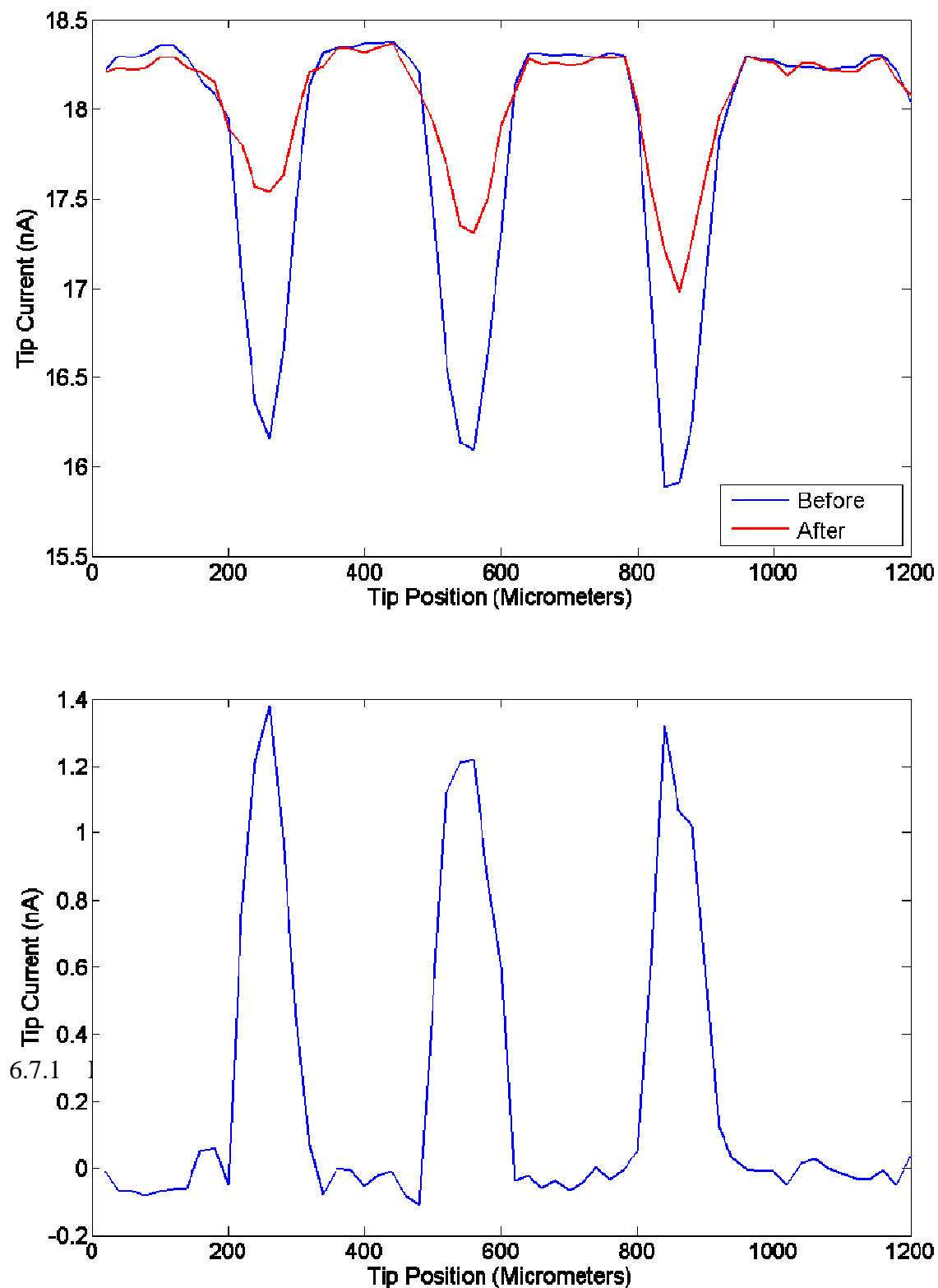


Figure 6.23: Linescans extracted from the area scans in A) Figure 6.21 and B) the array subtraction in Figure 6.22 – which is the difference of the two linescans in A)

Similarly to the complementary experiment described previously, on initial investigation, there appears to be little change in the feedback response measured before and after exposure of the ssDNA/PEI array to non-complementary ssDNA (Figure 6.24). On subtracting the 'before' area scan array from the 'after' after area scan array however, a much smaller increase in feedback current was observed, in the region of 0.2nA – a very small proportion of the initial feedback current (Figure 6.25).

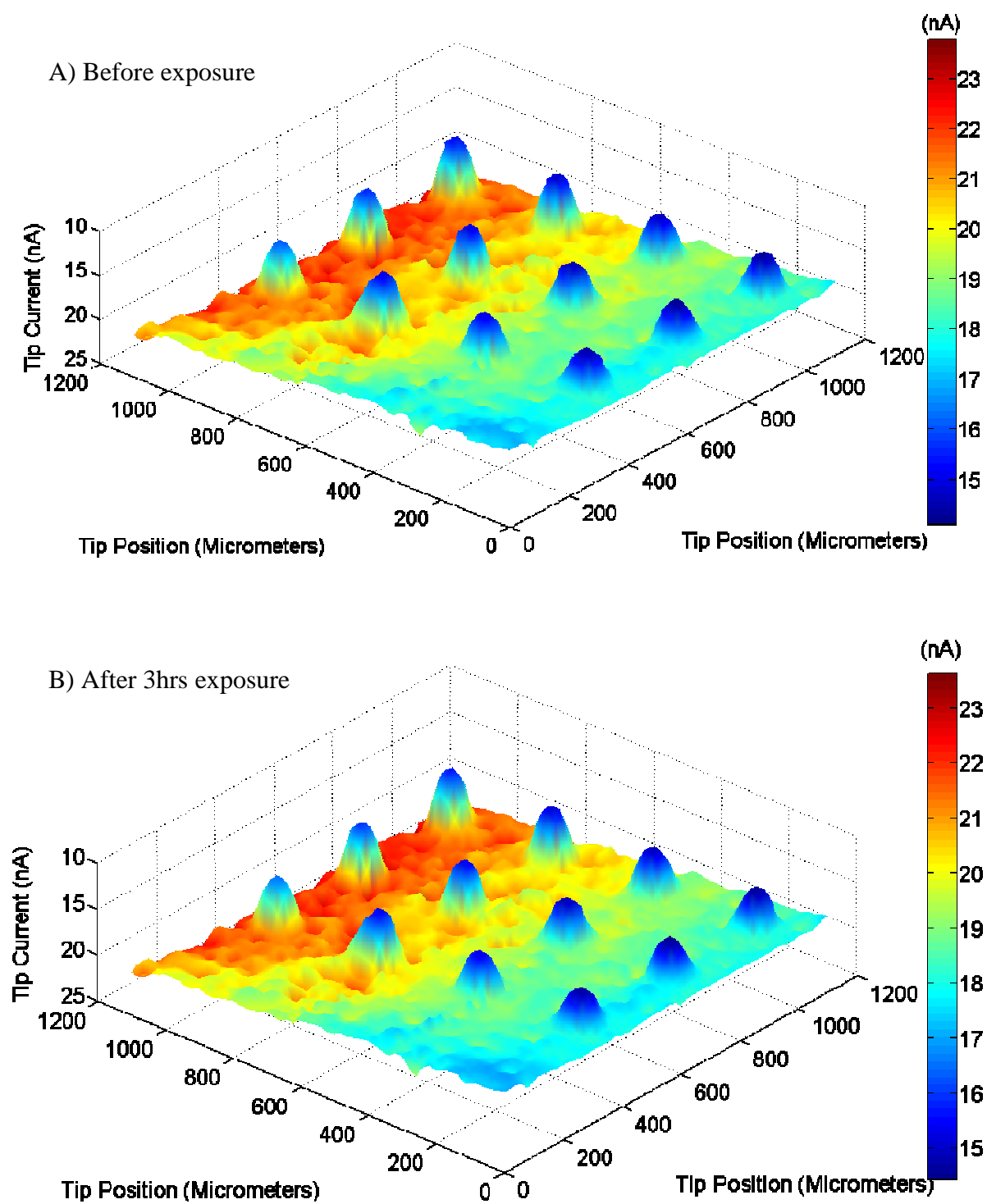


Figure 6.24: Area scans over ssDNA/PEI spotted array before and after exposure to non-complementary DNA

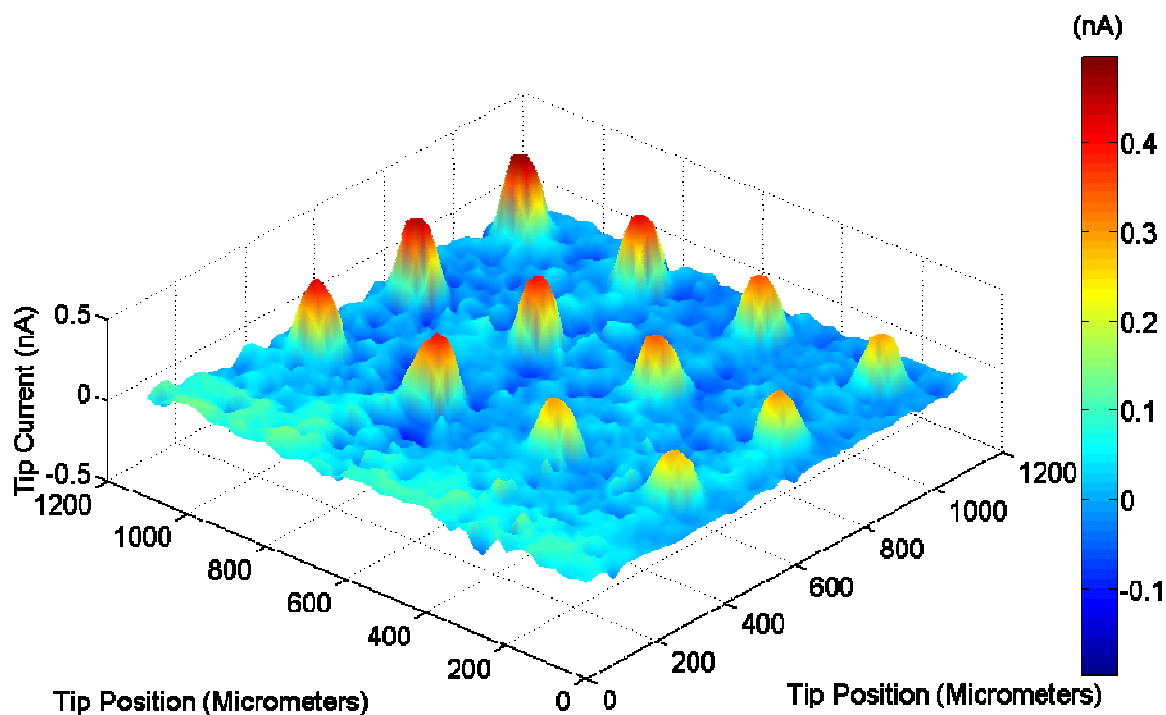


Figure 6.25: Absolute change in tip current after exposure to non-complementary DNA

To aid the comparison of the two scans and the change in current between them, a cross section of each scan was plotted on the same axis (Figure 6.26 (A)). It can be seen from these linescans that there is a very small enhancement in the feedback current obtained after exposure of the system to the complementary DNA, which is in contrast to the observation that the non-functionalised regions do not undergo such a change. The absolute change in the feedback current between each of these scans is given in Figure 6.26 (B).

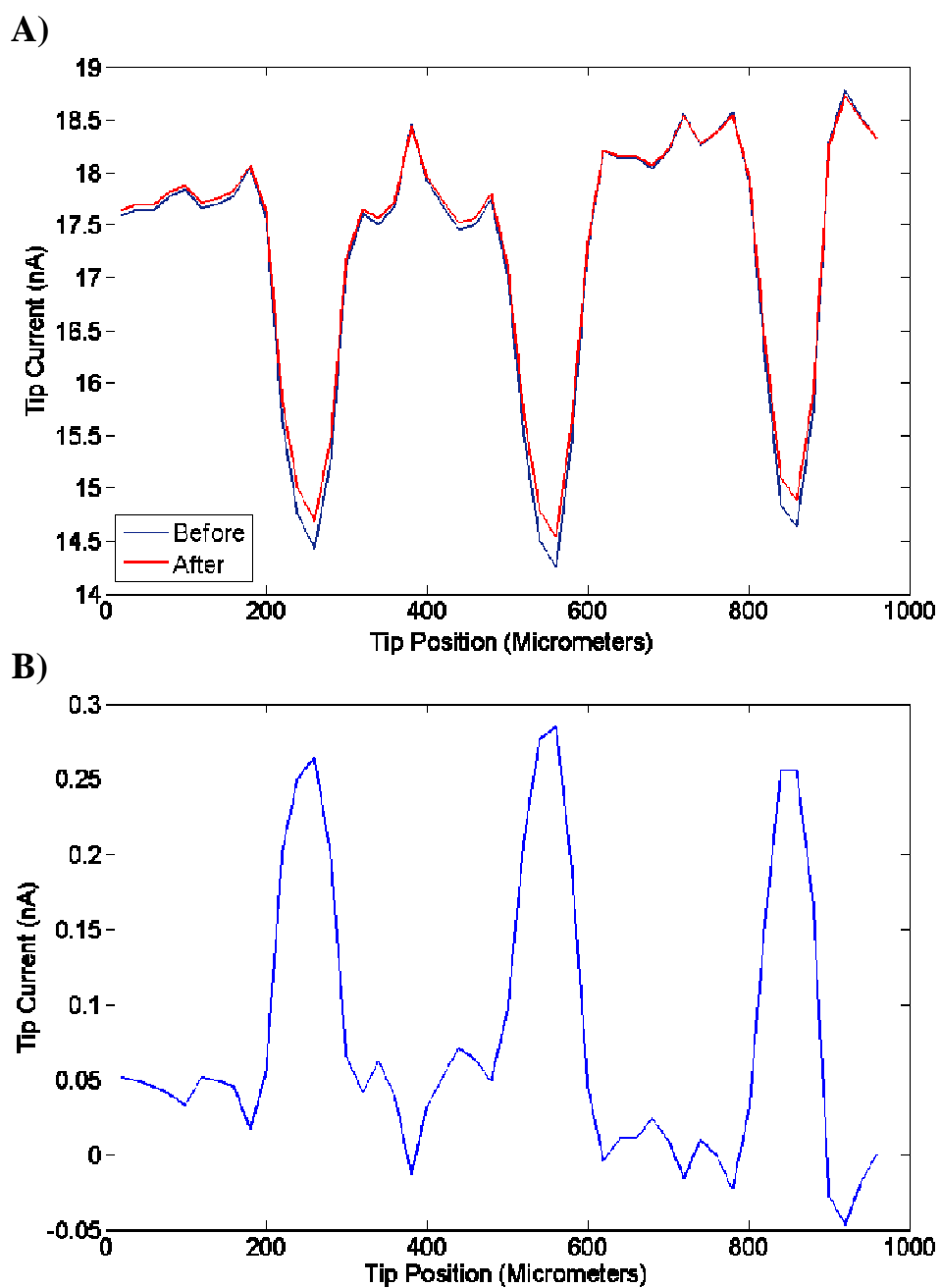


Figure 6.26: A) Series of linescans extracted from arrays represented in Figure 6.24 – the current profile across a spotted array before and after exposure to non-complementary DNA B) linescan extracted from Figure 6.25 depicting change in tip current after exposure to non-complementary DNA

The data presented in Figure 6.27 are representative linescans from the arrays formed by the subtraction of the array data obtained before and following the exposure of the PEI/ssDNA array to complementary and non-complementary DNA. It may be observed that the magnitude of the change is much more pronounced in the complementary experiment. This suggests that exposure of the PEI/ssDNA film to a hybridisation solution containing complementary DNA has a more significant effect on the feedback response of the polyelectrolyte film than the exposure of the film to non-complementary DNA.

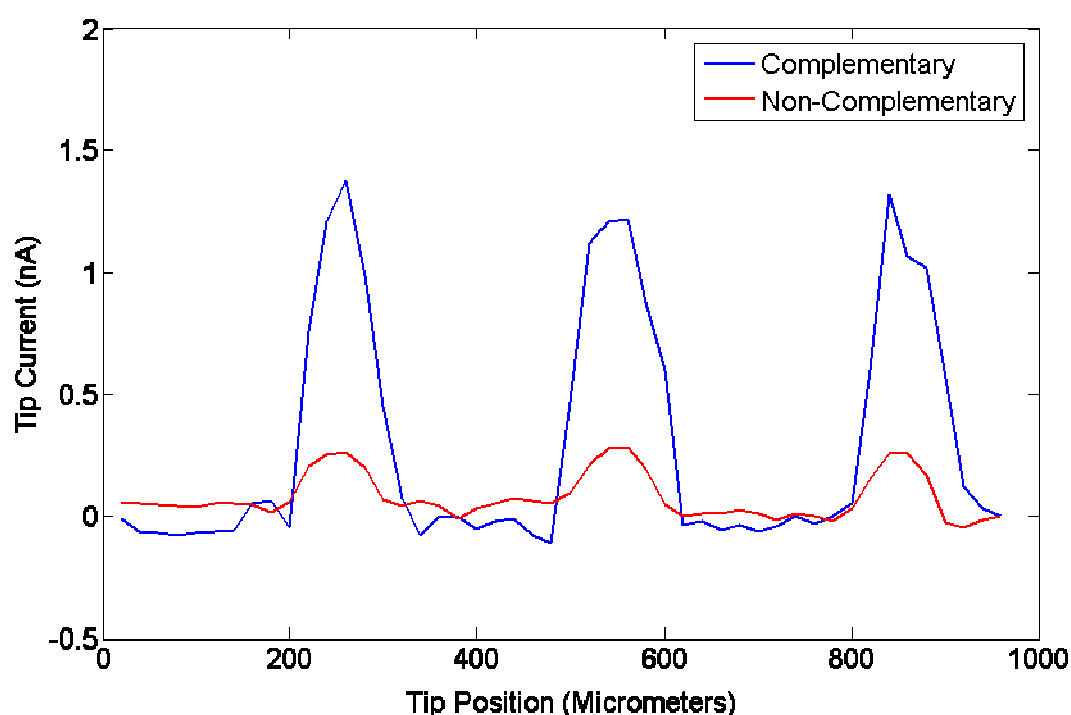


Figure 6.27: Linescans illustrating difference in feedback response after exposure to single stranded complementary and non-complementary DNA

Whilst these findings are evident in the representative data given above, to determine whether the differences observed in each replicate were statistically significant, the ROI GUI was used. Using the ROI analysis tool, the mean current value for each of the dots in the arrays before and following exposure to complementary and non-complementary DNA was calculated.

A single dataset was assembled from the average tip current over each dot in three experimental replicates (40 dots) and a paired t-test conducted on each merged data set before and following exposure to complementary and non-complementary DNA. The change in average tip current over each dot was found to be statistically significant for the complementary experiments ($t = 3.6536$; d.f. = 39; $p = 0.004$; CI = 0.14×10^{-9} to 0.5658×10^{-9}) and the non-complementary experiments ($t = 2.92$; d.f. = 39; $p = 0.0137$ CI = 0.074×10^{-9} to 0.5594×10^{-9}) - although the difference in p values suggests that the difference is more statistically significant in the complementary experiments.

On carrying out the same analysis on the same arrays but conducting a paired t-test on the minimum feedback current obtained over each dot, it was found that there was a statistically significant difference between the feedback current obtained before and after exposure to complementary DNA ($t = 6.092$; df=39; CI= 0.40×10^{-09} to 0.89×10^{-09} ; $p = 7.8262 \times 10^{-05}$). The same test on the non-complementary dataset revealed that there was also a statistically significant difference between the feedback current obtained before and following the exposure of the array to non-complementary DNA ($t = 19.4$; df=39; CI = 0.33×10^{-09} to 0.41×10^{-09} ; $p = 7.3993 \times 10^{-10}$).

To determine whether the changes in feedback current were significantly larger in either experiment, a one tailed t-test was conducted. The null hypothesis, that the enhancement in feedback current after exposure to the hybridisation solution was not significantly greater in the complementary experiment, was rejected. The alternative hypothesis, which states that the enhancement in feedback current was statistically significantly larger in the case of complementary hybridisation was hence accepted ($t = 2.36$; df = 38; $p = 0.0137$).

There are two suggestions as to why the observed changes in feedback current may have been observed. The first is based on the proposition that DNA is capable of conducting charge (Kliene *et al* 2004; Kelley *et al*, 1997; Williams, *et al* 2000; Jackson *et al*, 2001; Okada *et al*, 2003). On exposing the PEI/ssDNA film to a solution containing complementary genomic ssDNA, complementary binding occurs, where regions of the genomic DNA immobilised on the surface bind to complementary nucleotide sequences on genomic DNA suspended in the hybridisation solution. This complementary pairing forms double stranded regions of DNA at the surface of the sensor, enhancing the rate of electron

transfer from the carbon electrode surface to the mediator in solution as the double stranded regions act as ‘nano-wires’, allowing the transfer of electrons along its length with the effect of lowering the impedance of polyelectrolyte/solution interface.

The intrinsic conductivity of DNA and the migration of charge through the pi-stack has received much attention over the last decade – partly due to its increasing importance in the field of DNA biosensors and DNA based bioelectronics. As research continues, so does the divide between the findings. This is very much highlighted by the large body of research in photochemistry, radiation biology, electrochemistry and solid-state physics that now exists in the field of DNA-mediated charge transport (Jackson, 2001). An example of these disparate findings is highlighted by comparing the work of Barton’s group (Kelley *et al* 1999) and Meade *et al* (1995). In 1999, Barton and co-workers reported an intrinsic rate of $>10^9\text{s}^{-1}$ between photoinduced electron donors and electron acceptors held 15 base pairs apart on a double helix, whereas Meade *et al* reported a rate ~ 1000 times slower using reactants attached by electrostatic interaction to a duplex half as long.

A second hypothesis for the observed changes in the feedback current response however, is that on exposure to the ssDNA/PEI film, complementary ssDNA in solution becomes associated with the immobilised sections on the immobilised ssDNA on the sensor surface. As a result of this, the net charge on the sensor surface becomes more negative, which has the effect of allowing or ‘facilitating’ the diffusion of the positively charged ruthenium complex through the interpenetrating PEI/DNA film and towards the underlying conductive carbon electrode.

On imaging the DNA/polymer arrays, it is evident that despite the deposition of the polyanionic DNA onto the polycationic film, there is no apparent change in the polycationic properties of the film; using the $\text{Ru}(\text{NH}_3)_6^{3+}$ mediator, negative feedback is still observed. With reference to the images obtained using the ferrocenecarboxylic acid and ferricyanide mediators, the charges of the polymer and mediator are clearly important factors in determining whether a film will exhibit positive or negative feedback characteristics when interrogated. On depositing the initial, negatively charged ssDNA film on the polyethylenimine array, it may be expected that the apparent electrostatic charge would be reversed and that the film would exhibit positive feedback characteristics

as the positively charged mediator is attracted to the negatively charged DNA immobilised close to the electrode surface. This is not the case, however and despite ssDNA functionalisation, the film continues to exhibit negative feedback characteristics.

$\text{Ru}(\text{NH}_3)_6^{3+}$ has been used extensively in the electrochemical quantification of oligonucleotides on surfaces. In an investigation into the permeation of ions through DNA modified electrodes, a cyclic voltammogram of $\text{Ru}(\text{NH}_3)_6^{3+}$ at a DNA modified electrode showed that the mediator binds to the DNA at the sensor surface by charge interaction. On conducting a cyclic voltammogram for $\text{Ru}(\text{NH}_3)_6^{3+}$ using a DNA modified electrode, the cyclic voltammogram resembled that which may be obtained by using a surface bound species where the peak shape is symmetrical and lacks any kind of diffusive tail (Ceres *et al* 2007). These findings may be related to the observations in this series of experiments. On the interrogation of the initial ssDNA/PEI film, negative feedback is observed as the net charge of the film remains positive as a result of the neutralisation of the excess charge of the DNA above that compensated for by the polyethylenimine film.

The smaller enhancements observed with the non-complementary experiments may be explained by a lesser degree of binding occurring between non-complementary strands and mis-matching which may occur when non-complementary binding occurs. As the DNA used is genomic, there are considerable sections of the DNA used that contain long range repeats – sections of DNA that contain the same sequence repeated for thousands of base pairs. As the DNAs used are those for Herring and Salmon, it is likely that they share similar repeats. Attempts were made to determine the degree of homogeneity between these two organisms for a percentage similarity, using various DNA sequence databases but these organisms' genomes have not yet been sequenced. Also, the likelihood of binding occurring by chance collisions of matching sequences approximately similar is high when using genomic DNA. The argument is hence that binding may occur in the non-complementary system but to a lesser extent to that observed in the complementary system. This point is very much supported by the work conducted by Nabok and Davis *et al* (2007).

A point for consideration however, is whether the changes observed are due to any kind of binding at all, but to some other affinity interaction, in the form of some other property of

genomic DNA that gives it an enhanced structural affinity for DNA of its own 'type' (i.e. genomic DNA from the same species interacts more strongly than DNA from different species) (Martin and Hoyer 1966).

The sensitive optical method of total internal reflection ellipsometry (TIRE) and atomic force microscopy (AFM) was used to investigate the interactions between and within DNA / PEI films (Nabok *et al* 2007). In a separate study using TIRE ellipsometry, the thickness and refractive indexes of adsorbed DNA layers on polyethylenimine films were determined. On exposing herring-ssDNA to herring-ssDNA immobilised on the surface of the polyethylenimine film, a thickness change of approximately 20nm was observed in comparison to a smaller change in thickness of 3-5nm when Herring-ssDNA was exposed to non-complementary Salmon-ssDNA. This differential change in thickness suggests that a greater quantity of genomic DNA is adsorbed onto the surface by complementary than non-complementary interactions (such changes may be investigated further by using a quartz crystal microbalance). It hence follows that the larger increase in feedback current observed over arrays exposed to complementary DNA may be explained by the larger amount of negatively charged DNA drawing more positively charged ruthenium to the surface of the carbon electrode by electrostatic interactions.

In the experiments conducted by *Davis et al*, changes in the impedance of the polyethylenimine film were observed to plateau over the course of three hours to a relative impedance of approximately 90% of that observed at the beginning of the experiment. The aim of this work was to investigate whether SECM in feedback mode was capable of monitoring these changes after this time period.

A possible avenue of investigation was to investigate the change in feedback current following exposure to the non-complementary and complementary hybridisation solution. However, this was not possible for a number of reasons. Firstly, the arrays are interrogated by SECM in feedback mode, which necessitates the use of an electroactive mediator. To monitor the change in the feedback response with time, the hybridisation solution would have to be repeatedly removed and replaced with mediator, which would inevitably introduce error and increase the risk of disturbing the polyelectrolyte film. Secondly, unlike the impedimetric approach in which an impedance measurement is taken in a matter

of seconds, area scans of the arrays fabricated here took over 1.5hrs. Preliminary experiments employing approach curves were carried out with the aim of minimising the time required to interrogate each substrate, but due to the heterogeneous nature of the carbon, the feedback response varied significantly across the substrate as some regions exhibited positive feedback while others demonstrated negative feedback despite being exposed to the same treatment. The area scan method provides a better insight into the electrochemical properties of the surface.

6.8 Conclusions

The principle aim of this chapter was to explore the possibility of using SECM to characterise a previously optimised impedance based DNA biosensor developed within the group (Davis *et al* 2007). The sensor is based on the construction of a bio-polyelectrolyte film of polyethylenimine and single stranded genomic DNA on a carbon ink electrode surface. The impedance of the sensor was observed to drop by approximately 10% in 3hrs on exposure to a hybridisation solution containing single stranded complementary genomic DNA. In contrast, on exposing the sensor to a buffered solution of non-complementary ssDNA, the impedance was observed to marginally increase. One of the aims of the research reported in this chapter was hence to determine whether these small changes in the impedance of the system were detectable by SECM in feedback mode within this time frame. In addition, it was hoped that the results would provide a valuable insight into other aspects of the biosensor for consideration in later studies.

Using the area scan macro, the spatial heterogeneity of the carbon electrodes used in the fabrication of the biosensor was demonstrated. Whilst this substrate is suitable for impedimetric analyses and fulfils the requirements of a disposable biosensor such as ease of fabrication, cost effectiveness and mechanical robustness, if the SECM array system described within this chapter is to be considered for further development, it is suggested that alternative, more topographically homogenous electrode surfaces should be investigated including gold, silicon and glassy carbon.

A polyelectrolyte film was constructed using polycationic polyethylenimine and polyanionic single stranded genomic herring DNA. The initial polyethylenimine layer was patterned in an array format, demonstrating the ability of the SECM XYZ micropositioning system to fabricate polyelectrolyte arrays of differing densities. On the interrogation of the system by SECM, the potential of the SECM approach to monitoring polyelectrolyte film formation was demonstrated.

Using the area scan macro and a variety of differently charged mediators, the insulating properties of the polyelectrolyte film were investigated. On using alternately charged mediators, it was revealed that the insulating effect of the polyethylenimine film on the

carbon substrate could be reversed. When the PEI array was interrogated by an area scan using the positively charged hexamine ruthenium chloride mediator, a diminution in the feedback current was observed. However, on using the oppositely charged ferricyanide redox couple, the opposite was found – and was thought to be a result of the coulombic, electrostatic interactions of the film and the differently charged mediators. These results successfully demonstrate the polycationic properties of the polyethylenimine film and its suitability to immobilising polyanionic ssDNA.

After the characterisation of the carbon/polyethylenimine array and the identification of a suitable redox couple ($\text{Ru}(\text{NH}_3)_6^{3+}$), the complete platform was interrogated by SECM. In brief, this involved comparing area scan data obtained by scanning the PEI/ssDNA array before and after exposure to complementary and non-complementary genomic DNA. It was found that on exposure to the complementary genomic DNA, the charge transfer properties of the ssDNA/PEI film were enhanced. This was also true for non-complementary exposure, although to a lesser degree.

Within this series of experiments, large quantities of genomic DNA have been used, following the same protocol as that employed by Davis *et al.* Whilst small changes in the charge transfer properties of the arrays were detected, the reason behind these changes is not completely understood.

To examine the true potential of the SECM approach in the label-less detection of DNA hybridisation, shorter DNA sequences should be used which would have a higher probability of exhibiting complementary binding and allow an improved understanding of the changes in the charge transfer properties of the polyelectrolyte film.

Within this chapter, a sound methodology has been developed for the fabrication, interrogation and subsequent analysis of a previously developed genomic DNA biosensor based on the functionalisation of a polyelectrolyte film with single stranded genomic DNA.

Chapter 6

**Characterisation of DNA biosensor and
detection of changes in
DNA/polyelectrolyte film charge transfer
properties by SECM**

6. Characterisation of DNA biosensor and detection of changes in DNA/polyelectrolyte film charge transfer properties by SECM

6.1 Introduction

This chapter describes the use of scanning electrochemical microscopy for the characterisation of a DNA biosensor previously developed within the group (Davis *et al*, 2005). The work successfully demonstrates the usefulness of the technique in biosensor development, whilst also highlighting the possibility of using SECM for the label-less detection of DNA hybridisation.

The development of technologies capable of detecting specific DNA sequences in real time has significant implications for studies and diagnostic tests associated with clinical applications, environmental regulation, food science, agriculture and forensics (MacPherson *et al*, 1993; Wang, 1997; Lucarelli *et al*, 2002; Babkina, 2004).

The concept of the DNA biosensor was first introduced by Millan and Mikkelsen in 1993. The DNA biosensor is an analytical device which allows the recognition of a DNA hybridisation event and its conversion into a detectable signal (see Figure 6.1). Generally speaking, the system is composed of a detection component in which a single stranded DNA sequence is immobilised onto a surface which is then exposed to a hybridisation solution containing the target sequences. If the solution contains a sequence complementary to the immobilised probe DNA, complementary binding may occur. Complementary binding may then be detected by the transducer - which may be based on optical, gravimetric or electrochemical approaches (Okumura, 2005).

Electrochemical techniques for the detection of DNA hybridisation events have received a considerable amount of attention over recent years – partially as a result of the success of the blood-glucose sensing technologies - but also because of the numerous advantages they offer over alternative approaches to DNA assaying. Such techniques potentially offer high sensitivity and are compatible with modern microfabrication technologies.

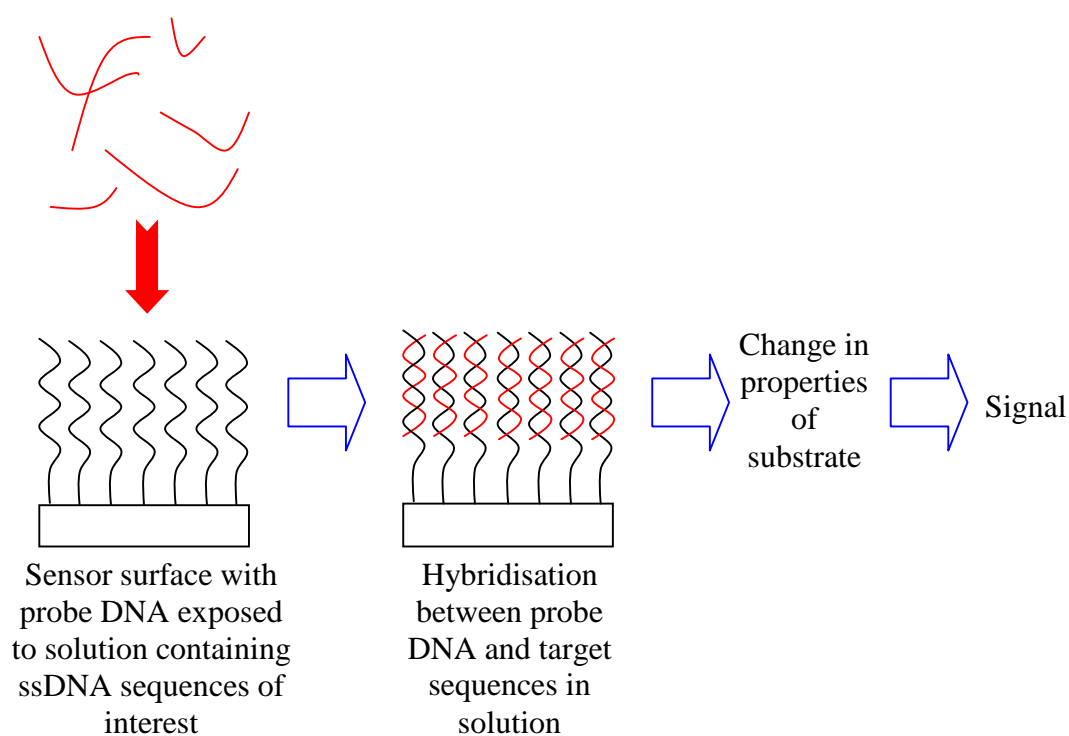


Figure 6.1: Schematic illustrating principle of DNA biosensor

The most frequently employed electrochemical strategies for detecting the hybridisation event rely on redox-active hybridisation indicators which have a greater affinity for double stranded rather than single stranded DNA (e.g. Hashimoto, 1994). In these systems, electrodes are functionalised with single stranded oligonucleotides with which target sequences bind to form a duplex. On the formation of a duplex, the indicator (which may be a cationic metal complex, a groove binder or intercalator) binds preferentially to the double stranded region, resulting in an increase in the local concentration of the indicator at the surface of the electrode. This may be detected by electrochemical approaches such as cyclic or chronoamperometric voltammetry (Hashimoto *et al*, 1994; Millan and Mikkelsen, 1993; Kelley *et al*, 1997). Zhou *et al* for example recently reported danthron (1,8-dihydroxy-anthraquinone) as having the ability to intercalate with DNA; due to its planar structure, it was found that Danthron slots between adjacent base pairs and in doing so, discriminates between DNA in its single and double stranded forms (Zhou *et al*, 2005). Daunomycin, a more well characterised intercalator, is known to bind to the guanine residue within the DNA duplex - Cheng *et al* recently reported a detection limit of 2.3 x

10^{-14} mol/L of target oligonucleotide using daunomycin and mercaptoacetic acid coated magnetite nanoparticles (Cheng, 2005;). Navarro *et al* directly labelled the probe DNA with ferrocene phosphoramidites (Navarro *et al*, 2004).

Whilst the electrochemical labelling approach has much potential in the development of a rapid sensing technology, there is much scope for the direct, label-less detection of DNA hybridisation by electrochemical methods. By removing the necessity for labelling, sensors are capable of offering faster responses and require fewer reagents, making them an extremely attractive route of investigation. A label-less detection mechanism such as this involves monitoring the changes in the physicochemical properties of the film by electrochemical methods. An example of a label-less system such as this was developed by Wang *et al*, who reported the label-free detection of DNA hybridisation by doping electropolymerised conducting polypyrrole films and monitoring the current-time profiles on the addition of complementary DNA sequences to the system (Wang *et al* 1999; see also Hui, 2005). In a similar system, detection limits of 1.6fmol of complementary oligonucleotide target in 0.1ml was reported by Komarova *et al* (2005). For a comprehensive review of electrochemical DNA biosensors, the reader is referred to Wang *et al* (1997), Thorp (1998), Pividori *et al* (2000), Gooding (2002) and Kerman *et al* (2004).

Within this chapter, a DNA biosensor previously developed within the group is interrogated by scanning electrochemical microscopy (Davis *et al* 2005). The biosensor is based on the modification of a carbon electrode with a genomic DNA/polyelectrolyte film which is then exposed to a solution containing either non-complementary or complementary single stranded genomic DNA. In this work, changes in the charge transfer properties of the film were monitored by impedimetric approaches. It was found that on exposing a carbon electrode modified with a polyethylenimine (PEI)/ssDNA film to a solution containing complementary ssDNA, the impedance of the system dropped approximately 10% over the course of three hours, after which time the impedance was observed to plateau. In contrast, on exposing the ssDNA/PEI film to non-complementary DNA, the impedance of the system increased slightly.

By interrogating the same system using SECM, valuable insights may be obtained regarding the fabrication of this biosensor and the applicability of SECM to detecting DNA hybridisation. SECM offers a route for non-contact electrochemical interrogation, negating the need for hard-wired electrodes; this in turn offers the potential for developing an array based approach which may be interrogated via a scanning probe tip.

In brief, the aim of the work presented in this chapter is two-fold:

1. To investigate the different components of the DNA biosensor developed by Davis *et al* by SECM, which will provide a useful insight into the methodologies employed in its fabrication.
2. To conduct a preliminary investigation into whether SECM may be used to differentiate between non-complementary and complementary DNA hybridisation.

6.2 Results and Discussion

6.2.1 Carbon electrode substrate

As described earlier, the substrate used in this series of experiments was the same as that used in the original study by Davis *et al.* An image of the sensor used is given below (Figure 6.2).

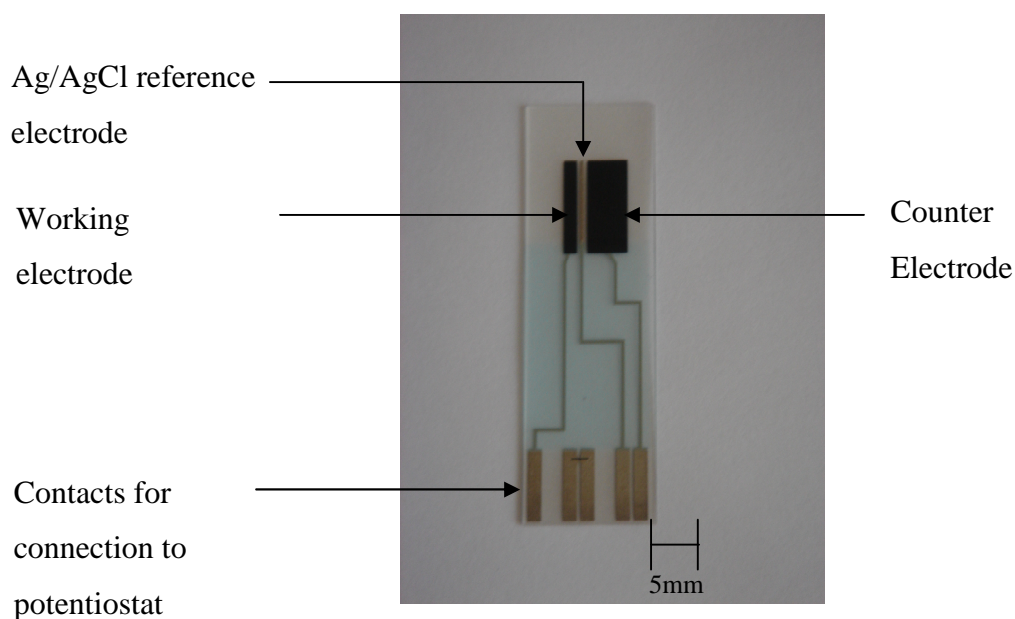


Figure 6.2: An image of the carbon paste electrode used in the study. The working electrode was patterned with the polyethylenimine array

The application of thick film, screen printing techniques to the fabrication of electrodes represents the most promising route towards the mass production of inexpensive yet highly reproducible biosensing devices (Alvarez-Icaza *et al.*, 1993).

As a result of the ease with which screen printed electrodes may now be fabricated and their application to blood glucose sensing, screen printing technologies have undergone intense development (Hart and Wring, 1997; Albareda-Silvert *et al.* 2000). Screen printed electrodes are now the substrate of choice for a wide range of sensing applications.

The screen printing of the functional sensing electrode has two main stages: the first is the deposition of the conductive film, which is achieved by forcing a conductive ink through a patterned screen. The second is the curing phase, achieved by either heating or photocuring; during this step, the solvent within the ink evaporates. This process is then repeated depending on how complex the pattern is. Insulating dielectric films may also be used to define electrode areas.

Silver based inks are generally used for reference electrodes, whilst carbon or metallic inks (e.g. Pt, Au, Ag) are used for the working and counter electrodes of the sensor.

There are various advantages associated with the use of carbon inks; they exhibit lower background currents over a wider potential window than metal electrodes which improves the signal/noise ratio and lowers the detection limits of the system under investigation (Niwa *et al*, 1994; Gilmartin *et al*, 1995). The graphite based carbon electrodes are also extremely robust and this allows them to be used in turbulent conditions (Wring *et al*, 1990). Moreover, they are extremely cost effective, making them ideal for single use applications. Screen printed electrodes additionally offer a clean electrode substrate electrode for each analyte and negate the need for electrode cleaning between analytical determinations.

6.2.2 Characterisation of carbon inks by SECM

Generally, carbon inks are composed of graphite particles bound by a polymer and a selection of additives which allow the dispersion, printing and adhesion of the ink to the base substrate (Adams, 1958; Svancara *et al*, 1996a, 1996b; Grennan *et al*, 2001). As a result of this heterogeneous composition, there is a great deal of topographical variation in the conductivity of the electrodes produced. These heterogeneities were investigated by SECM.

Prior to each area scan, the microelectrode tip was positioned at a height where the tip current was equal to half of that obtained in bulk solution. The area scan shown in Figure 6.3 was conducted using the hexamine ruthenium chloride redox couple (5mM). On scanning across the carbon/millinex border, a 30% increase in the tip current is observed as

a consequence of positive feedback due to the recycling of the hexamine ruthenium redox couple at the conductive substrate. On further interrogation of the carbon substrate at a decreased tip to substrate distance, (see Figure 6.4) it is evident that there is a considerable amount of variation in the feedback response.

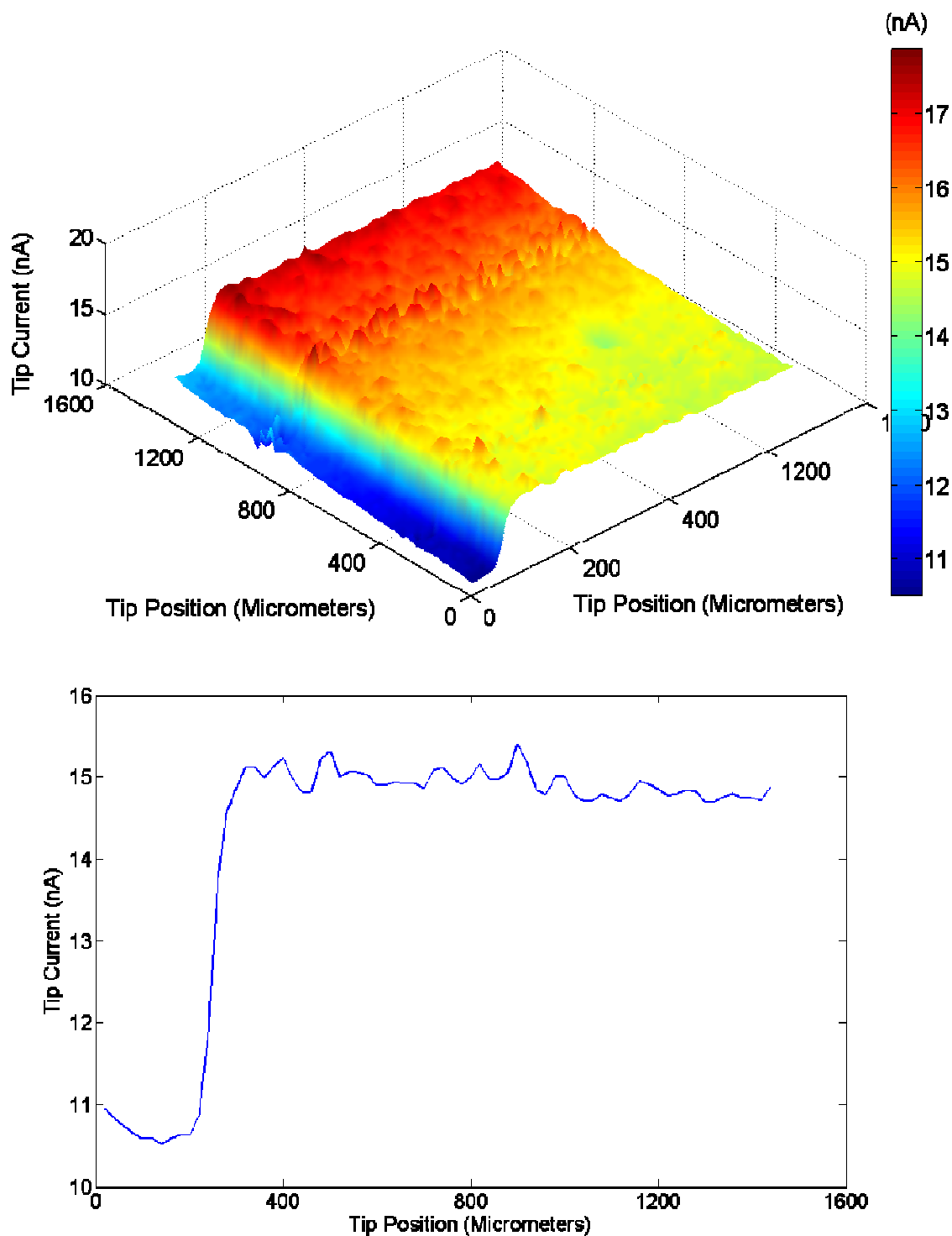


Figure 6.3: (A) Area scan over border between carbon (green/yellow region) substrate and millinex printing substrate (dark blue region) ; (B) Linescan across border at a tip position of 800microns

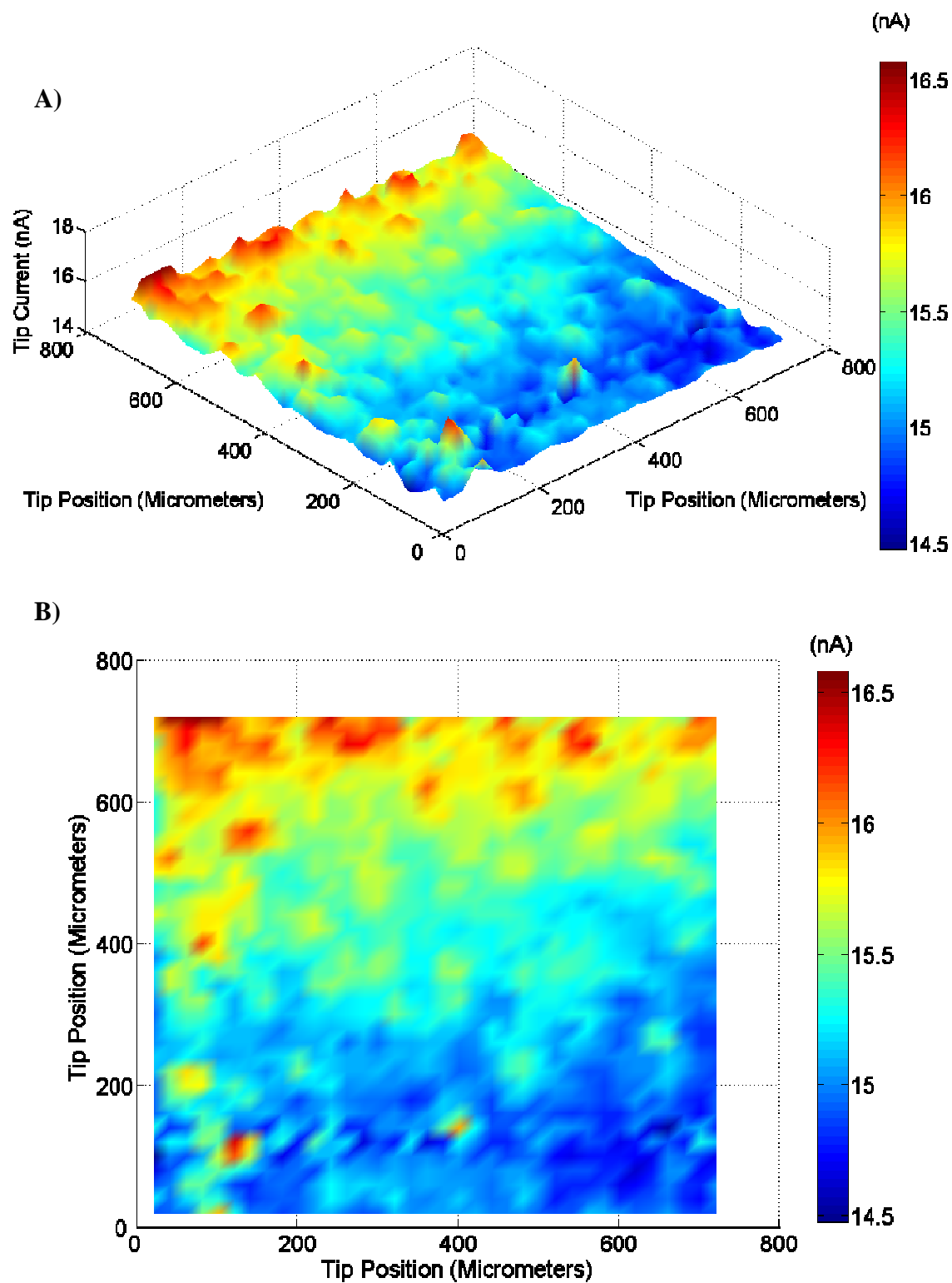


Figure 6.4: A) 3D representation of the data obtained from area scan images of a carbon ink electrode. Current hotspots show areas of raised topography and/or increased conductivity arising from the heterogeneous nature of the carbon ink used. B) A 'birds eye view' of 'A'

The observed heterogeneity may be due to variation in the conductivity of the substrate, arising as a result of the composition of the carbon ink. Electrical conductivity within the bulk system occurs by physical contact between graphite particles, providing a conductive route through the polymeric medium (Svancara *et al*, 2000), although an alternative mechanism involving indirect electron tunnelling between proximal particles has been suggested (Svancara *et al*, 2000). However, although the addition of conductive particles such as carbon black are added to the ink to enhance conductivity, regions of higher conductivities and hence, higher rates of heterogeneous charge transfer may still exist as a result of the physical properties of graphite. Graphite, an allotrope of carbon, consists of carbon atoms arranged in a hexagonal sheet, with each atom covalently bound to three other surrounding atoms; the remaining fourth electron is donated to a delocalised system of electrons between sheets. As a result of this delocalised system, there is high electron mobility parallel to the plane of the sheets, yielding excellent conductivity – of the order of $\sim 0.1 \Omega\text{cm}$ (McCreery, 1991). This is in contrast to the conductivity of graphite across the sheets – of the order of $\sim 1 \times 10^{-4} \Omega\text{cm}$. As a result of this differential conductivity, the edge plane of graphite exhibits excellent conductivity, whilst the basal plane is highly insulating. Considering that there is no mechanism by which to orientate the graphite particles in the carbon ink, the result of this differential conductivity is a surface with highly heterogeneous charge transfer, with some areas exhibiting higher rates of heterogeneous rates of charge transfer than others.

A further possible reason for the observed heterogeneity in feedback response is the variation in the topography of the substrate. When the tip is translated across the substrate, raised regions are closer to the tip, resulting in an enhanced positive feedback effect as the distance across which the recycled mediator has to travel is less than for areas that are topographically further away from the tip. This may either be as a result of the topography of the underlying millinex substrate, variation caused by the screen printing process, or be due to variations in the size of particles incorporated into the ink.

These two hypotheses for the observed variation in tip current highlight one of the central problems in interpreting SECM data. Without the aid of a constant distance approach, it is not possible to differentiate current variation due to differences in the electrochemical properties of the surface from those variations due to topographical variations.

6.2.3 Polyelectrolyte films

Polyelectrolyte films have been used extensively in the preparation of biosensing elements. Films such as these may be assembled by taking advantage of the strong forces of attraction between oppositely charged polyelectrolytes, a technique first reported by Decher *et al* (1992). The procedure is very simple and is demonstrated schematically in Figure 6.5. First, a charged solid substrate (in this case a negatively charged carbon ink electrode) is submerged in a dilute solution of an oppositely charged polymer (polyethylenimine) where strong multiple charge interactions result in the formation of a thin film of the polyelectrolyte across the substrate surface. After rinsing, the film coated sample is exposed to an alternately charged polymer (DNA) which has the effect of reversing (or perhaps only neutralising) the charge of the substrate by the adsorption of the polymer onto the substrate surface. If this process is repeated, a polyelectrolyte multilayer may be constructed.

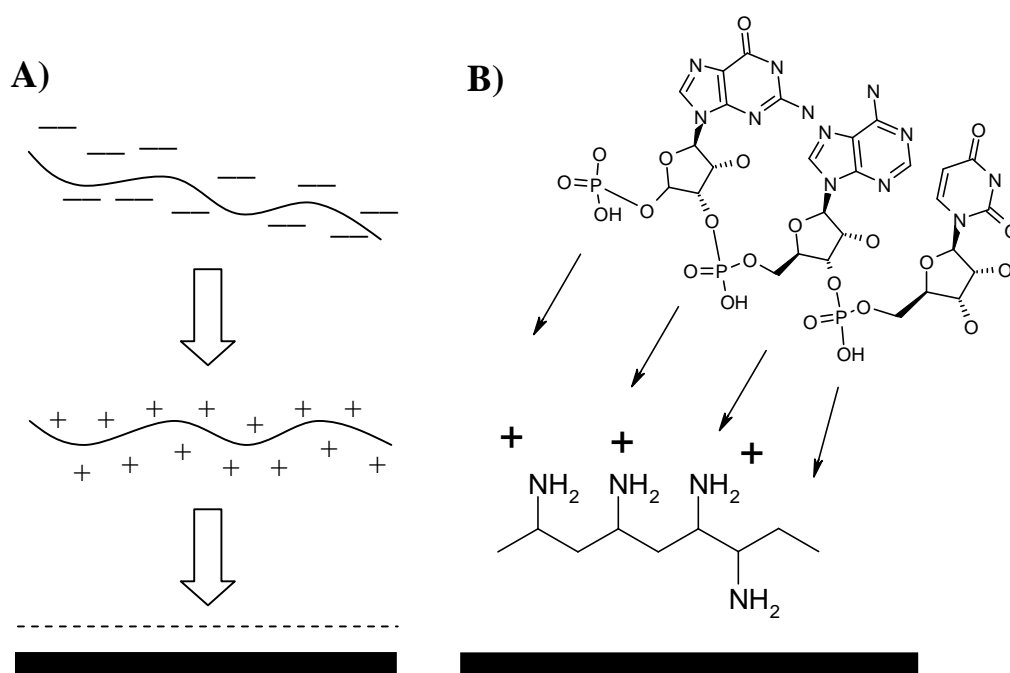


Figure 6.5: Schematic detailing construction of a A) general multilayer polyelectrolyte film B) DNA/polyethylenimine film

The use of polyelectrolyte films in the immobilisation of DNA was first reported in the early 1990s (Lvov *et al* 1993; Sukhorukov *et al* 1996). Since then, the technique has become widely employed in the development of DNA immobilisation and biosensing technologies, in which both oligonucleotides and complete DNA molecules have been used (Xi, *et al* 2000; Travas-Sejdic *et al* 2006). The technique has also been used to immobilise single stranded probe DNA on support structures, allowing hybridisation to complementary sequences in solution (Nicollini *et al*, 1997; Davis *et al* 2005).

In the biosensor developed within the group, a carbon ink electrode was dip coated with the polycationic polyethylenimine (Davis *et al* 2005). Whilst this was a suitable approach for sensor preparation for impedimetric analysis, it was not appropriate for the preparation of electrodes to be interrogated by SECM. The reason for this was that by imaging a homogeneously treated surface, it is not possible to compare a modified region with an unmodified region. Any changes in the tip current may be due to changes in the background current and not due to changes in the charge transfer properties of the modified substrate. It was therefore decided that for SECM interrogation, the polyelectrolyte film should be patterned in an array format. By producing this pattern, background changes in the feedback current could be determined by comparing the feedback signals over unmodified carbon (Figure 6.6).

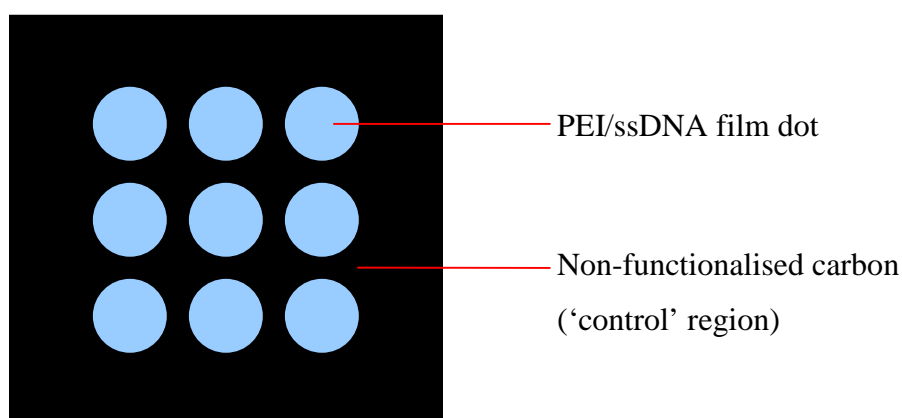


Figure 6.6: Schematic illustration of patterned polyelectrolyte film which allows the monitoring of the change in background current over an unmodified surface against the change in feedback response over PEI/DNA modified carbon

As described in the methods section (Chapter 3) the patterned array was achieved by using the SECM micro-positioning XYZ stage. A capillary was filled with the polyelectrolyte (polyethylenimine – PEI) and lowered towards the carbon substrate (Figure 6.7). The deposition process was accomplished by monitoring the tip to substrate distance by video microscope and by eye. By observing the small meniscus at the tip of the pulled capillary it was possible to determine the point at which contact was made and when the deposition of the PEI droplet was achieved. After deposition, the tip was retracted and moved in the X or Y direction respectively and the process repeated. Arrays with a variety of spot sizes and densities were possible (Figure 6.8). After deposition, arrays were rinsed. Problems arose with using larger dots however, as the surplus polymer attached to the non-functionalised regions during rinsing, resulting in poorly defined arrays.

As mentioned previously, this aspect of the work effectively illustrates the promise of the system to be used in micropatterning solution arrays and represents a significant route for investigation by Uniscan Instruments Ltd.

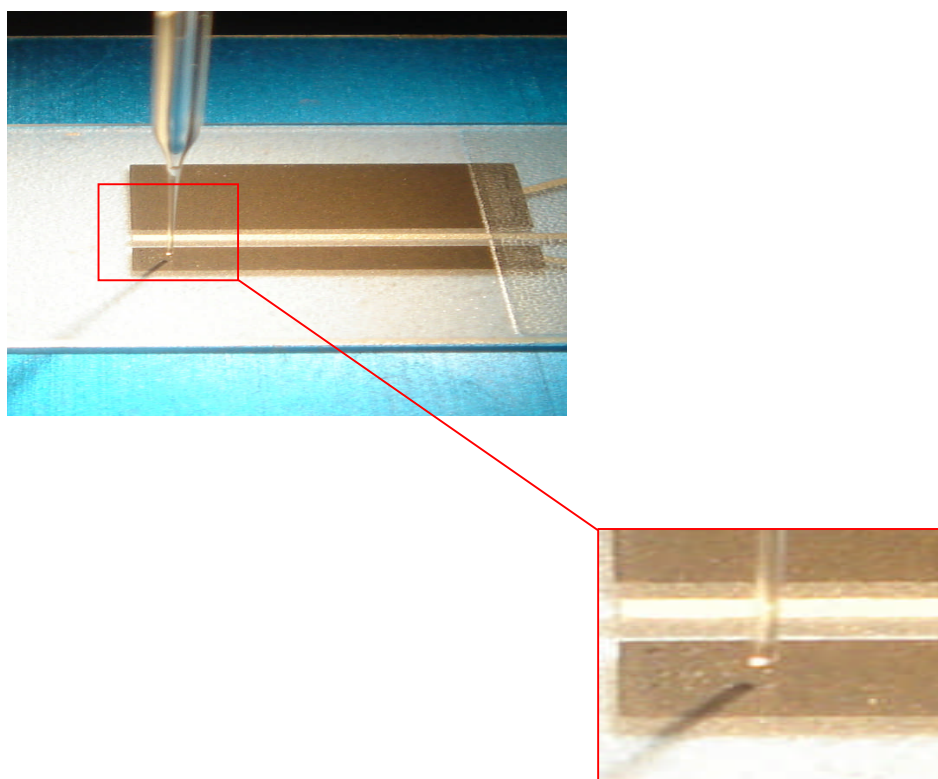


Figure 6.7: Photograph of polyethylenimine deposition on carbon electrode by pulled microcapillary using the XYZ micro-positioning stage of the SECM270

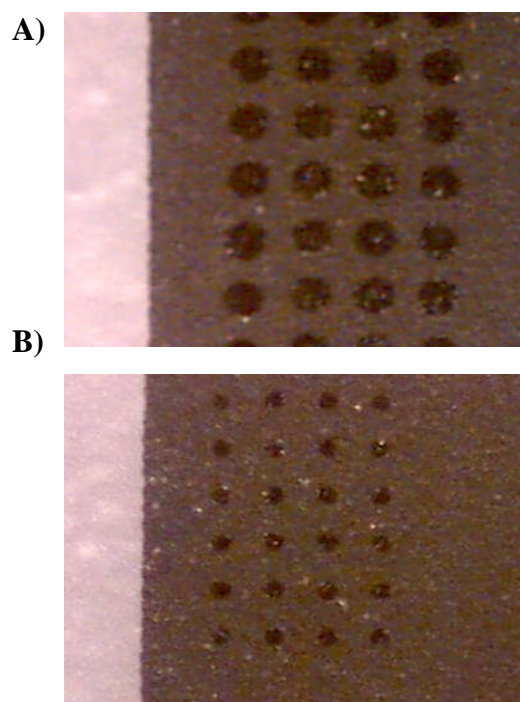


Figure 6.8: Optical Micrographs of polyethylenimine dots on carbon paste electrode using capillaries of differing internal diameters; 100micron (A) 30micron (B)

6.3 Mediator selection

A selection of mediators was considered for use in the interrogation of the DNA/PEI polyelectrolyte array, including ferrocenecarboxylic acid, ferricyanide and hexamine ruthenium chloride. Ruthenium bi-pyridine was not considered as it is known to irreversibly oxidise the guanine residue in DNA – and this could have implications for later use in the interrogation of DNA functionalised polyelectrolyte films.

6.3.1 Cyclic Voltammetry

To determine the suitability of each mediator to the study of a modified carbon electrode, the behaviour of each was characterised by cyclic voltammetry and then compared. Cyclic voltammetry was conducted using 5mM of the respective mediator dissolved in pH 7.1 phosphate buffer at a scan rate of 50mVs^{-1} . The cyclic voltammograms for these are shown in Figure 6.9.

The carbon ink was seen to exhibit quasi-reversible electron-transfer properties for both ferrocenecarboxylic acid and hexamine ruthenium (III) chloride. In contrast, the peak current for the potassium ferro/ferricyanide redox couple was significantly smaller than that obtained for the other two redox couples. This non-reversible electrochemical behaviour was exhibited in previous work involving the characterisation of inks. Erlenkotter *et al* (2000) for example reported peak separations of over 300mV, well beyond the 59mV expected for a Nernstian, diffusion controlled single electron transfer reaction.

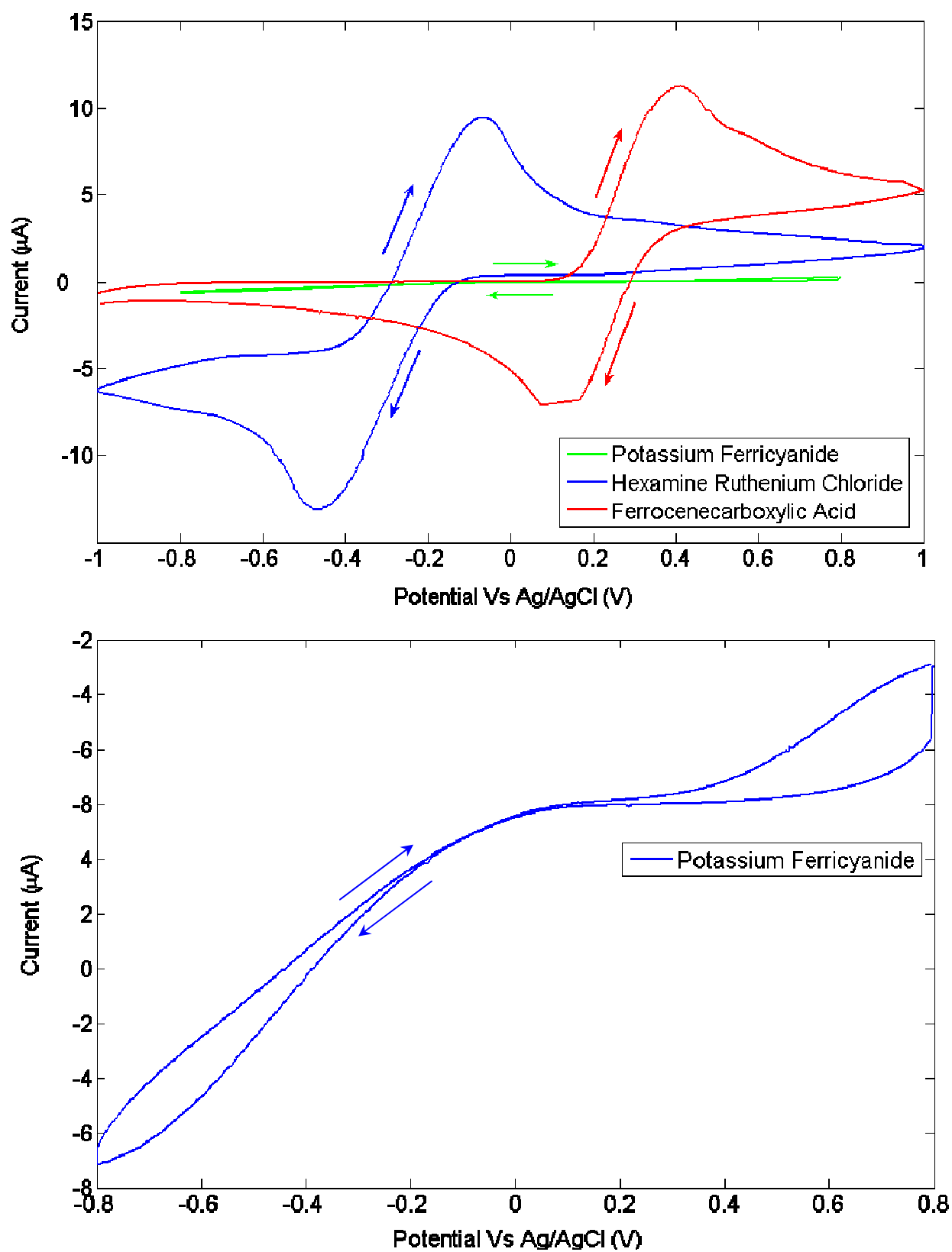


Figure 6.9: Cyclic voltammograms for A) hexamine ruthenium (III) chloride and ferrocenecarboxylic acid and potassium ferricyanide (III) and B) potassium ferricyanide only (5mM in pH 7.1 buffer)

The stark contrast between the cyclic voltammograms obtained for hexamine ruthenium chloride and ferrocencarboxylic acid and those obtained for potassium ferricyanide offers further support for the hypothesis that the carbon substrate has a slightly negative charge (Deakin *et al.*, 1985; Cui *et al.*, 2001). This negative charge hinders the diffusion of the negatively charged mediator species to the carbon substrate by electrostatic repulsion; as a consequence of this, charge transfer kinetics are slowed, resulting in the departure of the system from ideal behaviour. These results also exhibit the suitability of the carbon as a base substrate for the construction of a polyelectrolyte film due to its negative charge.

6.4 Scan height

A series of linescans were conducted across the border of the carbon ink substrate to determine the optimum height at which area scans could be conducted. Using 5mM hexamine ruthenium chloride, approach curves were conducted and line scans across the carbon border were performed where the tip current was equal to 80, 70, 60 and 50% of the current measured in bulk (Figure 6.10).

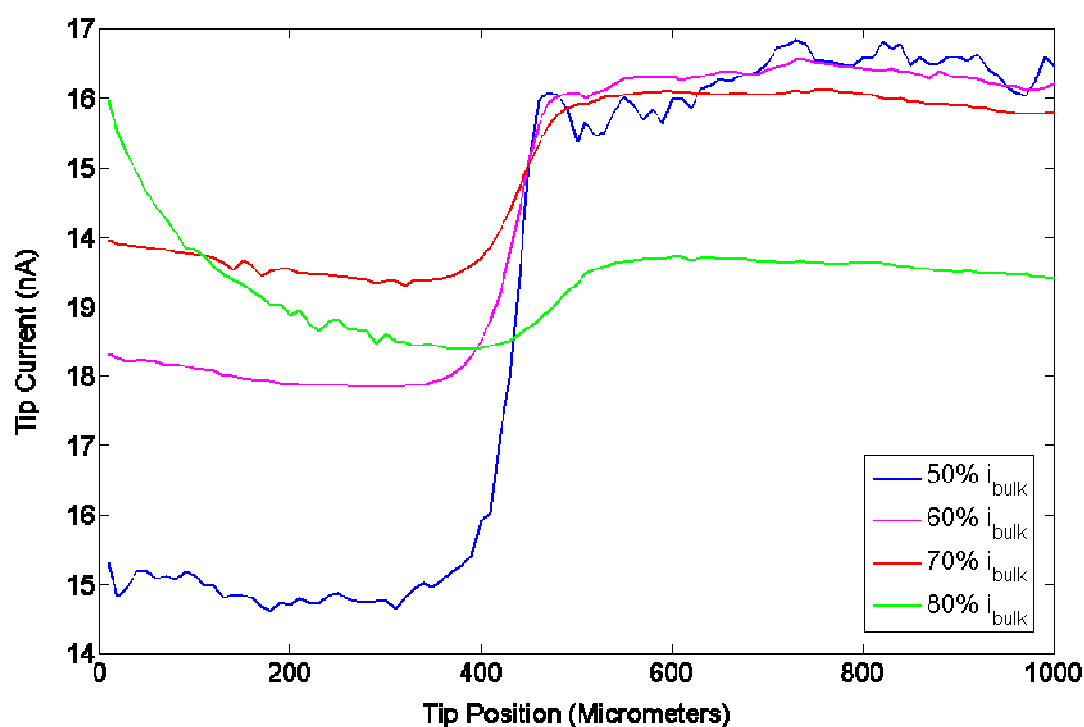


Figure 6.10: Consecutive linescans over carbon ink border. Scans were carried out at the height at which the tip current was equal to 80%, 70%, 60% and 50% of the tip current observed in bulk

The resolution of each linescan is observed to increase with a reduction in the tip to substrate distance (Figure 6.10). On comparing the gradient of the line over the region of inflexion, which represents the movement of the tip across the insulator/carbon border, it is evident that the scan which produces the greatest rate of change is the scan conducted at the height at which the tip current is equal to 50% of that obtained in bulk solution (see Table 6.1

This improved resolution is also apparent on observing the variation in tip current over the portion of the linescan conducted over the carbon surface. Because conducting linescans at lower scan heights increases the likelihood of tip crash, it was deemed prudent to conduct area scans within this work with the tip positioned where $i_{\text{tip}} = 0.5 \times i_{\text{bulk}}$.

Table 6.1: Resolution as a function of scan height – calculated over the 400-440 μm range of line scans

Scan height as a % of bulk current	Resolution ($\Delta I/\text{distance}$)(nA/ μm)
80	3.32×10^{-03}
70	1.48×10^{-03}
60	2.87×10^{-03}
50	6.29×10^{-03}

6.4.1 Effect of mediator charge on feedback response

The feedback response when interrogating polyelectrolyte films is strongly influenced by the charge of the mediator used. In the images below, ferricyanide and ferrocenecarboxylic acid were both used as the mediator to interrogate a polyethylenimine array patterned on a carbon ink electrode. The results also give greater insights into the observations made in section 6.3.1 where potassium ferricyanide was observed to exhibit poor electrochemical behaviour at the surface of the carbon electrode.

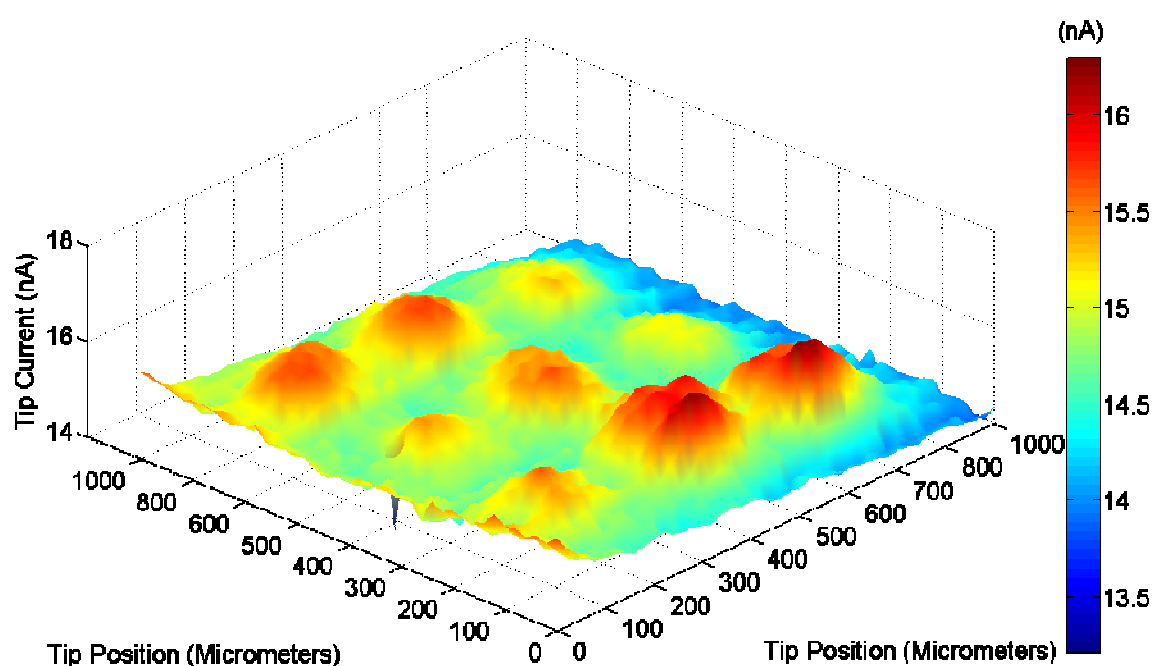


Figure 6.11: Area scan profile over polyethylenimine array patterned on a carbon ink electrode using 5mM potassium ferricyanide mediator

With reference to Figure 6.11, it is evident that the functionalisation of the carbon ink with the polyelectrolyte film had the effect of enhancing the rate of charge transfer between the carbon electrode and the ferricyanide mediator solution. In the case of unmodified carbon, following reduction at the tip of the microelectrode, the ferrocyanide mediator diffuses to the carbon surface, where it is recycled (oxidised) to ferricyanide and is made available for re-reduction. In the case of polyethylenimine functionalised carbon, however, the rate at which the ferrocyanide is oxidised to ferricyanide is enhanced. For an enhancement of current to be observed, there must be some mechanism by which the transfer of charge

from the carbon to the mediator is being facilitated. As polyethylenimine has no delocalised electron systems, the transfer of charge from the carbon substrate to the mediator is unlikely to occur by the passage of electrons through the polymer film. It is therefore thought that charge transfer occurs as a result of the diffusion of the mediator through the polymer, promoted by the electrostatic forces of attraction between the polymer and negatively charged mediator species. Polyelectrolyte films such as those used here are not highly ordered films with a crystalline structure – like Langmuir Blodgett films for example. Rather, they tend to be more amorphous in nature, with layers interpenetrating one another (Decher, 1997; Decher *et al.*, 1998). As a consequence of this, gaps in the film allow the diffusion of the mediator towards the electrode substrate, resulting in an enhancement in the faradaic current measured at the tip.

This enhancement of charge transfer properties is in contrast with the diminution in charge transfer properties observed when using the positively charged mediator, ferrocenecarboxylic acid. On modifying the carbon ink with the polyethylenimine array, the functionalised region is observed to behave similarly to an insulating substrate when interrogated by SECM (Figure 6.12). This is thought to be a result of the electrostatic forces of repulsion between the positively charged mediator and the positively charged polyethylenimine film. As a result of these repulsive forces, the mediator is inhibited from approaching the conductive carbon substrate, resulting in the diminution of positive feedback. The result is a lowering in the feedback current when compared to the feedback response over blank, unmodified carbon. This argument is illustrated schematically in Figure 6.13.

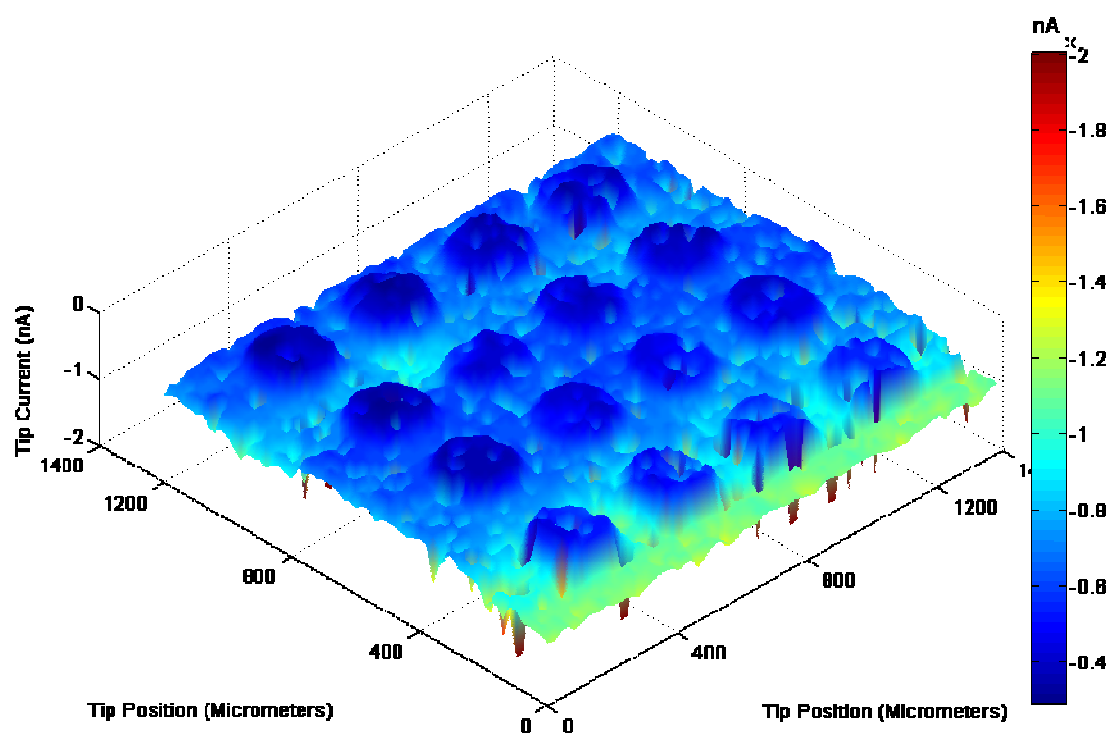


Figure 6.12: Area scan over polyethylenimine array using 5mM ferrocenecarboxylic acid.

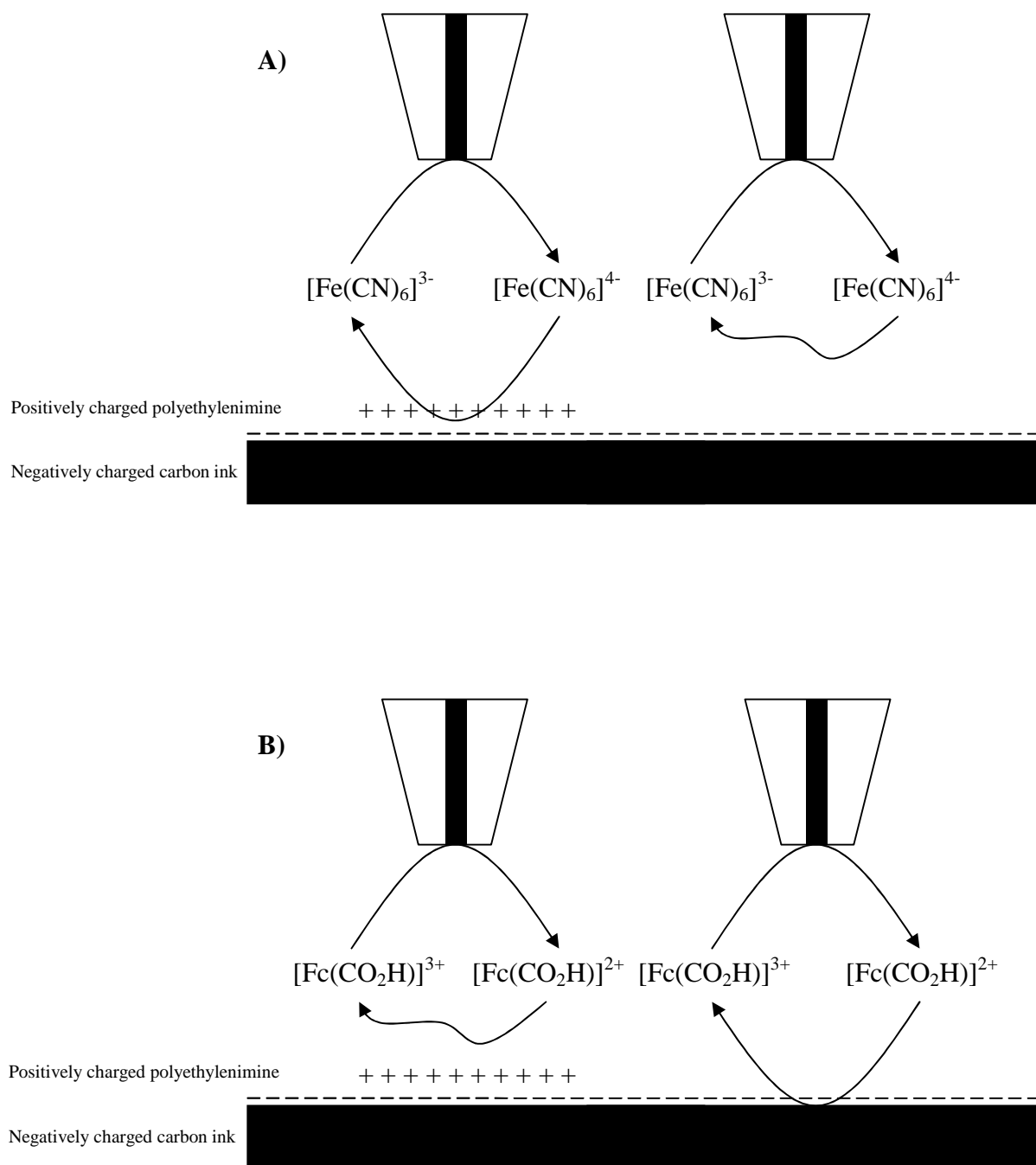


Figure 6.13: Schematic diagram illustrating the electrostatic forces of attraction and repulsion between the mediators A) ferricyanide and B) ferrocenecarboxylic acid with the positively charged polyethylenimine film and the negatively charged carbon substrate respectively

6.4.2 Interrogation of film integrity by SECM

To determine the stability of the polyethylenimine film during multiple scans, to the scanning process, the polyethylenimine film was scanned repeatedly over a period of time. If the integrity of the film was put at risk by the scanning process, it would not be possible to determine whether any changes occurring in the film were due to DNA hybridisation or not in future experiments. With reference to Figure 6.14, it is apparent that over the course of four area scans in which the polyethylenimine film was submerged in ferrocenecarboxylic acid mediator, the image became significantly distorted. Initially it was thought that this noise may have been a result of the degradation of the film, but because the distortion is seen to occur across the entire region, it is felt that this may be due to either the fouling of the electrode or the degradation of the substrate as a whole – perhaps as a consequence of precipitation of the ferrocenecarboxylic acid out of solution.

On performing the same experiment using hexamine ruthenium chloride however, there was no such distortion. Whilst a small increase in noise is apparent on comparing visually, there is little apparent change in the area scan data as a whole (Figure 6.15). A paired t-test was carried out on both datasets to determine whether there was any statistically significant difference between the change in feedback response using the mediators ferrocenecarboxylic acid and hexamine ruthenium chloride. It was found that there was no statistically significant difference between arrays at $T = 0\text{min}$ and $T = 300\text{min}$ using the hexamine ruthenium chloride mediator ($p \gg 0.05$), but there was a statistically significant difference between those scans obtained using ferrocenecarboxylic acid (the null hypothesis of no difference was rejected for 29 of the 76 columns of the array of data obtained by the use of ferrocenecarboxylic acid (p-value range 0 to 0.7746)).

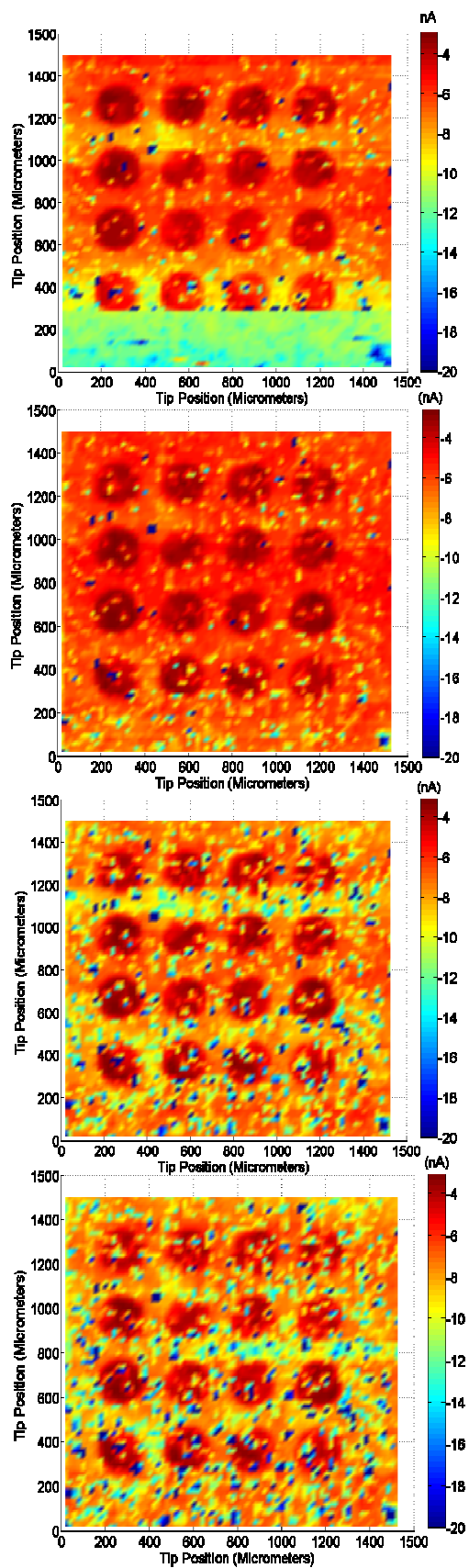


Figure 6.14: Consecutive area scans over PEI array on carbon at T=0min, T=100min, T=200min, T=300min using 5mM ferrocenecarboxylic acid

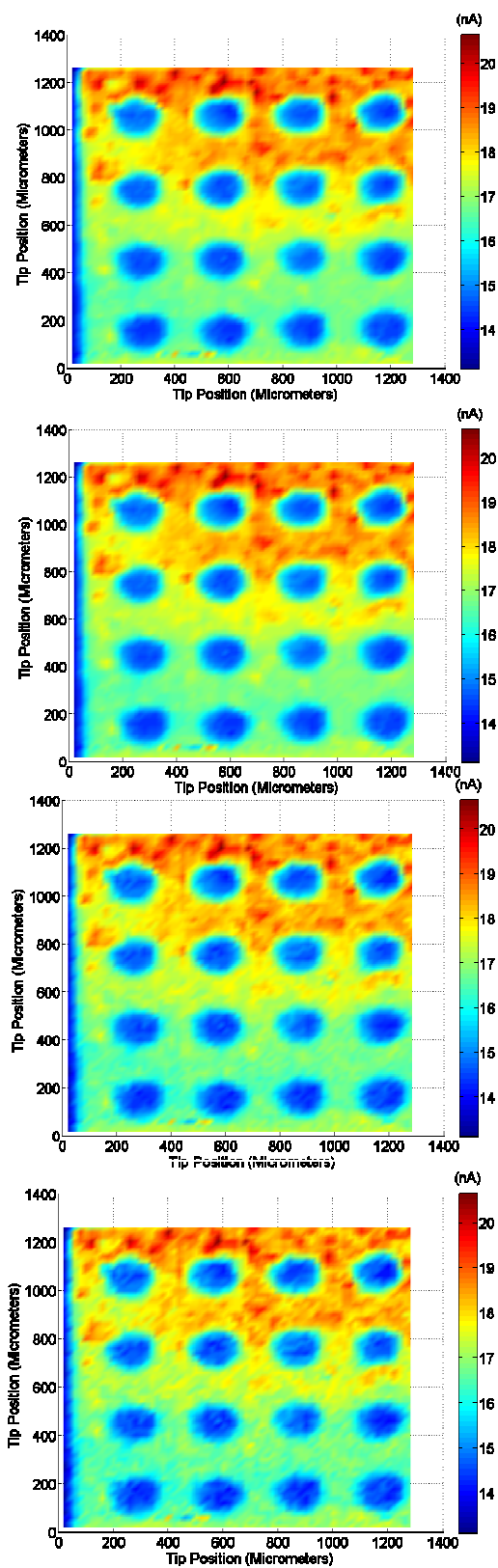


Figure 6.15: Consecutive scans over a PEI array on carbon at T=0min, T=100min, T=200min, T=300min using 5mM hexamine ruthenium chloride mediator

Building on this analysis, it was decided that hexamine ruthenium chloride would be used as the mediator in the interrogation of the DNA/polyethylenimine array as it has been shown that the films show good stability when immersed in the hexamine ruthenium chloride mediator.

6.5 Statistical interrogation of array data by region of interest (ROI) analysis tool

In the previous section, a simple statistical analysis was undertaken to determine whether the changes observed in the charge transfer properties of the surfaces before and after the exposure of the ssDNA/PEI film to complementary and non-complementary genomic DNA were statistically significant. The way in which this was initially achieved was by a simple paired t-test, in which each column of data was paired with its respective column in the second array. A significant problem with this is that by doing so, data points not exposed to the experimental treatment become part of the population dataset, which may affect the test statistic obtained. Whilst the test statistics obtained support the observations – i.e. the apparent enhancement in charge transfer properties over ssDNA/PEI regions, it was decided that an alternative approach to analysing these arrays should be developed. In conjunction with a bioinformatician within our department, a simple graphical user interface (GUI) tool was developed to allow the calculation of descriptive statistics about a specific region of the area scan (Clarke, 2007).

The ROI GUI was developed to allow the extraction of information about regions of interest (ROI) in an array of data obtained by the use of the area scan macro in the SECM270 software. Data is extracted from the SECM user interface and saved as an excel file which is then imported into the Matlab GUI. The user is then able to highlight a region of the area scan with a polygon. Information regarding the number of data points, the average current value and relevant statistics are then saved to a chosen excel file for further interpretation and analysis. The GUI, screen captures of which are shown in Figure 6.16, provided an ideal platform for the analysis of the PEI/DNA arrays fabricated in this study. Such a tool, which allows the interrogation of area scan data, would be an excellent addition to the SECM270 as it would significantly curtail the time spent by the user in post-scan analysis.

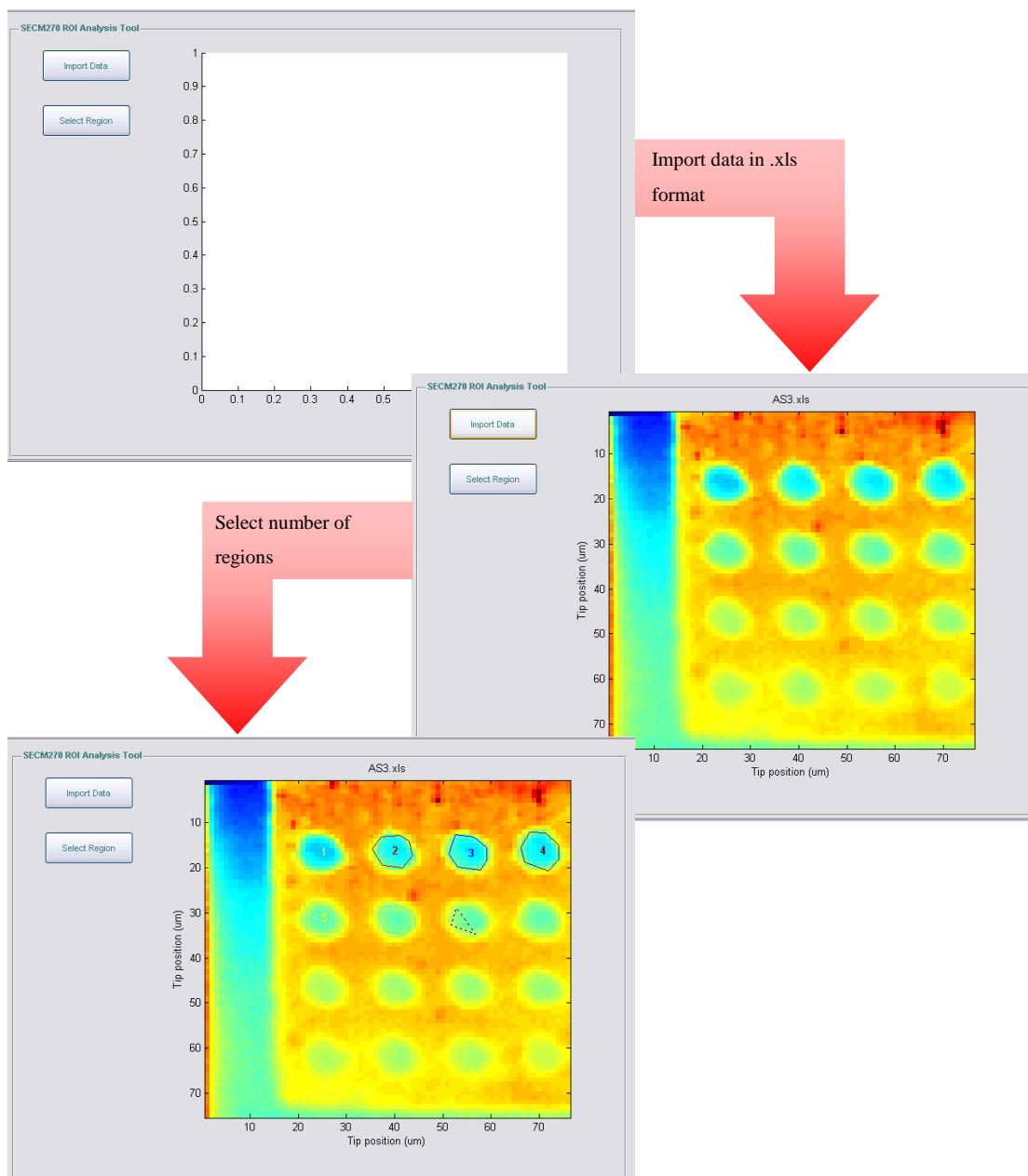


Figure 6.16: Screen captures of the GUI developed to allow extraction of data from area scan data

As the user highlights regions of the array, descriptive statistics are calculated for the highlighted regions encapsulated by the polygon, including the mean, minimum, maximum, range, standard deviation and ROI centre (coordinate). By the selection of the functionalised regions, discrete data points are obtained which may then undergo statistical analysis. A screen capture of the ROI GUI output in excel is given in Figure 6.17.

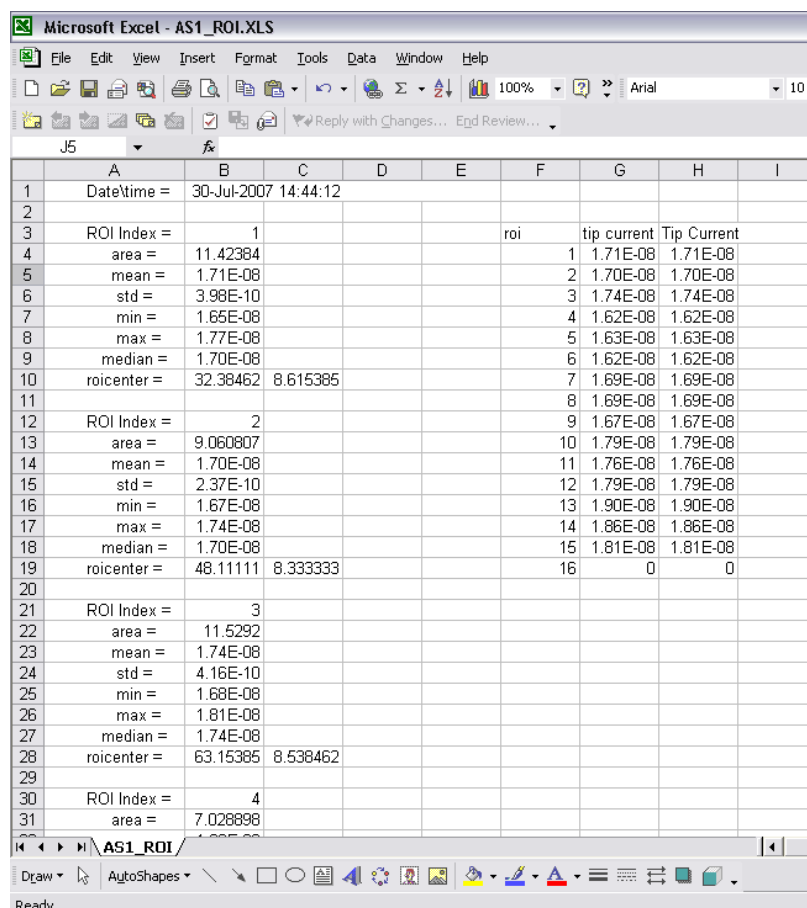


Figure 6.17: Screen capture of ROI output in excel, detailing extraction of data from an area scan array

6.6 Control experiments

In the hybridisation experiment, different solutions are introduced and removed from the polyelectrolyte substrate. To ensure that the introduction and removal of these solutions did not affect the integrity of the film or have an impact on its charge transfer properties, a control experiment was conducted. In this experiment, all steps of the hybridisation studies were replicated but with the omission of the single stranded DNA from the hybridisation solution. All other aspects of the investigation, from imaging to rinsing protocols were identical to those of the hybridisation studies. In Figure 6.18, the two area scans, before and after the 3hr exposure to the hybridisation solution, are presented. On subtracting the 'post-exposure' scan from the 'pre-exposure' scan, the resulting 'difference' array is relatively homogenous with an approximate range of 0 to 0.08nA Figure 6.19(A). If there was some change in the charge transfer properties of the film, then one would see larger changes over those regions functionalised with the ssDNA / polyethylenimine film. On conducting a paired t-test on the average current over each dot measured before and after exposure to the buffered control hybridisation solution, it was revealed that whilst there was a statistically significant difference between the average current value, it was very small ($t = 8.1$; $df = 15$; $p = 7.1 \times 10^{-7}$; $CI = 0.04 \times 10^{-9}$ to 0.07×10^{-9}). Representative linescans are also presented (Figure 6.19 (B)), which depict graphically the very small change in the feedback current after exposure to the buffered hybridisation solution (Figure 6.20). It may be concluded that the PEI/ssDNA film does not appear to undergo any changes on exposure to the hybridisation solution that would produce a significant change in the charge transfer properties of the film observable by SECM.

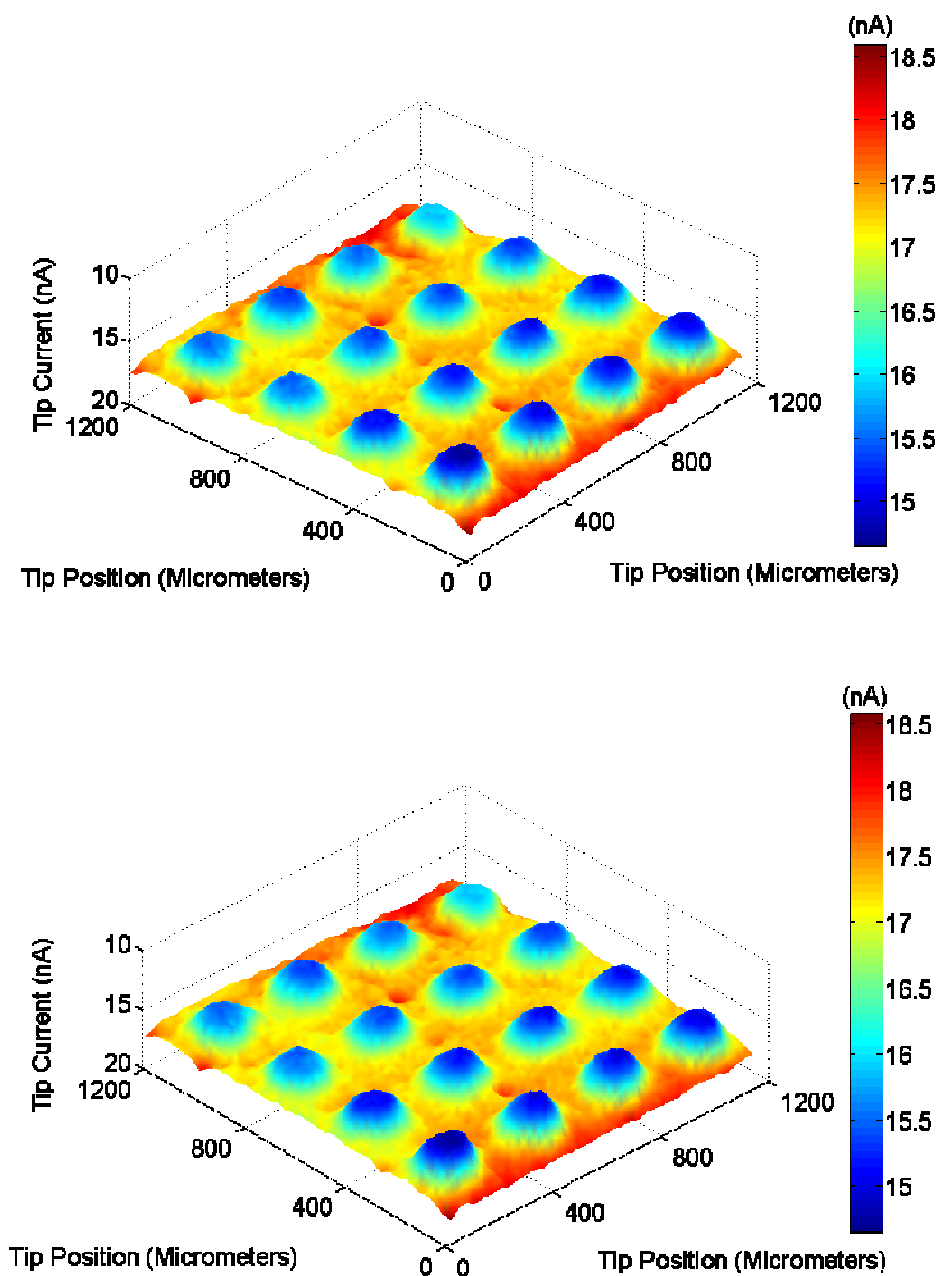
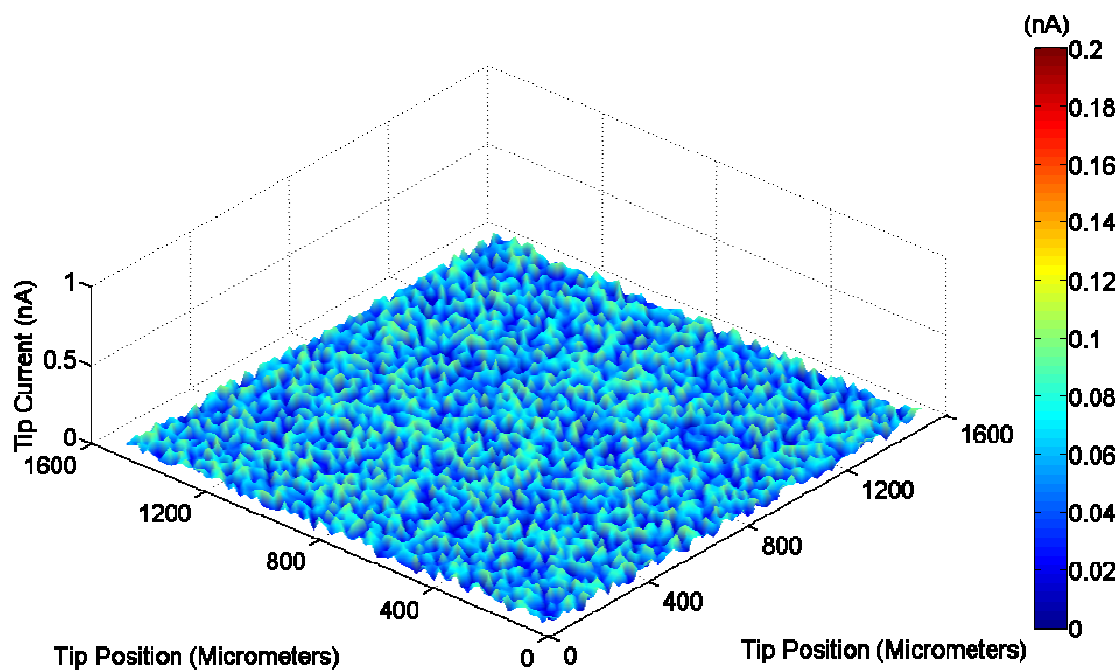


Figure 6.18: Area scan arrays before (A) and after (B) rinsing and 3hrs exposure to control solution (0.015mM phosphate buffer solution)



B)

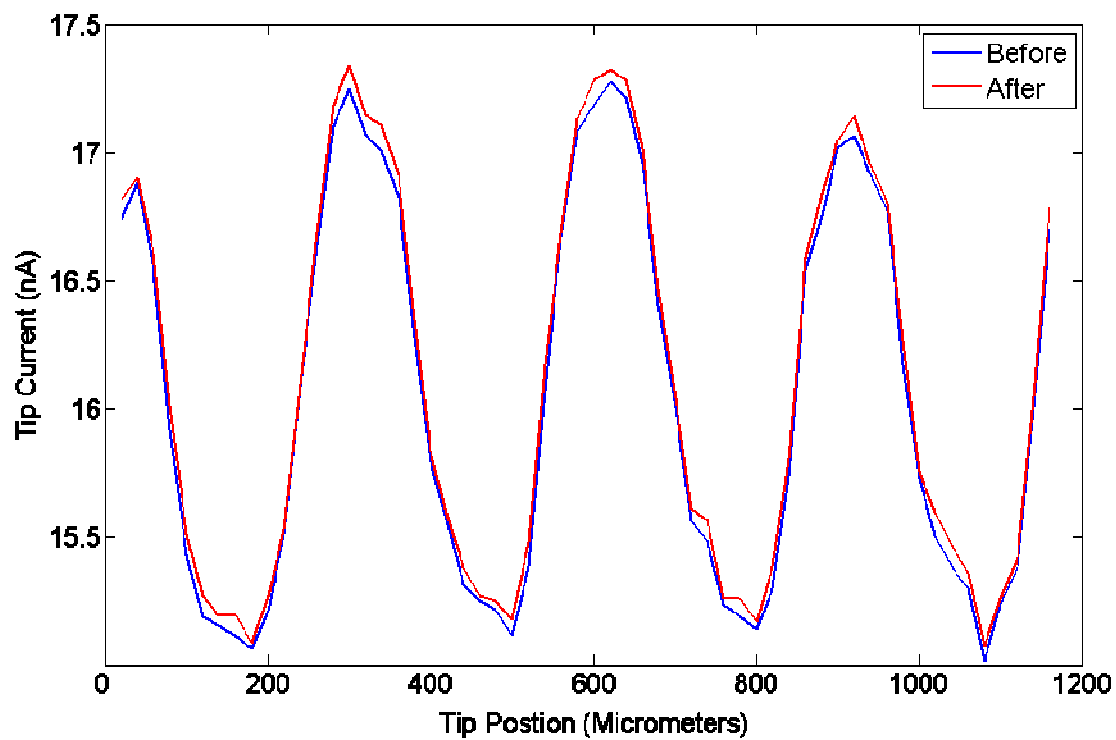


Figure 6.19: A) Array obtained from the subtraction of 'before' array from 'after' array; B) Representative linescans from before and after rinsing and exposure

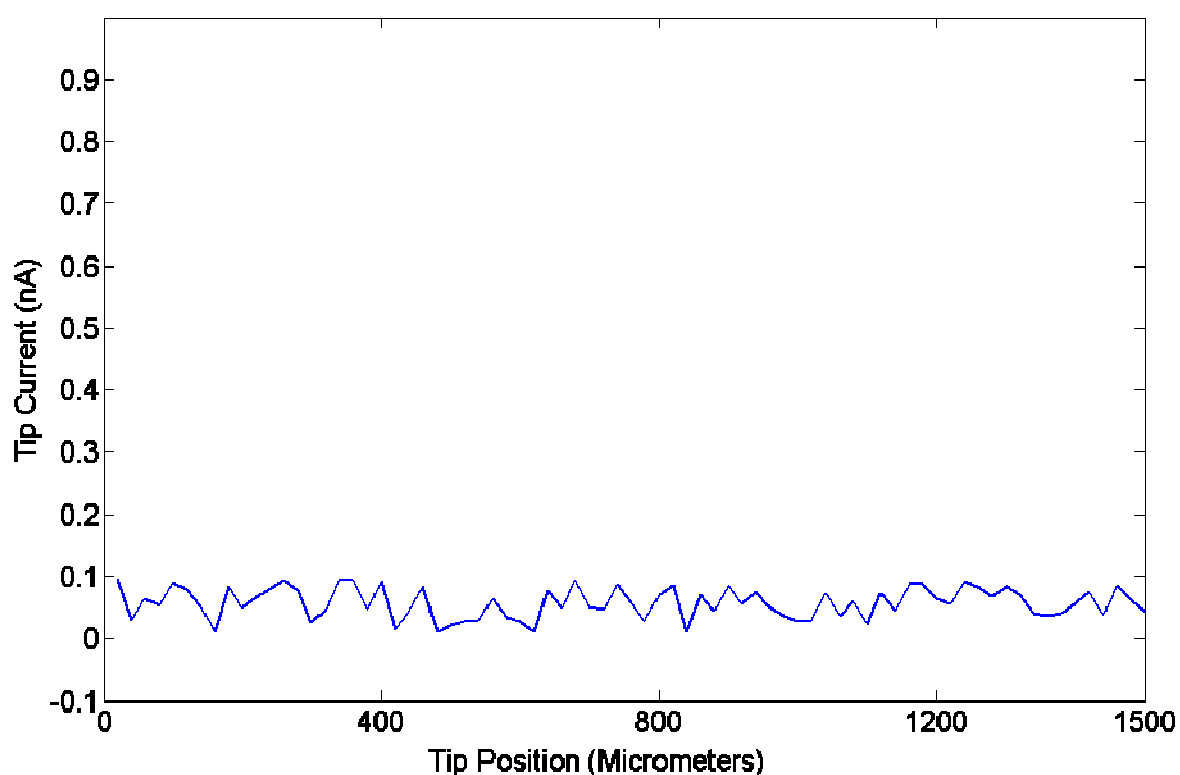


Figure 6.20: Linescan across array obtained by the subtraction of array 'before' and 'after' exposure to 'control' hybridisation solution

6.7 Hybridisation detection by SECM

After the preparation of the ssDNA/PEI arrays on the carbon electrode, the substrate was interrogated by SECM area scan. Following the successful completion of the scan, the mediator solution was removed and the substrate was rinsed with 5ml UHQ H₂O which was then also removed. 1ml of the hybridisation solution containing 0.015mM phosphate buffer and 0.2mg/ml of either complementary or non-complementary DNA in its single stranded form was then applied to the substrate and left at room temperature for 3hrs (ssDNA, formed by boiling dsDNA was also an approach used by Ding *et al* (2005)). After this time, according to Davis *et al*, changes in the impedimetric response are observed to plateau. Following the 3hr exposure period, the hybridisation solution was removed and the substrate rinsed once more with 5ml UHQ H₂O before the introduction of the electroactive mediator to the system – 5mM hexamine ruthenium chloride. Any possible

dilution effects were minimised by the removal and re-introduction of the mediator solution three times. Every precaution was taken in all cases to prevent moving the substrate and the tip. After the re-introduction of the mediator solution, the tip was re-positioned and the scan conducted once more using exactly the same parameters as the previous scan. Representative images of the data obtained by this technique are given in sections Figure 6.21.

Whilst the data used in the analysis of the arrays before and after exposure to complementary and non-complementary DNA were well resolved replicates, a number of problems arose relating to scanning height, substrate crash, tip fouling, and substrate slope. Much time was spent trouble-shooting these issues and making slight modifications to the experimental setup which would allow the collection of data of sufficient resolution and reproducibility for analysis. The dependence of the tip current on the tip to substrate distance was also a key consideration and care had to be taken to minimise any movement of the system.

On the initial comparison of the 'before' and 'after' scans (Figure 6.21), the exposure of the system to the complementary DNA solution appears to have had no effect on the charge transfer properties of the ssDNA/PEI film. However, on the subtraction of the 'before' scan from the 'after' scan, it becomes evident that there has indeed been a change (Figure 6.22).

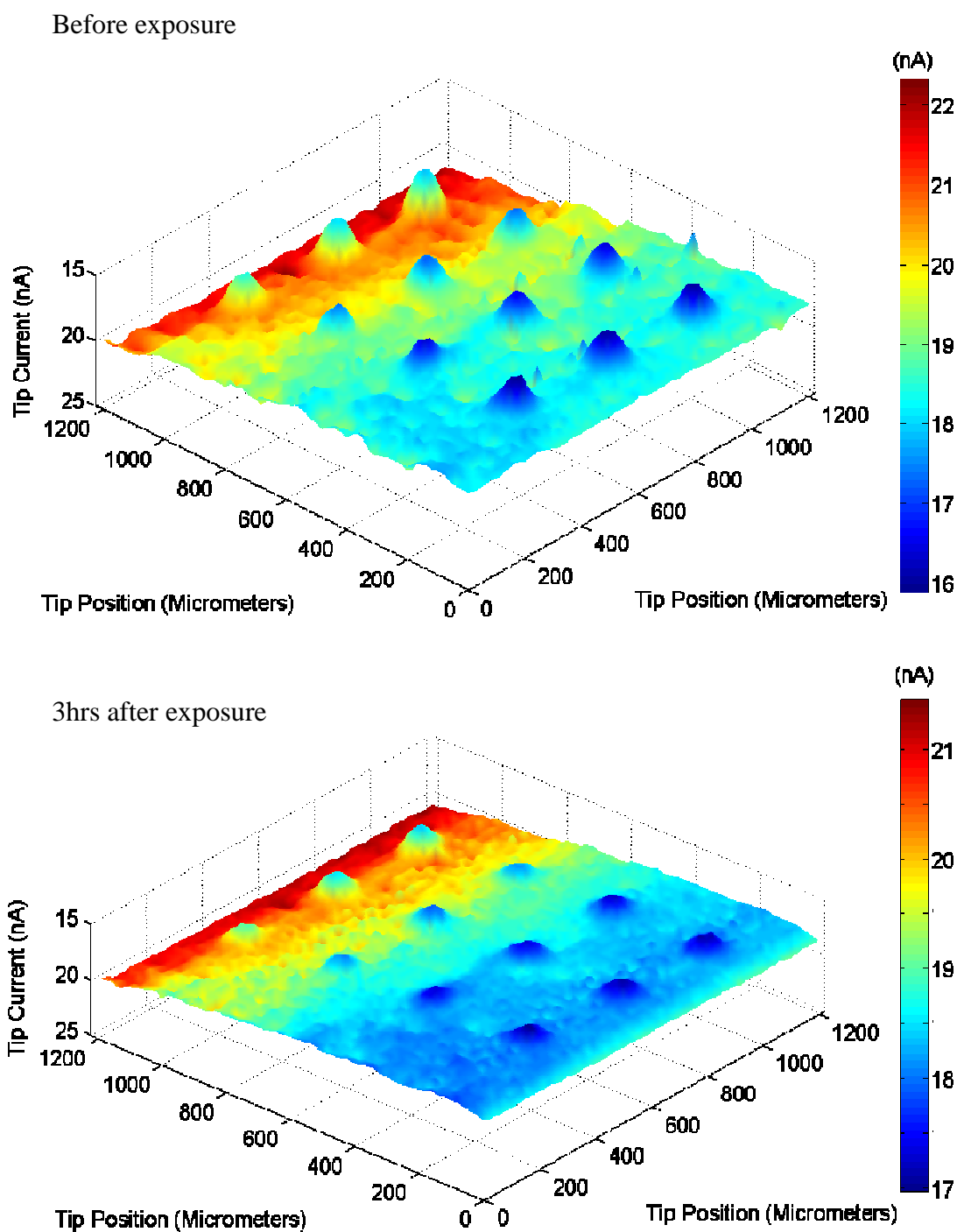


Figure 6.21: Area scans over PEI/ssDNA array before and after exposure to complementary ssDNA solution (0.2mg/ml)

Referring to Figure 6.22, the feedback current over the PEI/ssDNA array has increased – more specifically, the insulating effect of the PEI/ssDNA on the carbon electrode has fallen by 1.2nA, which represents an increase in the feedback current of approximately 7.5% in this representative example. In contrast, the feedback current over the non-functionalised carbon is unaffected.

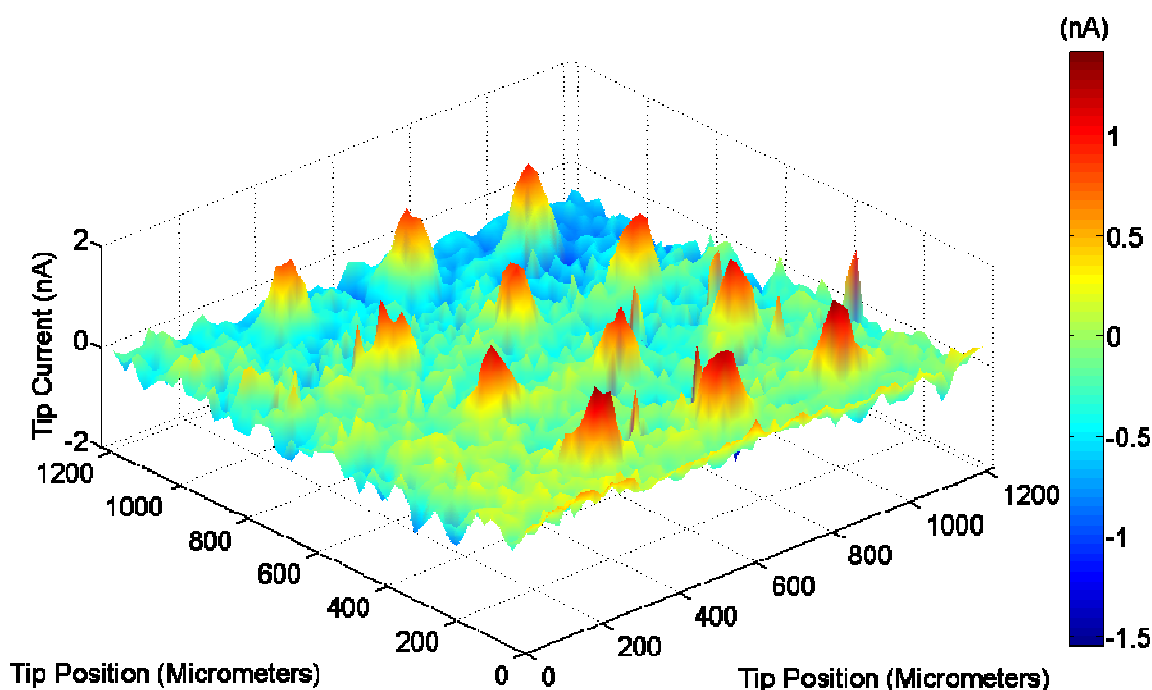


Figure 6.22: Absolute change in tip current after exposure to complimentary single stranded DNA

To aid the comparison of the two scans and the change in current between them, a cross section of each scan was plotted on the same axis (Figure 6.23 (A)). It can be seen from these linescans that there is a significant enhancement in the feedback current obtained following exposure of the system to the complementary DNA, which is in contrast to the observation that the non-functionalised regions do not given rise to such a change. The absolute change in the feedback current measured in each of these scans is given in (Figure 6.23 (B)).

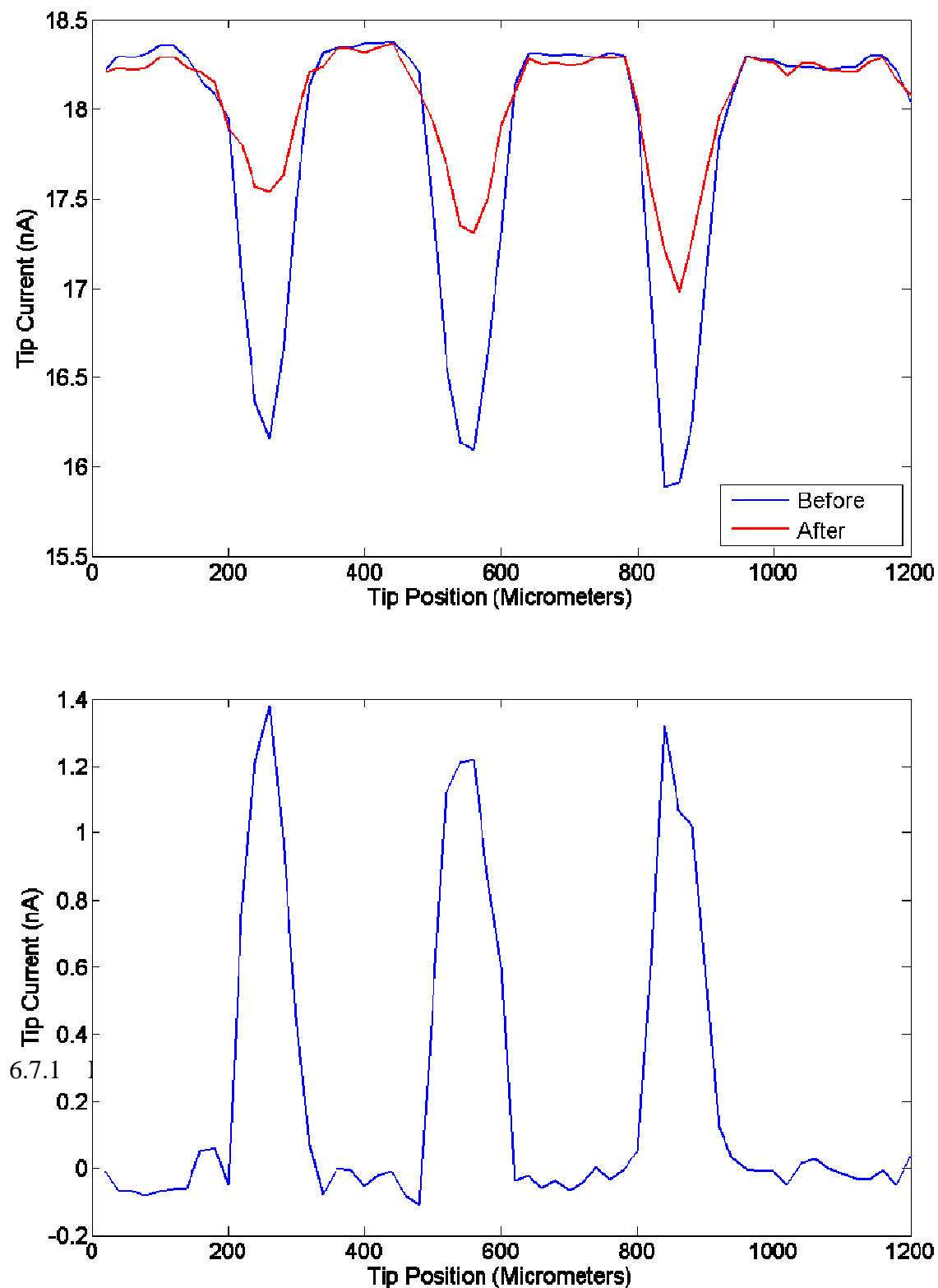


Figure 6.23: Linescans extracted from the area scans in A) Figure 6.21 and B) the array subtraction in Figure 6.22 – which is the difference of the two linescans in A)

Similarly to the complementary experiment described previously, on initial investigation, there appears to be little change in the feedback response measured before and after exposure of the ssDNA/PEI array to non-complementary ssDNA (Figure 6.24). On subtracting the 'before' area scan array from the 'after' after area scan array however, a much smaller increase in feedback current was observed, in the region of 0.2nA – a very small proportion of the initial feedback current (Figure 6.25).

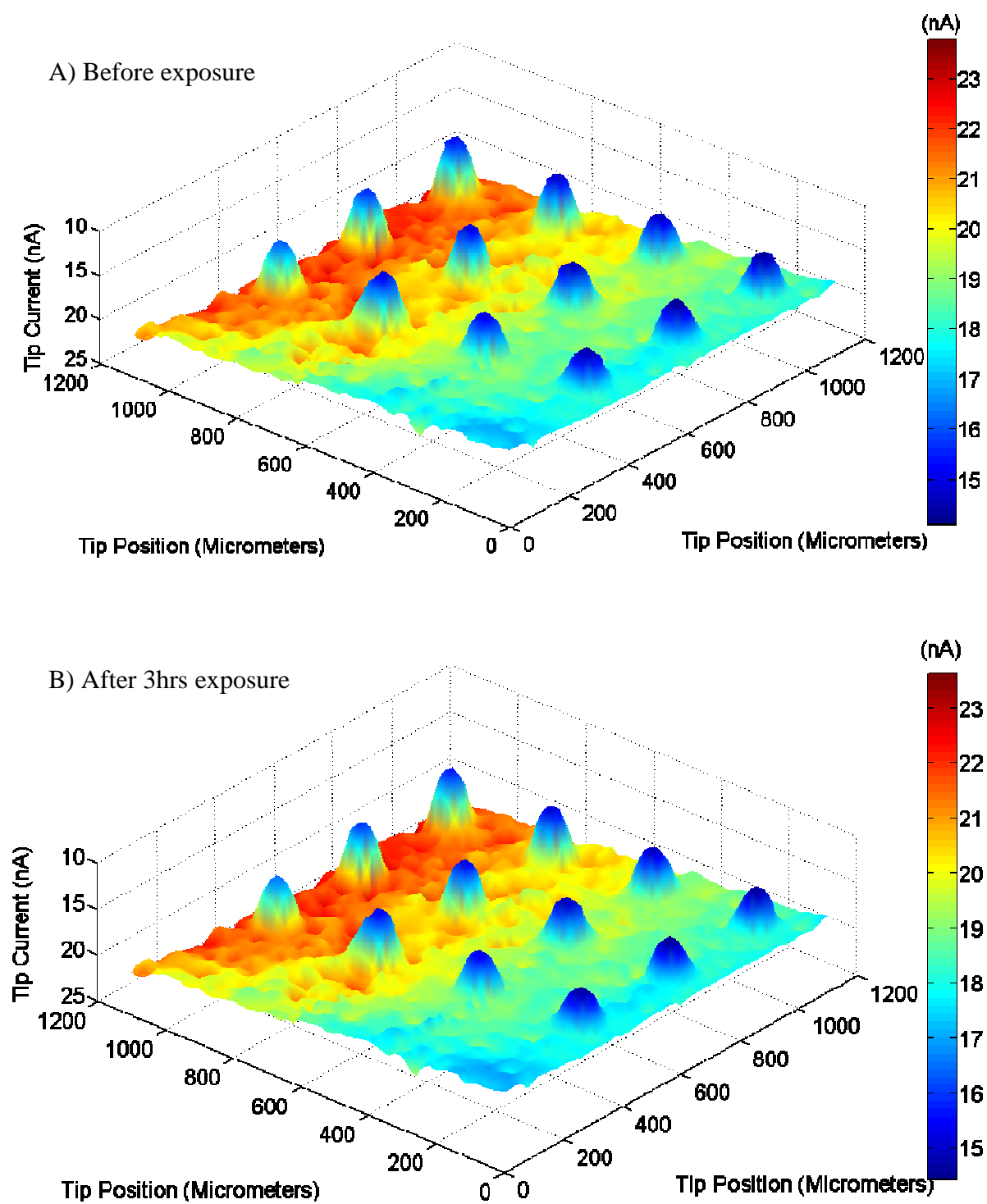


Figure 6.24: Area scans over ssDNA/PEI spotted array before and after exposure to non-complementary DNA

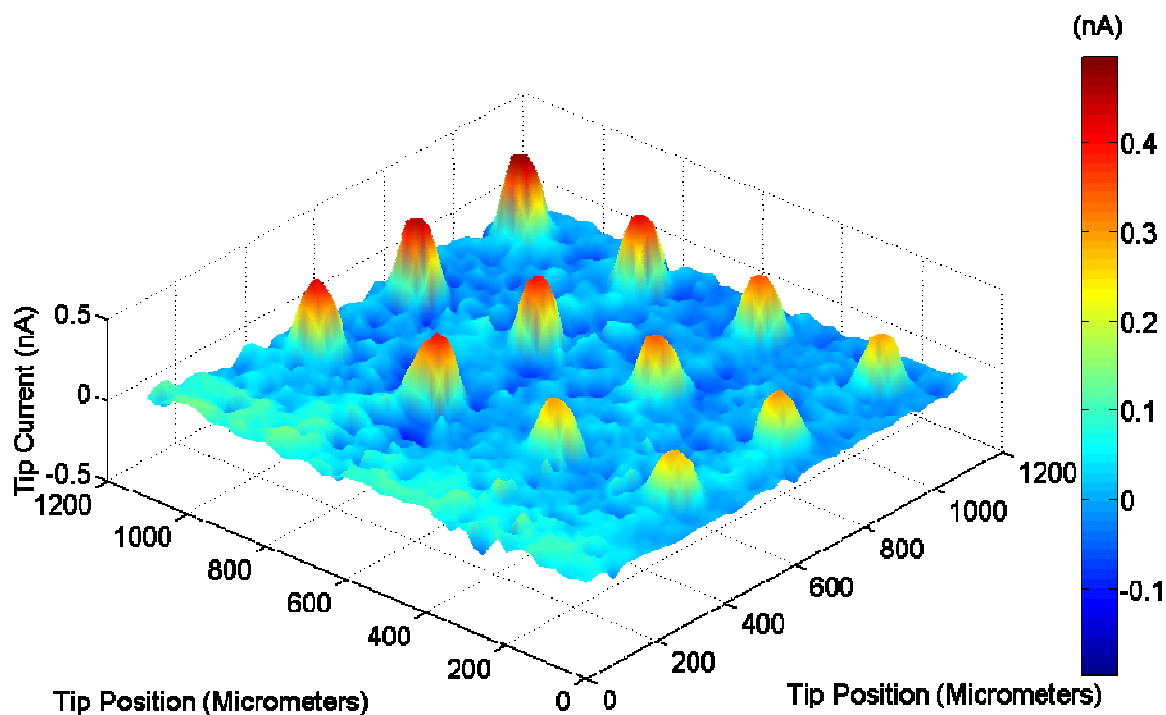


Figure 6.25: Absolute change in tip current after exposure to non-complementary DNA

To aid the comparison of the two scans and the change in current between them, a cross section of each scan was plotted on the same axis (Figure 6.26 (A)). It can be seen from these linescans that there is a very small enhancement in the feedback current obtained after exposure of the system to the complementary DNA, which is in contrast to the observation that the non-functionalised regions do not undergo such a change. The absolute change in the feedback current between each of these scans is given in Figure 6.26 (B).

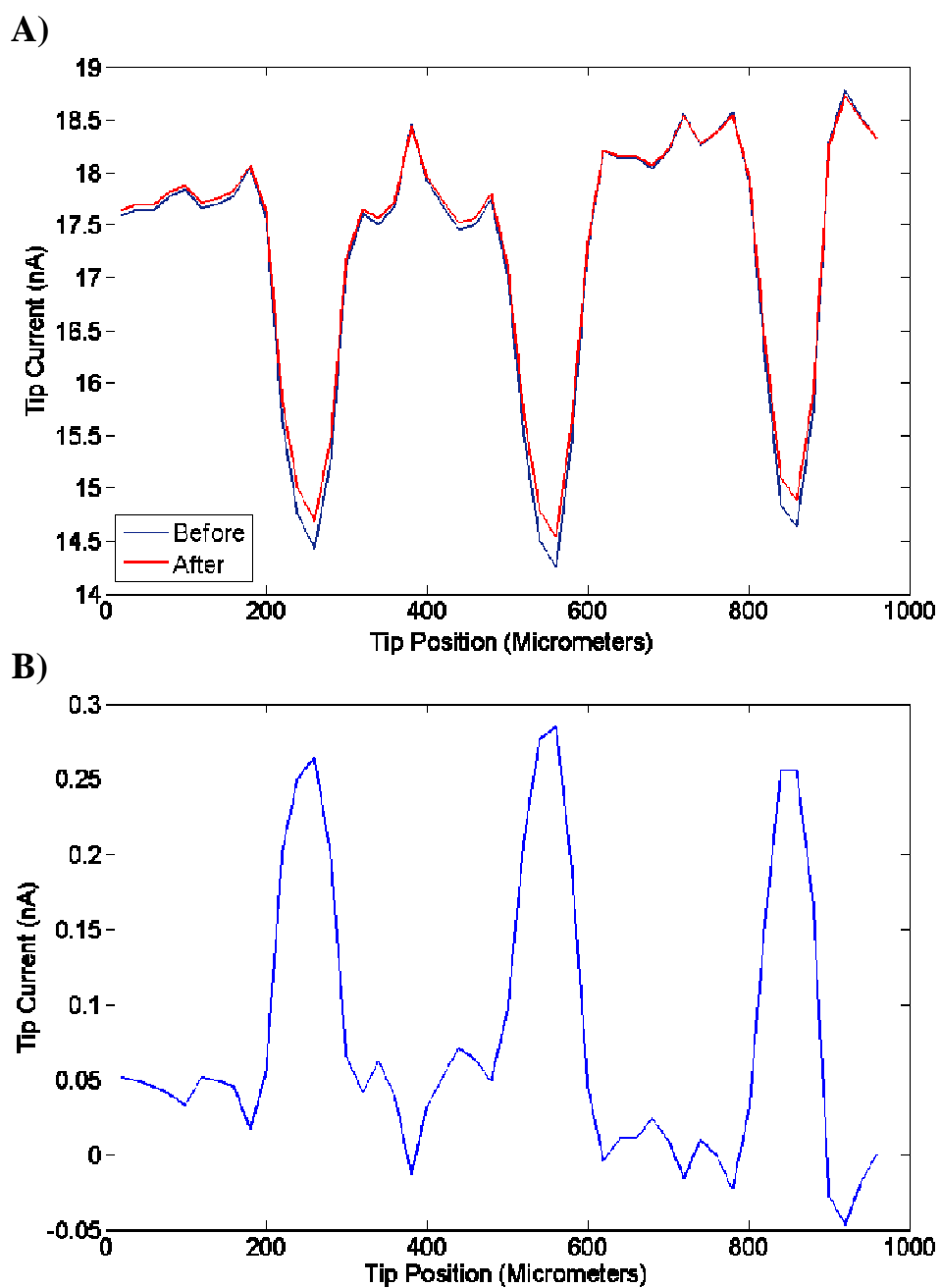


Figure 6.26: A) Series of linescans extracted from arrays represented in Figure 6.24 – the current profile across a spotted array before and after exposure to non-complementary DNA B) linescan extracted from Figure 6.25 depicting change in tip current after exposure to non-complementary DNA

The data presented in Figure 6.27 are representative linescans from the arrays formed by the subtraction of the array data obtained before and following the exposure of the PEI/ssDNA array to complementary and non-complementary DNA. It may be observed that the magnitude of the change is much more pronounced in the complementary experiment. This suggests that exposure of the PEI/ssDNA film to a hybridisation solution containing complementary DNA has a more significant effect on the feedback response of the polyelectrolyte film than the exposure of the film to non-complementary DNA.

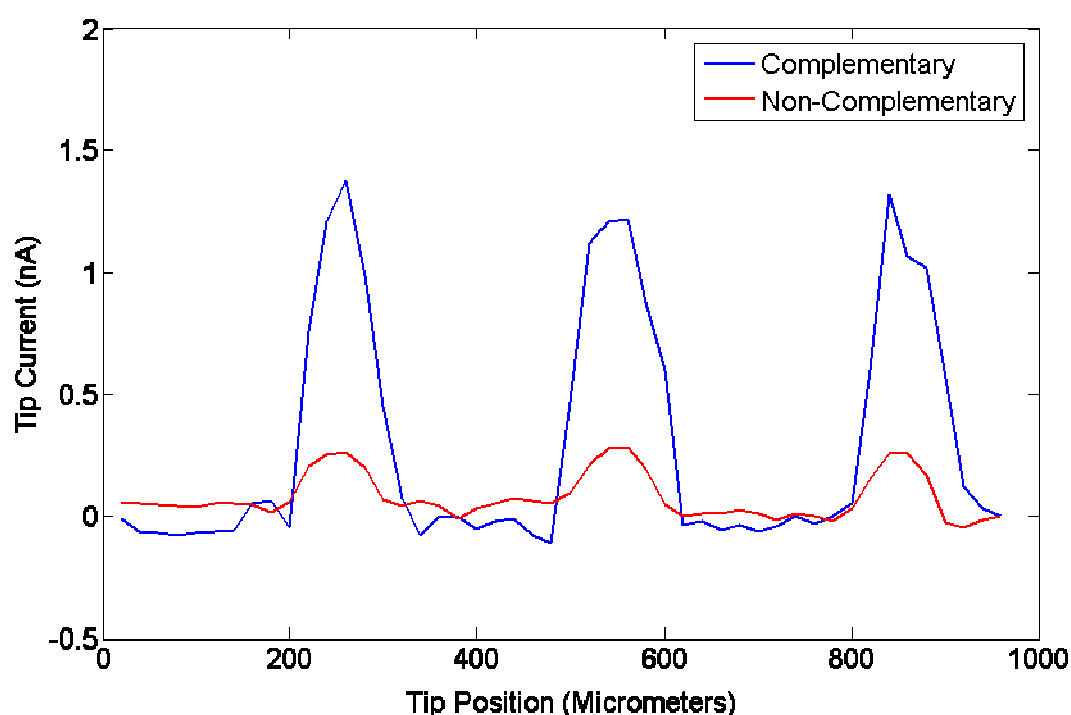


Figure 6.27: Linescans illustrating difference in feedback response after exposure to single stranded complementary and non-complementary DNA

Whilst these findings are evident in the representative data given above, to determine whether the differences observed in each replicate were statistically significant, the ROI GUI was used. Using the ROI analysis tool, the mean current value for each of the dots in the arrays before and following exposure to complementary and non-complementary DNA was calculated.

A single dataset was assembled from the average tip current over each dot in three experimental replicates (40 dots) and a paired t-test conducted on each merged data set before and following exposure to complementary and non-complementary DNA. The change in average tip current over each dot was found to be statistically significant for the complementary experiments and the non-complementary experiments - although the difference in p values suggests that the difference is more statistically significant in the complementary experiments.

Item	Test outcome for average feedback current		Test outcomes for minimum feedback current	
	Non-complementary	Complementary	Non-complementary	Complementary
t-value	2.92	3.6536	19.4	6.092
d.f	39	39	39	39
CI	0.074 x 10 ⁻⁹ to 0.5594x10 ⁻⁹	.14 x 10 ⁻⁹ to 0.5658 x 10 ⁻⁹	0.33x10 ⁻⁰⁹ to 0.41x10 ⁻⁰⁹	0.40 x 10 ⁻⁰⁹ to 0.89x10 ⁻⁰⁹
p	0.0137	0.004	7.3993x10 ⁻¹⁰	7.8262e-005

On carrying out the same analysis on the same arrays but conducting a paired t-test on the minimum feedback current obtained over each dot, it was found that there was a statistically significant difference between the feedback current obtained before and after exposure to complementary DNA. The same test on the non-complementary dataset revealed that there was also a statistically significant difference between the feedback current obtained before and following the exposure of the array to non-complementary DNA.

To determine whether the changes in feedback current were significantly larger in either experiment, a one tailed t-test was conducted. The null hypothesis, that the enhancement in feedback current after exposure to the hybridisation solution was not significantly greater in the complementary experiment, was rejected. The alternative hypothesis, which states that the enhancement in feedback current was statistically significantly larger in the case of complementary hybridisation was hence accepted ($t = 2.36$; $df = 38$; $p = 0.0137$).

There are two suggestions as to why the observed changes in feedback current may have been observed. The first is based on the proposition that DNA is capable of conducting charge (Kliene *et al* 2004; Kelley *et al*, 1997; Williams, *et al* 2000; Jackson *et al*, 2001;

Okada *et al*, 2003). On exposing the PEI/ssDNA film to a solution containing complementary genomic ssDNA, complementary binding occurs, where regions of the genomic DNA immobilised on the surface bind to complementary nucleotide sequences on genomic DNA suspended in the hybridisation solution. This complementary pairing forms double stranded regions of DNA at the surface of the sensor, enhancing the rate of electron transfer from the carbon electrode surface to the mediator in solution as the double stranded regions act as 'nano-wires', allowing the transfer of electrons along its length with the effect of lowering the impedance of polyelectrolyte/solution interface.

The intrinsic conductivity of DNA and the migration of charge through the pi-stack has received much attention over the last decade – partly due to its increasing importance in the field of DNA biosensors and DNA based bioelectronics. As research continues, so does the divide between the findings. This is very much highlighted by the large body of research in photochemistry, radiation biology, electrochemistry and solid-state physics that now exists in the field of DNA-mediated charge transport (Jackson, 2001). An example of these disparate findings is highlighted by comparing the work of Barton's group (Kelley *et al* 1999) and Meade *et al* (1995). In 1999, Barton and co-workers reported an intrinsic rate of $>10^9 \text{s}^{-1}$ between photoinduced electron donors and electron acceptors held 15 base pairs apart on a double helix, whereas Meade *et al* reported a rate ~ 1000 times slower using reactants attached by electrostatic interaction to a duplex half as long.

A second hypothesis for the observed changes in the feedback current response however, is that on exposure to the ssDNA/PEI film, complementary ssDNA in solution becomes associated with the immobilised sections on the immobilised ssDNA on the sensor surface. As a result of this, the net charge on the sensor surface becomes more negative, which has the effect of allowing or 'facilitating' the diffusion of the positively charged ruthenium complex through the interpenetrating PEI/DNA film and towards the underlying conductive carbon electrode.

On imaging the DNA/polymer arrays, it is evident that despite the deposition of the polyanionic DNA onto the polycationic film, there is no apparent change in the polycationic properties of the film; using the $\text{Ru}(\text{NH}_3)_6^{3+}$ mediator, negative feedback is still observed. With reference to the images obtained using the ferrocenecarboxylic acid

and ferricyanide mediators, the charges of the polymer and mediator are clearly important factors in determining whether a film will exhibit positive or negative feedback characteristics when interrogated. On depositing the initial, negatively charged ssDNA film on the polyethylenimine array, it may be expected that the apparent electrostatic charge would be reversed and that the film would exhibit positive feedback characteristics as the positively charged mediator is attracted to the negatively charged DNA immobilised close to the electrode surface. This is not the case, however and despite ssDNA functionalisation, the film continues to exhibit negative feedback characteristics.

$\text{Ru}(\text{NH}_3)_6^{3+}$ has been used extensively in the electrochemical quantification of oligonucleotides on surfaces. In an investigation into the permeation of ions through DNA modified electrodes, a cyclic voltammogram of $\text{Ru}(\text{NH}_3)_6^{3+}$ at a DNA modified electrode showed that the mediator binds to the DNA at the sensor surface by charge interaction. On conducting a cyclic voltammogram for $\text{Ru}(\text{NH}_3)_6^{3+}$ using a DNA modified electrode, the cyclic voltammogram resembled that which may be obtained by using a surface bound species where the peak shape is symmetrical and lacks any kind of diffusive tail (Ceres *et al* 2007). These findings may be related to the observations in this series of experiments. On the interrogation of the initial ssDNA/PEI film, negative feedback is observed as the net charge of the film remains positive as a result of the neutralisation of the excess charge of the DNA above that compensated for by the polyethylenimine film.

The smaller enhancements observed with the non-complementary experiments may be explained by a lesser degree of binding occurring between non-complementary strands and mis-matching which may occur when non-complementary binding occurs. As the DNA used is genomic, there are considerable sections of the DNA used that contain long range repeats – sections of DNA that contain the same sequence repeated for thousands of base pairs. As the DNAs used are those for Herring and Salmon, it is likely that they share similar repeats. Attempts were made to determine the degree of homogeneity between these two organisms for a percentage similarity, using various DNA sequence databases but these organisms' genomes have not yet been sequenced. Also, the likelihood of binding occurring by chance collisions of matching sequences approximately similar is high when using genomic DNA. The argument is hence that binding may occur in the non-complementary system but to a lesser extent to that observed in the complementary

system. This point is very much supported by the work conducted by Nabok and Davis *et al* (2007).

A point for consideration however, is whether the changes observed are due to any kind of binding at all, but to some other affinity interaction, in the form of some other property of genomic DNA that gives it an enhanced structural affinity for DNA of its own 'type' (i.e. genomic DNA from the same species interacts more strongly than DNA from different species) (Martin and Hoyer 1966).

The sensitive optical method of total internal reflection ellipsometry (TIRE) and atomic force microscopy (AFM) was used to investigate the interactions between and within DNA / PEI films (Nabok *et al* 2007). In a separate study using TIRE ellipsometry, the thickness and refractive indexes of adsorbed DNA layers on polyethylenimine films were determined. On exposing herring-ssDNA to herring-ssDNA immobilised on the surface of the polyethylenimine film, a thickness change of approximately 20nm was observed in comparison to a smaller change in thickness of 3-5nm when Herring-ssDNA was exposed to non-complementary Salmon-ssDNA. This differential change in thickness suggests that a greater quantity of genomic DNA is adsorbed onto the surface by complementary than non-complementary interactions (such changes may be investigated further by using a quartz crystal microbalance). It hence follows that the larger increase in feedback current observed over arrays exposed to complementary DNA may be explained by the larger amount of negatively charged DNA drawing more positively charged ruthenium to the surface of the carbon electrode by electrostatic interactions.

In the experiments conducted by Davis *et al*, changes in the impedance of the polyethylenimine film were observed to plateau over the course of three hours to a relative impedance of approximately 90% of that observed at the beginning of the experiment. The aim of this work was to investigate whether SECM in feedback mode was capable of monitoring these changes after this time period.

A possible avenue of investigation was to investigate the change in feedback current following exposure to the non-complementary and complementary hybridisation solution. However, this was not possible for a number of reasons. Firstly, the arrays are interrogated

by SECM in feedback mode, which necessitates the use of an electroactive mediator. To monitor the change in the feedback response with time, the hybridisation solution would have to be repeatedly removed and replaced with mediator, which would inevitably introduce error and increase the risk of disturbing the polyelectrolyte film. Secondly, unlike the impedimetric approach in which an impedance measurement is taken in a matter of seconds, area scans of the arrays fabricated here took over 1.5hrs. Preliminary experiments employing approach curves were carried out with the aim of minimising the time required to interrogate each substrate, but due to the heterogeneous nature of the carbon, the feedback response varied significantly across the substrate as some regions exhibited positive feedback while others demonstrated negative feedback despite being exposed to the same treatment. The area scan method provides a better insight into the electrochemical properties of the surface.

6.8 Conclusions

The principle aim of this chapter was to explore the possibility of using SECM to characterise a previously optimised impedance based DNA biosensor developed within the group (Davis *et al* 2007). The sensor is based on the construction of a bio-polyelectrolyte film of polyethylenimine and single stranded genomic DNA on a carbon ink electrode surface. The impedance of the sensor was observed to drop by approximately 10% in 3hrs on exposure to a hybridisation solution containing single stranded complementary genomic DNA. In contrast, on exposing the sensor to a buffered solution of non-complementary ssDNA, the impedance was observed to marginally increase. One of the aims of the research reported in this chapter was hence to determine whether these small changes in the impedance of the system were detectable by SECM in feedback mode within this time frame. In addition, it was hoped that the results would provide a valuable insight into other aspects of the biosensor for consideration in later studies.

Using the area scan macro, the spatial heterogeneity of the carbon electrodes used in the fabrication of the biosensor was demonstrated. Whilst this substrate is suitable for impedimetric analyses and fulfils the requirements of a disposable biosensor such as ease of fabrication, cost effectiveness and mechanical robustness, if the SECM array system described within this chapter is to be considered for further development, it is suggested that alternative, more topographically homogenous electrode surfaces should be investigated including gold, silicon and glassy carbon.

A polyelectrolyte film was constructed using polycationic polyethylenimine and polyanionic single stranded genomic herring DNA. The initial polyethylenimine layer was patterned in an array format, demonstrating the ability of the SECM XYZ micropositioning system to fabricate polyelectrolyte arrays of differing densities. On the interrogation of the system by SECM, the potential of the SECM approach to monitoring polyelectrolyte film formation was demonstrated.

Using the area scan macro and a variety of differently charged mediators, the insulating properties of the polyelectrolyte film were investigated. On using alternately charged mediators, it was revealed that the insulating effect of the polyethylenimine film on the

carbon substrate could be reversed. When the PEI array was interrogated by an area scan using the positively charged hexamine ruthenium chloride mediator, a diminution in the feedback current was observed. However, on using the oppositely charged ferricyanide redox couple, the opposite was found – and was thought to be a result of the coulombic, electrostatic interactions of the film and the differently charged mediators. These results successfully demonstrate the polycationic properties of the polyethylenimine film and its suitability to immobilising polyanionic ssDNA.

After the characterisation of the carbon/polyethylenimine array and the identification of a suitable redox couple ($\text{Ru}(\text{NH}_3)_6^{3+}$), the complete platform was interrogated by SECM. In brief, this involved comparing area scan data obtained by scanning the PEI/ssDNA array before and after exposure to complementary and non-complementary genomic DNA. It was found that on exposure to the complementary genomic DNA, the charge transfer properties of the ssDNA/PEI film were enhanced. This was also true for non-complementary exposure, although to a lesser degree.

Within this series of experiments, large quantities of genomic DNA have been used, following the same protocol as that employed by Davis *et al.* Whilst small changes in the charge transfer properties of the arrays were detected, the reason behind these changes is not completely understood.

To examine the true potential of the SECM approach in the label-less detection of DNA hybridisation, shorter DNA sequences should be used which would have a higher probability of exhibiting complementary binding and allow an improved understanding of the changes in the charge transfer properties of the polyelectrolyte film.

Within this chapter, a sound methodology has been developed for the fabrication, interrogation and subsequent analysis of a previously developed genomic DNA biosensor based on the functionalisation of a polyelectrolyte film with single stranded genomic DNA.

Chapter 7

Imaging horseradish peroxidase activity by SECM

7. Imaging horseradish peroxidase activity by SECM

7.1 Introduction

This chapter describes the use of SECM to image the activity of immobilised horseradish peroxidase (HRP). A brief introduction to the enzyme is given, after which, the experimental results are presented and discussed accordingly.

The principle aim of this chapter is the development of a method of imaging the enzymatic activity of horseradish peroxidase activity which may be taken forward into the following chapter which explores the possibility of using SECM to detect cell membrane protein expression by HRP labelling.

As discussed in chapter 2, scanning electrochemical microscopy has been used extensively in the characterisation of enzymatically patterned surfaces, providing valuable information about the effectiveness of the immobilisation and patterning techniques employed. With the possibility of using SECM in both feedback and generation/collection mode, the technique offers both spatial resolution and high sensitivity.

7.1.1 Horseradish peroxidase

In the early 1800s, Planché reported that a guaiacum tincture developed a stronger colour when a piece of fresh horseradish root was soaked in it. Since this time, horseradish peroxidase, the heme-containing enzyme responsible for Planché's observations, has been used extensively in the development of ideas on redox catalysis (Berglund *et al* 2002).

The direct electrochemistry of a variety of peroxidases have been investigated, including cytochrome C peroxidase, microperoxidase, lactoperoxidase, peroxidase from *Arthromyces ramosus* and chloroperoxidase from *Caldariomyces fumago* (Santucci *et al*, 1988; Kulys *et al*, 1990; Zamponi *et al*, 1990; Dunford *et al*, 1991; Razumas *et al*, 1992; Ruzgas *et al*, 1995; Csoregi *et al*, 1993; Mondal *et al* 1998). Horseradish peroxidase is the most well characterised enzyme of the peroxidase family and probably the most frequently used – due

to its fast kinetics and its subsequent exploitation in signal amplification. Its availability and high purity make it moreover, extremely cost effective – horseradish roots are now harvested on a relatively large scale due to the commercial use of the enzyme in clinical diagnostics and immunoassays.

All horseradish peroxidase enzymes are heme-containing glycoproteins with a molecular weight of approximately 42,000da. Although ‘horseradish peroxidase’ is the generally accepted term, a number of distinctive isozymes exist, of which the HRP isozyme C is the most prevalent and so, on which most of the HRP literature is based (Veitch, 2004). Originally sequenced by Welinder (1976), this enzyme is comprised of 308 amino acid residues, the 3D structure of which was published by Gajhede *et al* (1997). The structure was found to consist largely of α -helices and a smaller β -sheet region. The heme group - which is essential for the structural and functional integrity of the enzyme - is positioned between the distal and proximal domains (Figure 7.1).

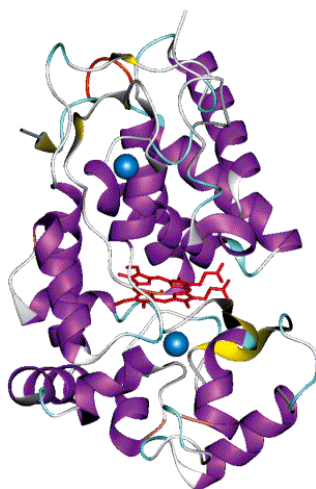


Figure 7.1: Three dimensional representation of X-ray crystal structure of HRP isozyme C (PDB Accession code 1H5A)

7.1.2 HRP enzymatic mechanism

The HRP catalysed reaction of hydrogen peroxide to water is given in Figure 7.2. AH and A[•] represent the reducing substrate and its reduced radical product respectively. Substrates identified to date include aromatic phenols, phenolic acids, indoles, amines and sulfonates (Veitch, 2004).

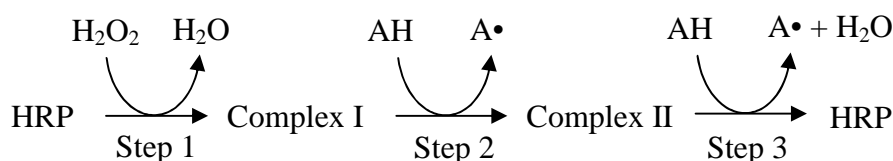


Figure 7.2: Simplified schematic of HRP enzymatic reaction

The catalytic mechanism has received much attention and has been investigated with high resolution by Berglund *et al* (2002) amongst others (i.e. intermediaries between the main step discussed here have been identified) (see reviews by Dunford, 1991; Veitch and Smith, 2001). The first step of the catalytic process involves the HRP-catalysed cleavage of the hydrogen peroxide molecule. In this step, one molecule of water leaves the complex, leaving a ferryl group and a porphyrin ring, each of which have accepted an electron from the hydrogen peroxide. Otherwise known as Complex I, this is two oxidation equivalents above the HRP in its ground state, so to return to its native form, it must be oxidised (an interesting point to note is that at low temperatures, a transient intermediate formed before Complex I, termed ‘Complex 0’ has been detected – described as an Fe(III)-hydroperoxy complex (Filizola *et al* 2000)). This is achieved via a two step process involving a reducing substrate, AH.

In step 2, on interaction with the substrate, an electron leaves the porphyrin ring radical cation, yielding Complex II. This then undergoes a further reaction with another reducing substrate molecule, at which point an electron leaves the ferryl group, releasing a reduced substrate molecule and another molecule of water. Within this work, the co-substrate used is hydroquinone, the interaction of HRP with which is given in Figure 7.3.

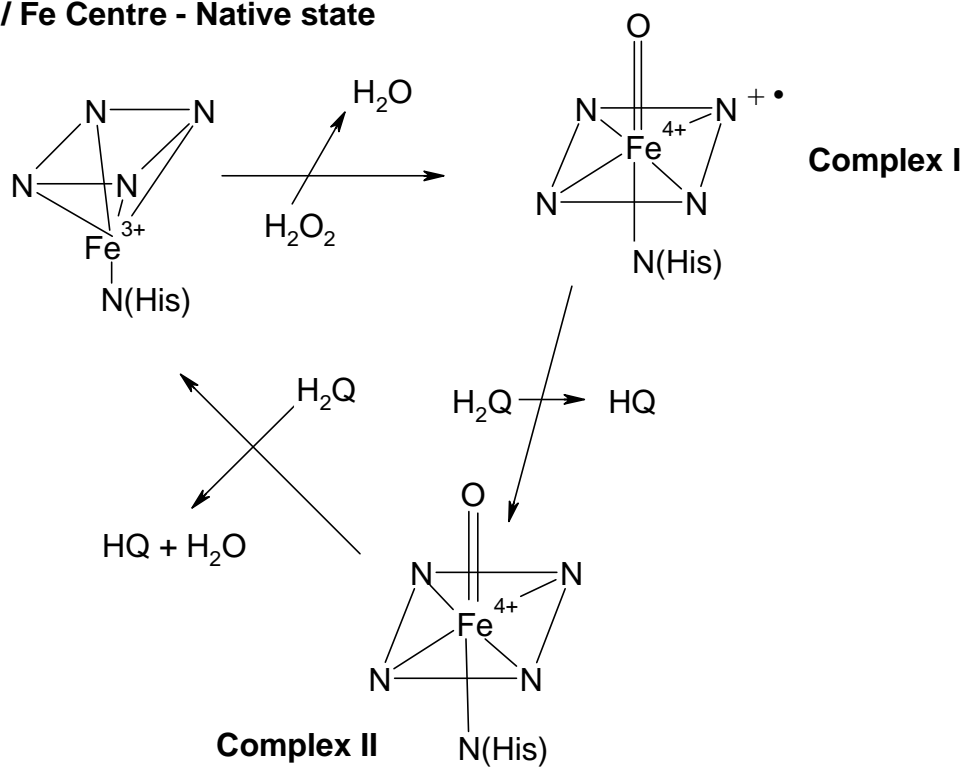
Porphyrin / Fe Centre - Native state

Figure 7.3: Catalysis of hydrogen peroxide by HRP, forming Complex I and its return to its native state via complex II

7.1.3 Hydroquinone / Benzoquinone redox couple

For the experiments in this chapter, the hydroquinone / benzoquinone redox couple is used. This redox couple is perhaps one of the most well characterised organic redox couples in the electrochemistry literature (e.g. Wipf, 1986; Aquino-Binaq, 1994; Raffie, 2007). With respect to its interaction with HRP, hydroquinone is thought to move into close proximity to the heme-edge on Complex I or Complex II where it receives an electron from the porphyrin ring or ferryl group respectively. It then moves away from the active site, at which point it undergoes disproportionation to form benzoquinone as shown in Figure 7.4.

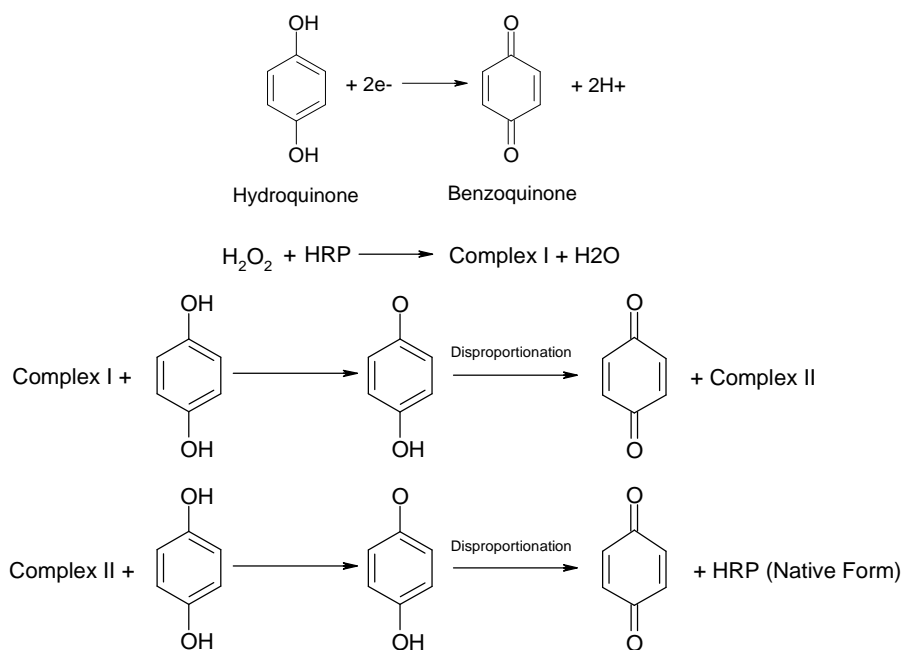


Figure 7.4: Proposed mechanism for the catalysis of hydrogen peroxide to water by HRP using hydroquinone as the oxidising substrate

7.1.4 Immobilisation of horseradish peroxidase on glass and SECM detection method

Horseradish peroxidase was crosslinked to a silanised glass microscope slide using glutaraldehyde (see Figure 7.5) and imaged by SECM using the hydroquinone/benzoquinone redox couple (Zhou *et al*, 2001).

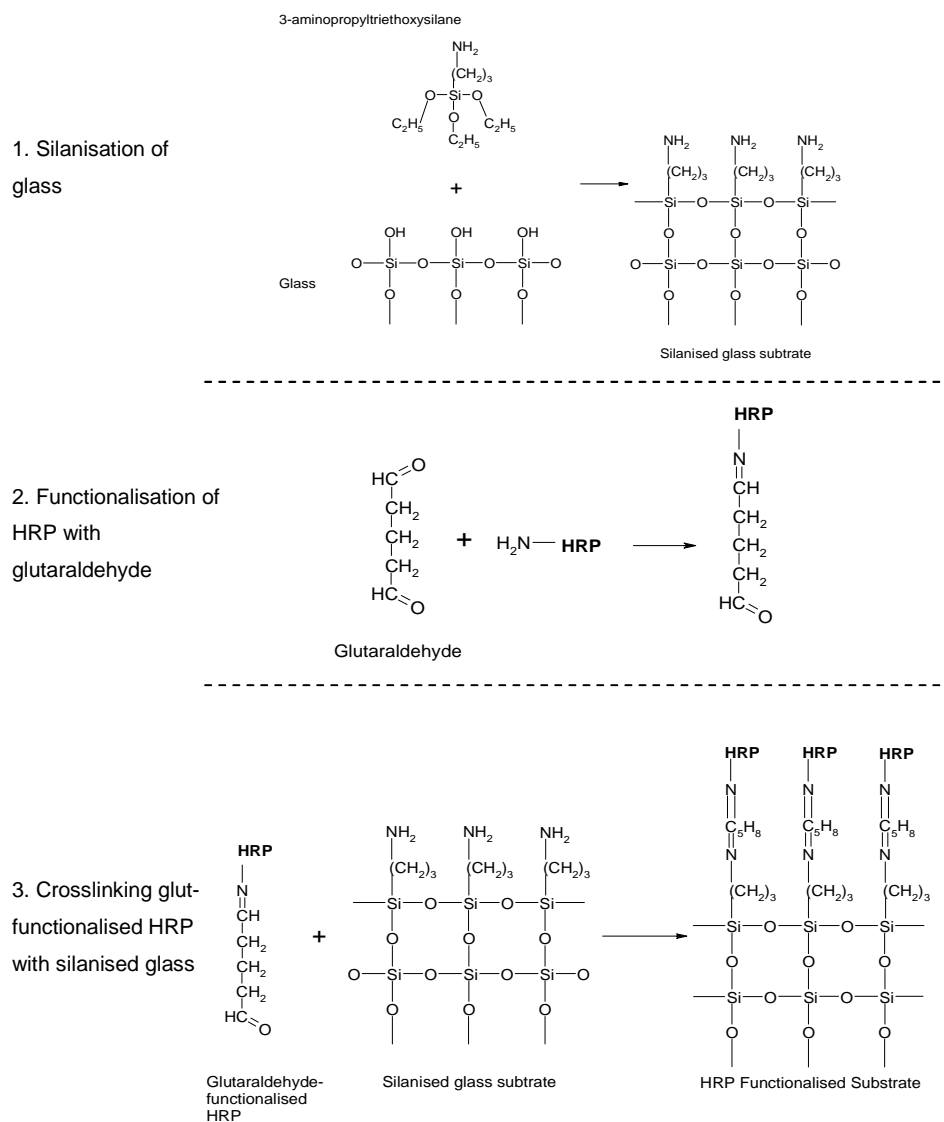


Figure 7.5: Reaction mechanism of HRP immobilisation

Both the enzyme-glutaraldehyde reaction and the subsequent glutaraldehyde-silane reaction occurs via nucleophilic attack by the amine group on the carbonyl group of the glutaraldehyde. The formation of these covalent bonds ensures the enzyme is immobilised strongly to the glass substrate for interrogation by SECM. Such a covalent method of attachment also reduces the risk of the patterned substrate ‘running’; due to the strong nature of this method of immobilisation, there is a reduced likelihood of the enzyme disassociating from the substrate and becoming attached to a non-functionalised region, allowing accurate, well defined and permanent substrate patterning in an array format.

To monitor and subsequently image the activity of the immobilised HRP moieties, SECM was used in generation/collection mode. The tip was set at -0.4V vs. Ag/AgCl , at which potential the reduced benzoquinone from the enzymatic reaction may be detected as per the schematic (Figure 7.6).

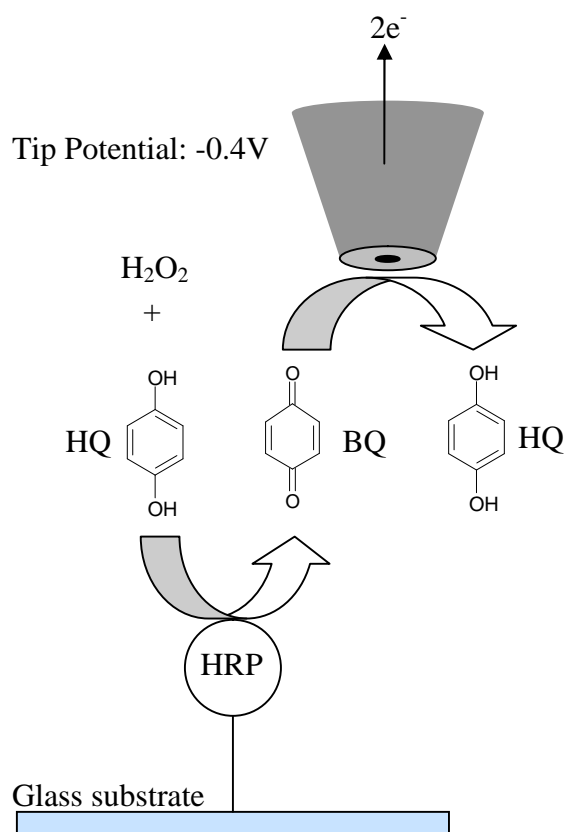


Figure 7.6: Schematic diagram of proposed detection mechanism of horseradish peroxidase using the hydroquinone / benzoquinone redox couple and the SECM in GC mode

The principle aim of this chapter is to develop a methodology by which the activity of the immobilised horseradish peroxidase may be imaged. By undertaking such a study, one may be afforded a valuable insight into the behaviour of immobilised horseradish peroxidase which may be subsequently used in the interpretation of information gathered in Chapter 8.

7.2 Results and Discussion

7.2.1 SECM approach curves

To determine the activity of the immobilised HRP, approach curves were conducted as follows. Firstly, the tip was positioned above the functionalised substrate and the reference and counter electrodes placed in close proximity. A 2mM pH 7.1 buffered solution of hydroquinone was then introduced to the system and an approach curve conducted with the tip biased at +0.8V which was sufficient for the reduction of hydroquinone to benzoquinone at the microelectrode disk. On approaching the substrate, the current was observed to fall, indicative of the negative feedback as the diffusion of hydroquinone to the tip is hindered by the proximity of the insulating glass (Figure 7.7). To prevent tip crash, the tip was halted when the faradaic current was equal to half of that in bulk (Figure 7.8). At this point, the position of the tip was zeroed and the tip was then retracted the required distance for the subsequent approach curves to be recorded.

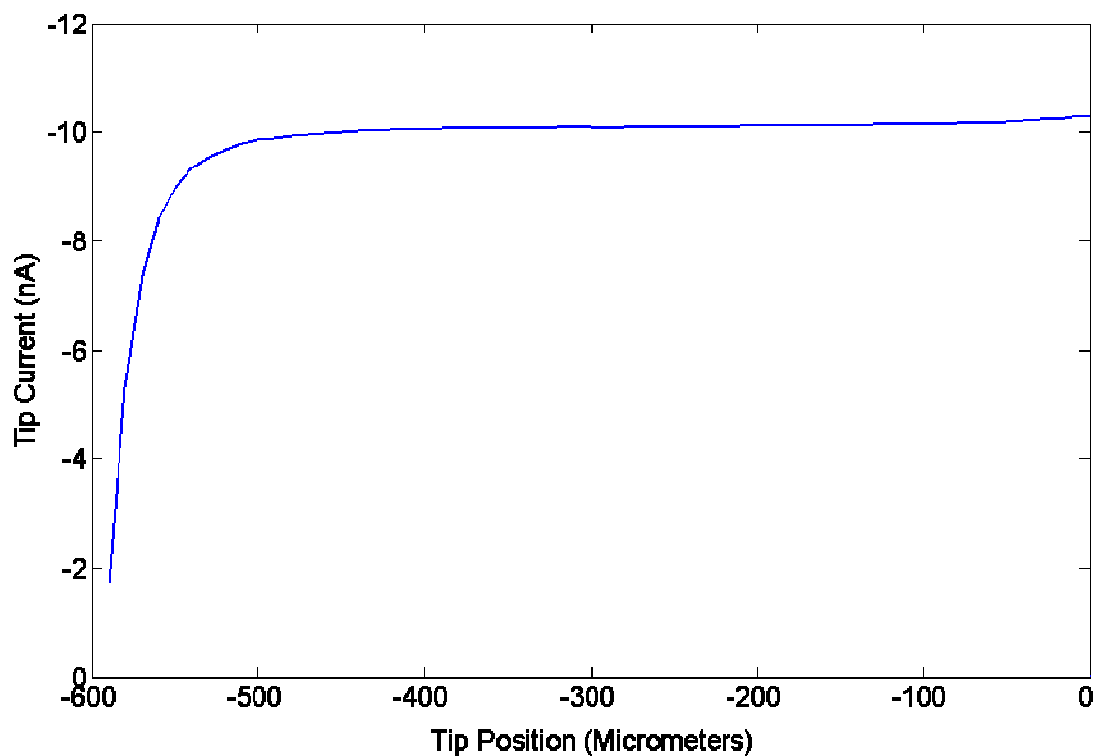


Figure 7.7: Approach curve over HRP functionalised glass in 2mM hydroquinone in pH 7.1 buffered solution

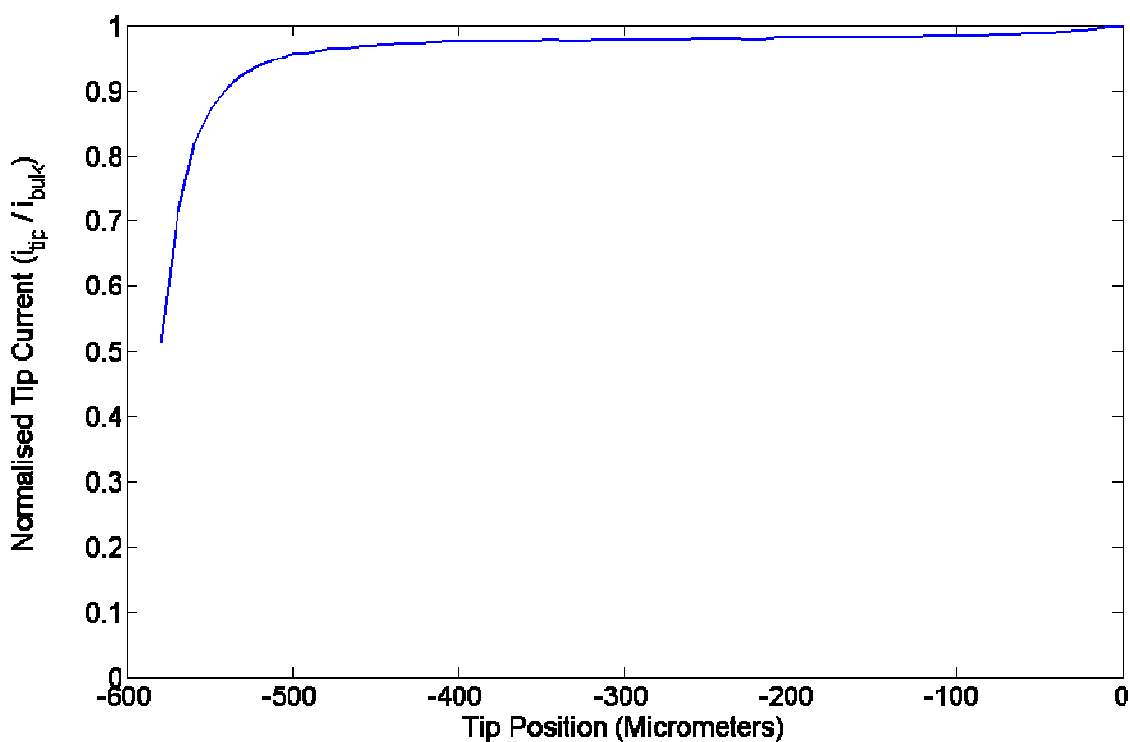


Figure 7.8: Normalised approach curve [i_{tip} / i_{bulk}] used to position tip over HRP-modified surface. Approach curves were conducted in pH 7.1 buffered 2mM hydroquinone; tip potential +0.8V; scan rate : 10 μ m increments

After positioning the tip, hydrogen peroxide solution was added to the system, which facilitates the enzymatic reaction. The tip potential was then polarised at -0.4V for the oxidation of benzoquinone and an approach curve towards the substrate was performed. The time between the addition of the hydrogen peroxide and the commencement of the approach curve was variable, depending on the experiment, but varied from 0 to 10 minutes (plus the duration for each approach curve, which was approximately 1.5 min). It was not possible to monitor the production of benzoquinone immediately after the introduction of the hydrogen peroxide using the approach curve because of the time delay between the commencement of the scan and the point at which the tip comes into close proximity to the immobilised enzyme.

7.2.2 Approach curve control experiments

Two substrates were used as controls in this study – a glass microscope slide along with a slide which had been functionalised with glutaraldehyde-crosslinked horseradish peroxidase and then exposed to a heat treatment (placed in an oven at 80°C for 15mins).

Approach curves were conducted over these substrates in a mediator solution containing 1mM hydroquinone and 1mM hydrogen peroxide in a pH 7.1 buffered solution. The resulting approach curves are presented in Figure 7.9. As the tip is moved into close proximity to the substrate, the tip current precipitously falls which is indicative of negative feedback due to the hindered diffusion of the mediator to the microelectrode and the absence of any detectable concentrations of enzymatic product.

These observations suggest that the heat treatment has denatured the HRP immobilised at the surface, diminishing its ability to catalyse the reduction of hydrogen peroxide to water via the reduction of hydroquinone to benzoquinone. As a consequence, the heat-treated surface behaves similarly to the unfunctionalised, insulating glass substrate.

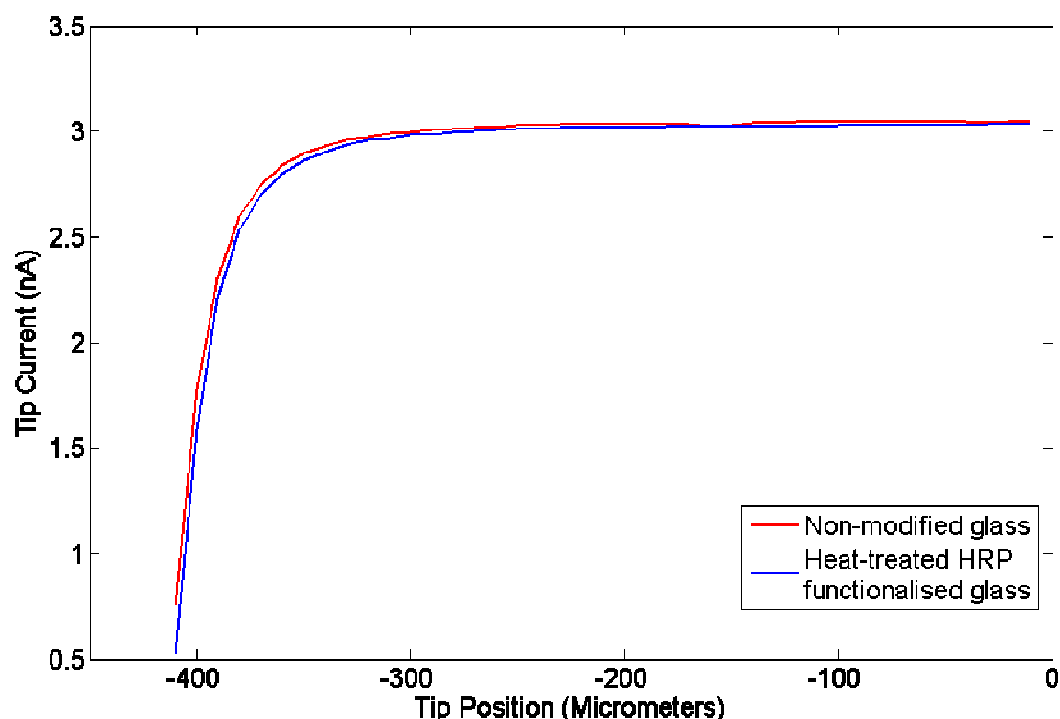


Figure 7.9: Control approach curves over a non-functionalised glass substrate and a heat treated, HRP functionalised substrate

7.2.3 Experimental approach curves

On approaching a HRP functionalised surface, the tip current is observed to increase to a peak value before exhibiting a sharp fall. This is in contrast to the negative feedback curves obtained when approaching an insulating, non-functionalised substrate or denatured substrate. The increase in current can be explained in terms of the generation of benzoquinone by the enzyme immobilised at the substrate surface. Since the rate at which the benzoquinone molecules can diffuse away from the surface is slower than the rate at which they are being produced by the enzyme, a concentration gradient arises and extends into solution; in this way, the concentration of benzoquinone at the functionalised surface is greater than that in bulk solution. As a result of this increase in concentration, there is a proportional increase in the faradaic current as the tip approaches the surface. However, as the tip comes into close proximity to the HRP-functionalised surface, the diffusion of the enzymatic product from the surface to the tip is hindered by the insulating glass sheath around the conductive disc, resulting in a lowering in current akin to that observed for a probe approaching an insulating

substrate. To allow comparison with the control curves, the approach curves were normalised to the current observed in bulk solution (Figure 7.10).

In this particular example, at a distance of 600 μm from the substrate surface, the tip current is equal to the tip current obtained in bulk solution. However, as the tip approaches the substrate, the tip current increases to a peak where the tip current is equal to 1.8 times the current obtained in bulk, indicating a local benzoquinone concentration 1.8 times that observed 600 μm away in bulk solution.

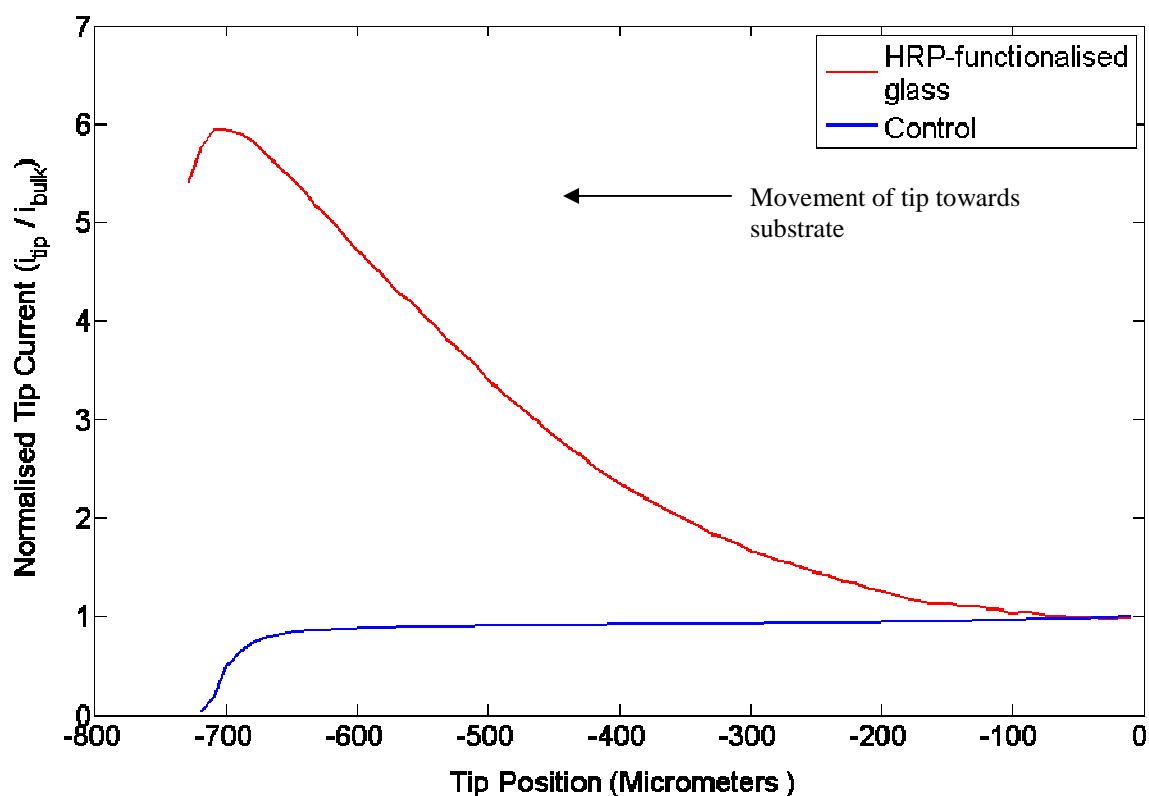


Figure 7.10: Normalised approach curves over a control substrate (heat treated HRP functionalised glass) and a normal, HRP functionalised glass substrate. Each approach curve was conducted in a pH 7.1 buffered mediator solution containing 1mM hydroquinone and 1mM hydrogen peroxide

7.2.4 Effect of enzyme concentration in loading solution on tip current

To determine the sensitivity of the technique, the silanised glass substrate was functionalised using solutions containing different concentrations of enzyme – specifically, 5, 4, 3, 2, 1, 0.75, 0.5, 0.05 and 0.025mg of HRP per ml of 1% glutaraldehyde solution. A 50 μ l droplet of each loading solution was pipetted onto the silanised glass surface and allowed to crosslink for five minutes before the substrate was rinsed and stored in pH 7.1 buffer until used. The average background subtracted peak currents were then plotted (Figure 7.11).

It may be seen from Figure 7.12 that on using a loading solution with an enzyme concentration of between 1 and 5mgml⁻¹, there appears to be no significant difference between the peak current measured by the approach curves over each substrate.

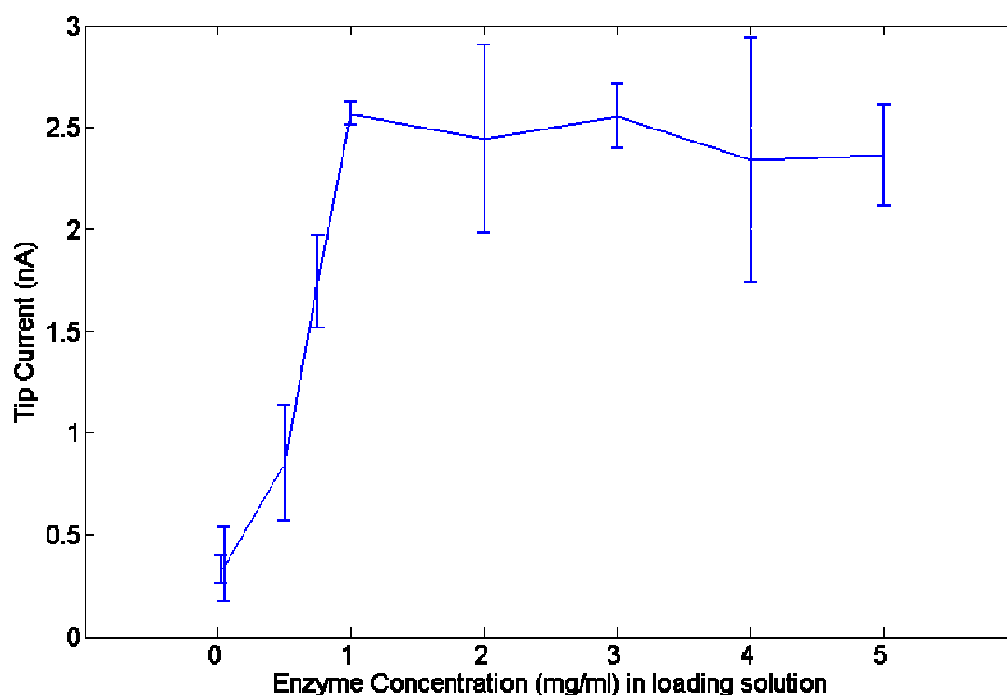


Figure 7.11: Variation in peak tip current with enzyme concentration in loading solution. Error bars are 95% confidence intervals for calculated means.

However, on reducing the concentration of the loading solution to 0.75mgml^{-1} and below, there is a concomitant decrease in the average peak current obtained by approach curve.

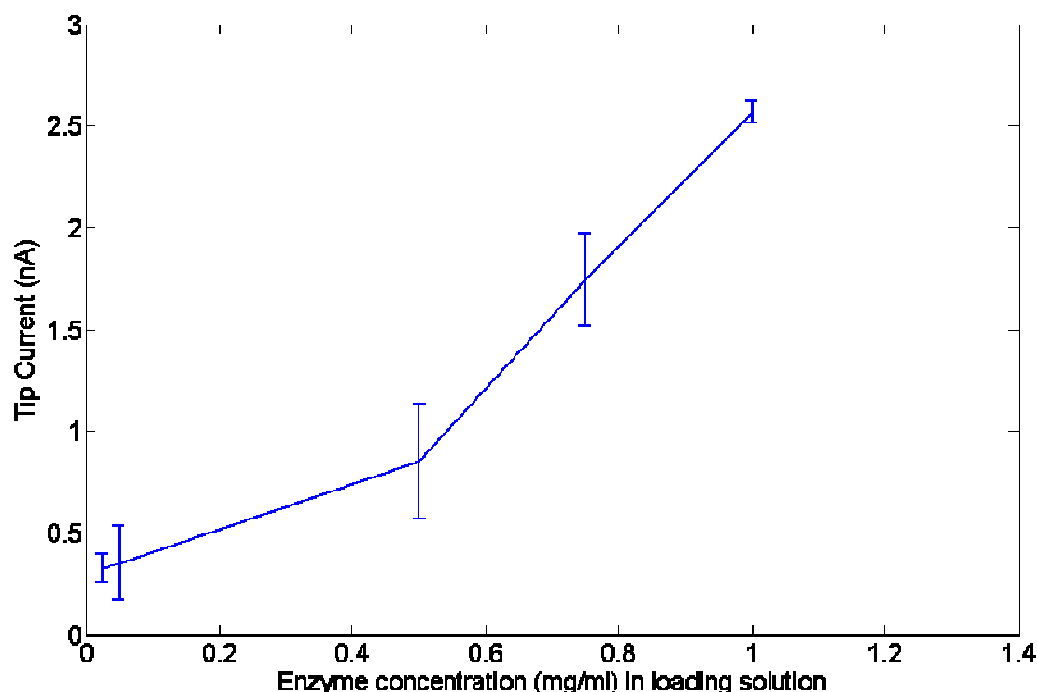


Figure 7.12: Variation in peak tip current with enzyme concentration in loading solution. Error bars are 95% confidence intervals for calculated means

The observed relationship between the average peak tip current and the enzyme concentration in the loading solution may be due to two possible reasons, as described below.

The first relates to the density of enzyme on the surface; on treating the silanised glass with a 1mgml^{-1} solution, if the surface is saturated with the enzyme and all cross linking sites are occupied, the use of enzyme loading solutions with 2, 3, 4 and 5mgml^{-1} may result in no further increase in the concentration of enzyme immobilised at the substrate surface. The effect of such surface saturation would be that the peak current observed over each of these saturated substrates was similar in magnitude.

A second hypothesis for this observation is based on the diffusional kinetics of the immobilised enzyme. When the rate of diffusion of the reactants to the enzyme is greater than the rate of the enzymatic reaction, the overall rate of the enzymatic reaction would be under the kinetic control of the enzyme. Under these conditions, if one was to increase the

concentration of the enzyme at the surface, the enzymatic activity per unit area would increase, resulting in an enhancement in the production of benzoquinone and a higher peak current when interrogated by SECM. At the lower enzyme concentrations, on increasing the concentration of enzyme at the surface, an incremental increase in the peak current would be observed. However, on increasing the concentration of the loading solution to 1mgml^{-1} and above, the peak current plateaus; this is thought to be due to the fact that at this level of enzymatic activity per unit area, the rate of the enzymatic reaction per unit area is faster than the rate at which the reactants, hydroquinone and hydrogen peroxide, can reach the immobilised enzyme by diffusion – i.e. the rate of the enzymatic reaction is limited by the rate of diffusion of the substrate to the enzyme.

As may be seen from these figures, there is a significant amount of variation in the peak tip current recorded. Whilst every precaution was made to minimise variation between experimental replicates, a significant amount of inter-replicate variation remained; this very much highlights the difficulty in interrogating diffusion layers above a substrate using SECM.

7.2.5 Effect of reaction time on product concentration

Approach curves were conducted at specific time periods to monitor the diffusion of the enzymatic product, benzoquinone, from the substrate with time. By conducting such experiments, valuable information may be provided which would aid the interpretation of area scan data. Approach curves were conducted at $t = 0, 2, 4, 6, 8$ and 10 minutes from the introduction of hydrogen peroxide to the mediator solution. An example of the resulting series of approach curves is given in Figure 7.13.

Approach curves were conducted at a scan rate of $5\mu\text{m}$ per point so as to minimise disturbance of the diffusion layer emanating from the HRP functionalised substrate. If approach curves were conducted at any greater speed, whilst they would allow measurements to be taken faster, the movement of the tip towards the surface may disturb the diffusion layer by mechanical convection.

In the example given (Figure 7.13), at $t = 0$ mins, the bulk concentration of benzoquinone is equal to the background concentration of benzoquinone, resulting in a low initial tip current up to $600\mu\text{m}$ from the surface. On approaching the enzyme functionalised substrate, the tip current was observed to increase to approximately 3.2nA above the background current. On conducting further approach curves at later time intervals, a similar current profile was obtained but the rate of change of tip current was not as great.

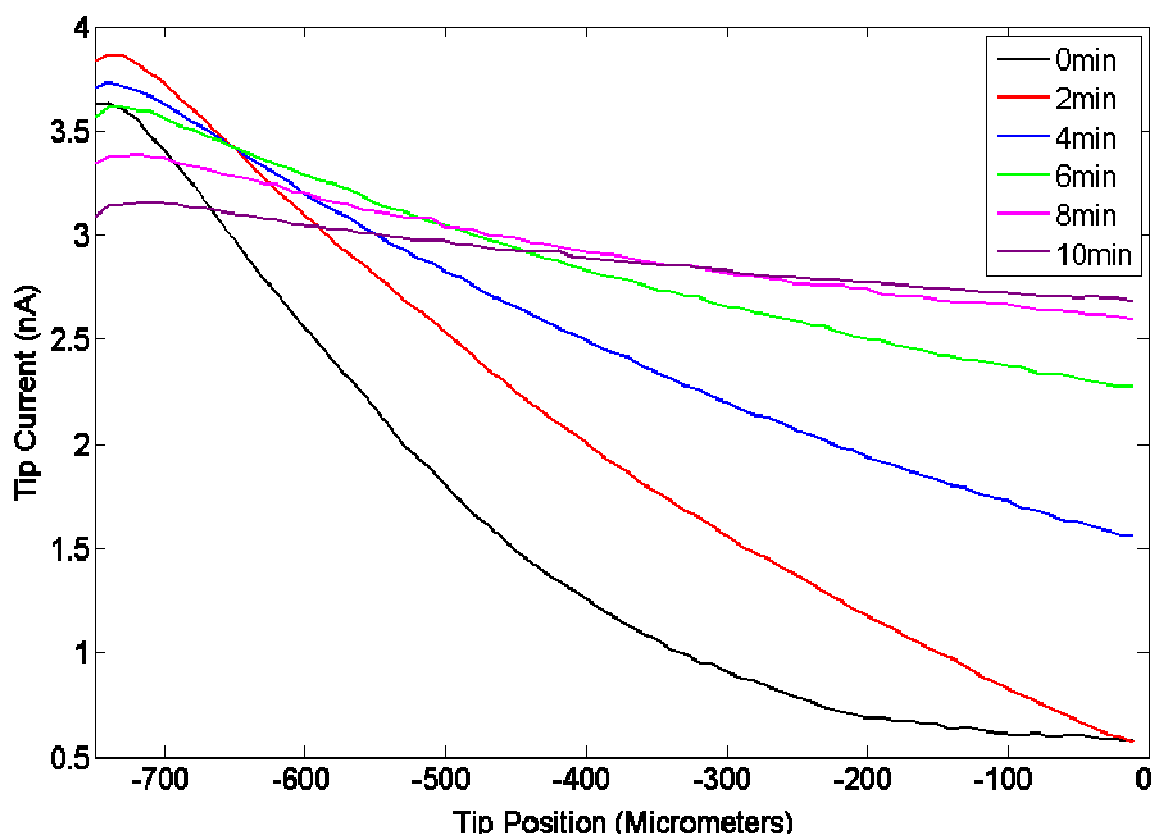


Figure 7.13: A series of approach curves obtained at various time intervals after the introduction of hydrogen peroxide to the system

An interesting observation is the temporal change in the tip current measured in close vicinity to the enzyme functionalised substrate. To illustrate these changes, the peak current recorded at each time interval was extracted from the data depicted in Figure 7.13 and plotted against time (Figure 7.14).

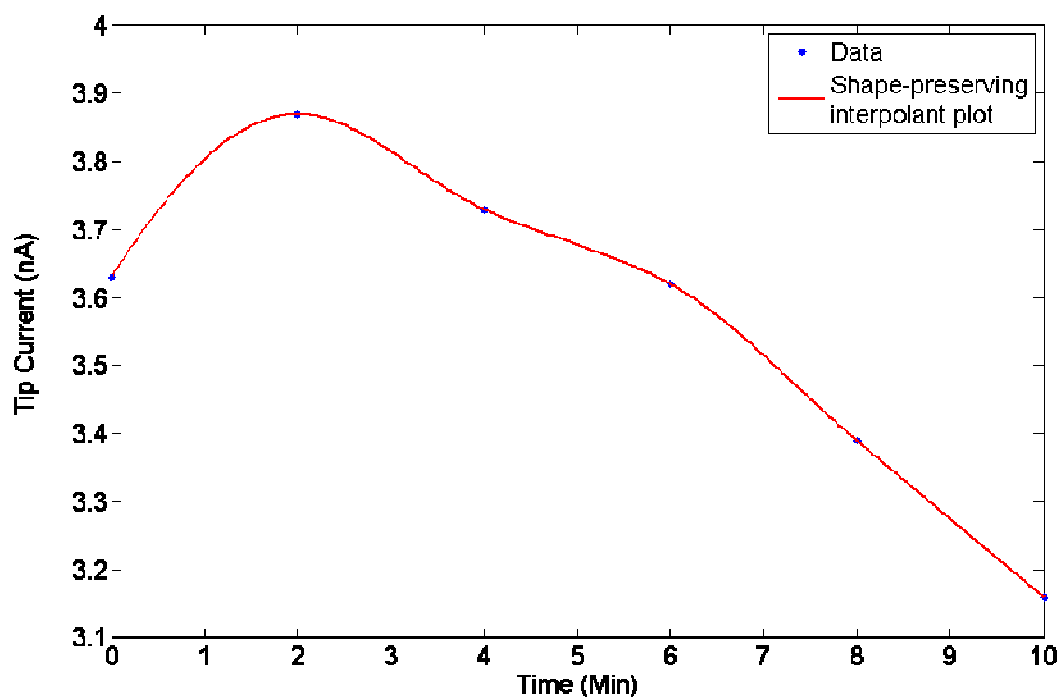


Figure 7.14: Graph illustrating change in peak tip current over time obtained by approach curve over HRP-functionalised glass

Initially, when $t = 0$, the rate of benzoquinone production by the immobilised enzyme is limited by the kinetics of the enzyme as reactants are present at a high concentration in close proximity to the enzyme. In this initial phase, the reaction proceeds rapidly and the concentration of the enzymatic product increases (i.e. $[BQ]_{t=2} > [BQ]_{t=0}$). However, as the reaction continues, the concentration of the reactants falls in the vicinity of the enzyme, resulting in a lowering of the rate of the enzymatic reaction. This fall in the rate of the enzymatic reaction is then manifested in a fall in tip current as this is in proportion to the concentration of benzoquinone in solution.

7.2.6 Calculation of benzoquinone concentration gradients

In order to estimate the concentration of benzoquinone in the diffusion layer emanating from the immobilised enzyme using the equation for the current at a microelectrode, it was necessary to first calculate the diffusion coefficient for benzoquinone. This was accomplished by conducting a cyclic voltammogram under the same solute conditions as those used for the approach curves and then using the peak current measured in the CV in the Randles-Sevcik equation (Equation 7.2.1).

In this relationship, the peak current (i_p) in a cyclic voltammogram for the species under interrogation is expressed as a function of n , the number of electrons involved in the charge transfer reaction, F , the Faraday constant ($96485.3415\text{Cmol}^{-1}$), A the electrode area (cm^2), ν the sweep rate, D the analyte's diffusion coefficient (cm^2/s), R the universal gas constant (8.134 J/mol), C the concentration in mol cm^{-3} , and T , the absolute temperature (K):

$$i_p = 0.4463nFAC\left(\frac{nF\nu D}{RT}\right)^{1/2}$$

Equation 7.2.1

At 25°C however, this equation may be simplified to:

$$i_p = (2.687 \times 10^5)n^{3/2}\nu^{1/2}D^{1/2}AC$$

Equation 7.2.2

Where the constant (2.687×10^5) has the units $\text{Cmol}^{-1}\text{ V}^{-1/2}$.

Analysis of the data obtained from a cyclic voltammogram, run using the same solute solution as described in Section 7.2.1 yielded the following values:

$$I_p = 2.01\text{e-}06\text{ A}$$

$$n = 2$$

$$A = 0.24\text{cm}^2$$

$$C = 0.002\text{mol l}^{-1} = 2\text{e-}06\text{ mol cm}^{-3}$$

$$\nu = 0.05\text{ Vs}^{-1}$$

Using the Randles-Sevcik equation, a diffusion coefficient of $2.46 \times 10^{-5} \text{ cm}^2 \text{ s}^{-1}$ for benzoquinone in buffer was calculated under these specific solute conditions. This figure is in good agreement with previous results (Rees *et al*, 1995; Martin *et al*, 1998).

The faradaic current observed at a microelectrode in bulk solution is described by the following equation:

$$i_{T\infty} = 4nFDCa$$

Equation 7.2.3

During the approach curves over HRP modified glass, at any point in bulk solution, the current may be described by the equation above. Given the tip current, the area of the working electrode and the diffusion coefficient for the species under detection, it is possible from this equation to estimate the concentration of benzoquinone at each point along each approach curve. The change in the benzoquinone concentration profile over time for a 5 mg ml^{-1} HRP functionalised substrate is presented in Figure 7.15.

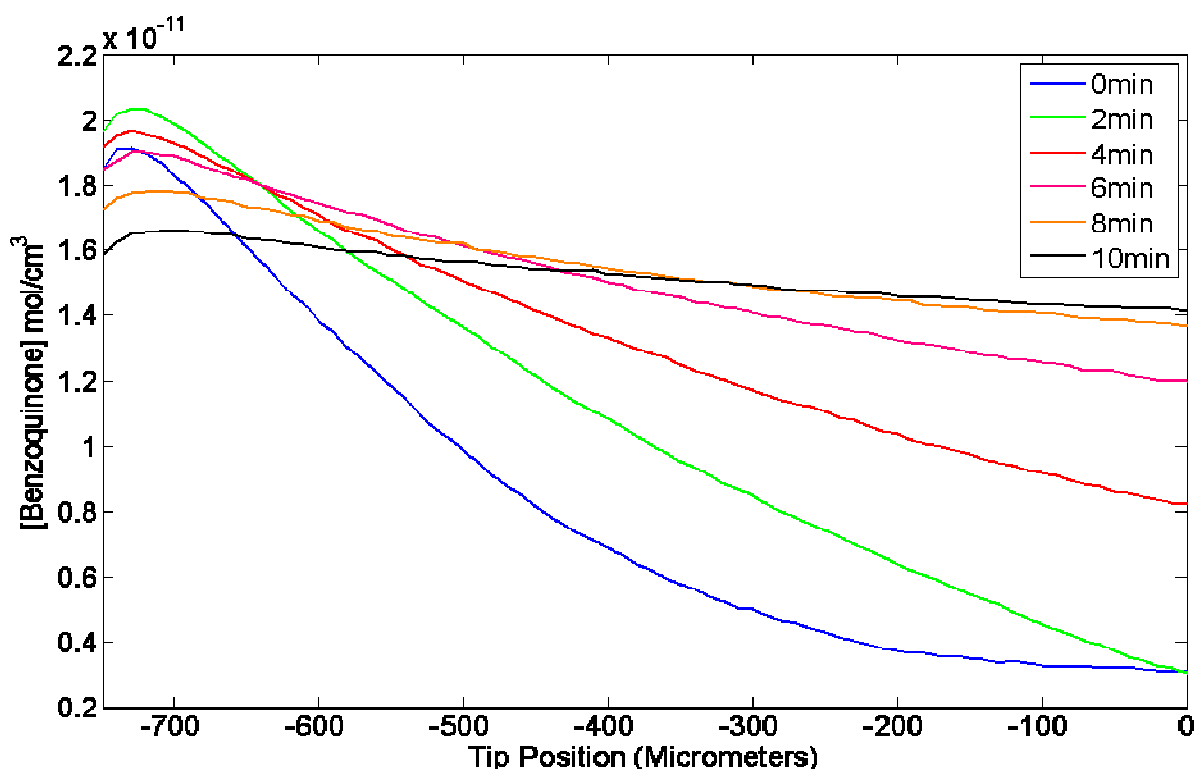


Figure 7.15: Linegraphs illustrating changing benzoquinone concentration from bulk solution towards the enzyme functionalised surface. These were calculated using approach curve data (5 mg ml^{-1})

As expected, the conformation of the concentration profiles in Figure 7.15 is exactly the same as that observed in Figure 7.13 as the tip current is proportional to the concentration of benzoquinone in the vicinity of the electrode. However, care must be taken in the interpretation of Figure 7.15 at tip positions lower than $-700\mu\text{m}$. The drop in current observed here is not due to a drop in benzoquinone concentration but due to negative feedback effects arising from the proximity of the tip to the surface. It is hence not possible to make an accurate estimation of the benzoquinone concentration in the immediate vicinity of the enzyme by this method.

The lowest measured current peak detected was for the substrate functionalised with 0.025mg/ml enzyme solution and was calculated to be $1.2 \times 10^{-12} \text{ mol cm}^{-3}$.

The differential changes in the concentration of benzoquinone in bulk and in close vicinity to the immobilised enzyme has interesting implications for interrogating enzyme activity by an area scan approach. By conducting an area scan at a smaller tip to substrate distance, one may minimise the effect of time on the current response as the temporal changes in tip current are smaller than those observed in bulk solution. The growth of the diffusion layer into solution also highlights the problem with the resolution of images obtained by SECM in generation/collection mode. Due to this diffusion of the enzymatic product from the surface, it is difficult to determine with any precision the location from which the product originated – i.e. the site of the enzymatic reaction.

By calculating the concentration of benzoquinone 300 μm from the enzyme functionalised surface and the concentration of benzoquinone obtained before the onset of negative feedback, the average concentration gradient, at two minute intervals, was calculated.

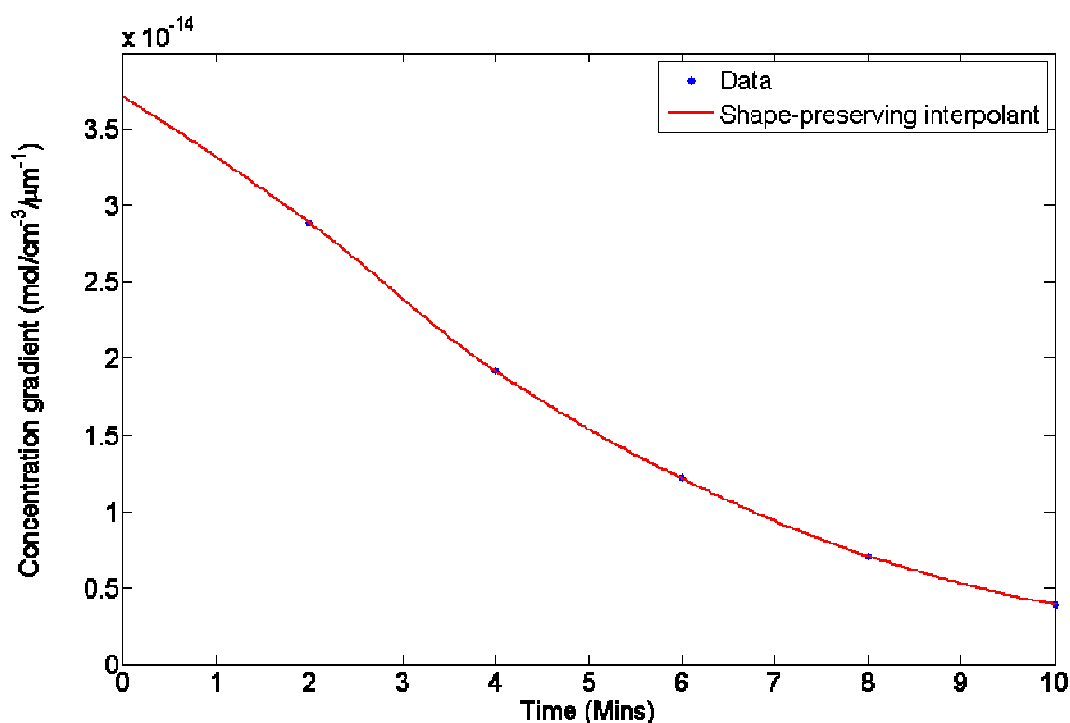


Figure 7.16: Average concentration gradient of benzoquinone plotted as a function of time, calculated using data from approach curves

At $t = 0$, the hydroquinone concentration in the enzyme's microenvironment will be high, meaning that initially, the reaction rate will be limited by the activity of the enzyme. As time elapses the concentration of hydroquinone in the vicinity of the enzyme will fall, since the rate of reaction is faster than the rate at which reactants can diffuse to the enzyme; this results in a concomitant decrease in the reaction rate. This decrease in reaction rate, combined with the diffusion of benzoquinone out into solution, causes a lowering of the benzoquinone concentration at the substrate.

This hypothesis is supported by observing Figure 7.15 which demonstrates the slow diffusion of the benzoquinone out into solution. Initially, the concentration gradient is high as the rate at which benzoquinone can diffuse away from the site of the enzymatic reaction is slower

than the rate at which it is produced by the enzyme. As time elapses however, the flux of benzoquinone from the surface becomes limited by the flux of fresh substrate to the enzyme. The result is that this decrease in the rate of benzoquinone production allows benzoquinone to become more evenly distributed in the volume of solution in the vicinity of the enzyme – i.e. the difference in benzoquinone concentration between any one point along the approach curve axis becomes smaller.

7.2.7 Imaging horseradish peroxidase activity

In order to move towards a method of imaging cell membrane protein expression, it was necessary to develop an appropriate method for imaging HRP activity. Using the same patterning techniques as those employed in chapter 6, patterned HRP arrays were fabricated using the XYZ micro-positioner. The spacing of the arrays was an essential consideration to avoid the merging of diffusion layers – which would affect the resolution of the array. If the array dots were placed too close together, there would be a risk of their diffusion layers overlapping, resulting in two dots appearing as one. It was found that by positioning them up to 500 μm apart, they were sufficiently distant from one another to appear as two distinct dots, as depicted in Figure 7.17

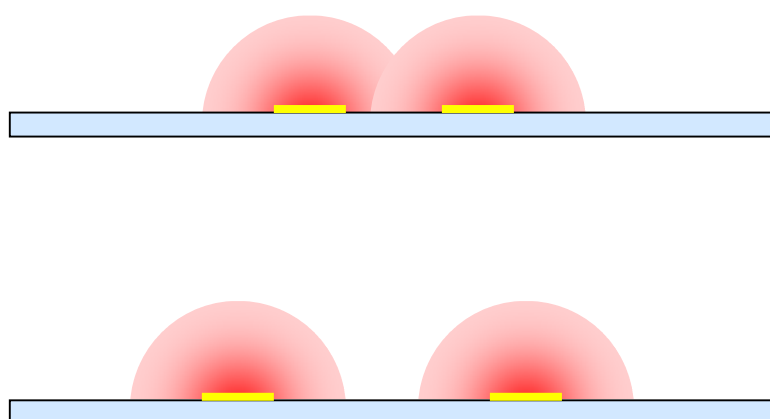


Figure 7.17: Schematic diagram illustrating the importance of distance in fabricating an array and avoiding merging of diffusion layers

7.2.8 Area scans

Before conducting area scans over the HRP arrays, approach curves were carried out over a non-functionalised region of the microscope slide patterned with the array. The tip was positioned 50 μ m above the point at which the tip current was 50% of that in bulk. The decision to position the probe at this height was based on observing the behaviour of the tip current when approaching the HRP functionalised substrate in the previous series of approach curves. It was at this height where the peak current was obtained and where negligible feedback effects were observed. After positioning the tip in the Z axis, the tip was then moved through solution and positioned proximal to the horseradish peroxidase array before hydrogen peroxide was introduced into the system. The area scan macro was then conducted over the functionalised substrate.

7.2.9 Effect of substrate concentration on area scan resolution

The aim of this series of experiments was to determine the effect of substrate concentration on the enzymatic reaction. Area scans were conducted in a buffered mediator solution comprising 1mM hydroquinone and hydrogen peroxide at concentrations of 1mM, 0.6mM, 0.4mM and 0.2mM.

It is evident that on using smaller concentrations of the hydrogen peroxide substrate, the resolution of the images obtained decreases. Using hydrogen peroxide concentrations of 0.6mM and above, the area scans recorded well defined regions of enzymatic activity (Figure 7.18). Those scans which have been obtained using hydrogen peroxide in lower concentrations however have poorly defined functionalised regions, indicative of lowered enzymatic activity (Figure 7.19).

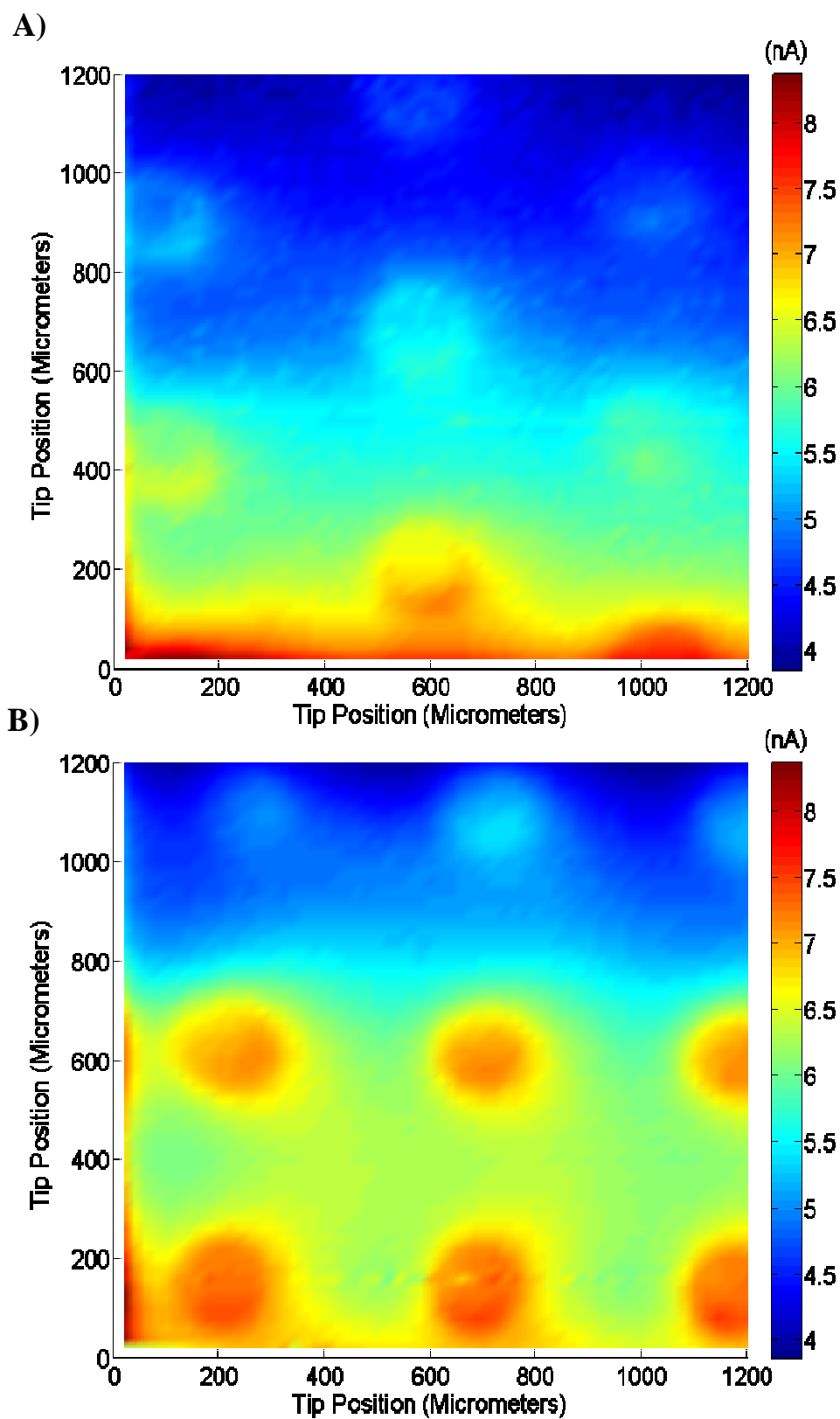


Figure 7.18: Area scans over HRP arrays. Scans were conducted in a pH 7.1 buffered solution containing 1mM hydroquinone and A) 1mM and B) 0.6mM H_2O_2 respectively.

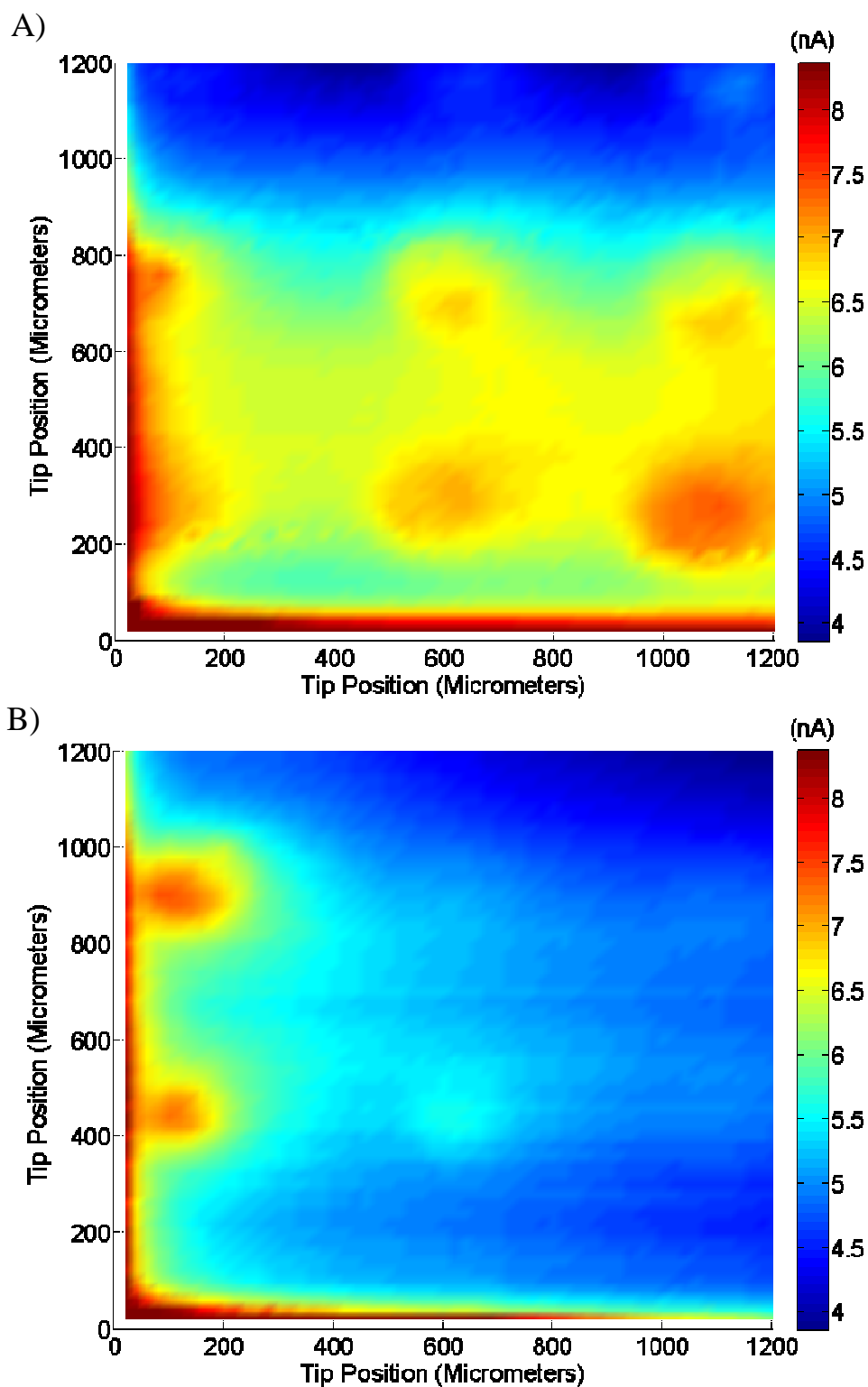


Figure 7.19: Area scans over HRP modified array. Scans were conducted in a pH 7.1 buffered solution containing 1mM hydroquinone and A) 0.4mM and B) 0.2mM H_2O_2 respectively

Background subtraction

Background subtractions were performed to improve the resolution of the area scan images obtained. In doing so, the current range of the images was lowered. The subtraction had the effect of removing the tip current variation due to substrate slope as well as taking into account the concentration of benzoquinone in bulk solution.

The subtraction was achieved post-scan by constructing a background array from a line of data extracted from the experimental area scans (Figure 7.20 and Figure 7.21). This background area was then subtracted from the original experimental area scan to obtain the background subtracted, optimally resolved area scan images of the array.

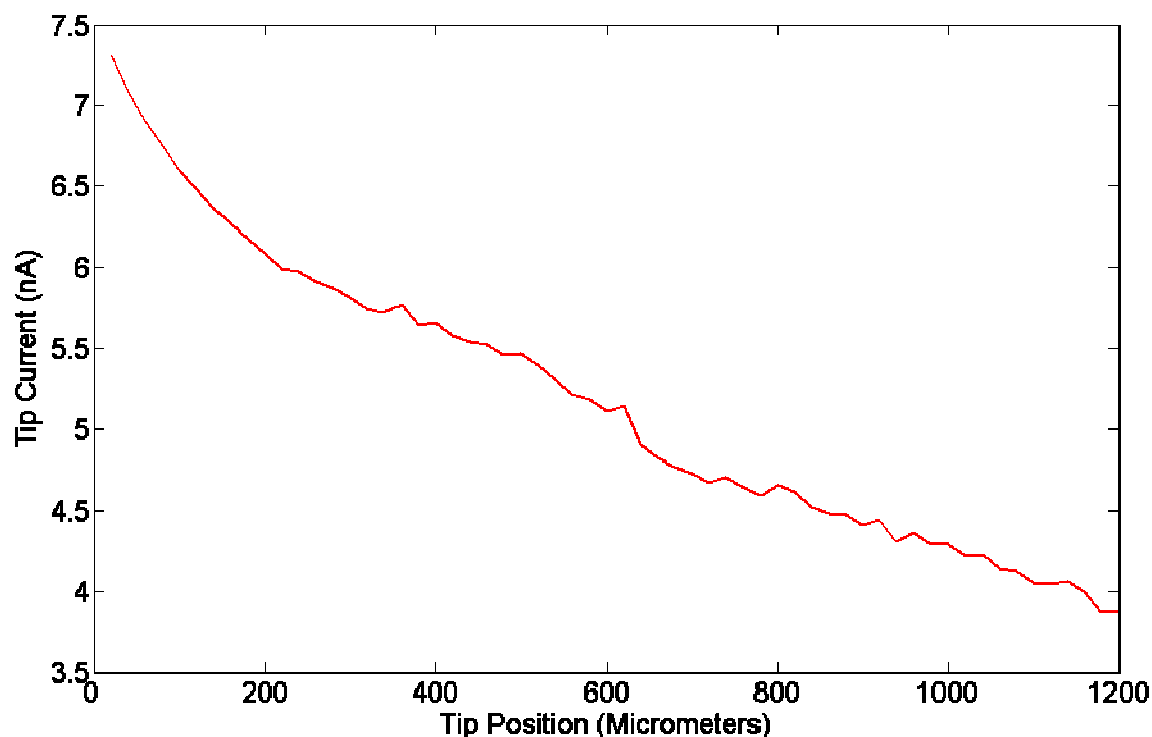


Figure 7.20: Linescan extracted from area scan data to allow construction of background current array

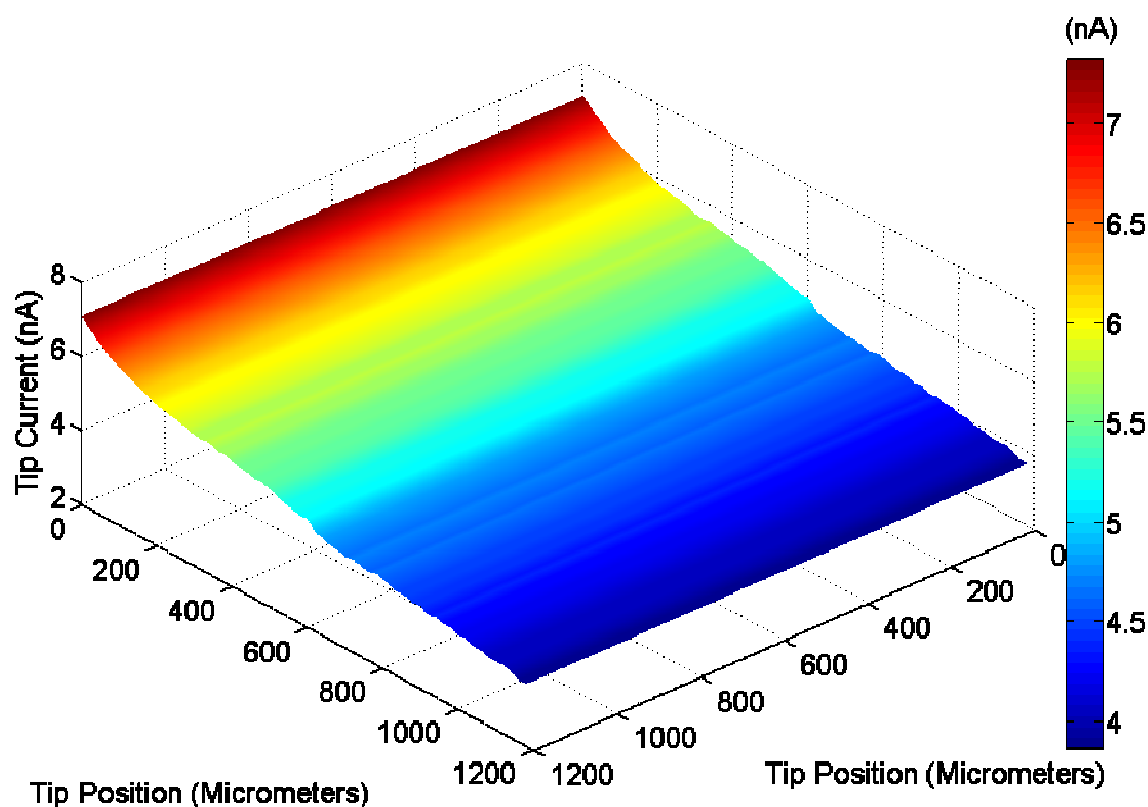


Figure 7.21: Background current array constructed from Figure 7.20, for subtraction from experimental array

An alternative approach to the background subtraction method employed here would be to have conducted an area scan before and following the addition of the hydrogen peroxide and then to have subtracted the ‘before’ scan from the ‘after’ scan. The reason for not doing so is two fold: firstly, although the un-catalysed reaction between hydroquinone and hydrogen peroxide is very slow, the addition of hydrogen peroxide to the system may have an effect on the concentration of benzoquinone in bulk, resulting in an increase in the bulk concentration of benzoquinone that would not have been catered for by the simple subtraction of the ‘before’ data. Secondly, on the addition of the hydrogen peroxide to the system, the bulk concentration of the mediator is altered, which would have implications for the validity of comparing the two scans. Thirdly, on conducting the first scan, there may be tip crash and the tip may become fouled on the first scan, which again would introduce error to the data, affecting the validity of the subtraction.

Using the methodology described, well defined, high resolution images were obtained which illustrate the applicability of the technique to imaging enzymatic activity. A significant limitation of the substrate generation, tip collection mode is that during scanning, the electrode is moved through the diffusion layers extending into solution around the area of interest, which may lead to the redistribution of electroactive species over the substrate. Such movement of these species may then lead to a poorly resolved image whereby it is difficult to determine where on the substrate the reaction is occurring. Despite this problem, it is apparent from the images below (Figure 7.22 to Figure 7.23) that well resolved images may be obtained.

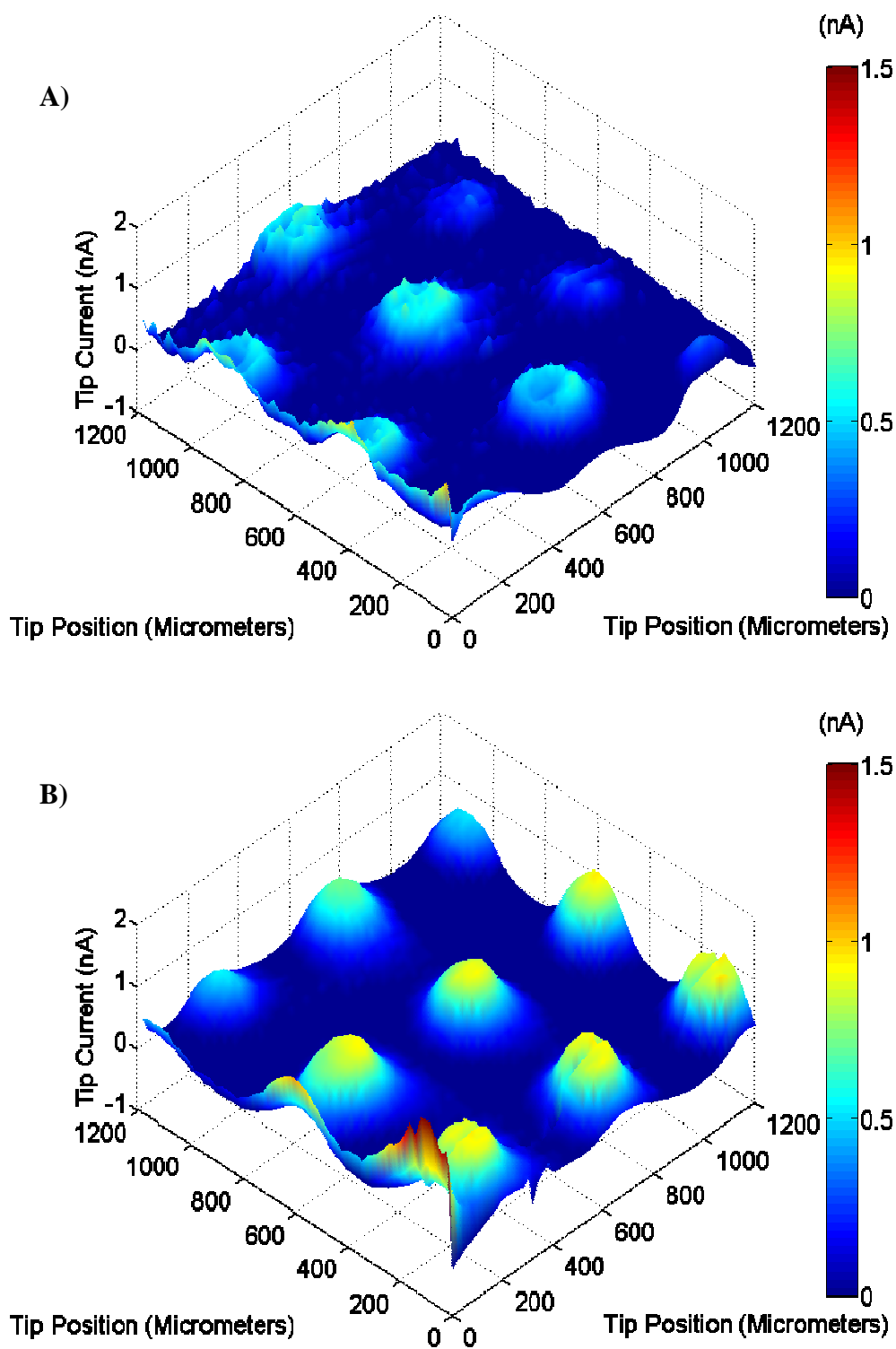


Figure 7.22: Background subtracted area scan over HRP modified arra using pH 7.1 buffered solution containing 1mM hydroquinone and A) 1mM H_2O_2 and B) 0.6mM H_2O_2

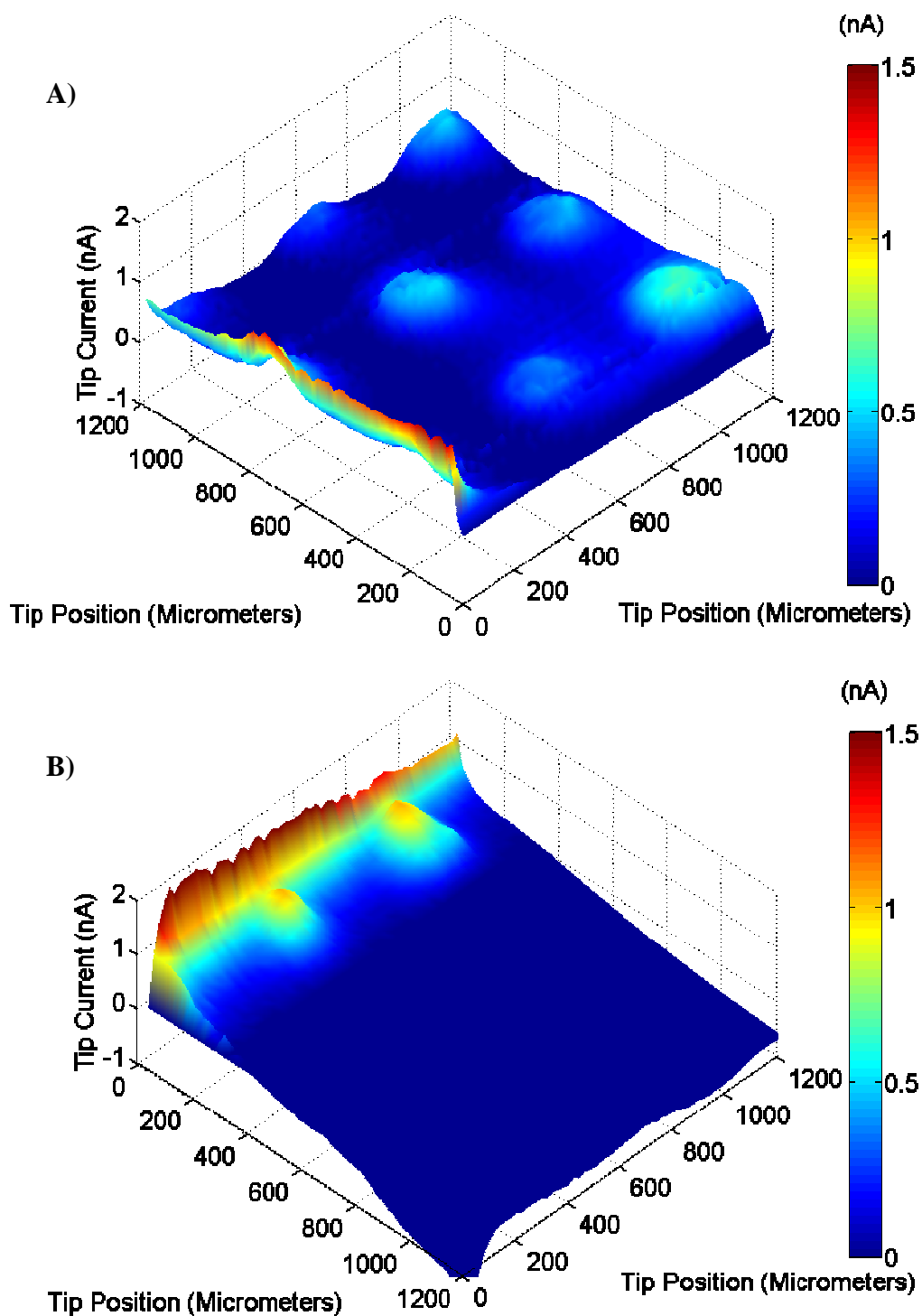


Figure 7.23: Background subtracted area scan over HRP modified arra using pH 7.1 buffered solution containing 1mM hydroquinone and A) 0.4mM H_2O_2 and B) 0.2mM H_2O_2

By lowering the concentration of hydrogen peroxide in the mediator solution, the rate of the enzymatic reaction is also lowered. As a consequence, the production of benzoquinone by the HRP immobilised at the substrate surface is lowered, resulting in a diffusion layer of lower benzoquinone concentration in the vicinity of the immobilised enzyme. The implication of this reduction in the diffusion layer concentration is that the effect of substrate slope is more pronounced. This is demonstrated in the schematic below - Figure 7.24.

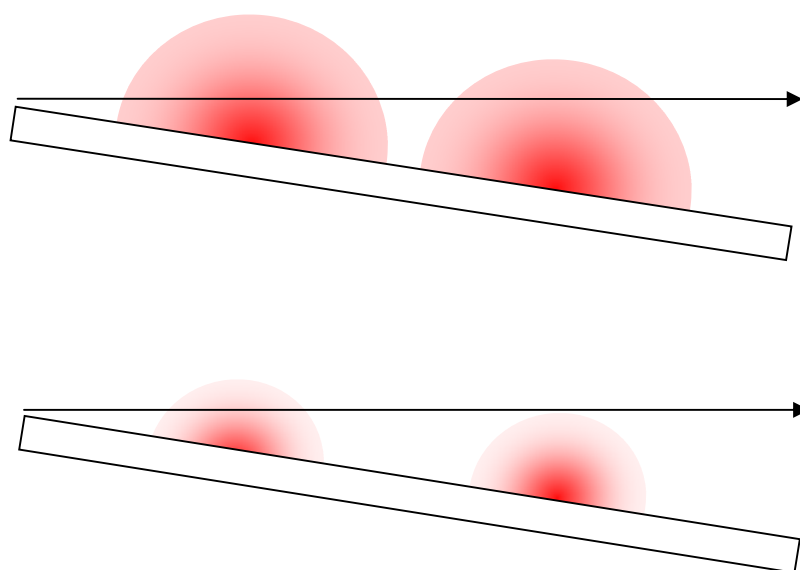


Figure 7.24: Schematic illustrating the effect of topography on interrogating diffusion layers of differing depths as a result of substrate concentration

When the diffusion layers are deep and of higher concentration gradient, when the probe moves from one diffusion layer to another, the difference in concentration between each point is less than that observed when the diffusion layers are smaller and of a lower concentration gradient (Figure 7.24).

To aid comparison of these images, a single cross-sectional line was extracted from each array as below (Figure 7.25) aligned appropriately and plotted on the same axis (Figure 7.26) using both background subtracted and raw area scan data.

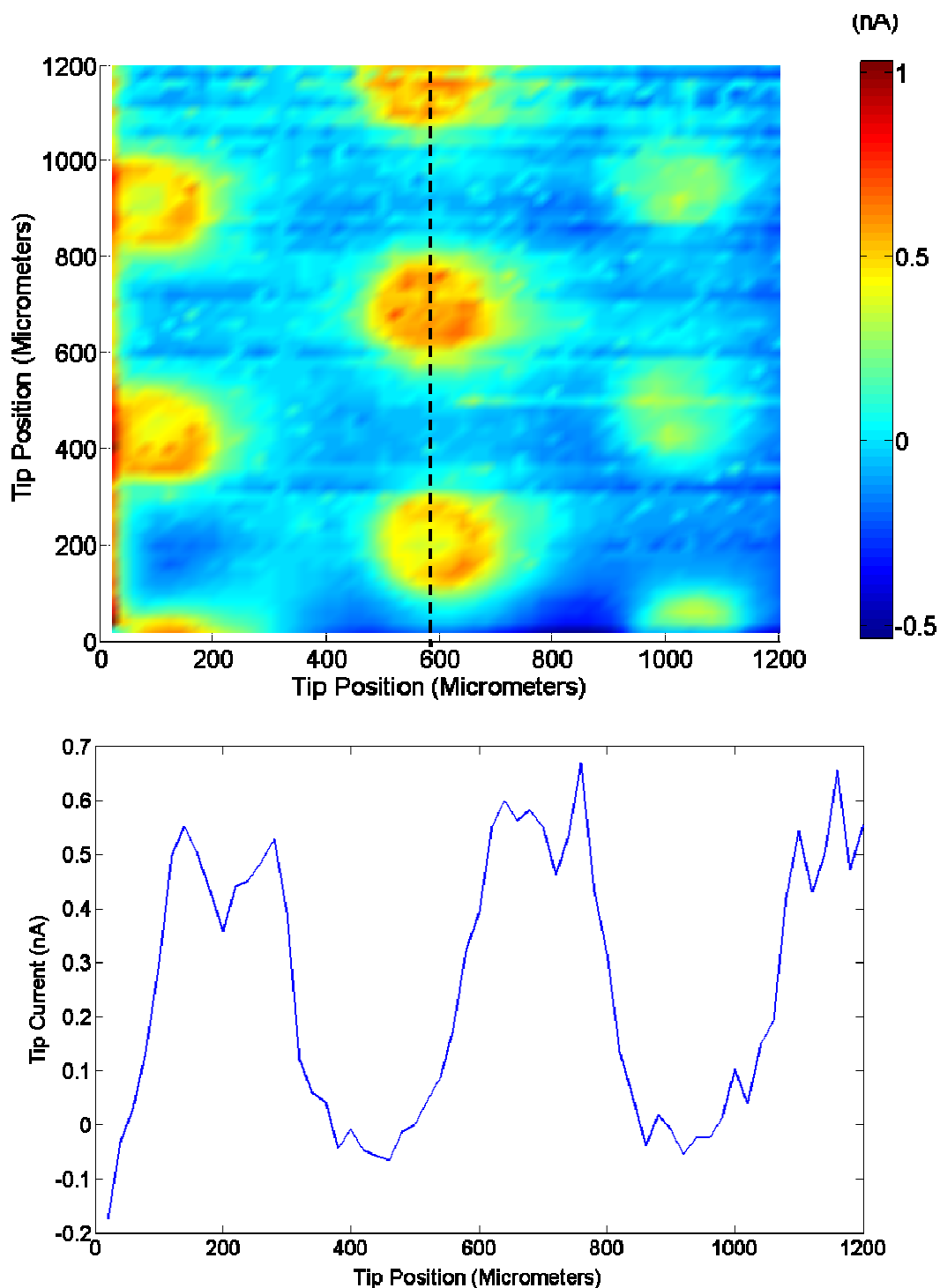


Figure 7.25: A) A cross section was extracted from the area scan array along the dotted line and the resulting data plotted as a line scan (B)

From Figure 7.26, it may be seen that there is a significant degree of variation between the current measured at the arrays interrogated using different concentrations of the enzymatic substrate, hydrogen peroxide, in the mediator solution. There is no apparent trend in the data either before or following background subtraction.

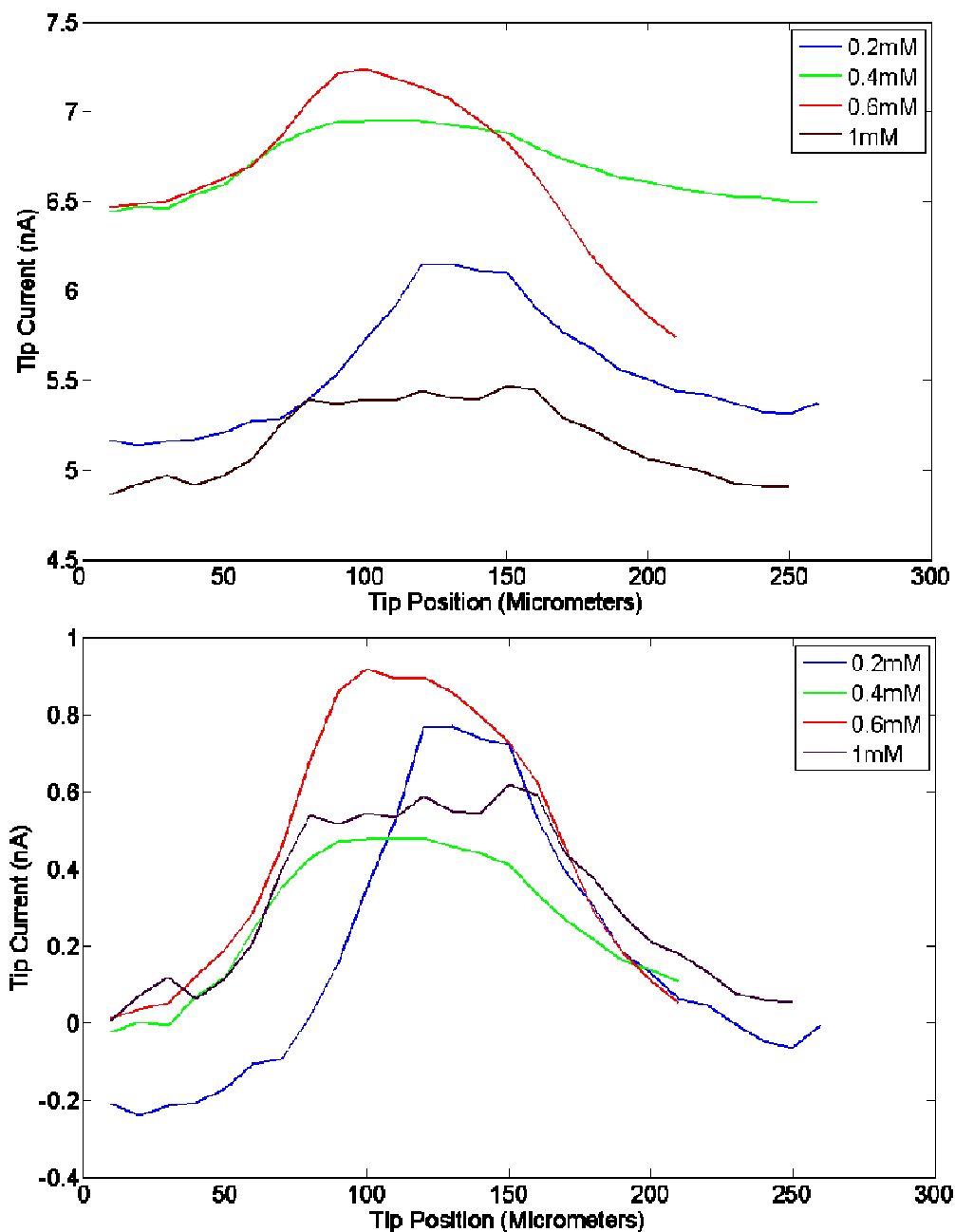


Figure 7.26: Linescans over HRP array. Data is extracted from area scans conducted in a pH 7.1 buffered solution of 1mM hydroquinone and hydrogen peroxide at concentrations of 0.2mM, 0.4mM, 0.6mM and 1mM hydrogen peroxide. A) Actual data B) same data as in 'A)' but with background subtraction

These findings very much highlight the problems associated with imaging enzyme activity by SECM in generation collection mode - at small tip to substrate distances, there may be a decrease in the tip current as a result of negative feedback whilst at larger distances, the resolution of the image may decrease as a consequence of the diffuse layer of enzymatic products.

This observation may, however, be expected considering the convective effects of scanning the probe across the substrate through the diffusion layers of different sizes extending from the immobilised enzymes at the substrate surface and out into solution. Whilst the magnitude of these currents differs between those substrates interrogated using mediator solutions containing different concentrations of substrate, the resolution of the images obtained is significantly improved using higher concentrations of hydrogen peroxide.

7.3 Conclusions

As discussed in chapter 2, scanning electrochemical microscopy has been used extensively in the study of immobilised enzymatic systems. Within this section, a methodology has been developed for the imaging of horseradish peroxidase by SECM that might be applied to the detection of cell membrane protein expression by HRP labelling. This work will be described in chapter 8.

SECM may be used to detect enzymatic activity by one of two methods – by feedback mode or by generation collection mode - each of which offers advantages in comparison to each other. Feedback imaging offers high resolution since there are no diffuse layers of enzymatic product (i.e. the reaction only occurs when the tip is in the vicinity of the enzyme) but suffers from low sensitivity, whereas generation collection mode offers excellent sensitivity but poor resolution since it detects the enzymatic product diffusing away from the enzyme functionalised surface (in this scenario the reaction occurs wherever there is active enzyme and substrate). In a feedback experiment, the tip current obtained includes the current due to the flux of mediator from bulk solution as well as the flux of recycled mediator generated by the enzymatic reaction.

In the series of experiments described here, the use of SECM in generation collection mode allowed for the sensitive imaging of HRP activity. Feedback imaging was attempted but without success. In this investigation, benzoquinone was used as the mediator. In this experiment, the microelectrode tip was polarised at a potential sufficient to oxidise benzoquinone and form hydroquinone. The hydroquinone would then diffuse to the enzyme modified substrate and participate in the charge transfer reaction with the immobilised HRP, where it was recycled to benzoquinone which would lead to an increase in the flux of benzoquinone to the microelectrode tip, increasing the tip current. This approach failed to detect any enzymatic activity – by area scan or by approach curve when using the same substrate preparation methods as those employed for the GC experiments.

On conducting approach curves over HRP modified glass, the low detection limits of the SECM approach were demonstrated. Silanised glass was loaded with glutaraldehyde-crosslinked horseradish peroxidase present in concentrations down to 0.025mgml^{-1} . This

approach to functionalising a surface with a variable concentration of enzyme has previously been used. Zhou et al (2002), for example, employed the technique in their study of HRP by a combined SECM/confocal system. Using luminol as the electron acceptor, chemiluminescence intensity was found to increase as a function of the concentration of HRP in the loading solution.

Observing the difference between the peak currents obtained by approach curve over substrates loaded with differing concentrations of HRP, it appears that this technique is capable of differentiating between surfaces functionalised using different concentrations of enzyme loading solution.

Using approach curves, benzoquinone concentrations down to as low as $1.2 \times 10^{-12} \text{ mol cm}^{-3}$ were detected, demonstrating excellent sensitivity. These concentration profiles along the Z axis of the diffusion layer emanating from the enzyme modified surface were calculated from the approach curves using microelectrode theory.

The imaging capabilities of the SECM approach have been demonstrated. Imaging an array fabricated by the deposition of a HRP/glutaraldehyde solution on glass allowed a well resolved array to be imaged. Dots spaced $500\mu\text{m}$ apart were clearly resolved from one another. Obtaining such a well resolved pattern was, however, surprising. As the generation/collection mode involves imaging the enzymatic product in the diffusion layer, it was expected that there would be a considerable lack of resolution in the images obtained as the tip 'dragged' enzymatic product from the vicinity in which it was produced as it was moved through the diffusion layer.

Imaging horseradish peroxidase in a mediator solution containing variable concentrations of hydrogen peroxide had a significant effect on the quality of image obtained. By limiting the concentration of enzyme substrate, the rate of enzymatic reaction was lowered, which in turn had the effect of lowering the quantity of enzymatic product generated by the enzyme and so, the size of the diffusion layer. The result of this effect was to lower the resolution of the image with significant inter-dot variation.

Whilst some very preliminary investigations into the diffusional kinetics of horse radish peroxidase are presented, the primary aim of this chapter was to develop a methodology by which horseradish peroxidase activity could be imaged by SECM for application in chapter 8; this has been achieved. It was also hoped that it may be possible to determine whether tip responses were dependent on the concentration of enzyme immobilised at the surface. On comparing the approach curve data, it was revealed that there was a great deal of variation in the peak currents obtained, with large confidence intervals around each mean value. Differences in activity per unit area were, however, observed between substrates functionalised using very low (0.025mgml^{-1}) and very high concentrations ($>2\text{mgml}^{-1}$) of enzyme - i.e. the resolution of the approach in terms of differentiating surfaces with similar concentrations of enzyme is quite poor. The fundamental problem hindering the study of this reaction is that the enzymatic reaction is exceptionally rapid, even though the rate of diffusion is relatively slow. Benzoquinone is produced rapidly by the enzyme, but the rate at which it diffuses from the substrate and into solution is slow, resulting in a difficulty in differentiating diffusion profiles due to substrates functionalised with similar surface enzyme concentrations.

However, as the intention is to use the enzyme as an electroactive label for following membrane protein expression, the results presented here demonstrate the suitability of the enzyme and the detection method as a viable route for the development of this assay. In addition, the micropatterning capabilities of the Uniscan micropositioning device have been further demonstrated.

Chapter 9

Exploitation of innovation networks as a resource to create and maintain competitive advantage

9. Exploitation of innovation networks as a resource to create and maintain competitive advantage

9.1 Introduction

In today's highly competitive business environment, technological innovations are hugely prevalent, with their introduction to the industry often representing a significant disruption to the competitive environment. With the continual introduction of potentially 'path-breaking' innovations to the industry's existing portfolio, hi-tech markets are highly dynamic. As a consequence of this inherent instability and dynamism, a successful company will be one which is sufficiently flexible in its resource structure so as to allow it to renew its offering in line with contemporary market conditions. This dynamic behaviour and organisational flexibility in times of market instability is a critical characteristic if a firm is to succeed, especially in the high-tech sector. Organisations which fail to recognise changing market conditions and to capitalise on the peripheral innovative momentum of the industry, whilst resting on past success are frequently overtaken by more vigorous, innovatively aggressive companies.

The absence of innovation is by no means the sole conspirator to a firm's decline however – rather, the problem lies in the translation of the product of the innovative process into a valuable, profit generating asset. The focus is hence not 'to innovate', but to *manage*, innovation, technological innovation, for profit. According to the DTI¹, innovation is broadly defined as “the successful exploitation of ideas into new products, processes, services or business practices - and is a critical process for achieving the two complementary business goals of performance and growth which in turn will help to close the productivity gap” (DTI's Innovation Report 2003). Innovation within this work is hence interpreted to be the generation and exploitation of new products, processes, services and business practices. With products becoming increasingly modular and as knowledge is spreading across organisations, firms are recognising the growing requirement for inter-firm collaboration both formally and informally. This delocalisation of the locus of innovation outside the boundary of the firm is

¹ Now the Department for Business Enterprise and Regulatory Reform (since 28th June 2007)

becoming increasingly apparent in a number of industries – the biotech sector being an excellent example. Within this industry, few firms have sufficient resources to undertake all the risk and work associated with getting an emergent technology or drug to the marketplace; firms within this rapidly changing complex industry form networks across a myriad of different organisations of varying sizes in a concerted effort to get their product to market (Riccaboni and Pammolli 2003).

Within this chapter, a comprehensive review of the innovation network literature is provided, framed within the existing theoretical frameworks of strategic management. In doing so, an insight is given into the many different aspects of innovation networks – their structure, their flexibility and the management and orchestration skills required to leverage value from them. The findings of an interview with the managing director of Uniscan Instruments Limited, Dr. Graham Johnson are then presented, together with a discussion presenting a number of suggestions regarding the proactive management of their innovation network that Uniscan may take into consideration over the course of their forthcoming strategic review.

9.2 Models of strategic management

Over the past three or so decades, many theories have been proposed centred on the firm and its strategic management to yield competitive advantage. Whilst these theories differ in their minutiae, they are all usually centred on one of three frameworks.

Pioneered by Porter, the competitive forces framework was the dominant theory in strategic management in the 1980s (Porter, 1979; Porter, 1980). The central tenet of his theory was that the strategies available to a firm are determined by the organisations environment - the industry or industries in which it competes. In this model, five industry-level forces determine the potential of the firm to generate economic rents in a particular industry, namely 1) barriers to entry 2) threat of substitution 3) bargaining power of buyers 4) bargaining power of suppliers and 5) rivalry between the industry incumbents (Figure 9.1). Primarily a defensive behavioural framework, this approach allows the firm to adopt a position from which it can most effectively defend itself against these five forces, or influence them to generate competitive advantage over industry incumbents. In outlining the major forces on an

incumbent, the framework represents a useful mechanism for the analysis of the profitability of different industries and sectors therein. Some industries for example, may have structural artefacts which impede some competitive forces which allow incumbent firms scope to build and maintain competitive advantage. A key point to this framework for comparison to others is that the rents generated are done so primarily at the level of the industry rather than at the level of the firm. Further, in comparison to other models, the focus is on external forces and entities rather than any firm specific assets.

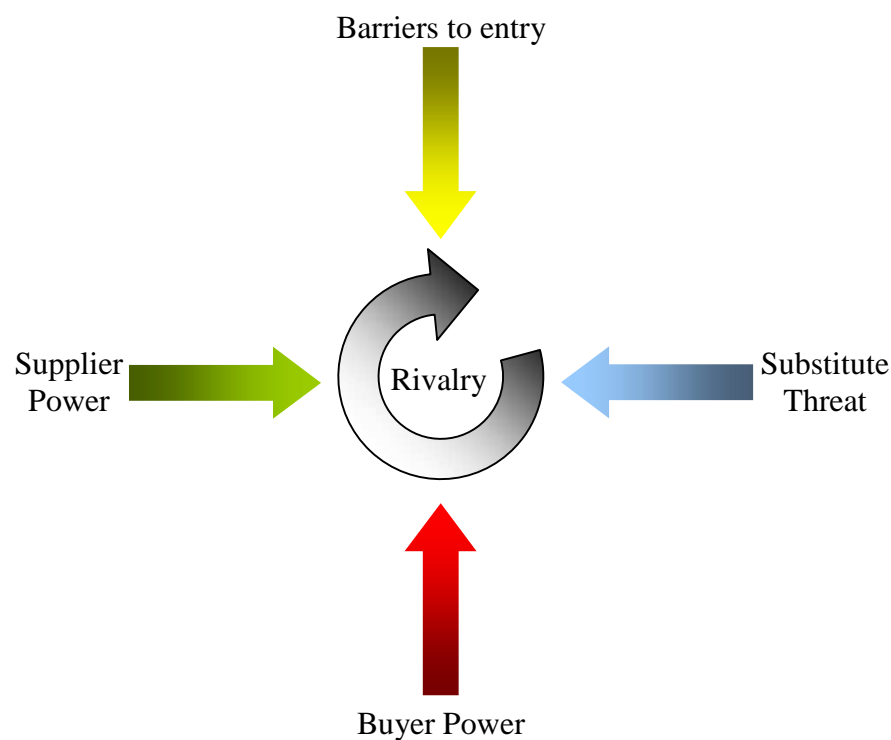


Figure 9.1: Schematic diagram illustrating Porter's Five Forces Model

Following the development of Porter's five forces model, Carl Shapiro's publication of his paper entitled 'The Theory of Business Strategy' in 1989 suggested an alternative approach to the strategic management of the firm. Utilising tools central to game theory, his 'Strategic Conflict' framework proposed that competitive outcomes were a product of how effective a firm was in wrong-footing competitors through pricing stratagems, pre-emptive signalling and strategic investments amongst other behaviours. Central to this school of thought is the use of signalling and the controlled flow of information from one incumbent to another to elicit a required response – how the behaviours of one firm may influence those of a

competitor. An investment in advertising (sunk costs) (Schmalensee, 1983), production capacity (Dixit, 1980) or a cut in retail price all represent well characterised tactics employed in Shapiro's strategic conflict model of management. A key assumption however, is that the strategic action must incur upon the issuer a cost; otherwise the action is easily copied by the competitive firm. If the action is not followed by its competitor, the action will hopefully result in the achievement of its strategic goal and the firm may increase profits. The execution of a particular strategic action is not always necessary however – simply signalling to the competitive market an intention or capability to undertake a particular route of action is often equally as effective. Overt, explicit signalling is sometimes not even necessary – the reputation of a firm, previous behavioural patterns or strategic alliances may often be enough to dampen any competitors' attempts to vie for competitive advantage. Whilst this framework yields many interesting questions about the role of strategic signalling and strategic behaviours in eliciting responses from competitive agents, it fails in that the result of a strategic pattern between industry agents is entirely dependant on the specification of each agent, resulting in un-testable outcomes. The essential flaw is that the framework will only work and produce a testable outcome if the agents are identical, i.e. the strategic engagement is symmetrical. When they are grossly asymmetric, the outcome is generally obvious – the stronger competitor will usually make aggressive advances until the challenger withdraws or submits. On the other hand, when they are more evenly matched, each with a comprehensive information portfolio, the different strategic behaviours employed and pre-emptive signalling make the outcome less predictable. In a technology-centred industry however, where competitive advantage may be obtained by innovation and rapid technological advance, the role of strategic conflict and the tactics it embodies is lessened. Nevertheless, in an environment where there is complete information about competitors and the strategic paths available to them, the model may provide the firm powerful insights into achieving its strategic goals. A concern raised by Teece *et al* however, is that in focussing effort on understanding competitors strategies and developing one's own - is that effort is no longer being devoted introspectively and being spent on developing the internal skills and core competencies necessary for gaining pure competitive advantage. These sentiments are echoed by Dierickx and Cool (1989) who have found that proponents of the strategic conflict model fail to note the importance of developing, accumulating and correctly aligning internal resources for the construction of firm level assets that leverage competitive advantage;

instead there is a preference to focus on market positioning relative to competitors and the development of Machiavellian stratagems to better those positions.

A commonality between these two models is that, whilst they allow useful insights into the different forces and behaviours prevalent in the competitive arena, they neglect to take into account the firm-specific resources and competencies which in themselves are often responsible for attaining long-run competitive advantage. According to Penrose, “a firm is more than an administrative unit; it is also a collection of productive resources the disposal of which between different users and over time is determined by administrative decisions” (Penrose, 1959). This Resource Based View (RBV) proposes that competitive advantage is a result of intra-firm systems, processes and cultural patterns that yield lower operational costs and better product performance. If these resources meet the VRIN criteria, abnormal rents may be achieved:

1. **Valuable:** when they allow the firm to implement value-adding strategies which improve efficiency or effectiveness
2. **Rare:** valuable resources which cannot be obtained easily by competing firms. Ubiquitous resources will not add any differential value
3. **Imperfectly Imitable:** due to unique historical pathways of development, social complexity or causal ambiguity.
4. **Non-Substitutable:** There is no other strategically equivalent valuable resource that is rare or inimitable.

A number of quantitative studies exist that demonstrate the RBVs applicability to strategic management. Rumelt *et al* (1991) for example found that differences in intra-industry profits are greater than inter-industry profits, emphasising the relevance of firm-specific factors and the relative unimportance of industry effects. An effective way of comparing the RBV and the competitive forces approach is to consider the decision making process leading to market entry. A key difference is that the RBV view is much more flexible in its approach to earning economic rents. It assesses where its operational strengths lie and exploits them where it can in the most suited environment. However, whilst existing skills and competencies may be the focus, efforts are also expended on developing these resources to build the core competencies

of the firm and enhance its competitive advantage. This may be through effective knowledge management, the acquisition of the right human capital or the development of the necessary organisational culture.

The possession, acquisition and development of a firm's core competencies is not however, always all that is needed for success in the market place. In a fast changing, dynamic environment in which the forces are changeable, the technologies being employed are rapidly evolving and the behaviours of competing organisations are always changing. An emerging view is that the possession and accumulation of resources is not in itself sufficient to gain competitive advantage. Rather, it is the organisations ability to respond rapidly and flexibly to changing market conditions, achieved by the re-bundling of existing internal and external core competencies and possible acquisition of other VRIN resources for a better strategic fit to the new environment (depicted schematically in Figure 9.2). This ability to re-organise a firms core competencies to achieve new forms of competitive advantage is termed 'dynamic capabilities' as championed by Teece *et al*, and represents an extension of the RBV framework (Teece *et al*, 1997).

Within this framework, 'dynamic' is used to emphasise the capacity to restructure competencies to achieve congruence with the new competitive environment. The term reflects the necessity for rapid flexibility and the entrepreneurial insight needed to meet the rate of change, be it technological or otherwise, required for the achievement of competitive advantage. A key problem that faces the management of a company with dynamic capabilities however is the selection of those VRIN capabilities for receipt of resources for development. The determination of how much to invest in each of these areas is hence a major strategic consideration, although there will be a historical aspect to the decision; i.e. what domain of competence has always been strong and worth more investment? How a firm acquires, grows and exploits its core competencies has been developed by a number of authors (e.g. Prahalad *et al* (1990)). In comparison to other frameworks, it is believed the dynamic capabilities approach to strategic management in rapidly changing, dynamic environments gives a more well balanced, adaptive framework. It gives managers the scope to effectively evaluate what they do well and apply these competencies in a different orientation to fit new market conditions. It negates the need to continually buy in new, often

non-VRIN competencies, encouraging investment in ‘sticky’, unique capabilities that will deliver true value in competitive advantage.

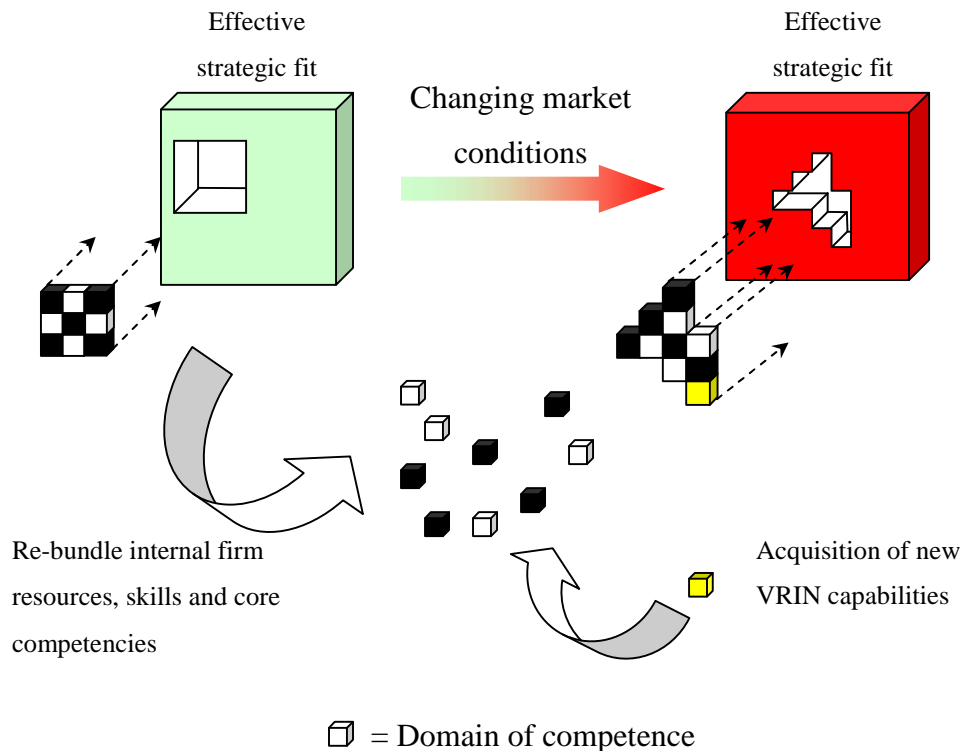


Figure 9.2: Schematic diagram illustrating the re-organisation and re-bundling of internal resources to meet new competitive environments

The competencies to which the DCV framework refers are inextricably linked to the firms operations; as a consequence of this, Teece organises these capabilities in three classes – processes, positions and paths, the relationship between which is depicted in Figure 9.3.

When a firm makes a decision about what competencies should be developed over the medium to long term, it casts a significant shadow over the terrain it may negotiate over the ensuing period. In following a specific trajectory of competency development, the firm limits the niche space it can exploit in the future. The choice of trajectory and the subsequent quasi-reversible decisions made along this path hence represent a major strategic problem for the firm. Whilst the competencies developed may allow the contemporary collection of rent from the current competitive environment, it does limit the company in what it can do in the future. Ideally, the firm would be sufficiently flexible and agile as well as having the

absorptive capacity for these strategic decisions to have an immediate effect but with minimal inertia to allow their rebundling / re-alignment in congruence with fluctuations in the competitive environment. As discussed by Horari (1997) (cited in van Aken *et al*, 2000):

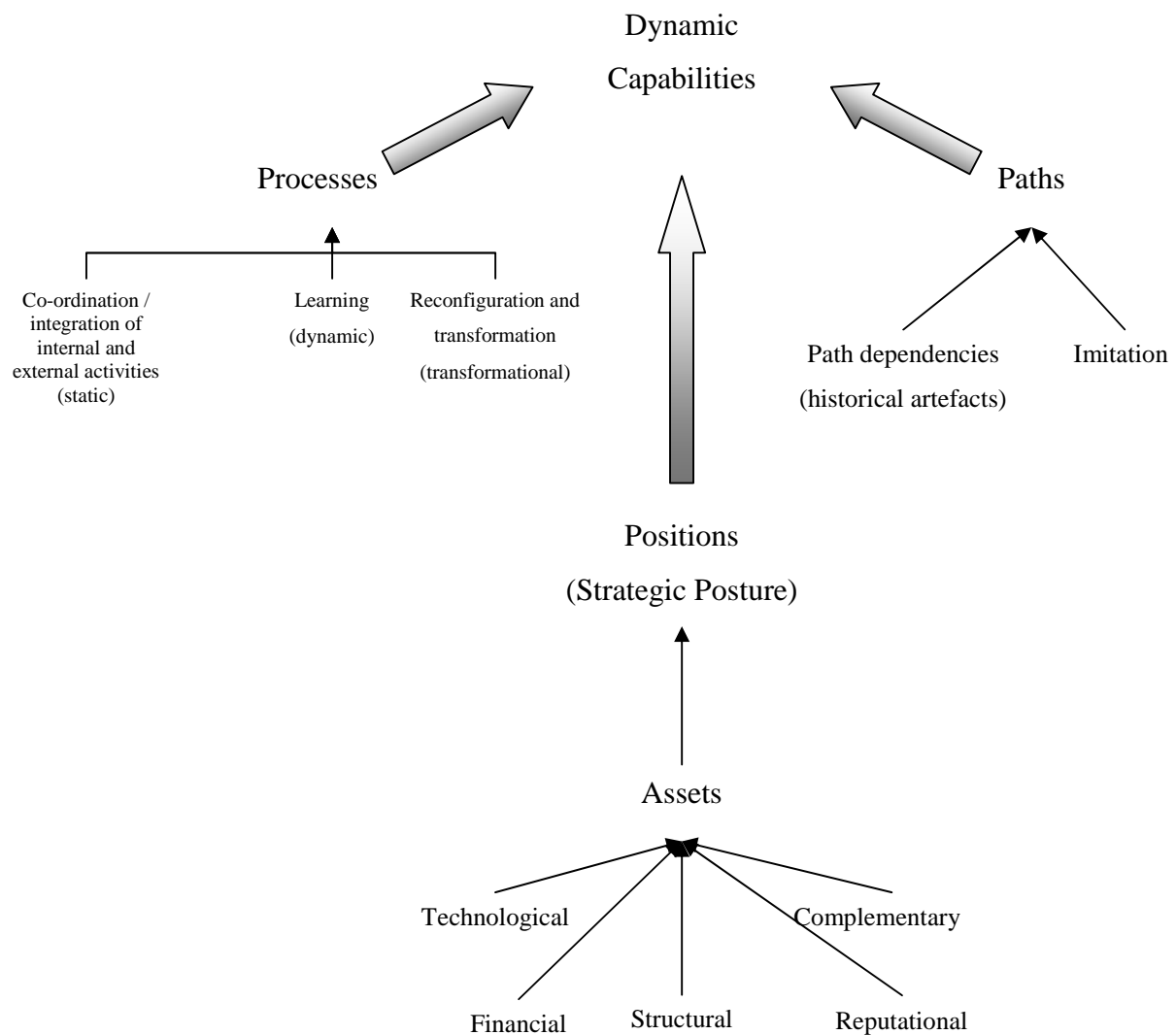


Figure 9.3: Schematic diagram illustrating the three kinds of dynamic capabilities

'World wide competition continues to compress profits on anything that is uniform, routine and standard; intangible assets and facets of knowledge like expertise and intelligence, speed, agility, imagination, manoeuvrability, responsiveness and networking skills, become more important than the tangibles of traditional balance sheet perspectives'.

The idea of larger bodies being capable of more innovative activity is embedded in the earliest perspectives on firm behaviour – Schumpeter (1942) suggested three reasons for assuming a link between firm size and innovation: 1) larger firms are more capable of meeting the high costs associated with the design and development of innovative products and processes; 2) they are more able to absorb high failure rates and technological setbacks associated with these innovations; 3) larger firms will have more power in determining behaviour of competitive market, allowing greater exploitation of innovative activity (Teece *et al* 1992; Tracey *et al* 2003). The role of the smaller company is however, coming to the fore in today's information and knowledge based economy – and although they are small and lack the substantial resources of the larger conglomerates, they do not have their inherent rigidity. As a result of this, they are able to develop strategies reliant on networks of interaction and innovation to succeed in complex, uncertain and changeable competitive arenas.

Porter's five forces, the strategic conflict and the resource base view of strategic management all make valuable contributions to the development of a framework towards wealth creation. The five forces model approaches the problem via industry structure, defensive positioning and entry deterrence; the strategic conflict model tackles the question using signalling and strategic actions to manipulate relationships between market competitors and the RBV framework focuses on the role of firm-specific assets as a route to gaining competitive advantage.

There is no hard and fast rule, however, stipulating that a firm should be managed steadfastly according to any one of these frameworks. Rather than representing different, distinct approaches, they should be used together to produce a synergistic tool of management as each approach asks different, often complimentary questions of the firm, its competitors and the arena in which they compete. This is of particular relevance to complex strategic

problems which will gain significant benefit from insights obtained from all angles. Strict adherence to just one framework will inevitably lead to strategic blind spots, so there is much scope for the appropriate selection of tools from each of the strategic toolboxes proposed.

The resource based view, and its extension in the dynamic capabilities model does not, however, according to Eisenhart and Martin (2000), contribute much to explaining the achievement of long term competitive advantage in dynamic markets. Rather, there is the suggestion that the locus of knowledge and value creation is shifting within supply and demand chains in response to variable industry dynamics. It follows that competitive advantage and the innovative processes by which it is derived, may not be entirely controlled by the individual firm, as in the RBV framework. Rather, it is proposed that the locus of innovation lies within a network of individual actors/nodes in a boundary-less organisation. When control of competitive advantage leaves the firms boundaries, innumerable questions arise relating to how it may leverage value from the network of which it is part. How may it manage relationships, orchestrate the network in such a way that it may benefit from the network's innovative output and receive a return on investment into it?

The role of inter-firm alliances in gaining competitive advantage is partially tackled in the increasing volume of alliance literature based on observation driven research, but a gap still exists between the theoretical descriptions of firm behaviour (as independent actors) and the observed phenomenon of the creation of alliances and the resultant success and failure of the resultant network (Lavie, 2006).

The movement of the locus of innovation and value creation outside the boundaries of the firm is becoming an increasingly frequently observed phenomenon. This movement may be illustrated in the schematic given in Figure 9.4. Consider the first grid: here, the grid represents a multidimensional space, where the mix of skills and competencies firm A has, gives it a unique, specific co-ordinate. Now, consider product P. For the successful production and exploitation of P to generate economic rents, a firm with the skills mix closest to that required by P is required – firm A. The result is that the product demands and the firms capabilities are highly congruent, meaning that A may successfully generate rents by production of P. Now, consider an industry, a group of firms with highly VRIN resources –

they occupy a unique, distinct location in the multidimensional space. When the opportunity arises for the production of product Q, neither have the capabilities to achieve it alone. On forming a network however, they form one in such a way that between them they construct a delocalised web with a spectrum of skills and competencies allowing the production of Q.

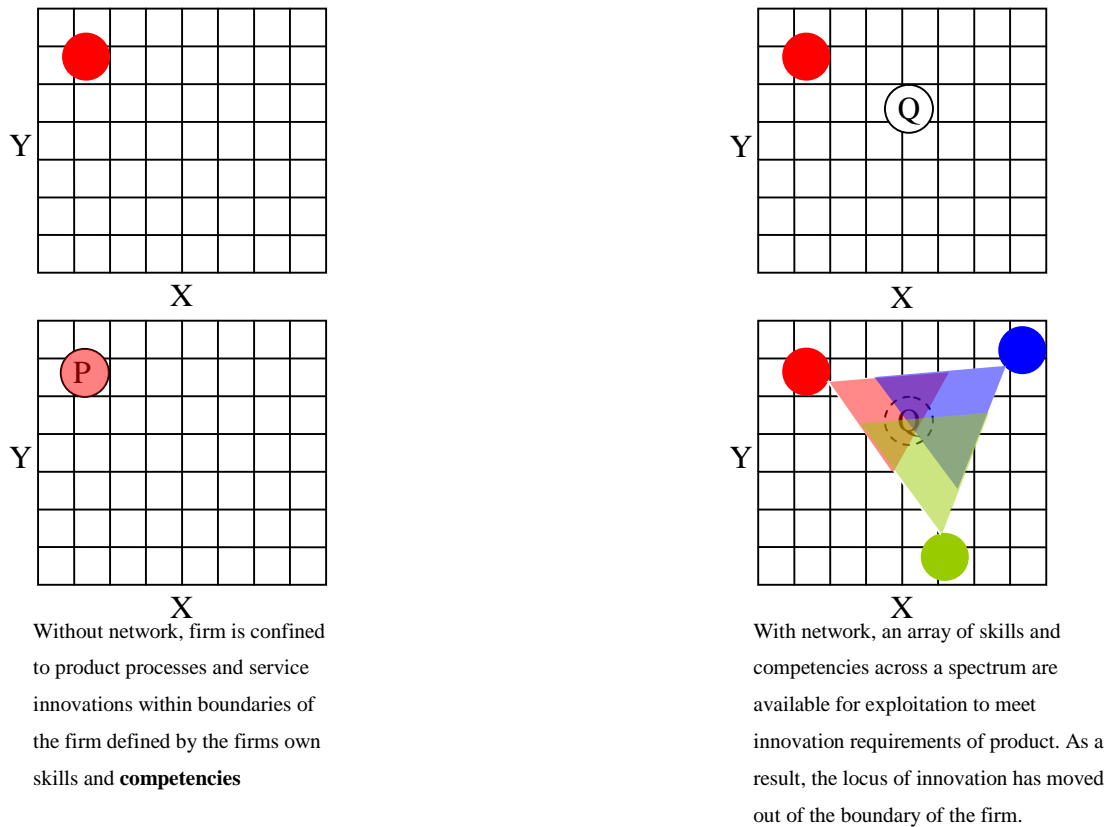


Figure 9.4: Schematic illustration of the concept of innovation networks and the movement of the locus of innovation outside the boundary of the firm

9.3 Innovation networks

Innovation is the successful introduction of products, processes or services that are new to the firm: novel innovators introduce products, processes or services that are completely new to the industry. Within the following section, how an organisation may enhance the rate and quality of innovative activities by association with an innovation network is explored.

9.3.1 Innovation networks – a definition

According to van Aken, an innovation network is a special case of organisational network (ON), which in itself, may be defined as ‘a system of autonomous and legally equal organisations connected by select and persistent business relations’. The relations are select in that the network is often not industry-wide and they show durability against environmental perturbations. In most ONs, there is an explicit or implicit division of labour between partners and the synergies created by them may be positive or negative. Generally speaking, ONs may be one of two types – emergent or designed. An emergent network is one which is not created by overt actions, but is organic, arising from frequent, positive transactions between network actors (Granovetter, 1985) - or by social interactions between organisational representatives (Eisenhart and Schoonoven, 1990). A designed ON on the other hand, is a network formed as a result of deliberate actions by single or multiple mobilisers where network actors undertake collaborative actions based on explicit collaboration agreements. Alliances within these networks may involve a myriad of different partners. They may be between functional departments or subsidiaries of the same organisation, between competitive firms, complementary firms such as suppliers, customers and subcontractors, between private firms and universities and regional/national governments, or indeed between other industry stakeholders like trade unions, consumers and even activists (Dunning, 1998).

Innovation networks are different in that one of the key objectives of their existence is competitive advantage through innovative output from the network of which they are part. Whilst this is very much an outcome-related definition, there is little consensus in the network literature. DeBresson and Amesse (1991) for example, regard innovation networks simply as innovating companies working together; van Aken defines them equally as simply as ‘an organisation network engaged in product or process innovation or both’. Similarly to ONs, these too may be of different types. They may be formal, designed networks, in which

the actors' behaviour is governed by formal collaboration agreements, or they may be more informal; the trading of technological know-how, customer-supplier learning pathways, and the exchange of knowledge between academic bodies and technological sponsors all represent informal innovation networks (van Aken 2000).

In forming a network with other organisations, the benefits an organisation may subsequently reap are numerous (e.g. Hotz-Hart, (2000);

1. *Improved access to information, knowledge, skills and experience*

Networks provide routes to learning new operational techniques, reducing adoption time and lowering cost of new products and processes.

2. *Strengthened linkages and cooperation between network members*

Leading firm competencies can form new benchmarks for others; effective networks can encourage interactive learning, synergy and complementarities between specialist groups across participating firms e.g. design, production, marketing, finance.

3. *Improved response capacity*

Networks allow participants to lower response times to changing environmental conditions, to anticipate changes and to learn quickly about new enabling technologies.

4. *Reduced risk, information and transaction costs, and moral hazards*

Networks with complementary assets and skill sets share resources to lower costs. Risks may be assessed and shared across the network, resulting in lowered inhibition of innovative activity and more complete information.

5. *Enhanced trust and social cohesion*

By forming an alliance, firms may share values, goals, norms and operation methods which allow enhanced problem solving, collective action and innovative behaviour – often through a complex pattern of competition and cooperation.

Further benefits are highlighted by Pittaway (2004) and include obtaining access to new markets and technologies, and safeguarding property rights when complete or contingent contracts are not possible.

In knowledge intensive industries, product and process innovation is a hugely important factor. It allows companies to gain significant competitive advantage over competitors, delivering higher quality products, with higher specification and or at a more competitive price. Increasingly, as initially illustrated by the SAPPHO-project, external relationships with customers, suppliers and other sources of technological knowledge are becoming essential in the achievement of this. Further, this need for process and product innovation is especially relevant in the rapid, fast moving, dynamic environment of high end technology (Hauschildt, 1992; Jonash *et al*, 1996; Chatterji, 1996). This pattern of innovative behaviour is particularly well highlighted in a study conducted by Jonash *et al* (1996), who, via interviews with in excess of 50 CEOs and CTOs, found that the majority of companies achieved over 50% of technological competitiveness from external alliances (Jonash *et al*, 1996). In a further study by Oerlmans *et al*, it was found that the use of both internal and external resource bases is positively related to innovation output – the higher the contribution of the internal resource base, the contributions of private knowledge infrastructure and the suppliers and buyers, the greater the innovative result; the study exemplified how key the use of internal *and* external resources was to innovative performance (Oerlmans *et al*, 2001).

Whilst networks are valuable in their contribution to product and process innovation, they are also highly useful in the communication of innovative working practices and in-house ‘ways of working’ that they could adopt. Whilst homogeneity in this sense may lead in the long run to single loop learning and a settling with the status quo, such communications may in the short term be useful and secondly, may lead to a strengthening of the relationship through trust and social interactions, an essential component of knowledge transfer (Almeida and Kogut 1999).

An excellent empirical example of networks in action is that of Novartis’ development of Gleevec, an anti-cancer drug. After extensive collaboration with Dana Faber Cancer Institute, the drug was successfully produced with sales of US\$2.2bn in 2005, making it the number one selling drug in its therapeutic category (Cross *et al* 2005; www.novartis.com).

Whilst innovation networks have significant approval in the value they may deliver to an organisation, a number of problems associated with their use have been highlighted.

Often, network ties are made between organisations with similar working practices and standard operating procedures (SOPs) – initially, collaboration between these firms may generate a valuable output, but sometimes the innovating firm may experience a loss in flexibility. This comes as a result of granted norms and ways of thinking imposing noticeable restrictions on decision making and behaviour within and between the organisations which are frequently sustained and reinforced through observations of others’ behaviour, social interaction and consensus building (Figure 9.5). In creating these suffocating behaviours, firms become paralysed by single loop learning – SOPs are just one example. Network functioning may further be hindered by political factors – opportunistic behaviours may elicit hostile responses and a reduction of trust in the network.

A thorough appreciation of these disruptive elements and the risk they pose to a network is an important part of network management – understanding organisational assumptions, norms, frameworks and paradigms all represent key steps toward agents successfully influencing their environment effectively.

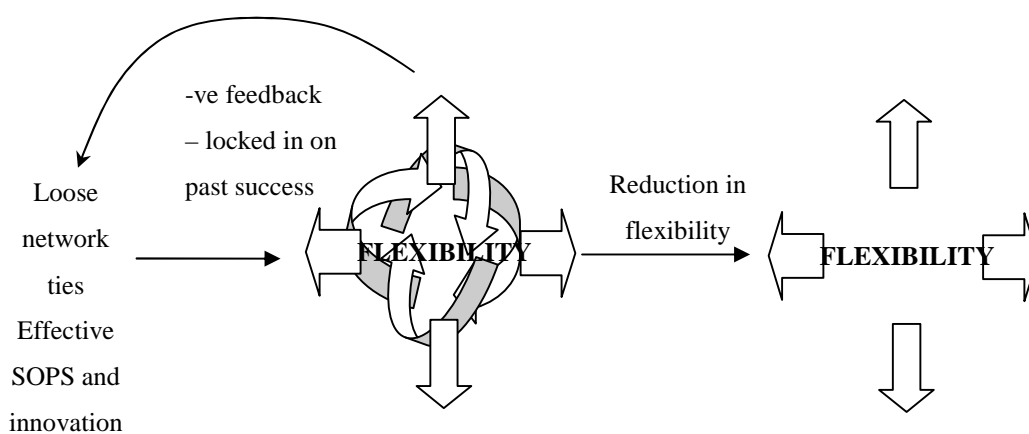


Figure 9.5: A schematic illustrating the potential loss of flexibility a firm may experience as a result of collaboration and single loop learning

9.4 Relationship strength

An important issue for consideration when building innovation networks is the strength of the ties within that network. In an essay by Granovetter (1973), on the ‘strength of weak ties’, weak ties were cited as ‘indispensable to individuals opportunities and to their integration into communities; strong ties, breeding local cohesion, lead to overall fragmentation’. Building on this work, Burt (1992) developed the theory that the strength of the tie was not important; what was key was the ‘information benefits’ a new relationship may bring as well as the levels of control assumed by firms after connection. Whatever the argument of each, the underlying assumption was that distance is a key parameter in network formation if the maximum yield is to be obtained in terms of exploitation and identification of innovative ideas and concepts. Following on from this work, there has been much scholarly focus on network ties (e.g. Grabher 1993). The principle arguments are thus: weak ties represent a link to other firms and networks with alternative perspectives on the world and as such, are a good source of new ideas and perspectives and are crucial for innovative behaviours; strong ties on the other hand are effective conduits of information between networks actors but tend to be poor sources of innovative ideas and new ways of working – and this rigidity grows with familiarisation over time as firms come to view situations from increasingly similar situations. This latter perspective is in contrast to many other scholars who argue that close, strong ties are required for innovation and competitiveness. This may be true in some instances, but a definition of ‘close’ and ‘strong’ is needed. If ‘close’ means close in knowledge spheres and competencies, then innovative output will be limited – if it is close as in the commitment to a common goal, a commitment to each other, and disparate in what skills and knowledge they offer the alliance, then the relationship stands a more significant chance of yielding the required innovative output. This is an area of definition that the literature lacks.

Taking these different perspectives forward, Tracey proposes that two ‘prototypical approaches’ to relationships in innovation networks exist – weak and strong ties (Tracey, 2003). In a network of weak ties, ideas are sourced from other networks and other network members with whom they have rudimentary relationships. As the relationship ages, they may become closer as they decide to collaborate on a project, or they may remain distant. With respect to strong ties, innovation within these networks is derived from the close interaction

between members with shared values and approaches to problem solving and decision making. The value of these ties may wane with time however, and become weakened. The treatment of strong and weak ties as distinct entities is somewhat flawed however. Firms should not be confined to making one kind of tie.

Before making a ‘strong’ tie, a weak relationship should exist to allow firms to assess each other and establish congruency. It is hence suggested that Tracey’s model be extended to one in which all relationships begin as weak ties before then staying as such or strengthening (Figure 9.6). However when one considers these ties, one thing is clear – innovative firms which show dynamism in the midst of environmental change have a mix of ties of differing strengths. In doing so, they are able to reposition themselves within their network to achieve the optimum strategic position for the given competitive context. The tie-mix is very much dependant on the nature of the industry sector. For instance, a firm in a fast moving, technology based industry like software development would benefit greatly from weaker ties, whereas firms in industries where changes are more predictable – i.e. linear, may be better suited to alliances with stronger ties.

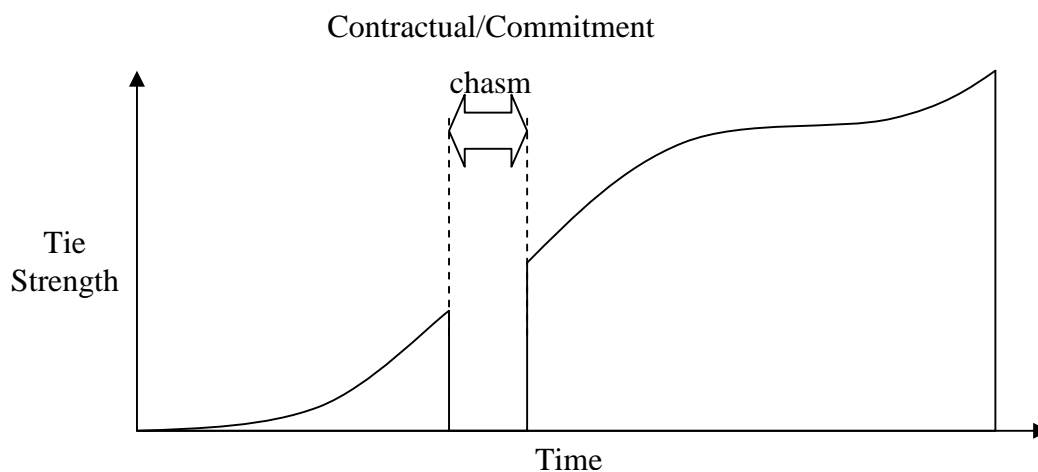


Figure 9.6: Schematic diagram illustrating the transition from weak informal tie to strong tie. Ties may either be lost, or they may traverse the ‘chasm’ to form a strong relationship with other members of the network

The strength and directness of alliances in networks is also discussed by Salman and Saives (2005). In their paper, it is proposed that in high tech sectors, indirect linkages or ties can deliver significant innovative power to a firm. Defining an indirect tie as a tie between two bodies who have a direct tie with a common network actor, it is believed that these indirect linkages act as a channel of information between the firm and other indirect contacts - they provide a strong form of social capital for access to knowledge and skills.

One may consider that a firm has only a finite absorptive capacity – an absolute amount of resources it can allocate to network relationship management. If the amount of resource required to manage a strong tie is larger than that required for a weak indirect tie, it follows that a firm's pool of information and number of channels of communication are larger and more numerous in a network of indirect linkages than direct.

In the early stages of network formation, there is much overlap with the theory developed for informal innovation networks. Informal innovation networks may be utilised in any phase of the innovation process for technology exchange and synergised problem solving. This is in contrast to formal innovation networks which are based on formal collaborative agreements in the mainstream innovation of the current range of products and processes. At the front end of the innovation pipeline, informal networks provide the creative capacity to allow the development of routes of development (see Figure 9.7). In doing so, in creating this 'fuzzy front end', more uncertainties, more routes to success are generated, which in turn, demand more know-how from outside the current knowledge sphere (e.g. Khurana *et al* 1997). There is considerable risk at this front end, in this informal network, of leakage and subsequent exploitative / opportunistic behaviours however, which has implications for the evaluation of the network by constituent firms. In spite of these possible risks, considerable advantages lie with informal innovation networks; they are easier to create and are more congruent with the uncertain nature of the 'fuzzy end' of the innovation pipeline. Further, by their combination with in-house R&D resources at the fuzzy end, they may allow the sharing of risk, the leverage of resources across all constituents and add technological and competence diversity. Informal innovation networks and the collaborative activities within them are more about information exchange and the creation and testing of ideas and concepts which may then be fed into the innovation pipeline.

By creating an innovative environment, high potential ideas for products and processes are then fed into the innovation pipeline for development, a stage which may utilise a different network of collaborating bodies.

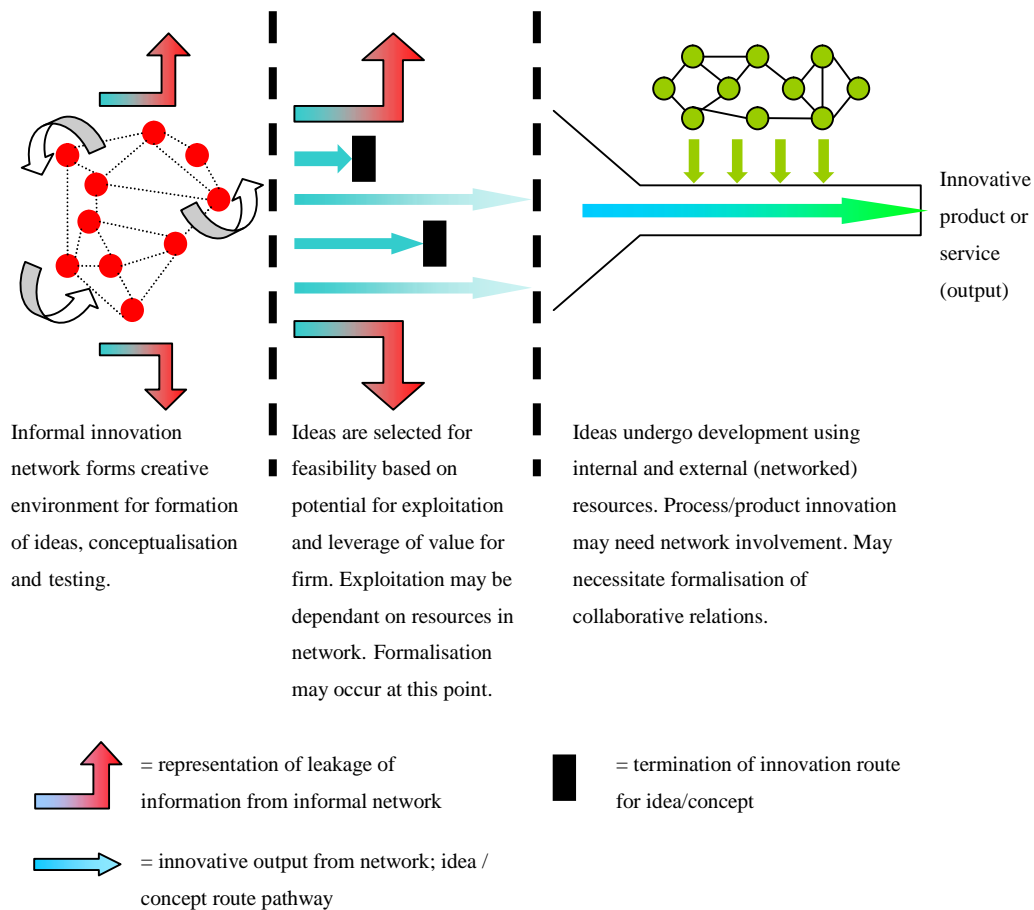


Figure 9.7: Schematic representation of role of weak and strong ties in the innovation pipeline

9.5 Network configuration

On reviewing the literature, it becomes evident that there is no ‘one size fits all’ approach to configuring an innovation network. The optimum configuration and the nature of the network are hugely dependent on the context of the firm and how it wishes to extract value from the network. Several different themes emerge from the literature (1) Firms’ strategies will be different and the value they wish to derive from the alliances within the network will be different in nature (e.g. Ostgaard and Birley, 1994); (2) Network configurations will be different as firms’ need for different relationships changes with environmental variations (e.g. Kash and Rycroft, 2002); (3) the configuration a network adopts is dependant on what kind of innovation is required – specifically, whether it is process or product innovation (Gemunden *et al*, 1995); (4) The performance of a firm can be strongly affected by the network of alliances it forms during its formation (Baum *et al*, 2000); (5) networks are in a state of continual flux, changing configuration according to changes in the competitive environment (e.g. Kash and Rycroft, 2002). Pittaway, following an in depth analysis of the literature, states “research has not yet clearly demonstrated which configurations most effect innovation in particular contexts” (Pittaway *et al*, 2004). Whilst this is very much the case, perhaps we should perhaps look at the *process* by which these networks are initiated and built rather than the configuration of the final networked product. Network actors are complex entities, with often unique abilities and aims and objectives – trying to analyse the final product after their interaction is perhaps a step too far – understanding the decision making process in network design is where the focus should be.

9.6 Centrality

A firms position within a network – i.e. its degree of centrality – can have a significant impact on the value it can leverage from the network of which it is part.

By increasing the number of network ties, its degree of centrality is increased. Benefits that come as a result of this include an enhancement in reputation, increased visibility and improved access to resources via benefit rich networks. Further, by their central location, they are optimally positioned for the diffusion of knowledge and associated innovations from all parts of the network, where the competitive advantage they leverage is proportional to their

ability to collaborate. This is further enhanced by the success with which they identify and internalise new project opportunities, ideas and concepts. As a consequence of the nature of networks, the face of competition is changing relationships that may once have been focussed on rivalry to those based on co-operation. For a firm that is positioned centrally, this allows it to diffuse its understandings of competition and collaboration through the network with the effect that all members act with a shared set of collaborative principles and contractual and non-contractual honour (a collaborative code of conduct).

Over a series of 40 interviews with biotech firms, it was found that through central positioning, a firm is more likely to access scientific and technological expertise, leading to an increase in innovation related activities. Since innovation is an information intense activity, the more information a firm has, the more opportunities may arise for innovative action (Salman and Saives, 2005).

The concept of centrality is partially illustrated by Albrecht (1991) who found that two types of network members exist - the 'elite' insiders, who wield power, gain resources and make decisions that impact those around them in obvious and subtle ways and the 'outsiders'-network members who follow behaviours and the innovative direction taken by the 'behavioural elite' (Hage and Dewar, 1973). In Albrecht's paper, results were presented of a study into the nature of communication patterns based on innovation. The findings supported previous work – the existence of a central group of core, integrated members with a high degree of interaction surrounded by a less dominant group of outsiders. Elite cliques perceived other elites as more trustworthy, supportive, influential, credible and receptive to new ideas than they did outsiders. Interestingly, the views were the same of outsiders on elites. Innovative behaviour of elites may create a highly valuable stance for sustained power and influence in the organisation – they may monopolise a valuable but fragile aspect of the network and manipulate the level of uncertainty in the system, reinforcing their own relational positions of privilege power and influence (Albrecht, 1991).

9.7 Network diversity

An increasing amount of literature is emerging detailing the importance of network diversity, with many illustrating quantitatively that the innovation process benefits significantly from engagement with a diverse range of allies. Being integral to such a network allows for access for learning to different knowledge bases, behaviours and approaches to thinking. Diverse groups with an array of orthogonal skills and competencies stand a much more significant chance of developing a novel concept and exploiting it accordingly. By having both formal and informal channels of communication between diverse partners with different knowledge spheres, skills and competencies, there is an increased chance of novel combinations of systems and applications that can lead to radical, disruptive technologies.

An awareness of the indirect linkages the organisation acquires on building this network interface is also a huge strategic advantage. Ideally the organisation with whom the linkage is made should itself have a diverse array of linkages, with ties to possibly completely unrelated fields.

The upward integration of firms with up-stream suppliers has been highlighted as being a key factor in disruptive innovations (Figure 9.8). With a strong supplier network, firms report significantly higher levels of productivity than those with a weak network. By the integration of the firm with its suppliers, open, trusting communications can lead to significant improvements in the timely provision of products and services to the firm's customer base. Whilst there has been much focus on the role of suppliers and co-suppliers in a firm's innovation process, firms most frequently turn to customers when seeking insights into the innovation. Without this key alliance with their customer base, companies would be driving the innovation engine blind.

As highlighted by Von Hippel (1978), customers play a pivotal role in the innovation process. In his paper, he argues that customer-centric approaches to innovation are more effective than those which are product focussed. By the integration of the customer into the innovation process, a continual and open exchange of insights, ideas and developments in both directions will offer the firm a significant route to the identification of novel ideas for development and subsequent exploitation. This point of information is similarly put forward by Ragatz *et al*

(1997) who showed that customers are the most important partners during incremental innovation. A key consideration when innovating is that by following the current innovation trajectory, a product will be of a specification which is in considerable excess of existing requirements, leading to a slow adoption of the technology. By constant communication with the customer base, this risk is lowered, or at least, an awareness of the absorptive capacity of the market is identified. The prominence of the customer is also emphasised as being key to product innovation success by Gemunden *et al* (1995), who conducted an empirical analysis into the relationship between innovation success and the intensity and structure of a firms technological network. The value that customers can yield however, should not be overestimated – whilst they may provide feedback on the current product, giving scope for incremental innovation, they may not offer a great deal in frame-breaking disruptive innovations.

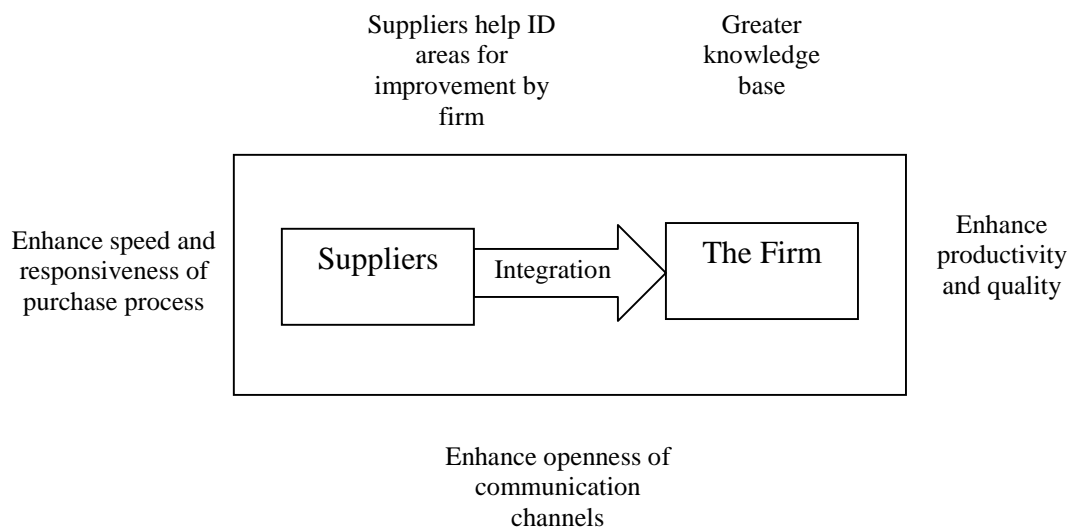


Figure 9.8: Schematic illustration of innovation associated advantages of upstream interaction with suppliers

9.8 Communication environment

An organisations communication structure is defined by Johnson (1992) as “the relatively stable configuration of communication relationships between entities within an organisational context”. It is essential as it enables action, providing a framework whereby knowledge gets to the right people at the right time to promote the innovation process. The most elementary distinction between the different types of structure is between formal and informal channels, where organisations are composed of elements of both.

The communication environment within a firm, be it informal or formal, can have a significant impact on the organisation’s members’ perception regarding the degree to which they work in an innovative organisation. These perceptions can significantly influence the innovative climate within a firm and subsequently, have a significant effect on how they manage relationships with other external network members. Installing and promoting the right communication structure for an organisation is hence essential. How organisations construct these channels and how they are perceived by the organisation’s members is essential to the innovative environment within the firm.

9.9 Geographical clustering in innovation networks & embeddedness

The majority of studies into agglomeration and clustering have emphasised the importance of geographical proximity for the promotion and maintenance of the relationships necessary for innovation (Tracey 2003). According to Storper (1997), this is due to issues such as trust, shared norms and familiar values that stem from common localisation. Further, in networks where the knowledge is highly embedded and immobilised with the firm as tacit knowledge, such tight, intense social interaction may be the only way to learn from one another. Building on this, and knowing the high importance of tacit knowledge, the importance of face to face interactions perhaps cannot be exaggerated enough – as Feldman put it, the common hypothesis is that “knowledge traverses corridors and streets more easily than continents and oceans”. If the innovative and research activities are knowledge intensive, the more face to face (F2F) relationship management is necessary; it then follows that the higher the frequency of these meetings, the greater the necessity for permanent physical proximity. The hypothesis that different actors of innovation need to be in close physical proximity for the

transfer of tacit knowledge was investigated further by Rallet and Torre (1999). Working through a series of case studies, it was found that there is considerable need for close location at specific stages of the innovation process – in the early stages, informal interactions are valuable, creating ideas and transferring contemporary information and developments. As work progresses however and as tasks are divided between organisations, the possibility of remote coordination increases. Whilst the weight of tacit knowledge to the frequency of F2F meetings may vary in line with the nature of the activity and the stage of development, an increasingly emerging question is whether Information and Communication Technology (ICT) can change this situation. Whilst ICT may be effective for the communication of tangible, codified knowledge, its congruence with the accurate communication of tacit knowledge is less well fitting. The reasons are multiple: tacit knowledge is constantly changing and being updated, so there is cost in its conversion to codified form; also, tacit and explicit knowledge are complementary – in transferring codified knowledge, tacit knowledge must frequently accompany it to allow the user to get most value from it. Through advances in ICT however, such as video conferencing, there is bridging the gap between face to face meetings and distant coordination. With the adoption of ICT, firms may run the risk of losing the advantages that may arise from inter-cultural interactions, cultural heterogeneity and the different perspectives these phenomena offer.

It is clear that networks are dispersing further – advances in communication technologies, transportation links and shared platforms are making for a smaller world. Ties today are becoming increasingly international, as firms are seeking the most appropriate partners, regardless of geography, in order to improve their competitive stance although it should be noted that these networking behaviours are hugely dependant on the nature of the industry. With different working practices, cultural norms and best practices, international networks may constitute a crucial source of innovative ideas.

In terms of the empirical findings on the effect of geographical proximity on the propensity to network, these are quite variable. Gilley and Rasheed (2000) for example, suggest that by being in close geographical proximity to each other, the outsourcing decision (and hence the propensity to network) may be positively influenced by affecting the costs or by changing the risks associated with information asymmetry, bounded rationality and opportunism. Love's

findings were quite different – it was found that locational influences on shaping the level of outsourcing and inter-firm collaboration played a lesser role than organisational and strategic factors in shaping outsourcing in the innovation process (Love et al 2001). Regional clusters and the creation of policies that promote their formation is also a significant area of interest (Park 2001).

9.10 Strategic Relationship Management

The different properties of network ties and alliances are an essential mechanism for the transfer of knowledge across a network. Their characteristics however – their strength, their flexibility - are significantly affected by the way they are managed by each of the constituent firms. As network ties evolve from social interaction, to informal collaboration, to formal, contractual agreements on innovation processes, trust is engendered which enhances the flow of information between network actors. As this grows, open ended contracts become more apparent and relationships become temporally long, yielding value for all parties (Lipparini and Sobrero 1994). For firms to form these long term alliances however, there must be appropriate rules of governance in place. By highlighting to each other aims and objectives, driving forces for network membership and their perceived position in the network, a comprehensive, well thought out set of governance mechanisms may be designed and put in place (Grandori 1997). The level of governance that will deliver the most value is, however, very much a variable in this process, as under- and over- governance and formalisation may be detrimental to innovation. To be an effective manager of these networks, a firm must be able to identify when an agreement should be formalised as opposed to remaining a good faith feature, how this formalisation should manifest itself, in what detail, and the role of different variables – relationship duration, degree of friendship and strength of reputation (Shaw, 1998). Collaboration, like any process, gives scope for a learning curve – as time passes, a firm should get better at managing its relationships. However, this is only going to be achieved if they have the appropriate absorptive capacity to learn (Cohen, 1990). What is prevalent in this review is that firms who shape and subsequently manage their network in line with their innovation requirements increase their innovation capacity. As found by Powell et al (1996), the extent to which firms participate in networks is strongly related to the degree to which firms learn about new opportunities.

9.11 Network Orchestration

In order to extract value from a network, firms may orchestrate network activities without a hierarchical arrangement by the performance of deliberate, purposeful behaviours and actions. Whilst the focus in the literature is on the orchestration behaviours undertaken by the ‘hub’ (Jarillo, 1988) or ‘strategic centre’ (Lorenzoni *et al* 1995) firm, the recommended behavioural traits may be adopted by less central network actors – although the efficacy of their actions may be limited. Whilst there is a wealth of research and associated literature on the structure and relational aspects of innovation networks however, relatively little exists on their orchestration. In order to leverage value from an innovation network, a firm must undertake 3 main managerial tasks – namely the management of knowledge mobility, innovation appropriability and network stability (Dhanaraj and Parkhe, 2006). The meaning of these, together with how these tasks may be performed is briefly discussed below (also see Figure 9.9).

9.11.1 Knowledge Mobility (KM)

For the actor to extract knowledge developed by the innovation network, mechanisms must be in place which allows it to be shared, acquired and effectively deployed to the network constituents. They must distribute the relevant knowledge to the relevant members of the network at the right time. Once this information is released, the firm must be able to assess its value and arrange its appropriate transfer to relevant bodies. By increasing the fluidity of knowledge, they increase the probability of it getting to network members who can use it to add value. Specifically, to enhance knowledge mobility, a firm focuses on three specific processes – knowledge absorption, network identification and inter-organisational socialisation. In doing so, they increase the likelihood of advantageous innovations via the combination of new combinations of existing competencies (Kogut and Zander, 1996).

9.11.2 Appropriability

First coined by Teece (1986) and Pisano (1990), ‘appropriability’ refers to a firm’s ability to generate profits from a network innovation. Whilst ensuring they have the right mix of internal resources to do this, it is also essential that environmental factors are in place too. The firm must look at mechanisms to prevent cheating and opportunistic behaviours and also, the leakage of network innovative output to other competing networks.

9.11.3 Network stability

In loosely coupled networks, dynamic relationships between network members when combined with competitive pressures, may lead to network instability. When such problems arise, inter-actor communication may be hindered, as may collaborative activities in general.

Network instability arises from the weakening of ties between members, and may be the result of isolation, migration of actors to other networks or the formation of cliques, a result of high levels of interaction between non-hub firms. However, by the appropriate management of the future shadow, the networks reputation and the enhancement of the complexity of relationship ties (multi-member relationships – multiplexity), it is believed that the stability of the network may be enhanced, which has the effect of enhancing the network’s value creation capabilities.

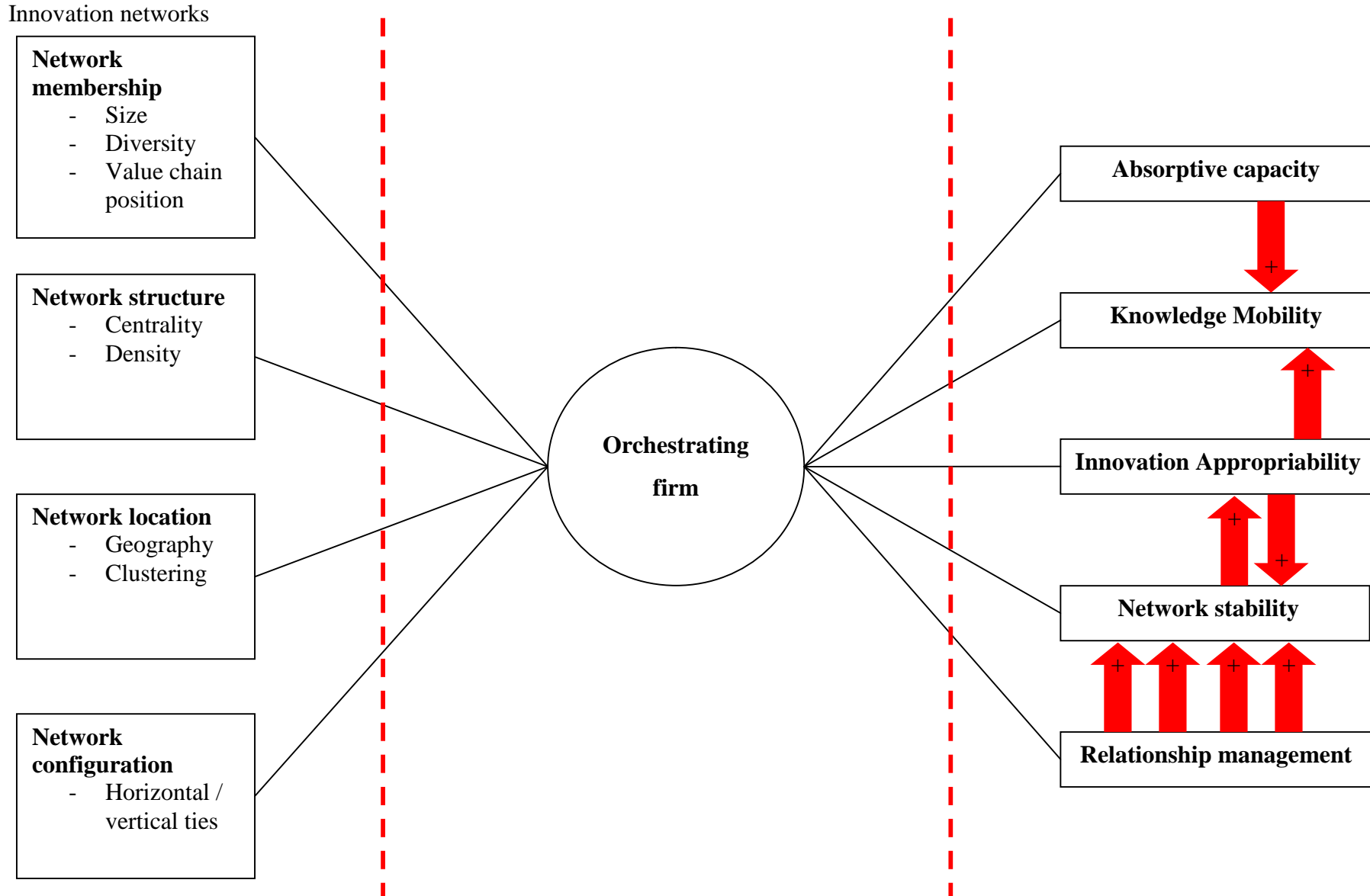


Figure 9.9: Schematic diagram illustrating the factors involved in the orchestration of an innovation network by a firm

9.12 Uniscan Instruments Limited

9.12.1 Introduction

The aim of this section is to draw on particular themes emergent from the literature review and to determine their applicability to Uniscan Instruments Ltd, the industrial sponsors of this research programme.

9.12.2 Company profile

Uniscan Instruments Ltd was formed in 1989 and has since become a market leader in the design and development of electrochemical and optical instrumentation for use in precision measurement applications.

Their product portfolio includes electrochemistry instrumentation and scanning probe platforms including a scanning electrochemical microscope (SECM270), a scanning vibrating electrode system (SVP370), a scanning Kelvin probe system (SKP) and a Localised Electrochemical Impedance System (LEIS370). However, in the last year, Uniscan Instruments Ltd released the M370 scanning electrochemical workstation, which represents a significant step change in the scanning probe market. This innovative concept is an entirely configurable system which allows the user to perform all the techniques mentioned above using a single platform. The ergonomically designed instrument has flexibility at its core and each functionality may be added all at once or as and when it is required by the user. The M370 offers the electrochemical research community a unique, high performance product unmatched by the offerings of other industry incumbents. Additionally, there is a series of surface profiling systems which allow high resolution non-contact surface imaging (OSP100A and OSP500LM).

It is the success of the M370 to which the company's strong growth has been primarily attributed. Uniscan's turnover was reported to increase by 50% over the last year to £1.3m.

9.12.3 Skills and core competencies

Workforce

Uniscan Instruments Ltd is a high technology, knowledge based company, manufacturing niche products for application in the electrochemistry and surface measurement domain. Their occupation of this niche in the instrumentation market necessitates that their staff are highly focussed, very highly qualified and put simply, very good at what they do.

By the recruitment of highly capable engineers, Uniscan have built a proactive, agile and results oriented team, the quality of which represents a significant resource in building competitive advantage over competitors in the electrochemistry instrumentation market.

The Directors of the firm also represent a significant strategic asset. Again, they are highly qualified with extensive experience in the instrumentation field.

Marketing ethos and targeted value creation

Being a relatively small company, delivering a product to the market with the right combination of specifications is at the core of Uniscans strategy. The perception of the Managing Director, Dr. Graham Johnson, is that the larger, more mature companies in Uniscan's field drift away from the market, losing touch with changes in the demands and requirements of the modern day customer. Instead of creating products with the user in mind, the relationship is reversed and products are developed with functionalities deemed useful by in-house product development teams but are found to be redundant to the customer. In response to this, Uniscan has put targeted value creation at the forefront of their strategy. They are in constant contact with current and prospective customers, determining what specifications they would like to see incorporated into their systems. They also fund research projects such as this to allow more focussed feedback regarding what areas of the product may be improved, test new software functions and investigate new applications for their instrument.

Reputational assets

As a result of the development of high quality instrumentation and a driven presence in the electrochemistry community, Uniscan Instruments Ltd has risen to become one of the major brands within this industry. They actively seek opportunities to raise the profile of the firm in Pan-European projects (e.g. ELISHA project) and attend a wide range of conferences, electrochemistry courses, symposiums and workshops.

Size & Agility

In contrast to larger industry incumbents, Uniscan has just 11 employees. This has significant advantages at many levels of the organisation. Firstly, because the firm is small, individuals have significant opportunities to interact with one another. A multi-disciplinary team, engineers have the opportunity to interact across function boundaries many times a day, providing enhanced problem solving capabilities. Secondly, the firm does not overly suffer with organisational inertia - new ideas, concepts or project directions are easily communicated and the resulting changes are potentially easily monitored. Also, should an engineer have an idea for a new product or product improvement, this may be quickly communicated to management who may subsequently reject the concept or suggest further scoping. Additionally, Uniscan's business model is such that every individual is stretched, meaning that there is minimum organisational slack and each increment of effort brings a similar return.

9.12.4 Strategic direction

The development and provision of high quality, high performance equipment of a specification that exceeds the expectation of the customer is central to Uniscan's strategy. Over the past decade, much effort has been focussed on the development of a comprehensive portfolio of products which demonstrate exceptional performance on all fronts. However, the trajectory of each product was very similar to that of competing products – i.e. the products were undergoing development in areas that were being similarly developed by competitors. In 2007 however, Uniscan launched the M370 (Figure 9.10).

This product significantly changes the competitive landscape of the electrochemical scanning probe market being able to perform all four functions using the same platform.

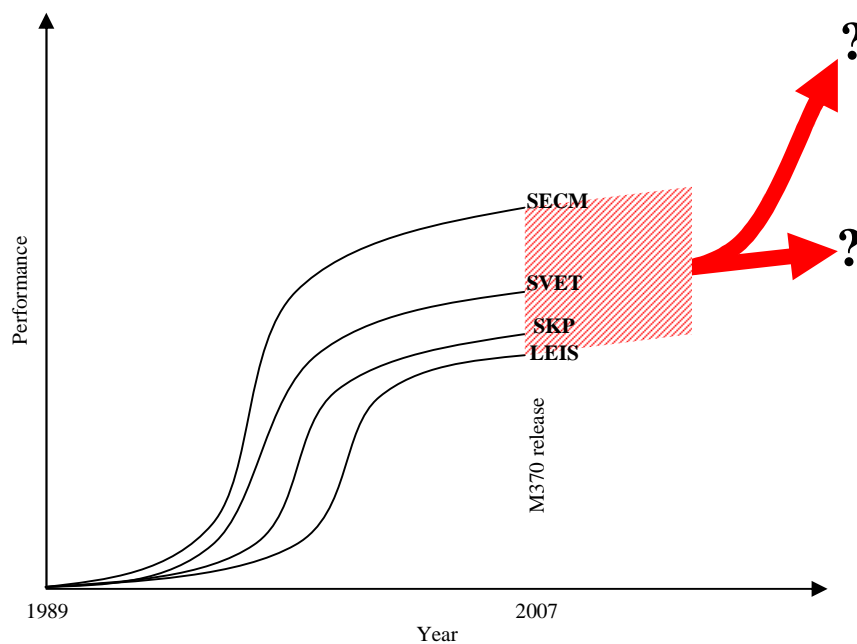


Figure 9.10: Schematic illustration of the innovation trajectories of the SVET, SECM, SKP and LEIS before and after the M370. The red, shaded area depicts the new innovation trajectory of the M370 which is a combination of all four previous innovation trajectories

As a result of the popularity of the M370, it is predicted that there will be a greater amount of feedback and input into the product development process from current and prospective customers. As a result of the incorporation of these new ideas and concepts into the design of the M370, there may be a concomitant increase in the rate of enhancement in the performance of the system. However, there is the risk that the improvements that may be made are only incremental, suggesting that the return on investment in product development may be lessened.

Following on from Uniscan's success with the M370, the firm must now, however, look beyond the current horizon for the next product innovation. Key to their success in achieving this is the relationships and alliances they have outside the boundaries of their organisation. By the creation and appropriate management of these relationships, Uniscan may benefit significantly by internalising ideas, concepts, visions on future market trends and ways of working to deliver the next innovative product that is going to further fuel their growth.

9.13 The Uniscan Network

Network diversity is an essential network property. Being integral to a diverse network allows access to different knowledge bases, behaviours and approaches to thinking. Diverse groups with an array of orthogonal skills and competencies stand a much more significant chance of developing a novel concept and exploiting it accordingly. A schematic representation of Uniscan’s network is given below (Figure 9.11).

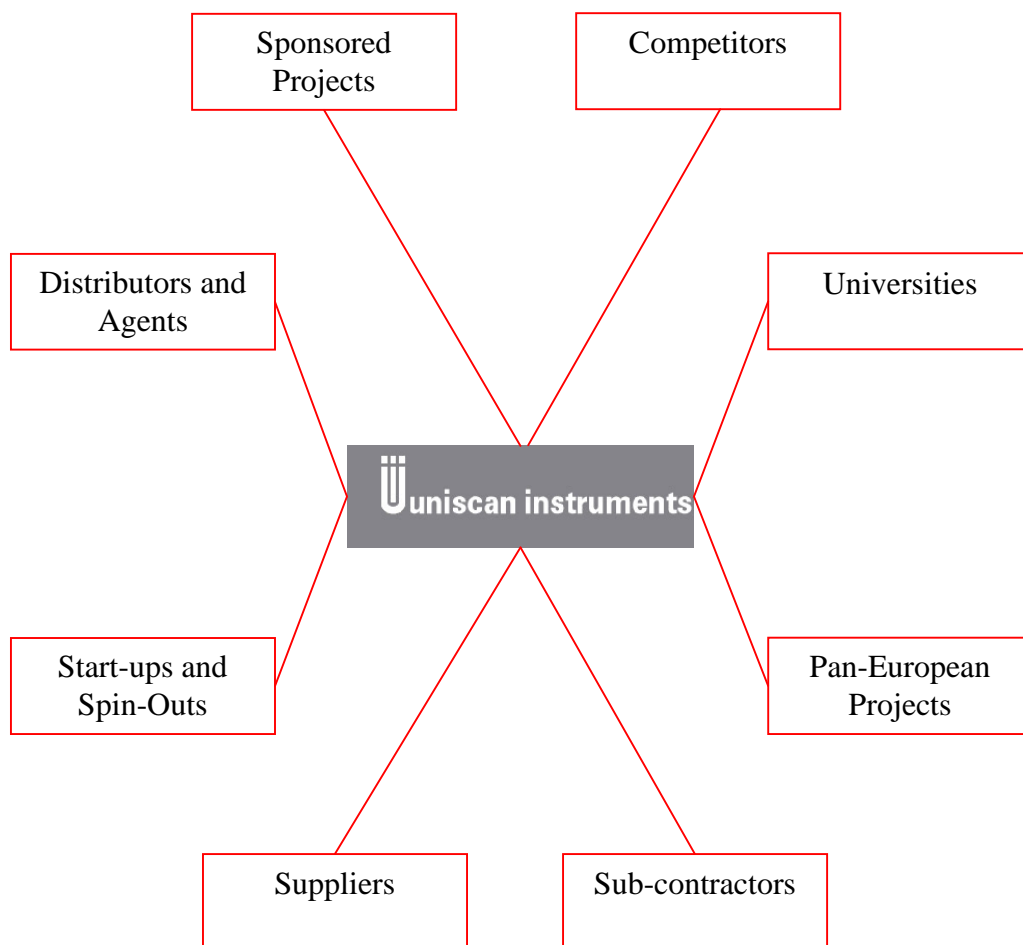


Figure 9.11: Schematic illustration of Uniscan's innovation network

9.13.1 Universities and research institutes

Universities and research institutes not only represent a significant target market for the sale of Uniscan's products and services – they are an excellent source of innovative ideas that may be incorporated into the product offering. It hence follows that Uniscan expends a great deal of effort on maintaining a constant dialogue with the academic community. Such a dialogue allows Uniscan to keep a finger on the pulse of developments in the research community and to perhaps detect underlying trends in research which may give scope to the development of future products. Additionally, Uniscan may get invaluable feedback on product performance and desirable features. In maintaining such a close relationship with the academic community, Uniscan successfully differentiates itself from the mature industry incumbents.

9.13.2 Sponsored Projects

Although these may be projects undertaken in Universities, the relationship is fundamentally different to that above, whereby the relationship is based on social interaction or after sales service. Sponsored projects allow Uniscan to generate focussed feedback on particular aspects of the system, beta test new product developments and raise the profile of the Uniscan brand within that particular institution. In particular, these projects allow Uniscan to benefit from the wide range of skills and competencies a University or group may have that it lacks. Uniscan's skills and competencies lie in the design and manufacture of complex measurement instrumentation – not necessarily the application of this instrumentation. By the involvement of creative individuals in the academic environment, valuable insights may be obtained into the use of the technology in previously un-thought of research applications. This is especially so in institutions which have a collaborative approach to research and the diffusion of research capabilities across functional boundaries. When entering these relationships, Uniscan should look at the opportunity for the project to cross departmental boundaries and ensure that the project group is as diverse as possible. Such diversity will add depth to the project and raise awareness of the brand and technology across the institution.

Sponsored projects also represent a key marketing mechanism in that they may result in the publication of research papers which further raise the awareness of the brand and its instrumentation in the target market.

9.13.3 Start-ups and spin outs

Involvement with University spin-outs and young start up companies is one of Uniscan's significant interests – the company is currently associated with several early stage companies. In the majority of cases, Uniscan play a quite central role, whereby they develop the instrumentation – usually for a sensing application which involves the detection of a signal by electrochemical means.

This small scale 'corporate venturing' of relatively high risk projects holds many opportunities for Uniscan. Firstly, there is the possibility that the project results in a marketable product, in which case Uniscan benefit financially via an equity stake in the company or royalties on each subsequent transaction. Secondly, and most importantly, these projects give Uniscan the opportunity to introduce variety to the workforce – allowing them scope to use their diverse range of skills in the scoping, design and manufacture of an innovative product. By undertaking these projects they may internalise new technologies and approaches to 'doing things' with the effect of improving the NPD process within the organisation. Such variety is also a key factor in maintaining a motivated workforce. Additionally, by interacting with a new group of individuals, Uniscan may learn about new emergent technologies and see opportunities for product developments further a field.

By their very nature, the spin out projects and start up companies are centred around new, innovative product offerings. Uniscan, by their involvement in these projects not only have the opportunity to play an instrumental part in the creation of a novel product, but they also have the opportunity to develop the unique skills and competencies on which Uniscan's competitive advantage is built. In playing a central role in the product development process, they are following a unique path, acquiring unique skills and competencies that form the dynamic capabilities required in their competitive environment (see Figure 9.3).

There are also the reputational benefits associated with entering these relationships – they are perceived as an approachable, innovative company with the skills and resources necessary to develop new technologies.

9.13.4 Distributors and Agents

These bodies essentially represent the mechanism by which Uniscan distributes its instrumentation across the globe. By actively promoting the product portfolio at tradeshows, conferences and by direct contact with potential customers, awareness of the Uniscan brand is increased, as are sales and the possibility of further interaction via projects and spin outs. As distributors are also highly competent in their own particular field, they provide Uniscan with useful insights into new opportunities to which they would otherwise be blind.

9.13.5 Joint research initiatives

A relatively new initiative in the research community, EC projects involve the assemblage of a research committee composed of a variety of different agents. The ELISHA project for example is composed of a number of Universities and research groups in addition to Uniscan. Whilst these projects often end with a product which is quite different to the product in the initial brief, the process by which it is achieved allows Uniscan the opportunity to work closely with organisations outside its area of specialisation. Working with both academic and commercial partners, they are provided with a creative insight into possible product development paths. These initiatives are also often composed of eminent academics that are at the forefront of their field and who may play a ‘visionary’ role in predicting future market trends and research directions.

9.13.6 Sub-contractors

Uniscan has recruited a highly competent workforce which has the stand-alone capabilities to develop high quality instrumentation. However, because the work force is particularly small, each engineer is stretched to their limit. As a consequence, if a single project requires a significant amount of software development for example, this may be sub-contracted out to

another firm or individual. The use of a sub-contractor as opposed to the recruitment of another member of personnel is because these jobs are generally one-offs and the use of a sub-contractor is the most financially viable option. Also, sub-contractors may be used if the project demands a level of specialisation beyond that of the internal resources.

9.13.7 Suppliers

Due to Uniscans size, there is limited scope for them to collaborate with firms up the value chain. They simply do not have the buying power to initiate such a relationship with the majority of their suppliers. However, they do have some interaction with companies with whom they 'have control over' – more specifically, companies that produce specialist components for their instrumentation.

The observation that Uniscan's size and buying power is a significant barrier to collaboration up the value chain is quite a valuable finding. Considering that the interaction of firms with up-stream suppliers has been highlighted as being a key factor in the development of innovative products, overcoming this limitation may allow the formation of relationships from which Uniscan may leverage significant innovative value.

One way in which this may be achieved would be to increase its buying power by forming an alliance with companies using similar components. In doing so, the financial value of their custom and the accompanying need for customer oriented services would increase the likelihood of the up-stream suppliers entering a collaborative relationship with Uniscan to yield innovative outcomes.

9.13.8 Network Infrastructure

The network infrastructure may be defined as the mechanism by which networks are created and to a certain extent, maintained. With the primary aim of the development and sale of innovative measurement technologies, Uniscan is hugely proactive in seeking out opportunities to collaborate on new projects and to sell their existing portfolio of products. By their involvement and interaction with a number of different bodies within academic, professional and commercial environments (see Figure 9.12), Uniscan exposes itself to a variety of organisations composed of people with very different skills and competencies – an extremely valuable resource to the innovating firm.

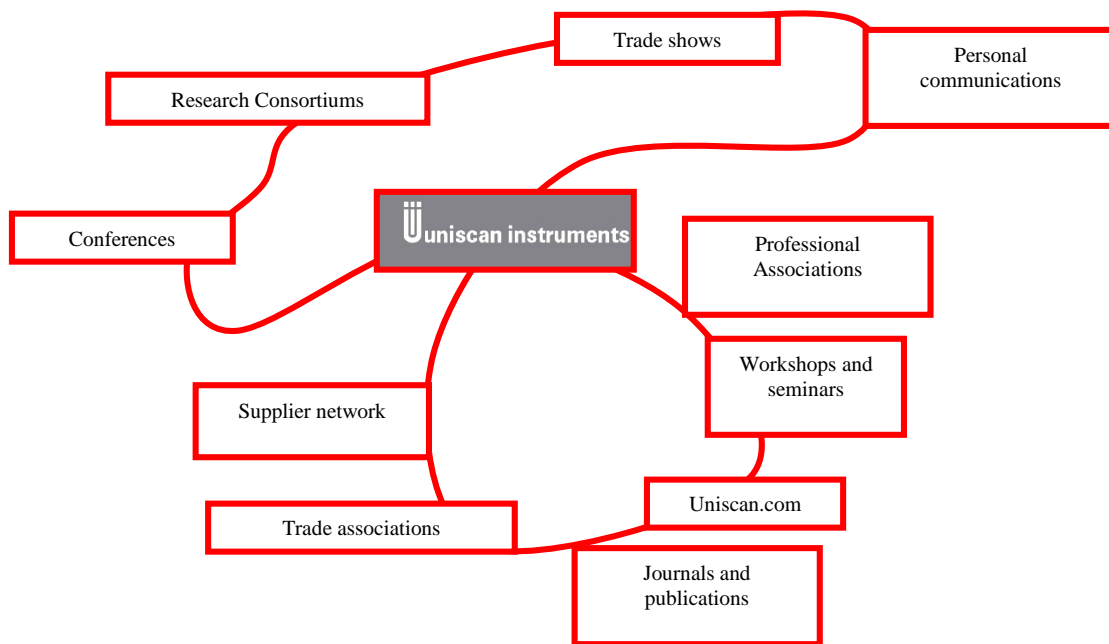


Figure 9.12: Schematic depicting Uniscan's network infrastructure - the mechanism by which alliances may be initiated and maintained.

Uniscan's website (www.uniscan.com) is an essential tool in acquiring business. By continually optimising the site, it is now in the top 5 search results in Google™ for “SECM” and “potentiostat”, two of Uniscan's major product lines. Whilst it represents a very important tool for acquiring custom and showcasing Uniscan's product portfolio, in today's social e-networking environment, there is perhaps the potential to extract much more value from this versatile customer interface. A possible suggestion is to make Uniscan.com an electronic hub for existing customers to showcase their work. Customers with Uniscan kit (and even, perhaps, simply prospective customers) would be invited to upload a profile and detail the nature of their research, place of work and aims and objectives – to publicise and market themselves and the organisation of which they are part. In doing so, potential customers not only see the number of satisfied customers Uniscan have supplied equipment to, but they also become aware of groups involved in related work (Figure 9.13). As a consequence, Uniscan plays a central, integral role in catalysing collaborative relationships between existing customers which will not only have a positive effect on the perception of the Uniscan brand (as one which actively promotes and engages in collaborative, exciting projects), but also increase the possibility of Uniscan being involved in more innovative projects; perhaps openly promoting and rewarding inter-customer collaboration.

In creating their own collaborative infrastructure, Uniscan would become a highly centralised body in this global network and in doing so, be increasingly able to orchestrate and manage network relationships to extract innovative value in the form of ideas and potential products. Additionally, the networking tool could be extremely valuable in the acquisition of engineers and scientists for employment within Uniscan – again, another source of competitive advantage.



Figure 9.13: Illustration of what the Uniscan Innovation Net may look like

9.13.9 Relationship ties

It is of significant benefit to the innovating firm to have a mix of weak and strong relational ties during the innovation process. As illustrated in Figure 9.7, weak ties, which may stem from social interactions and are not centred on contractual agreements are key to the production of innovative ideas and concepts, whereas strong ties are essential later in the innovation process.

From observing the relationships in which Uniscan is involved, it is apparent that they benefit from ties of varied strengths. Weak ties built upon social interaction via membership of projects and consortiums provide new concepts, ideas and indicate new trends, whereas stronger ties, which may be sponsored projects and corporate venturing for example allow the development and continual improvement of products which require contractual enforcement.

Whilst the mix of strength and type of tie between Uniscan and its network members is currently good, it is important that they have an overt awareness of the importance of a good balance between weak and strong ties. Whilst strong ties are effective forces in the latter stages of the innovation process, the potential for weak ties to be incorporated down the innovation pipeline and continue to deliver innovative insights should not be discounted.

9.13.10 Network management

The major force driving the formation of alliances between Uniscan and members of its network is the generation of novel, innovative ideas which it may incorporate into its product development pipeline. By interacting with a diverse range of individuals, they are provided with a unique and invaluable insight into how their product may be improved, what aspects of it may be redundant, or how it may be used in a new field of application.

However, whilst these sources of information and insight are exceptionally important, they must be managed in such a way that the maximum value possible may be extracted from them.

Knowledge Mobility

Knowledge mobility, as described earlier, refers to an organisations ability to access and internalise information from its network of alliances.

A fortunate outcome of Uniscan's small but highly technologically competent workforce is that when network members interact with Uniscan, they do so via these individuals. Because the customer base is composed of people who are highly proficient in their respective fields, they are able to talk to Uniscan engineers at the technical level that they require and value. This is especially important for the management of customer interactions – which are truly essential in driving product development.

Uniscan's approach to managing the customer is in significant contrast to the way these relationships may be brokered by larger, more mature companies. Often, sales representatives are used who may not be as technologically competent and are hence unable to communicate with the customer at the level that they require.

The result of this highly competent interface is that not only is the right information communicated to the customer – opportunities or ideas for product development arising from interaction with the customer are much more likely to be internalised and exploited within Uniscan. By adding a layer of separation between the engineers and the customer through

adding a sales/marketing function with less technological experience, there is a considerable risk that really innovative, useful information may be filtered out and the true value of the relationship may not be realised. Although Uniscan does not have a discrete sales/marketing function, it is performed by an individual with extensive experience in the field of scanning probe microscopy and electrochemical measurement instrumentation.

An exceptionally important skill is also a degree of emotional and cultural intelligence. By understanding how academics for example, work, then they may adjust their approach to managing that relationship. Uniscan appears to very much value what academics have to offer and their underlying principles on the progression of human knowledge. They therefore understand that there may be incongruence between the ways in which they and academics work and behave and adjust their style of interaction accordingly to extract knowledge from and relay knowledge to the academic community.

As a result of these attributes, the absorptive capacity of the company is improved – it is able to recognise, internalise and assimilate knowledge from its network and apply it to commercial ends.

Knowledge appropriability

Knowledge appropriability refers to Uniscan's ability to extract value from an alliance with a member of its network.

Uniscan very much appreciates that each organisation, each individual it works with is different. As a consequence of this, it does not have a prescriptive way in which it deals with potential allies. However, if the relationship involves the development of a new product or system, Uniscan will tailor a contract according to what it wishes to extract from the relationship, be it technological know how, an equity stake or royalty. It will also build in contractual agreements which prohibit the flow of sensitive information outside of the alliance network.

9.13.11 The academic/commercial boundary

The academic environment is exceptionally important to Uniscan. They represent a market for the sale of their products and an invaluable source of ideas and concepts that they may incorporate into their new product offerings. However, whilst they continue to enter alliances with a variety of different academic institutions, they continue to experience the same problems over and over again. The reasons for these problems are based on the simple fact that the goals of the academic and those of the commercial entity are fundamentally different.

Commercial entities exhibit goal oriented, focussed behaviours that are driven by the unerring need to generate value for stakeholders. Academics however, whilst they are being increasingly forced to generate income in the form of funding and studentships, are focussed on the publication of papers, enhancing their reputation, the reputation of their group and that of the academic institution of which they are part. With different goals, come different behaviours.

With the aim of pushing forth the boundaries of human knowledge, academics may actively pursue different avenues of research during a project based on areas of interest and the possibility that further investigation may yield a novel finding. In contrast, a project within industry would have been undertaken in a pragmatic, logical manner with a single goal – the development of a product, process or service that would add value to the operations of the firm.

It is clear from the continual interplay between academia and industry that these relationships do deliver value to the industrial partners, although not always in the way it was intended. However, with a clear incongruence between the goals driving the behaviours of the academic workforce and those of the industrial partners, there is a clear possibility that with the appropriate management of this boundary, both industrial and academic parties can stand to reap significantly greater benefits from their collaborative agreements. This is not only with reference to goal delivery but also to ways of working.

9.13.12 Enhancing learning across the commercial / academic boundary and the development of best practice

Taking forward the observations of Uniscan and its perception of interacting with the academic environment, it may be argued that Uniscan, (and commercial organisations in general) and the academic organisations with whom they are allied, may extract more value from the relationship by an increased understanding of the principles that govern inter-organisational learning.

The majority of prior research on inter-organisational learning has focussed on the principle of ‘absorptive capacity’ – defined as a firm’s ability to “recognise the value of new, external knowledge, assimilate it and apply it to commercial ends” (Cohen and Levinthal, 1990).

There are broadly three methods by which an organisation may internalise the knowledge present in the network of which it is part – passive, active and interactive learning. Passive learning occurs when a firm acquires tangible codified knowledge from journals, seminars and accepted industry norms. Active learning on the other hand, involves processes such as bench-marking and competitive intelligence which is achieved by the observation of other organisations and the internalisation of their observable behaviours. However, both active and passive learning are limited - because the knowledge is codified and in the public domain, it is no longer a VRIN resource and may be internalised by other organisations. This may, however, be overcome by interactive learning whereby the two organisations work in close proximity to one another and learn not only the observable components of the organisations capabilities but also the more tacit aspects the ‘how and why’ knowledge.

It may hence be of value to both the industrial organisations and the academic partner if a method of ‘best practice’ was to be developed. In this framework of best practice, recommendations would be made as to how the relationship may be managed to try and ensure both parties extract the optimum amount of value from the relationship. Not only does this enhance the extraction of value from the current project – it also enhances the probability of repeated interaction.

The best practice framework may be built by a co-ordinated effort by the academic and industrial partners to integrate the best parts of each organisation's approach to relationship management and knowledge transfer. On the completion of each project, this best practice framework may then be reviewed using industrial and academic focus groups and improved upon if necessary.

When employed, the framework would suggest mechanisms which would have the effect of increasing the permeability of the boundary between the two organisations, allowing each to extract as much value from the other as possible, whether this be new ways of working, ensuring any project related idea or concept is captured and internalised or the application of new approaches to project management.

9.14 Conclusions

Innovation networks are emerging as a key resource in today's competitive environment. By their appropriate design and subsequent management, a firm may gain significant competitive advantage if they can successfully extract and leverage innovative outcomes from them.

Emergent from the network literature is the importance of a number of factors in the design and management of innovation networks. Design considerations include degree of centrality, network diversity, relationship strength and geographical location, whereas management considerations include variables such as knowledge mobility, knowledge appropriability and absorptive capacity.

Whilst the concepts of 'network design' and 'network management' are not currently terms employed at Uniscan, their theoretical principles are very much emergent in the organisation. This is especially so with respect to absorptive capacity and network diversity.

With a highly skilled workforce and a myriad of relationships outside the boundary of the organisation, Uniscan is highly competent in the production of high quality, innovative instrumentation that exceeds the requirements of the end user. However, there is an aspect of the organisation which may be perceived to hinder innovative activity – specifically, the size of the workforce. The Uniscan business model is designed so that each member of the organisation is stretched. Whilst this ensures that each employee is delivering value to the organisation, it does not allow any slack which would allow employees to pursue ideas or concepts they may have arrived at or thought of. Whilst the management of the organisation appreciates the need for such 'creative time', the work load is such that after working to troubleshoot a problem with an instrument or to construct an instrument for shipping, there is not sufficient time. This is no doubt a function of their small size, but with growth, perhaps a small amount of operational slack may allow more innovative activity to take place.

The production of innovative products is a key value driver within Uniscan. The innovative M370 for example has contributed massively to the recent financial success of the company. However, the bottom line continues to be the measure of success, despite the fact that it was driven by this product innovation. It is hence proposed that Uniscan looks to develop a more

balanced scorecard of performance, looking at drivers of value, including metrics which are aligned with innovative output. These may include, for example, the number of incremental improvements made per month, the number of hours spent interacting with end users, or the number of hours spent developing new macros for a new instrument. In doing so, if there is any deviation in the bottom line, there may be an increased understanding in what drove those changes and how resources may be distributed to alter this deviation.

In recent years, the internet has become a major commercial tool. Uniscan's website is a key marketing device, allowing prospective customers to browse their product portfolio and learn of the innovative product offerings available. In light of the current collaborative and social networking climate, the suggestion is made that Uniscan develops its site as an electronic hub for researchers and academics to showcase their work and invite collaborative activities. Customers are invited to form a collaborative community with Uniscan as the commonality. As the Uniscan Collaborative Network grows, so does the awareness of the brand and its perception as an innovative, pro-collaboration entity.

A further finding of this research is the importance of the appropriate management of the academic/commercial boundary. By the appreciation that these organisations are fundamentally different it is suggested that through work with both commercial and academic bodies, a framework of best practice is developed which allows both parties to extract the maximal amount of value from the collaborative relationship. This framework would suggest mechanisms which would allow each body to develop the absorptive capacity to internalise valuable information from its partners and leverage value from it.

Chapter 10

General conclusions

10. General conclusions

Scanning electrochemical microscopy (SECM) is a scanning probe technique which allows the interrogation of the electrochemical and topographical properties of a variety of surfaces. The technique has been used in a variety of fields and its application to studying biological systems is well documented. Within this thesis, two applications for the SECM technique are explored.

The first application involved the characterisation of a previously optimised impedance based DNA biosensor developed within the group (Davis *et al* 2005). The sensor consists of a bio-polyelectrolyte film of polyethylenimine and single stranded DNA on a carbon ink. In the original study, the impedance of the film was observed to drop by approximately 10% in 3hrs when exposed to complementary DNA, but increase marginally when exposed to non-complementary DNA. One aim of the work presented within this thesis was hence to determine whether these small changes in the charge transfer properties of the film were detectable by SECM in feedback mode.

For interrogation by SECM, the polyelectrolyte/ssDNA array was fabricated using the polycationic polymer polyethylenimine (PEI); using the SECM micropositioning stage, the PEI film was patterned in an array format and then functionalised with ssDNA by exposure of the array to ssDNA in solution.

Following the characterisation of the PEI array and the identification of hexamine ruthenium chloride as a suitable redox couple, the complete biosensing platform was interrogated by SECM area scan. On comparing the feedback current obtained over the PEI/DNA array before and after exposure to complementary and non-complementary DNA, it was found that on exposure to the complementary genomic DNA, the charge transfer properties of the PEI/DNA film were enhanced. This was also the case for non-complementary exposure, although to a lesser degree.

This work clearly demonstrates the applicability of SECM to detecting changes in the charge transfer properties of a film and highlights the potential of the technique to feature strongly in the development of a label-less approach to detecting DNA hybridisation. Although the

technique currently has limitations in comparison to the fluorescence technique for example, it holds great promise in terms of providing a sensitive, cost effective platform for detecting DNA hybridisation and also, characterising DNA biosensors based on electrochemical techniques.

The second SECM application explored in this research project involved the implementation of SECM as a means by which protein expression in cells may be detected. The work clearly demonstrates the promise offered by SECM to become a powerful tool in immunochemistry.

Immunochemistry involves the use of antibodies linked to an enzymatic or fluorescent label to detect antigens of interest in cytological or histological preparations. It is an invaluable tool in the diagnosis of disease and in the investigation of the localisation of protein expression in cells and tissues. Described within this thesis is a new, innovative approach to imaging protein expression which involves the electrochemical detection of the immunochemical enzymatic label horseradish peroxidase (HRP).

Horseradish peroxidase is already extensively used in immunochemistry in conjunction with the DAB (diaminobenzidine) staining method. After the enzyme linked antibodies are allowed to bind to the antigen of interest expressed in the cell or tissue preparation, the preparation is exposed to hydrogen peroxide and DAB. In the presence of HRP, the DAB is reduced to form a brown precipitate which indicates the presence of the antigen in the sample. Although this technique is probably the most frequently employed, there are problems associated with this approach. In light of this, the use of scanning electrochemical microscopy was investigated for the detection and localisation of horseradish peroxidase activity.

In Chapter 7, a method was developed by which HRP may be imaged by SECM. A glutaraldehyde-crosslinked HRP pattern was fabricated on silanised glass using the micropositioning stage on the SECM270. The immobilised HRP was then imaged using hydroquinone as the oxidising co-factor. In the presence of hydrogen peroxide, hydroquinone is reduced to benzoquinone which is subsequently oxidised at the microelectrode tip held in the vicinity of the enzyme. Following the development of this HRP-imaging methodology,

the same approach to imaging enzymatic activity was used in the development of SECM as a tool by which protein expression may be imaged.

The transmembrane protein, CD44, plays a pivotal role in anchoring cells to the surrounding extra-cellular matrix and growth factors. It is unique as it facilitates both cell to cell and cell to matrix interactions and is expressed on a variety of cell types including epithelial cells. In chapter 8, the expression of CD44 in RT112 is detected using the SECM in the generation/collection mode.

By using a well defined immunochemical protocol, CD44 expressed at the surface of cultured RT112 cells was labelled with HRP via a biotinylated primary/secondary antibody complex. Following labelling and taking care not to allow the cells to dry out, the cells were then submerged in a buffered solution of hydroquinone. After the subsequent introduction of hydrogen peroxide, a series of approach curves and area scans were carried out over the HRP-labelled CD44-expressing RT112 cells. Using highly confluent fields of cells grown on slide flasks and cells patterned on poly-L-lysine functionalised glass, SECM successfully imaged the enzymatic activity of the HRP labels linked to the CD44 molecules by the primary/secondary antibody complex. It was found that by using secondary antibodies of a lower concentration, the resolution of scans over highly confluent cells may be improved.

The work clearly demonstrated the promise the SECM technique offers the detection of proteins expressed by immobilised cells.

The scanning electrochemical microscope used in this research programme was designed and manufactured by Uniscan Instruments Limited, the industrial sponsors of this research programme. Their involvement was primarily based on their desire to obtain feedback on the performance of their instrument and to glean ideas which may be incorporated into future product developments. Some of these recommendations are detailed in chapter 4. Additional requirements were the development of a microelectrode probe fabrication and characterisation protocol (chapter 5) as well as beta testing new product innovations such as, for example, the sloping scan macro described in chapter 4.

The extraction of value from relationships with organisations like Cranfield University is a significant consideration for Uniscan Instruments Ltd. Not only do organisations like Cranfield represent a customer base – they also represent an invaluable source of ideas and concepts that are instrumental to the creation of innovative products, processes and services. The importance of such collaborative relationships is becoming increasingly apparent in the high technology market. Being able to exploit resources both within and outside the boundary of the firm is essential if a firm is to create and maintain competitive advantage over other industry incumbents. As a result, the locus of innovation is moving outside the boundary of the firm and the design and management of the network of organisations around this locus is a significant strategic consideration. In chapter 9, a literature review is presented of the emergent principles of network theory which is then drawn upon in a cursory analysis of the network of organisations associated with Uniscan Instruments Ltd. An interesting finding was the importance of common working principles in brokering an inter-organisational relationship, with particular emphasis on the relationship between Uniscan and academic institutions.

As commercial and academic bodies are fundamentally different kinds of organisation, the transfer of knowledge, especially tacit knowledge, between the two *may* be hindered. It was hence suggested that each kind of organisation develops a code of best practice whereby each develops and codifies an understanding of the workings of the other with the effect of working better, side by side and extracting more value from the relationship.

An additional suggestion was made regarding how Uniscan may increase their degree of centrality and hence, their capability to orchestrate their network of relational ties to extract more innovative value. It was suggested that Uniscan develop a web-based networking tool whereby customers are able to showcase their research and advertise potential collaboration opportunities. Not only will this endorse the perception of Uniscan as an innovative, collaborative company, but it will also give them the opportunity to identify and orchestrate new collaborative relationships themselves.

Chapter 11

Suggestions for further work

Development of SECM as a high throughput DNA microarray platform

The work reported in chapter 6 involved the development of an SECM based DNA hybridisation sensor using genomic DNA. With the aim of developing this technique as a high throughput hybridisation technology, further work may include:

- the use of short oligonucleotides of a known sequence and length.
- the investigation of the hybridisation of same system using another, non-electrochemical analytical technique – such as, for example, QCM or fluorescence microscopy.
- a study of the use of alternative, topographically flat substrates to serve as an immobilisation platform for the bio-polyelectrolyte film.

Development of SECM as a novel approach to detecting protein expression in cells

In chapter 8, the potential for the exploitation of SECM as a novel approach to detecting protein expression in cells is clearly demonstrated. With the aim of exploring the true potential of this technique, further work may include:

- the application of the technique to detecting different proteins expressed in different locations within the cell.
- the application of the technique to histological samples.
- the use of different enzymatic labels such as alkaline phosphatase and glucose oxidase.
- the growth of monolayers of cultured cells in well defined patterns which, when combined with approach curve data and mathematical models of the diffusional profiles, may allow for an approximation of the concentration of enzyme and hence, the concentration of the expressed protein of interest in the patterned cells.

Chapter 12

References

- Abe, H. and Hoshi, H. (2003) Evaluation of bovine embryos produced in high performance serum-free media. *Journal of Reproduction and Development* 49, 193-202.
- Adams, R.N. (1958) Carbon Paste Electrodes, *Analytical Chemistry*, 30, 1576-1576.
- Aguilar, Z.P., Vandaveer, W.R. and Fritsch, I. (2002) Self-contained microelectrochemical immunoassay for small volumes using mouse IgG as a model system. *Analytical Chemistry*, 74, 3321-3329.
- Agung, B., Otoi, T., Abe, A., Hoshi, H., Murakami, M., Karja, N.W.K., Murakami, M.K., Wongsrikeao, P., Watri, H. and Suzuki, T. (2005) Relationship between oxygen consumption and sex of bovine *in vitro* fertilized embryos. *Reproduction in Domestic Animals*, 40, 51-56.
- Albrecht, H. (1991) Relational and Content Differences Between Elites and Outsiders in Innovation Networks. *Human Communication Research*, 17(4), 535-561.
- Almeida, P., Kogut, B. (1999) Localisation and knowledge and the mobility of engineers in regional networks. *Management Science*, 45, 905-917.
- Alpuche-Aviles, M.A., Wipf, D.O. (2001) Impedance feedback control for scanning electrochemical microscopy. *Analytical Chemistry*, 73, 4873-4881.
- Alvarez-Icaza, M., Bilitewski, U. (1993) A mediated amperometric enzyme electrode using tetrethiafulvalene and L-glutamate oxidase for the determination of L-glutamic acid. *Analytica chimica acta*, 282, 353-361.
- Amemiya, S., Guo, J., Xiong, H. and Gross, D.A. (2006) Biological applications of scanning electrochemical microscopy: Chemical imaging of single living cells and beyond. *Analytical and Bioanalytical Chemistry* 386, 3, 458-471.
- Aoyagi, S., Utsumi, Y., Masudaira, M., Yamada, H., Kaachi, M., Shiku, H., Abe, H., Hoshi, H., Matsue, T. (2006) Quality evaluation of *in vitro*-produced bovine embryos by respiration measurement and development of semi-automatic instrument. *Bunseki Kagaku*, 55 (11) 847-854.
- Aquino-Binag, C., Pigram, P.J., Lamb, R.N., Alexander, P.W. (1994) Surface studies of quinhydrone pH sensors. *Analytica Chimica Acta* 291, 65-73.
- Aruffo, A., Stamenkovic, I., Melnick, M., Underhill, C.B., Seed, B. (1999) CD44 is the principal cell surface receptor for hyaluronate. *Cell* 61(7), 1303-1313.
- Babkina, S.S., Ulakhovich, N.A. (2004) Amperometric biosensor based on denatured DNA for the study of heavy metals complexing with DNA and their determination in biological, water and food samples. *Bioelectrochemistry*, 63, 261-265.
- Bard, A.J., Fan, F.R., Kwak, J. and Lev, O. (1989) Scanning electrochemical microscopy. Introduction and principles. *Analytical Chemistry* 61, 132-138.
- Bard, A.J., Denault, G., Lee, C., Mandler, D. and Wipf, D.O. (1990) Scanning electrochemical microscopy: A new technique for the characterization and modification of surfaces. *Accounts of Chemical Research* 23, 357-363.
- Bard, A.J., Denault, G., Friesner, R.A., Dornblaser, B.C. and Tuckerman, L.S. (1991) Scanning electrochemical microscopy: Theory and application of the transient (chronoamperometric) SECM response. *Analytical Chemistry* 63, 1282-1288.
- Bard, A.J., Mirkin, M.V., Unwin, P.R. and Wipf, D.O. (1992) Scanning electrochemical microscopy. 12. Theory and experiment of the feedback mode with finite heterogeneous electron-transfer kinetics and

- arbitrary substrate size. *Journal of Physical Chemistry* 96, 1861-1875.
- Bard, A.J., Faulkner, L.R., (2001) *Electrochemical Methods, Fundamentals and Applications* (2nd Ed.) John Wiley & Sons, Inc.
- Bard, A.J. and Mirkin, M.V. (2001) *Scanning Electrochemical Microscopy*. Printed by Marcel Dekker, Inc. New York.
- Baum, J., Calabrese, T. Silverman, B. (2000). Don't go it alone: alliance network composition and start-ups performance in Canadian biotechnology. *Strategic Management Journal*, 21, 267-294.
- Bath, B.D., Scott, E.R., Phipps, J.B. and White, H.S. (2000) Scanning electrochemical microscopy of iontophoretic transport in hairless mouse skin. Analysis of the relative contributions of diffusion, migration, and electroosmosis to transport in hair follicles. *Journal of Pharmaceutical Science* 89, 1537-1549.
- Berger, C.E.M., Rathod, H., Gillespie, J.I., Horrocks, B.R. and Datta, H.K. (2001) Scanning electrochemical microscopy at the surface of bone-resorbing osteoclasts: Evidence for steady-state disposal and intracellular functional compartmentalization of calcium. *Journal of Bone and Mineral Research* 16, 2092-2102.
- Bond, A.M., Oldham, K.B., Zoski, C.G. (1988) Theory of electrochemical Processes at an inlaid disc microelectrode under steady-state conditions. *Journal of Electroanalytical Chemistry*, 245, 71-104.
- Bond, A.M., Luscombe, D., Oldham, K.B., Zoski, C.G. (1988b) A comparison of the chronoamperometric response at inlaid and recessed disc microelectrodes, 249, 1-14.
- Bond, A.M., Oldham, K.B., Zoski, C.G. (1989) Steady state voltammetry. *Analytica Chimica Acta*, 216, 177-230.
- Borgmann, S., Radtke, I., Erichsen, T., Blochl, A., Heumann, R. and Schumann, W. (2006) Electrochemical high-content screening of nitric oxide release from endothelial cells. *ChemBioChem* 7, 662-668.
- Buchler, M., Kelley, S.C. and Smyrl, W.H. (2000) Scanning electrochemical microscopy with shear force feedback. Investigation of the lateral resolution of different experimental configurations. *Electrochemical and solid state letters* 3, 35-38.
- Burgland, G.I., Carlsson, G.H., Smith, A.T., Szoke, H., Henriksen, A., Hajdu, J. (2002) The catalytic pathway of horseradish peroxidase at high resolution. *Nature*, 417, 463-468.
- Burt, R.S. (1992). *Structural holes: The social structure of competition*. Cambridge MA: Harvard University Press.
- Cai, C.X., Liu, B., Mirkin, M.V., Frank, H.A. and Rusling, J.F. (2002) Scanning electrochemical microscopy of living cells. 3. *Rhodobacter sphaeroides*. *Analytical Chemistry* 74, 114-119.
- Camp, R.L., Kraus, T.A., Pure, E. (1991) Variations in the cytoskeletal interaction and post-translational modification of the CD44 homing receptor in Macrophages. *Journal of Cell Biology*, 115(5), 1283-1292.
- Ceres, D.M., Udit, A.K., Hill, H.D., Hill, M.G., Barton, J.K. (2007) Differential Ionic Permeation of DNA-Modified Electrodes. *Journal of Physical Chemistry B*, 111, 663-668.
- Chapman, D.L. (1913) A contribution to the theory of electrocapillarity. *Philosophical Magazine*, 25, 475-481.

- Chatterji, D. (1996) Accessing external sources of technology. *Research, Technology Management*, 39(2) 48-56.
- Cheng, G.F., Qu, H.y., Zhang, D.M., Zhang, J.D., He, P.G., Fang, Y.Z. (2002) Spectroelectrochemical study of the interaction between antitumor drug daunomycin and DNA in the presence of antioxidants. *Journal of Pharmaceutical Biomedical Analysis* 29, 361.
- Cheng, G.C. Zhao, J., Tu, Y., Pingang, H., Fang, Y. (2005) A sensitive DNA electrochemical biosensor based on magnetite with a glassy carbon electrode modified by multi-walled carbon nanotubes in polypyrrole. *Analytica Chimica Acta*, 533, 11-16.
- Clarke, C. (2007) Personal Communication.
- Cohen, W.M., Levinthal, D.A. (1990). Absorptive capacity: A new perspective on learning and innovation. *Administrative Science Quarterly*, 35, 128-152.
- Cui, G., Yoo, J.H., Lee, J.S., Yoo, J., Uhm, J.H., Cha, G.S., Nam, H. (2001) Effect of pre-treatment on the surface and electrochemical properties of screen-printed carbon printed carbon paste electrodes, *Analyst* 126, 1399-1403.
- Cross, R. Liedka, J., Weiss, L. (2005) A Practical Guide to Social Networks. *Harvard Business Review*, March.
- Csoka, B. Kovacs, B., Nagy, G. (2003a) Scanning electrochemical microscopy inside the biocatalytic layer of biosensors: investigation of a double function complex multienzyme reaction layer, *Electroanalysis* 15(15-16) 1335-1342.
- Csoka, B. Kovacs, B., Nagy, G. (2003b) Investigation of concentration profiles inside operating biocatalytic sensors with scanning electrochemical microscopy (SECM), *Biosensors and Bioelectronics*, 18(2-3), 141-149.
- Csoregi, E., Jonsson-Peterson, G., Gorton, L. (1993) Mediatorless electrocatalytic reduction of hydrogen peroxide at graphite electrodes chemically modified with peroxidases. *Journal of Biotechnology*, 30, 315-337.
- Davis, F., Higson, S.P.J., (2005) Structured thin films within biosensors. *Biosensors and Bioelectronics* 21(1), 1-20.
- Davis, F., Nabok, A.V., Higson, S.P.J. (2005) Species differentiation by DNA-modified carbon electrodes using an ac impedimetric approach. *Biosensors and Bioelectronics* 20(8), 1531-1538.
- Dayton, M.A., Brown, J.C., Stutts, K.J., Wightman, R.M. (1980) Faradaic electrochemistry at microvoltammetric electrodes. *Analytical Chemistry*, 52, 946-950.
- Dayton, M.A., Brown, J.C., Stutts, K.J., Wightman, R.M. (1980b) Response of microvoltammetric electrodes to homogenous catalytic and slow heterogeneous charge-transfer reactions. *Analytical Chemistry*, 52, 2392-2396.
- Deakin, M.R., Stutts, K.J., Wightman, R.M. (1985) The effect of pH on some outer-sphere electrode reactions at carbon electrodes. *Journal of Electroanalytical Chemistry* 182, 113-122.
- Debresson, C., Amesse, F. (1991) Networks of Innovators – A Review and Introduction to the Issue. *Research Policy*, 20 (5), 363-379.

- Decher, G., Hong, J.D., Schmitt, J. (1992) Build up of ultrathin multilayer films by a self-assembly process. 3. Consecutively alternating adsorption of anionic and cationic polyelectrolytes on charged surfaces, *Thin Solid Films* 210, 504-507.
- Decher, G. (1997) Molecular multilayer films: The quest for order, orientation and optical properties. *Photonic and Optoelectronic Polymers ACS Symposium Series* 672, 445-459.
- Decher, G., Eckle, M., Schmitt, J., Struth, B. (1998) Layer-by-layer assembled multicomposite films. *Current opinion in Colloid and Interface Science*, 3(1), 32-39.
- Demaille, C., Brust, M., Tsionsky, M. and Bard A.J (1997) Fabrication and characterisation of self-assembled spherical gold UMEs. *Analytical Chemistry*, 69(13), 2323-2328.
- Dhanaraj, C., Parkhe, A. (2006) Orchestrating Innovation Networks. *Academy of Management Review*. 31(3), 659-669.
- Dierickx, I., Cool, (1989) Asset stock accumulation and sustainability of competitive advantage. *Management Science*, 35(12), 1504-1511.
- Ding, X., Hu, J., Li, Q. (2006) Direct electrochemistry and superficial characterisation of DNA-cytochrome *c*-MUA films on chemically modified gold surface. *Talanta* 68, 3, 653-658.
- Dixit, A. (1980) The role of investment in entry deterrence. *Economic Journal*, 90, 95-106.
- Dobson, P.S. Weaver, J.M.R., Holder, M.N. (2005) Characterisation of batch-microfabricated scanning electrochemical-atomic force microscopy probes. *Analytical chemistry*, 77(2), 424-434.
- DTI (2003). Competing in the global economy: The innovation challenge, December 2003. (www.dti.gov.uk/innovationreport/index.htm)
- Dunford, H.B., In Everse, S.L., Everse, K., Grisham, M.B. (Eds) (1991) Peroxidases in Chemistry and Biology, Vol.2, CRC Press, Boca Raton, Fl. 1-23.
- Dunning, J.H., (1998). Globalisation, technological change and the spatial organisation of the economic activity. In *The dynamic firm*, edited by A.D. Chandler, P. Hagstrom and O. Solvell. Oxford: OUP.
- Edwards, M.A., Martin, S., Whitworth, A.L., Macpherson, J.V., Unwin, P.R. (2006). Scanning electrochemical microscopy: principles and applications to biophysical systems. *Physiological Measurement* 27, R63-R108.
- Eisenhart, K., Schoonhoven, C.B. (1996) Resource-based view of strategic alliance formation: strategic and social effects in entrepreneurial firms. *Organisational Science*, 7, 136-150.
- Eisenhart K., Martin, J. (2000) Dynamic capabilities: what are they? *Strategic Management Journal*, 21, 10-11.
- Engstrom, R.C. (1984). Spatial Resolution of Electrode Heterogeneity Using Iontophoresis. *Analytical Chemistry* 56, 890-894.
- Engstrom, R.C., Weber, M., Wunder, D.J., Burgess, R. and Winquist, S. (1986) Measurements within the diffusion layer using a microelectrode probe. *Analytical Chemistry* 58, 844-848.
- Engstrom, R.C., Meaney, T., Tople, R. (1987). Spatiotemporal Description of the Diffusion Layer with a Microelectrode Probe. *Analytical Chemistry*, 59(15) 2005-2010
- Erlenkotter, A., Kottbus, M., Chemnitz, G.C. (2000). Flexible amperometric transducers for biosensors

- based on a screen printed three electrode system. *Journal of Electroanalytical Chemistry*, 481, 82-94.
- Etienne, M., Anderson, E.C., Evans, S.R. (2006) Feedback-independent Pt nanoelectrodes for shear force-based constant-distance mode scanning electrochemical microscopy. *Analytical Chemistry*, 78(20): 7317-7324.
- Evans, S.A.G., Brakha, K., Billon, M., Mailley, P. and Denuault, G. (2005) Scanning electrochemical microscopy (SECM): Localized glucose oxidase immobilization via the direct electrochemical microspotting of polypyrrole-biotin films. *Electrochemistry Communications* 7 (2), 135-140.
- Fan, F.-R.F., (2001) SECM Imaging. *In Scanning Electrochemical Microscopy*. Ed. Bard, E.J. and Mirkin, M.V. Printed by Marcel Dekker, Inc. New York.
- Fasching, R.J., Tao, Y. and Prinz, F.B. (2005) Nanoscale electrochemical probes for single cell analysis. *Sensors and Actuators B: Chemical* 108 (1-2), 964-972.
- Fasching, R.J., Bai, S.-J., Fabian, T. and Prinz, F.B. (2006) Cantilever tip probe arrays for simultaneous SECM and AFM analysis. *Microelectronic Engineering*, 83, 1638-1641.
- Feng, W.J., Rotenberg, S.A. and Mirkin, M.V. (2003) Scanning electrochemical microscopy of living cells. 5. Imaging of fields of normal and metastatic human breast cells. *Analytical Chemistry*, 75, 4148-4154.
- Fernandez, J.L. and Bard, A.J. (2003) Scanning Electrochemical Microscopy. 47. Imaging Electrocatalytic Activity for Oxygen Reduction in an Acidic Medium by the Tip Generation-Substrate Collection Mode. *Analytical Chemistry*, 75, 2967-2974.
- Fernandez, J.L., Mano, N., Heller, A. and Bard, A.J. (2004) Optimization Of Wired Enzyme O₂-Electroreduction Catalyst Compositions by Scanning Electrochemical Microscopy. *Angewandte Chemie* 116, 6515-6517.
- Fick, A., (1855) Ueber diffusion. *Annalen der physik*, Leipzig, 170, 59-86.
- Filizola, M., Loew, G.H. (2000) Role of protein environment in horseradish peroxidase compound I formation: molecular dynamics simulations of horseradish peroxidase-HOOH complex. *Journal of the American Chemical Society*, 122, 18-25.
- Fleishmann, M., Ghoroghchian, J., Pons, S. (1985) Electrochemical Behaviour of Dispersions of Spherical Ultramicroelectrodes. 1. Theoretical Considerations. *Journal Physical Chemistry*, 89, 5530-5536.
- Fuyun, G., Tenent, R.C. and Wipf, D.O. (2001) Fabricating and imaging carbon-fiber immobilized enzyme ultramicroelectrodes with scanning electrochemical microscopy. *Analytical Sciences*, 17, 27-35.
- Gajhede, M., Schuller, D.J., Henriksen, A., Smith, A.T., Poulos, T.L. (1997). Crystal structure of horseradish peroxidase C at 2.15 Angstrom resolution. *Nature Structural Biology*, 4, 1032-1038.
- Garay, M.F., Ufheil, J., Borgwarth, K., Heinze, J., (2004) Retrospective chemical analysis of tree rings by means of the scanning electrochemical microscopy with shear force feedback. *Physical Chemistry Chemical Physics*, 6, 4028-4033.
- Gaspar, S., Mosbach, M., Wallma, L., Laurell, T., Csoregi, E. and Schumann, W. (2001) A method for the design and study of enzyme microstructures formed by means of a flow-through microdispenser. *Analytical Chemistry*, 73, 4254-4261.
- Gemunden, H.G., Heydebreck, P. (1995) The influence of business strategies on technological network activities. *Research Policy*, 24(6), 831-849.

- Gilley, K.M., Rasheed, A. (2000) Making more by doing less: An analysis of outsourcing and its effects on firm performance. *Journal of Management*, 26(4),763-790.
- Gilmartin, M., Hart, J.P. (1995) Development of one-shot biosensors for the measurement of uric-acid and cholesterol. *Analytical Proceedings*, 32(8), 341-345.
- Glidle, A.T., Yasukawa, C.S., Hadyoon, N. , Anicet, T. , Matsue, M., Nomura, M., Cooper, J.M. (2003) Analysis of Protein Adsorption and Binding at Biosensor Polymer Interfaces Using X-ray Photon Spectroscopy and Scanning Electrochemical Microscopy. *Analytical Chemistry* 75(11), 2559–2570.
- Gonsalves, M., Macpherson, J.V., O'Hare, D., Winlove, C.P. and Unwin, P.R. (2000) High resolution imaging of the distribution and permeability of methyl viologen dication in bovine articular cartilage using scanning electrochemical microscopy. *Biochimica et Biophysica Acta (BBA) - General Subjects*, 1524 (1), 66-74.
- Gooding, J.J., (2002) Electrochemical DNA hybridisation biosensors. *Electroanalysis* 14, 1149-1156.
- Grabher, G. (1993). Rediscovering the social in the economics of interfirm relations. In *The Embedded Firm: on the Socioeconomics of Industrial Networks*, edited by G.Grabher. London: Routledge.
- Grahame, D.C. (1947) The electrical double layer and the theory of electrocapillarity. *Chemical reviews*, 41, 441-501.
- Grandori, A., (1997) An organisational assessment of interfirm coordination modes. *Organisational Studies*, 18, 897-925
- Granovetter, M., (1973) Strength of weak ties. *American Journal of Sociology*. 78(6), 1360-1380.
- Granovetter, M. (1985) Economic action and social structure: The problem of embeddedness. *American Journal of Sociology*, 91, 481-510.
- Grennan, B., Killard, A.J., Smyth, M.R. (2001) Physical characteristics of a screen printed electrode for use in an amperometric biosensor system. *Electroanalysis* 13(8-9), 745-750.
- Guo, J.D. and Amemiya, S. (2005) Permeability of the Nuclear Envelope at Isolated *Xenopus* Oocyte Nuclei Studied by Scanning Electrochemical Microscopy. *Analytical Chemistry* 77 (7), 2147-2156.
- Guoy, G. (1910) Sur la constitution de la charge électrique a la surface d'un électrolyte. *Comptes Rendus*, 149, 654-657.
- Gyurcsanyi, R.E., Jagerszki, G., Kiss, G. and Toth, K. (2004) Chemical imaging of biological systems with the scanning electrochemical microscope.. *Bioelectrochemistry*, 63 (1-2), 207-215.
- Hage, J., Dewar, R. (1973) Elite values versus organisational structure in predicting innovation.. *Administrative science quarterly*, 18(3), 279-290.
- Hart, J.P., Wring, S.A. (1997) Recent developments in the design and application of screen-printed electrochemical sensors for biomedical, environmental and industrial analyses. *Trends in analytical chemistry*, 16(2), 89-103.
- Hashimoto, K., Ito, K., Ishimori, Y., (1994) Sequence-Specific Gene Detection With A Gold Electrode Modified With DNA Probes and an Electrochemically Active Dye *Analytical Chemistry*, 66(21), 3830-3833.
- Hauschildt, J. (1992) External acquisition of knowledge for innovation – a research agenda. *R&D Management*, 22(2), 105-110

- Hirata, Y., Yabuki, S. and Mizutani, F. (2004) Application of integrated SECM ultra-micro-electrode and AFM force probe to biosensor surfaces. *Bioelectrochemistry*, 63 (1-2), 217-224.
- Holt, K. (2005) Using Scanning Electrochemical Microscopy (SECM) to Measure the Electron-Transfer Kinetics of Cytochrome c Immobilised on a COOH-terminated Alkanethiol Monolayer on a Gold Electrode. *Biochemistry*, 44, 13214-13223.
- Holt, K. (2006) Using Scanning Electrochemical Microscopy (SECM) to Measure the Electron-Transfer Kinetics of Cytochrome c Immobilized on a COOH-Terminated Alkanethiol Monolayer on a Gold Electrode. *Langmuir*, 22, 4298-4304.
- Horari, O. (1997) Column in *Management Review*, November.
- Kulys, J., Schmid, R.D. (1990) Mediatorless Peroxidase electrode and preparation of bienzyme sensors. *Bioelectrochemistry and Bioenergetics*, 24(3), 305-311.
- Hoshi, H. (2003) In vitro production of bovine embryos and their application for embryo transfer. *Theriogenology*, 59, 675-685.
- Hotz-Hart, B. (2000) Innovation networks, regions and globalisation. In *The Oxford Handbook of Economic Geography*, edited by G.L. Clark, M.P. Feldman and M.S. Gertler. Oxford: OUP.
- Invitrogen Corporation, (2006). *The Handbook – A Guide to Fluorescent Probes and Labelling Technologies*.
- Jalkonen, S., Bargatze, R.F., De-Los-Toyos, J., Bucher, E.C. (1987) Lymphocyte recognition of high endothelium: anti-bodies to distinct epitopes of an 85-95kD glycoprotein antigen differentially inhibit lymphocyte binding to lymph node, mucosal or synovial endothelial cells. *Journal of Cell Biology*, 105: 983-990.
- Jackson, N.M., Hill, M.G. (2001) Electrochemistry at DNA-modified surfaces: new probes for charge transport through the double helix. *Current Opinion in Chemical Biology*, 5, 209-215.
- Jarillo, C. (1988) On strategic networks. *Strategic Management Journal*, 9, 31-41.
- Jan, C., McCreery, R.L., Gamble, F.T. (1985) Diffusion Layer Imaging: Spatial Resolution of Electrochemical Concentration Profiles. *Analytical Chemistry* 57, 1763-1765.
- Johnson, J.D. (1992) Approaches to organisational communication structure. *Journal of Business Research*, 25, 99-113.
- Jonash, R.S. (1996) Strategic technology leveraging: making outsourcing work for you. *Research-Technology Management*, 39(2), 19-25.
- Kaji, H., Kanada, M., Oyamatsue, D., Matsue, T. and Nishiwaza, M. (2003) Microelectrochemical approach to induce local cell adhesion and growth on substrates. *Langmuir* 20, 16-19.
- Kasai, S., Yokota, A., Zhou, H., Nishizawa, M., Niwa, K.O.T. and Matsue, T. (2000) Immunoassay of the MRSA-Related Toxin Protein, Leukocidin, with Scanning Electrochemical Microscopy. *Analytical Chemistry* 72, 5761-5765.
- Kasai, S., Shiku, H., Torisawa, Y-S., Noda, H., Yoshitake, J., Shiraishi, T., Tomoyuki, Y., Watanabe, T., Matsue, T., Yoshimura, T. (2005) Real-time monitoring of reactive oxygen species production during differentiation of human monocytic cell lines (THP-1). *Analytica Chimica Acta* 549, 1-2, 14-19.

- Kash, D.E., Rycroft, R. (2002) The emergence of corporate integrated innovation systems across regions: the case of the chemical and pharmaceutical industry in Germany, the UK and Belgium. *Journal of International Management*, 8(1), 97-119.
- Katemann, B.B. and Schuhmann, W. (2002) Fabrication and characterisation of needle-type Pt-disk nanoelectrodes. *Electroanalysis*, 14, 22-28.
- Katemann, B.B., Schulte, A. and Schuhmann, W. (2003) Constant-Distance Mode Scanning Electrochemical Microscopy (Secm) - Part I: Adaptation of a Non-Optical Shear-Force-Based Positioning Mode for Secm Tips. *Chemistry-a European Journal*, 9, 2025-2033.
- Kaya, T., Nishizawa, M., Yasukawa, T., Nishiguchi, M., Onouchi, T. and Matsue, T. (2001) A microbial chip combined with scanning electrochemical microscopy. *Biotechnology and Bioengineering*, 76, 391-394.
- Kaya, T., Nagamine, K., Oyamatsu, D., Shiku, H., Nishizawa, M. and Matsue, T. (2003a) Fabrication of Microbial Chip Using Collagen Gel Microstructure. *Lab on a Chip*, 3, 313-317.
- Kaya, T., Nagamine, K., Oyamatsu, D., Nishizawa, M. and Matsue, T. (2003b) A Microbial Chip for Glucose Sensing Studied With Scanning Electrochemical Microscopy (SECM). *Electrochemistry*, 71, 436-438.
- Kaya, T., Torisawa, Y.S., Oyamatsu, D., Nishizawa, M. and Matsue, T. (2003c) Monitoring the Cellular Activity of a Cultured Single Cell by Scanning Electrochemical Microscopy (SECM). A Comparison With Fluorescence Viability Monitoring. *Biosensors & Bioelectronics*, 18, 1379-1383.
- Kaya, T.D., Numai, K., Nagamine, K., Aoyagi, S., Shiku, H. and Matsue, T. (2004) Respiration activity of *Escherichia coli* entrapped in a cone-shaped microwell and cylindrical micropore monitored by scanning electrochemical microscopy (SECM). *Analyst*, 129, 529-534.
- Kelley, S.O., Barton, J.K., Jackson, N.M., Hill, M.G. (1997) Electrochemistry of methylene blue bound to a DNA-modified electrode. *Bioconjugate Chemistry*, 8, 3-37.
- Kelley, S.O., Jackson, N.M., Hill, M.G., Barton, J.K., Jackson, N.M., Hill, M.G. (1999) Long range electron transfer through DNA films. *Angewandte Chemie International Edition*, 38, 941-945.
- Kelley, S.O., Barton, J.K. (1999) Electron transfer between bases in double helical DNA. *Science*, 283(5400), 375-381.
- Kerman, K., Kobayashi, M., Tamiya, E. (2004) Recent trends in electrochemical DNA biosensor technology. *Measurement Science Technology*, 15, R1-R11.
- Khurana, A., Rosenthal, S.R. (1997) Integrating the fuzzy front end of new product development. *Sloan Management Review*, 38(2): 103-120.
- Kleine, H., Wilke, R., Pelargus, C., Rott, K., Puhler, A., Reiss, G., Ros, R., Anselmetti, D. (2004) Absence of intrinsic electric conductivity in single dsDNA molecules. *Journal of Biotechnology*, 112, 91-95.
- Kogut, B., Zander, U. (1996) What do firms do? Coordination, identity and learning. *Organisational Science*, 7:502-518
- Komaraova, E., Aldissi, M., Anastasia, B. (2005) Direct electrochemical sensor for fast reagent-free DNA detection. *Biosensors and Bioelectronics*, 21, 182-189
- Komatsu, M., Yamashita, K., Uchida, K. (2006) Imaging of DNA microarray with scanning

electrochemical microscopy. *Electrochimica Acta*, 51 (10), 2023-2029.

Kranz, C., Lotzbeyer, T., Schmidt, H.-L. and Schuhmann, W. (1997) Mapping of enzyme activity by detection of enzymatic products during AFM imaging with integrated SECM-AFM probes. *Biosensors and Bioelectronics* 12 (4), 257-266.

Kranz, C., Friedbacher, G. and Mizaikoff, B. (2001) Integrating an Ultramicroelectrode in an Afm Cantilever: Combined Technology for Enhanced Information. *Analytical Chemistry* 73, 2491-2500

Kranz, C., Kueng, A., Lugstein, A., Bertagnolli, E. and Mizaikoff, B. (2004) Mapping of enzyme activity by detection of enzymatic products during AFM imaging with integrated SECM-AFM probes. *Ultramicroscopy* 100 (3-4), 127-134.

Kueng, A., Kranz, C., Lugstein, A., Bertagnolli, E. and Mizaikoff, B. (2003) Integrated Afm-Secm in Tapping Mode: Simultaneous Topographical and Electrochemical Imaging of Enzyme Activity. *Angewandte Chemie-International Edition*, 42, 3238-3240.

Kulys, J., Schmid, R.D. (1990) Mediatorless Peroxidase electrode and preparation of bienzyme sensors. *Bioelectrochemistry and Bioenergetics*, 24(3), 305-311.

Kurulugama, R.T., Wipf, D.O., Takacs, S.A., Pongmayteegul, S., Garris P.A. and Baur, J.E. (2005) Scanning electrochemical microscopy of model neurons: Constant distance imaging. *Analytical Chemistry*, 77, 1111-1117.

Kwak, J. and Bard, A.J. (1989) Apparatus and two dimensional scans of conductive and insulating substrates. *Analytical Chemistry*, 1794-1799.

Kwak, J.B., A.J. Bard (1989b) Scanning Electrochemical Microscopy. Theory of the feedback mode. *Analytical Chemistry*, 61, 1221-1227.

Lavie, D. (2006) The competitive advantage of interconnected firms: an extension of the resource-based view. *Academy of Management Review*, 31(3), 638-658.

Lee, C. and Bard, A.J. (1990) Scanning electrochemical microscopy. Application to polymer and thin metal oxide films. *Analytical Chemistry* 62, 1906-1913.

Lee, C., Kwak, J. and Bard, A.J. (1990) Application of SECM to biological samples. *PNAS USA* 87, 1740-1743.

Lee, C., Miller, C.J. and Bard, A.J. (1991) Scanning electrochemical microscopy: Preparation of sub-micrometer electrodes. *Analytical chemistry*, 63(1), 78-83.

Lee, Y., Ding, Z.F. and Bard, A.J. (2002) Combined Scanning Electrochemical/Optical Microscopy With Shear Force and Current Feedback. *Analytical Chemistry*, 74, 3634-3643.

Lee, S., Zhang, Y. and White, H.S. (2004) Electrophoretic capture and detection of nanoparticles at the opening of a membrane pore using scanning electrochemical microscopy. *Analytical Chemistry*, 76, 6108-6115.

Liebeskind, J., Porter, O., Zucker, L., Brewer, M. (1996) Social networks learning and flexibility: sourcing scientific knowledge in new biotechnology firms. *Organisation Science*, 7, 428-443.

Liebetrau, J.M., Miller, H.M. and Baur, J.E. (2003) Scanning Electrochemical Microscopy of Model Neurons: Imaging and Real-Time Detection of Morphological Changes. *Analytical Chemistry*, 75, 563-571.

- Liljeroth, P., Johans, C., Slevin, C.J., Quinn, B.M. and Kontturi, K. (2002) Disk-Generation/Ring-Collection Scanning Electrochemical Microscopy: Theory and Application. *Analytical Chemistry*, 74, 1972-1978.
- Liljeroth, P., Johans, C., Slevin, C.J., Quinn, B.M. and Kontturi, K. (2002) Micro Ring-Disk Electrode Probes for Scanning Electrochemical Microscopy. *Electrochemistry Communications*, 4, 67-71.
- Lipparini, A., Sobrero, M. (1994) The glue and the pieces: entrepreneurship and innovation in small-firm networks. *Journal of Business Venturing*, 9, 125-140.
- Lorenzoni, G., Baden-Fuller, C. (1995) Creating a strategic centre to manage a web of partners. *Californian Management Review*, 37 (3), 146-163.
- Love, J. (2001) The theory of innovation. *Review of Industrial Organisation*, 18(1), 137-139.
- Liu, B., Rotenburg, S.A. and Mirkin, M.V. (2000) Scanning electrochemical microscopy of living cells: different redox activities of non-metastatic and metastatic human breast cells. *PNAS* 97, 9855-9860.
- Liu, B., Cheng, W., Rotenberg, S.A. and Mirkin, M.V. (2001) Scanning Electrochemical Microscopy of Living Cells - Part 2. Imaging Redox and Acid/Basic Reactivities. *Journal of Electroanalytical Chemistry* 500, 590-597.
- Liu, B., Bard, A.J., Li, C.J. and Kraatz, H.B. (2005) Scanning electrochemical microscopy. 51. Studies of self-assembled monolayers of DNA in the absence and presence of metal ions. *Journal of Physical Chemistry B* 109, 5193-5198.
- Liu, H.-Y., Fu-Ren, F.F., Lin, C.W. and Bard, A.J. (1986) Scanning Electrochemical and Tunnelling Ultramicroelectrode Microscope for High-Resolution Examination of Electrode Surfaces in Solution. *Journal of the American Chemical Society* 108, 3838-3839.
- Longobardi, F., Cosma, P., Milano, F., Agostiano, A., Mauzeroll, J., Bard, A.J. (2006) Scanning electrochemical microscopy of the photosynthetic reaction center of *Rhodobacter sphaeroides* in different environmental systems. *Analytical Chemistry*, 78(14), 5046-5051.
- Lucarelli, F., Palchetti, I., Marrazza G., Mascini, M. (2002) Electrochemical DNA biosensor as a screening tool for the detection of toxicants in water and wastewater samples, *Talanta*, 56, 949.
- Lvov, Y., Decher, G., Sukhorukov, G. (1992) Assembly of Thin Films by Means of successive Deposition of Alternate Layers of DNA and Poly(allylamine). *Macromolecules*, 26, 5396-5399.
- Lyons, A.J., Jones, J. (2007) Cell adhesion molecules, the extracellular matrix and oral, squamous carcinoma. *International Journal of Oral Maxillofacial Surgery*, 36, 671-679.
- Maciejewska, M., Schäfer, D., Schuhmann, W. (2006a) SECM imaging of spatial variability in biosensor architectures. *Electrochemistry Communications*, 8, 1119-1124.
- Maciejewska, M., Schäfer, D., Schuhmann, W. (2006b). SECM visualization of spatial variability of enzyme-polymer spots. Part 2: Complex interference elimination by means of selection of highest sensitivity sensor substructures and artificial neural networks. *Electroanalysis*, 18(19-20), 1916-1928.
- Macpherson, J.M., Gajadhar, A., (1993) Variability Of The Random Amplified Polymorphic DNA Assay Among Thermal Cyclers, And Effects Of Primer And DNA Concentration Molecular Cellular Probes, 7, 97.

- Macpherson, J.V. and Unwin, P.R. (2005) Scanning Electrochemical Microscopy as an In Vitro Technique for Measuring Convective Flow Rates Across Dentine and the Efficacy of Surface Blocking Treatments. *Electroanalysis* 17, 197-204.
- Malone, K.S., Wiggers, T.B., Spence, L.M. (2004) Monoclonal Anti-CD 20 Antibody Used in Non-Hodgkins Lymphoma: A Case Study. *Clinical Laboratory Science*, 17(4): 197.
- Mano, N., Fernandez, J.L., Kim, Y., Shin, W., Bard A.J. and Heller, A. (2003) Oxygen is Electroreduced to Water on a "Wired" Enzyme Electrode at a Lesser Overpotential than on Platinum. *Journal of the American Chemical Society*, 125, 15290-15291.
- Martin, R.D. Unwin, P.R. (1998) Theory and Experiment for the substrate generation/tip collection mode of the scanning electrochemical microscope: Application as an Approach for Measuring the Diffusion Coefficient Ratio of Redox Couple. *Analytical Chemistry*, 70, 276-284.
- Matsui, N., Kaya, T., Nagamine, K., Yasukawa, T., Shiku, H. and Matsue, T. (2006) Electrochemical mutagen screening using microbial chip. *Biosensors and Bioelectronics* 21, 1202-1209.
- Mauzeroll, J., Bard, A.J. (2004a) Scanning electrochemical microscopy of menadione-glutathione conjugate export from yeast cells. *PNAS USA*, 101(21), 7862-7867.
- Mauzeroll, J., Bard, A.J., Owhadian, O., Monks, T.J. (2004b) Menadione metabolism to thiodione in hepatoblastoma by scanning electrochemical microscopy. *PNAS USA* 101 (51) 17582-17587.
- McConnell, H.M., Owicki, J.C., Parce, J.W., Miller, D.L., Baxter, G.T., Wada, H.G. and Pitchford, S. (1992) The Cytosensor Microphysiometer: Biological Applications of Silicon Technology. *Science* 257, 1906-1912.
- McCreery, R.L. (1991) Carbon electrodes: Structural effects on electron transfer kinetics, Dekker, New York, US.
- Meade, T.J., Kayyem, J.F. (1995) Electron-Transfer through DNA- Site-specific Modification of Duplex DNA with Ruthenium Donors and Acceptors. *Angewandte Chemie-International Edition* 34(3): 352-354.
- Millan, K.M., Mikkelsen, S.R. (1993) Sequence-selective biosensor for DNA based on electroactive hybridisation indicators. *Analytical Chemistry*, 65, 2317.
- Millan, K.M., Saraullo, S., Mikkelsen, S.R. (1994) Voltammetric DNA biosensor for cystic fibrosis based on a modified carbon paste electrode. *Analytical Chemistry*, 66, 2943-8.
- Miles, D.T., Knedlik, A. and Wipf, D.O. (1997) Construction of Gold Microbead Ultramicroelectrodes. *Analytical Chemistry*, 69, 1240-1243.
- Mirkin, M.V., Liu, B., Rotenberg, S.A. (2002) Probing redox activity of human breast cells by scanning electrochemical microscopy. *Redox Cell Biology and Genetics. Part a* 352, 112-122.
- Mondal, M.S. Goodlin, F.A., Armstrong, F.A. (1998). Simultaneous Voltammetric Comparisons of Reduction Potentials, Reactivities, and Stabilities of the High-Potential Catalytic States of Wild-Type and Distal-Pocket Mutant (W51F) Yeast Cytochrome *c* Peroxidase. *Journal of the American Chemical Society*, 120, 6270-6276.
- Mori, Tomari, T., Koshikawa, N. (2002) CD44 directs membrane-type matrix metalloproteinase to lamellipodia by associating with its hemopexin-like domain. *EMBO Journal* 21(15), 3949-3959.

- Nabok, A. Tsargorodskaya, A., Davis, F., Higson, S.P.J. (2007) The study of genomic DNA adsorption and subsequent interactions using total internal reflection ellipsometry. *Biosensors and Bioelectronics*, 23(3), 377-383.
- Nagamine, K., Onodera, S., Torisawa, Y-S., Yasukawa, T., Shiku, H. and Matsue, T. (2005a) On-Chip Transformation of Bacteria. *Analytical Chemistry*, 77, 4278-4281.
- Nagamine, K., Kaya, T., Yasukawa, T., Shiku, H. and Matsue, T. (2005b) Application of microbial chip for amperometric detection of metabolic alteration in bacteria. *Sensors and Actuators B: Chemical*, 108 (1-2): 676-682.
- Navarro, A-E., Spinelli, N., Chaix, C., Moustrou, C., Mandrand, B., Brisset, H. (2004) Supported synthesis of ferrocene modified oligonucleotides as new electroactive DNA probes. *Bioorganic and Medicinal Chemistry Letters*, 14 (2004) 2439-2441.
- Nicollini, C., Erokhin, V., Facci, P., Guerzoni, S., Ross, A., Pashkevich, P. (1997) Quartz balance DNA sensor. *Biosensors and Bioelectronics*, 12, 613-618.
- Niculescu, M., Gaspar, S., Schulte, A., Csoregi, E. and Schuhmann, W. (2004) Visualization of micropatterned complex biosensor sensing chemistries by means of scanning electrochemical microscopy. *Biosensors and Bioelectronics*, 19, 1175-1184.
- Nishizawa, M., Takoh, K. and Matsue, T. (2002) Micropatterning of HeLa Cells on Glass Substrates and Evaluation of Respiratory Activity Using Microelectrodes. *Langmuir* 18, 3645-3649.
- Niwa, O., Tabei, H. (1994) Voltammetric measurements of reversible and quasi-reversible redox species using carbon film based interdigitated array microelectrodes. *Analytical Chemistry*, 66,285-289.
- Oerlemans, L.A.G., Meeus, M.T.H. Boekema, F.W.M. (2001) Firm clustering and innovation: Determinants and effects. *Papers in Regional Science*, 80, 337-356.
- Okada, A., Yokojima, S., Kurita, N., Sengoku, Y., Tanaka, S. (2003) Charge transfer in duplex DNA containing mismatch. *Journal of Molecular Structure (Theochem)* 630, 283-290.
- Okumura, A., Sato, Y., Kyo, M., Kawaguchi H. (2005) Point mutation detection with the sandwich method employing hydrogel nanospheres by the surface plasmon resonance imaging technique. *Analytical Biochemistry*, 339, 328-337.
- Oldham, K.B., Zoski, C.G., Bond, A.M. (1988) Measurement of ultrafast electrode kinetics via steady state voltammograms at microdisc electrodes. *Journal of Electroanalytical Chemistry* 248, 467-473.
- Oldham, K.B., Zoski, C.G. (1988) Comparison of voltammetric steady states at hemispherical and disc microelectrodes. *Journal of electroanalytical chemistry*, 256, 11-19.
- Ostgaard, T.A., Birley, S. (1996) New venture growth and personal networks. *Journal of Product Innovation Management*, 13, 557-558.
- Oyamatsu, D., Hirano, Y., Kanaya, N., Mase, Y., Nishizawa, M. and Matsue, T. (2003a) Imaging of enzyme activity by scanning electrochemical microscope equipped with a feedback control for substrate-probe distance. *Bioelectrochemistry*, 60, 115-121.
- Oyamatsu, D., Kanaya, N., Shiku, H., Nishizawa, M. and Matsue, T. (2003b) Electrochemical/Photochemical Formation of Enzyme Patterns on Glass Substrates Using a Scanning Electrochemical/Confocal Microscope. *Sensors and Actuators B-Chemical*, 91, 199-204.
- Oyamatsu, D., Kanaya, N., Hirano, Y., Nishizawa, M. and Matsue, T. (2003c) Area-Selective

- Immobilization of Multi Enzymes by Using the Reductive Desorption of Self-Assembled Monolayer. *Electrochemistry*, 71, 439-441.
- Pailleret, A., Oni, J., Reiter, S., Isik, S., Etienne, M., Bedioui, F. and Schuhmann, W. (2003) In Situ Formation and Scanning Electrochemical Microscopy Assisted Positioning of No-Sensors Above Human Umbilical Vein Endothelial Cells for the Detection of Nitric Oxide Release. *Electrochemistry Communications*, 5, 847-852.
- Park, S.O. (2001) Regional innovation strategies in the knowledge-based economy. *Geo Journal* 53(1), 29-38.
- Peach, R.J., Hollenbaugh, D., Stamenkovich, I., Aruffo, A. (1993) Identification of hyaluronic acid binding sites in the extracellular domain of CD44. *Journal of Cell Biology*. 122, 257-264.
- Penrose, E. (1959) *The theory of the growth of the firm*. Basil Blackwell, London.
- Parra, A., Casero, E., Vazquez, L., Jin, J., Pariente, F., Lorenzo, E. (2006) Microscopic and voltammetric characterisation of bioanalytical platforms based on lactate oxidase. *Langmuir* 22, 5443-5450.
- Pendley, B.D. and Abruna, H.D. (1990) Construction of submicrometer voltammetric electrodes. *Analytical Chemistry*, 62, 782-784.
- Pierce, D.T., Unwin, P.R. and Bard, A.J. (1992) Scanning Electrochemical Microscopy. 17. Studies of Enzyme-Mediator Kinetics for Membrane- and Surface-Immobilised Glucose Oxidase. *Analytical Chemistry*, 64, 1795-1804.
- Pierce, D.T. and Bard, A.J. (1993) Scanning Electrochemical Microscopy. 23. Reaction Localisation of Artificially Patterned and Tissue-Bound Enzymes. *Analytical Chemistry*, 65, 3598-3604.
- Pisano, G.P. (1990) The R&D boundaries of the firm: An empirical analysis. *Administrative Science Quarterly*, 35, 153-176.
- Pittaway, L., Robertson, M., Munir, K., Denyer, D., Neely, A. (2004) Networking and innovation: a systematic review of the evidence. *International Journal of Management Review*, September/December 2004, 5/6(3&4), 137-168.
- Pividori, M.I., Merkoci, A., Alegret, S. (2000) Electrochemical genosensor design: immobilisation of oligonucleotides onto transducer surfaces and detection methods. *Biosensors and bioelectronics*, 15, 291-303.
- Ponchon, J-L., Gespuglio, R., Gonon, F., Jouvét, M., Pujol, J-F., (1979). Normal Pulse Polarography. *Analytical Chemistry*, 51, 1483-1486
- Ponta, H., Sherman, L., Herrlich, P.A. (2003) CD44: From adhesion molecules to signalling regulators. *Nature reviews molecular cell biology*, 4(1), 33-45
- Porter, M. (1979) "How competitive forces shape strategy". *Harvard Business Review*, March/April.
- Porter, M. (1980) *Competitive strategy: Techniques for analysing industries and competitors*. New York: Free Press.
- Powell, W.W., Koput, K.W., Smith-Doerr, L. (1996) Interorganisational collaboration and the locus of innovation: Networks of learning in biotechnology. *Administrative Science Quarterly*, 41(1), 116-145.
- Pruksma, R., McCreery, R.L. (1979) Observation of Electrochemical Concentration Profiles by Absorption Spectroelectrochemistry. *Analytical Chemistry* 51, 2253-2257.

- Pruksma, R., McCreery, R.L. (1981) Spectroelectrochemical Observation of Diffusion Profiles by the Parallel Absorption Method. *Analytical Chemistry* 53, 202-206.
- Rabinowitz, J.D., Vacchino, J.F., Beeson, C. and McConnell, H.M. (1998) Potentiometric Measurement of Intracellular Redox Activity. *Journal of the American Chemical Society*, 120, 2464-2473.
- Raffie, M., Nematollahi, D. (2007) Voltammetry of Electroinactive species using quinone/hydroquinone redox: A known Redox system viewed in a New Perspective. *Electroanalysis*, 19(13), 1382-1386.
- Ragatz, G., Handfield, R., Scannel, T. (1997) Success factors for integrating suppliers into new product development. *Journal of Product Innovation Management*, 14, 190-202.
- Rallet, A., Torre, A. (1999) Is geographical proximity necessary in the innovation networks in the era of global economy? *Geo Journal*, 49(4), 373-380.
- Razumas, V., Kazlauskaitė, T., Ruzgas, T., Kulys, J. (1992) Bioelectrochemistry of Microperoxidases. *Bioelectrochemistry and Bioenergetics*, 28(1-2), 159-176.
- Rees, N.V., Alden, J.A., Dryfe, R.A., Coles, B.A., Compton, R.G.J. (1995) Voltammetry Under High Mass Transport Conditions. The High Speed Channel Electrode and Heterogenous Kinetics. *Journal of Physical Chemistry*, 99, 14813-14818.
- Riccaboni, M., Pammolli, F., (2003). Technological regimes and the evolution of networks of innovators. Lessons from Biotechnology and Pharmaceuticals. *International Journal of Technology Management*, 25, 334-349.
- Rossi, P., McCurdy, C.W., McCreery, R.L. (1981) Diffractive Spectroelectrochemistry - Use Of Diffracted Light For Monitoring Electrogenerated Chromophores. *Journal of the American Chemical Society*, 103, 2524.
- Rossi, P., McCreery, R.L. (1983) Diffractive Spectroelectrochemistry - A Sensitive Probe Of The Electrochemical Diffusion Layer. *Journal of Electroanalytical Chemistry*, 151, 47- 64.
- Rumelt, R.P. (1991) How much does industry matter? *Strategic Management Journal*, 12(3), 167-185.
- Ruzgas, T., Gorton, L., Emneus, J., Csoregi, E., Marco-Varga (1995) Direct bioelectrocatalytic reduction of hydrogen peroxide at chloroperoxidase modified graphite electrode. *Analytical proceedings*, 32, 207-208.
- Salman, N., Saives, A.L. (2005) Indirect networks: an intangible resource for biotechnology innovation. *R&D Management*, 35(2), 203-215.
- Santucci, R., Reihard, M., Brunori, M., Marassi, R. (1988) Direct electrochemistry of the undecapeptide from cytochrome c (microperoxidase) at a glassy carbon electrode. *Journal of the American Chemical Society*, 110, 8536-8537.
- Scheller, F. and Renneberg, R. (1983) Glucose-Eliminating Enzyme Electrode for Direct Sucrose Determination in Glucose-Containing Samples. *Analytica Chimica Acta*, 152, 265-269.
- Schmalensee, R. (1983) Advertising and entry deterrence: An exploratory model. *Journal of Political Economy*, 91(4), 636-653.
- Schumpeter, J.A. (1942) *Capitalism, Socialism and democracy*. New York: Harper.
- Shapiro, C. (1989) The theory of business strategy. *RAND Journal of Economics*, 20(1), 125-137.

- Shaw, B. (1998) Innovation and new product development in the UK medical equipment industry. *International Journal of Technology Management*, 15, 433.
- Shiku, H., Takeda, T., Yamada, H., Matsue, T. and Uchida, I. (1995) Oxygen Consumption of Single Bovine Embryos Probed by Scanning Electrochemical Microscopy. *Analytical Chemistry*, 67, 312-317.
- Shiku, H., Matsue, T. and Uchida, I. (1996) Detection of Microspotted Carcinoembryonic Antigen on a Glass Substrate by Scanning Electrochemical Microscopy. *Analytical Chemistry*, 68, 1276-1278.
- Shiku, H., Hara, Y., Matsue, T., Uchida, I. and Yamauchi, T. (1997) Dual immunoassay of human chorionic gonadotropin and human placental lactogen at a microfabricated substrate by scanning electrochemical microscopy. *Journal of Electroanalytical Chemistry*, 438 (1-2):187-190.
- Shiku, H., Shiraishi, T., Ohya, H., Matsue, T., Abe, H., Hoshi, H. and Kobayashi, M. (2001) Oxygen Consumption of Single Bovine Embryos Probed by Scanning Electrochemical Microscopy. *Analytical Chemistry*, 73, 3751-3758.
- Shiku, H., Shiraishi, T., Aoyagi, S., Utsumi, Y., Matsudaira, M., Abe, H., Hoshi, H., Kasai, S., Ohya, H. and Matsue, T. (2004) Respiration activity of single bovine embryos entrapped in a cone-shaped microwell monitored by scanning electrochemical microscopy. *Analytica Chimica Acta*, 522, 51-58.
- Shiku, H., Torisawa, Y.S., Takagi, A. (2005) Metabolic and enzymatic activities of individual cells, spheroids and embryos as a function of the sample size. *Sensors and Actuators B-Chem*, 108 (1-2): 597-602.
- Soderlind, K.J., Gorodetsky, B., Singh, A.K., Bachur, N.R., Miller, G.G. and Lown, J.W. (1999) Bis-benzimidazole anticancer agents: targeting human tumour helicases. *Anti-Cancer Drug Design*, 14, 19-36.
- Stamenkovic, I., Aruffo, A., Amiot, M. (1991) The hemtopoietic and epithelial forms of CD44 are distinct polypeptides with different adhesion potentials for hyaluronate bearing cells. *EMBO Journal*, 10(2), 343-348.
- Stern, O., (1924) Zur theorie der elektrolytischen doppelschicht. *Zietschrift Elektrochemia*, 30, 508-516.
- Storper, M. (1997). *The regional world: Territorial development in a global economy*. New York: The Guildford Press.
- Strike, D., Hengstenberg, A., Quinto, M., Kurzawa, C., Koudelka-Hep, M. and Schuhmann, W. (1999) Localized visualisation of chemical cross-talk in microsensor arrays by using SECM (Scanning Electrochemical Microscopy). *Microchimica Acta*, 131, 47-55.
- Stulik, K., Amatore, C., Holub, K., Marecek, V., Kutner, W. (2000) Microelectrodes. Definitions, characterisation and applications. *Pure and Applied Chemistry*, 72(8), 1483-1492.
- Subriamaniam, V., Vincent, I.R., Gardner, H., Chan, E., Dhamko, H., Jothy, S. (2007) CD44 regulated cell migration in human colon cancer cells via Lyn kinase and AKY phosphorylation. *Experimental and Molecular Pathology*, 83, 207-215.
- Sukhorukov, G.B., Möhwald, H., Decher, G., Lvov, M.V. (1996) Assembly of polyelectrolyte multilayer films by consecutively alternating adsorption of polynucleotides and polycations. *Thin Solid Films*, 284-285, 220-223.
- Sun, P., Laforge, F.O., Mirkin, M.V. (2007) Scanning electrochemical microscopy in the 21st century. *Physical Chemistry Chemical Physics* 21;9 (7): 802-23.
- Suzuki, M., Yasukawa, T., Mase, Y., Oyamatsu, D., shiku, H. and Matsue, T. (2004) Dielectrophoretic

- Micropatterning with Microparticle Monolayers Covalently linked to Glass Surfaces. *Langmuir* 20, 11005-11011.
- Svancara, I., Kalcher, K., Diewald, W. (1996a) Voltammetric determination of silver at ultratrace levels using a carbon paste electrode with improved surface characteristics. *Electroanalysis*, 8(4), 336-342.
- Svancara, I., Hvizdalova, M., Vytras, K. (1996b) A microscopic study on carbon paste electrodes. *Electroanalysis*, 8(1), 61-65.
- Svancara, I., Vytras, K. (2000) Physico-chemical processes in analytical electrochemistry with carbon paste electrodes. An overview. *Chemija*, 11(1), 18-27.
- Tafel, J. (1905) Über die polarisation bei kathodischer Wasserstoffentwicklung. *Zeitschrift für Physikalische Chemie*, 50, 641-712.
- Takahashi, Y., Hirano, Y., Yasukawa, T., Shiku, H., Yamada, H., Matsue, T. (2006) Topographic, electrochemical, and optical images captured using standing approach mode scanning electrochemical/optical microscopy. *Langmuir*, 22 (25) 10299-10306
- Takii, Y., Takoh, K., Nishizawa, M. and Matsue, T. (2003) Characterization of Local Respiratory Activity of Pc12 Neuronal Cell by Scanning Electrochemical Microscopy. *Electrochimica Acta*, 48, 3381-3385.
- Takoh, K., Takahashi, A., Matsue, T. and Nishizawa, M. (2004) A porous membrane-based microelectroanalytical technique for evaluating locally stimulated culture cells. *Analytica Chimica Acta*, 522 (1):45-49.
- Thorp, H.H. (1998) Cutting out the middleman: DNA biosensors based on electrochemical oxidation. *TIBTECH*, March 1998 (Vol 16)
- Teece, D.J. (1986). Profiting from technological innovation: Implications for integration, collaboration, licensing and public policy. *Research Policy*, 15, 285-305.
- Teece, D.J. (1992) Competition, cooperation and innovation: Organisational arrangements for regimes of rapid technological progress. *Journal of Economic Behaviour and Organisation*, 18(1), 1-25.
- Teece, D.J., Pisano, G., Shuen, A. (1997) Dynamic capabilities and strategic management. *Strategic management journal*, 18, 509-533.
- Thiebaud, P., Beuret, C., Rooij, N.F.d. and Koudelka-Hep, M. (2000) Microfabrication of PT-tip Microelectrodes. *Sensors and Actuators*, 70, 51-56
- Torisawa, Y.-S., Kaya, T., Takii, Y., Oyamatsu, D., Nishizawa, M. and Matsue, T. (2003) Scanning Electrochemical Microscopy-Based Drug Sensitivity Test for a Cell Culture Integrated in Silicon Microstructures. *Analytical Chemistry*, 75, 2154-2158.
- Torisawa, Y.-S., Shiku, H., Kasai, S., Nishiwaza, M. and Matsue, T. (2004) Proliferation assay on a silicon chip applicable for tumors extirpated from mammals. *International Journal of Cancer*, 109, 302-308.
- Torisawa, Y., Shiku, H., Yasukawa, T., Nishizawa, M. and Matsue, T. (2005a) Metabolic and enzymatic activities of individual cells, spheroids and embryos as a function of the sample size. *Sensors and Actuators B: Chemical*, 108 (1-2), 654-659.
- Torisawa, Y., Shiku, H., Yasukawa, T., Nishizawa, M. and Matsue, T. (2005b) Multi-channel 3-D cell culture device integrated on a silicon chip for anticancer drug sensitivity test. *Biomaterials*, 26 (14):2165-2172.

- Tracey, P., Clark, G.L. (2003). Alliances, Networks and Competitive Strategy: Rethinking Clusters of Innovation. *Growth and Change*, 34, (1) 1-16.
- Travas-Sejdic, J., Soman, R., Peng, H. (2006) Self-assembled polyaniline thin films: Comparison of poly(styrene sulphonate) and oligonucleotide as a polyanion. *Thin Solid Films*, 497, 96-102
- Treichel, D.A., Mirkin, M.V. and Bard, A.J. (1994) Three-dimensional micro-culture system with a silicon-based cell array device for multi-channel drug sensitivity test. *Journal of Physical Chemistry*, 88, 5751-5757.
- Tsionsky, M., Cardon, Z.G., Bard, A.J. and Jackson, R.B. (1997) Photosynthetic Electron Transport in Single Guard Cells as Measured by Scanning Electrochemical Microscopy. *Analytical Chemistry*, 113, 895-901.
- Turcu, F., Schulte, A., Hartwich, G. and Schuhmann, W. (2004) Imaging immobilised ssDNA and detecting DNA hybridisation by means of the repelling mode of scanning electrochemical microscopy (SECM). *Biosensors and Bioelectronics*, 20(5), 925-932.
- Turcu, F., Schulte, A., Hartwich, G. and Schuhmann, W. (2004b) Label-free electrochemical recognition of DNA hybridization by means of modulation of the feedback current in SECM. *Angewandte Chemie-International Edition*, 43, 3482-3485.
- Turcu, F., Hartwich, G., Schafer, D. and Schuhman, W. (2005) Ink-Jet Microdispensing for the formation of gradients of immobilised enzyme activity. *Macromolecular rapid Communications*, 26, 325-330.
- Turyan, I., Matsue, T. and Mandler, D. (2000) Patterning and characterisation of surfaces with organic and biological molecules by the Scanning Electrochemical Microscope. *Analytical Chemistry*, 72, 3431-3435.
- Uitto, O.D. and White, H.S. (2003) Electroosmotic Pore Transport in Human Skin. *Pharmaceutical Research*, 20, 646-652.
- Unwin, P.R. and Bard A.J (1991) Scanning electrochemical microscopy. 9. Theory and application of the feedback mode to the measurement of following chemical reaction rates in electrode processes. *Journal of Physical Chemistry*, 95, 7814-7824.
- Van Aken, J.E., Weggeman, M.P. (2000). Managing learning in informal innovation networks: overcoming the Daphne-dilemma. *R&D Management*, 30(2), 139-149.
- Van Aken, J.E. (2005) Management Research as a Design Science: Articulating the Research Products of Mode 2 Knowledge Management. *British Journal of Management*, 16, 19-36.
- Veitch, N.C., Smith, A.T. (2001) Horseradish peroxidase. *Advanced Inorganic Chemistry*, 51, 107-162.
- Veitch, N.C. (2004) Horseradish peroxidase: a modern view of a classic enzyme. *Phytochemistry*, 65, 249-259.
- Von Hippel, E. (1978) Successful industrial products from customer ideas: a paradigm, evidence and implications. *Journal of marketing*, 42 (1), 39_49.
- Wang, J. (1997) DNA electrochemical biosensors for environmental monitoring: a review. *Analytical Chimica Acta*, 347, 1-8.
- Wang, J., Jian, M., Fortes, A., Mukherjee, B., (1999) New label-free DNA recognition based on doping nucleic-acid probes within conducting polymer films. *Analytica Chimica Acta*, 402(1-2), 7-12.
- Wang, J. (2001) *Analytical Electrochemistry*, 2nd edn.

- Wang, J. and Zhou, F.M. (2002a) Scanning electrochemical ,microscopic imaging of surface- confined DNA probes and their hybridization via guanine oxidation. *Journal of Electroanalytical Chemistry*, 537, 95-102.
- Wang, J., Song, F.Y. and Zhou, F.M. (2002b) Silver-Enhanced Imaging of DNA Hybridization at DNA Microarrays With Scanning Electrochemical Microscopy. *Langmuir* 18, 6653-6658.
- Wang, K., Xu, J.-J., Sun, D.-C., Wei, H. and Xia, X.-H. (2005) Selective glucose detection based on the concept of electrochemical depletion of electroactive species in diffusion layer. *Biosensors and Bioelectronics* 20(7), 1366-1372.
- Wang, S., Tuzhi, P. and Yang, C.F. (2002) Electrochemical Studies for the Interaction of DNA with an Irreversible Redox Compound - Hoescht 33258. *Electroanalysis*, 14, 1648-1653.
- Wang, X.L., Shi, Y.X., Bai, Z.L., Jin, W.R. (2004). *Chinese Chemical Letters*, 15(2) 214-215.
- Welinder, K.G. (1976) Covalent structure of the glycoprotein horseradish peroxidase. *FEBS Letters*, 72, 19-23.
- Wightman, R.M. (1981) Microvoltammetric electrodes. *Analytical Chemistry*, 53, 1125A.
- Wijayawardhana, C.A., Wittstock, G., Halsall, H.B. and Heinman, W.R. (2000a) Electrochemical Immunoassay with Microscopic Immunomagnetic Bead Domains and Scanning Electrochemical Microscopy. *Electroanalysis*, 12, 640-644.
- Wijayawardhana, C.A., Wittstock, G., Halsall, H.B. and Heinman, W.R. (2000) Spatially Addressed Deposition and Imaging of Biochemically Active Bead Microstructures by Scanning Electrochemical Microscopy. *Analytical Chemistry*, 72, 333-338.
- Wilhelm, T. and Wittstock, G. (2003) Analysis of interaction in patterned multienzyme layers by using scanning electrochemical microscopy. *Angewandte Chemie-International Edition*, 42, 2247-2250.
- Wilhelm, T. and Wittstock, G. (2002) Generation of Periodic Enzyme Patterns by Soft Lithography and Activity Imaging by Scanning Electrochemical Microscopy. *Langmuir*, 18, 9485-9493
- Wilhelm, T., Wittstock, G. and Szargan, R. (1999) Scanning Electrochemical microscopy of enzymes immobilised on structured glass-gold substrates. *Fresenius Journal of Analytical Chemistry*, 365, 163-167.
- Wipf, D.O., Wehmeyer, K.R., Wightman, R.M. (1986) Disproportionation of Quinone Radical Anions in Protic Solvents at High pH. *Journal of Organic Chemistry*, 51, 4760-4764.
- Wittstock, G. (2001) Modification and characterisation of artificially patterned enzymatically active surfaces by scanning electrochemical microscopy. *Fresenius Journal of Analytical Chemistry*, 370, 303-315.
- Wittstock, G., Wilhelm, T., Bahrs, S. and Steinrucke, P. (2001) SECM Feedback Imaging of Enzymatic Activity on Agglomerated Microbeads. *Electroanalysis*, 13, 669-675.
- Wittstock, G., Burchardt, M., Pust, S.E., Shen, Y., Zhao, C. (2007) *Angewandte Chemie International Edition*, 46,1584-1617.
- Wolff, E.A., Greenfield, B., Taub, D.D. (1999) Generation of artificial proteoglycans containing glycoaminoglycan-modified CD44 – Demonstration of the interaction between RANTES and chondroitin sulphate. *Journal of Biological Chemistry*, 274(4),2518-2524.

- Wring, S.A., Hart, J.P. (1990) Development of screen-printed carbon electrodes, chemically modified with cobalt phthalocyanine, for electrochemical sensor applications. *Analytica Chimica Acta*, 231, 203-212.
- Yamada, H., Fukumoto, H., Yokoyama, T. and Koike, T. (2005) Immobilised Diaphorase Surfaces Observed by Scanning Electrochemical Microscope with Shear Force Based Tip-Substrate Positioning. *Analytical Chemistry* 77, 1785-1790.
- Yamashita, K., Takagi, M., Uchida, K., Kondo, H. and Takenaka, S. (2001) Visualization of Dna Microarrays by Scanning Electrochemical Microscopy (SECM). *Analyst*, 126, 1210-1211.
- Yasukawa, T., Kondo, Y., Uchida, T. and Matsue, T. (1998) Imaging of cellular activity of single cultured-cells by scanning electrochemical microscopy. *Chemistry Letters*, 767-768.
- Yotter, R.A. and Wilson, D.M. (2004) Sensor technologies for monitoring metabolic activity in single cells - Part II: Nonoptical methods and applications. *Ieee Sensors Journal*, 4, 412-429.
- Yu, Q., Stamenkovic, I. (1999) Localisation of matrix metalloproteinase 9 to the cell surface provides a mechanism for CD44-mediated tumor invasion. *Genes and Development*, 13 (1) 35-48.
- Zamponi, S., Santucci, R., Brunori, R. (1990) A spectroelectrochemical study of microperoxidase at bare and gold-plated RVC thin-layer electrodes. *Biochimica et Biophysica Acta*, 1034, 294-297.
- Zaumseil, J., Wittstock, G., Bahrs, S. and Steinrucke, P. (2000) Imaging the activity of nitrate reductase by means of a scanning electrochemical microscope. *Fresenius J Anal Chem*, 352-355.
- Zhang, H., Gao, Y.G., Vandermarel, G.A., Vanboom, J.H., Wang, A.H.J. (1999) Simultaneous incorporation of 2 anticancer drugs into DNA – the structures of formaldehyde-cross-linked adducts of daunorubicin-d(CG(ARAC)GCG) and doxorubicin-d(CA(ARAC)GTC) complexes at high resolution. *Journal of Biological Chemistry*, 268, 10095-10101.
- Zhang, J., Chi, Q., Albecht, T., Kuznetsov, A.M., Grubb, M., Hansen, A.G., Wackerbath, H., Welinder, A.C. and Ulstrup, J. (2005) Electrochemistry and bioelectrochemistry towards the single-molecule level: Theoretical notions and systems. *Electrochimica Acta*, 50, 3143-3159.
- Zhang, X., Peng, X. and Wenrui, J. (2006) Scanning Electrochemical Microscopy with enzyme immunoassay of the cancer-related antigen CA15-3. *Analytica Chimica Acta*, 558, 110-114.
- Zhan, W., Bard, A.J. (2006) Scanning electrochemical microscopy. 56. Probing outside and inside single giant liposomes containing Ru(bpy)₃(2+). *Analytical Chemistry*, 78(3), 726-733.
- Zhao, G., Giolande, J.R. and Kirchoff, J. (1995) Chemical Vapor Deposition Fabrication and Characterization of Silica-Coated Carbon Fiber Ultramicroelectrodes. *Analytical Chemistry*, 67, 2592-2598.
- Zhao, C. and Wittstock, G. (2004a) Scanning Electrochemical Microscopy of Quinoprotein Glucose Dehydrogenase. *Analytical Chemistry*, 76, 3145-3154.
- Zhao, C. and Wittstock, G. (2004b) An SECM Detection Scheme with Improved Sensitivity and Lateral Resolution: Detection of Galactosidase Activity with Signal Amplification by Glucose Dehydrogenase. *Angewandte Chemie*, 43, 4170-4172.
- Zhao, C. and Wittstock, G. (2005) Scanning electrochemical microscopy for detection of biosensor and biochip surfaces with immobilized pyrroloquinoline quinone (PQQ)-dependent glucose dehydrogenase as enzyme label. *Biosensors and Bioelectronics*, 20 (7), 1277-1284.

Zhou, H.F., Kasai, S. and Matsue, T. (2001) Imaging Localized Horseradish Peroxidase on a Glass Surface With Scanning Electrochemical/Chemiluminescence Microscopy. *Analytical Biochemistry*, 290, 83-88.

Zhou, J.F., Campbell, C., Heller, A. and Bard, A.J. (2002) Scanning Electrochemical Microscopy. 44. Imaging of Horseradish Peroxidase Immobilized on Insulating Substrates. *Analytical Chemistry*, 74, 4007-4010.

Zhou, H., Sun, Z., Hoshi, T., Kashiwagi, Y., Anzai, J-I., Li, G. (2005) Electrochemical studies of danthron and the DNA-danthron interaction. *Biophysical Chemistry*, 114(1), 21-26.

Zoski, C.G. (1990) A survey of steady state microelectrode and experimental approaches to a voltammetric steady state. *Journal of electroanalytical chemistry*, 296(2), 317-333.

Zoski, C.G. Rodgers, R.S. (2000) Current amplification with signal averaging at steady state microelectrodes. *Electroanalysis*, 12(6), 420-424

Zoski, C.G. (2002) Ultramicroelectrodes: design, fabrication and characterisation. *Electroanalysis*, 14(15-16), 1041-1051.

Zhu, R., Macfie, S.M. and Ding, Z. (2005) Cadmium-induced plant stress investigated by scanning electrochemical microscopy. *Journal of Experimental Botany*, 56, 2831-2838.

Websites

www.uniscan.com

www.novartis.com



Review

Advances in the application of scanning electrochemical microscopy to bioanalytical systems

William S. Roberts^a, Daniel J. Lonsdale^b, John Griffiths^b, Séamus P.J. Higson^{a,*}^a *Cranfield Health, Cranfield University, Barton Road, Silsoe, Bedfordshire MK45 4DT, United Kingdom*^b *Uniscan Instruments Ltd., Sigma House, Burlow Road, Buxton, SK17 9JB, United Kingdom*

Received 8 March 2007; received in revised form 11 June 2007; accepted 27 June 2007

Available online 31 July 2007

Abstract

Scanning electrochemical microscopy (SECM) is a powerful surface characterisation technique that allows for the electrochemical profiling of surfaces with sub micrometer resolution.

While SECM has been most widely used to electrochemically study and profile non-biological surfaces and processes, the technique has in recent years, been increasingly used for the study of biological systems – and this is the focus of this review.

An overview of SECM and how the technique may be applied to the study of biological systems will first be given. SECM and its application to the study of cells, enzymes and DNA will each be considered in detail. The review will conclude with a discussion of future directions and scope for further developments and applications.

© 2007 Elsevier B.V. All rights reserved.

Keywords: Scanning electrochemical microscopy; Cells; Enzymes; DNA; Biological applications

Contents

1. Introduction	301
2. Principles of SECM	302
3. SECM applications	304
3.1. Living cells	304
3.1.1. Mammalian cells	306
3.1.2. Monitoring cellular status and drug viability testing	308
3.1.3. Multicellular organisms and their interrogation by SECM	308
3.1.4. Single celled organisms, microbial chips and bioassays	309
3.1.5. Cellular models	309
3.2. Enzymes	310
3.3. DNA Imaging by SECM	314
4. Conclusions and future outlook	315
Acknowledgements	316
References	316

1. Introduction

Scanning electrochemical microscopy (SECM) is a surface scanning probe technique that allows for the collection of high

resolution electrochemical data at a variety of surfaces. SECM exploits several of the unique electrochemical properties of microelectrodes, including the hemispherical diffusion profile of solutes towards a microelectrode and the stir independence of microelectrodes responses. SECM builds on a body of work conducted by Engstrom et al. and Liu et al. in the late 1980s in which the possibility of using microelectrodes to probe diffusion

* Corresponding author. Tel.: +44 1525 863455; fax: +44 1525 863533.
E-mail address: s.p.j.higson@cranfield.ac.uk (S.P.J. Higson).

layers and study conductor and semi-conductor surfaces was first demonstrated (Engstrom et al., 1986; Liu et al., 1986). During these early years much of the theory underpinning SECM was developed and expanded by Bard and co-workers allowing a theoretical description of (i) how the faradaic current measured at the tip may be described as a function of substrate charge transfer properties, (ii) the relationship between the faradaic current detected at the tip and the tip to substrate distance and (iii) the relationship between mass transport and homogenous reaction kinetics in the inter tip-substrate gap (Kwak and Bard, 1989a,b; Bard et al., 1989, 1990, 1991; Unwin and Bard, 1991; Bard et al., 1992).

SECM, since its earliest days, has been applied to a diverse array of bio-analytical problems and represents a tool that is capable of bringing together a number of previously dissociated analytical techniques. SECM is capable of providing quantitative information about the topography and electrochemical properties of a surface, however, the resolution of the image is very much dictated by the geometry and size of the ultramicroelectrode used. Whilst the majority of experiments conducted on biological specimens have used tips in the 5–25 μm range, much attention has been focussed towards the development of smaller, submicron probes since these allow smaller areas to be studied with a corresponding increase in resolution. Techniques increasingly employed in the fabrication of small probes include electrochemical etching, laser pipette pulling and photolithographic techniques, with many similarities to techniques employed in the fabrication of ultra fine AFM tips.

In contrast to other microscopic techniques such as fluorescence or scanning electron microscopy, SECM does not require the biological sample to undergo complex pre-treatment, with a sample only having to be submerged in a mediator solution or thin film. SECM moreover does not suffer from artefacts such as background fluorescence since the technique is not optically based. A further advantage of SECM over alternative imaging technologies, is that the system under interrogation may be numerically modelled, allowing the subsequent capture of information relating to the kinetics of the reaction under observation. This makes SECM uniquely suitable for the study of biological specimens, since they may be studied under simulated conditions close to those experienced *in vivo* and may be interrogated repeatedly due to the non-destructive nature of the imaging process. SECM has allowed numerous, distinctly different bioanalytical problems to be tackled, and these have included; determining the electroosmotic flow of ions through mouse and human skin (Bath et al., 2000; Uitto and White, 2003), the imaging of methyl viologen permeability in bovine cartilage (Gonsalves et al., 2000), bone reabsorption by osteoclasts (Berger et al., 2001), convective flow rates through dentine (Macpherson and Unwin, 2005), the interrogation of redox activities of cancer cells – and as a quality control tool for biosensor fabrication.

Other techniques, however, have undergone rigorous development and have established, well characterised protocols. Further, as a consequence of this and their greater commercial availability, they are more widely used in academic and other research laboratories. A significant caveat to SECM imaging

however, (which is one experienced by most scanning probe techniques), is the slow scanning speed and hence, low sample throughput. The use of a probe as opposed to a lens is also a significant issue – for positive feedback to occur, the tip must be positioned within one critical dimension of the working electrode from the surface under interrogation. This in itself gives rise to the problem of tip crash and the potential damage of the tip and substrate, which can lead to wasted time and effort. A key point to remember, however, is that one should not be tempted to directly compare SECM against other imaging technologies. SECM is a technique which does not directly image these biological entities, but the processes in which they are involved. When SECM is used to image an enzyme immobilised on a surface for example, it is the enzyme mechanism and the behaviour of products, co-factors or substrates that it is imaging, not the enzyme itself. The technique gives complementary information that can allow an improved understanding of the images obtained by other techniques such as fluorescence.

This review will cover the principles on which the SECM technique is based, before focussing on recent advances in the application of SECM to biological systems. For additional reviews on SECM and biological systems, the reader is also directed to Gyurcsanyi et al. (2004), Edwards et al. (2006), Wittstock et al. (2001, 2007), Amemiya et al. (2006) and Sun et al. (2007).

2. Principles of SECM

A schematic for a typical SECM arrangement is illustrated in Fig. 1. Here, an ultramicroelectrode is used within a three electrode system, in a solution containing (a) a redox active mediator (generally present in millimolar concentrations) together with (b) an electrolyte in excess. Under initial conditions, we shall assume that the redox couple is present in one form only, R/O ($R \leftrightarrow O + ne^-$). When polarised at the appropriate potential for the oxidation/reduction of the redox mediator, a diffusion-limited current will be detected at the tip. The current for an embedded disk ultramicroelectrode, may be given by:

$$i_{\infty} = 4nFDc^b a \quad (1)$$

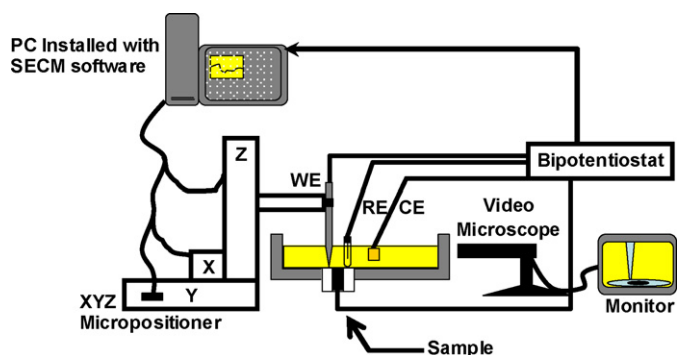


Fig. 1. Schematic diagram of an SECM system. The microelectrode probe is clamped into a high resolution XYZ micropositioning device and scanned across the sample surface. Scan parameters and tip electrochemistry is controlled via a PC interface.

where n is the number of electrons transferred per molecule of redox couple, F is the Faraday constant, D is the diffusion coefficient of R/O, c^b is the bulk concentration of R/O, a is the disk radius. Using a micro-positioning stage the tip (the microelectrode) is rastered across a surface in micrometer steps. When the tip is in bulk solution, the tip current observed follows the relationship described in Eq. (1). However, on moving the tip towards the substrate using a micro-positioning stage, the diffusion limited tip current (i_T) is observed to rise or fall, depending on the charge transfer properties of the substrate (Fig. 2). If the substrate is insulating or electrochemically inert, the diffusion of the R/O couple to the embedded electrode from bulk solution is physically hindered by the substrate, resulting in a decrease in current to a level less than that observed in bulk ($i_T < i_\infty$). As the tip approaches the substrate, the diffuse layer of the electrode is disturbed and the current falls precipitously as the tip-substrate gap narrows and the mass transport processes become increasingly hindered. On the other hand, if the substrate is conductive or electrochemically active, the mediator is recycled at the substrate, making it available once again to undergo the reaction at the tip resulting in an increase in the faradaic current observed. This approach, in which the tip acts as the source and detector of the mediator in its relevant redox state is termed feedback (FB) imaging, where positive and nega-

tive feedback signals are obtained over conductive/redox active and insulating/inert substrates respectively. The key parameter for positive feedback to occur however, is not the necessarily the electrical conductivity of the substrate, but the rate of heterogeneous electron transfer. This is demonstrated in a study by Lee et al., who switched layers of chromium between the pure metal and an oxide-covered surface, which resulted in the exhibition of positive and negative feedback respectively (Lee et al., 1990). For positive feedback to occur however, all it requires is that at the surface under interrogation, electron transfer to or from the respective half of the redox couple can occur, allowing their regeneration for re-oxidation or reduction at the electrode. This regeneration may occur due to the mediator's interaction with, for example, an oxidoreductase enzyme, a redox centre in an immobilised cell, or an electrochemical reaction at another electrode interface.

A particularly important mode of operation for SECM when used for studying biological entities is the substrate generation, tip collection mode (SG/TC) where, in contrast to feedback imaging, the tip acts solely as the detector of electroactive species produced by the substrate (the mode is also referred to as generation/collection mode, GC) (Fig. 2C). Here, the biochemical process under investigation by SG/TC mode is independent of the presence of the tip.

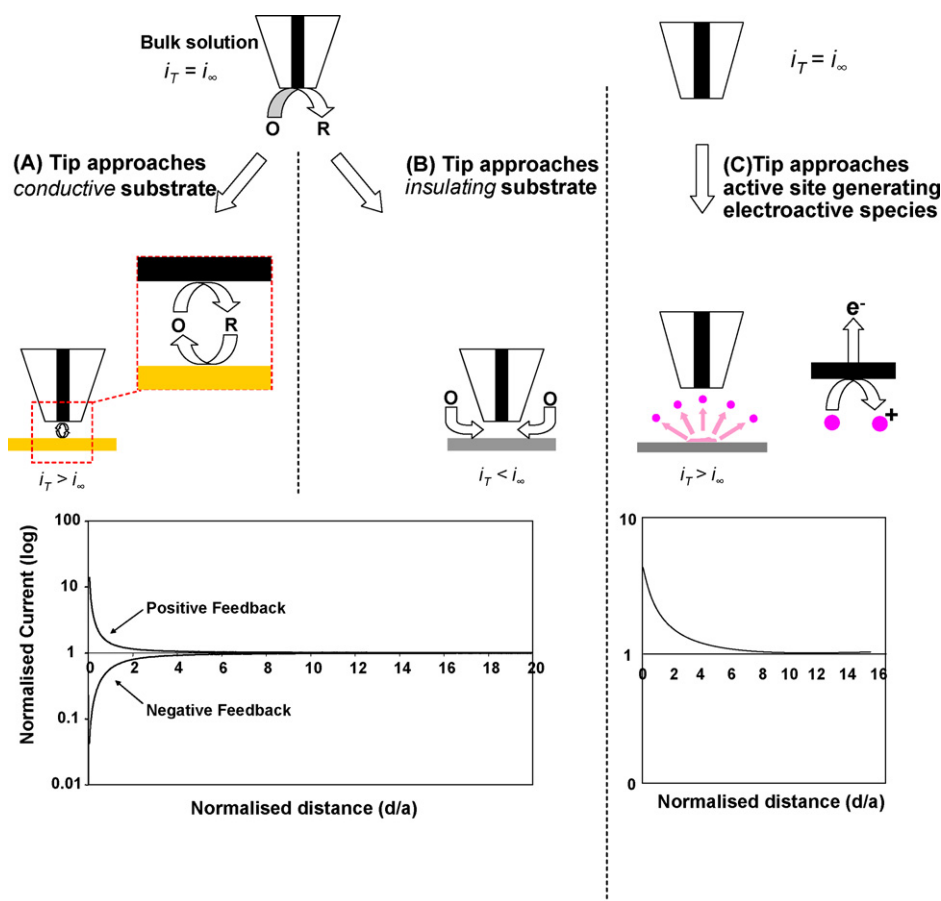


Fig. 2. Schematic illustrating the principles of positive and negative feedback (A and B) and of SECM in substrate generation, tip collection mode (C). (A) Mediator recycling at the boundary interface results in enhanced mass transport and increase in faradaic current. (B) Hindered diffusion of mediator to active electrode results in decrease in faradaic current. (C) SECM may be used to detect electroactive species generated at an active site (SG/TC mode).

Two varieties of this mode of imaging have been described – the first is where the tip radius is less than the specimen dimensions while the second is where the tip dimension is greater than the specimen dimensions. The latter approach has been little explored although the detection efficiency of species generated at the specimen may be close to 100%. An approach such as this can be useful when the analyte is present at low concentrations and spatially resolved data are not required. A second approach involves a small tip being rastered across the specimen surface to produce a map of the local concentration of a molecule that is being generated or consumed at the substrate.

Each of these approaches has distinct advantages in comparison to one another: in feedback mode, the image resolution achieved is typically much greater, as the reaction at the surface can only occur proximal to the tip since it is the sole source of the reactant. A significant caveat to this however, is that feedback imaging necessitates the use of a mediator which may either affect the behaviour of the substrate – or react with the substrate products. Additionally, the sensitivity of the FB mode is limited as the redox species is recycled at the substrate and must be detected against the signal arising from the initial oxidation/reduction of the mediator diffusing to the tip from bulk. Furthermore, as a result of the occurrence of positive feedback, the possibility for using this mode to interrogate functionalised conductive substrates like gold is limited since the positive feedback may be arising from regeneration via interaction with both the gold and the immobilised entity. These problems associated with the feedback mode of imaging are overcome by the use of the SG/TC mode however, where the ultramicroelectrode is used solely as the detector and is much more sensitive to electroactive species produced at the substrate, to allow the imaging of functionalised conductive substrates. The resolution of this technique is, however, often limited due to the diffuse nature of the substrate products.

The two imaging techniques do not have to remain distinct techniques though and it is possible to combine the sensitivity of SG/TC together with the high resolution of the feedback mode, although the applications to which this may be applied are somewhat limited. In an example such as this, Zhao and Wittstock (2004a) used the FB-SG/TC mode to image the activity of the enzyme glucose dehydrogenase (GDH). With reference to Fig. 3, PQL, a cofactor to GDH, diffuses to the substrate and is converted to PAP by GDH in the presence of D-glucose. PAP then diffuses back to the ultramicroelectrode, closing the feedback loop. The ultramicroelectrode tip current may in this way be attributed to the oxidation of PAP from galactosidase activity (GC mode) and from PQL at the GDH modified surface (FB mode); GC mode provides the sensitivity and FB allows signal amplification over GDH regions only, so enhancing resolution (Zhao and Wittstock, 2004a,b).

3. SECM applications

3.1. Living cells

Unlike many other microscopic techniques, SECM may be used to image living specimens under *in vivo* conditions, so

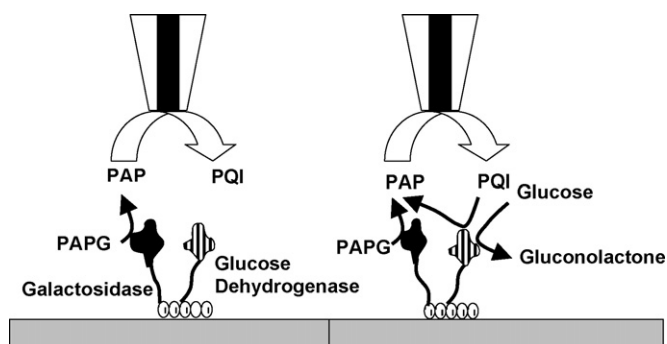


Fig. 3. Schematic diagram illustrating the combination of FB mode with SG/TC to combine the sensitivity of the SG/TC mode with the high resolution of the FB mode (Zhao and Wittstock, 2004a,b). Figure depicts and immobilised Gal-GDH multi-enzyme system. (A) Conventional GC mode for Galactosidase in the absence of glucose. (B) Signal amplification in the presence of glucose.

negating the need for complex preparation techniques that can give rise to artefacts. Combined with its ability to interrogate substrates non-invasively, SECM offers a unique approach to the study of intracellular processes with high spatial resolution (Yotter and Wilson, 2004). Using SECM, Lee et al. (1990) studied the photosynthetic activity of a variety of plant leaf structures by monitoring the concentration profiles of oxygen evolved during photosynthesis and their topography via negative feedback imaging using potassium ferricyanide (Lee et al., 1990). Since this first application of SECM to a biological substrate, the technique has since been considerably refined and subsequently applied to a variety of biological systems. Here we discuss how SECM techniques have been applied to derive information on living cells and the processes that occur within them.

The first approach to monitoring cellular activity by SECM is based upon monitoring the depletion of molecular oxygen in the immediate environment of cells as they respire (Yasukawa et al., 1998). In bulk solution, oxygen is present at higher concentrations than in the immediate vicinity to a respiring cell as oxygen moves down a concentration gradient and is consumed by the cell (Fig. 4). If an electrode is placed in close vicinity to a respir-

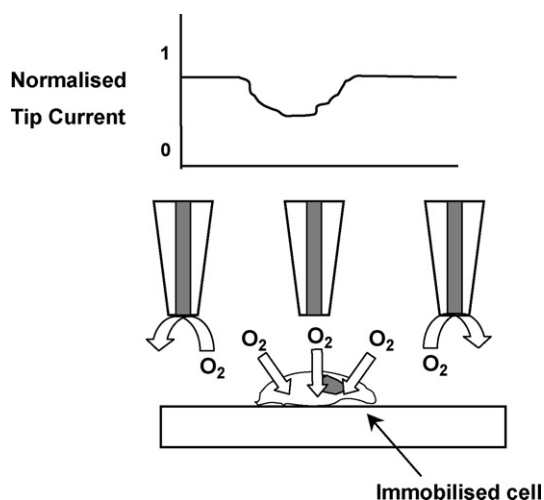


Fig. 4. Schematic diagram detailing imaging of cells by detection of reduction in oxygen concentration in the vicinity of the immobilised cell.

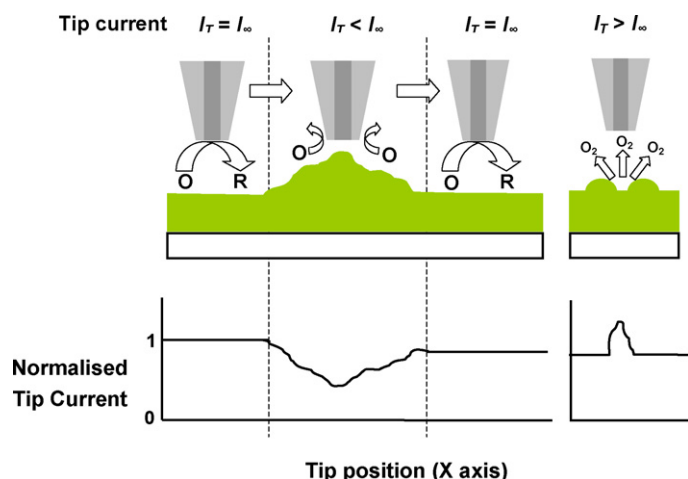


Fig. 5. (A) ‘O’ represents the mediator in its oxidised form and ‘R’ in its reduced form. In bulk solution, faradaic current is maximal at the applied potential and diffusion controlled; however, when brought into close proximity to a cell or a raised region of the specimen surface the diffusion of the mediator to the UME is hindered and negative feedback is observed. (B) When interrogating stomatal behaviour, an increase in tip current is observed over oxygen-generating regions of the specimen surface, i.e. over stomata.

ing cell, the faradaic current arising from the reduction of oxygen near the specimen will be less than that recorded by the electrode in bulk solution. Conversely, if a cell is producing oxygen, as in the case of a photosynthetic cell, oxygen concentration around the cell increases (Fig. 5). This approach may be used in the study of plant physiology (Tsionsky et al., 1997); SECM’s ability to obtain high resolution electrochemical maps of a surface has enabled the activity of single stomata to be monitored and has allowed an investigation into the effects of Cadmium induced stress on the plant *Brassica juncea* (Zhu et al., 2005) (Fig. 6). It was also used in the retrospective chemical analysis of tree rings by modifying the amino groups on the wood surface with glucose oxidase; using a shear force feedback approach, it was possible to obtain both topographical and chemical composition information about the sample wood surface obtained from the spruce, *Picea abies* (Garay et al., 2004) (Fig. 7). The 2–4% difference observed between early and late wood regions was attributed to a greater deposition of nitrogen during high growth phases (during early wood growth in spring and summer). The results were in strong agreement with other, more classical analyses of the wood, illustrating SECM’s applicability to a wide variety of bioanalytical problems. It is perhaps surprising that to date SECM has not been employed more widely in the study of plant physiology.

Oxygen was used further by SECM in a study of the differentiation process of human monocytic cell lines (THP-1). Leukocytes, which play a central role in the immune system, produce reactive oxygen species (ROS), ($O_2^{\bullet-}$, H_2O_2 and OH^-) during “respiratory burst” which involves the conversion of molecular oxygen to $O_2^{\bullet-}$ by NADPH oxidase in human monocytic leukaemia cells. Using SECM, the rate of ROS production was found to be reflective of the cellular differentiation process and when combined with chemiluminescence methodologies, could represent an easy approach to

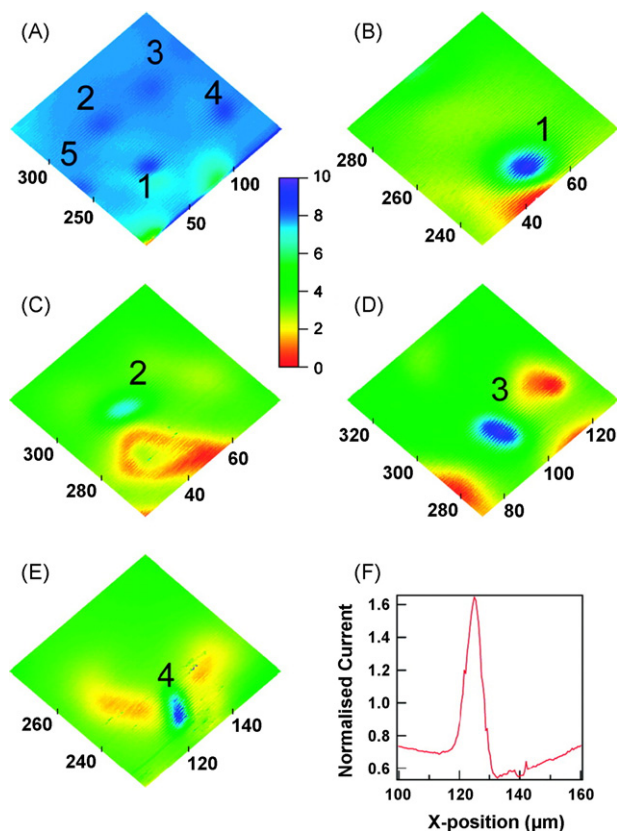


Fig. 6. (A) SECM image of a $150 \mu\text{m} \times 150 \mu\text{m}$ area of *Brassica juncea* (tip current, i_T was normalised by: i_T/i_∞ where $i_\infty = 0.77$ nA). (B–E) Zoomed in image of areas 1–4 in (A). (F) Cross-sectional linescan over stomata with high peripheral oxygen concentration (Zhu et al., 2005 with permission of Oxford University Press).

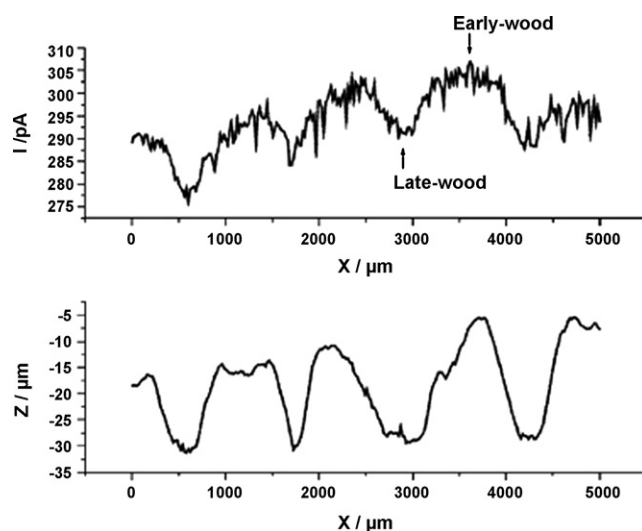


Fig. 7. Linescans over wood surface achieved simultaneously by using SECM in GC mode with shear force feedback. Glucose oxidase was immobilised on nitrogenous compounds on the wood surface and imaged under a 0.1 M phosphate buffer + 50 mM glucose solution (Garay et al., 2004 with permission of the PCCP Owner Societies).

monitoring the differentiation process in real time (Kasai et al., 2005).

An alternative method to the imaging of cells using oxygen is described by Liu et al. (2001). The approach involves the depletion of oxygen in the vicinity of the cell and monitoring the resultant increase in tip current as oxygen diffuses from the cell into its immediate surroundings. Whilst this is not necessarily a direct measurement of respiratory activity, it was only used here as a means of locating cells in the absence of a potentially harmful mediator. The tip current near the cell surface is enhanced as a result of the diffusion of oxygen trapped within the cell membrane to the tip down a concentration gradient, so increasing the effective mass transport rate.

Cellular activity may also be followed by approaches including the monitoring of the efflux of acid species from cells, since this is often an indicator used to monitor metabolic rate (McConnell et al., 1992). Using antimony electrodes to monitor the efflux of acid from immobilised cells, pH measurements were possible which allowed pH profiles to be composed and inferences about cellular activity to be made (Liu et al., 2001). Given advances in the detection of pH changes at the molecular level, it is possible that more spatially resolved data may be able to be obtained to allow more detailed inferences to be drawn about the role of pH in cellular and metabolic regulation (Petersen et al., 2004).

All of the approaches discussed so far do not include the use of electroactive mediators, i.e. redox active species that act as intermediaries between the ultramicroelectrode probe and the substrate under interrogation. The advantage of this approach is that the use of potentially harmful reagents can be avoided, maintaining conditions as close as possible to those experienced *in vivo*. Whilst this type of experiment is useful for studying cellular respiration and has been used extensively in SECM experiments, their usefulness in probing cellular biology and physiology is somewhat limited. There is hence much scope for the development of alternative techniques, such as the use of electroactive mediators. By introducing a mediator to the sys-

tem it is possible to interrogate the topography of cells, changes in morphology and changes in intracellular processes – as well as the mixed intracellular potentials, concentration and location of redox centres (Liu et al., 2001).

Of the vast array of tightly regulated cellular metabolic pathways, many function by the involvement of specific redox couples such as NAD^+/NADH , cysteine/cystine and the oxidised and reduced forms of glutathione and metalloenzymes (Rabinowitz et al., 1998). It follows that as extracellular conditions vary and these pathways are regulated to allow the cell to tolerate these changes, the intracellular concentrations of these couples also change. SECM techniques were first applied to investigating transmembrane charge transfer in a study into the different redox activities of nonmetastatic and metastatic human breast cells; this followed work in which intracellular redox activity was probed by detecting ferri/ferrocyanide regeneration by menadione/menadiol redox membrane permeable mediators at a gold electrode (Rabinowitz et al., 1998; Liu et al., 2000; Mirkin et al., 2002).

A schematic detailing some of the ways in which mediators of differing hydrophobicities may be utilised to interrogate living cells are shown in Fig. 8.

3.1.1. Mammalian cells

It has become possible to conduct studies exploring the intracellular redox potential of cells and the redox reactions that take place within them through the use of mediators with differential hydrophobicities – and hence abilities to permeate through cellular membranes.

Using a range of hydrophilic mediators, namely $\text{Ru}(\text{NH}_3)_6^{3/2+}$, $\text{Fe}(\text{CN})_6^{3/4}$ and $\text{Ru}(\text{CN})_6^{3/4}$, the topography and intracellular redox behaviour of metastatic and non-metastatic breast cell lines has been investigated (Liu et al., 2001). Metastatic and non-metastatic cell lines were observed to exhibit significantly different intracellular redox behaviour; normal, healthy MCF-10A cells regenerated naphthoquinone at a substantially greater rate than the metastatic MDA-MB-231

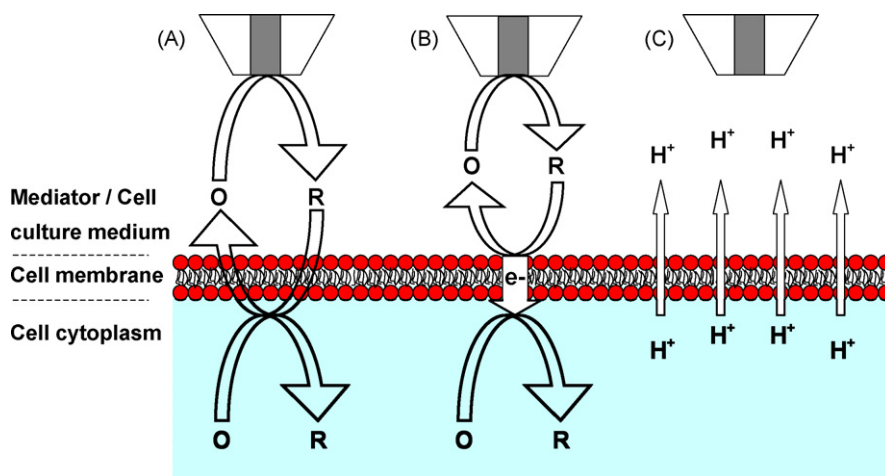


Fig. 8. (A) Positive feedback is observed as the hydrophobic reduced species generated at the tip diffuses through the cell membrane and is re-oxidised by a different intracellular redox centre confined within the boundaries of the cell. (B) Positive feedback is observed as a result of a self-exchange electron transfer reaction. Hydrophobic mediator diffuses to the cell membrane where it is re-oxidised by ET occurring across the cell membrane. (C) Schematic diagram illustrating the potentiometric measurement of the pH profile around a single cell.

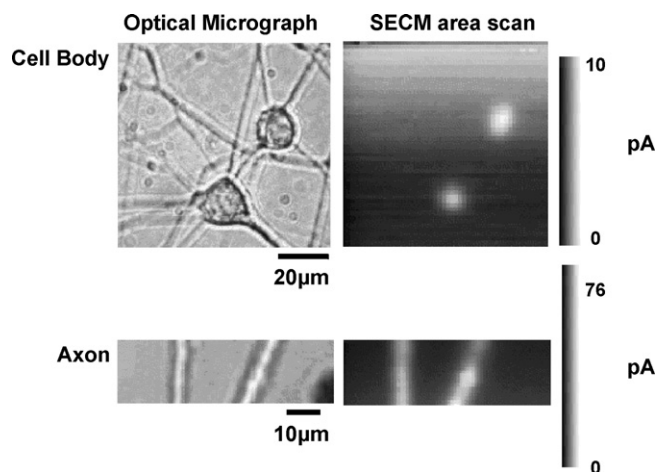


Fig. 9. Optical Micrographs and the corresponding SECM images of the cell bodies and axons of NGF-differentiated PC12 neuronal cells. SECM images were recorded with a Pt microelectrode scanned at $9.8 \mu\text{m s}^{-1}$ in a HEPES based saline solution. This figure was published in Takii et al. (2003). ©Elsevier (2003).

cells, a pattern which was observed with each of the other mediators used. Using SECM in combination with single cell chronocoulometry, it was established that the difference in the redox activity between non-transformed breast cells and metastatic breast cells arose from different concentrations of redox-active moieties in the cells and that the same intracellular moieties participate in the oxidation of all three quinols used as mediators. The occurrence of ‘hotspots’ of mediator regeneration within the cell also raised the question of whether specific redox events are confined to specific spatial localities

in the cell (Liu et al., 2001). The capability of SECM to detect hotspots of activity is highlighted further by Takii et al. (2003) who employed SECM techniques to characterise the spatial distribution of respiratory activity in PC12 neuronal cells (Fig. 9). Using the oxygen reduction current as an indicator of respiratory intensity, areas in which negative feedback was obtained were correlated to areas of high respiratory activity as the cell consumes oxygen from its immediate environment. Using this technique, the location of mitochondria in the axon could be identified together with the role of neuronal growth factor (NGF) in mitochondrion distribution and excitation (Takii et al., 2003). A significant limitation on this study however, was that it was not possible to simultaneously image the axon and cell body due to the height differential between the two cell structures. This problem was later overcome by the use of a ‘standing approach mode’, a feedback mechanism which allowed the simultaneous imaging of PC12 cell topography and respiratory activity for the first time (Takahashi et al., 2006) (Fig. 10). SECM has also been used in the development of a sensor for the neurotransmitter acetylcholine (Lin et al., 2004).

SECM provides information at the single cell level that may be very difficult to obtain by observing the average response from fields of cells – as well as allowing measurements on a much smaller time scale. However, SECM may be applied to larger fields of cells with good effect. By measuring the redox activity of a heterogeneous field of cells, it is possible to identify cancerous cells and so identify malignant cells in human tissues. Metastatic breast cells were loaded with fluorescent nanospheres and placed in a densely packed monolayer with unlabelled normal breast cells. Fluorescent images and SECM profiles were then superimposed on one another to show that SECM was capa-

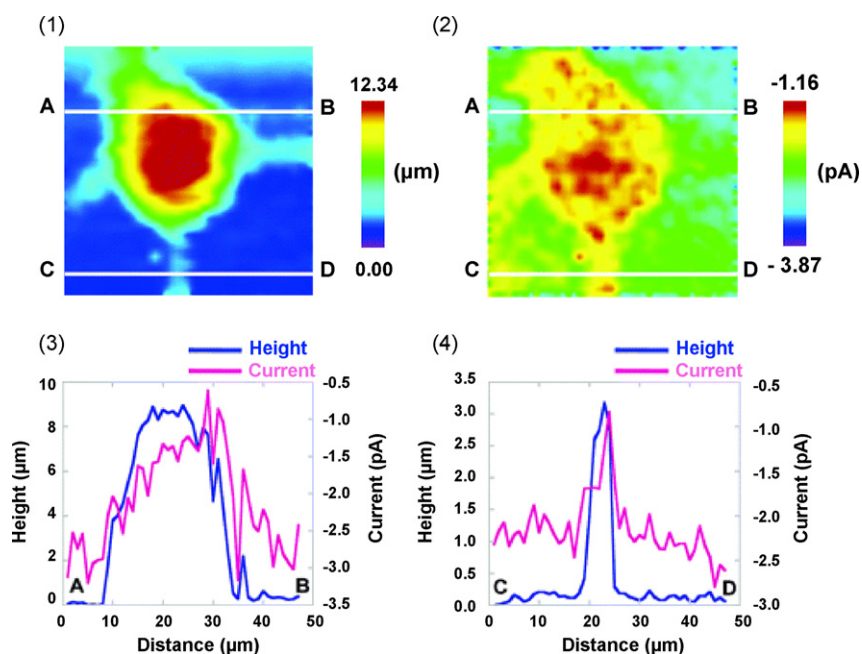


Fig. 10. Topographical (1) and electrochemical (2) images of live PC12 neuronal cells in PBS solution. Cross sections (white lines on images, A–B, C–D) across these images yield profiles (3 and 4) across the cell body and axon respectively. Images were recorded by SECM in STA (standing approach mode) using a capillary electrode probe, which allowed constant distance imaging. Scan range: $47 \mu\text{m} \times 47 \mu\text{m}$; step size: $1.0 \mu\text{m}$. Reprinted with permission from Langmuir 22 (25) (2006) 10299–10306. ©American Chemical Society (2006).

ble of differentiating between the two closely packed cell lines (Feng et al., 2003).

It is possible via the use of hydrophobic mediators, to obtain quantitative information relating to the morphology of living cells by observing changes in the tip current arising from variations in topography. Using SECM, cell structure–function relationships may be investigated. With a specific interest in the differentiation of PC12 cells into a neuron phenotype on exposure to nerve growth factor, Liebetrau et al. (2003) found that the images produced by the occurrence of negative feedback gave valuable insights into cell topography that could not be attained via light microscopy. SECM successfully recorded real-time morphological changes ($\pm < 1 \mu\text{m}$) induced by modulating the ionic strength of the surrounding medium. However, using the constant height approach to image the cells, it was not possible to image a complete neuron with the cell body and associated neurites due to the height difference between the two types of structure, much like the aforementioned study of Takii et al. (2003). To image samples with such a height differential, the SECM must be used in the constant distance mode and was later adopted to study undifferentiated and differentiated PC12 neurons. Here, the tip to substrate distance was maintained by monitoring the impedance of the solution between the tip and substrate and then moving the tip in the Z plane accordingly (Kurulugama et al., 2005).

3.1.2. Monitoring cellular status and drug viability testing

There are various approaches available for monitoring the physiology of cultured cells, including following pH changes through to impedance measurement and extracellular potential recording. The principal technique for measuring drug efficacy is however via fluorescence imaging. Stains such as GFP, Calcein-AM and propidium iodide interact with intracellular components to emit fluorescence which may subsequently be measured by a fluorometer. A drop in fluorescence may be attributed either to a decrease in cellular status or the photo-degradation of the fluorescing species, which means that care must be taken since the data can be ambiguous. This creates a perfect niche for the use of SECM since the approach does not depend on such chronodependent reactions – but rather measures respiratory activity directly through the uptake of oxygen. A further advantage of using this non-invasive approach over these other approaches, is that continuous monitoring of the dose effect is possible – and so there is no need for loading the system with cytotoxic fluorescent dyes.

In a study by Kaya et al. (2003c), SECM was used to study the impact of KCN, ethyl alcohol and Antimycin A on HeLa cells (see also Nishizawa et al., 2002). Measuring cellular activity by observing the oxygen reduction current, SECM successfully monitored cellular activity and the effects of cellular inhibitors. In a similar manner, Torisawa et al. (2003) used the SECM imaging system to investigate the differential anticancer drug sensitivity of the human erythroleukemia (K562) cell line and its adriamycin-resistant subline (K562/ADM). On comparing the results obtained to the succinic dehydrogenase inhibition (SDI) assay, it was found that they were highly correlated, despite the underlying principles of the tests being fundamentally different.

The same SECM assay was later applied to cancer cells isolated from xenografts implanted into severe combined immunodeficiency (SCID) mice as a model of a human tumor (Torisawa et al., 2004). By using SECM, the substrate and the sensing equipment are separated, so removing the necessity to incubate the cell with the chip, which in turn allows results to be attained in 4 days as opposed to 9 using the CD-DST assay.

SECM has been used in the development of a multi-channel 3-D cell culture device for use in an anticancer drug sensitivity test. The device, which consisted of 4×5 panels of pyramidal activities micromachined on a silicon wafer, when combined with SECM allowed for the continuous quantification of the oxygen consumption rate by the immobilised cells (Torisawa et al., 2005). Using this 3-D culture system combined with SECM, the simultaneous detection of the effects of multiple chemical stimuli on the cells arrayed in the chip was possible (Torisawa et al., 2005b). The results obtained via the continual monitoring of cellular viability by the measurement of the oxygen reduction current were in both cases well correlated with those obtained using the SDI assay.

3.1.3. Multicellular organisms and their interrogation by SECM

SECM has been used to study several different multi-cellular systems in a similar manner to the approach used for individual cells. For example, SECM has been used to quantify the embryogenesis, oxygen consumption and quality of individual bovine embryos and the respiratory, photosynthetic and peroxidase (POD) activities of *Bryopsis plumosa*, an algal protoplast, breast cancer spheroids and bovine embryos (Shiku et al., 2001, 2004a,b, 2005; Aoyagi et al., 2006; Agung et al., 2005; Abe and Hoshi, 2003; Hoshi, 2003). With reference to the work on bovine embryos, this is of particular interest since it involved the entrapment of the embryos within a cone-shaped microwell to amplify the oxygen concentration changes due to respiration, giving considerable support for the use of this substrate in constructing multi-sample arrays. SECM has also been used to quantify the local permeability of the nuclear envelope of *Xenopus oocyte* nuclei (Guo and Amemiya, 2005). Using approach curve and chronoamperometric experiments, findings supported existing conclusions that most nuclear pore complexes spanning the nuclear envelope are open. An advantage of using SECM over alternative methods used to study membrane transport such as patch clamping, is that SECM is non-destructive and this allows the same nucleus or membrane to be used for several different experiments.

An alternative approach for monitoring the activity of specific electrochemically active species is by chemically modifying the tip of the bare ultramicroelectrode. Tip modifications such as these were undertaken by Pailleret et al. (2003) to target nitric oxide, a key intracellular messenger, which is generated by adherently grown human umbilical vein endothelial cells (HUVEC) upon stimulation with bradykinin. Using SECM approach curves it was possible to position the tip accurately and non-destructively near the cell population and allow the detection of spontaneous NO release by the HUVEC population on stimulation by bradykinin. In a later study, a $50 \mu\text{m}$

diameter platinum disk probe was modified by the electrodeposition of Ni^{II} tetrakis (*p*-nitrophenylporphyrin) and combined in a double-barrel electrode arrangement to study the signal transduction pathway of NO release from transformed HUVEC cells (Borgmann et al., 2006).

Whilst SECM is capable of imaging fields of cells, problems arise in comparing cells with differing treatments. A technique has been developed that allows for a local dose to be administered to part of the cell culture, allowing the simultaneous comparison of cellular status of neighbouring cells undergoing different treatments. By juxtaposing a microporous alumina membrane with a poly-(dimethoxysilane) (PDMS) mask, ethanol was administered to a well defined area of a HeLa cell culture which was subsequently imaged by SECM via the measurement of the oxygen reduction current (Takoh et al., 2004). Additionally, SECM has been used quite extensively in patterning cells on substrates, examples of which involved switching the cytophobic behaviour of albumin-coated substrates to cell adhesive by exposure to HBrO, an oxidising agent, generated at an ultramicroelectrode held in close proximity to the surface (Kaji et al., 2003).

3.1.4. Single celled organisms, microbial chips and bioassays

SECM has been used extensively in the characterisation of microbial behaviour, largely due to its ability to facilitate non-invasive studies. As a consequence, SECM offers many advantages for both studying and incorporation into microbial bio-sensing systems. SECM has been used to interrogate the impact of the antibiotics ampicillin and streptomycin on the electron transport chain and membrane synthesis of *Escherichia coli* (Kaya et al., 2001), the effect of high osmotic stress on bacterium *E. coli* and *Staphylococcus aureus* (Nagamine et al., 2005b) and the respiratory activity of immobilised *E. coli* in response to exposure and subsequent uptake of Ag⁺, which is known to be an antibacterial agent (Holt, 2005). In the latter study, the well characterised ferricyanide mediator was used to monitor cellular status as bacteria are known to reduce ferricyanide to ferrocyanide during respiration; it was found that Ag⁺ affected cellular viability by inhibiting electron transfer. The possibility of using *E. coli* microbial chips as sensors for glucose was explored using SECM (Kaya et al., 2003a). On scanning a microelectrode across the collagen microstructure in which the *E. coli* cells were immobilised, a significant increase in the oxidation current was observed on the addition of D-(+)-glucose. This increase in oxidation current indicates the localised increase in the concentration of ferrocyanide released from the embedded *E. coli* cells. In the same study, the potential of the SECM to detect changes in microbial population size, and hence, growth rates, was investigated and a detection limit of just 100 cells was achieved in a later study (Kaya et al., 2003b,c), revealing the sensitivity of the technique and its potential for application to interrogating microbial arrays (Kaya et al., 2004).

Whilst the evolution of DNA microarray technologies has allowed the survey of intracellular gene networks and pathways by the comparison of transcriptional profiles in response to environmental stimuli, the data it provides is discontinuous and as

such, it is not suitable for the investigation of temporal changes in cellular behaviour. Taking this into account, it would be of great benefit if we could probe genetic changes that eventually manifest themselves at the cellular level. SECM, by its non-invasive nature and wide applicability offers a novel way to probe microbial behaviour on array chips, (Nagamine et al., 2005a,b). Using a microfluidic device, *E. coli* cells were transformed with various plasmid DNAs and the resulting change in phenotype monitored by a variety of techniques, including SECM. By monitoring β -galactosidase activity induced by the insertion of different plasmid DNAs, SECM successfully allowed differentiation between transformed and normal *E. coli* cells (Nagamine et al., 2005a). The approach was later applied to screening for mutagens in a whole cell sensor containing *Salmonella typhimurium*. Using *p*-aminophenyl- β -D-galactopyranoside (PAPG) as the enzymatic substrate, in comparison to the conventional *umu* assay, the SECM measurements were taken in a much smaller volume, were less time consuming and offered a lower detection limit for the mutagens used (Matsui et al., 2006). SECM was also used to investigate the production of ferrocyanide by *Paracoccus denitrificans* in response to a changing carbon source.

The technique also been used in the study of menadione uptake in the yeast *Saccharomyces cerevisia*. As menadione is toxic to yeast, the cell employs a defence system, based on glutathione (GSH), a non-protein sulfhydryl compound that conjugates with menadione to form a complex (thiodone) which is then exported from the intracellular space by a specific membrane pump. As thiodone is detectable by electrochemical means, it was possible to determine its rate of efflux from the cell and from that, to calculate the rate of uptake of menadione by the yeast cells, which, it was found, was the rate determining process (Mauzeroll and Bard, 2004). The technique was similarly used to detect the efflux of the same compound from hepatocytes (Mauzeroll et al., 2004). These studies highlight the unique potential for the use of SECM techniques in studying cellular behaviour and response to environmental stress.

By investigating the difference in the charge transfer mechanism between mammalian cells and bacteria, SECM has been used to probe the redox behaviour of *Rhodobacter sphaeroides*, a purple bacteria that contains a number of bound redox cofactors and a membrane bound reaction centre protein (Cai et al., 2002). By using a variety of hydrophobic and hydrophilic mediators it was possible to both interrogate different compartments of the cell due to their differential permeabilities and secondly to establish the effective concentration of intracellular redox centres. SECM revealed that the irradiation of the bacteria with visible light affects their redox response and that rate constants for the regeneration of mediators were being significantly lowered by illuminating the cells. The same membrane bound reaction centre was interrogated further but in chromatophores and liposomes (Longobardi et al., 2006).

3.1.5. Cellular models

Cells interrogated by SECM described so far, have primarily consisted of the positioning of an ultramicroelectrode in close proximity to a cell and the measurement of the resultant current

due to changes in topography, the emission of cellular products – or the recycling of a redox mediator. However, whilst this provides a great deal of information regarding the redox state of the cell, it would be hugely beneficial to monitor redox processes occurring within the cell directly. This would allow the more precise determination of the location of redox activities and their subsequent characterisation – and may even allow the development of techniques that would enable the study of the redox behaviour of intracellular compartments. With the long term aim of one day carrying out such an intracellular investigation, a simpler analogous system was interrogated to determine the viability of monitoring the intracellular redox conditions by SECM (Zhan and Bard, 2006). Giant liposomes of diameters 30–50 μm were constructed by the double-emulsion method and filled with $\text{Ru}(\text{bpy})_3^{2+}$; their redox properties were then probed by a flame-etched Carbon fibre SECM ultramicroelectrode tip. Over the course of the experiments, the tip current was monitored as the tip was firstly lowered into close proximity and then through the lipid membrane. The results illustrate SECM's suitability to studying membrane transport and its potential as an alternative technique to those based on fluorescence and radioactivity. The application of this technique to studying membrane transport also represents a departure from the current paradigm of membrane transport investigations via the use of bi-layer lipid membranes and allows measurements to be conducted over a longer period of time (Zhan and Bard, 2006). One of the first SECM studies involving the penetration of a cell with an electrode was reported by Fasching et al. (2006). Tips of a radius <50 nm were fabricated using focus ion beam technology and inserted into an 8 micron diameter rat fibroblast cell (Fasching et al., 2005, 2006). Using the ultra small tip, it was possible to penetrate the cell membrane and so to measure the potential of the cytosolic cell environment. A key area for consideration for

future 'overlap' with single cell analysis by SECM is that of ITIES (interface between two immiscible fluids) and the study of membrane transfer, a key process in cellular processes. Lee et al., for example describe the stochastic electrophoretic capture of individual nanometer-scale particles at a pore in a synthetic membrane (Lee et al., 2004).

3.2. Enzymes

With a strong trend towards the development of miniaturised analytical devices, there is much scope for the use of SECM in the fabrication (with regards to substrate patterning), characterisation and optimisation of enzyme based sensing systems. Through the determination of enzymatic activity, SECM may be used to characterise a variety of different sensors with various applications, from those that use enzymes as a label for a binding event through to sensors in which the enzyme forms the primary recognition element (Turcu et al., 2005; Zhang et al., 2006). By obtaining spatially resolved data relating to the distribution of electrochemical activity on the sensor substrate, the effectiveness of the patterning technique may be established and problems associated with cross talk between different sensing regions may be detected (Strike et al., 1999). For example, SECM was recently used to validate an ink-jet microdispensing technique for the production of a sensor with differently composed sensing regions (Turcu et al., 2005). Here, we give a brief overview of imaging enzyme activity and highlight recent advances in the field since the publication of the comprehensive review of enzymatic imaging by Wittstock (2001), whilst a summary of these developments may be seen in Tables 1 and 2.

An immobilised enzyme may be imaged by SECM in either feedback or SG/TC mode of operation, with the usual trade-off between resolution and sensitivity. Enzyme mediated feed-

Table 1
Proteins interrogated by SECM in feedback mode

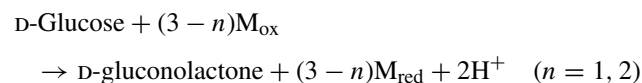
Protein	Substrate	Mediator	Reaction at UME	Ref.
Cytochrome <i>c</i> NADH-cytochrome <i>c</i> reductase	NADH	$\text{Fe}(\text{CN})_6^{4-}$	Oxidation	Holt (2006)
		TMPD ⁺	Oxidation	Pierce et al. (1992)
Glucose oxidase	β -D-Glucose	FcCOOH	Oxidation	Pierce et al. (1992)
Glucose dehydrogenase	Glucose	FcCH ₂ OH	Oxidation	Zhao et al. (2004), Zhao and Wittstock (2005)
		FcCOOH	Oxidation	Zhao et al. (2004)
		<i>p</i> -Aminophenol	Oxidation	Zhao et al. (2004)
Glucose oxidase	Glucose	Dimethylaminomethyl ferrocene Hydroquinone (HQ)	Oxidation	Wittstock (2001) Pierce and Bard (1993)
PQQ-dependant glucose dehydrogenase (GDH)	Glucose	$\text{Fe}(\text{CN})_6^{3-/4-}$ (with Os-redox relay)	Oxidation	Niculescu et al. (2004a)
		PAPG/PAP ^a	Oxidation	Zhao et al. (2004)
Quinohemoprotein alcohol dehydrogenase	Ethanol	$\text{Fe}(\text{CN})_6^{3-/4-}$ (with Os-redox relay)	Oxidation	Niculescu et al. (2004a)
Diaphorase (Dp)	NADH	FMA ⁺	Oxidation	Shiku et al. (1995, 2004a), Oyamatsu et al. (2003a,b,c)
Nitrate reductase	NO_3^-	Methyl viologen	Reduction	Zaumseil et al. (2000), Wittstock (2001)
Lactate oxidase	L-Lactate	Hydroxymethylferrocene (HMF)	Oxidation	Parra et al. (2006)

PAPG: *p*-aminophenyl- β -D-galactopyranoside; PAP: *p*-aminophenol.

Table 2
Proteins interrogated using SECM in generation collection mode

Protein	Substrate	Signal product	Reaction at UME	Ref.
Horse radish peroxidase (HRP)	Hydrogen peroxide	Hydroxyl methyl ferrocene (FMA)	Oxidation	Kranz et al. (2004), Wilhelm and Wittstock (2002), Glidle et al. (2003), Oyamatsu et al. (2003c)
HRP	Hydroquinone (H ₂ Q)	Benzoquinone (BQ)	Reduction	Zhang et al. (2006), Zhou et al. (2002)
Glucose oxidase	D-Glucose	Hydrogen peroxide (H ₂ O ₂)	Oxidation	Turcu et al. (2005), Kueng et al. (2003), Wilhelm and Wittstock (1999, 2002), Evans et al. (2005), Turyan et al. (2000), Strike et al. (1999), Hirata et al. (2004), Kasai (2002), Csoka et al. (2003a,b), Fuyun et al. (2001)
	D-Glucose (<i>p</i> -benzoquinone as co-substrate)	Hydroquinone	Oxidation	
GOx in multienzyme step (mutarose + glucosidase)	D-Glucose	Hydrogen peroxide		Gaspar et al. (2001)
Diaphorase	NADH	FMA	Reduction	Yamada et al. (2005)
Bilirubin oxidase	Oxygen	Hydrogen peroxide	Oxidation	Mano et al. (2003)
Glucose dehydrogenase	Glucose	Fe(CN) ⁴⁻	Oxidation	Zhao et al. (2004)
Galactosidase (in multienzyme system with GOx)	PAPG	<i>p</i> -Aminophenol	Oxidation	Zhao et al. (2004)
Uricase	Uric acid	Hydrogen peroxide	Oxidation	Kasai (2002)

back imaging, or ‘enzyme-mediated positive feedback’ involves the replacement of the enzymes co-factor, or ‘electron acceptor’ by a mediator. To illustrate this principle of feedback imaging through mediator regeneration, we use the catalysis of glucose to gluconolactone by glucose dehydrogenase (GDH) using the redox active mediator ferrocenemethanol as a cofactor (Zhao and Wittstock, 2005). Biotinylated GDH was immobilised on streptavidin coated paramagnetic microbeads at a surface concentration of 2.8×10^6 molecules/ $4\pi r_{\text{bead}}^2$ (1.8×10^{-11} mol cm⁻²) and deposited in a well defined, mound-shaped 100 μm diameter microspot. Polarised at a potential of 400 mV at a scan height of 30 μm above the surface, the scan was conducted in a buffered solution of Ca²⁺, D-glucose and FcCH₂OH. Positive feedback was obtained as a result of the reduction of the ferroceniummethanol (Fc) complex that occurs with the oxidation of glucose and its subsequent diffusion to the tip (see Fig. 11). On the removal of the D-glucose from the system, the feedback signal was halted. The detailed catalytic mechanism of GDH has not yet been fully defined due to the limited structural information available, however, a simplified over-arching mechanism has been proposed as (Zhao and Wittstock, 2004a):



For enzymatic activity to be detected by SECM in FB mode, the system must, however, obey the following equation, developed by Pierce et al. (1992).

$$k_{\text{cat}}\Gamma_{\text{enz}} \geq 10^{-3} \frac{D_{\text{R}}c_{\text{R}}}{r_{\text{T}}} \quad (2)$$

where k_{cat} is the enzyme reaction rate, Γ_{enz} is the enzyme surface concentration, D_{R} is the diffusion coefficient of

reactant, c_{R} is the concentration of reactant, r_{T} is the tip radius.

For feedback imaging to be possible not only must the parameters be of the correct magnitude to permit Eq. (2) but also, further to this, none of the mediator solution components should undergo oxidation or reduction at the working electrode or be capable of interfering with enzyme activity in any way (Wittstock, 2001). Taking into account the observation that SECM in feedback mode is somewhat less sensitive than SG/TC mode, the detection limit of the technique in feedback mode was

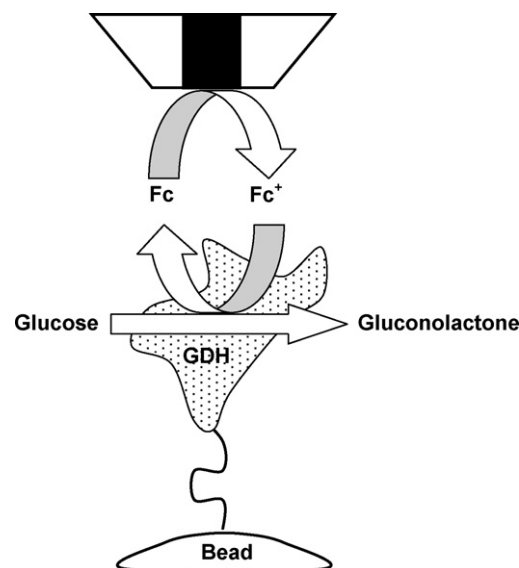


Fig. 11. Schematic diagram detailing the principle of enzyme mediated positive feedback. The mediator replaces oxygen as the electron acceptor, resulting in mediator recycling over a GDH-functionalised surface and hence, positive feedback. In this system, the reaction only occurs if the tip is present, which has the effect of increasing the resolution of the system.

determined. Horseradish peroxidase (HRP) was immobilised both within a hydrogel in a polycarbonate filter membrane and by biotin-avidin chemistry to a glass slide; both were subsequently imaged using the benzoquinone/hydroquinone redox couple. The work demonstrated a detection limit of less than 7×10^5 HRP molecules within a $\sim 7 \mu\text{m}$ diameter area (Zhou et al., 2002).

Until recently, a significant limitation to the use of oxidases as a recognition element in biosensors has been their dependence on the oxygen concentration in the surrounding media. However, significant improvements have been achieved by the replacement of the oxidase with a quinoprotein – one example being the pyrroloquinoline quinone-dependent glucose dehydrogenase (PQQ-GDH). The potential of this enzyme to replace its oxygen dependent predecessor, glucose oxidase is illustrated in a study by Zhao and Wittstock (2004a,b), who undertook a qualitative and quantitative study into the activity of this immobilised enzyme by SECM. Using four different mediators, of which *p*-aminophenol was found to be the most sensitive, they found that despite a degree of deactivation (during the biotinylation and immobilisation steps), PQQ-GDH had a turnover rate significantly larger than immobilised glucose oxidase. It was hence concluded that the high activity of PQQ-GDH and its independence of oxygen make this enzyme a very promising substitute for glucose oxidase as the recognition element in glucose sensors and as the labelling enzyme in chip-based bioassays.

The second mode of imaging enzymatic activity, substrate generation/tip collection (SG/TC) mode, is different to the feedback mode in that it does not involve the use of a mediator but rather the direct reduction or oxidation of the enzymatic product. Here, the microelectrode tip is rastered across the specimen surface to produce a map of the local concentration of a molecule generated or consumed by the enzyme. In contrast to the feedback mode, the biochemical process in this mode is independent of the presence of the tip. A distinct advantage of GC over the feedback mode is that the background current detected at the tip is negligible, increasing the signal to noise ratio by allowing any change in the faradaic current to be attributed to enzymatic activity. Additionally, many immobilisation techniques involve the immobilisation of the enzyme on gold substrates, meaning that if the feedback approach was to be adopted, the contribution of mediator regeneration by the electrochemical reaction at the gold surface under the enzyme layer would have to be decoupled from the faradaic current arising from the oxidation or reduction of electroactive species generated by the immobilised enzyme (Kranz et al., 1997; Oyamatsu et al., 2003a).

Despite its high sensitivity however, in contrast to the FB mode, this technique does suffer from a lack of spatial resolution; this comes as a result of the diffuse distribution of the biocatalytic products which diffuse away from the substrate down a concentration gradient into the surrounding medium preventing the accurate determination of the location of the enzyme. This may further be distorted by the movement of the electrode through the surrounding medium and the disturbance of the diffusion shell around the enzyme functionalised region. A further disadvantage of this technique arises when the process at the tip is reversible which means that there may be a feedback component to the current. This problem may be overcome by increasing the

tip to substrate distance or by using a potentiometric tip which does not perturb the local concentration of the reactant. The sensitivity of the GC mode may be enhanced by increasing the concentration of the generated product, which may be achieved by reducing the volume of solution between the tip and the substrate. A problem with this however, is that the diffusion of the substrate or cofactor from bulk to the enzyme may be physically hindered by the tip, resulting in a reduction in the tip current akin to that observed when approaching an insulating substrate (Zhao and Wittstock, 2004a). Further, unless the SECM system is equipped with a constant distance mechanism, by positioning the tip closer to the substrate, the user increases the risk of tip crash and hence damaging the microelectrode probe and substrate.

To illustrate the principle behind GC mode, we will look at the interrogation of horseradish peroxidase by Zhang et al. (2006) who demonstrate the use of the GC mode in an SECM-enzyme immunoassay. Designed to detect the circulating CA15-3 antigen, a specific marker used by clinicians to identify and diagnose breast cancer patients, this immunoassay was constructed with the aim of simplifying the conventional, time consuming, costly and complex assays currently being adopted. The assay, depicted schematically in Fig. 12, involves the sandwiching of the antigen between an antibody immobilised on a streptavidin coated plate and an antibody labelled with horseradish peroxidase. On exposure of the complete system (Ab-Ag-Ab*HRP) to H_2O_2 and hydroquinone, HRP catalyses the reduction of hydrogen peroxide to water via the oxidation of hydroquinone to benzoquinone which then diffuses to the microelectrode and is reduced, thus generating a faradaic current. The immunoassay was sensitive to 2.5 U/mL, which makes the approach suitable for detecting CA15-3 antigens (Fig. 13). Similarly, SECM has been used in a number of other immunoassays and immunosensors involving the use of a variety of other enzyme linked

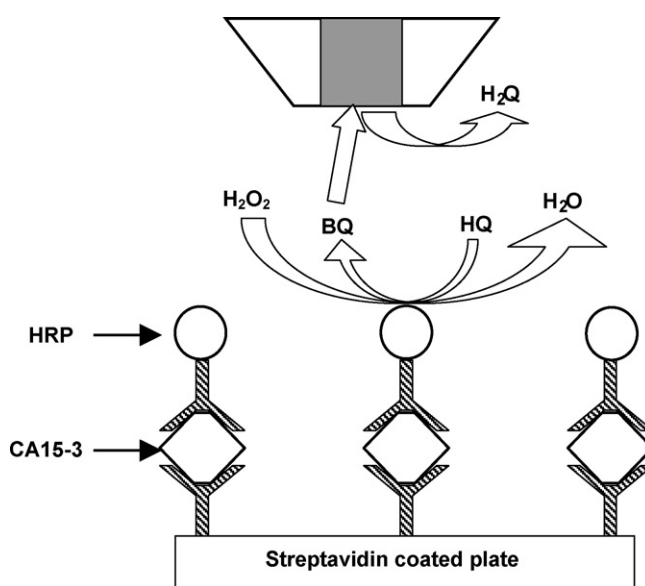


Fig. 12. Schematic diagram illustrating the principle of generation collection mode to image horseradish peroxidase (HRP) activity and here, to use it in an immunoassay to signal a binding event.

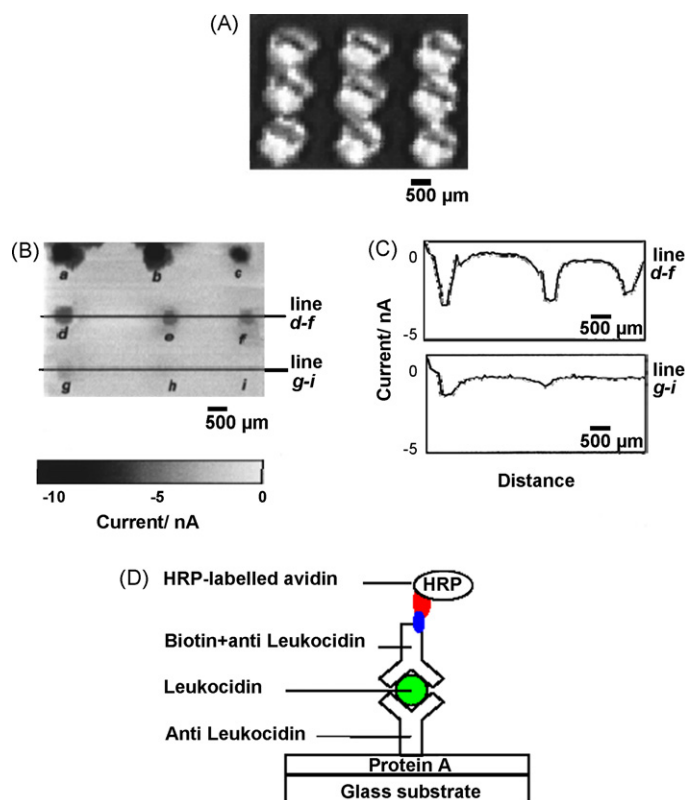


Fig. 13. A series of images illustrating the use of SECM in the development of an immunoassay for leukocidin, a toxic product of the MRSA bacterium. (A) Optical micrograph of 3×3 array containing different conc. leukocidin. (B) SECM image of leukocidin spots of differing concentrations. (C) Linescans over corresponding dots. Concentrations: (a) $52.5 \mu\text{g mL}^{-1}$, (b) $5.25 \mu\text{g mL}^{-1}$, (c) 525 ng mL^{-1} , (d) 52.5 ng mL^{-1} , (e) 5.25 ng mL^{-1} , (f) 525 pg mL^{-1} , (g) 52.5 pg mL^{-1} , (h) 5.25 pg mL^{-1} , (i) 0 pg mL^{-1} . (D) Schematic representation of leukocidin immunoassay. (A–C) Reprinted with permission from *Anal. Chem.* 72 (23) (2000) 5761–5765. ©American Chemical Society (2000).

systems including alkaline phosphatase (Wittstock et al., 1995; Wijayawardhana et al., 2000a), horseradish peroxidase (Shiku et al., 1996, 1997; Kasai et al., 2000) and biotinylated glucose oxidase (Wijayawardhana et al., 2000b). Building on the advantageous analytical properties that the SECM provides the immunoassay analyst, a self contained microelectrochemical enzyme-linked immunosorbant assay device was developed – the integration of all electrodes in the microwell in very close proximity to the modified surface allowed reproducible low detection limits of 9 pg/mL of mouse IgG in a $1 \mu\text{L}$ drop (Aguilar et al., 2002).

Similar to the feedback mode the functionalised area must obey the following detection limit model developed by Horrocks and Wittstock (2001) to allow the enzyme to be imaged by SECM:

$$k_{\text{cat}} \Gamma_{\text{enz}} \geq \frac{c' D}{r_s} \quad (3)$$

where r_s is the radius of enzyme-functionalised area, c' is the detection limit for species detected at the UME and D is the diffusion coefficient of c . Using this equation it is estimated that on a $100 \mu\text{m}$ diameter disk functionalised with a single layer of

enzyme, enzymes with a specific activity of $k_{\text{cat}} \geq 1 \text{ s}^{-1}$ may be imaged by SECM in GC mode (Horrocks and Wittstock, 2001).

SECM imaging is unique in the information it can provide and serves as an excellent complimentary technique, allowing an opportunity for hybridisation with other imaging techniques. By hybridisation it may also be possible to address the recurrent problem of differentiating the variation in current due to surface reactivity from that due to surface topography. For example, SECM was combined with a scanning chemi-luminescence microscope (SCLM) to generate electrochemical/chemiluminescence maps of HRP activity; the SCLM images generated are based on the detection of localised chemi-luminescence and show the activity and distribution of the immobilised enzyme, whereas the SECM image based on the reduction current of oxygen gives information on the topography of the area of enzyme immobilisation (Zhou et al., 2001). In a further example, Oyamatsu et al. (2003b) utilised a novel hybrid SECM/scanning confocal microscope (SCFM) system to image diaphorase (Dp) patterns generated by spotting, laser induced patterning and patterning through the electrogeneration of HOBr in order to deactivate the immobilised enzyme. Unlike the SECM which only generates an image when NADH is introduced to the system, SCFM is capable of imaging Dp alone, which makes these ideal complimentary techniques since one can image the localised enzyme and the *activity* of the enzyme only. Together however, these techniques could be used to good effect in the patterning and imaging of enzymes in the fabrication and characterisation of bio-devices.

In order to describe the function of different enzyme based biosensors, or to design optimal, efficient devices, it is necessary to determine the distribution of the different electroactive species inside the differently made, sized and formed reaction layers during their operation. Using SECM it is possible to make these determinations, in order to allow for the optimisation of the biosensor. Such is the effectiveness and usefulness of the technique, this area of research is one of the most frequent situations where SECM is used as a quality control technique.

In this context, in a series of papers by Csoka et al., SECM has been used to quantify the effectiveness of an interference-eliminating layer and to determine the reaction layer thickness to give an optimum enzyme response ($100 \mu\text{m}$) and to calculate the distribution of enzyme products within a less complex glucose oxidase biosensor in order to determine the optimum polymer:enzyme ratio in a wired enzyme electrode (Csoka et al., 2003a; Csoka et al., 2003b). The research demonstrated the capability of SECM in determining the distribution of different species within the reaction layer of biosensors which may allow their optimisation by the alteration of the structure of the sensor. Interference elimination was also the focus for Maciejewska et al. who used SECM to visualise the spatial variability of GOx/resydrol dots; using selected data collected from SECM area scans, principle component analysis (PCA) and trained neural networks were used to successfully quantify the concentration of glucose, 2-deoxy-D(+)-glucose and ascorbic acid in a solution (Maciejewska et al., 2006a,b; Wang et al., 2005). SECM was used further in the visualisation of redox hydrogel-based micropatterned complex biosensor architec-

tures; using SECM in feedback mode, the biochemical activity of immobilised enzyme microstructures were determined with high spatial resolution through the use of $K_4[Fe(CN)_6]$ as the electroactive mediator (Niculescu et al., 2004a,b).

Extensive work has also been conducted on evaluating the efficiency of different linkage chemistries and methods for the immobilisation of enzymes on a variety of substrates. In a comprehensive review by Wittstock (2001), a variety of techniques available for the immobilisation of enzymes are described, including enzyme-modified patterned monolayers, polymer and metal microstructures (e.g. Suzuki et al., 2004). SECM studies published after this review which detail new immobilisation combinations include: GOx immobilisation on biotinylated polypyrrole films deposited by SECM in direct mode (Evans et al., 2005; see also Kranz et al., 1997); biotinylated β -Galactosidase on streptavidin coated paramagnetic beads (Zhao et al., 2004); ‘wired’ spots of bilirubin oxidase (laccase) in a redox hydrogel (Fernandez et al., 2004); horseradish peroxidase in β -cyclodextrin (Wang et al., 2004); horseradish peroxidase and glucose oxidase immobilisation on amino-, thiol- and disulphide-functionalised gold patterned by a variety of soft lithographic techniques (Wilhelm and Wittstock, 2002, 2003; Oyamatsu et al., 2003c; see also Gaspar et al., 2001). Also, recently, lactate oxidase, LOx absorbed directly on glassy carbon and highly ordered pyrolytic graphite was detected by SECM and AFM, giving scope for the development of these materials as platforms for a biosensor for lactate, an important analyte in food and clinical science (Parra et al., 2006).

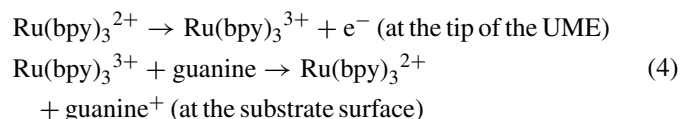
On reviewing the extensive literature concerning the application of SECM to the interrogation of immobilised enzymes, it is clear that only a limited number of enzymes have been characterised to date. There is clearly a vast array of proteins that remain uncharacterised by SECM.

3.3. DNA Imaging by SECM

As discussed by Fan (2001), the first SECM images of DNA were reported by Guckerberger et al. in 1994. Since these images were first produced, much progress has been made and effort devoted to, the development of the fabrication techniques of DNA microarrays and their associated high-throughput DNA microarray chip detectors. The reliable detection of mismatched base pairs is critical for the study, diagnosis and treatment of genetic disease, as well as the identification of single nucleotide polymorphisms (SNPs). Of the assays proposed for large scale mutational analysis those employing “DNA chips” are by far the most widely investigated. Existing techniques often rely on the detection of a label tagged on to the target sequence on the formation of a duplex between the probe sequence (on the chip) and targets in the sample analyte (which may have a fluorophore or a chemiluminescent label). However, the size, complexity and capital-intensive nature of these techniques represent major drawbacks, meaning there is plenty of scope for the development of alternative methods of detecting hybridisation events (Turcu et al., 2004a). As a consequence of this, numerous electrochemical biosensors and assays have been successfully developed which represent realistic alternatives to identifying

sequence specific DNA in addition to the mass-sensitive devices and optical biosensors dominating this biomedical niche today.

The employment of SECM techniques in studying hybridisation events is extremely appealing for a number of reasons – the detection level is potentially sufficiently low for most applications involving gene expression and SECM detection is relatively inexpensive and substrate general. With regards to its suitability in comparison to other modes of scanning probe microscopy, it represents the most viable approach because of the congruency of the spatial resolution of SECM tips with dimensions of microarray wells or spots. Micro arrays printed by ink jet technology, for example, produce droplets $\sim 67 \mu\text{m}$ in diameter, which is well within the resolution capabilities of an SECM and does not require the possibly costly fabrication of sub-micrometer UME tips. The simplest form of nucleic acid detection has been described by Wang et al. who exploit the intrinsic electrochemical properties of the guanine residue in the DNA duplex (Wang et al., 2002a; Wang and Zhou, 2002). Surface-confined DNA molecules were detected through the guanine oxidation induced by the tip-generated $Ru(bpy)_3^{3+}$:



On the application of a sufficient potential at the tip (+1.1 V), $Ru(bpy)_3^{3+}$ is generated which then diffuses to the substrate and irreversibly oxidises the guanine residues on the immobilised substrate, generating $Ru(bpy)_3^{2+}$ for re-oxidation at the tip. In this way positive feedback is observed over the surface confined DNA molecules. In the same study, the applicability of SECM to the detection of DNA hybridisation was illustrated also by exposing a Poly[G] target to an immobilised Poly[C] probe sequence. A distinct disadvantage of this approach is that due to the irreversible oxidation of the guanine residue, the same surface cannot be repeatedly scanned. In addition to this, the success of the technique is wholly dependent on the DNA sequence containing a significant amount of guanine residues in order to produce a sufficiently large oxidation current, which somewhat limits its applicability (Wang et al., 2002a).

The second approach to imaging DNA and the hybridisation event is to use electrochemically active labels. Yamashita et al. (2001) were one of the first teams to investigate the SECMs applicability to visualising DNA microarrays. Using an amino based ligand to immobilise DNA duplexes on glass in a mediator solution of ferrocenyl naphthalene, the microarray was imaged. This ligand was concentrated on the double stranded DNA region of the DNA array only, meaning that because of the ligand’s electrochemistry, it can interact with the scanning tip to generate a signal (the reader is also referred to Komatsu et al., 2006). The DNA hybridisation detection levels of this system however, were significantly less than those reported for alternative, existing techniques. In a later study by Wang et al. (2002b), these weaknesses of Yamashita et al. were highlighted. They subsequently reported using the silver staining approach in combination with SECM to image a DNA microarray. Here, silver nanoparticles were deposited at sites where hybridisation had occurred as they

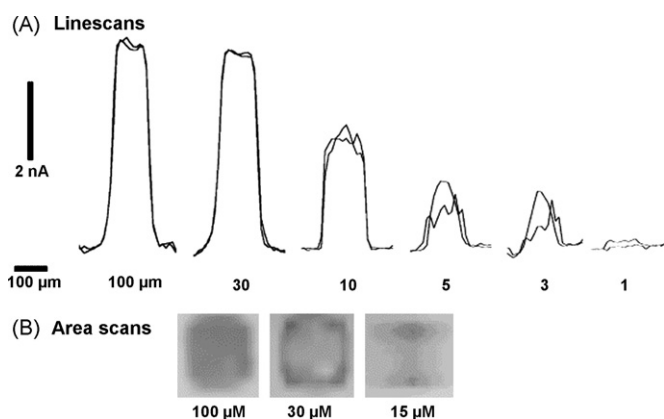


Fig. 14. Linescans over a DNA modified gold surface. Dots represent different concentrations of DNA solution ranging from 1 to 100 μM . Linescans were obtained in a mediator solution of 5 mM $[\text{Fe}(\text{CN})_6]^{3-}$ in 3 M NaCl/0.1 M phosphate buffer, pH 5.7; area scans obtained using a solution of 5 mM $[\text{Fe}(\text{CN})_6]^{3-}$ in 1 M NaCl/0.1 M phosphate buffer, pH 6.3. SECM probe: 10 μm Pt; scan rate: 10 $\mu\text{m s}^{-1}$ (Turcu et al., 2004a). This figure was published in Turcu et al. (2004a). ©Elsevier (2004).

conjugate onto the biotin/streptavidin-colloidal gold conjugate that has been sequentially constructed at the site of hybridisation. The result was an area over which positive feedback could occur as a consequence of mediator recycling at the site of silver deposition. Hence, the SECM can be used to detect hybridisation events. In addition to these findings, it was also revealed that by altering the hybridisation temperature, highly sequence-specific DNA analysis was possible down to the single base-mismatch level.

A significant caveat of current approaches to imaging DNA microarrays is the use of numerous reagents – a costly and time consuming factor. The development of reagentless means by which DNA hybridisation could be detected would clearly be highly beneficial. Exploiting the highly negatively charged properties of the sugar phosphate backbone of DNA, Turcu et al. (2004a) developed an electrostatic approach to visualising the status of surface bound DNA probes (Turcu et al., 2004a,b). Hybridisation detection was achieved through coulomb interactions between the negatively charged sugar phosphate backbone of the immobilised oligonucleotide and the free diffusing redox mediator. Using $[\text{Fe}(\text{CN})_6]^{3-}$ as a mediator, it was found that when the tip was scanned across a gold electrode functionalised with DNA, the tip current dropped as a result of the repulsive forces preventing the diffusion of the mediator to the gold electrode beneath for recycling (Fig. 14). On using a positively charged mediator however, such as $[\text{Ru}(\text{NH}_3)_6]^{3+}$, no fall in current was observed. Additional differences were found between the repulsive forces of ssDNA dots and dsDNA, indicating that the increase in repellent charges due to duplex formation is sufficient for detection by their repellent mode of SECM operation. In a further study by Liu and Bard et al., the role of mediator charge in investigating DNA films was highlighted further (Liu et al., 2005). Using the anionic mediators $\text{Fe}(\text{CN})_6^{3-/4-}$ and $\text{Fe}(\text{III})\text{EDTA}^-$, they interrogated ds-DNA and M-DNA immobilised on thiolated gold (M-DNA is dsDNA in which a divalent metal cation is inserted in place of one of the

protons at the interface between two of the nitrogenous bases at the centre of the duplex – which has been shown by electrochemical methods to enhance the ET properties of the DNA strand). Whilst initial results from approach curves suggested that M-DNA showed enhanced ET transfer properties, it was later revealed that this observation may be due to changes in the electrostatic repulsion forces between the mediator and the polyanionic sugar-phosphate backbone of the DNA; on adding the metal cations they may have been attracted to the phosphate groups, resulting in charge compensation, diminishing the overall negative charge on the immobilised DNA and allowing anionic mediators to diffuse through the film to the gold substrate, resulting in the surface exhibiting positive feedback when interrogated by SECM approach curves.

Preliminary experiments were conducted in order to evaluate the feasibility of SECM for detecting hybridisation events via the use of enzyme labelling (Gyurcsanyi et al., 2004). Complementary probe sequences were first dropped onto a microarray slide and allowed to hybridise. A 2.5% glutaraldehyde solution was then applied to the surface for the subsequent covalent crosslinking and attachment of GOx via the amino group on the complementary nucleotide. By monitoring the activity of the enzyme labels, it was possible to follow the hybridisation event.

As our knowledge of the human genome expands, there is an accompanying drive to develop increasingly specific DNA-targeting drugs, possibly acting on specific genes, effectively switching them on or off by preventing their transcription. With this comes the need to develop techniques that allow the characterisation of their behaviour to answer questions regarding the nature of the drug and characteristics of the binding site. Using electrochemical methods, including SECM approach curves, the electrochemical behaviour of minor-groove binding electroactive, antitubercular compound Hoechst 33258 was characterised (Wang et al., 2002a; also see Soderlind et al., 1999). Using these techniques they successfully developed a relationship for examining the interaction of irreversible redox active compounds intercalated with DNA.

4. Conclusions and future outlook

Since the first description of SECM in the late 1980s, SECM has become a key tool in the interrogation of a variety of biological systems. Since samples require little or no pre-treatment, the technique permits high resolution imaging of electrochemical processes under *in situ* conditions, making this technique an invaluable tool for studying living cells. Using mediators with different hydrophobicities, a number of studies have been conducted into the redox behaviour of cells. Additionally, SECM has been used extensively to study transmembrane processes and the role of trans-membrane pumps. The further interrogation of intracellular domains is a significant possibility with the fabrication of increasingly small electrodes – Takahashi et al. for example have just recently reported the successful imaging of biological samples using an electrode with an effective radius of just 35 nm (Takahashi et al., 2006) – it has already been demonstrated that it may be sensitive enough to determine the locus of enhanced mitochondrial activity within a cell;

with developments in SECM probes capable of insertion into the intracellular domain, more accurate determination of the locus of redox activity may be attained. However, with the fabrication of these electrodes must come the development of the accompanying theory, since electrodes with progressively smaller critical dimensions may exhibit electrochemical behaviour that departs from existing models.

The major group of organisms not yet interrogated by SECM are the fungi – major, extra-cellular producers of enzymes which play a central role in the major nutrient cycles. Given SECM's ability to detect enzymatic activity in both generation collection- and feedback-mode, it is believed that the technique is ideally suited to mapping the extracellular production of enzymes by fungi. By doing so, the technique may give a useful insight into the metabolism of fungi, with specific relevance to selecting the appropriate organisms with the optimal suitability to industrial processes. Capable of performing chemically difficult reactions under harsh conditions, many fungal enzymes have been harnessed in a variety of industrial processes, including pulp and paper processing, bioremediation and biocatalysis in the production of fine chemicals.

Since SECM has been successfully used in monitoring cellular respiration by measuring the oxygen oxidation current in the vicinity of a living cell, it is apparent SECM has significant potential as a research tool for use within drug discovery. Since the technique may be used to non-invasively monitor cellular status, it is believed that it will be increasingly adopted in this field.

There is a strong trend towards the exploitation of developments in manufacturing techniques to allow the miniaturisation of biological devices such as biosensors, micro-fluidic devices and “lab-on-a-chip” sensing technologies. Whilst the fabrication techniques are available, it is important that for these systems there is a technique sufficiently flexible to characterise the resulting product appropriately, with particular reference to imaging immobilised enzymes by SECM. Using this technique it is possible to locate immobilised entities, determine their spatial distribution and to interrogate the movement of substrates and products in and around the functionalised surface. The SECM is hence a hugely versatile system for application to sensor development, not only in their characterisation and quality control of sensing systems, but also in their fabrication via the controlled direct deposition of polymers and other biosensor scaffolds. The SECM's capability to pattern substrates, either by selective desorption of self assembled monolayers or by the localised deposition of polymers, has significant implications for the construction of multi-enzyme arrays.

A significant amount of effort is continuing to be focussed towards the development of electrochemical methods by which to detect DNA hybridisation. The reasons are several; the technique potentially offers great sensitivity, the sensors themselves exploit micro-fabrication techniques and they are also highly cost effective. With the current drive to develop electrochemical approaches for monitoring DNA, it is possible that the spatial resolution attainable using SECM offers great potential for the development of DNA microarray sensing systems to rival the benchmark fluorescent approach currently used.

As a stand-alone technique, SECM is a powerful tool for particular applications, but beyond this, when combined with other imaging tools such as atomic force and confocal microscopy, the power and resolution of the technique, in terms of information provided, is very much enhanced. By this ‘hyphenation’ or ‘hybridisation’ with other techniques, the shortcomings of the technique in tackling bioanalytical problems are partly addressed.

Acknowledgements

The authors would like to acknowledge the Engineering and Physical Sciences Research Council (EPSRC) of the UK and Uniscan Instruments Ltd., Buxton, UK, for the funding and sponsorship of an EngD studentship for W.S.R.

References

- Abe, H., Hoshi, H., 2003. *J. Reprod. Dev.* 49, 193–202.
- Aguilar, Z.P., Vandaveer, W.R., Fritsch, I., 2002. *Anal. Chem.* 74, 3321–3329.
- Agung, B., Otoi, T., Abe, A., Hoshi, H., Murakami, M., Karja, N.W.K., Murakami, M.K., Wongsrikeao, P., Watri, H., Suzuki, T., 2005. *Reprod. Domest. Anim.* 40, 51–56.
- Amemiya, S., Guo, J., Xiong, H., Gross, D.A., 2006. *Anal. Bioanal. Chem.* 386 (3), 458–471.
- Aoyagi, S., Utsumi, Y., Masudaira, M., Yamada, H., Kaachi, M., Shiku, H., Abe, H., Hoshi, H., Matsue, T., 2006. *Bunseki Kagaku* 55 (11), 847–854.
- Bard, A.J., Fan, F.R., Kwak, J., Lev, O., 1989. *Anal. Chem.* 61, 132–138.
- Bard, A.J., Denault, G., Lee, C., Mandler, D., Wipf, D.O., 1990. *Acc. Chem. Res.* 23, 357–363.
- Bard, A.J., Denault, G., Friesner, R.A., Dornblaser, B.C., Tuckerman, L.S., 1991. *Anal. Chem.* 63, 1282–1288.
- Bard, A.J., Mirkin, M.V., Unwin, P.R., Wipf, D.O., 1992. *J. Phys. Chem.* 96, 1861.
- Bath, B.D., Scott, E.R., Phipps, J.B., White, H.S., 2000. *J. Pharmaceut. Sci.* 89, 1537–1549.
- Berger, C.E.M., Rathod, H., Gillespie, J.I., Horrocks, B.R., Datta, H.K., 2001. *J. Bone Miner. Res.* 16, 2092–2102.
- Borgmann, S., Radtke, I., Erichsen, T., Blochl, A., Heumann, R., Schumann, W., 2006. *Chem. Biol. Chem.* 7, 662–668.
- Cai, C.X., Liu, B., Mirkin, M.V., Frank, H.A., Rusling, J.F., 2002. *Anal. Chem.* 74, 114–119.
- Csoka, B., Kovacs, B., Nagy, G., 2003a. Scanning electrochemical microscopy inside the biocatalytic layer of biosensors: investigation of a double function complex multienzyme reaction layer. *Electroanalysis* 15 (15–16), 1335–1342.
- Csoka, B., Kovacs, B., Nagy, G., 2003b. Investigation of concentration profiles inside operating biocatalytic sensors with scanning electrochemical microscopy (SECM). *Biosens. Bioelectron.* 18 (2–3), 141–149.
- Edwards, M.A., Martin, S., Whitworth, A.L., Macpherson, J.V., Unwin, P.R., 2006. *Physiol. Meas.* 27, R63–R108.
- Engstrom, R.C., Weber, M., Wunder, D.J., Burgess, R., Winquist, S., 1986. *Anal. Chem.* 58, 844–848.
- Evans, S.A.G., Brakha, K., Billon, M., Mailley, P., Denuault, G., 2005. *Electrochem. Commun.* 7 (2), 135–140.
- Fan, F.-R.F., 2001. In: Bard, E.J., Mirkin, M.V. (Eds.), *Scanning Electrochemical Microscopy*. Marcel Dekker, Inc., New York.
- Fasching, R.J., Tao, Y., Prinz, F.B., 2005. *Sens. Actuators B: Chem.* 108 (1–2), 964–972.
- Fasching, R.J., Bai, S.-J., Fabian, T., Prinz, F.B., 2006. *Microelectron. Eng.* 83, 1638–1641.
- Feng, W.J., Rotenberg, S.A., Mirkin, M.V., 2003. *Anal. Chem.* 75, 4148–4154.
- Fernandez, J.L., Mano, N., Heller, A., Bard, A.J., 2004. *Angew. Chem.* 116, 6515–6517.
- Fuyun, G., Tenent, R.C., Wipf, D.O., 2001. *Anal. Sci.* 17, 27–35.

- Garay, M.F., Ufheil, J., Borgwarth, K., Heinze, J., 2004. *Phys. Chem. Chem. Phys.* 6, 4028–4033.
- Gaspar, S., Mosbach, M., Wallma, L., Laurell, T., Csoregi, E., Schumann, W., 2001. *Anal. Chem.* 73, 4254–4261.
- Glidle, A.T., Yasukawa, C.S., Hadyoon, N., Anicet, T., Matsue, M., Nomura, M., Cooper, J.M., 2003. *Anal. Chem.* 75 (11), 2559–2570.
- Gonsalves, M., Macpherson, J.V., O'Hare, D., Winlove, C.P., Unwin, P.R., 2000. *Biochim. Biophys. Acta (BBA) – Gen. Subj.* 1524 (1), 66–74.
- Guo, J.D., Amemiya, S., 2005. *Anal. Chem.* 77 (7), 2147–2156.
- Gyurcsanyi, R.E., Jagerszki, G., Kiss, G., Toth, K., 2004. *Bioelectrochemistry* 63 (1–2), 207–215.
- Hirata, Y., Yabuki, S., Mizutani, F., 2004. *Bioelectrochemistry* 63 (1–2), 217–224.
- Holt, K., 2005. *Biochemistry* 44, 13214–13223.
- Holt, K., 2006. *Langmuir* 22, 4298–4304.
- Horrocks, B.R., Wittstock, G., 2001. In: Bard, A.J., Mirkin, M.V. (Eds.), *Scanning Electrochemical Microscopy*. Marcel Dekker, New York, p. 462.
- Hoshi, H., 2003. *Therigenology* 59, 675–685.
- Kaji, H., Kanada, M., Oyamatsue, D., Matsue, T., Nishiwaza, M., 2003. *Langmuir* 20, 16–19.
- Kasai, S., Yokota, A., Zhou, H., Nishizawa, M., Niwa, K.O.T., Matsue, T., 2000. *Anal. Chem.* 72, 5761–5765.
- Kasai, S., Shiku, H., Torisawa, Y.-S., Noda, H., Yoshitake, J., Shiraishi, T., Tomoyuki, Y., Watanabe, T., Matsue, T., Yoshimura, T., 2005. *Anal. Chim. Acta* 549 (1–2), 14–19.
- Kaya, T., Nishizawa, M., Yasukawa, T., Nishiguchi, M., Onouchi, T., Matsue, T., 2001. *Biotechnol. Bioeng.* 76, 391–394.
- Kaya, T., Nagamine, K., Oyamatsu, D., Shiku, H., Nishizawa, M., Matsue, T., 2003a. *Lab Chip* 3, 313–317.
- Kaya, T., Nagamine, K., Oyamatsu, D., Nishizawa, M., Matsue, T., 2003b. *Electrochemistry* 71, 436–438.
- Kaya, T., Torisawa, Y.S., Oyamatsu, D., Nishizawa, M., Matsue, T., 2003c. *Biosens. Bioelectron.* 18, 1379–1383.
- Kaya, T.D., Numai, K., Nagamine, K., Aoyagi, S., Shiku, H., Matsue, T., 2004. *Analyst* 129, 529–534.
- Komatsu, M., Yamashita, K., Uchida, K., 2006. *Electrochim. Acta* 51 (10), 2023–2029.
- Kranz, C., Lotzbeyer, T., Schmidt, H.-L., Schuhmann, W., 1997. *Biosens. Bioelectron.* 12 (4), 257–266.
- Kranz, C., Kueng, A., Lugstein, A., Bertagnolli, E., Mizaikoff, B., 2004. *Ultramicroscopy* 100 (3–4), 127–134.
- Kueng, A., Kranz, C., Lugstein, A., Bertagnolli, E., Mizaikoff, B., 2003. *Angew. Chem.-Int. Ed.* 42, 3238–3240.
- Kurulugama, R.T., Wipf, D.O., Takacs, S.A., Pongmayteegul, S., Garris, P.A., Baur, J.E., 2005. *Anal. Chem.* 77, 1111–1117.
- Kwak, J., Bard, A.J., 1989a. *Anal. Chem.*, 1794–1799.
- Kwak, J.B., Bard, A.J., 1989b. *Anal. Chem.* 61, 1221–1227.
- Lee, C., Kwak, J., Bard, A.J., 1990. *Proc Natl. Acad. Sci. U.S.A.* 87, 1740–1743.
- Lee, S., Zhang, Y., White, H.S., 2004. *Anal. Chem.* 76, 6108–6115.
- Liebetrau, J.M., Miller, H.M., Baur, J.E., 2003. *Anal. Chem.* 75, 563–571.
- Lin, S., Liu, C., Chou, T.C., 2004. *Biosens. Bioelectron.* 20 (1), 9–14.
- Liu, H.-Y., Fu-Ren, F.F., Lin, C.W., Bard, A.J., 1986. *J. Am. Chem. Soc.* 108, 3838–3839.
- Liu, B., Rotenberg, S.A., Mirkin, M.V., 2000. *PProc Natl. Acad. Sci. U.S.A.* 97, 9855–9860.
- Liu, B., Cheng, W., Rotenberg, S.A., Mirkin, M.V., 2001. *J. Electroanal. Chem.* 500, 590–597.
- Liu, B., Bard, A.J., Li, C.J., Kraatz, H.B., 2005. *J. Phys. Chem. B* 109, 5193–5198.
- Longobardi, F., Cosma, P., Milano, F., Agostiano, A., Mauzeroll, J., Bard, A.J., 2006. *Anal. Chem.* 78 (14), 5046–5051.
- Maciejewska, M., Schäfer, D., Schuhmann, W., 2006a. *Electrochem. Commun.* 8, 1119–1124.
- Maciejewska, M., Schäfer, D., Schuhmann, W., 2006b. *Electroanalysis* 18 (19–20), 1916–1928.
- Macpherson, J.V., Unwin, P.R., 2005. *Electroanalysis* 17, 197–204.
- Mano, N., Fernandez, J.L., Kim, Y., Shin, W., Bard, A.J., Heller, A., 2003. *J. Am. Chem. Soc.* 125, 15290–15291.
- Matsui, N., Kaya, T., Nagamine, K., Yasukawa, T., Shiku, H., Matsue, T., 2006. *Biosens. Bioelectron.* 21, 1202–1209.
- Mauzeroll, J., Bard, A.J., 2004. *Proc Natl. Acad. Sci. U.S.A.* 101 (21), 7862–7867.
- Mauzeroll, J., Bard, A.J., Owhadian, O., Monks, T.J., 2004. *Proc Natl. Acad. Sci. U.S.A.* 101 (51), 17582–17587.
- McConnell, H.M., Owicki, J.C., Parce, J.W., Miller, D.L., Baxter, G.T., Wada, H.G., Pitchford, S., 1992. *Science* 257, 1906–1912.
- Mirkin, M.V., Liu, B., Rotenberg, S.A., 2002. *Redox Cell Biol. Genet., Part a* 352, 112–122.
- Nagamine, K., Onodera, S., Torisawa, Y.-S., Yasukawa, T., Shiku, H., Matsue, T., 2005a. *Anal. Chem.* 77, 4278–4281.
- Nagamine, K., Kaya, T., Yasukawa, T., Shiku, H., Matsue, T., 2005b. *Sens. Actuators B: Chem.* 108 (1–2), 676–682.
- Niculescu, M., Gaspar, S., Schulte, A., Csoregi, E., Schuhmann, W., 2004a. *Biosens. Bioelectron.* 19, 1175–1184.
- Niculescu, M., Gaspar, S., Schulte, A., Csoregi, E., Schuhmann, W., 2004b. *Biosens. Bioelectron.* 19 (10), 1175–1184.
- Nishizawa, M., Takoh, K., Matsue, T., 2002. *Langmuir* 18, 3645–3649.
- Oyamatsu, D., Hirano, Y., Kanaya, N., Mase, Y., Nishizawa, M., Matsue, T., 2003a. *Bioelectrochemistry* 60, 115–121.
- Oyamatsu, D., Kanaya, N., Shiku, H., Nishizawa, M., Matsue, T., 2003b. *Sens. Actuators B: Chem.* 91, 199–204.
- Oyamatsu, D., Kanaya, N., Hirano, Y., Nishizawa, M., Matsue, T., 2003c. *Electrochemistry* 71, 439–441.
- Pailletet, A., Oni, J., Reiter, S., Isik, S., Etienne, M., Bedioui, F., Schuhmann, W., 2003. *Electrochem. Commun.* 5, 847–852.
- Parra, A., Casero, E., Vazquez, L., Jin, J., Pariente, F., Lorenzo, E., 2006. *Langmuir* 22, 5443–5450.
- Petersen, J., Boldt, F.M., Diez, M., Heinze, J., Borsch, M., 2004. *Biochimica Et Biophysica Acta. Bioenergetics* 1658, 118.
- Pierce, D.T., Bard, A.J., 1993. *Anal. Chem.* 65, 3598–3604.
- Pierce, D.T., Unwin, P.R., Bard, A.J., 1992. *Anal. Chem.* 64, 1795–1804.
- Rabinowitz, J.D., Vacchino, J.F., Beeson, C., McConnell, H.M., 1998. *J. Am. Chem. Soc.* 120, 2464–2473.
- Shiku, H., Takeda, T., Yamada, H., Matsue, T., Uchida, I., 1995. *Anal. Chem.* 67, 312–317.
- Shiku, H., Matsue, T., Uchida, I., 1996. *Anal. Chem.* 68, 1276–1278.
- Shiku, H., Hara, Y., Matsue, T., Uchida, I., Yamauchi, T., 1997. *J. Electroanal. Chem.* 438 (1–2), 187–190.
- Shiku, H., Shiraishi, T., Ohya, H., Matsue, T., Abe, H., Hoshi, H., Kobayashi, M., 2001. *Anal. Chem.* 73, 3751–3758.
- Shiku, H., Shiraishi, T., Aoyagi, S., Utsumi, Y., Matsudaira, M., Abe, H., Hoshi, H., Kasai, S., Ohya, H., Matsue, T., 2004a. *Anal. Chim. Acta* 522, 51–58.
- Shiku, H., Shiraishi, T., Aoyagi, S., Utsumi, Y., Matsudaira, M., Abe, H., Hoshi, H., Kasai, S., Ohya, H., Matsue, T., 2004b. *Anal. Chim. Acta* 522 (1), 51–58.
- Shiku, H., Torisawa, Y.S., Takagi, A., et al., 2005. *Sens. Actuators B: Chem.* 108 (1–2), 597–602.
- Soderlind, K.J., Gorodetsky, B., Singh, A.K., Bachur, N.R., Miller, G.G., Lown, J.W., 1999. *Anti-Cancer Drug Design* 14, 19–36.
- Strike, D., Hengstenberg, A., Quinto, M., Kurzawa, C., Koudelka-Hep, M., Schuhmann, W., 1999. *Microchim. Acta* 131, 47–55.
- Sun, P., Laforge, F.O., Mirkin, M.V., 2007. *Phys. Chem. Chem. Phys.* 21 (7), 802–823, 9.
- Suzuki, M., Yasukawa, T., Mase, Y., Oyamatsu, D., shiku, H., Matsue, T., 2004. *Langmuir* 20, 11005–11011.
- Takahashi, Y., Hirano, Y., Yasukawa, T., Shiku, H., Yamada, H., Matsue, T., 2006. *Langmuir* 22 (25), 10299–10306.
- Takii, Y., Takoh, K., Nishizawa, M., Matsue, T., 2003. *Electrochim. Acta* 48, 3381–3385.
- Takoh, K., Takahashi, A., Matsue, T., Nishizawa, M., 2004. *Anal. Chim. Acta* 522 (1), 45–49.
- Torisawa, Y.-S., Kaya, T., Takii, Y., Oyamatsu, D., Nishizawa, M., Matsue, T., 2003. *Anal. Chem.* 75, 2154–2158.
- Torisawa, Y.-S., Shiku, H., Kasai, S., Nishiwaza, M., Matsue, T., 2004. *Int. J. Cancer* 109, 302–308.
- Torisawa, Y., Shiku, H., Yasukawa, T., Nishizawa, M., Matsue, T., 2005. *Sens. Actuators B: Chem.* 108 (1–2), 654–659.

- Torisawa, Y., Shiku, H., Yasukawa, T., Nishizawa, M., Matsue, T., 2005b. *Biomaterials* 26 (14), 2165–2172.
- Tsionsky, M., Cardon, Z.G., Bard, A.J., Jackson, R.B., 1997. *Anal. Chem.* 113, 895–901.
- Turcu, F., Schulte, A., Hartwich, G., Schuhmann, W., 2004a. *Biosens. Bioelectron.* 20 (5), 925–932.
- Turcu, F., Schulte, A., Hartwich, G., Schuhmann, W., 2004b. *Angew. Chem.-Int. Ed.* 43, 3482–3485.
- Turcu, F., Hartwich, G., Schafer, D., Schuhman, W., 2005. *Macromol. Rapid Commun.* 26, 325–330.
- Turyan, I., Matsue, T., Mandler, D., 2000. *Anal. Chem.* 72, 3431–3435.
- Uitto, O.D., White, H.S., 2003. *Pharmaceut. Res.* 20, 646–652.
- Unwin, P.R., Bard, A.J., 1991. *J. Phys. Chem.* 95, 7814–7824.
- Wang, J., Zhou, F.M., 2002. *J. Electroanal. Chem.* 537, 95–102.
- Wang, S., Tuzhi, P., Yang, C.F., 2002a. *Electroanalysis* 14, 1648–1653.
- Wang, J., Song, F.Y., Zhou, F.M., 2002b. *Langmuir* 18, 6653–6658.
- Wang, X.L., Shi, Y.X., Bai, Z.L., Jin, W.R., 2004. *Chin. Chem. Lett.* 15 (2), 214–215.
- Wang, K., Xu, J.-J., Sun, D.-C., Wei, H., Xia, X.-H., 2005. *Biosens. Bioelectron.* 20 (7), 1366–1372.
- Wijayawardhana, C.A., Wittstock, G., Halsall, H.B., Heinman, W.R., 2000a. *Electroanalysis* 12, 640–644.
- Wijayawardhana, C.A., Wittstock, G., Halsall, H.B., Heinman, W.R., 2000b. *Anal. Chem.* 72, 333–338.
- Wilhelm, T., Wittstock, G., 2002. *Langmuir* 18, 9485–9493.
- Wilhelm, T., Wittstock, G., 2003. *Angew. Chem.-Int. Ed.* 42, 2247–2250.
- Wittstock, G., Yu, K.J., Halsall, H.B., Ridgway, T.H., Heineman, W.R., 1995. *Anal. Chem.* 67 (19), 3578–3582.
- Wittstock, G., 2001. *Fresenius J. Anal. Chem.* 370, 303–315.
- Wittstock, G., Wilhelm, T., Bahrs, S., Steinrucke, P., 2001. *Electroanalysis* 13, 669–675.
- Wittstock, G., Burchardt, M., Pust, S.E., Shen, Y., Zhao, C., 2007. *Angew. Chem. Int. Ed.* 46, 1584–1617.
- Yamada, H., Fukumoto, H., Yokoyama, T., Koike, T., 2005. *Anal. Chem.* 77, 1785–1790.
- Yamashita, K., Takagi, M., Uchida, K., Kondo, H., Takenaka, S., 2001. *Analyst* 126, 1210–1211.
- Yasukawa, T., Kondo, Y., Uchida, T., Matsue, T., 1998. *Chem. Lett.*, 767–768.
- Yotter, R.A., Wilson, D.M., 2004. *IEEE Sensors J.* 4, 412–429.
- Zaumseil, J., Wittstock, G., Bahrs, S., Steinrucke, P., 2000. *Fresenius J. Anal. Chem.*, 352–355.
- Zhan, W., Bard, A.J., 2006. *Anal. Chem.* 78 (3), 726–733.
- Zhang, X., Peng, X., Wenrui, J., 2006. *Anal. Chim. Acta* 558, 110–114.
- Zhao, C.J., Sinha, J.K., Wijayawardhana, C.A., Wittstock, G., 2004. *J. Electroanal. Chem.* 561 (1–2), 83–91.
- Zhao, C., Wittstock, G., 2004a. *Anal. Chem.* 76, 3145–3154.
- Zhao, C., Wittstock, G., 2004b. *Angew. Chem.* 43, 4170–4172.
- Zhao, C., Wittstock, G., 2005. *Biosens. Bioelectron.* 20 (7), 1277–1284.
- Zhou, H.F., Kasai, S., Matsue, T., 2001. *Anal. Biochem.* 290, 83–88.
- Zhou, J.F., Campbell, C., Heller, A., Bard, A.J., 2002. *Anal. Chem.* 74, 4007–4010.
- Zhu, R., Macfie, S.M., Ding, Z., 2005. *J. Exp. Bot.* 56, 2831–2838.